

Research reactor core conversion guidebook

Volume 4: Fuels (Appendices I–K)



INTERNATIONAL ATOMIC ENERGY AGENCY

IAEA

RESEARCH REACTOR CORE CONVERSION GUIDEBOOK
VOLUME 4: FUELS (APPENDICES I-K)
IAEA, VIENNA, 1992
IAEA-TECDOC-643
ISSN 1011-4289

Printed by the IAEA in Austria
April 1992

FOREWORD

In view of the proliferation concerns caused by the use of highly enriched uranium (HEU) and in anticipation that the supply of HEU to research and test reactors will be more restricted in the future, this guidebook has been prepared to assist research reactor operators in addressing the safety and licensing issues for conversion of their reactor cores from the use of HEU fuel to the use of low enriched uranium (LEU) fuel.

Two previous guidebooks on research reactor core conversion have been published by the IAEA. The first guidebook (IAEA-TECDOC-233) addressed feasibility studies and fuel development potential for light-water-moderated research reactors and the second guidebook (IAEA-TECDOC-324) addressed these topics for heavy-water-moderated research reactors. This guidebook, in five volumes, addresses the effects of changes in the safety-related parameters of mixed cores and the converted core. It provides an information base which should enable the appropriate approvals processes for implementation of a specific conversion proposal, whether for a light or for a heavy water moderated research reactor, to be greatly facilitated.

This guidebook has been prepared at a number of Technical Committee Meetings and Consultants Meetings and coordinated by the Physics Section of the International Atomic Energy Agency, with contributions volunteered by different organizations. The IAEA is grateful for these contributions and thanks the experts from the various organizations for preparing the detailed investigations and for evaluating and summarizing the results.

EDITORIAL NOTE

In preparing this material for the press, staff of the International Atomic Energy Agency have mounted and paginated the original manuscripts as submitted by the authors and given some attention to the presentation.

The views expressed in the papers, the statements made and the general style adopted are the responsibility of the named authors. The views do not necessarily reflect those of the governments of the Member States or organizations under whose auspices the manuscripts were produced.

The use in this book of particular designations of countries or territories does not imply any judgement by the publisher, the IAEA, as to the legal status of such countries or territories, of their authorities and institutions or of the delimitation of their boundaries.

The mention of specific companies or of their products or brand names does not imply any endorsement or recommendation on the part of the IAEA.

Authors are themselves responsible for obtaining the necessary permission to reproduce copyright material from other sources.

This text was compiled before the unification of Germany in October 1990. Therefore the names German Democratic Republic and Federal Republic of Germany have been retained.

PLEASE BE AWARE THAT
ALL OF THE MISSING PAGES IN THIS DOCUMENT
WERE ORIGINALLY BLANK

PREFACE

Volume 4 consists of detailed Appendices I - K, which contain useful information on the properties, irradiation testing, and specifications and inspection procedures for fuels with reduced uranium enrichments. Summaries of these appendices can be found in Chapters 9 - 11 of Volume 1 (SUMMARY) of this guidebook.

Appendix I contains information on the properties of aluminide, oxide, and silicide dispersion fuel materials, cladding and structural materials, corrosion resistance of aluminum alloy claddings, exothermic reactions, and structural stability of MTR fuel elements. Descriptions are also provided on the design, development, and qualification of LEU(8%) "Caramel" fuel and on the development, testing, and general specifications of uranium-zirconium hydride TRIGA-LEU fuel.

Appendix J summarizes requirements on the reliability of LEU fuel from the point of view of a reactor operator and outlines the philosophy and procedures that were utilized by the U.S. RERT Program for non-destructive and destructive PIE of miniplates and full-size elements. Extensive data are provided on the irradiation and post-irradiation examination of HEU and LEU dispersion fuels with high uranium density ($\geq 1.7 \text{ g/cm}^3$). Data includes burnup results, swelling and blister threshold temperature behavior, results of metallographic examinations, and fission product release behavior.

Appendix K discusses standardization of specifications and inspection procedures for LEU plate-type fuels. Detailed examples of fuel specifications and inspection procedures are provided for several fuel element geometries and fuel types. Methodology for determination of cladding thickness is also described.

The topics which are addressed in Volume 4, the appendices in which detailed information can be found, and the summary chapters of Volume 1 are listed below.

<u>Topic</u>	<u>VOLUME 4 APPENDIX</u>	<u>VOLUME 1 SUMMARY Chapter</u>
Fuel Materials Data	I	9
Irradiation and Post-Irradiation Examination (PIE) of Dispersion Fuels with High Uranium Density	J	10
Examples of Fuel Specifications and Inspection Procedures	K	11

CONTRIBUTING ORGANIZATIONS

Argonne National Laboratory	ANL	United States of America
Atlas-Danmark A/S	ATLAS	Denmark
Babcock & Wilcox	B&W	United States of America
Chalk River Nuclear Laboratories	CRNL	Canada
Comisión Nacional de Energía Atómica	CNEA	Argentina
Commissariat a l'Énergie Atomique	CEA	France
Compagnie Pour l'Étude et la Réalisation de Combustibles Atomiques	CERCA	France
EG&G - Idaho	EG&G	United States of America
GA Technologies Inc.	GA	United States of America
GEC Energy Systems, Ltd.	GEC	United Kingdom
GKSS-Forschungszentrum Geesthacht GmbH	GKSS	Federal Republic of Germany
Japan Atomic Energy Research Institute	JAERI	Japan
Kernforschungsanlage Julich	KfA	Federal Republic of Germany
Kernforschungszentrum Karlsruhe	KfK	Federal Republic of Germany
Kyoto University Research Reactor Institute	KURRI	Japan
Netherlands Energy Research Foundation	ECN	Netherlands
NUKEM GmbH	NUKEM	Federal Republic of Germany
Oak Ridge National Laboratory	ORNL	United States of America
Risø National Laboratory	RISØ	Denmark
United Kingdom Atomic Energy Authority	HARWELL	United Kingdom
United Kingdom Atomic Energy Authority	DOUNREAY	United Kingdom
University of Michigan - Ford Nuclear Reactor	FNR	United States of America

The IAEA is grateful for the contributions volunteered by these organizations and thanks their experts for preparing the detailed investigations and for evaluating and summarizing the results presented in this Guidebook.

CONTENTS

APPENDIX I. FUEL MATERIALS DATA

I-1. Properties of fuel meat materials	
I-1.1. ANL: Selected thermal properties and uranium density relations for alloy, aluminide, oxide, and silicide fuels	13
<i>J.E. Matos, J.L. Snelgrove</i>	
I-1.2. ANL: Phases in U-Si alloys	31
<i>R.F. Domagala</i>	
I-2. Properties of cladding and structural materials	
I-2.1. CERCA: Description and qualification of some aluminum alloys used by CERCA as cladding materials	41
I-2.2. NUKEM: NUKEM cladding and structural materials	45
I-2.3. B&W: Babcock and Wilcox cladding and structural materials	47
I-3. Corrosion resistance and experience with aluminum alloy claddings	
I-3.1. ANL: Water corrosion of aluminum alloy claddings	49
I-3.2. GKSS: Point corrosion defects of FRG-2 fuel elements	53
<i>W. Krull</i>	
I-3.3. HARWELL: Note on UK experience relating to corrosion of MTR fuel	57
<i>R. Panter</i>	
I-3.4. GEC: Aluminium corrosion data	59
<i>C. Baglin</i>	
I-3.5. CRNL: CRNL experience with aluminum cladding corrosion	61
<i>R.D. Graham</i>	
I-3.6. KfA: Water and corrosion technology of light water research reactors	69
<i>H. Pieper</i>	
I-4. Exothermic reactions	
I-4.1. ANL/ORNL: Exothermic reactions in U_3O_8 dispersion fuel	79
I-4.2. ANL: A differential thermal analysis study of U_3Si-Al and U_3Si_2-Al reactions	89
<i>R.F. Domagala, T.C. Wiencek, J.L. Snelgrove, M.I. Homa,</i> <i>R.R. Heinrich</i>	
I-4.3. KfK: Reaction behaviour of U_xSi_y-Al and U_6Fe-Al dispersions	107
<i>S. Nazaré</i>	
I-4.4. ATLAS: Differential thermal analysis and metallographic examinations of U_3Si_2 powder and U_3Si_2/Al (38 w/o) miniplates	115
<i>P. Toft, A. Jensen</i>	
I-5. Structural stability	
I-5.1. ANL: Structural stability of plate-type fuel elements used in US research and test reactors	123
I-5.2. JAERI: Hydraulic tests on dummy fuel elements for JAERI reactors	133
<i>K. Tsuchihashi, T. Sato, K. Simizu, K. Kurosawa, M. Banba,</i> <i>S. Yamaguchi, J. Tsunoda, F. Nakayama, Y. Itabashi, H. Kanekawa,</i> <i>R. Oyamada, M. Saito, T. Nagamatsuya</i>	
I-6. CEA: 'Caramel' — French LEU fuel for research reactors with emphasis on the OSIRIS experience of core conversion	143
I-7. GA: Uranium-zirconium hydride TRIGA-LEU fuel	161
I-7.1. GA/ORNL: Final results from TRIGA LEU fuel post-irradiation examination and evaluation following long term irradiation testing in the ORR	187
<i>G.B. West, M.T. Simnad, G.L. Copeland</i>	

APPENDIX J. IRRADIATION AND POST-IRRADIATION EXAMINATION (PIE) OF DISPERSION FUELS WITH HIGH URANIUM DENSITY

J-1. Irradiation and PIE of MTR HEU dispersion fuels with uranium densities up to 1.7 g/cm ³	
J-1.1. ANL: PIE data for HEU (93%) aluminide and oxide fuels	197
J-1.2. KfK: A statistical evaluation of the irradiation performance of HEU-based UAl _x -Al dispersion fuels	205
<i>S. Gahlert, S. Nazaré</i>	
J-1.3. CEA: Irradiation experiments	217
J-2. GKSS: Reliability of LEU fuel	229
<i>W. Krull</i>	
J-3. ANL: Post-irradiation examinations of dispersion fuels with reduced enrichment	231
<i>J.L. Snelgrove</i>	
J-4. Irradiation and PIE of test plates, rods, and full sized elements	
J-4.1. ORNL/ANL: The Oak Ridge Research Reactor	
J-4.1.1. Miniplate irradiations in the Oak Ridge Research Reactor	239
J-4.1.2. Full-sized element irradiations in the Oak Ridge Research Reactor	269
Part I. Irradiation performance of low-enriched uranium fuel elements	271
<i>G.L. Copeland, G.L. Hofman, J.L. Snelgrove</i>	
Part II. Performance of low-enriched uranium aluminide-aluminum thick-plate fuel elements in the Oak Ridge Research Reactor	283
<i>G.L. Copeland, J.L. Snelgrove</i>	
Part III. Examination of U ₃ Si ₂ -Al fuel elements from the Oak Ridge Research Reactor	303
<i>G.L. Copeland, G.L. Hofman, J.L. Snelgrove</i>	
J-4.2. CEA: LEU and MEU fuel testing in CEA reactors	315
<i>C. Baas, M. Barnier, J.P. Beylot, P. Martel, F. Merchie</i>	
J-4.3. ECN: Final report on the irradiation testing and post-irradiation examination of low enriched U ₃ O ₈ -Al and UAl _x -Al fuel elements by the Netherlands Energy Research Foundation (ECN)	329
<i>H. Pruimboom, E. Lijbriek, K.H. van Otterdijk, R.J. Swanenburg de Veye</i>	
J-4.4. GKSS: Full size element irradiations in the FRG-2	367
<i>W. Krull</i>	
J-4.5. CRNL: The conversion of NRU from HEU to LEU fuel	369
<i>D.F. Sears, M.D. Atfield, I.C. Kennedy</i>	
J-4.6. DOUNREAY: Development of low enrichment MTR fuel at Dounreay	381
<i>D. Sinclair</i>	
J-4.7. RISØ: Part I. Irradiation of MEU and LEU test fuel elements in DR 3	385
<i>K. Haack</i>	
Part II. Irradiation in DR 3 of the three Danish manufactured LEU silicide test fuel elements	397
J-5. Fission product release	
J-5.1. ANL: Fission product release from alloy, aluminide, oxide and silicide fuels	413
<i>D. Stahl, J.L. Snelgrove</i>	
J-5.2. KURRI/ORNL/ANL: Release of fission products from irradiated aluminide fuel at high temperatures (<i>Abstract</i>)	419
<i>T. Shibata, T. Tamai, M. Hayashi, J.C. Posey, J.L. Snelgrove</i>	
J-5.3. ORNL: Release of fission products from miniature fuel plates at elevated temperature	421
<i>J.C. Posey</i>	

J-5.4. JAERI: Further data of silicide fuel for the LEU conversion of JMTR	433
<i>M. Saito, Y. Futamura, H. Nakata, H. Ando, F. Sakurai, N. Ooka,</i>	
<i>A. Sakakura, M. Ugajin, E. Shirai</i>	

APPENDIX K. EXAMPLES OF FUEL SPECIFICATIONS AND INSPECTION PROCEDURES

K-1. GKSS: Standardization of specifications and inspection procedures for LEU plate-type research reactor fuels	445
<i>W. Krull</i>	
K-2. ANL/FNR: Fuel elements with LEU UAl_x -Al fuel for the Ford Nuclear Reactor	
K-2.1. Specifications	457
K-2.2. Inspection scheme	477
K-3. RISØ: Fuel elements with LEU U_3O_8 -Al fuel for the DR-3 reactor	
K-3.1. Specifications	505
K-3.2. Inspection scheme	515
K-4. ANL/ORNL: Specifications for fuel plates with LEU U_3Si_2 -Al fuel for the Oak Ridge Research Reactor	553
K-5. DOUNREAY: Notional specification for MTR fuel plates/tubes at uranium densities up to 1.6 g/cm^3	563
<i>B. Hickey</i>	
K-6. KURRI/CERCA: Fabrication of medium enriched uranium fuel plate for KUCA critical experiment: Design, fabrication, inspection and transportation	565
<i>K. Kanda, Y. Nakagome, T. Sagane, T. Shibata</i>	
K-7. JAERI: Specifications for fuel elements with MEU UAl_x -Al fuel for the JMTRC reactor	577
<i>R. Oyamada, Y. Yokemura, K. Takeda</i>	
K-8. CRNL: Summary of specifications for Canadian enriched U-Al pin-type fuel	585
<i>R.D. Graham</i>	
K-9. NUKEM: Determination of cladding thickness in fuel plates for material test and research reactors (MTR)	589
<i>T. Görgenyi, U. Huth</i>	

Appendix I

FUEL MATERIALS DATA

Abstract

Information is provided on the properties of aluminide, oxide, and silicide dispersion fuel materials, cladding and structural materials, corrosion resistance of aluminum alloy claddings, exothermic reactions, and structural stability of MTR fuel elements.

Descriptions are also provided on the design, development, and qualification of LEU(8%) "Caramel" fuel with emphasis on the OSIRIS experience of core conversion and on the development, testing, and general specifications of uranium-zirconium hydride TRIGA-LEU fuel with up to 45 wt-% U.

Appendix I-1

PROPERTIES OF FUEL MEAT MATERIALS

Appendix I-1.1

SELECTED THERMAL PROPERTIES AND URANIUM DENSITY RELATIONS FOR ALLOY, ALUMINIDE, OXIDE, AND SILICIDE FUELS

J.E. MATOS, J.L. SNELGROVE
RERTR Program,
Argonne National Laboratory,
Argonne, Illinois,
United States of America

Abstract

This appendix presents data on the specific heat, thermal conductivity, and other properties of fuel meat materials commonly used, or considered for use, in research and test reactors. Also included are formulae relating the density of uranium in the fuel meat with the weight fraction of uranium and the volume fraction of the dispersed phase.

1.0 URANIUM DENSITY RELATIONS

In general, the density and weight fraction of uranium in fuel meat composed of aluminum, a dispersed phase, and voids can be written as:

$$\rho_U = \frac{(1 - P) W_U}{\frac{1}{\rho_{Al}} - a W_U} \qquad W_U = \frac{\rho_U / \rho_{Al}}{(1 - P) + a \rho_U} \qquad (1)$$

where

$$a = \frac{1}{W_U^D} \left(\frac{1}{\rho_{Al}} - \frac{1}{\rho_D} \right) \qquad (2)$$

$$P = \text{Porosity} = \frac{\text{Volume of Voids}}{\text{Volume of Solids} + \text{Volume of Voids}}$$

W_U = Weight Fraction of Uranium in the Fuel Meat

W_U^D = Weight Fraction of Uranium in the Dispersed Phase

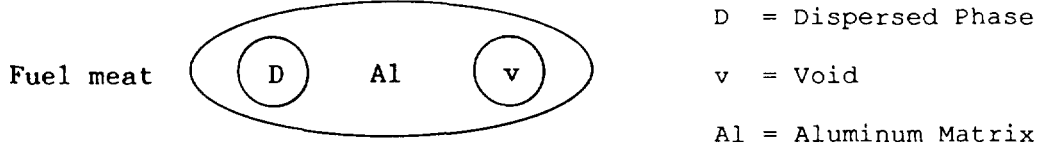
ρ_{Al} = Density of Aluminum = 2.7 g/cm³

ρ_D = Density of the Dispersed Phase

A useful formula in relating the terminology used by physicists and the terminology used by fuel fabricators is the relationship between the uranium density in the fuel meat and the volume fraction (V_f^D) of the dispersed phase:

$$\rho_U = w_U^D \rho_D V_f^D \quad (3)$$

The derivation of these formulae is given below.



Volume Balance for Fuel Meat: $V_m = V_D + V_{Al} + V_v$

Divide by M_m (mass of meat): $\frac{V_m}{M_m} = \frac{V_D}{M_m} + \frac{V_{Al}}{M_m} + \frac{V_v}{M_m}$

Substitute: $\frac{V_m}{M_m} = \frac{1}{\rho_m}$, $\frac{V_D}{M_m} = \frac{V_D}{M_D} \frac{M_D}{M_m} = \frac{w_D}{\rho_D}$,

$$\frac{V_{Al}}{M_m} = \frac{V_{Al}}{M_{Al}} \frac{M_{Al}}{M_m} = \frac{w_{Al}}{\rho_{Al}} = \frac{1 - w_D}{\rho_{Al}} \quad \text{and} \quad \frac{V_v}{M_m} = \frac{V_v}{V_m} \frac{V_m}{M_m} = \frac{P}{\rho_m}$$

to obtain:

$$\frac{1 - P}{\rho_m} = \frac{w_D}{\rho_D} + \frac{1 - w_D}{\rho_{Al}} = \frac{1}{\rho_{Al}} - w_D \left(\frac{1}{\rho_{Al}} - \frac{1}{\rho_D} \right)$$

Substitute: $\rho_U = \frac{M_U}{M_m} \frac{M_m}{V_m} = w_U \rho_m$ and $w_U = w_U^D w_D$

to obtain:

$$\frac{(1 - P) w_U}{\rho_U} = \frac{1}{\rho_{Al}} - w_U \left[\frac{1}{w_U^D} \left(\frac{1}{\rho_{Al}} - \frac{1}{\rho_D} \right) \right] = \frac{1}{\rho_{Al}} - a w_U$$

= a

Solve for ρ_U :

$$\rho_U = \frac{(1 - P) w_U}{\frac{1}{\rho_{Al}} - a w_U} \quad \text{which is Eq. (1)}$$

Also:

$$\rho_U = \frac{M_U}{V_m} = \frac{M_U}{M_D} \frac{M_D}{V_D} \frac{V_D}{V_m} = w_U^D \rho_D V_f^D \quad \text{which is Eq. (3).}$$



The uranium-aluminum system¹ (Fig. 1) contains three compounds - UAl_2 , UAl_3 , and UAl_4 - which are formed during cooling down from the molten state. Some properties² of these compounds are listed in Table 1:

<u>Compound</u>	Density, <u>g/cm³</u>	<u>W_U^D</u>	<u>Melting</u> <u>Point, °C</u>
UAl ₂	8.1	0.813	1590
UAl ₃	6.8	0.744	1350
UAl ₄ [*]	6.1 (Theoretical)	0.685	730
	5.7 ± 0.3 (Measured ³)	0.640	

Since UAl_2 and UAl_3 react with an excess of aluminum at moderate temperatures to form UAl_4 , the relative amounts of these compounds that are present in the fuel meat of a finished plate or tube is a function of the wt-% of the uranium and the fabrication processes and heat treatments that are utilized.

3.0 URANIUM-ALUMINUM ALLOY FUEL

For uranium-aluminum alloy fuel with less than ~25 wt-% U, the alloy is mostly aluminum and UAl₄. Above ~25 wt-% U, a considerable amount of meta- stable UAl₃ may be present. The amount of retained metastable UAl₃ increases with increasing uranium content and with increasing impurity content. If it is advantageous, the brittle UAl₄ phase can be suppressed⁴ in favor of the more ductile UAl₃ phase through the use of ternary additions such as silicon.

3.1 Uranium Density Relations for U-Al Alloy Fuel

The densities of UAl₃ and UAl₄, the corresponding weight fractions of uranium in each compound, and the value of the parameter a in Eq. (2) are:

Uranium Compound	Density, g/cm ³	W _U ^D	a
UAl ₃	6.8	0.744	0.300
UAl ₄	5.7 ± 0.3	0.640	0.305

The relationships between the uranium density and the weight fraction of uranium in the fuel meat, and between the uranium density and the volume fraction of the uranium compound are:

$$\rho_U = \frac{(1 - P) W_U}{0.370 - a W_U} \quad W_U = \frac{0.370 \rho_U}{(1 - P) + a \rho_U}$$

$$\rho_U = 5.1 v_f^{UAl_3} \quad \rho_U = 3.7 v_f^{UAl_4}$$

3.2 Specific Heat of U-Al Alloy Fuel

The specific heat of U-Al alloy fuel meat depends on the relative amounts of its constituents and their respective specific heats. The specific heat of "pure" aluminum is given by:⁵

$$C_{p,Al} = 0.892 + 0.00046 T \quad \text{J/g K, } T \text{ in } ^\circ\text{C} \quad (4)$$

Measured specific heats for pure uranium-aluminum compounds such as UAl₃ and UAl₄ are not available. The best data available are calculated⁶ from specific heat data⁷ for uranium and aluminum employing Kopp's law⁸ and values of excess heat capacity.⁹ The data presented in Ref. 6 yield the following specific heats for UAl₃ and UAl₄:

$$C_{p,UAl_3} = 0.329 + 0.00021 T \quad \text{J/g K, } T \text{ in } ^\circ\text{C} \quad (20-600 ^\circ\text{C}) \quad (5)$$

$$C_{p,UAl_4} = 0.473 + 0.00024 T \quad \text{J/g K, } T \text{ in } ^\circ\text{C} \quad (20-600 ^\circ\text{C}) \quad (6)$$

Using $W_U^D = 0.744$ for fully-enriched UAl₃ and $W_U^D = 0.640$ for fully-enriched UAl₄:

$$C_{p,U-Al \text{ alloy}} = (1.0 - W_U/0.744) C_{p,Al} + (W_U/0.744) C_{p,UAl_3}$$

(100% UAl₃)

$$= 0.892 + 0.00046 T - W_U (0.757 + 0.00034 T) \text{ J/g K, } T \text{ in } ^\circ\text{C}$$

$$C_{p,U-Al \text{ alloy}} = (1.0 - W_U/0.640) C_{p,Al} + (W_U/0.640) C_{p,UAl_4}$$

(100% UAl₄)

$$= 0.892 + 0.00046 T - W_U (0.655 + 0.00034 T) \text{ J/g K, } T \text{ in } ^\circ\text{C}$$

Since most plate-type research reactor fuels contain < 25 wt-% U, the uranium compound in the fuel meat is mostly UAl₄. At 25 wt-% U and 40°C, for example, specific heats for U-Al alloy calculated assuming 100% UAl₄ and 100% UAl₃ differ by less than 4%. In practice, only a small fraction of the uranium compound is likely to be UAl₃.

3.3 Thermal Conductivity of U-Al Alloy Fuel

The thermal conductivity of U-Al alloy fuel meat decreases with increasing weight fraction of uranium¹⁰ as shown in Fig. 2. A linear regression of the data points for the as-cast material yields the relation:

$$K = 2.17 - 2.76 W_U$$

K = thermal conductivity of fuel meat, W/cm K

W_U = weight fraction of uranium in the fuel meat.

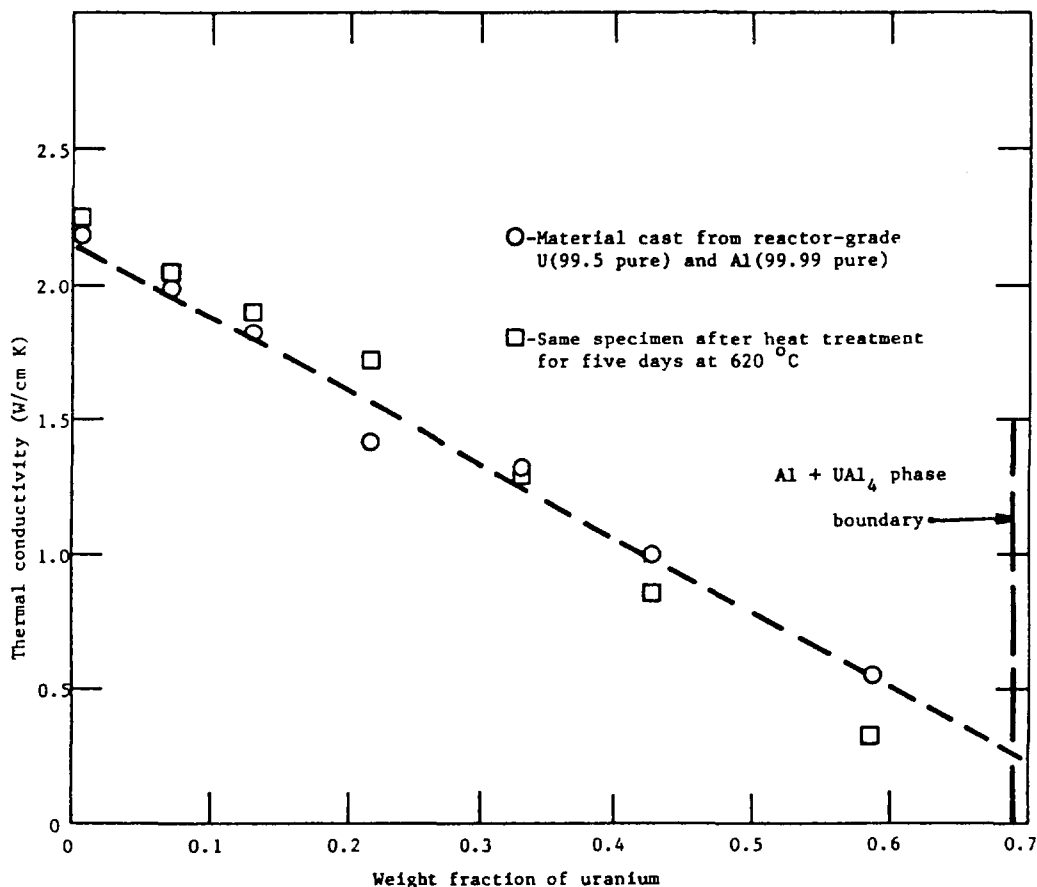
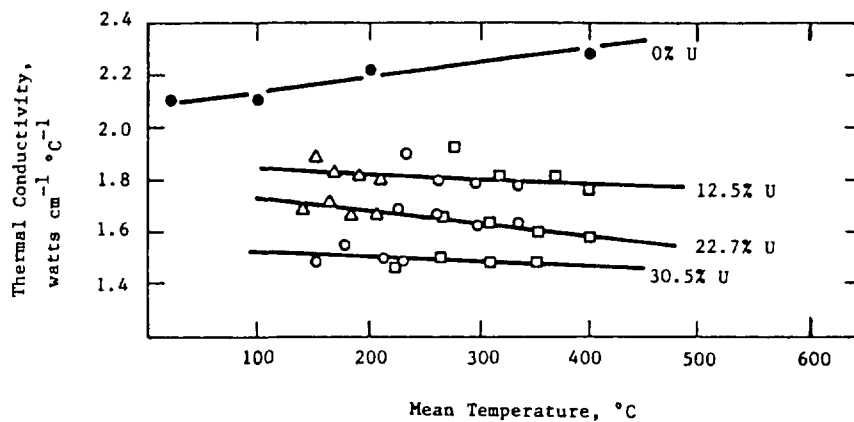


Fig. 2. Thermal Conductivity of U-Al Alloy at 65°C (Ref. 10).



(Δ, O, and □ Denote Results Obtained on Different Runs)

Fig. 3. Thermal Conductivity versus Temperature for Various Loadings (in Wt%U) of U-Al Alloy Fuel (Ref. 10).

Data presented in Fig. 3 for various uranium weight loadings in uranium-aluminum alloy fuel indicate only a small decrease in thermal conductivity with increasing temperature. Over the temperature ranges expected in research and test reactors, the thermal conductivity of U-Al alloy fuel meat can be assumed to be constant.

The thermal conductivity of a fuel plate can be calculated using:

$$\frac{t_{\text{plate}}}{K_{\text{plate}}} = \frac{t_{\text{meat}}}{K_{\text{meat}}} + \frac{2 t_{\text{clad}}}{K_{\text{clad}}} \quad (7)$$

where t_{plate} , t_{meat} , and t_{clad} are the thicknesses of the plate, fuel meat, and cladding, respectively.

The thermal conductivity of 1100 Al cladding, for example, is 2.22 W/cm K. For U-Al alloy fuel meat containing 21 wt-% U with a thickness of 0.51 mm and 1100 Al cladding with a thickness of 0.38 mm, the thermal conductivity of the fuel plate would be 1.92 W/cm K.

4.0 UAl_x-Al DISPERSION FUEL

The information presented in Section 2.0 on the uranium-aluminum system also applies to UAl_x-Al dispersion fuel. The three broad steps in the manufacture of UAl_x-Al dispersion fuel are production of the UAl_x powder, fabrication of the UAl_x-Al core compacts, and fabrication of the fuel plates.

Specified and typical properties¹¹ of the UAl_x powder and UAl_x-Al core compacts that are used to manufacture finished fuel plates with uranium densities up to 1.7 g/cm³ for the Advanced Test Reactor (ATR) are shown in Table 2. Typical UAl_x powder consists of about 6 wt-% UAl₂, 61 wt-% UAl₃, and 31 wt-% UAl₄. During the hot rolling and annealing steps in fabricating fuel plates, almost all of the UAl₂ reacts with aluminum from the matrix to form UAl₃ and some of the UAl₃ reacts with aluminum to form UAl₄. Thus, the core (fuel meat) of a finished plate contains UAl₃ and UAl₄ as the fuel compounds. The actual fractions of UAl₃ and UAl₄ in a

Table 2. Properties of Uranium Aluminide (UAl_x) Powder and Core Compacts Used to Manufacture Fuel for the ATR Reactor (From Ref. 11).

Powder	Specified	Typical
Isotopic Composition:		
^{235}U content	$93.0 \pm 1.0 \text{ wt}\%$	93.19
^{238}U content	$6.0 \pm 1.0 \text{ wt}\%$	5.37
^{236}U content	$0.3 \pm 0.2 \text{ wt}\%$	0.44
^{234}U content	1.2 maximum wt%	1.00
Chemical Composition:		
Uranium	$69.0 \pm 3.0 \text{ wt}\%$	71.28
Oxygen	0.60 wt% maximum	0.25
Carbon	0.18 wt% maximum	0.05
Nitrogen	0.045 wt% maximum	0.032
Hydrogen	0.020 wt% maximum	0.005
Nonvolatile matter	99.0 wt% minimum	99.9
Easily extracted fatty and oily matter	0.2 wt% maximum	0.09
EBC ^a	30 ppm maximum	<6
Physical Properties:		
Particle size, U.S. standard mesh	-100 +325 mesh = 75% minimum -325 mesh = 25% maximum	76.0 24.0
Crystalline constituents- by x-ray diffraction	50% UAl_3 minimum no unalloyed U	6% UAl_2^b 63% UAl_3 31% UAl_4
Core Compacts		
For ATR zone loaded		
core fuel loading, g $^{235}\text{U}/\text{cm}^3$ core	1.00, 1.30, 1.60	
(maximum) wt% UAl_3 in core	1.00 g $^{235}\text{U}/\text{cm}^3$ 1.30 g $^{235}\text{U}/\text{cm}^3$ 1.60 g $^{235}\text{U}/\text{cm}^3$	46.4 54.4 62.8
Uranium concentration, U atom/ cm^3 of core (maximum)	1.00 g $^{235}\text{U}/\text{cm}^3$ 1.30 g $^{235}\text{U}/\text{cm}^3$ 1.60 g $^{235}\text{U}/\text{cm}^3$	2.76×10^{21} 3.58×10^{21} 4.41×10^{21}

^aEBC = equivalent boron content

^bEither UAl_2 or UAl_3 reacts with an excess of aluminum at moderate temperatures to form UAl_4 . Thus, the finished fuel plate cores, ready for reactor use, contain UAl_3 and UAl_4 as the fuel compound.¹¹

finished plate will vary from manufacturer to manufacturer depending on the processes and heat treatments that are utilized in fabricating the powder, core compacts, and fuel plates.

In the following discussions, it is assumed that the UAl_x in the fuel meat of finished fuel plates consists of 60 wt-% UAl_3 and 40 wt-% UAl_4 .

4.1 Uranium Density Relations for Aluminide Fuel

For UAl_x in the meat of finished fuel plates that consists of 60 wt-% UAl_3 and 40 wt-% UAl_4 , the density of the UAl_x is:

$$\begin{aligned}\rho_{UAl_x} &= w_{UAl_3} \rho_{UAl_3} + w_{UAl_4} \rho_{UAl_4} \\ &= 0.6 (6.8) + 0.4 (5.7) = 6.4 \text{ g/cm}^3\end{aligned}$$

using the measured densities of UAl_3 and UAl_4 from Table 1. Additionally, the weighted value of x in UAl_x (taking 4.9 aluminum atoms per uranium atom in UAl_4) is about 3.8 and the uranium weight fraction (w_U^D) in the UAl_x is about 0.70.

Substituting these values into Eq.(2), a value of "a" = 0.306 is obtained. The relationships between the uranium density and the weight fraction of uranium in the fuel meat, and between the uranium density and the volume fraction of the dispersed phase are then:

$$\rho_U = \frac{(1 - P) w_U}{0.370 - 0.306 w_U} \quad w_U = \frac{0.370 \rho_U}{(1 - P) + 0.306 \rho_U}$$

$$\rho_U = 4.5 v_f^{UAl_x}$$

A plot¹¹ of the fuel meat (core) density and porosity of uranium aluminide fuel for different uranium densities is shown in Fig. 4. The figure indicates that at constant core density, the porosity increases with increasing uranium loading. For calculational purposes, an average porosity of 7 vol-% is commonly used.

4.2 Specific Heat of Aluminide Fuel

Using Eqs.(5) and (6), the specific heat of UAl_x that consists of 60 wt-% UAl_3 and 40 wt-% UAl_4 is given by:

$$\begin{aligned}C_p \text{ } UAl_x &= w_{UAl_3} C_p \text{ } UAl_3 + w_{UAl_4} C_p \text{ } UAl_4 \\ &= 0.387 + 0.00022 T \quad \text{J/g K, } T \text{ in } ^\circ\text{C}\end{aligned}$$

The specific heat of UAl_x -Al fuel meat is obtained by summing the specific heats of the UAl_x and aluminum phases, weighted by their respective fractions:

$$\begin{aligned}C_{p, UAl_x-Al} &= (1.0 - w_U/0.7) C_{p, Al} + (w_U/0.7) C_{p, UAl_x} \\ &= C_{p, Al} + 1.43 w_U (C_{p, UAl_x} - C_{p, Al}) \\ &= 0.892 + 0.00046 T - w_U (0.722 + 0.00034 T) \quad \text{J/g K, } T \text{ in } ^\circ\text{C}\end{aligned}$$

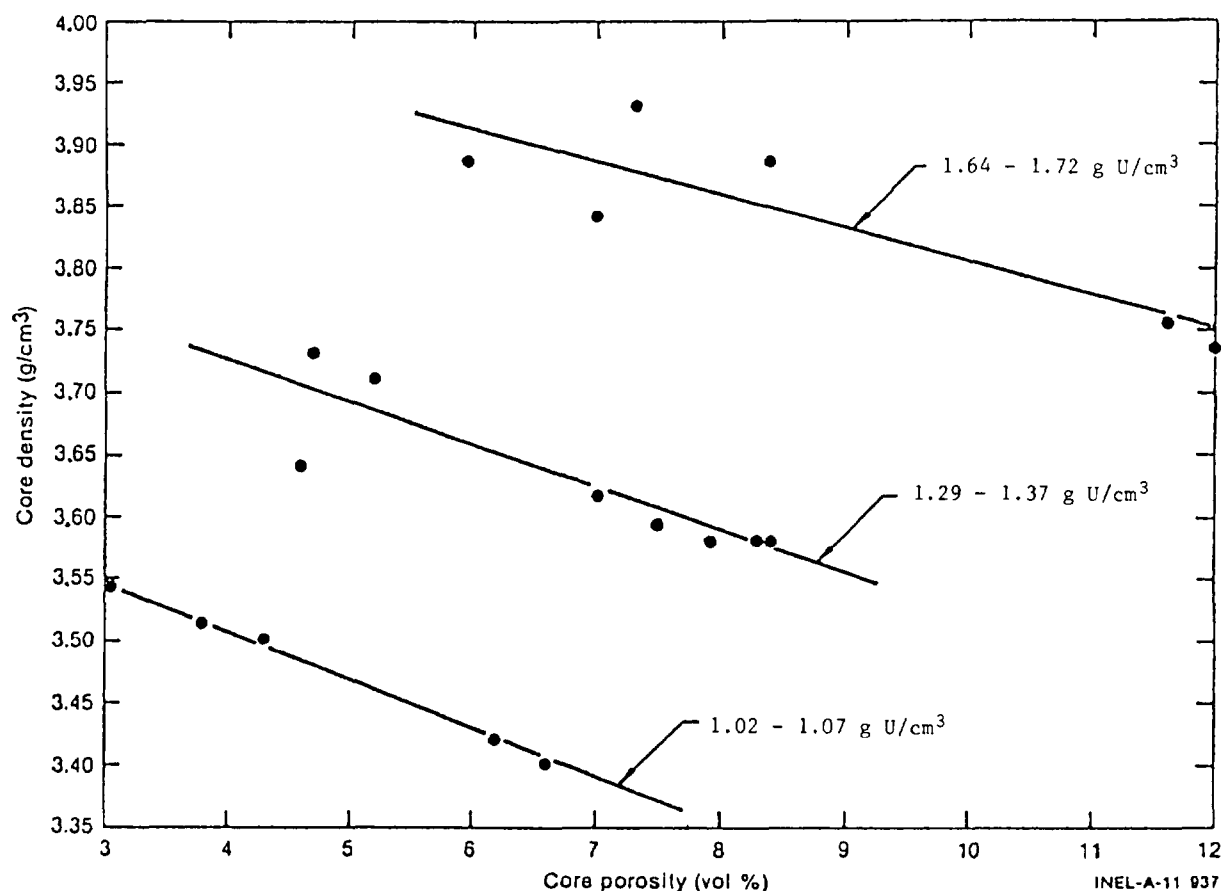


Fig. 4. Core Density and Porosity of Uranium Aluminide Fuel Plates with Different Fuel Loadings (Ref. 11).

4.3 Thermal Conductivity of Aluminide Fuel

Available data on the thermal conductivity of aluminide fuels (that are typical of those in reactor use) are limited to three data points (Ref. 6) calculated for ATR sample fuel plates using thermal diffusivity measurements (Ref. 10) at Battelle Northwest Laboratories on MTR-ETR type fuel plates. The data from Table II of Ref. 6 are reproduced in Table 3 below.

Table 3. Thermal Conductivity of ATR Sample Fuel Plates Calculated (Ref. 6) from Thermal Diffusivity Measurements (Battelle Northwest, Ref. 10).

Plate	Fuel	Thermal Diffusivity, cm^2/s		Fuel Plate Density, g/cm^3		Heat Capacity, $\text{J}/\text{g } ^\circ\text{C}$		Thermal Conductivity, $\text{W}/\text{cm K}$	
		25°C	600°C	25°C	600°C	25°C	600°C	25°C	600°C
P-1-1047	UAl _x	0.32	0.25	2.953	2.830	0.766	0.996	0.724	0.703
P-1-1048	UAl _x	0.38	0.33	2.980	2.855	0.758	0.984	0.858	0.925
P-5-576	UAl _x	0.33	0.24	3.00	2.872	0.737	0.963	0.728	0.661

Thermal conductivities in Table 3 were obtained using the relation:

$$K = \alpha \rho C_p$$

where K is the thermal conductivity, α is the thermal diffusivity, ρ is the density of the plate, and C_p is the heat capacity.

The sample fuel plates in Table 3 had a thickness of 1.296 mm, with a 6061 Al cladding thickness of about 0.394 mm and an assumed fuel meat thickness of 0.508 mm. The fuel meat contained about 35.4 vol-% UAl_x (57.7 wt-% UAl_x) and had a porosity of about 6 vol-%. The matrix material was X8001 aluminum alloy and the uranium density in the fuel meat was about 1.6 g/cm³.

The thermal conductivity of the UAl_x-Al fuel meat can be calculated from the fuel plate data in Table 3 using the relation:

$$\frac{t_{\text{plate}}}{K_{\text{plate}}} = \frac{t_{\text{meat}}}{K_{\text{meat}}} + \frac{2 t_{\text{clad}}}{K_{\text{clad}}}$$

where t_{plate} , t_{meat} , and t_{clad} are the thicknesses of the plate, fuel meat, and cladding, respectively. 6061 Al cladding has a thermal conductivity of 1.80 W/cm K and is essentially constant over the temperature range considered. The thermal conductivity of the UAl_x-Al fuel meat for the three fuel plates listed in Table 3 is then:

Table 4. Calculated Thermal Conductivities of the UAl_x-Al Fuel Meat in the Three Sample Fuel Plates in Table 3.

Plate	Fuel Meat	Vol-% UAl _x	Percent Porosity	Thermal Conductivity of Fuel Meat, W/cm K	
				25°C	600°C
P-1-1047	UAl _x -Al	35.4	6	0.376	0.361
P-1-1048	UAl _x -Al	35.4	6	0.474	0.527
P-5-576	UAl _x -Al	35.4	6	0.378	0.334

The thermal conductivity data for UAl_x-Al fuel at 25°C are plotted in Fig. 8 (Section 6), which compares the thermal conductivities of U₃O₈-Al, U₃Si₂-Al, and U₃Si-Al fuel meats as a function of the volume percent of fuel dispersant plus voids. From the data in Fig. 7, we conclude that all four of these dispersion fuels have approximately the same thermal conductivity. Since the thermal conductivities of UAl_x and U₃Si₂ and the metallurgical properties of UAl_x-Al fuel and U₃Si₂-Al fuel are very similar, we suggest that the measured thermal conductivity data for U₃Si₂-Al fuel be used for UAl_x-Al fuel as well.

5.0 U₃O₈-Al DISPERSION FUEL

5.1 Uranium Density Relations for Oxide Fuel

The density of the high-fired U₃O₈ used by the High Flux Isotope Reactor (HFIR) at ORNL is 8.22 g/cm³ and $W_U^D = 0.846$. Substituting these data into Eq. (2), one obtains $a = 0.294$. The relationships between the uranium density and the weight fraction of uranium in the fuel meat, and

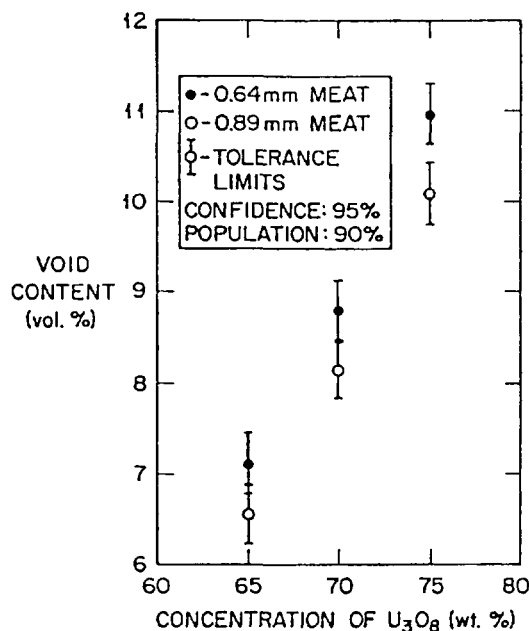


Fig. 5. Void Content of U₃O₈-Al Fuel Meat versus Concentration of U₃O₈ and Fuel Meat Thickness.

between the uranium density and the volume fraction of the dispersed phase are then:

$$\rho_U = \frac{(1 - P) w_U}{0.370 - 0.294 w_U} \quad w_U = \frac{0.370 \rho_U}{(1 - P) + 0.294 \rho_U}$$

$$\rho_U = 7.0 V_f^{U_3O_8}$$

The void content of U₃O₈-Al fuel meat depends on the concentration of U₃O₈ and to a lesser extent on the fuel meat thickness. The void content as a function of U₃O₈ concentration for plates with two fuel meat thicknesses fabricated by ORNL¹² are shown in Fig. 5. Appropriate values of P for use in the uranium density relations should be obtained from this figure or from similar data supplied by the fuel manufacturer.

5.2 Specific Heat of Oxide Fuel

Specific heat data¹³ for U₃O₈ in the temperature range from 0-300°C is represented approximately by the linear relationship:

$$C_{p,U_3O_8} = 0.27 + 0.00030 T \quad \text{J/g K, } T \text{ in } ^\circ\text{C}$$

If w_U is the uranium weight fraction and $C_{p,Al}$ is the specific heat of aluminum [Eq.(4)], the specific heat of the U₃O₈-Al fuel meat is given by:

$$\begin{aligned} C_{p,U_3O_8-Al} &= (1 - w_U/0.848) C_{p,Al} + (w_U/0.848) C_{p,U_3O_8} \\ &= 0.892 + 0.00046 T - w_U (0.734 + 0.00019 T) \quad \text{J/g K, } T \text{ in } ^\circ\text{C} \end{aligned}$$

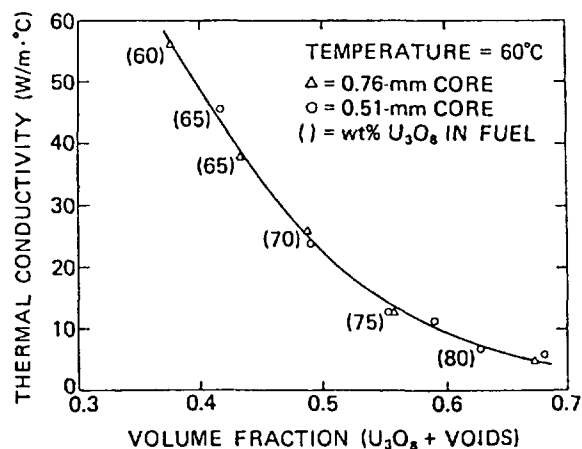


Fig. 6. Thermal conductivity of U₃O₈-Al core region depends significantly on the volume fraction of U₃O₈ + voids.

5.3 Thermal Conductivity of Oxide Fuel

Figure 6 shows a curve of measured¹⁴ thermal conductivity versus uranium loading for U₃O₈-Al dispersion material. For the lightly loaded dispersions, the decrease in conductivity with increasing volume fraction of U₃O₈ is linear, primarily due to the substitution of the low conductivity oxide ($k \sim 0.3\text{--}0.5$ W/m K)¹⁵ for aluminum. As more U₃O₈ is added, however, the thermal conductivity drops more dramatically. In the range of uranium loadings between 2.5 and 3.1 g/cm³, the thermal conductivity ranges from 30 to 12 W/m K.

6.0 U₃Si₂-Al AND U₃Si-Al DISPERSION FUELS

The development and testing of uranium silicide fuels has been an international effort, involving national reduced enrichment programs, several commercial fuel fabricators, and several test reactor operators. Numerous results of this effort have been published previously. Some of the results are summarized in this section.

As with the uranium-aluminum system, the uranium-silicon system normally consists of a mixture of intermetallic compounds, or phases. The quantity of each phase present depends upon the composition and homogeneity of the alloy and on its heat treatment. Since the different phases behave differently under irradiation, knowledge of the phases to be expected in the fuel is necessary to correctly interpret test results and to prepare specifications. For this reason, a detailed discussion of the phases in the uranium-silicon system is presented in Appendix I-1.2 (Ref. 16). Further properties of uranium silicide fuels can be found in Refs. 17-19.

6.1 Uranium Density Relations for Silicide Fuels

The densities of the U₃Si₂ and U₃Si dispersants that were measured at ANL, the corresponding weight fractions of uranium in each dispersant, and the value of the parameter "a" in Eq. (2) are given below.

Silicide Dispersant	wt-% Si	Measured Density g/cm ³	w_U^D	a
U ₃ Si ₂	7.5	12.2 ^a	0.925	0.312
U ₃ Si	4.0	15.2 ^b	0.960	0.317

^aAs-arc-cast.

^bAfter heat treatment of 72 h at 800°C.

The relationships between the uranium density and the weight fraction of uranium in the fuel meat, and between the uranium density and the volume fraction of the dispersed phase are then:

$$\rho_U = \frac{(1 - P) w_U}{0.370 - a w_U} \quad w_U = \frac{0.370 \rho_U}{(1 - P) + a \rho_U}$$

with appropriate values of the parameter "a" for each dispersant.

$$\rho_U = 11.3 v_f^{U_3Si_2} \quad \rho_U = 14.6 v_f^{U_3Si}$$

Porosity remaining after fabrication of dispersion fuel meat provides space to accommodate the initial swelling of the fuel particles under irradiation. Data obtained at ANL from measurements²⁰ on U₃Si₂ miniplates are plotted in Fig. 7. These data are well fit¹⁷ by the cubic function:

$$V_P = 0.072 V_F - 0.275 V_F^2 + 1.32 V_F^3$$

where V_P and V_F are the volume fractions of porosity and fuel dispersant in the meat, respectively. The amount of as-fabricated porosity increases significantly as the volume loading of fuel dispersant increases because it becomes more difficult for the matrix aluminum matrix to flow completely around all fuel particles, especially those in contact with one another²⁰.

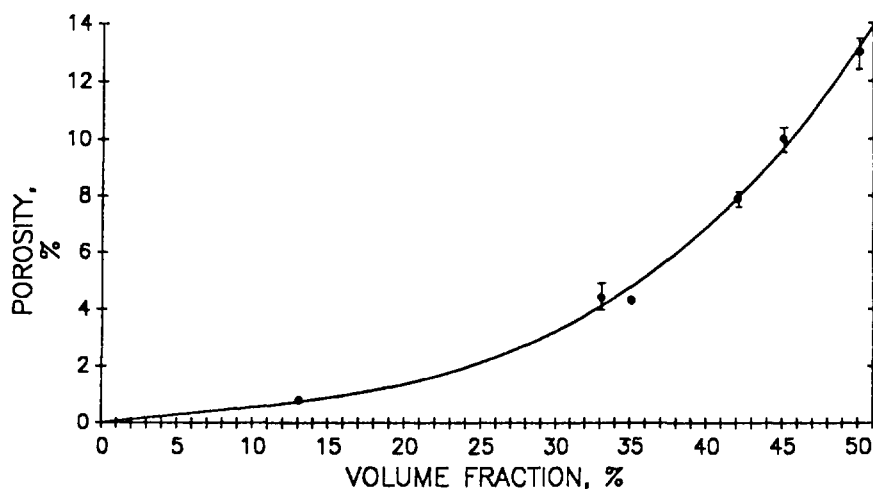


Fig. 7. Percent Porosity as a Function of the Volume Percent of U₃Si₂ in U₃Si₂-Al Fuel Meat.

It is important to note that the porosity in the fuel meat of fabricated fuel plates varies from fabricator to fabricator due to differences in manufacturing techniques in the aluminum alloys of the cladding. For example, consider the nominally identical U_3Si_2 fuel elements fabricated by B&W, CERCA, and NUKEM for irradiation testing in the Oak Ridge Research Reactor. The porosity content of the fuel cores produced by a given fabricator remained virtually constant, but there was a variation from fabricator to fabricator: 4 vol-% for CERCA, 7-8 vol-% for NUKEM, and 9-10 vol-% for B&W. Differences in material or fabrication parameters which might have contributed to the different amount of porosity include: (1) strength of the aluminum alloy used for frames and covers -- the CERCA alloy was by far the strongest while the B&W alloy was the weakest; (2) the rolling temperature -- 425°C for CERCA and NUKEM and ~500°C for B&W; (3) the amount of fines in the U_3Si_2 powder -- 40 wt-% for CERCA and 17-18 wt-% for NUKEM and B&W; (4) the rolling schedule, especially the amount of cold reduction; and (5) the relationship between the size of the compact and the size of the cavity in the frame.

6.2 Specific Heats of Silicide Fuels

The specific heats of U_3Si_2 and U_3Si as a function of temperature have been derived¹⁷ from plots of specific heat data²¹ for stoichiometric U_3Si and for a U-Si alloy at 6.1 wt-% Si:

$$C_{p,U_3Si_2} = 0.199 + 0.000104 T \quad \text{J/g K, } T \text{ in } ^\circ\text{C}$$

$$C_{p,U_3Si} = 0.171 + 0.000019 T \quad \text{J/g K, } T \text{ in } ^\circ\text{C}$$

If W_U is the uranium weight fraction and $C_{p,Al}$ is the specific heat of aluminum [Eq.(4)], the specific heats of U_3Si_2 -Al and U_3Si -Al fuel meat are given by:

$$\begin{aligned} C_{p,U_3Si_2-Al} &= (1 - W_U/0.925) C_{p,Al} + (W_U/0.925) C_{p,U_3Si_2} \\ &= 0.892 + 0.00046 T - W_U (0.749 + 0.00038 T) \quad \text{J/g K, } T \text{ in } ^\circ\text{C} \end{aligned}$$

$$\begin{aligned} C_{p,U_3Si-Al} &= (1 - W_U/0.960) C_{p,Al} + (W_U/0.960) C_{p,U_3Si} \\ &= 0.892 + 0.00046 T - W_U (0.751 + 0.00046 T) \quad \text{J/g K, } T \text{ in } ^\circ\text{C} \end{aligned}$$

6.3 Thermal Conductivity of Silicide Fuels¹⁷

Both U_3Si_2 and U_3Si have a thermal conductivity of ~15 W/m K²². Values of the thermal conductivities of the fuel meat in unirradiated U_3Si_2 -Al dispersion fuel plates, measured at 60°C, are listed in Table 5 and are plotted in Fig. 8.²³ Most of the samples were cut from miniature fuel plates produced at ANL for use in out-of-pile studies. Two samples came from a full-sized plate from a lot of plates fabricated by CERCA for the ORR test elements. The porosities of these miniplates follows the trend discussed in Section 6.1 but are somewhat larger, owing, presumably, to the different shape of the fuel zone than in the miniplates fabricated for irradiation testing (cylindrical rather than rectangular compacts were used).

Table 5. Thermal Conductivities of U_3Si_2 -Aluminum Dispersions

Sample Identification	Fraction of Fuel -325 Mesh, wt-%	U_3Si_2 Volume ¹ Fraction, %	Porosity, ² vol-%	Thermal Conduct.of Dispersion at 60°C, W/m K	Temperature Coefficient, W/m K ²
CS148	15	13.7	1.9	181	0.148
CS106	15	32.3	6.0	78	0.029
CS140	0	39.4	9.2	40	0.014
CS141	15	37.0	9.3	48	5×10^{-4}
CS142	25	39.1	9.5	40	0.017
CERCA #1	41.5	46.4	4.0	59	0.161
CERCA #2	41.5	46.4	4.0	59	0.076
CS143	15	46.4	15.4	13.9	0.010

¹Determined on the thermal conductivity specimens using a radiographic technique.

²Average value for roll-bonded fuel plate.

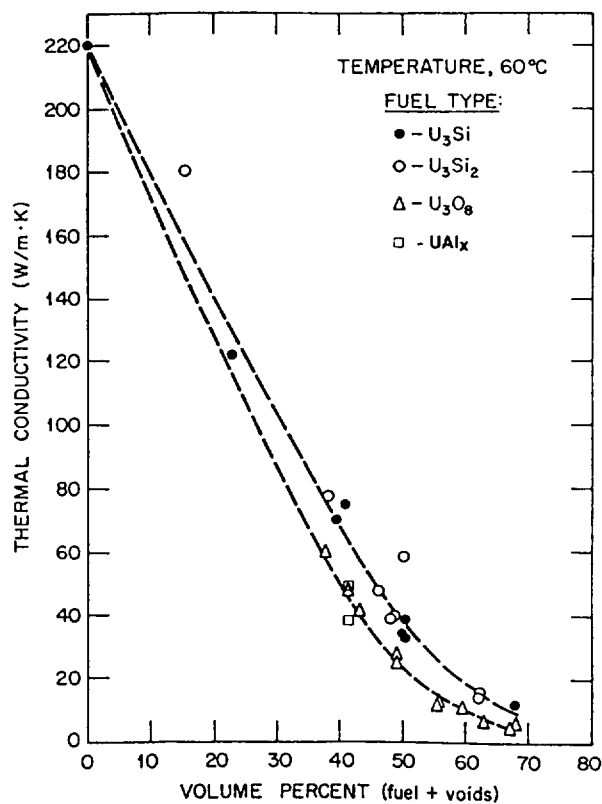


Fig. 8. Thermal Conductivities of Uranium Silicide-, U_3O_8 -, and UAl_x -Aluminum Dispersion Fuels as a Function of Volume Fraction of Fuel Particles Plus Voids (Porosity).

In Fig. 8, the thermal conductivity decreased rapidly as the volume fraction of fuel plus porosity increases (and the volume fraction of aluminum matrix decreases), owing to the ~14 times larger thermal conductivity of aluminum than U_3Si_2 . For very low volume loading of U_3Si_2 , it would be expected that the thermal conductivity of the dispersion would be proportional to the amount of aluminum present, since the aluminum matrix should provide a continuous thermal path. Indeed, this is the case for sample CS148. At higher volume fractions of U_3Si_2 plus void, however, the aluminum ceases to be the continuous phase, and the thermal conductivity decreases more rapidly than the volume fraction of aluminum. At very high loadings the aluminum ceases to play a significant role, and the thermal conductivity approaches that of the fuel. It may even become lower than that of the fuel alone because of poor thermal contact between fuel particles. The microstructure of the meat, specifically the distribution of the voids, can significantly affect the thermal conductivity. It appears that thin planar regions in which voids are associated with fractured fuel particles are responsible for the large difference in thermal conductivity exhibited by the CERCA samples and sample CS143. The larger void content of the CS samples than measured in the miniplates fabricated for irradiation testing or in full-sized plates most likely indicated the presence of more of such planar void regions. Therefore, it is believed that the thermal conductivity curve in Fig. 8 for U_3Si_2 -Al fuel meat represents essentially a lower limit for the thermal conductivities of full-sized fuel plates.

The data for U_3Si_2 -Al dispersions are virtually indistinguishable from those obtained in the same series of measurements for U_3Si -Al dispersions. They are also quite similar to data obtained in other measurements of thermal conductivities of UAl_x -Al dispersions⁶ and U_3O_8 -Al dispersions.¹⁴ The U_3O_8 -Al data fall somewhat below the U_3Si_2 -Al data, possibly because the friable nature of U_3O_8 leads to the formation of more planar void regions than are present in U_3Si_2 -Al fuel.

REFERENCES

1. Metals Handbook, Eighth Edition, Volume 8, "Metallography, Structures, and Phase Diagrams" (1973).
2. H.S. Kalish et al., "Uranium Alloys" in Reactor Handbook, Vol. I, Materials, p. 174, C.R. Tipton, Ed., Interscience Publishers, Inc., New York (1960).
3. B.S. Borie, "Crystal Structure of UAl_4 ", Journal of Metals, Vol. 3, September 1951, p. 800.
4. D. Stahl, "Fuels for Research and Test Reactors, Status Review, July 1982", ANL-83-5, December 1982.
5. CRC Handbook of Chemistry and Physics, 58th Edition (1977).
6. R.R. Hobbins, "The Thermal Conductivity and Heat Capacity of UAl_3 and UAl_4 ", Aerojet Nuclear Company Interoffice Correspondence, January 4, 1973.
7. Handbook of Chemistry and Physics, 40th Ed., Chemical Rubber Publishing Co. (1958).
8. L.S. Darken and R.W. Gurry, Physical Chemistry of Metals, McGraw-Hill (1953) p. 158.

9. P. Chiotti and J.A. Kateley, "Thermodynamic Properties of Uranium-Aluminum Alloys", J. Nucl. Mat. 32, 135 (1969).
10. J.L. Bates, "Thermal Diffusivity of MTR-ETR Type Fuel Plates, Battelle Pacific Northwest Laboratories Report BNWL-CC-456 (Jan. 10, 1966).
11. J.M. Beeston, R.R. Hobbins, G.W. Gibson, and W.C. Francis, "Development and Irradiation Performance of Uranium Aluminide Fuels in Test Reactors", Nuclear Technology 49, 136 (1980).
12. G.L. Copeland and M.M. Martin, "Fabrication of High-Uranium-Loaded U3O8-Al Developmental Fuel Plates," Proc. International Meeting on Development, Fabrication, and Application of Reduced-Enrichment Fuels for Research and Test Reactors, Argonne National Laboratory, Argonne, Illinois, November 12-14, 1980.
13. Y.S. Youloukian and E.H. Buyco, Thermophysical Properties of Matter, Vol. V, "Specific Heat - Nonmetallic Substances" (1970).
14. G.L. Copeland and M.M. Martin, "Development of High-Uranium-Loaded U3O8-Al Fuel Plates," Nucl. Tech. 56, 547 (1982).
15. Y.S. Youloukian and E.H. Buyco, Thermophysical Properties of Matter, Vol. I, "Thermal Conductivity" (1970).
16. R.F. Domagala, "Phases in U-Si Alloys", Proc. 1986 Int. Mtg. on Reduced Enrichment for Research and Test Reactors, Gatlinburg, Tennessee, November 3-6, 1986, Argonne National Laboratory Report ANL/RERTR/TM-9, CONF-861185 (May 1988) p. 45.
17. J.L. Snelgrove, R.F. Domagala, G.L. Hofman, T.C. Weincek, G.L. Copeland, R.W. Hobbs, and R.L. Senn "The Use of U3Si2 Dispersed in Aluminum in Plate-Type Fuel Elements for Research and Test Reactors", ANL/RERTR/TM-11, October 1987.
18. R.F. Domagala, T.C. Weincek, and H.R. Thresh, "Some Properties of U-Si Alloys in the Composition Range from U3Si to U3Si2", Proc. 1984 Int. Mtg. on Reduced Enrichment for Research and Test Reactors, Argonne, Illinois, October 15-18, 1984, Argonne National Laboratory Report ANL/RERTR/TM-6, CONF-8410173 (July 1985) p. 47.
19. T.C. Weincek, R.F. Domagala, and H.R. Thresh, "Thermal compatibility Studies of Unirradiated Uranium Silicide Dispersed in Aluminum", Proc. 1984 Int. Mtg. on Reduced Enrichment for Research and Test Reactors, Argonne, Illinois, October 15-18, 1984, Argonne National Laboratory Report ANL/RERTR/TM-6, CONF-8410173 (July 1985) p. 61.
20. T.C. Weincek, "A Study of the Effect of Fabrication Variables on the Quality of Fuel Plates," Proc. 1986 Int. Mtg. on Reduced Enrichment for Research and Test Reactors, Gatlinburg, Tennessee, November 3-6, 1986, Argonne National Laboratory Report ANL/RERTR/TM-9, CONF-861185 (May 1988) p. 54.
21. H. Shimizu, "The Properties and Irradiation Behavior of U3Si2", Atomics International Report NAA-SR-10621, p.14 (July 25, 1965).
22. A.G. Samoilov, A.I. Kashtanov, and V.S. Volkov, Dispersion-Fuel Nuclear Reactor Elements, (1965), translated from the Russian by A. Aladjem, Israel Program for Scientific Translations Ltd.. Jerusalem, pp. 54-57 (1968).
23. R.K. Williams, R.S. Graves, R.F. Domagala, and T.C. Weincek, "Thermal Conductivities of U3Si and U3Si2-Al Dispersion Fuels", Proc. 19th Int. Conf. on Thermal Conductivity, Cookeville, Tennessee, October 21-23, 1985, in press.

Appendix I-1.2

PHASES IN U-Si ALLOYS*

R.F. DOMAGALA
RERTR Program,
Argonne National Laboratory,
Argonne, Illinois,
United States of America

Abstract

The binary (two-component) U-Si system contains a total of seven "compounds." The most U-rich compounds are of interest to the RERTR community because they are now being employed as fuels in research and test reactors. The nomenclature used in describing these fuels and the metallurgical significance of the notations recorded may have different meanings to people from different technical backgrounds. This paper is a succinct exploration of the principles of phase equilibria and the realities of commercial fabrication as applied to U-Si alloys. It is an attempt to record in referenceable and retrievable form information of value to the continued development, application and understanding of silicide fuels.

INTRODUCTION

Discussions of silicide fuels as applied to the RERTR Program often involve considerations of the relative amounts of the various phases (distinguishable crystalline entities) present in U-Si alloys at different Si levels. This topic is being reexamined more carefully as the requirements for certain reactors exceed the U levels possible with "pure" U_3Si_2 . In many ways this report is a supplement to the paper on the properties of selected U-Si alloys¹ as well as the work of A. E. Dwight on the U-Si and U-Si-Al systems.² It is intended to serve as a brief exposition of the nature of binary systems as applied to an understanding of the microstructural situations likely to be encountered in utilizing U-Si alloys as fuels for nuclear reactors.

Within this paper certain rules and principles of binary diagrams are employed. More detailed discussions of these principles may be found in any textbook on physical metallurgy. Two "classic" monographs on the subject may be of interest to those who wish to pursue the subject in depth.^{3,4}

DISCUSSION

Table 1 is a list of the calculated and experimentally measured compositions of U_3Si , U_3Si_2 and USi , the three most U-rich phases in the U-Si system, which is shown in Fig. 1.

* Work supported by the US Department of Energy, Office of Spent Fuel Management and Reprocessing Systems, under contract W-31-109-Eng-38.

Table 1. Weight Percent Silicon and Density for
 U_3Si , U_3Si_2 and USi

Phase	wt.% Si			Density Determined at ANL, g-cm ⁻³
	Method (a)	Method (b)	Method (c)	
U_3Si	3.78	3.79	3.9	15.2 ^d
U_3Si_2	7.29	7.31	7.3	12.2 ^e
USi	10.56	10.58	10.6	10.9 ^f

(a) Calculated for natural U (a.w. 238.03).

(b) Calculated for 20% enriched U (a.w. 237.4).

(c) Experimentally determined for depleted U.

(d) For 4.0 wt.% Si alloy heat treated at 800°C, presumed to be at equilibrium.

(e) For 7.3 wt.% Si as-arc-cast alloy.

(f) For 10.6 wt.% Si as-arc-cast alloy.

In all calculations and plots that follow, I have used the 3.9 wt.% Si figure for the composition of U_3Si and have rounded off the value for U_3Si_2 at 7.3 wt.% Si and for USi at 10.6 wt.% Si. The densities recorded in Table 1 for these phases have been used as necessary.

The density figures and the microstructural conditions they represent require some amplification. The three compounds (the terms "phases," "intermetallic compounds," and "intermediate phases" may be used interchangeably) of interest here are often described as "line compounds." In the language of phase diagrams this means that within the experimental ability to define composition, a single formula and composition is assigned to each compound. They are represented, therefore, as vertical lines in the diagram. From a practical point of view -- even in terms of research activity -- it may be considered essentially impossible to produce an alloy at the exact stoichiometry of a line compound and of such atomistic homogeneity that only the "pure" phase is present. One always expects to see in a microstructure a small but finite amount of the phase to the left or the right of the compound of interest. It is even possible, with minor perturbations in the distribution of the two components (U and Si in this case), that there may be regions where the phase to the left of the compound of interest is present and other regions in the same piece of material where the phase to the right of the compound is present.

The statement in the preceding paragraph regarding the possible presence of three (or more) phases in a binary (two-component) system violates one of the fundamental tenets of phase equilibria -- Gibbs's Phase Rule. This rule states that in a binary system at equilibrium, there may be at most two phases coexisting in any area of the diagram. Three phases may exist at equilibrium only along a horizontal line in such a diagram. Such horizontal lines in a binary system are called "invariant reaction lines" or "invariant reaction isotherms." The boundary conditions for Gibbs's Phase Rule as stated above are as follows: the alloy is at equilibrium, the pressure is constant, and the vapor phase is considered non-existent. "Constant pressure" for systems

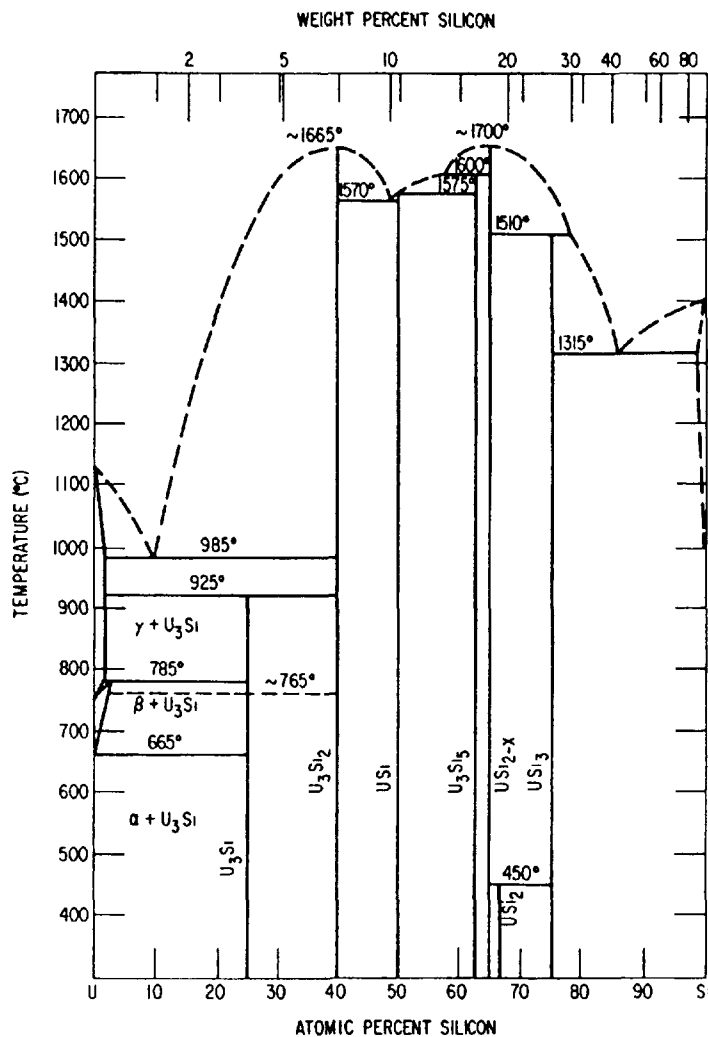


Fig. 1. U-Si Phase Diagram.

of the U-Si type may be considered to encompass values ranging from very high vacuum to pressures of several hundred atmospheres.

Gibbs's Rule further demands that at constant pressure and equilibrium, no more than three phases can coexist in a binary alloy under any conditions. Therefore, any discussion regarding more than two phases coexisting in a binary alloy (except on an invariant reaction isotherm) describes, by definition, a non-equilibrium state.

To potentially complicate the story a bit more, the presence of impurities (and they are inevitably present) can lead to the existence of other phases which may or may not be distinguishable under the microscope, depending on their size and the magnification employed. Impurities must also be expected to be in "solid solution" (i.e., within the crystalline lattice) in each of the phases present. The presence of such impurities in solid solution is discernible only with analytical procedures capable of accurately detecting very small quantities of a foreign species. Often such equipment and techniques are not available, or simply do not exist.

The density figures recorded in Table 1 were used for all calculations. The value of 10.9 g-cm^{-3} for USi is probably accurate to $\pm 0.1 \text{ g-cm}^{-3}$. Values determined for U_3Si_2 have varied from ~ 11.9 to 12.2 g-cm^{-3} ; I have arbitrarily used the 12.2 figure. The value of 15.2 g-cm^{-3} for U_3Si represents our best

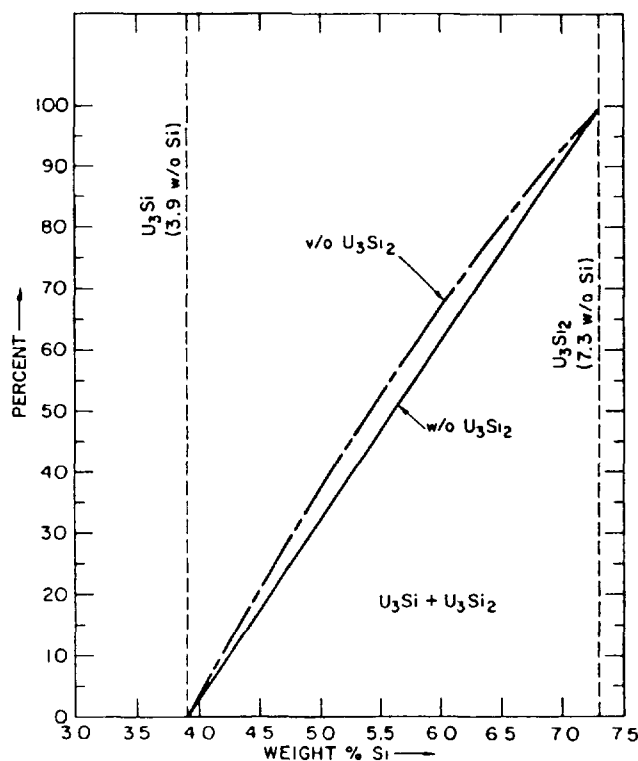


Fig. 2. Weight % (w/o) and vol.% (v/o) of U_3Si_2 vs. w/o Si. Alloys at equilibrium. Temperature $< 925^\circ C$.

value for an equilibrated alloy at 4.0 wt.% Si. We know that there is a finite amount of U_3Si_2 in such an alloy, but I chose not to adjust the density figure accordingly.

Figure 2 is a plot of wt.% and vol.% (w/o and v/o) U_3Si_2 as a function of Si content, based on application of the tie line and lever principles for alloys at equilibrium. Figure 3 is a similar plot for USi as function of Si content at Si levels between U_3Si_2 and USi , also for equilibrium conditions. Equilibrium is emphasized because neither of the principles may be quantitatively applied to a non-equilibrium state. Nevertheless, for arc-cast alloys in the range 7.3 to 10.6 wt.% Si and for properly heat treated (e.g., $800^\circ C$ for 72 h, air cool) alloys in the range 3.9 to 7.3 wt.% Si, it is reasonable to presume that a macroscopically homogeneous melt (alloy) will approach the equilibrium condition. The formulas used to generate these plots are presented in the Appendix.

One concern is with alloys between U_3Si and U_3Si_2 . As vendors consider the fabrication of fuel elements at total ^{235}U loadings exceeding those possible with U_3Si_2 , they must move into the two-phase ($U_3Si + U_3Si_2$) field to take advantage of the higher U density possible with U_3Si . The sacrifice, however, is to accept the presence of a phase (U_3Si) which has been demonstrated to develop large fission gas bubbles at high ^{235}U burnups. Our experimental data for irradiated fuels in this two-phase field are somewhat limited. At ANL we have produced eight miniplates with " $U_3Si_{1.5}$ " (a formula used to designate a composition of nominally 5.5 wt.% Si). Seven of these have been sent to ORNL for irradiation in the ORR. Our analyzed compositions for " $U_3Si_{1.5}$ " are 93.32 wt.% U + 5.86 wt.% Si (MEU alloy) and 93.74 wt.% U + 5.70 wt.% Si (LEU alloy). Postirradiation examination studies have only recently been initiated.

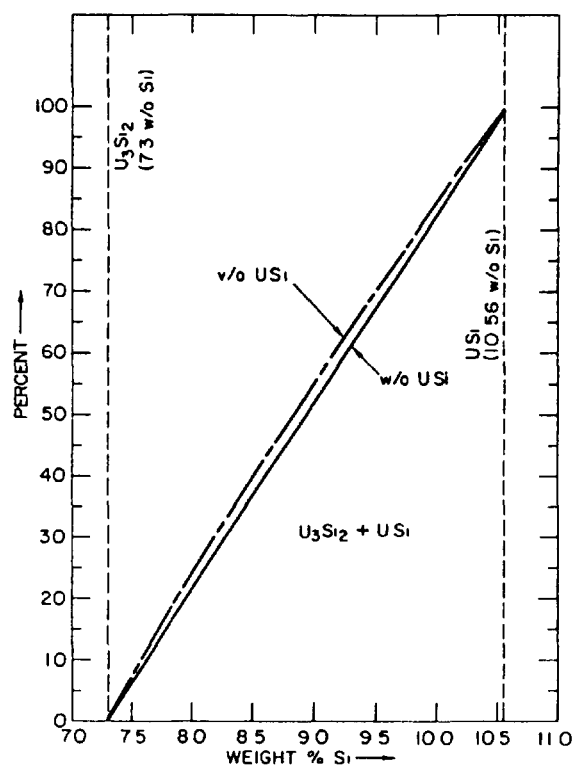


Fig. 3. Weight % (w/o) and vol.% (v/o) of USi vs. Weight Percent Si. Alloys at equilibrium.

For equilibrated (properly heat treated) compositions between U_3Si and U_3Si_2 , we see that at 5.41 wt.% Si we have exactly 50 vol.% of each phase. In simplest terms, compositions greater than 5.41 wt.% Si will have microstructures in which U_3Si_2 is volumetrically the dominant phase. Nevertheless, U_3Si may be a continuous phase even though it is a minor constituent. Because of the way U_3Si_2 crystallizes from the liquid state and because of the morphology of the annealed microstructures, there is evidence that the U_3Si phase is continuous (interconnecting) up to ~6 wt.% Si.

Under non-equilibrium conditions, alloys between 3.9 and 7.3 wt.% Si may be expected to contain ($U_{ss} + U_3Si_2 + U_3Si$), where U_{ss} designates uranium solid solution, in percentages that cannot be calculated quantitatively. It is possible to say, though, that the amounts of U_{ss} and U_3Si_2 will diminish with heat treatment (below 925°C) and the amount of U_3Si will increase, ultimately reaching the equilibrium value.

It is important to remember that U_3Si is formed by a peritectoid reaction (the horizontal line at 925°C in Fig. 1) and that any as-cast alloy in the range 0 to 7.3 wt.% Si will have some U_{ss} present in the microstructure. This is true even if the molten alloy is perfectly homogeneous, and irrespective of the melting or casting techniques used. The amount of U_{ss} in an as-cast alloy may be calculated by the same procedures used to produce Figs. 2 and 3, and a plot of such data is shown in Fig. 4. In generating Fig. 4, I have simplified the presentation by assuming no solid solubility of Si in U. Formulas for calculating wt.% and vol.% U_{ss} in this composition range are shown in the Appendix.

The peritectoid formation of U_3Si suggests, but does not guarantee, that U_3Si will not be present in an as-cast alloy. Peritectoid reactions in metallic systems are usually sluggish and require long-time anneals to initiate and

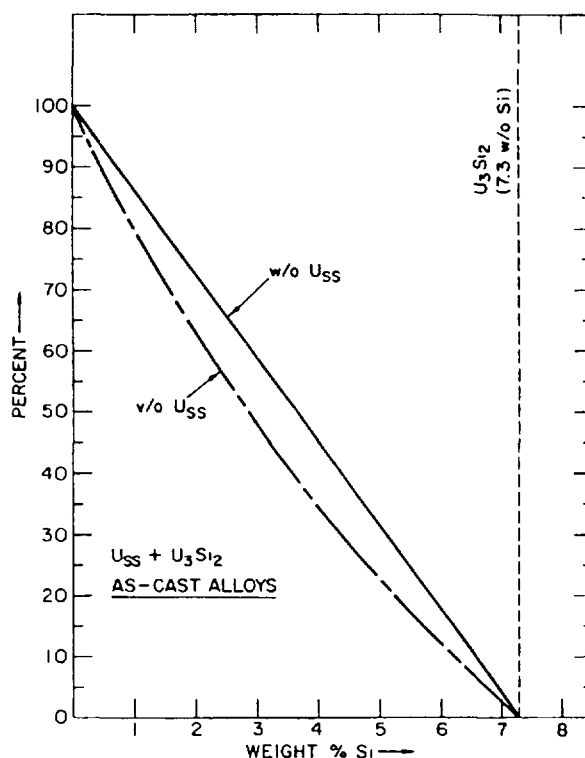


Fig. 4. Weight % (w/o) and vol.% (v/o) of Uranium Solid Solution (U_{ss}) vs. Weight Percent Si. As-cast alloys.

complete. As a matter of record, this author has never seen U_3Si present in an as-cast structure of a binary alloy, no matter what casting technique was used or section size (mass) produced.

For alloys heat treated below $925^{\circ}C$, the peritectoid reaction $U_{ss} + U_3Si_2 \rightarrow U_3Si$ occurs and at equilibrium, there is no U_{ss} remaining in alloys with >3.9 wt.% Si. All heat-treated alloys in the composition range 0-3.9 wt.% Si will have no U_3Si_2 remaining. The wt.% of U_{ss} will be a linear function of the Si content in the stated range with 100% U_{ss} at 0% Si and 0% U_{ss} at 3.9 wt.% Si. The kinetics of the peritectoid reaction have been studied by G. Kimmel et al.⁵

Concern has been periodically expressed about the possible existence of Si-rich compounds (e.g., USi_3) in U-Si alloys with ~ 7.5 wt.% Si. Such a circumstance violates the rules of phase equilibria unless the molten alloy was grossly heterogeneous before freezing. During irradiation or prolonged heat treatment of fuel powders dispersed in Al, however, $U(AlSi)_3$ will form. This is in fact the phase that is predicted by Dwight's study of the U-Al-Si system.² $U(AlSi)_3$ is a shorthand notation for UAl_3 with some of the Al positions occupied by Si atoms.

In some fuel alloy specifications, the fabricator may be required to identify the amount of each phase present in a fuel alloy as determined, for example, by x-ray diffraction analysis. It is important to recognize that under the best of conditions, at least 5 vol.% of a phase must be present to show up in a diffraction pattern. More likely, 10 vol.% is required before lines from that phase will be evident. Also, the pattern is generated by diffraction from approximately the top 20 Å layer of each particle. Thus,

depending on particle size, the diffraction pattern may represent the phases present in only a small percentage of the bulk of the sample. Therefore, x-ray diffraction of powders is not a good analytical tool for the identification of the amount of each phase present in a multiple-phase alloy.

SUMMARY AND CONCLUSIONS

A principal point of this paper as it applies to RERTR fuel alloy development and fabrication is simply this:

Whenever a U-Si fuel is described, a notation such as U_3Si , $U_3Si_{1.5}$, U_3Si_2 , or USi may be recorded or spoken. For other fuels, equivalent notations might be U_6Fe , U_6Mn , or U_3SiAl , for example. The descriptive formulas must not be taken literally. In all cases, at least one other phase is present; the amount of the second phase is quantitatively related to the content of deliberate additions (and impurities) in the alloy.

In all the development and fabrication work with U-Si alloys, compositions have always been selected to be on the Si-rich side of the stoichiometric compound. This choice was deliberately made to preclude the presence of U_{ss} in the alloy and therefore in the fuel particles. Uranium solid solution will be absent only if the molten alloy is homogeneous before freezing and, in the case of alloys between 3.9 and 7.3 wt.% Si, after proper heat treatment. It had been presumed that the presence of U_{ss} would be detrimental to the irradiation performance of silicide fuels. However, recent evidence from postirradiation examinations indicates that the presence of some U_{ss} is not detrimental to the performance of an Al-matrix dispersion fuel. The U_{ss} primarily reacts with Al to form uranium-aluminide, a very stable fuel, ss during irradiation.

Recognizing that perfect homogeneity and equilibrium are goals which one can approach but cannot achieve, we must always expect to have more than one phase in a fuel alloy.

APPENDIX

Given below are formulas for calculating percentages of phases present in the U-Si system. Densities and compositions are rounded off to the first decimal. w/o = wt.%; v/o = vol.%.

1. For alloys in the two-phase field U_3Si (3.9 w/o Si) plus U_3Si_2 (7.3 w/o Si), annealed below the peritectoid temperature (925°C) for the "proper" equilibration time:

$$(a) \quad w/o \ U_3Si_2 = \frac{w/o \ Si - 3.9}{3.4} \times 100$$

$$w/o \ U_3Si = 100 - w/o \ U_3Si_2$$

$$(b) \quad v/o \ U_3Si_2 = \frac{\frac{w/o \ U_3Si_2}{12.2}}{\frac{100 - w/o \ U_3Si_2}{15.2} + \frac{w/o \ U_3Si_2}{12.2}} \times 100$$

$$v/o \ U_3Si = 100 - v/o \ U_3Si_2$$

2. For equilibrated alloys in the two-phase field U_3Si_2 (7.3 w/o Si) plus USi (10.6 w/o Si):

$$(a) \quad w/o \ USi = \frac{w/o \ Si - 7.3}{3.3} \times 100$$

$$w/o \ U_3Si_2 = 100 - w/o \ USi$$

$$(b) \quad v/o \ USi = \frac{\frac{w/o \ USi}{10.9}}{\frac{100 - w/o \ USi}{12.2} + \frac{w/o \ USi}{10.9}} \times 100$$

3. For as-cast alloys between U (0 w/o Si) and U_3Si_2 (7.3 w/o Si), not heat treated:

$$(a) \quad w/o \ U_{ss} = \frac{7.3 - w/o \ Si}{7.3} \times 100$$

$$w/o \ U_3Si_2 = 100 - w/o \ U_{ss}$$

$$(b) \quad v/o \ U_{ss} = \frac{\frac{w/o \ U_{ss}}{19.1}}{\frac{100 - w/o \ U_{ss}}{12.2} + \frac{w/o \ U_{ss}}{19.1}} \times 100$$

$$v/o \ U_3Si_2 = 100 - v/o \ U_{ss}$$

REFERENCES

1. R. F. Domagala, T. C. Wiencek and H. R. Thresh, "Some Properties of U-Si Alloys in the Composition Range U_3Si to U_3Si_2 ," in Proceedings of the 1984 Intl. Meeting on Reduced Enrichment for Research and Test Reactors. ANL/RERTR/TM-6 CONF-8410173 (July 1985), pp. 47-60.
2. A. E. Dwight, A Study of the Uranium-Aluminum-Silicon System, ANL-82-14 (Sept. 1982).
3. F. E. W. Wetmore and D. J. LeRoy, Principles of Phase Equilibria, McGraw-Hill Book Co., New York (1951). Reprinted by Dover Publications, New York (1969).
4. A. Prince, Alloy Phase Equilibria, Elsevier Publ. Co. (1966).
5. G. Kimmel, A. Tomer and A. Bar-Or, "The Kinetics of U_3Si Formation in Cast U_3Si Alloy," J. Nucl. Mater. **40**, 242-248 (1971).

Appendix I-2

PROPERTIES OF CLADDING AND STRUCTURAL MATERIALS

Appendix I-2.1

DESCRIPTION AND QUALIFICATION OF SOME ALUMINUM ALLOYS USED BY CERCA AS CLADDING MATERIALS

COMPAGNIE POUR L'ETUDE ET LA REALISATION
DE COMBUSTIBLES ATOMIQUES (CERCA)
France

Abstract

The specifications, physical and mechanical properties, and qualification of some of the aluminum alloys used by CERCA as cladding materials for MTR fuel elements are described.

The aluminum alloys used in France for cladding MTR elements produced by CERCA were specially developed in the early sixties by the French CEA to resist water corrosion in operating conditions of research reactors.

I - Specifications and Properties

I - 1 AG 1 N.E. - AG 2 N.E. and AG 3 N.E. aluminum alloys⁽¹⁾

The three alloys are aluminum - magnesium alloys with the following chemical composition :

AG 1 NE	1.1 ≤	Mg	≤ 1.4 w %
AG 2 NE	1.8 ≤	Mg	≤ 2.3 w %
AG 3 NE	2.5 ≤	Mg	≤ 3.0 w %

Other elements specifications are the same for the two alloys, namely, in weight percentage :

	B	≤	0,001
	Cd	≤	0,001
	Cu	≤	0,008
0,2 ≤	Fe	≤	0,4
	Si	≤	0,3
0,2 ≤	Fe + Si	≤	0,5
	Li	≤	0,001
	Cr	≤	0,3
	Mn	≤	0,7

Other elements (each) ≤ 0,03

⁽¹⁾ NE means " Nuclear Grade - water ".

Physical and mechanical properties are not part of specifications. Information about these properties can be derived from published data relating to standard, non nuclear, AG alloys, although it should be pointed out that tolerances on their impurities levels are different from those specified for the nuclear grade N.E. alloys :

	Standard AG 2 (mean values)	Standard AG 3
Density (g/cc)	≈ 2.7	≈ 2.7
Melting Point (deg. C)	≈ 650	≈ 650
Specific Heat (J/g/deg. C)	-	≈ 0.96
Thermal conductivity (w/cm/deg. C)	-	≈ 1.3
Linear Expansion Coefficient between 20 and 300°C (10 ⁶ /deg. C)	-	≈ 25.7
Average Tensile Strength(hbars) (1)		
at 20°C	≈ 20	≈ 24
at 200°C	≈ 16,5	≈ 20
Average Yield Strength (at 0,2% elongation in h bars)		
at 20°C	≈ 9.5	≈ 13
at 150°C	≈ 9	≈ 12
at 200°C	≈ 8	≈ 11.5
at 250°C	≈ 7.5	≈ 10

(1) Some references indicate significantly lower values for these characteristics.

I - 2 AlFeNi (N.E. grade) alloy

This alloy is generally preferred to AG 2 NE and AG 3 NE in cases where unusually high coolant or plate surface temperature are to be expected.

Chemical composition (weight per cent)

0.8	≤	Fe	≤	1.2
0.8	≤	Ni	≤	1.2
1.8	≤	Fe + Ni		
0.8	≤	Mg	≤	1.2
0.2	≤	Cr	≤	0.5
0.2	≤	Mn	≤	0.6
0.06	≤	Zn	≤	0.14
0.02	≤	Ti	≤	0.08

OPERATING EXPERIENCE IN FRANCE WITH AL ALLOYS CLADDINGS FOR PLATE ELEMENTS

Reactor Name	Thermal power (MW)	Cladding	Exposure time in core(approx.)	Total immersion time (core+pool)	Operating experience with this type of cladding	Number of CERCA plates irradiated
SILOE	35	AG1,AG2 and AG3	150 days	mini 2 years maxi 5 years	14 years	30.000
OSIRIS	70	"	90 days average	av. 2 years max. 4 years	13 years	>40.000
PEGASE	35	"			12 years	15.000
TRITON	1.5	"			13 years	> 6.000
ULYSSE ISIS	0.1 0.8	"	> 10 years	>10 years	18 years	170 > 400
ORPHEE	14	"	120 days		6 months	~ 800
EL 3	18	"	57 days		9 years	~ 3.000
RHF	57	ALFENI	44 days	240 days minimum	10 years	8.500

The maximum permissible content for other elements are the same as for AG 3 NE.

B	0.001
Cd	0.001
Cu	0.008
Li	0.001
Si	0.3
Zn	0.03

Regarding mechanical properties, the following minimum values are guaranteed for AlFeNi N.E. alloy at 20°C, in the annealed state :

Tensile strength	at least 18 hbars
Yield strength (0,2% elongation) -	8 hbars
Elongation	- 16 %

Furthermore the AlFeNi (Ne grade) alloy has been tested succesfully for corrosion resistance at temperature as high as 250°C.

II - Performances and operating experience

The three type of alloys have demonstrated excellent stability under neutron irradiation and such a good corrosion resistance in normal reactor operating conditions that they are always used in their normal state (i. e. without protective coating of any kind).

Their safety as cladding materials is backed by many years operation in French and Foreign reactors without any single plate failure. This operating experience is best exemplified in the following table limited to MTR reactors located in France. When it is remembered that a number of other reactors in the world are also using them with equally good results, it appears in conclusion that these aluminum alloys are well qualified for use as cladding materials of MTR fuel elements.

Appendix I-2.2

NUKEM CLADDING AND STRUCTURAL MATERIALS

NUKEM GmbH
Hanau,
Federal Republic of Germany

Abstract

The composition and maximum content of some of the aluminum alloys used by NUKEM as cladding and structural materials for MTR fuel elements are described.

SHEETS OF Al Mg 1

Composition and Maximum Content of Alloys

The alloy AlMg1 (Material No. 3.3315) DIN 1725 Tl. 1 is produced from the material Al 99.5 H (Material No. 3.0250) DIN 1712 Tl. 1 by adding magnesium whereby the special tolerances as to boron, cadmium, lithium, cobalt, copper, and zinc have to be adhered to.

Composition in Weight Percentage

Mg	0.7 - 1.1
Al	rest

Maximum Content of Alloys in Weight Percentage

B	0.001	Fe	0.45
Cd	0.001	Li	0.001
Co	0.003	Mn	0.15
Cr	0.10	Si	0.30
Cu	0.008	Zn	0.05
Other elements	0.05	each	
Other elements	0.15	in total	

SHEETS OF Al Mg 2

Composition and Maximum Content of Alloys

The alloy AlMg2 (as Material No. 3.3525 DIN 1725 Tl.1 edition 1967) is produced from the material Al 99.5 H (Material No. 3.0250) DIN 1712 Tl.1 by adding magnesium whereby the special tolerances as to boron, cadmium, lithium, cobalt, copper, and zinc have to be adhered to.

Composition in Weight Percentage

Mg	1.7 - 2.4
Al	rest

Maximum Content of Alloys in Weight Percentage

B	0.001	Fe	0.40
Cd	0.001	Li	0.001
Co	0.003	Mn	0.30
Cr	0.30	Si	0.30
Cu	0.008	Zn	0.03
		Ti	0.1
Other elements	0.05	each	
Other elements	0.15	in total	

SHEETS AND PLATES OF AL 6061-T0

Composition and Maximum Content of Admixtures

The Alloy 6061 is produced according to ASTM B-209, whereby the special tolerances for boron, cadmium, cobalt, and lithium must be observed.

Composition in % by Weight

Mg	=	0.80 - 1.20
Si	=	0.40 - 0.80
Cu	=	0.15 - 0.40
Cr	=	0.04 - 0.35
Fe	=	0.70
Mn	=	0.15
Zn	=	0.25
Ti	=	0.25
Al	remainder	
Other elements		
Individual	:	0.05
Total	:	0.15

Special Conditions in % by Weight

B	≤	0.001
Cd	≤	0.001
Co	≤	0.003
Li	≤	0.008

Mechanical Characteristics According to Condition T0 (Soft)

Tensile strength	max.	150 N/m ²
0.2 proof stress	max.	85 N/m ²
Elongation	min.	18 %

Appendix I-2.3

BABCOCK AND WILCOX CLADDING AND STRUCTURAL MATERIALS

BABCOCK AND WILCOX
United States of America

Abstract

A listing of specifications for the aluminum alloys used by Babcock & Wilcox as cladding and structural materials for fabrication of research reactor fuel elements is provided.

The following table shows materials used by B&W for research reactor element fabrication. The list is not inclusive but represents materials used successfully to fabricate research reactor elements. The current revision of the specifications listed is used.

<u>Aluminum Alloy</u>	<u>Specifications</u>
<u>Plate Cladding, Dummy Plates, Side Plates</u>	
1100F	ASTM B209 aluminum-alloy plate
6061 Clad with 1100, 6061-T6, 6061-T0 6061-T651	QAA-200 aluminum alloy bar, rod, shapes, and extruded tube 6061, 6062 (U.S. Federal Specification) ASTM B221-81, extruded tubing
6061-T6511 (Tubes)	
6063-T5 (Tubes)	
<u>End Fittings (adapters, combs, bails, handles, etc.)</u>	
356-T6 356-T21	ASTM B26 aluminum alloys and casting or ASTM B618 aluminum alloy investment casting
5G70A-T6 5G70A-68	ASTM B108-68 aluminum alloy permanent mold casting
6061-T651	ASTM B211 or B221 aluminum alloy
6061-T6	bars, rods, wire ASTM B209 aluminum alloy sheet and plate

The maximum impurity content for aluminum components except end fittings is reported in ppm with boron not to exceed 15 ppm. Otherwise the material composition must conform to the standard specification (ASTM).

For aluminum cladding and structurals, the chemistry specification is based on the chemistry of the melt. Results of the chemical analyses and mechanical property tests, including yield strength, are also provided by the supplier and overchecked as necessary by B&W.

Appendix I-3

CORROSION RESISTANCE AND EXPERIENCE WITH ALUMINUM ALLOY CLADDINGS

Appendix I-3.1

WATER CORROSION OF ALUMINUM ALLOY CLADDINGS

ARGONNE NATIONAL LABORATORY
RERTR Program,
Argonne, Illinois,
United States of America

Abstract

Literature applicable to the water corrosion of aluminum alloy claddings in research reactors is reviewed for the purposes of specifying operating parameters and estimating reasonable service lifetimes.

Introduction

Aluminum alloys have been, and are, being used in water-cooled production, research, and test reactors since the beginning of the nuclear enterprise. Thus, there is a voluminous literature dealing with the aqueous corrosion of aluminum and its alloys under a variety of conditions. It is not the purpose of this section to present a comprehensive review of this literature. Rather, a portion of the literature relevant to research reactors, i.e. that applicable to corrosion in recirculatory systems operating below 200°C and with provision for pH and impurity control, will be considered for the purposes of specifying operating parameters and estimating reasonable service lifetimes.

Corrosion Behavior

The corrosion behavior of aluminum alloys is sensitive to temperature, pH, and flow rate. The behavior of alloy 1100 (99% min. Al) at temperatures up to 95°C is summarized in Fig. 1.¹ Figure 2 summarizes the corrosion behavior of the same alloy over a wider range of temperatures.² In evaluating the relevance of the data in Figs. 1 and 2 to particular cases it should be noted that 1 MDD (mg/cm²/day) is equivalent to 13.5 μm/yr (0.53 mils/yr).

The data summarized in Figs. 1 and 2 were obtained in high purity water (except for the acid and alkali used for pH control) and in the absence of reactor radiation. Chlorides and heavy metals e.g. Ni, Cu, Co, Pb, Sn and Hg, in concentrations above ~0.1 ppm (above 0.02 ppm for Cu), particularly in solutions of pH below 6 lead to severe pitting.^{1,3} At temperatures up to ~150°C, water velocities up to 7.6 m/sec (25 ft/sec) do not adversely affect corrosion behavior.² At higher temperatures, the effects of flow rate and surface/volume ratio are complex.⁴ Corrosion rate increases slightly with temperature in the range of interest to research reactors and increases also with flow rate in an unsaturated (with respect to corrosion product) system.⁵

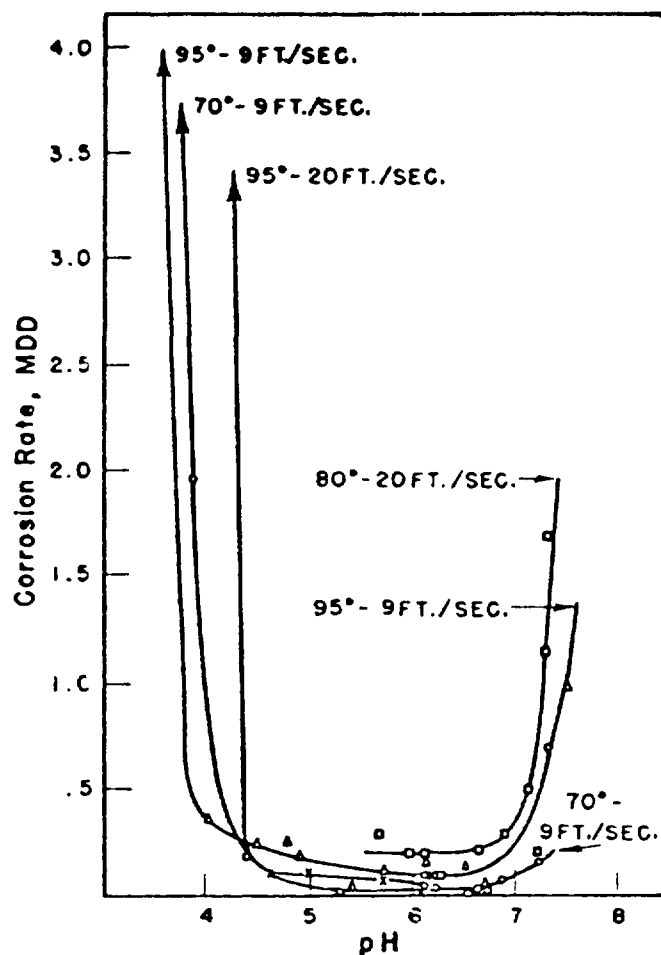


Fig. 1. Effect of pH and Other Variables on the Aqueous Corrosion of 1100 Aluminum

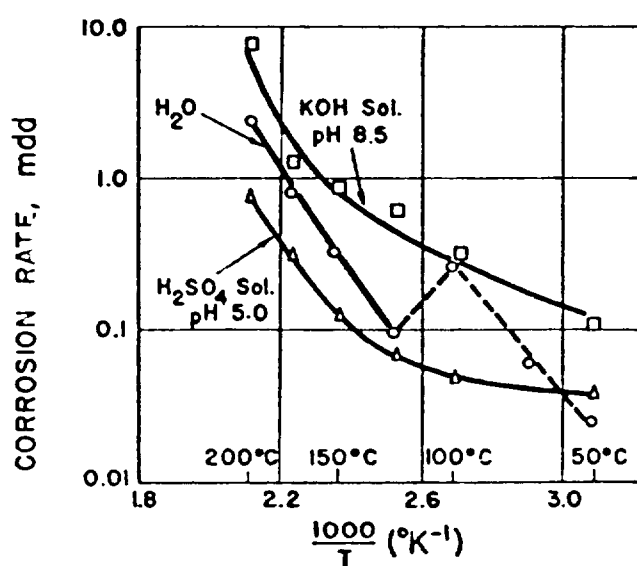


Fig. 2. Aqueous Corrosion of 1100 Aluminum

The corrosion rate of freshly exposed alloy is rapid, but it decreases parabolically to a lower constant rate as corrosion product builds up.⁶ This corrosion product is a multi-layered aluminum oxide and there is evidence that dissolution of at least one of these layers can have a significant effect on the corrosion rate.⁷⁻¹¹ The dissolution rate is a function at least of temperature, pH, and refreshment rate but there is no generally acceptable model of the detailed behavior.

Alloys with improved corrosion behavior at higher temperatures have been developed.^{2,4,12} However, it is expected that the commonly used aluminum alloys (e.g. 6061 - 0.25 Cu, 0.6 Si, 1.0 Mg, 0.25 Cr and 5052 - 2.5 Mg, 0.25 Cr) will behave similarly to 1100 and these improved alloys under research reactor conditions.² Although quantitative data are limited, there is evidence that reactor irradiation does not adversely affect the corrosion behavior of aluminum alloys.¹² For example, specimens of 6061 aluminum exposed in the core of the ORR at 57°C (135°F) for one year showed a very low corrosion rate of less than 1.3 $\mu\text{m}/\text{yr}$ (<0.1 mils/yr).¹³

Conclusions and Recommendations

Based upon the data presented above it is clear that research reactors can be operated in such a manner that corrosion of the aluminum cladding is not a practical limit on fuel element lifetime. The recommended conditions to achieve the desired long service life are pH between ~5 and ~6.7, preferably ~6, and chloride and heavy metal concentrations as low as can be achieved, at least ~0.02 ppm for Cu and below 0.1 ppm for the others. It is emphasized that these recommendations apply to periods of down-time as well as to those periods when the reactor is operating. The effect on uniform corrosion rate of periods of exposure at pH outside the recommended range can be estimated from the data in Figs. 1 and 2. Increase in concentration of chlorides and/or heavy metals will lead to severe pitting, including complete penetration of the cladding, in relatively short time.

It is also worth noting that care should be taken during storage in air to keep humidity or contamination (e.g., from fingerprints) from plate surfaces, particularly if the plates have not been cleaned and passivated.

REFERENCES

1. J. E. Draley and A. Greenberg, "The Applications of Materials in Low Temperature Water and Organic Liquid Cooled Reactors," Nuclear Metallurgy, IMD, Special Report No. 2, AIME (Feb. 1956).
2. J. E. Draley and W. E. Ruther, "Aqueous Corrosion of Aluminum Alloys at Elevated Temperatures," Geneva Conference Paper 535 (1955).
3. C. R. Schmitt, J. M. Schneyer, and J. M. Googin, "Corrosion Behavior of Aluminium in Water," Report Y/DA-7055 (Feb. 1977).
4. J. E. Draley and W. E. Ruther, "The Corrosion of Aluminum Alloys in High-Temperature Water," in Corrosion of Reactor Materials, Vol. 1, pp. 477-498, IAEA (June 1962).
5. R. L. Dillon, "Dissolution of Aluminium Oxide As A Regulating Factor in Aqueous Aluminum Corrosion," HW-61089 (August 31, 1959).

6. H. P. Godard, W. B. Jepson, M. R. Bothwell, and R. L. Kane, "The Corrosion of Light Metals," Corrosion Monograph Series, John Wiley & Sons, 1967.
7. R. L. Dillon, "Dissolution of Aluminum Oxide As A Regulating Factor in Aqueous Aluminum Corrosion," AEC-Euratom Conference on Aqueous Corrosion of Reactor Materials, TID-7587, pp. 134-152 (July 1960).
8. J. E. Draley, Shiro Mori, and R. E. Loess, "The Corrosion of 1100 Aluminum and of Aluminum-Nickel Alloys, *ibid.*, pp. 165-187.
9. J. E. Draley, Shiro Mori, and R. E. Loess, "The Corrosion of 1100 Aluminum in Oxygen-Saturated Water at 70°C," J. Electrochemical Society, Vol. 110, p. 622 (June 1963),
10. Shiro Mori and J. E. Draley, "Oxide Dissolution and Its Effect on the Corrosion of 1100 Aluminum in Water at 70°C, *ibid.*, Vol. 114, p. 352 (April 1967).
11. A. Berzins, J. V. Evans and R. T. Lowson, "Aluminum Corrosion Studies: II Corrosion Rates in Water," Aust. J. Chem., 30, 721-31 (1977).
12. K. Viden, "Aluminum Alloys with Improved Resistance in High-Temperature Water," in Corrosion of Reactor Materials, Vol. 1, pp. 499-537, IAEA (June 1962).
13. P. D. Neumann, "The Corrosion of Aluminum Alloys in the Oak Ridge Research Reactor," ORNL-3151 (June 23, 1961).

POINT CORROSION DEFECTS OF FRG-2 FUEL ELEMENTS

W. KRULL

GKSS — Forschungszentrum Geesthacht GmbH,
Geesthacht, Federal Republic of Germany

Abstract

Experience with point corrosion defects of FRG-2 fuel elements is described along with the measures that were taken to overcome point corrosion problems.

At the end of 1970 an increasing activity concentration in the air of the reactor hall of the FRG-reactors was measured. Using the wet sipping method, defect fuel elements could be localized in the reactor core of the FRG-2 (15 MW). Point defects ($\emptyset < 1,2$ mm) have been detected in the hot cells. Typical defects are shown in fig. 1-3. The electric conductivity of the primary coolant (light) water was below $1 \mu\text{S}$ and e.g. no Cl^- and Cu -ions could be found.

The FRG-1 (5 MW) and the FRG-2 (15 MW) use the same MTR-type fuel element: 23 plates, UAl_x meat, 180 g U-235, 93 % enriched, Al 99,5 canning material and anodic treatment coating.

To overcome the point corrosion problems the following parameters were changed

- canning material
Al 99,5 to Al 99,85, AlFeNi, AlMg1
- surface treatment
anodic treatment to chromatisation, only etching, cooking 0,5 h and cooking 16 h (to provide a so-called corrosion resistant boehmite coating /1/)
- reduction of the max. permissible surface defects from 100μ to 60μ .

By far the best experience was obtained with fuel elements with Mg-based Al-alloy canning materials and 16 h cooked (boehmite) surface treatment.

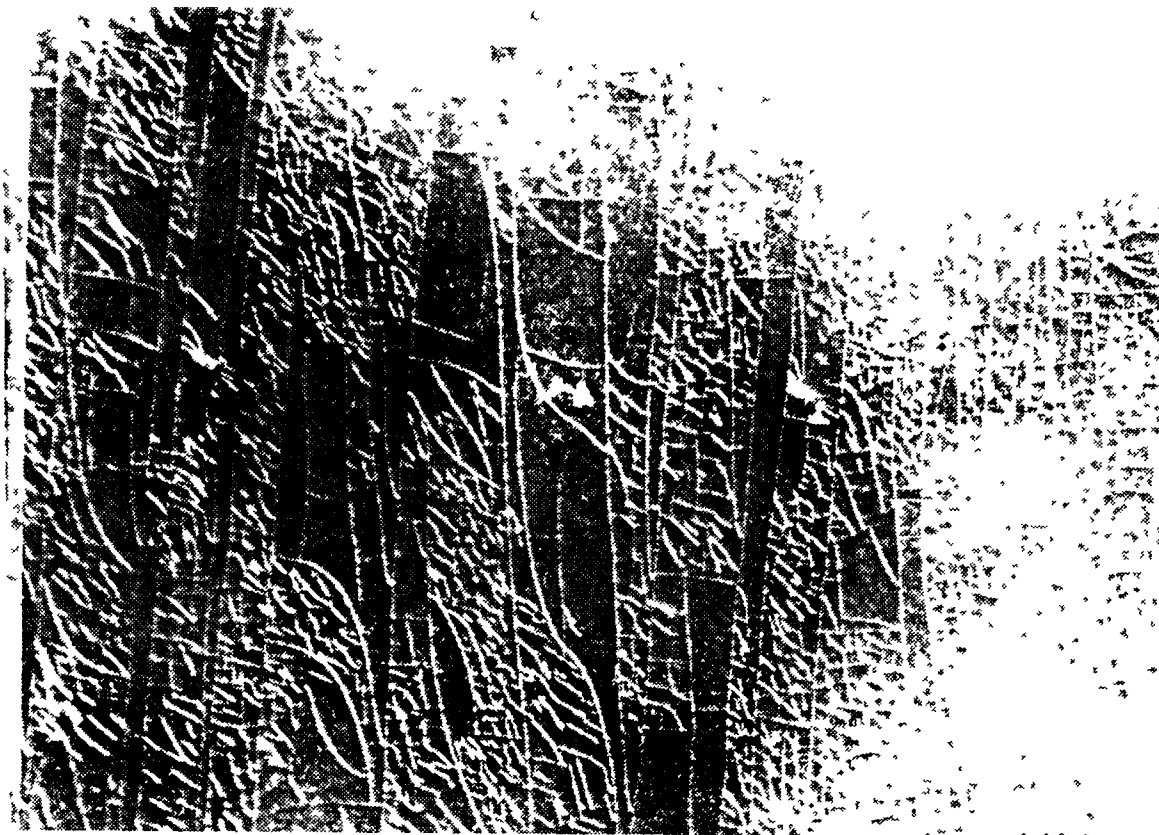


Fig. 1 Cracks in the anodic treatment coating

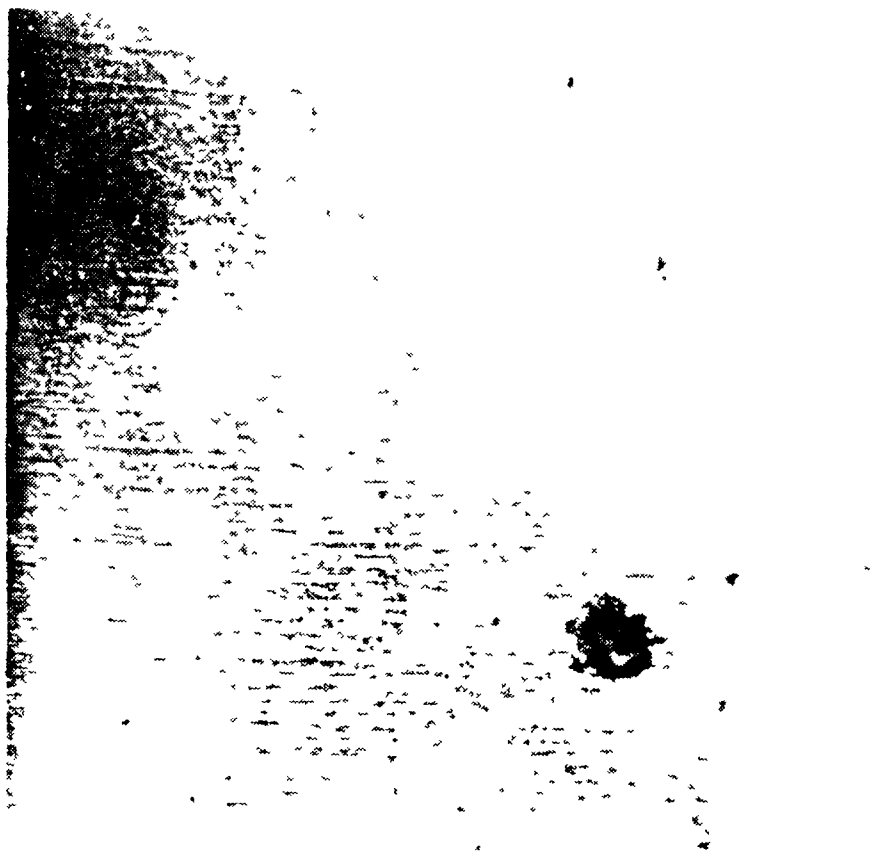


Fig. 2 Point defects without washout

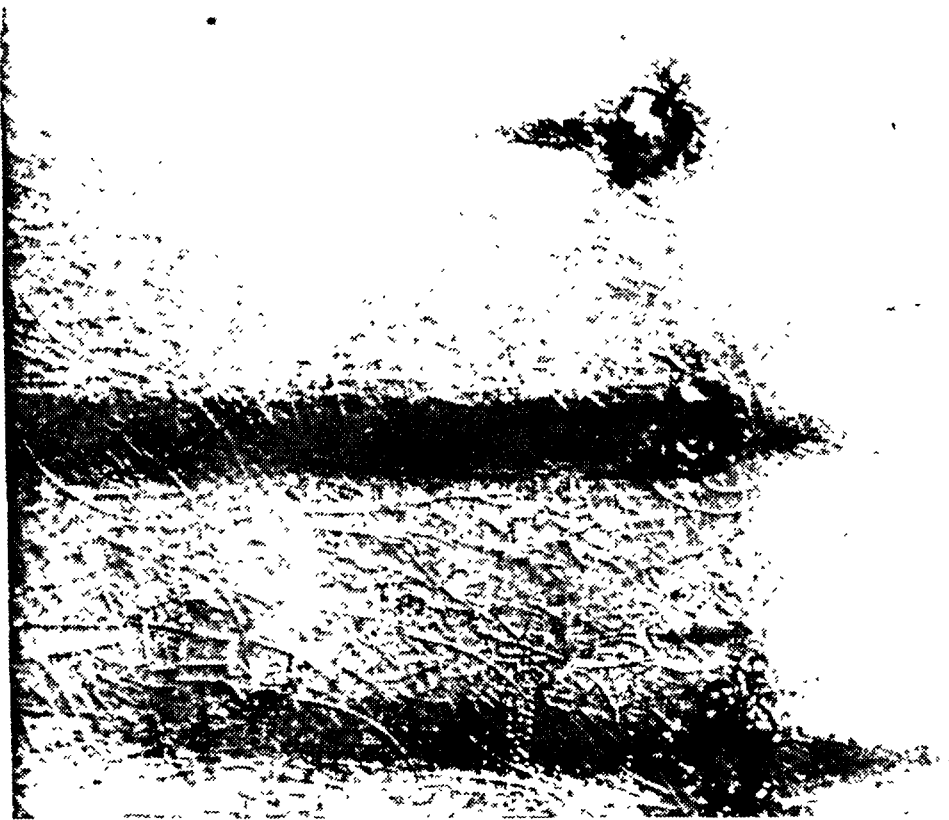


Fig. 3 Point defects with washout

Such fuel elements have been in operation since 1975 in the FRG-2 reactor and no further defects have occurred. It should be noted that point corrosion defects initiated by surface defects have never been found and that the FRG-1 reactor using the same fuel elements as the FRG-2 reactor and having a similar water quality was free from fission product release all over the years.

More information about failed fuel elements can be found in the literature /2 - 9/.

REFERENCES

- /1/ D.G. Altenpohl: Use of boehmite films for corrosion protection of aluminium, Corrosion 18 (1962) 4, p. 143-153
- /2/ W. Krull, G. Röbert: The operation and utilization of the research reactors at the research center Geesthacht, Conference on research and test reactors, ANS-Transactions (1974), p. 26-27
- /3/ M.H. Brooks: Detection and identification of failed fuel elements - HFBR, ANS-Transactions, Conference of Reactor Operating Experience /1977) 37-38
- /4/ D.R. Boisblanc, C.F. Leyes, M.H. Barts: Process water fission product activity from MTR fuel assemblies, MTRL-54-62
- /5/ L.J. Harrison: In-pile mechanical failure of MTR fuel assemblies, (1963) IDO 16862
- /6/ J.W. Dykes, J.D. Ford, K.R. Hoopingarner: A summary of the 1962 fuel element fission break in the MTR, /1965) IDO 17064
- /7/ R.H. Clark, J.W. Cure: Detecting leaks in plate-type elements, ANS-Transactions Supplement 2 p. 5-6 (1971)
- /8/ H.R. Hilker, F.C. Fogarty: Test reactor operating experiences with failure-prove fuel, ANS-Transactions Supplement 2 p. 20-22 (1971)
- /9/ J.L. Eagan: Multiple failure of MTR-type fuel elements at LPTR, ANS-Transaction Supplement to Volume 12 p. 61-62 (1969)

Remarks More experiences with fuel elements failures are well known. As these defects are not documented in the open literature no citation can be given.

Appendix I-3.3

NOTE ON UK EXPERIENCE RELATING TO CORROSION OF MTR FUEL

R. PANTER

United Kingdom Atomic Energy Authority,
Harwell, Didcot, Oxfordshire,
United Kingdom

Abstract

Experience in the U.K. related to corrosion of MTR fuel elements clad in pure aluminium is described. Recommended conditions for demineralized water are provided along with the surface treatment used to passivate complete Harwell fuel elements.

U.K. experience relates only to fuel clad in pure aluminium, assembled by mechanical means or by inert gas shielded welding or brazing with either pure aluminium or aluminium-silicon alloy.

Elements have been used for up to 15 years in low power reactors, in some cases followed by high power use to normal burn-up. Prior to reprocessing, elements are stored in water for between two and five years. No cases of corrosion failure have been experienced in water of good quality.

The conditions recommended are demineralised water of

conductivity 0.2 to 1.5 μ mho/cm²

pH 5.5 to 6.5

Fe not more than 0.01 ppm

Cu " " " 0.01 ppm

Cl " " " 0.2 ppm

Any particles of rust from unprotected mild steel in the water cause rapid pitting corrosion of aluminium.

It is worth noting that storage in air prior to use also requires dry and clean conditions, particularly if the aluminium surface has not been chemically cleaned and passivated. Some cases of failure prior to irradiation, in elements assembled by salt-bath dip brazing, were due to brazing flux trapped in crevices in the structural elements. This method of assembly is no longer used.

It has been found advantageous to passivate complete elements to remove any particles of foreign metal on the surface and to reduce the initial oxidation in the reactor water. The treatment used for Harwell elements is:

1. Clean mechanically if necessary, degrease using methanol and blow off any dust with compressed air.
2. Soak in 10% w/w nitric acid at 40°C for 5 minutes.
3. Rinse in running water.
4. Soak in demineralised water at 40°C for 5 minutes.

5. Soak in clean demineralised water at 70°C for 15 minutes - this provides an opportunity to check that no contamination has been carried over.
6. Dry in air at 100°C.

The visual result of this treatment is less attractive than mechanical or chemical cleaning, but the surface is less susceptible to corrosion in damp air or in water.

Appendix I-3.4

ALUMINIUM CORROSION DATA

C. BAGLIN

GEC Energy Systems Limited,
Whetstone, Leicester,
United Kingdom

Abstract

Literature related to pitting corrosion of the aluminium used in the cladding of research reactor fuel elements is reviewed. Key data and conclusions are summarized.

The corrosion rate of aluminium and its alloys under normal research reactor conditions of relatively low temperature and high water purity, can be kept very low. Generally the higher the degree of purity of the aluminium the greater its corrosion resistance. However, certain elements such as magnesium and zinc can be alloyed in amounts up to 1% with refined (99.99%, AA-1099) aluminium without reducing the corrosion resistance of the pure metal (Ref. 1). Under research reactor conditions either commercial - purity aluminium or 2S (99.0%, AA-1100) are used because high-purity aluminium is susceptible to intergranular corrosion in deoxygenated water at slightly elevated temperature (Ref. 2). A corrosion rate of 0.01 ml/yr at 50°C has been achieved using AA-1100 (Ref. 3). The control of the pH of the water system between 5 and 7 is essential and this produced little significant changes in the latter corrosion rate (Ref. 3). An increase in the temperature of the water system causes an increase in the film formation on the surface of the aluminium, which at 80°C was sufficient to prevent further pitting corrosion to AA-1100 (Ref. 4). Pitting corrosion was found to be sensitive to water composition at different temperatures with even a small addition of copper to the water causing some pitting to occur even at higher temperatures (Ref. 4). The initiation and rate of pitting are influenced by the flowrate of the water and a velocity of only 8 fpm suppresses the pitting of AA-1100 sheet completely (Ref. 5). The effects of water conductivity on the corrosion resistance of aluminium has been little documented, but a value of between 0-5 μ mho is generally desirable.

Low Temperature References

1. Godard, H. P., W. B. Jepson, M. R. Bothwell and R. L. Kane. The corrosion of light metals. Corrosion monograph series 1967.
2. Perryman, E. C. W., J. Inst. Met., 88, 62 (1959/60).
3. Draley, J. E., and W. E. Ruther, Corrosion, 12, 441 (1956).
4. Porter, F. C., and S. E. Hadden, J. Appl. Chem., 3, 385 (1953).
5. Wright, T. E., and H. P. Godard, Corrosion, 10, 195 (1954).

High Temperature References

6. Huddle, R. A. U., and N. J. M. Wilkins, U.K. Atomic Energy Establishment Report - M/R-1669 (1955).
7. Huddle, R. A. U., and N. J. M. Wilkins, U.K. Atomic Energy Establishment Report - M/R-1669A (1956).
8. Bowen, H. C., U.S. Atomic Energy Commission Report HW-68253, March 1961.
9. Lobsinger, R. J., U.S. Atomic Energy Commission Report HW-59778, Feb. 1, 1961.
10. Draley, J. E., AEC Euratom Conf. Aq. Corrosion Reactor Materials, Brussels, TID-7587, (1960) 165.
11. Troutner, V. H., U.S. Atomic Energy Commission Report HW-50133, June 10, 1957.
12. Dillion, R. L., Corrosion, 15, 13 (1959).
13. Krenz, F. H., Corrosion, 13, 575 (1957).
14. Draley, J. E., C. R. Bredon, and W. E. Ruther, Conference on Peaceful Uses of Atomic Energy, Geneva, 1958, A/Conf./15, page 714.
15. Wilkins, N. J. M., J. T. Dalton, and J. N. Wanklyn, U.K. Atomic Energy Establishment Report-R-3649 (1961).
16. Dillon, R. L., et al., Hanford Works (USA) HW-37636 (1956).
17. Strom, P. O., and M. H. Boyer, Livermore Lab. (USA), LRL-64 (1953).

Appendix I-3.5

CRNL EXPERIENCE WITH ALUMINUM CLADDING CORROSION

R.D. GRAHAM

Reactor Technology Branch,
Chalk River Nuclear Laboratories,
Atomic Energy of Canada Limited,
Chalk River, Ontario,
Canada

Abstract

CRNL experience with corrosion of the aluminum fuel cladding used in the NRU and NRX research reactors is described. Both reactors currently use HEU(93%) uranium-aluminum alloy rod-type fuel.

NRU has had no problems with corrosion of the aluminum fuel cladding. NRX, which uses single pass, untreated water for fuel cooling and for which the fuel residence time is much longer than NRU, has generally had good performance from aluminum cladding. However, from 1975 to 1979, NRX had considerable trouble with cladding corrosion. That problem appears to have been resolved.

1. INTRODUCTION

The Chalk River Nuclear Laboratories (CRNL) at Chalk River, Canada, have two high power research reactors, NRX which began operation in 1947, and NRU which began operation in 1957 (see Table 1). Both reactors have used aluminum fuel cladding throughout their lives. Both reactors currently use highly enriched (93% U-235) uranium-aluminum alloy rod-type fuel.

NRU has had no problems with corrosion of aluminum fuel cladding. NRX, which uses single pass, untreated water for fuel cooling, and for which the fuel residence time is much longer than NRU, has generally had good performance from aluminum cladding, but from 1975 to 1979 NRX had considerable trouble with cladding corrosion. That problem now appears to have been solved.

2. NRX

2.1 Fuel Cladding Corrosion

The current NRX fuel design, the Mark IV, has been in regular use since 1971. Details of the design and operating conditions of the Mark IV, and the previous Mark I design which was in use from 1962 to 1974, are given in Table 2. Briefly, both designs consist of bundles of seven fuel rods*, the Mark IV fuel being 274 cm long and clad with 0.076 cm of Alcan 6102 aluminum, compared to a fuel length of 245 cm and a clad thickness of 0.114 cm of Alcan 2S (AA #1100) aluminum for the Mark I design.

*Alcan 6102 is a "customer alloy" having purity similar to or higher than 1S, but with more rigid specifications of alloy content.

TABLE 1. HIGH POWER RESEARCH REACTORS AT CRNL

	NRX	NRU
<u>General:</u>		
- Reactor type	Tank type	Tank type
- Moderator	D ₂ O	D ₂ O
- Reflector	Graphite	H ₂ O
- Coolant	H ₂ O	D ₂ O
- Nominal power	25 MW (thermal)	135 MW (thermal)
- Neutron flux: thermal	Avg. 4.8×10^{13} n/(cm ² ·s)	Avg. 1.4×10^{14} n/(cm ² ·s)
	Max. 1.3×10^{14} n/(cm ² ·s)	Max. 4.0×10^{14} n/(cm ² ·s)
	Avg. 1.6×10^{12} n/(cm ² ·s)	Avg. 1.3×10^{13} n/(cm ² ·s)
	Max. 4.3×10^{12} n/(cm ² ·s)	Max. 4.5×10^{13} n/(cm ² ·s)
fast		
- First critical	July, 1947	November, 1957
<u>Vessel:</u>		
- Shape	Vertical cylinder	Vertical cylinder
- Dimensions (inside)	D. 267 cm x H. 320 cm	D. 349 cm x H. 366 cm
- No. of lattice sites	Vert. 199 (through-tubes)	Vert. 227 (not through-tubes)
		Horiz. 2
		NOTE: Bottom of vessel forms coolant distribution header for fuel.
<u>Control and Safety:</u>		
- Regulation method	- Moderator level control	- Sequential control rods (6)
- Shutdown devices	- 6 B ₄ C shut-off rods	- 18 gravity fall control rods
	gravity fall plus partial moderator dump (6 valves)	(11 cadmium, 7 cobalt)
- Poison compensation and flux adjustment	- 4 Co adjuster rods	- on-power refuelling and 4 adjuster rods
<u>Fuel Coolant:</u>		
- Type	H ₂ O, single pass, untreated	D ₂ O (in series with moderator)
- Flow	150 kg/s	2000 kg/s
- Direction of flow	Down	Up (exits into vessel)
- Pressure: inlet	1.2 MPa	0.65 MPa
	0.3 MPa	0.15 MPa
- Inlet temperature	2-20°C	25-35°C
- Chemistry	pH 6.5-7.5	- min. purity 99.75% D ₂ O
	Conductivity 400-600 μS/m	- Conductivity approx. 20 μS/m
	Total solids 45-65 ppm	- Al less than 2 ppm
	Fe 0.1-0.4 ppm	- O ₂ less than 0.3 ppm
	Cu 0.01-0.04 ppm	
	Chloride 0.1-0.2 ppm	
	O ₂ 5-15 ppm	

A total of about 270 Mark IV assemblies have been irradiated to date, including about 60 presently in the reactor. Cladding failures, as detected by increased radioactivity in the coolant, have occurred in 74 of these assemblies. Examination of several of these assemblies indicates the failures were due to aggressive external pitting corrosion. In comparison, only three cladding failures occurred out of a total of 340 Mark I fuel assemblies irradiated.

As indicated in Tables 3 and 4, the early Mark IV assemblies were not affected: none of the fuel installed during 1971 and 1972 failed, and only three of the assemblies installed during 1973 suffered cladding failures, at essentially full burnup. However, the majority of fuel

TABLE 2. REACTOR FUEL ASSEMBLIES

	Mark I	NRX Mark IV	NRU
<u>Fuel Material:</u>			
- Type	U-Al alloy	U-Al alloy	U-Al alloy
- Composition	72 wt% Al- 28 wt% U	72 wt% Al- 28 wt% U	79% wt% Al-21 wt% U
- U density	0.97 g/cm ³	0.97 g/cm ³	0.69 g/cm ³
- % U-235	93%	93%	93%
<u>Fuel Elements:</u>			
- Type	Rods (pencils)	Rods (pencils)	Rods (pencils)
- Diameter (unclad)	0.635 cm	0.635 cm	0.549 cm
- Length	245 cm	274 cm	274 cm
<u>Cladding:</u>			
- Type	Extruded Aluminum	Extruded Aluminum	Extruded Aluminum
- Material	2 S (AA 1100)	Alcan #6102	Alcan #6102
- Thickness	0.114 cm	0.076 cm	0.076 cm
- No. fins/rod	3 (helical)	Outer 4 (hel.) Inner 6 (hel.)	6 (straight)
- Fin size: W	0.102 cm	0.076 cm	0.076 cm
H	0.094 cm	0.127 cm	0.127 cm
<u>Assembly:</u>			
- General	Rods suspended inside Al flow tube	Rods suspended inside Al flow tube	Rods suspended inside Al flow tube
- No. rods/assembly	7 (1 central, 6 outer)	7 (1 central, 6 outer)	12 (3 inner, 9 outer)
- Spacing of fuel centres	-1.12 cm	-1.054 cm	Inner - on radius 0.65 cm Outer - on radius 1.72 cm
Maintained by	Spacers every 43 cm	Fins (hel.)	Spacers (6 over length)
- Coolant area over fuel	-5.7 cm ²	-4.2 cm ²	-14.3 cm ²
<u>Operating Conditions:</u>			
- Coolant flow	2.1-2.4 kg/s	2.1-2.4 kg/s	12-14.5 kg/s
- Coolant velocity	3.7-4.2 m/s	5.0-5.7 m/s	7.7-9.1 m/s
- Maximum power to coolant (Limit)	740 kW	800 kW	2100 kW
- Max. surface heat flux	180 W/cm ²	200 W/cm ²	260 W/cm ²
- Max. clad surface temperature (calculated)	140°C	135°C	135°C
- Residence time in reactor	600-800 d	900-1500 d	Approx. 300 days
- Lifetime energy output	180-240 MW·d	290-350 MW·d	305 MW·d
- Fuel management scheme	(Normally) assembly starts life near centre of core - moved (about 5 times) progressively to outside of core		Assembly starts near outside of core - moved towards centre

assemblies installed in 1974, 1975 and 1976 failed. The failure rate declined for fuel installed during 1977 and 1978 although there was a tendency to schedule removals earlier than usual. As of June 1982, no cladding failures have occurred in fuel assemblies installed after the third quarter of 1978, and no cladding failures at all have occurred since the end of 1979.

TABLE 3. NRX FUEL CLADDING FAILURES BY DATE OF INSTALLATION (MARK IV ASSEMBLIES)

Year Installed	Total Installed	Cladding Failures			Scheduled Removals			Other Removals
		No.	Days in Reactor	Burnup (MW·d)	No.	Days in Reactor	Burnup (MW·d)	
1971	4	0	-	-	4	1070	293	0
1972	32	0	-	-	30	1170	309	2
1973	27	3	1100	311	16	1515	352	8
1974	26	19	785	275	6	1310	353	1
1975	25	23	625	250	2	1245	340	0
1976	28	15	690	245	7	925	288	6
1977	31	8	635	225	12	950	287	11
1978	20	6	460	194	5	800	274	6
1979	33*	0	-	-	0	-	-	13
1980	20*	0	-	-	0	-	-	3
1981	21*	0	-	-	0	-	-	1

* Some of these assemblies were still in reactor as of June 1982 (about 60 assemblies in reactor).

TABLE 4. NRX FUEL CLADDING FAILURES BY DATE OF REMOVAL (MARK IV ASSEMBLIES)

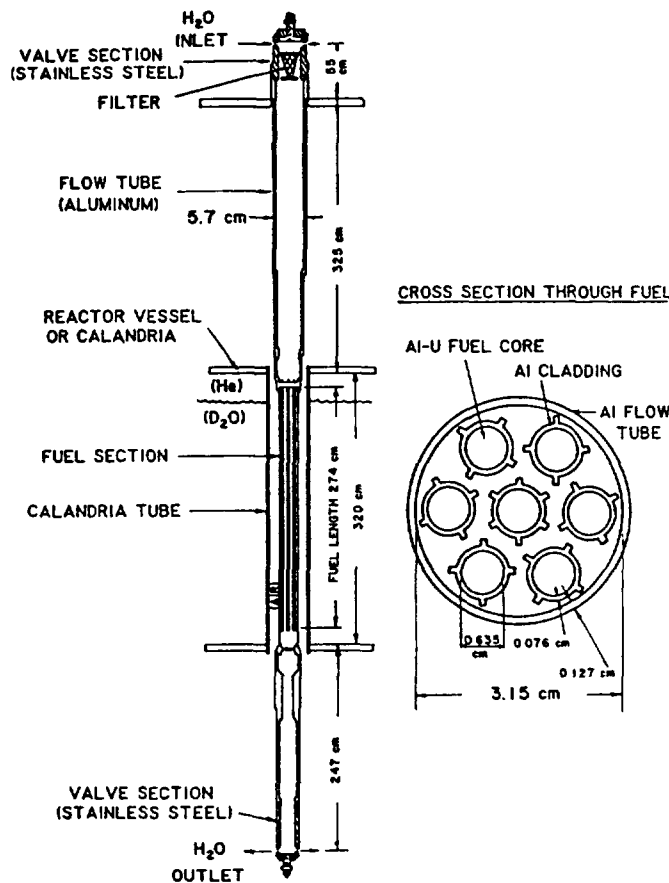
Year Removed	Total Rods Removed	Cladding Failures			Scheduled Removals			Other Removals
		No.	Days in Reactor	Burnup (MW·d)	No.	Days in Reactor	Burnup (MW·d)	
1974	12	0	-	-	9	1020	292	3
1975	26	5	465	228	17	1060	298	4
1976	23	17	700	255	2	1090	310	4
1977	59	26	745	270	29	1465	348	4
1978	17	10	680	237	3	1135	324	4
1979	39	16	650	235	11	955	291	12
1980	24	0	-	-	11	885	283	13
1981	8	0	-	-	3	1141	303	5
1982	4	0	-	-	1	1360	320	3
to June 1)								
Total Avg.	210	74	686	251	85	1170	313	51

2.2 Examination of Failed Fuel

Several Mark IV assemblies with cladding failures were examined. All failures appeared to be due to localized pitting corrosion leading to penetration of the cladding, with longitudinal slits developing in the worst cases. All failures occurred at the base of the fins, although some less severe pitting was observed away from the fins as well. Failures generally occurred slightly downstream of the maximum flux position, in the region of highest cladding temperatures. No failures were observed on central fuel elements which operate at slightly lower power than the outer elements due to flux depression. All fuel elements examined were covered with a layer of crud deposits, consisting of roughly 70% iron oxides, 20% aluminum oxides, and 10% organics. It was noted that little or no crud build-up was present at the base of the fins.

2.3 Cause of Failure

Since the early Mark IV assemblies were not affected, it was concluded that some change had occurred to produce corrosive conditions in



NRX Mark IV fuel assembly (not to scale).

later fuel assemblies. Investigation of operating conditions, water chemistry, materials and fabrication did not reveal any major changes corresponding to the start of the cladding failures. One of the most likely suspects discovered was the use of a lubricant containing a high proportion of nickel as an anti-seize compound on the threads of the stainless steel valve sections attached to both ends of the flow tube. While the corrosion mechanism has not been definitely confirmed, it is believed that the region at the base of the fins was susceptible to pitting and a small amount of impurities, probably nickel leached from the valve lubricant, depositing on the cladding was sufficient to cause localized galvanic corrosion preferentially in that region.

The nickel-bearing lubricant was in use for an undetermined length of time. Since it is applied by the reactor operators during the final assembly prior to installation it escaped the normal quality control checks of the fabrication process. Use of this compound was recognized as a potential cause of the corrosion and stopped in November, 1978. It was replaced with a silicone dielectric. No failures have occurred in fuel assemblies installed after that time.

A sharp corner at the base of the fins is believed to have contributed to the susceptibility of that region because of erosion of the protective oxide film by turbulent flow of hot coolant, slightly higher surface temperatures than elsewhere, and some residual stress from extrusion. The corners of the extrusion die have been rounded to produce a larger radius of curvature at the base of the fins on all NRX fuel elements produced since February 1979.

Other things probably contributing to the general susceptibility of the cladding to corrosion are the general water chemistry particularly the traces of copper and the long residence time of the Mark IV assemblies in the reactor.

2.4 Activity Releases Due to Cladding Failures

Releases of radioactivity to the NRX coolant as a result of these cladding failures are relatively small. Typically the failures are initially almost undetectable on monitoring instruments and the release rate slowly increases over a period of 2 to 4 weeks (occasionally longer) until a failure is confirmed, and the failed fuel assembly located and removed.

Routine analysis of non-gaseous fission product releases indicate that the average cladding failure resulted in releases in the order of 0.005% of the inventory for each fission product nuclide in the entire fuel assembly. In general the fission products appear to be retained in the metal matrix of the fuel alloy, being released only through erosion of the alloy and recoil from the exposed surface. In one of the worst cladding failures examined, about 0.08 cm³ of fuel meat had been eroded away and it was estimated that this represented a release of about 0.017% of the fission product inventory of that fuel assembly. In all cases the quantities of fission products released were very small fractions of the release limits for the CRNL site.

Releases of individual gaseous fission product nuclides have not been measured, but the fact that no significant release of activity is initially detectable suggests that there is little or no diffusion of gases out of the fuel. It is believed that gaseous fission product releases are of the same order of magnitude as non-gaseous releases.

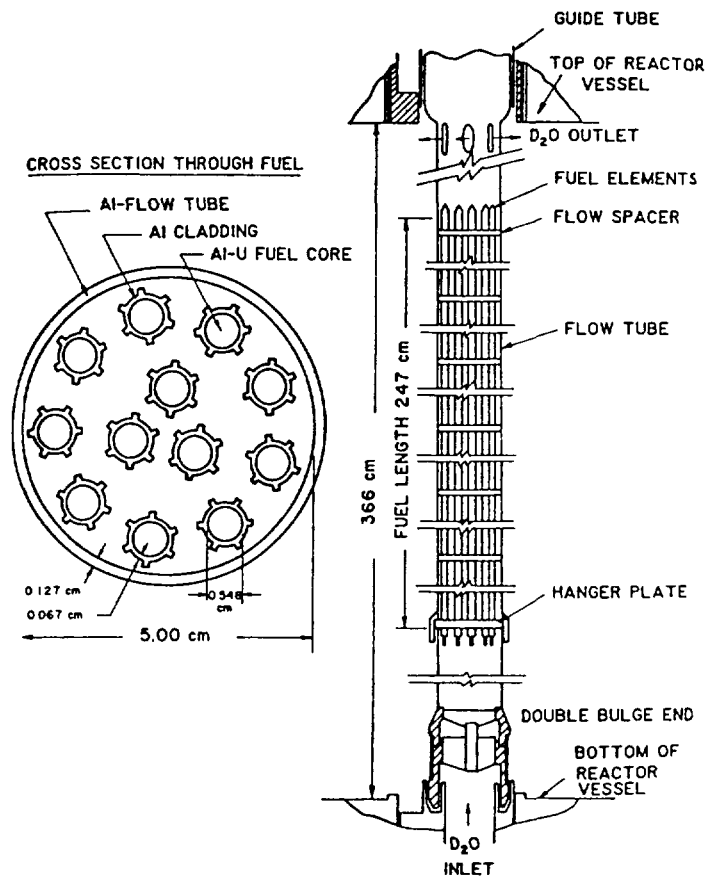
3. NRU

The present NRU fuel design has been in use since 1964, although the uranium density has changed several times: from 0.29 g/cm³ to 0.42 g/cm³ in 1966, to 0.54 g/cm³ in 1968, and to the present 0.69 g/cm³ in 1969. The fuel assembly consists of twelve rods, with fuel length 274 cm, and clad with 0.076 cm of Alcan 6102 aluminum (see Table 2).

Operating conditions for NRU fuel assemblies are slightly more severe than for NRX fuel, but there is a much shorter residence time in the reactor and better quality coolant. Over 1200 of these assemblies have been irradiated in the reactor. To date there has been no evidence of cladding failure or excess corrosion.

4. CONCLUSIONS

Aluminum has been used successfully at CRNL as a cladding material for highly enriched fuel, with surface heat flux to 260 W/cm², with in-reactor residence times in some cases over four years, and in both good quality and untreated coolant. General operating limits applied to this cladding at CRNL are: coolant velocity less than 9.1 cm/s; and surface temperature less than 135°C for Alcan 6102, or less than 160°C for 2S (AA 1100).



NRU fuel assembly (not to scale).

Experience with corrosion indicates that sharp corners should be avoided, and care taken to maintain quality control throughout fabrication, assembly, and operation of the fuel to avoid introducing impurities.

WATER AND CORROSION TECHNOLOGY OF LIGHT WATER RESEARCH REACTORS

H. PIEPER

Kernforschungsanlage Jülich GmbH,
Jülich, Federal Republic of Germany

Abstract

Light water is used as primary coolant and as moderator in most of the research reactors. In order to keep the corrosion of the structural materials used in the reactor as small as possible, specific requirements must be fulfilled both with respect to the water quality and also the engineering design of the system. The values which are associated with the fulfillment of these objectives may be termed "chemical parameters."

Suitable measures will be discussed which influence these chemical parameters and which satisfactorily fulfill the requirement to be met by water chemistry. In addition, experience gained in operating the Jülich FRJ-1 reactor will be demonstrated.

Light water used in the reactor as a primary coolant serves as a heat transfer medium and as a moderator. The influence of this water on the structural materials normally used such as:

- austenitic chrome nickel steels (weld claddings, piping, pumps, fittings and heat exchangers),
- and high-purity aluminium or aluminium-magnesium alloys (fuel element cladding, reactor vessel, internals etc.)

must in this case be as slight as possible.

The following requirements must be fulfilled by the water quality quite generally:

1. No or only little aggressiveness in order to maintain a minimal rate of metal loss from the structural materials -
2. The probability of the occurrence of selective corrosion forms through ionogenic or solid water impurities should be as small as possible -
3. Radiochemical hydrogen and oxygen formation (radiolysis) must be suppressed by suitable measures.

In addition the engineering design of the system should guarantee that the formation of activated corrosion products can be minimized, which means that:

4. Transport and deposition of corrosion products should be influenced in such a way that contamination of the primary circuit remains slight, i.e. if possible no material should deposit in the core zone and only short residence times should occur here -
5. The deposition of corrosion products on the heat transfer surfaces (fuel elements and heat exchangers) should therefore also be avoided as far as possible.

The de-ionized water used in the reactor primary coolant loop is more or less aggressive towards the structural materials used in the research reactor, especially if it is contaminated with oxygen and other substances such as chloride, sulphide or also traces of heavy metals. In order to minimize these impurities' chemical attack on the structural material as far as possible water chemistry for its part aims at preventing damage and operational impairments by an appropriate mode of operation.

The data exhibiting a connection with the fulfillment of this objective can be designated "chemical parameters". By suitable measures which influence the chemical parameters the demands made on water chemistry can be satisfactorily fulfilled.

Among these measures is the definition of directly measurable quantities. In the Federal Republic of Germany these measurable quantities are for example laid down in the water specifications for reactor primary cooling water in BWR's and PWR's.

Even today these values are strictly speaking not guidelines for research reactors, although some of the reactors have been in operation for more than 20 years. In this respect one adheres rather to the various operating regulations, usually taken over from other reactor stations, to the manufacturers' technical specifications, as well as to the fuel element warranty clauses, which as a rule all determine the maximum permis-

Table 1: VGB*standards for reactor water and reactor feed water in BWR installations in continuous operation (1973)

			reactor water	reactor feed water
conductivity	25°C	µS/cm	< 1	< 0.15
chloride	(Cl)	mg/kg	< 0.2	-
silica	(SiO ₂)	mg/kg	< 4	-
total iron	(Fe)	mg/kg	-	0.025
total copper	(Cu)	mg/kg	-	0.003
sodium and potassium		mg/kg	-	-

* VGB = Technische Vereinigung der Großkraftwerksbetreiber e.V.
 -Technical Association of Major Power Station
 Operators

sible concentrations of various substances in the reactor primary water and feed water which may not be exceeded in operation.

Stainless steel as a structural material in the primary system is susceptible to stress-corrosion cracking if chloride is also present in the water in addition to oxygen. In the case of aluminium and aluminium-magnesium alloys there is a danger of pitting corrosion at higher chloride concentrations. Since research reactors favour a swimming pool design as a reactor type one does not in any case have any influence on the oxygen concentration in the pool water, and therefore only the chloride concentration can be limited as a function of the oxygen content. However, selective forms of corrosion can be largely eliminated by such a restriction of the chloride concentration. The maximum permissible concentration of chloride ions in the primary cooling water is identical to the value of the VGB guideline. Today, however, in the operation of a research reactor with a well-functioning purification system values remain clearly below this limit.

Other ionogenic impurities or dissolved substances need not necessarily be specified with respect to their maximum permissible concentration. Nevertheless, with careful monitoring they can give indications of whether the behaviour of the primary cooling water which is to be expected on the basis of the given water chemistry actually occurs. This behaviour could in principle

also be observed from the analysis of certain activation products (e.g. Co-60, Co-58, Mn-54, Na-24), if this examination were carried out regularly.

The determination of limits becomes senseless however, if orders of magnitude are thereby obtained which are no longer analytically detectable. Therefore the observation of the water specification is not always sufficient to avoid damage. The consideration of further, not directly measurable values is equally important.

There are substances which cause detrimental effects even if present in non-analytically detectable amounts. Table 2 gives a rough survey of this type of substance; it does not claim to be exhaustive. A closer quantification is not normally carried out. The introduction of these substances into the primary cooling water can only be prevented, or rather kept under control, by countermeasures.

The following are among the necessary measures for influencing the chemical parameters:

1. Plant operation

In respect of the chemical parameters the plant operation will concentrate on the observation of the water specification. The values are monitored by instrumentation and laboratory analyses and can be controlled by means of the water purification systems' mode of operation and the flow of water in the circuit.

2. Plant engineering measures

Among these are the correct design and the proper functioning of the water purification system (filtration, ion exchanger), reliable make-up water conditioning, an optimal circulation system (purification bypass) and sufficient dimensioning in terms of flow mechanics (no dead legs).

3. Selection of materials

The composition of the high-grade steels, aluminium and aluminium-magnesium alloys used with respect to their content

Table 2: Survey of "forbidden" substances

substance	typical occurrence	effect
halogen-containing materials	degreasing agents, Teflon, PVC, Neoprene	decomposition to form halogen stress-corrosion cracking
mercury	thermometers, pressure gauges	intercrystalline corrosion
lead, cadmium, tin	shieldings, tools	intercrystalline corrosion
sulphide	molybdenum disulphide	pitting
cobalt, zinc, silver	materials, absorber materials	extensive activation in the neutron field
oil, grease	preserving agents, lubricants	decomposition into acids corrosion
mechanical dirt	drops of sweat, Kleenex-tissues, residues of foils, disposable gloves	clogging, jamming
ionogenic contaminants	salts, chemicals	increased conductivity corrosion
detergents	soaps, derusting agents, organic solvents	increased conductivity, pH value change, corrosion foaming
antistatic agents	new plastic filter cartridges	increased conductivity, corrosion, foaming
ion exchange resins	leakages from purification systems	decomposition corrosion

of alloying constituents and normal impurities must be specified in such a way that, in the case of corrosion, if possible no long-lived activation products can occur, or rather that no selective corrosions (local elements, pitting) can take place under the prevailing conditions. This includes e.g. the specifications about the maximum cobalt, zinc or copper contents in these materials. Furthermore, attention must be paid that no "forbidden" substances (Table 2) be introduced into the cooling system by means of auxiliary devices, tools, measuring instruments etc. (mercury, halogens, molybdenum sulphide, heavy metals).

4. Cleanliness

Particular care must be exercised when working on the open cooling system and reactor vessel. Basically only parts and

experimental devices perfectly clean, indeed as a rule only with pickled surfaces, should be introduced into the primary cooling water.

The water purification system was specially mentioned among the plant engineering measures for influencing the chemical parameters in the reactor primary coolant loop. It is a particular task of this purification system to ensure the observation of the water specifications during the operation of the reactor. This is why we shall here once more consider the major sources of the possible occurrence of contamination.

- Make-up water conditioning

Slippage of unwanted ions: (Cl^- , SO_4^{--} , Na^+ , SiO_3^{--} , CO_3^{--}) with depleted exchanger materials,

- leakages

In the heat exchanger in the case of pressure differences between the primary and secondary or ancillary coolant loop,

- structural materials

Surface erosions or the normal corrosion rates of high-grade steel and aluminium (these are approx. 0.005 mm/year). These dissolving impurities are activated (Cr-51, Mn-54, Na-24) and form a not inconsiderable radiation source,

- activation products

of the water, especially the nitrogen isotopes N-16 (half-life = 7.2 sec.) and N-17 (half-life = 4.2 sec.), which because of their short half-life are only effective during operation, neither should the argon isotope A-41 be forgotten, which is formed as an activation product due to the continual air contact between the pool water surface and the hall air. The hydrogen isotope H-3, which is also obtained in the case of light water moderated research reactors

with a slight build-up rate, only plays a minor role as an activation product and radiation source, however it may on the basis of its long half-life cause problems with respect to release during primary cooling water leakages or system drainages.

- and finally the impurities due to fissile materials from leaky fuel claddings (corrosion, hairline cracks, diffusion processes during film boiling) must also be mentioned. Above all iodine, the inert gases xenon and krypton, but also uranium itself or Np-239 must be mentioned here. Even though the fissile product activity does not influence the chemistry of the reactor water, it has no significance in terms of weight, it does however have a considerable effect on the handling of the reactor water during analysis, leakages or disturbances. The possible high specific activities always affect the radiation protection measures which have to be taken and therefore require particular attention during operation.

In respect of these possible sources of contamination in the reactor primary cooling water specified above it is therefore the major task of the water purification system to efficiently remove these impurities from the reactor water where they have dissolved or have appeared in the form of solids or colloids, and thereby to achieve safe operation of the reactor and a good availability of the plant.

The combination of a mechanical cartridge filter with a 2 - 5 μm filter fineness (as a preliminary filter) with a mixed-bed ion exchanger, whereby the ratio of the absorption capacity cation- to anion-exchange resin varies between 1 : 1, 1.5 : 1 up to 3 : 1 depending on the reactor plant, has proved successful in all research reactors. The throughput of the purification system is as a rule between 0.1 - 1 %, in the case of individual systems even up to approx. 10 % of the hourly cooling water circulation. In the same way purification variations are being operated in which the throughput through the mechanical filter amounts to several times (e.g. 4 - 5 times) that of the mixed-bed filter. It is necessary to additionally install a collecting filter for decomposed resin particles (approx. 10 - 25 μm fineness) behind the mixed-bed filter.

We can report from our own experience on FRJ-1 that the primary cooling water is operated with the addition of free silica at a concentration between 10 - 30 mg/kg. Extensive laboratory tests at the beginning of the sixties showed that corrosion damage to aluminium as a structural material in contact with high-grade steel or ferritic surface impurities could largely be avoided by the addition of silica. Our many years' experience with FRJ-1 have completely confirmed this inhibiting property of silica as a protective colloid.

One of the accidents which occurred must be mentioned whereby slight traces of chloride, which had been left behind on the aluminium cladding after the hot water sealing of the finished fuel plates, led to considerable pitting corrosion in the core after the fuel elements in question had been briefly utilized. This brought about an extensive contamination of the primary cooling water by escaping fission products. With respect to time the detection of damage and exact preservation of evidence for the cause of corrosion presented a much greater problem than the elimination of contamination in the primary system.

Another case of contamination, namely with Ag - 110, resulted from the fact that the galvanically applied nickel cladding of approx. 50 μm on the absorber rods previously used in our facility was not completely non-porous. On this occasion only a structural modification to the rods utilizing a solid encasing made from high-grade steel plate could provide the necessary impermeability.

We did not have any other type of corrosion problem in the previous operating years. We can however in general mention that a deterioration in water quality can occur relatively rapidly as a result of the elution of ions which have already been taken up if the ion-exchange resins in the purification system are not renewed in good time. This can indeed lead to increased corrosion rates in the core zone, possibly even to pitting. Therefore the most important task of chemical system monitoring is to register the beginnings of resin depletion in good time and to arrange for appropriate measures to be taken. Nevertheless, it must be emphasized that such processes do not take place at short notice, rather they are indicated as a rule by certain tendencies.

In our case the chemical analytical monitoring comprises one weekly laboratory investigation during which the pH value, conductivity, silica and chloride content, turbidity and γ -activity are determined. The determination of all the ionogenically dissolved impurities and the γ -spectrum is undertaken once during each operating period.

In summing up one can say that with appropriate efforts and the present state of knowledge - there are no basic difficulties in producing good and satisfactory conditions on the primary side of a light water moderated research reactor from a corrosion chemistry point of view and that these conditions can be fulfilled over a long period of time. Individual difficulties which may occur are part of the chemist's bread and butter and must in each case be individually overcome.

Appendix I-4

EXOTHERMIC REACTIONS

Appendix I-4.1

EXOTHERMIC REACTIONS IN U_3O_8 DISPERSION FUEL

ARGONNE NATIONAL LABORATORY

RERTR Program,
Argonne, Illinois

OAK RIDGE NATIONAL LABORATORY

Oak Ridge, Tennessee

United States of America

Abstract

A summary is provided of the experiments conducted since 1963 to study exothermic reactions in the U_3O_8 -Al system.

1. INTRODUCTION

A dispersion of uranium oxide (U_3O_8) in an aluminum matrix has been used as the fuel material for several research and test reactors. Higher uranium loadings in such material can be achieved by increasing the relative amount of the U_3O_8 phase.^[1]

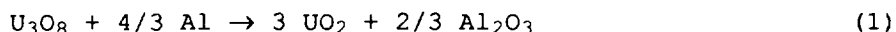
The fact that a U_3O_8 and aluminum mixture is not in chemical equilibrium was recognized very early. The possibility of a chemical reaction between the oxide and the metal phase has been investigated by several independent experimental efforts over two decades. The first experiments at Georgia Tech indicated a potential for a rapid exothermic reaction when a U_3O_8 -Al mixture reached a sufficiently high temperature. Subsequent tests at the Oak Ridge National Laboratory, Argonne National Laboratory, and Savannah River Laboratory yielded much more information and understanding.

This appendix summarizes the experiments conducted since 1963 to study exothermic reactions in the U_3O_8 -Al system.

2. EXPERIMENTAL STUDIES OF EXOTHERMIC REACTION

2.1 Georgia Tech Experiments

The exothermic reactions in the U_3O_8 -Al system have been studied by Fleming and Johnson.^[2,3] As indicated by X-ray diffraction studies, the reactions occur in two stages. The first is the reduction of U_3O_8 to UO_2



which releases 798 kJ/mole of U_3O_8 (based on heats of formation of U_3O_8 , UO_2 , and Al_2O_3 of 3574.8,^[4] 1085.0,^[4] and 1676.8^[5] kJ/mole, respectively).

This reaction was observed in heating experiments within minutes after the specimens reached a temperature of 649°C, slightly less than the aluminum melting temperature of 660°C. The rate of reaction was independent of U_3O_8 content, but increased with decreasing U_3O_8 particle size.

The second stage in the reaction is the further reduction of UO_2 to one or more of the uranium-aluminum intermetallic compounds



This reaction releases 125, 141, or 158 kJ/mole of UO_2 for $x = 2, 3,$ or 4 , respectively (based on heats of formation of UAl_2 , UAl_3 , and UAl_4 of 92.5, 108.4, and 124.7 kJ/mole, respectively)^[6]. Fleming and Johnson's estimate of the maximum credible energy release from both reactions as a function of the U_3O_8/Al composition, is shown in Fig. 1. Their calculation was based on UAl_x thermochemical data from 1958 which yielded significantly larger energy releases for reaction (2), namely, 188, 214, or 252 kJ/mole of UO_2 for $x = 2, 3,$ or 4 , respectively. (Their value for the energy release from reaction (1), 810 kJ/mole of U_3O_8 , agrees reasonably well with current values.)

Reaction (2) first occurs at temperatures ranging from 927°C to 982°C, although a few specimens reacted several seconds after reaching a temperature of only 815°C. As in reaction (1), the reaction rate increased as oxide particle size decreased. Unlike the first reaction, however, the second depends on composition (U_3O_8 loading) not only to determine the product mix, but also the reaction speed. Fleming and Johnson postulated two reasons for this increase in reaction rate with oxide loading. First, the thermal conductivity decreases as the U_3O_8 volume fraction increases. Thus, for higher U_3O_8 loadings, the fuel retains more of the heat generated by reaction (1) for a longer time, and higher temperatures are attained. Secondly, as shown in Fig. 1, there is a rapid increase of energy available for release with U_3O_8 loading. The line gives the energy release, per

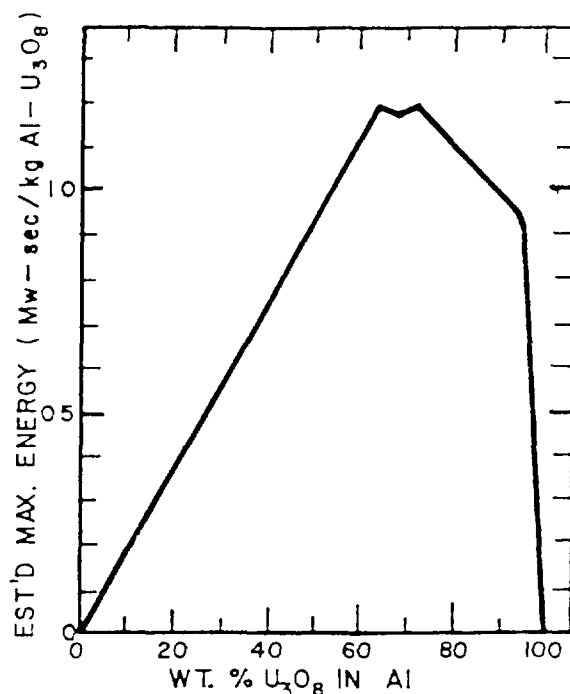


Fig. 1 Energy Available for Release by Complete Thermite Reaction (Reference 7)

Table 1. Effect of U₃O₈ Particle Size on Ignition Temperature

U ₃ O ₈ Particle Size (μm)	Ignition Temperature (°C)	Peak Area (mv-sec)	Peak Height (mv)
>149 (+100 mesh)	1,065	0	0
105-149 (100+140 mesh)	1,050	93	1.48
74-105 (-140+200 mesh)	1,015	130	1.85
53-74 (-200+270 mesh)	995	181	2.96
44-53 (-270+325 mesh)	970	165	2.18
<44 (-325 mesh)	970	118	1.16
Source: Reference 2			

Table 2. Effect of U₃O₈ Content on Ignition Temperature

U ₃ O ₈ Content w/o	Ignition Temperature (°C)	Peak Area (mv-sec)	Peak Height (mv)
85.4	993	184	2.98
79.5	932	319	4.56
74.5	815	401	2.85
Source: Reference 2			

kilogram of fuel material, computed from the previously stated heats of reaction, assuming the reactions proceed to the stoichiometric product mix. Post-experiment analysis found no free uranium metal in the fuel specimens.

Fleming and Johnson utilized the technique of differential thermal analysis^[8] (DTA) to study the effect of U₃O₈ particle size and composition (wt% U₃O₈) on the exothermic reaction. In DTA, reactions in a material during slow heating are indicated by comparing the outputs of thermocouples imbedded in the test specimen and in a nonreacting reference material. Phase transitions and chemical reactions are indicated by variations in the difference of the thermocouple readings. In the U₃O₈ exothermic reaction experiments, a peak in the temperature difference indicated the exothermic reaction.

The DTA results for various U₃O₈ particle sizes showed that ignition temperatures decreased with decreasing particle size in specimens containing 85.4 wt% U₃O₈ (see Table 1). It was postulated that smaller particle sizes resulted in a larger specific surface area and better contact between the U₃O₈ and aluminum phases. This enhances their reactivity as indicated by the decline in ignition temperatures in Table 1. The unexpected decline in DTA peak area and peak height for particle sizes smaller than 53 μm was attributed to poor mixing of fine powders during specimen fabrication, which caused the incomplete reaction.

The effect of fuel composition was also studied. Three samples, with U₃O₈ contents shown in Table 2, were heated and DTA indicated lower ignition temperatures for lower loadings (in the composition range shown).

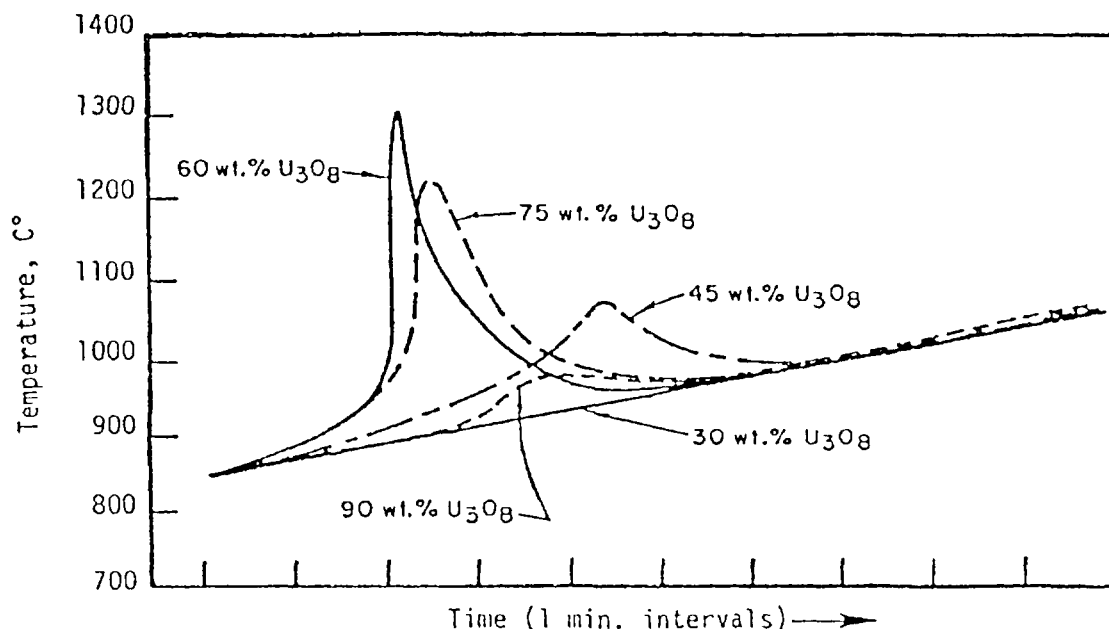


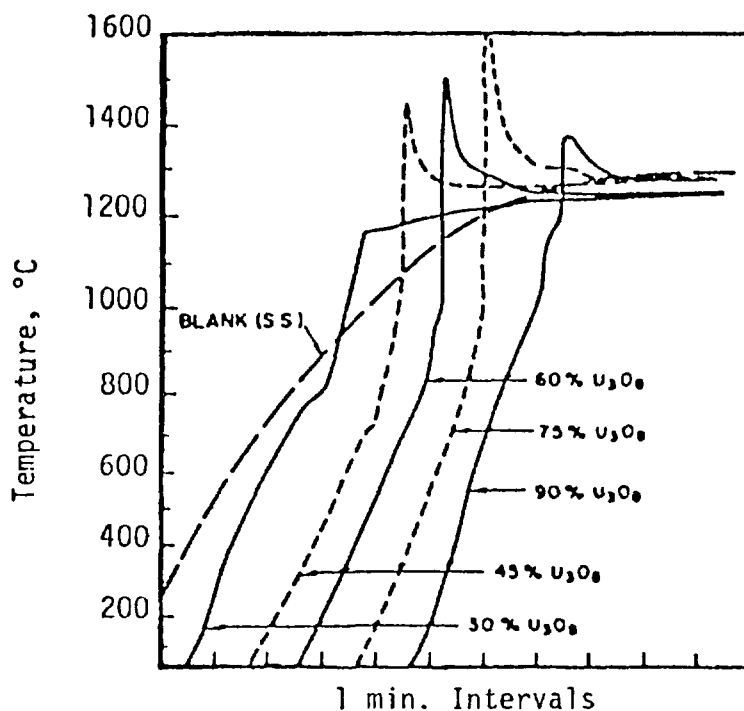
Fig. 2 Temperature of U_3O_8 -Al Specimens Heated at a Rate of 25°/minute (Reference 7)

Smaller U_3O_8 content would allow better contact with the relatively larger aluminum fraction and, like the smaller particle sizes, lower ignition temperatures would result. This reaction would also be facilitated by enhanced mass-action effects. The peak area data were consistent with the specific energy release data of Fig. 1, with peak area increasing with decreased U_3O_8 content, since these high loadings were well beyond the maximum specific energy release at about 60-70 wt% U_3O_8 .

2.2 Experiments at Argonne

Fleming and Johnson also reported^[2] that the reactions in some specimens were violent, with surface temperatures of over 2200°C observed by optical techniques. This prompted studies of a wider composition range in experiments at Argonne National Laboratory (ANL).^[9] Pellets were fabricated by cold-pressing U_3O_8 powder (median particle size of 12 μm) with aluminum powder to obtain specimens with 30, 45, 60, 75, and 90 wt% U_3O_8 . In one series of experiments, specimens of each composition were heated in an induction heater at a rate of 25°C/minute in an argon atmosphere. The specimen temperature, as measured by an imbedded thermocouple during the heating experiments, is shown in Fig. 2. Self-heating is especially apparent for the 60 and 75% wt% U_3O_8 specimens. A maximum temperature of 1300°C, nearly 400°C above the maximum furnace temperature, was observed for the 60 wt% U_3O_8 sample.

In a second series of heating experiments at ANL, the samples were placed in an induction heater which was preset to achieve an equilibrium temperature of 1250°C as rapidly as possible. The graphite container in this heater reached the desired temperature in less than one minute. The sample temperatures during these more rapid heating experiments as shown in Fig. 3. The curves for successively higher U_3O_8 content are displaced by one minute intervals for clarity of presentation; the heating curve for an inert stainless steel sample is shown for comparison. Self-heating is again observed, with maximum temperatures of 1450°C, 1500°C, and 1600°C achieved with 45, 60, and 75 wt% U_3O_8 samples, respectively. The exothermic reaction in the dispersions begins at about the melting point of aluminum (660°C), as shown by the change in slope of the curves in Fig. 3.



(successive curves displaced 1 min. further to the right)

Fig. 3 Temperatures of U_3O_8 -Al Specimens During Rapid Heating Experiments (Reference 9)

Chemical analysis of the specimens after heating indicated that the reaction went to completion, with UAl_3 as the favored reaction product. However, the violent reactions reported by Fleming and Johnson,^[2] with peak temperatures of 2200°C, self-heating rates of several thousand degrees per second, and an ignition temperature of about 1000°C, were not observed in the ANL experiments. A possible explanation, suggested by J. D. Fleming,^[6] was that the powder used by the ANL group (average particle size of 12 μm) was much finer than that used by Fleming and Johnson in their experiments (44 μm). This may allow the reaction to begin slowly at comparatively lower temperatures and leave less energy for rapid liberation at higher temperatures.

These differences in experimental results prompted further study at ANL. A series of experiments was designed to investigate the effects of varying particle size, the possibility of oxygen release during the reaction, and the effect of pre-heating the specimens in nitrogen atmosphere^[10]. Powders with average particle sizes in the range of 74 to 149 μm , 44 to 53 μm , and less than 44 μm were formed with aluminum into samples containing 75 to 85 wt% U_3O_8 . Contrary to Fleming's hypothesis, the coarser powders produced less rapid reactions and lower peak temperatures. In agreement with earlier ANL results, the highest peak temperature of 1700°C was obtained with the smallest particles (44 μm). The possibility that oxygen gas was being evolved, making it unavailable for further reaction, was explored but none was found.

Some explanation of the discrepancies was offered by another series of rapid heating experiments performed at ANL. This time the specimens, containing 85 wt% U_3O_8 with average particle size of 12 μm , underwent various pretreatments. One sample had no pretreatment, the second contained aluminum powder which had been previously heated for 4 hours in air at 600°C, and the third was pressed and then subjected to the same heat treatment (4 hours at 600°C). Upon rapid heating, the third specimen

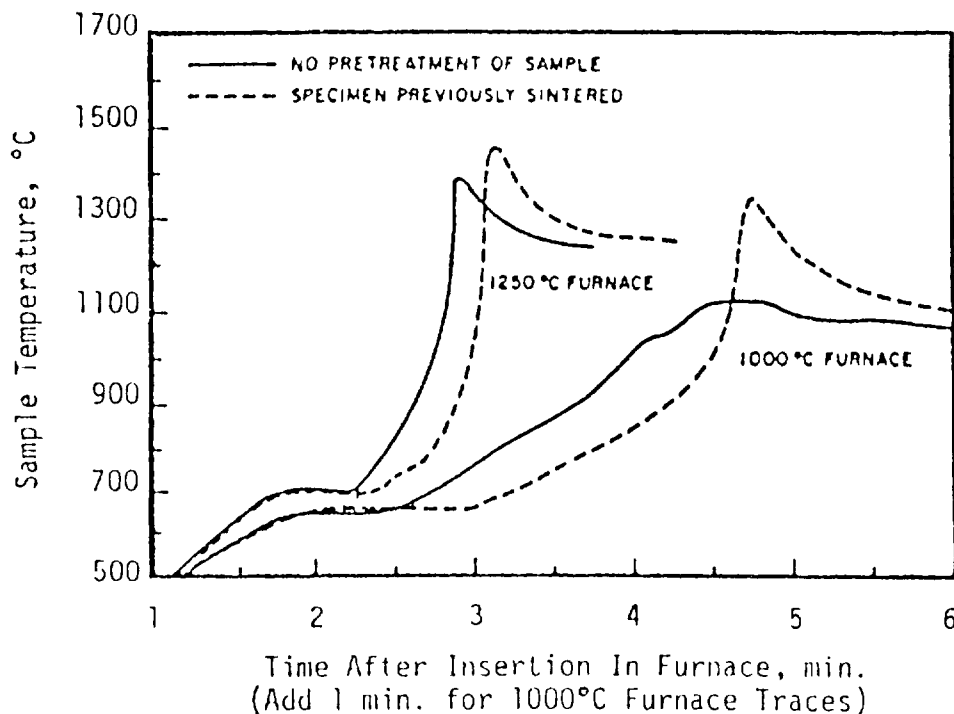


Fig. 4 Temperatures of 40 wt.% U_3O_8 Samples During Heating Experiments (Reference 10)

exhibited a violent reaction with a temperature peak of approximately 2200°C and a heating rate similar to the thousands of degrees per second observed by Fleming and Johnson. A fourth sample, containing only 75 wt% U_3O_8 , but sintered in the same fashion as the third specimen, also exhibited this rapid energy release, with a peak near 1900°C. Thus, the sintering of the sample, or some phenomenon induced by sintering, seems to be the cause, at least in part, of the violent energy release. To check the ramifications of this conclusion on the conventional U_3O_8 dispersion fuels, specimens containing 40 wt% U_3O_8 were fabricated and half were sintered while the remainder were left untreated. Rapid heating experiments indicated an increase in reactivity in the sintered samples, as seen in Fig. 4. Also, the self-heating rates were only 100 to 200°C per second, much lower than those observed by Fleming and Johnson.

2.3 Experiments at Oak Ridge

The potential use of highly loaded U_3O_8 -Al cermet fuel to achieve enrichment reduction, and the theoretical potential for large energy releases from the exothermic reaction in such fuel prompted additional experiments at Oak Ridge National Laboratory.^[11] Differential thermal analysis was employed to determine the temperature of onset, and enthalpy changes during, the exothermic and other reactions. Also, X-ray diffraction was used to determine which reactions were occurring during the heating of U_3O_8 -Al powder, and the mechanical properties of U_3O_8 -Al fuel plates were observed as the plates were heated past the temperatures at which the exothermic reactions occur. Power mixtures and miniature fuel plates of loadings ranging from 50 to 79 wt% U_3O_8 were studied.

The Oak Ridge group reported that differential thermal analysis indicated that the U_3O_8 -Al mixture underwent an exothermic reaction between 600°C and the melting point of aluminum. X-ray diffraction studies of the samples loaded with 50 wt% U_3O_8 showed no reaction products (Al_2O_3),

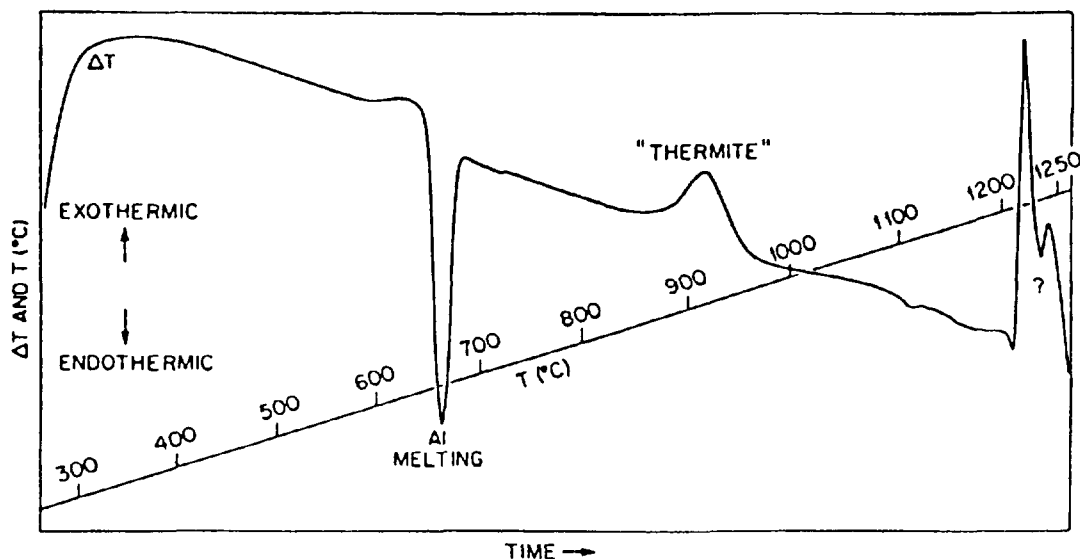


Fig. 5 Differential Thermal Analysis Results for U_3O_8 -Al Sample Loaded at 79 wt.% U_3O_8 (Reference 11)

however, even after heating to 725°C. The diffraction technique was sufficiently sensitive to detect Al_2O_3 if more than 10% of the mixture had reacted, setting an upper limit on the degree of reaction attained up to that temperature.

The melting of aluminum produced an endotherm at an onset temperature of 654°C, while the exothermic reaction caused by an exotherm with an onset temperature near 880°C. Two more exotherms were observed at temperatures greater than 1200°C. These features can be seen in Fig. 5, which presents the results for a cold-pressed mixture containing 79 wt% U_3O_8 . The areas under the peaks can be analyzed to provide the enthalpy changes of the reactions. This procedure is validated by the aluminum endotherm calculations, which yield results very close to the heat of melting, as shown in Table 3. The same procedure yields exothermic reaction heats for the exotherm near 900°C of 445 ± 232 kJ/mole of U_3O_8 for fuel plate samples containing ~46 wt% U_3O_8 and 171 ± 43 kJ/mole of U_3O_8 for fuel plate samples containing ~35 wt% U_3O_8 . No calibration was available for the higher-temperature exotherms. The Oak Ridge group speculated that this failure to even approach completion of the exothermic reaction may be due to (1) reaction rate being inversely proportional to U_3O_8 particle size; (2) Fleming and Johnson have overestimated the heats of reaction; (3) part of the exothermic reaction energy being released at higher temperature exotherms around 1200°C; or (4) the reaction being diffusion controlled. The last possibility results from the likely reaction sequence of aluminum atoms diffusing through an Al_2O_3 crust before reaching and reacting with the core material of a particle of U_3O_8 .

Since the heat evolved by the exothermic reaction was shown to be relatively small, its effect should be negligible compared to: (1) the sensible heat required to reach the aluminum melting point from operating temperatures; (2) the aluminum heat of melting; and (3) the sensible heat required to attain the exothermic reaction threshold at about 880°C. However, if another energy source, like decay heat, could bring the fuel temperature to the exothermic reaction threshold, reaction energy sufficient to heat the material to the second reaction stage at about 1200°C may be liberated. This hypothesis was tested by heating miniature

Table 3. Thermite Energy Release Data Derived from Differential Thermal Analysis Results for 79 wt% U₃O₈ (Reference 8)

Run Number	Aluminum Melting Onset Temperature (°C)	Calculated ΔH^a (J/g)	Thermite Reaction Heat (J/g)	
			Calculated	From Fleming and Johnson ^b
1	654	394	79.1	1090
2	654	390	76.1	1090
15	654	357	55.6	1090
17	654	403	85.4	1090

^aCompare to 397 J/g literature value.
^bJ.D. Fleming and J.W. Johnson, "Exothermic Reactions in Al-U₃O₈ Composites," pp. 649-66 in *Research Reactor Fuel Element Conference*, TID-7642, Book 2, (1962).

fuel plates in air in an electrical resistance furnace. The investigators observed that:

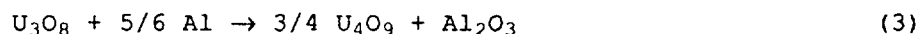
- 1) The aluminum cladding melted and flowed away from the fuel meat after reaching 640°C.
- 2) The fuel meat, under heating to 1400°C, remained solid but warped under its own weight.
- 3) There were no violent thermal effects, explosions, or gas releases.

The Oak Ridge group concluded that the use of higher U₃O₈ loading fuel meat to permit conversion from HEU to LEU does not present additional safety concerns due to the potential for exothermic reactions. Their results extend to higher loadings (up to 79 wt% U₃O₈) the observation that the diffusion-controlled exothermic reaction is too slow to contribute significantly to the severity of a fuel melting accident, even if the exothermic threshold near 900°C is reached.

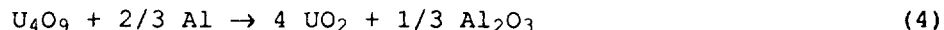
2.4 Experiments at Savannah River

A series of experiments performed at the Savannah River Laboratory^[12, 13] using both cold-pressed pellets and pieces of clad fuel tubes have yielded results very similar to those of the experiments at Argonne and Oak Ridge. The energy released from the exothermic reaction when a cold-pressed pellet containing 53 wt% of fine (<44 μm) U₃O₈ particles was plunged into a 1000°C preheated furnace was estimated from the time-temperature graph to be ~230 kJ/mole of U₃O₈. This is less than 20% of the total energy available according to reactions (1) and (2). As in the Oak Ridge work, the exothermic reaction in fuel tubes was found to be less than in cold-pressed powder mixtures. In addition, two experiments related to the self-propagation of the exothermic reaction were performed. No evidence of a self-propagating reaction was found when a fuel tube was heated with an acetylene torch or when a fuel tube was lowered into 1000°C aluminum.

An important discovery made at Savannah River provides at least a partial explanation of why the exothermic reaction in fabricated fuel plates is less energetic than in cold-pressed powder mixtures. They found that, during processing, a solid-state reaction converts U_3O_8 to U_4O_9 :



Approximately 50% of the U_3O_8 was converted to U_4O_9 during fuel tube fabrication. U_4O_9 also reacts with Al to form UO_2 and Al_2O_3 , as follows:



but the reaction only releases ~387 kJ/mole of U_4O_9 . Therefore, the exothermic reaction (4) of the U_4O_9 produced from one mole of U_3O_8 releases only 290 kJ of energy compared to the 798 kJ produced had it reacted directly.

3. IMPLICATIONS FOR ADVANCED FUELS

Consideration of the exothermic reaction between U_3O_8 and aluminum indicate the following:

- 1) The reactor occurs in two stages: the reduction by aluminum of U_3O_8 to UO_2 , followed by reaction of UO_2 with aluminum to produce intermetallic compounds of the form UAl_x . The first reaction proceeds slowly at temperatures around the melting of aluminum, but both reactions may occur rapidly once the fuel temperature rises above 850°C.
2. If the U_3O_8 -aluminum mixture is heated at temperatures and for times typical of fabrication of fuel plates, approximately 50% of the U_3O_8 is converted to U_4O_9 . The exothermic reaction of U_4O_9 also occurs in two stages, but releases significantly less energy than the direct exothermic reaction of U_3O_8 and aluminum.
3. Thermodynamically, the maximum energy available from the exothermic reaction of U_3O_8 and aluminum is 1271 kJ/mole of U_3O_8 (~81% of the value estimated by Fleming and Johnson using the data available at that time). The corresponding value of the maximum energy available from the exothermic reaction of U_4O_9 and aluminum is 1017 kJ/mole of U_4O_9 . Since one mole of U_3O_8 produces only 3/4 of a mole of U_4O_9 , the U_4O_9 -aluminum reaction releases an equivalent of 763 kJ/mole of original U_3O_8 .
4. The reaction is diffusion-controlled and therefore cannot add significant, rapidly liberated thermal energy during a high temperature transient.
5. The exothermic reaction is not a barrier to utilization of highly loaded U_3O_8 -Al dispersion fuel to reduce the uranium enrichment in research and test reactors.

REFERENCES

1. D. Stahl, "The Status and Development Potential of Plate-Type Fuels for Research and Test Reactors," ANL-79-11 (March 1979).
2. J. D. Fleming and J. W. Johnson, "Aluminum- U_3O_8 Exothermic Reactions," Nucleonics 21 (5), 84-87 (May 1963).

3. J. D. Fleming and J. W. Johnson, "Reactions in Al/U₃O₈ Dispersions," Trans. of the Amer. Nuc. Society 6, 158-159 (1963).
4. E. H. P. Cordfronke and R. J. M. Konings, eds., Thermochemical Data for Reactor Materials and Fission Products, North Holland Publishing Company, Amsterdam (1990).
5. G. V. Samsonov, ed., The Oxide Handbook 2nd Ed., Trans by R. K. Johnston, IFI/Plenum, New York, pp. 20-31 (1982).
6. P. Chiotti and J. A. Kateley, "Thermodynamic Properties of Uranium-Aluminum Alloys," J. Nucl. Mat. 32, pp. 135-145 (1969).
7. L. Baker and R. Liimatainen, "Chemical Reactions," Chapter 17 in T. J. Thompson and J. G. Beckerley, eds., The Technology of Nuclear Reactor Safety, Vol. 2, 495-497, The M.I.T. Press (1973).
8. C. B. Murphy and J. A. Hill, "Detection of Irradiation Effects by Differential Thermal Analysis," Nucleonics 18 (2), 78-80 (February 1960).
9. L. Baker, et al., "Aluminum-U₃O₈ Thermite Reaction," in ANL/CEN Semiannual Report for July/December 1963, ANL-6800, 390-402 (1964).
10. L. Baker, and J. D. Bingle, "Aluminum-U₃O₈ Thermite Reaction," in ANL/CEN Semiannual Report for January/June 1964, ANL-6900, 298-303 (1964).
11. A. E. Pasto, et al., A Quantitative Differential Thermal Analysis Study of U₃O₈-Al Thermite Reaction, ORNL-5659 (June 1980).
12. H. B. Peacock, "Study of the U₃O₈-Al Thermite Reaction and Strength of Reactor Fuel Tubes," Proc. of the International Meeting on Reduced Enrichment for Research and Test Reactors, October 24-27, 1983, Tokai, Japan, Japan Atomic Energy Research Institute Report, JAERI-M 84-073 (May 1984).
13. H.B. Peacock, "Properties of U₃O₈-Aluminum Cermet Fuel," Westinghouse Savannah River Laboratory Report WSRC-RP-89-981, Rev. 1, pp. 32-45 (March 1990).

Appendix I-4.2

A DIFFERENTIAL THERMAL ANALYSIS STUDY OF U₃Si-Al AND U₃Si₂-Al REACTIONS

R.F. DOMAGALA, T.C. WIENCEK, J.L. SNELGROVE,
M.I. HOMA, R.R. HEINRICH
RERTR Program,
Argonne National Laboratory,
Argonne, Illinois,
United States of America

Abstract

As part of the Reduced Enrichment Research and Test Reactor (RERTR) Program, high density uranium compounds are being evaluated as possible replacements for the fuels currently in use. U₃Si and U₃Si₂ powders dispersed in an Al matrix and roll bonded within 6061 Al alloy clad have performed well under irradiation in the ORR. A consideration of the heats of reaction between the silicides and the Al components of a reactor fuel plate has now been addressed.

By following standard quantitative differential thermal analysis (DTA) procedures, it has been demonstrated that neither silicide shows any measurable heat of reaction until the solidus temperature of 6061 (582°C) is exceeded. On heating, the exothermic reaction is quenched by the endothermic change of state as the Al species melt. All detectable events take place in the temperature regime from ~580 to ~660°C.

The heats of reaction per gram of fuel ranged from 304 ± 18 J for samples with 32 vol.% U₃Si₂ in the fuel zone to 486 ± 54 J for samples containing 45 vol.% U₃Si in the fuel zone.

I. INTRODUCTION

The Argonne National Laboratory (ANL) is managing the U.S. Reduced Enrichment Research and Test Reactor (RERTR) program to develop proliferation-resistant fuels. The main thrust of this effort is directed toward a reduction of ²³⁵U enrichment of the uranium employed in the fuel alloys from >90% (currently employed) to <20% (typically 19.7 ± 0.2%). As a consequence of this enrichment reduction, an increase in the total amount of uranium contained in a fuel element is required. However, at the lower enrichment, the total U required in an element for the most advanced reactors exceeds the amount that can be fabricated with present fuels and manufacturing techniques. For plate-type elements, the present fuels include powders of U₃O₈ or "UAl" (a U-Al alloy at about the composition of UAl₃, i.e., ~70 wt.% U) dispersed in a matrix of commercially pure Al powder and roll bonded within a cladding of 6061 aluminum alloy. The plates so generated, which might typically be ~3 in. (~76 mm) wide by ~26 in. (~660 mm) long and 0.050 to 0.060 in. (1.27 to 1.52 mm) thick, are assembled into a fuel element for insertion into the reactor core.

In order to meet the requirements of the most demanding reactors, a fuel alloy development effort was, and still is, an important aspect of the RERTR Program. The work in the Materials Science and Technology Division of ANL has focused on uranium silicides, U_3Si , U_3Si_2 , and " U_3SiAl " (a ternary alloy of $U + 3.5 \text{ wt.}\% \text{ Si} + 1.5 \text{ wt.}\% \text{ Al}$).³ The silicides have high densities and high uranium contents and are quite corrosion resistant in hot water -- the normal coolant for these reactors.

A description of the fuel alloy development work with silicide powders and "miniplates" is detailed in Ref. 1; comparable information on work with low-enrichment U_3O_8 may be found in Ref. 2. As a result of irradiation experience with fuel plates containing uranium silicides, the fuel alloys U_3Si and U_3Si_2 have emerged as contenders for satisfying the goals of the program; U_3SiAl has been abandoned as a fuel alloy powder for plate-type elements.

Once the silicides were determined to have a significant potential for commercial use, considerations beyond those of fabricability and stability in a normal irradiation environment had to be addressed. One such concern is the stability of the silicide-plus-aluminum mixture under off-normal conditions where the fuel element might be heated up to and beyond the melting point of Al. That is, what reactions might occur and what heat evolution might be expected to accompany such reactions? One report suggests that uranium silicides react rapidly with Al at $\sim 620^\circ\text{C}$.³

The purpose of this study, then, was to determine by differential thermal analysis (DTA) techniques the temperature regime and enthalpies associated with reactions that occur between the silicide fuel particles and the aluminum matrix as well as the 6061 clad at elevated temperatures. A similar study has already been conducted for U_3O_8 -type fuel plates.⁴

II. REACTIONS

In Al plus U_3Si or U_3Si_2 dispersion fuels (in the absence of oxygen), three possible reaction products are UAl_2 , UAl_3 , and UAl_4 . At least three concurrent possibilities may be examined. First, the formation of free Si can be postulated, although it has never been observed to form. Second, the Si may form USi_3 . Third, the Si may substitute in the lattice of UAl_3 to form $U(Al,Si)_3$.⁵ The third possibility is the one that has been documented in phase equilibria studies by A. E. Dwight.

For a reaction between one mole of U_3Si and a stoichiometric amount of Al, at least six equations can be written and balanced for a complete reaction. These are recorded in Table I. In Eqs. (4) through (6) the formation of USi_3 in combination with UAl_2 , UAl_3 , or UAl_4 is shown. This is a bookkeeping simplification since, as noted above, it has been demonstrated that USi_3 as a discrete phase is not formed, but $U(Al,Si)_3$ is the product.

Table II summarizes a similar set of six equations for possible reactions between U_3Si_2 and Al. Completely analogous to the discussion of $U_3Si + Al$ reactions, the most predictable event is the formation of UAl_3 which dissolves Si to form $U(Al,Si)_3$, i.e., reaction (11).

All reactions are diffusion controlled, and in each case the reaction products are less dense than the reacting phases. This inevitably leads to a growth of the fuel zone volume and, consequently, the fuel plate.

Table I. Possible U_3Si + Aluminum Reactions

$U_3Si + 6 Al$	\rightarrow	$3 UAl_2 + Si$	(1)
$U_3Si + 9 Al$	\rightarrow	$3 UAl_3 + Si$	(2)
$U_3Si + 12 Al$	\rightarrow	$3 UAl_4 + Si$	(3)
$U_3Si + \frac{16}{3} Al$	\rightarrow	$\frac{8}{3} UAl_2 + \frac{1}{3} USi_3$	(4)
$U_3Si + 8 Al$	\rightarrow	$\frac{8}{3} UAl_3 + \frac{1}{3} USi_3$	(5)
$U_3Si + \frac{32}{3} Al$	\rightarrow	$\frac{8}{3} UAl_4 + \frac{1}{3} USi_3$	(6)

Table II. Possible U_3Si_2 + Aluminum Reactions

$U_3Si_2 + 6 Al$	\rightarrow	$3 UAl_2 + 2 Si$	(7)
$U_3Si_2 + 9 Al$	\rightarrow	$3 UAl_3 + 2 Si$	(8)
$U_3Si_2 + 12 Al$	\rightarrow	$3 UAl_4 + 2 Si$	(9)
$U_3Si_2 + \frac{14}{3} Al$	\rightarrow	$\frac{7}{3} UAl_2 + \frac{2}{3} USi_3$	(10)
$U_3Si_2 + 7 Al$	\rightarrow	$\frac{7}{3} UAl_3 + \frac{2}{3} USi_3$	(11)
$U_3Si_2 + \frac{28}{3} Al$	\rightarrow	$\frac{7}{3} UAl_4 + \frac{2}{3} USi_3$	(12)

III. SAMPLE PREPARATION

The materials used to produce the samples for this study included Alcan MD101, a nominally -325 mesh commercially pure Al powder, and -100 mesh U_3Si (U + 4 wt.% Si) and U_3Si_2 (U + 7.5 wt.% Si) powders. The silicide powders were produced at ANL using high purity depleted uranium following procedures described in Ref. 1.

The powders were combined in accordance with the matrix shown in Table III. Silicide fuel was 15% -325 mesh (<45 μm , "fines") and 85% -100 + 325 mesh (<150 μm and >45 μm).

Individual charges were weighed into screw-top glass vials, sealed, and mixed in a V-blender for a minimum of 3 h. After mixing, the charges were compacted with pressures ranging from 9 to 31 tons per in.² (~12 to ~44 kg/mm²) in a cylindrical die [0.75 in. (19.0 mm) diameter]. The compacts were ~0.133 in. (~3.38 mm) high x 0.753 in. (19.0 mm) diameter with ~14 vol.% porosity. After compacting, the samples were placed into holes

Table III. Test Matrix for Differential Thermal Analysis (DTA) Specimens

Identification Code	Matrix	Fuel	Vol.% Fuel in Fuel Zone	Total U in Fuel Zone, g-cm ³
CS-6061-16 thru 24	None	None	0	0
CS-MD101-29 thru 32	MD101	None	0	0
CS-B-89 thru 94	MD101	U ₃ Si	32	4.7
CS-B-95 thru 100	MD101	U ₃ Si	45	6.6
CS-X-105 thru 110	MD101	U ₃ Si ₂	32	3.6
CS-X-113 thru 118	MD101	U ₃ Si ₂	45	5.1

drilled in a 6061 Al frame [6 x 8 in. (152 x 203 mm)] and covered top and bottom with 6061 Al cover plates. All 6061 hardware was chemically cleaned just prior to assembly to remove the oxide film. The assembly was then peripherally welded (leaving some gaps for air to escape) and roll-bonded by hot rolling, 20-25% reduction per pass, for seven passes. The hot rolling was followed by a one-hour blister test anneal at 485°C. Finally, the assemblies were cold rolled ~19% to 0.060 in. (1.52 mm). Hardware at various steps in the fabrication procedure is shown in Fig. 1.

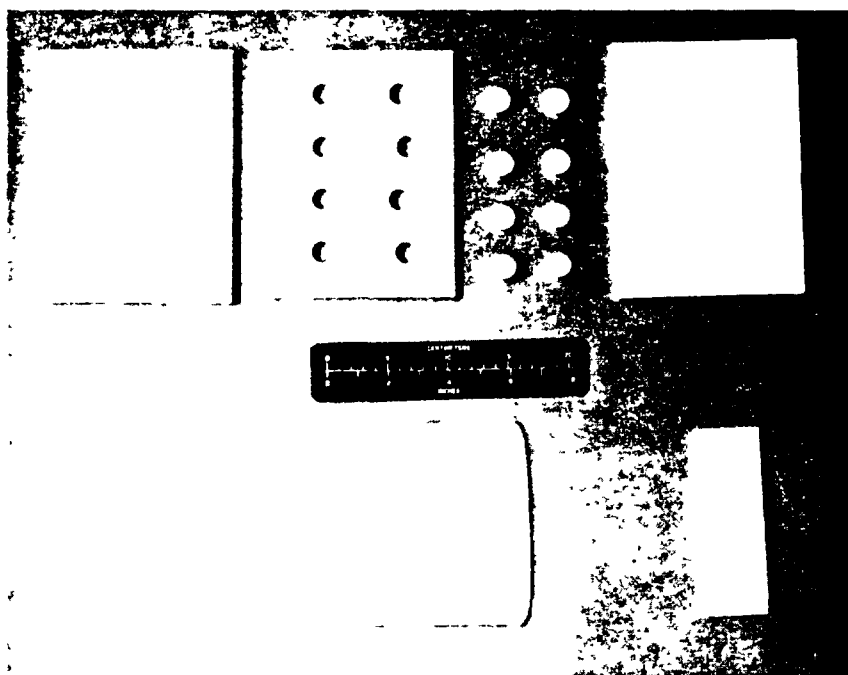


Fig. 1. Compatibility Study Components before Assembly (Top), after Rolling and Partial Shearing (Lower, Left), and Finished Plate (Bottom, Right).

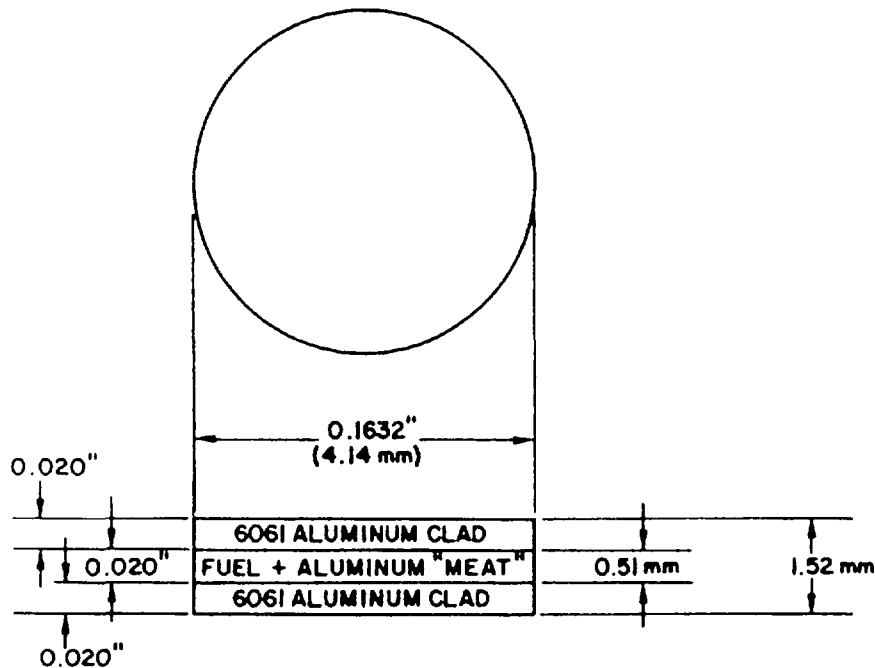


Fig. 2. Geometry of Samples Used for DTA Study.
Dimensions are Nominal.

The finished plates have an elliptical fuel zone [$\sim 0.75 \times 4.8$ in. ($\sim 19 \times 122$ mm)]; the overall dimensions are $\sim 2 \times 6$ in. ($\sim 51 \times 152$ mm).

Fuel zone volumes, silicide concentration values, and porosities of the fuel zones were calculated from the known quantities, chemistries, and densities of the components, and immersion densities measured in distilled water for several plates in each category. Radiographic films of the silicide plates were made to determine fuel location and homogeneity. Samples were manually punched out of uniform areas using a commercially available punch; the resulting sample geometry is illustrated in Fig. 2. As reference standards, similar discs were produced from plates which contained no "fuel." That is, samples were taken from plates wherein the fuel zone was 100% MD101 Al and from plates that were solid 6061 Al or pure Al. All samples, with or without fuel, were 0.060 in. (1.52 mm) thick.

IV. EQUIPMENT AND CALIBRATION

The system employed for this study was a Rigaku TG 2000 - a unit capable of being heated to 1500°C . Sample and reference pans were aluminum oxide and the atmosphere was high purity helium obtained by passing 99.999% pure helium through a six-foot (~ 2 meters) length of $3/16$ in. (4.8 mm) copper tubing filled with 60/80 mesh chromatographic grade molecular sieve material. The copper tubing was coiled and immersed in liquid nitrogen.

The thermo-gravimetric analysis (TGA) section of the system, which was not used for this study, was joined to the DTA portion and terminated in a $3/4$ in. (14.0 mm) "T" at the back of the unit. One leg of the "T" was connected to a 1405 Sargent-Welch mechanical vacuum pump while the other leg went to a flow meter that could be isolated from the vacuum by a three-port stopcock. The system is illustrated schematically in Figs. 3 and 4.

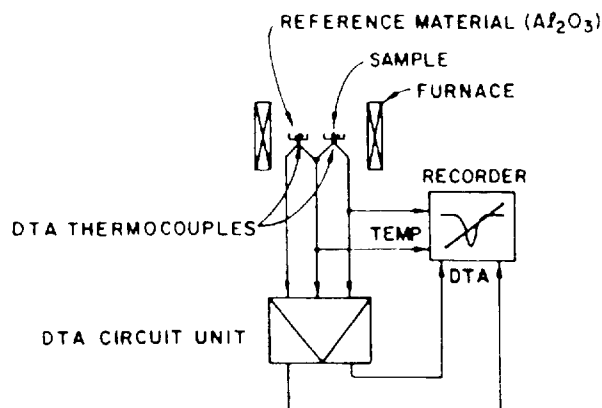


Fig. 3. Schematic Representation of DTA Unit.

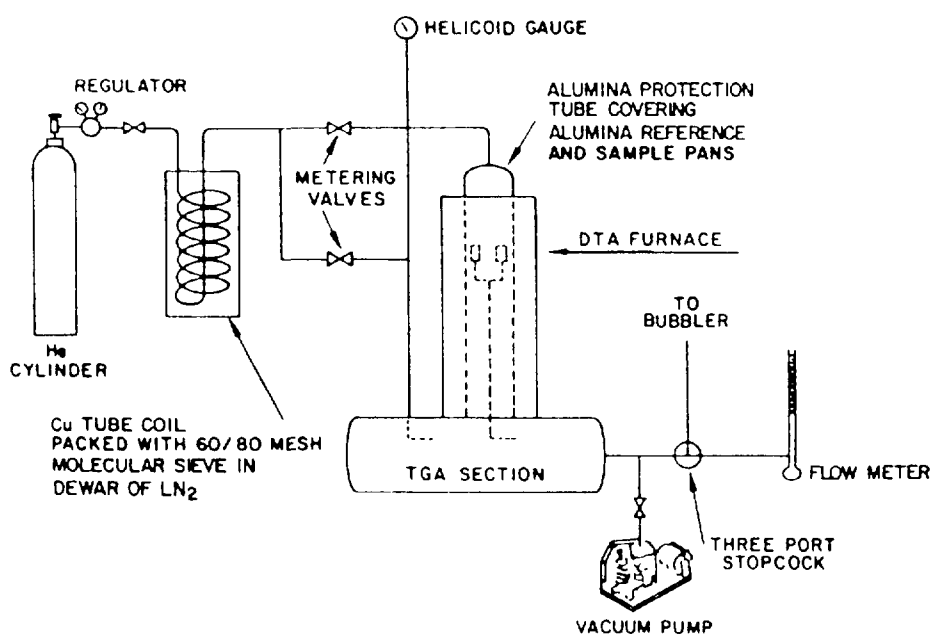


Fig. 4. Detailed Schematic of DTA Apparatus.

Helium flow was split, each half controlled by a Nupro metering valve and measured by the flow meter. One half of the helium (total flow rate 100 cm³/min) was directed down through the alumina protection tube which enclosed the sample and reference pans while the other half purged the TGA section. Prior to initiating helium flow, the entire system, including the 1/8 in. (3.2 mm) copper line leading to the main valve on the helium cylinder, was evacuated to approximately "0" torr (as read on a 0-1500 torr Helicoid absolute pressure gage). The vacuum pump was then isolated and the helium flow initiated. When the absolute pressure reached approximately 800 torr, the packless valve on the delivery side of the regulator (Matheson 3104-580) was closed and the vacuum pumping reinitiated. Three evacuation and purge cycles preceded each DTA run.

Once every seven to ten days the molecular sieve trap was regenerated. This regeneration consisted of heating the copper coil in place in an

electrical resistance furnace to 200°C while purging with helium. The duration of heating was at least overnight (16 h) and occasionally over the weekend (64 h).

Techniques and procedures described in Ref. 4 were used as guides for calibration in this work; all heating and cooling were controlled at the rate of 10°C per minute. Initially an instrument factor vs. temperature curve was generated using zinc, aluminum, silver, gold, copper, uranium, and gadolinium. During these calibrations it was found that copper wetted the alumina pan and gadolinium reacted with the alumina. Therefore, the Cu and Gd points were not used. The results of the calibration are shown in Table IV.

The instrument factor (I.F.) is defined in the following way:

$$I.F. = \frac{(\Delta H_f)(\text{Mass of Sample})(\text{Chart Speed})}{(\text{Instrumentation Amplification Setting})(\text{Endotherm Area})}$$

Heat of Fusion (ΔH_f) in joules per gram.

Mass of sample in grams.

Chart Speed in centimeters per minute.

Instrument Amplification Setting in microvolts (usually 25 or 50).

Endotherm area (on melting) in square centimeters (measured by cut-and-weigh and/or calibrated planimeter).

When making calibration runs, the specimen was cycled through at least two melts and two freezes to approximately 150°C above and below the melting (freezing) point. The five point calibration plot was tested with a high-purity antimony sample. Because of its relatively high vapor pressure, antimony was melted only once and then heated to ~675°C. The experimentally determined heat of fusion for Sb was 158 J/g, which compares very well with a literature value of 163 J/g.

After observing that the reaction temperature range for fuel plate pellets was always in the 600-700°C range for all of the different types of specimens, internal standards of Sb and Al were run frequently during this study to ensure that minor instrument calibration deviations were being properly monitored and used in the calculations.

V. RESULTS AND DISCUSSION

Having established an instrument factor-vs.-temperature relationship, the heats of fusion (ΔH_f) were determined for samples taken from a piece of "pure" 6061 as well as from a plate that only had MD101 Al as the "meat." Following procedures described for the instrument calibration, the data summarized in Table V were generated. The onset of melting and peak temperatures recorded for these runs compare with literature values of 582°C for the solidus temperature and 652°C for the liquidus temperature of 6061; the melting point of pure Al is 660°C.

Table IV. Calibration Results

Metal	Mass, mg	Accepted ΔH_f , J/g	Measured ΔH_f , J/g	Onset of Melting, °C	Peak Temp., °C	Accepted Melting Point, °C	Instrument Factor	
							Calculated	Regression Best Fit ^a
Zn	51.0	112.0 ^{b,c}	-	429 429	435 435	419.6	0.02636 0.02720	0.02677
Al	49.5	397.0 ^c	-	e 666	e 675	660.4	0.02636 0.02576	0.02618
Ag	51.0	104.7 ^b	-	963 963	975 972	961.9	0.02808 0.02766	0.02732
Au	49.6	63.7 ^b	-	1068 1068	1080 1077	1064.4	0.03113 0.03265	0.03281
U	49.0	38.4 ^d	-	1134	1140	1133	0.03852	0.03806
Sb	51.3	163.2 ^b	158.1	633	639	630.8	0.0266	

^aStatistically derived from the calculated instrument factors and used as the IF for calculating ΔH values for test samples.

^bSupplement to Selected Values of Thermodynamic Properties of Metals and Alloys, Hultgren, Orr, and Kelley, Univ. of California, Berkeley, CA, Nov. 1970.

^cJANAF Thermochemical Tables. Dow Chemical Co., Midland, MI. Al - June 30, 1979, Zn - Dec. 31, 1978.

^dThe Chemical Thermodynamics of Actinide Elements and Components, Part 1, The Actinide Elements, Oetting, Rand, Ackerman, International Atomic Energy Agency, Vienna, 1976.

^eMechanical failure of temperature plot but not of differential temperature plot.

Table V. Summary of Data from Plate Samples with No Silicide Fuel^a

Sample Type	No. of Runs	ΔH_f , J/g	Onset of Melting, °C	Peak Temperature, °C
6061	4	349 ± 23	633 ± 2	657 ± 2
6061 + MD101 Meat	2	372 ± 3	642 ± 3	660 ± 0

^aAll data determined from heating thermograms.

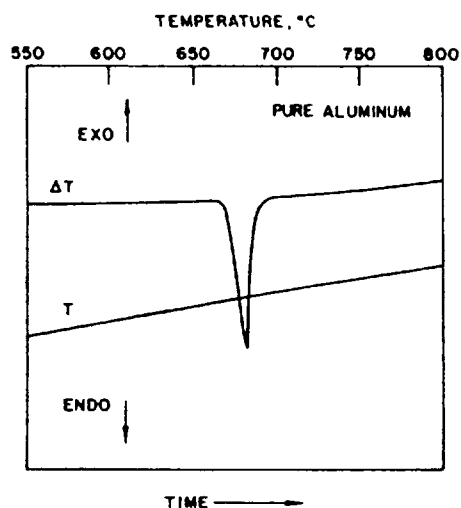


Fig. 5. Thermogram for Pure Aluminum.

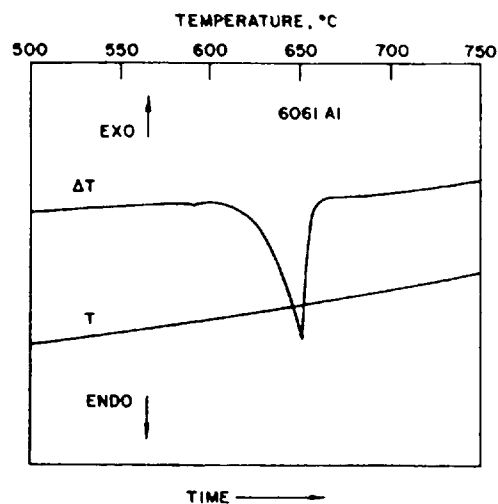


Fig. 6. Thermogram for 6061 Al.

Illustrative thermograms for pure Al and 6061 are shown in Figs. 5 and 6; a similar plot for a MD101 Al meat disc is shown in Fig. 7.

Three discs produced from each of four compatibility study plates were run next. The first heating cycle was initiated at room temperature and carried to $\sim 850^\circ\text{C}$. The sample was then cooled at the rate of 10°C per minute to $\sim 400^\circ\text{C}$, and a second heating cycle to 850°C followed. After a second cool to $\sim 400^\circ\text{C}$, a third and final heating cycle to 850°C was conducted. For one sample of each fuel and volume percent, heating was allowed to proceed to $\sim 1300^\circ\text{C}$, at which point the study of that particular material was considered complete and the sample was cooled to room temperature.

Typical curves for the first and second heating cycles of a 32-vol.% U_3Si disc and a 45-vol.% U_3Si_2 disc are shown in Figs. 8 through 11. What was uniformly clear in all thermograms is that with two exceptions no distinguishable event was ever observed at a temperature below the solidus temperature of 6061 (582°C) and that the reaction between the silicide and the aluminum (MD101 + 6061) proceeded at a detectable rate only after liquid had formed in the sample. No event (exothermic or endothermic) was ever detected above $\sim 660^\circ\text{C}$.

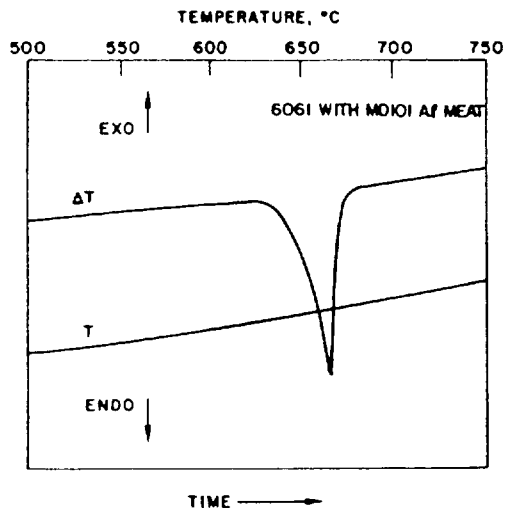


Fig. 7. Thermogram for MD101 Meat Sample.

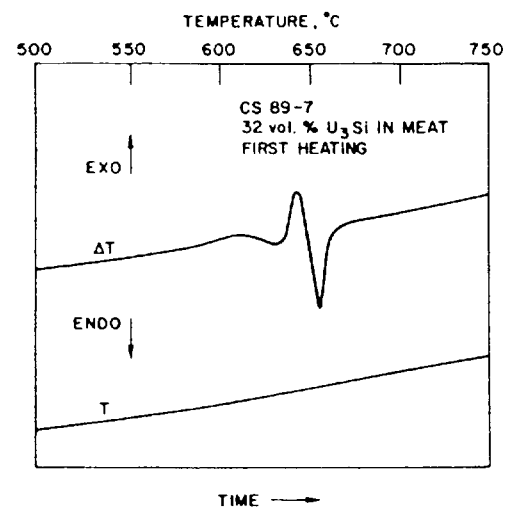


Fig. 8. Thermogram for 32-vol.% U_3Si in Meat Sample.

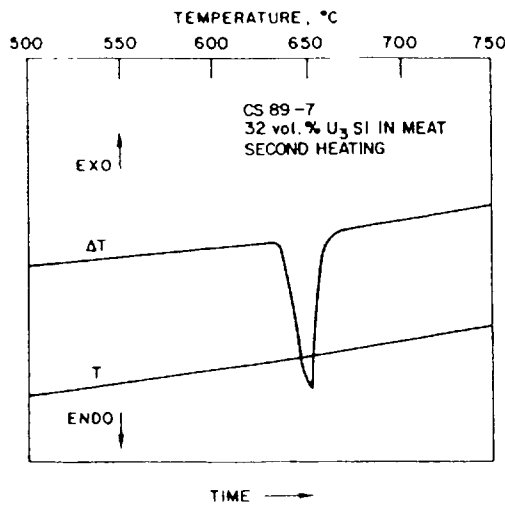


Fig. 9. Thermogram for Second Heating of the Same Specimen as Shown in Fig. 8.

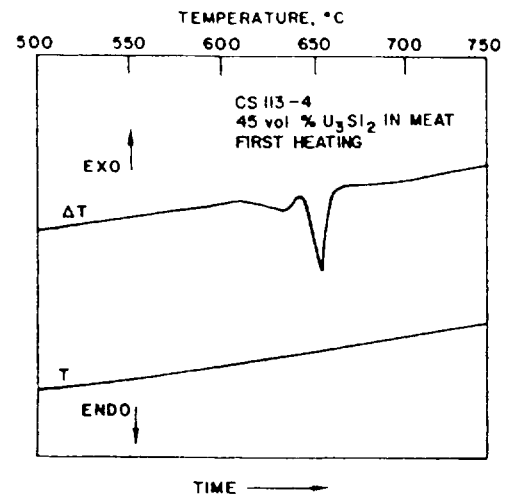


Fig. 10. Thermogram for 45-vol.% U_3Si_2 in Meat Sample.

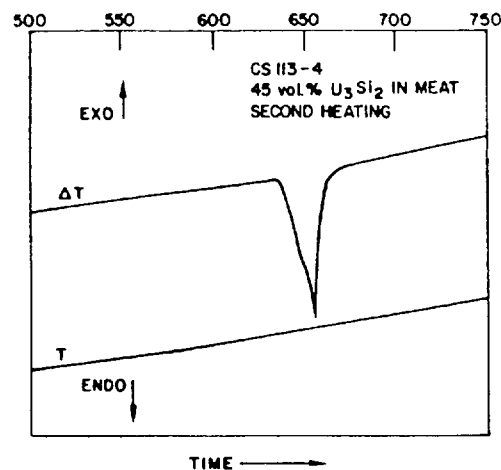


Fig. 11. Thermogram for Second Heating of the Same Specimen as Shown in Fig. 10.

There must have been some solid state reaction between the particles and the aluminum. The degree of reaction and amount of heat liberated during this solid state reaction, however, was too small to be detected by the DTA apparatus. The total heating time for a sample taken from room temperature to 600°C was only one hour, and it has been demonstrated in other studies that no metallographically detectable reaction zone has been observed in specimens heated for this length of time in the solid state.

The data for the twelve fuel alloy discs are summarized in Tables VI and VII. Unfolding the exothermic heat of reaction of the silicide from the endothermic heat of fusion of the aluminum was done in the following manner:

1. Each sample was assumed to be exactly of the geometry shown in Fig. 2. Numerous measurements supported this. Each disc was assumed to contain in its "meat" the volume percents of fuel, MD101, and voids shown in Table VI. These numbers were derived from the known quantities of material used and immersion density measurements made on plates in each category.

2. Each pellet was weighed to the nearest 0.1 mg. The volume of the meat in each pellet was calculated as follows:

$$M_s = V_m \rho_m + V_c \rho_c \quad (13)$$

$$V_s = V_m + V_c \quad (14)$$

$$\text{Substituting for } V_c, \quad M_s = V_m \rho_m + (V_s - V_m) \rho_c \quad (15)$$

$$\text{Rearranging Eq. (15), } V_m \rho_m - V_m \rho_c = M_s - V_s \rho_c \quad (16)$$

$$\text{Simplifying Eq. (16), } V_m (\rho_m - \rho_c) = M_s - V_s \rho_c \quad (17)$$

$$\text{Solving for } V_m, \quad V_m = \frac{M_s - V_s \rho_c}{\rho_m - \rho_c} \quad (18)$$

In Eqs. (13) through (18), the following apply:

M_s = Mass of sample in grams,

V_s = Volume of sample in cubic centimeters ($= 0.020568 \text{ cm}^3$),

V_m = Volume of meat in sample in cubic centimeters,

V_c = Volume of clad in sample in cubic centimeters,

ρ_c = Density of 6061 clad ($= 2.71 \text{ g/cm}^3$), and

ρ_m = Density of meat in sample in grams per cubic centimeter.

Table VI. Data on Fuel Containing Samples for DTA Study

Sample No.	Type of Fuel	Vol.% Fuel in Meat ^a	Vol.% Voids in Meat	Vol.% MD101 in Meat	Mass of Sample, mg	Mass of Fuel, mg	Mass of MD101, mg	Mass of 6061 Clad, mg	Calculated ΔH_f for MD101 + 6061, J
CS105-4	U_3Si_2	32.0 (3.6 gU/cm ³)	6.0	62.0	73.5	24.16	10.36	38.98	17.72
-5					72.6	22.94	9.84	39.83	17.81
-8					74.0	24.84	10.65	38.51	17.67
CS113-1	U_3Si_2	45.0 (5.1 gU/cm ³)	12.4	42.6	82.1	36.83	7.72	37.56	16.17
-2					81.2	35.57	7.45	38.18	16.28
-4					82.2	36.97	7.74	37.49	16.16
CS89-4	U_3Si	32.0 (4.7 gU/cm ³)	7.0	61.0	81.6	33.10	11.21	37.29	17.46
-5					79.1	29.90	10.13	39.07	17.66
-7					78.9	29.65	10.04	39.21	17.67
CS96-1	U_3Si	45.0 (6.6 gU/cm ³)	13.9	41.1	91.5	46.68	7.57	37.24	16.00
-3					92.1	47.46	7.70	36.93	15.95
-5					90.7	45.64	7.40	37.66	16.08

^aParentetical values are total U contained per unit volume of the fuel zone (= meat).

Table VII. DTA Data and Heats of Reaction for Fuelled Samples

Sample No.	Fuel in Heat	Calculated ΔH_f for MD101 + 6061, J	Onset Temperature First Heating, °C	Endothermic			Exothermic				Mean, J/g of fuel	Sample Standard Deviation, J/g
				ΔH_1 First Heating, J	ΔH_2 Second Heating, J	ΔH_3 Third Heating, J	ΔH_f (MD101 + 6061) - ΔH_1 , J	$\Delta H_3 - \Delta H_2$, J	$[\Delta H_f$ (MD101 + 6061) - ΔH_1] + $(\Delta H_3 - \Delta H_2)$, J	ΔH for Reaction, J/g of fuel		
CS105-4	32 vol.% U_3Si_2	17.72	595	9.75	15.84	15.98	7.97	0.14	8.11	336		
-5		17.81	600	11.10	14.43	14.91	6.71	0.48	7.19	313		
-8		17.67	585	7.78	16.17	16.04	9.89	-	9.89	398	349	± 44
CS113-1	45 vol.% U_3Si_2	16.17	575	5.69	13.29	(a)	10.48	-	10.48	285		
-2		16.28	590	5.31	11.08	(a)	10.97	-	10.97	308		
-4		16.16	595	4.53	11.21	11.41	11.63	0.20	11.83	320	304	± 18
CS 89-4	32 vol.% U_3Si	17.46	560	3.54	11.47	11.93	13.92	0.46	14.38	435		
-5		17.66	590	4.07	11.16	11.96	13.59	0.80	14.39	481		
-7		17.67	580	2.04	12.40	12.87	15.63	0.47	16.10	543	486	± 54
CS 96-1	45 vol.% U_3Si	16.00	570	-0.77	7.15	7.47	16.77	0.32	17.09	366		
-3		15.95	605	-2.12	8.65	9.12	18.07	0.47	18.54	391		
-5		16.08	600	-0.66	9.38	9.94	16.74	0.56	17.30	379	379	± 13

^aThird melting cycle not run.

Values for ρ_m were calculated using the volume percent (fractions) of fuel and MD101 shown in Table VI and the established densities of the meat components:

$$\begin{aligned}U_3Si_2 &= 12.2 \text{ g/cm}^3, \\U_3Si &= 15.2 \text{ g/cm}^3, \text{ and} \\MD101 &= 2.70 \text{ g/cm}^3.\end{aligned}$$

The ρ_m values for 32 and 45 vol.% U_3Si_2 in the meat are 5.58 and 6.64 g/cm³, respectively. For 32 and 45 vol.% U_3Si in the meat, the ρ_m values are 6.51 and 7.95 g/cm³, respectively.

Having established V_m , the masses of fuel, MD101, and 6061 were easily calculated by substituting the densities and volume fractions of each of the components into a simple conversion formula.

3. The heating thermograms for each of the three heating cycles were analyzed, and the net ΔH values for each were determined. The values are shown in Table VII.

4. A ΔH value was calculated for the mass of MD101 and 6061 in each pellet. For these calculations a ΔH_f value of 397 J/g was used for the MD101, and the experimentally determined value of 349 J/g was used for the ΔH_f of 6061.

5. The ΔH value measured for the first heating cycle (ΔH_1) was subtracted from the ΔH_f value for (MD101 + 6061). This became the ΔH value for the exothermic reaction between the silicide and the MD101 + 6061 during the first heating cycle and is shown in Table VII.

6. If no further reaction occurred, the thermograms for ΔH_2 and ΔH_3 should have been identical. That is, if the reaction was completed on the first heating, then subsequent thermograms would be a result of the ΔH of melting of the remaining aluminum species. However, with one exception (CS-105-8) there was a greater endothermic ΔH in heating cycle three than for the same sample in the second heating cycle. Therefore, the difference between ΔH_3 and ΔH_2 ($\Delta H_3 - \Delta H_2$ in Table VII) was ascribed to the completion of the reaction of the fuel with the aluminum. These (small) ΔH values were added to the value noted in Item 5 above and became the total ΔH for the fuel-aluminum reaction.

7. The total ΔH values described in Item 6 were divided by the grams of fuel present in each disc and became the enthalpy of reaction for the fuel. These values are shown in Table VII. Note that the values are recorded without a negative sign but are described as exothermic.

The arithmetic mean value for each set of samples is shown as is the sample standard deviation calculated for the three discs from each plate.

According to the phase equilibria work of A. E. Dwight,⁵ the reaction should place the composition of the reacted disc in the $U(Si,Al)_3 + Al$ field for all four conditions tested. Thus, the heat of reaction for each fuel type should be a constant and not depend on the volume percent of fuel present, at least within the limits studied in this work.

Nevertheless, for each fuel type the mean enthalpies of reaction are higher for the lower volume percent fuel. This might, for example, be the

result of a change in reaction kinetics as the fuel-to-aluminum ratio is changed. If part of the reaction occurred at a very slow rate, DTA might not detect the heat released. If this was in fact the case, the true heats of reaction would be somewhat larger than the measured values. No analytical modeling has been performed on which to base such an extrapolation.

The column in Table VII identified as "Onset Temperature First Heating, °C" requires some amplification. As stated in Sec. IV, the conventions for treating DTA thermograms described in Ref. 4 were used for all calibrating pure metals as well as for 6061. The procedure requires drawing tangents to the ΔT line and the "V"-shaped curve resulting from the endothermic (on melting) ΔH of fusion. Because the melting of the 6061 and Al initiates and is superimposed on the reaction exotherm, it is very difficult to define accurately an "onset of reaction" temperature. It was not unusual to have thermograms of the type shown in Fig. 8, where the onset of the reaction caused a very slight but detectable exotherm which was immediately quenched by the endotherm of melting of the aluminum components of the specimen. However, other thermograms displayed no initial exotherm; instead, the "onset temperature" was that for an endothermic event. Therefore, the "Onset ..." temperatures recorded in Table VII represent the first event on heating identified by the tangent-construction technique and in effect identify the first departure from linearity for the ΔT plot.

It is clear that all detectable exothermic as well as endothermic events take place in the $\sim 570^\circ$ to $< 700^\circ\text{C}$ temperature regime.

VI. SOURCES OF UNCERTAINTY

A number of assumptions and calculations were made in determining the heats of reaction. Each assumption is a potential source of error in the final value. For example, the description of each fuel zone as being exactly of the volume percent of fuel and porosity indicated and being uniformly of the geometry shown in Fig. 2 cannot be proven; it is, nevertheless, a reasonable assumption.

Tests were run with pure Al samples at 5°C as well as 20°C per minute heating and cooling rates. In some cases the instrument amplification setting was changed. None of these experimental runs resulted in data different from those recorded in Table V. It is possible that the heats of reaction could have been different from those recorded here if other heating rates had been used for fueled samples. It is believed that if differences do exist as a function of heating rate, such differences would be small.

The variations in ΔH value from disc to disc for a given fuel and concentration and for different concentrations of fuel in the meat might be a function of fuel particle size. There was no way to define the effect of this variable in this study.

A. Instrumentation Calibration

As mentioned elsewhere in the text, the instrument calibration curve was checked frequently during the data collection period using Sb and pure Al as reference points covering the major temperature range of interest (650 – 660°C) for these fuels. The uncertainty in the instrument constant did not exceed $\pm 2\%$.

B. Temperature Calibration of Thermograms

Uncertainties in determining relative temperature readings for endotherms (and exotherms) using the Rigaku scale are estimated to be $\pm 0.5\%$. Absolute temperatures are measured by the instrument platinum-rhodium thermocouple and during this study were reproducible to $\pm 0.5\%$.

C. Measurement of Peak Areas

Measurement of peak areas was done by two methods: by the cut-and-weigh technique and by planimeter. The differences in the two methods was less than $\pm 1\%$. Reproducibility of a particular method was dependent upon which event was being evaluated or, basically, the size of the endotherm (or exotherm) area. Typically, the reproducibility of the "first event" was $\pm 2.5\%$. The second melt, usually being better defined than the first, was reproducible to $\pm 1\%$. Very small exotherms associated with some specimens (e.g., CS-89-7) were difficult to measure precisely but this area represented only a small fraction ($< 1\%$) of the total area determined for the calculations. The combined uncertainty in the calculations due to measurement of peak areas is estimated to be $\leq \pm 3\%$.

VII. COMPARISONS WITH THE LITERATURE

The only other DTA studies of the uranium silicide plus aluminum reactions were conducted by S. Nazaré.⁶ Nazaré's work was with samples similar to the ones used in this study as well as with pellets without clad which consisted of pressed powders of U_3Si or U_3Si_2 with an amount of Al powder to simulate a U loading of 4.0 gU/cm^3 . The tests were conducted in an "inert gas" with a heating rate of 5°C per minute up to a maximum temperature of $\sim 740^\circ\text{C}$. Most notably, Nazaré also found that the melting of the matrix plus clad did occur in the same temperature regime as the silicide plus aluminum reaction. On heating, he shows an "onset of exotherm" for plate discs at 620°C and a peak exotherm at 630°C to 635°C , followed immediately by an endotherm of larger magnitude, peaking at 650° to 660°C . No reaction of any type is indicated above 660°C .

Nazaré did not thermally cycle the samples in his DTA work, but he does state that the reaction was presumably not totally completed after one heating and cooling cycle. The scope of his studies did not include unfolding the ΔH for the fuel plus Al reaction from the data. Therefore, a quantitative comparison of his work and the studies recorded here is not possible. The data presented by Nazaré appear to be in consonance with the results of this study.

VIII. SUMMARY AND CONCLUSIONS

The heats of reaction between U_3Si or U_3Si_2 and an Al + 6061 matrix have been determined by quantitative differential thermal analysis. Using discs punched from 0.060 in. (1.52 mm) plates with a 0.020 in. (0.51 mm) thick fuel zone, the enthalpies at two concentrations of each silicide were determined.

The exothermic ΔH values unfolded from the experimental curves are:

<u>Meat</u>	<u>ΔH, J per gram of fuel</u>
32 vol.% U_3Si_2	349 ± 44
45 vol.% U_3Si_2	304 ± 18
32 vol.% U_3Si	486 ± 54
45 vol.% U_3Si	379 ± 13

On heating, the $U_3Si + Al$ as well as the $U_3Si_2 + Al$ reactions are initiated by the formation of some liquid. That is, no event was observed in the DTA plots until the solidus temperature of 6061 (582°C) was exceeded. In the temperature regime from 582°C to ~660°C the endothermic melting of 6061 and the MD101 Al is superimposed on the exothermic reaction between the fuel₃ and the aluminum species. The net effect for fuel loadings up to ~5 gU/cm₃ is always an endotherm. For samples at 45 vol.% U_3Si in the fuel zone (~6.6 gU per cm³), the net effect for the first heating was a very slight exotherm.

For all specimens tested, a very slight reaction between the fuel particles and the aluminum occurred during a second heating cycle during which the reaction is completed; subsequent heating cycles up to as high as 1300°C demonstrated only the endothermic melting of the residual aluminum species.

The results of this study are in agreement with qualitative DTA studies conducted by one other independent investigator.⁶

ACKNOWLEDGMENTS

The work described in this paper could not have been successfully accomplished without the efforts of many individuals in ANL's Materials Science and Technology Division, the Analytical Chemistry Laboratory and the Chemical Technology Division. Special thanks are due to D. R. Schmitt, J. A. Zic, F. J. Karasek, C. Steves, G. K. Johnson, and J. L. Settle for their contributions.

REFERENCES

1. R. F. Domagala, T. C. Wiencek, and H. R. Thresh, *J-Si and J-Si-Al Dispersion Fuel Alloy Development for Research and Test Reactors*, Nucl. Tech. 62, 383 (1983).
2. G. L. Copeland and M. M. Martin, *Development of High-Uranium-Loaded U_3O_8 -Al Fuel Plates*, Nucl. Tech. 56, 547 (1982).
3. C. E. Weber, *Progress on Dispersion Elements*, in *Progress in Nuclear Energy*, Ser. V, 2, Pergamon Press, N.Y. (1959).
4. A. E. Pasto, G. L. Copeland, and M. M. Martin, *A Quantitative Differential Thermal Analysis Study of the U_3O_8 -Al Thermite Reaction*, Oak Ridge National Laboratory Report, ORNL-5659 (June 1980). Also, *Cermit Bulletin*, 61, No. 4, 491 (1982).

5. A. E. Dwight, *A Study of the Uranium-Aluminum-Silicon System*, Argonne National Laboratory Report, ANL-82-14 (Sept. 1982).
6. S. Nazaré, *Low Enrichment Fuels for Research and Test Reactors*, J. Nucl. Mat., 124, 14 (1984).

Appendix I-4.3

REACTION BEHAVIOUR OF U_xSi_y -Al AND U_6Fe -Al DISPERSIONS

S. NAZARÉ

Institut für Material- und Festkörperforschung,
Kernforschungszentrum Karlsruhe GmbH,
Karlsruhe, Federal Republic of Germany

Abstract

The paper describes the experiments carried out using differential thermal analysis (DTA) to investigate the reactions in fuel plates with U_3Si -, U_3Si_2 - and U_6Fe -Al dispersions up to and beyond clad melting. In all cases, exothermic reactions are observed at about $630^\circ C$. In the case of the silicides, UAl_3 with silicon in solution is the main reaction product; in the case of U_6Fe , UAl_4 is the main reaction product. The enthalpies of reaction were determined after calibration with suitable standards. The values obtained reveal the largest energy release in the case of the U_6Fe -Al dispersions. Reactions in the U_3Si_2 -Al system are less exothermic than in the U_3Si -Al system.

INTRODUCTION

It was well known at the outset, that the high U-density dispersants U_3Si , U_3Si_2 and U_6Fe are thermodynamically unstable in conjunction with an Al-matrix. Investigations were therefore initially focussed on the study of the compatibility of these dispersants with the Al-matrix under equilibrium conditions /1-4/, as well as the consequences of the reactions for the dimensional stability of the fuel plates after prolonged heat treatment. Post irradiation examination of the irradiated plates with the silicides revealed however, that under the test conditions only minor reaction zones (3-6 μm) between the particles and the matrix occurred even at high burnup /5/. Apart from the irradiation enhanced Al-diffusion, which particularly in the case of U_3Si -Al dispersions could be a cause of fission gas bubble nucleation /6/, the reaction behaviour and the energy release involved is important from the safety viewpoint in the case of an overtemperature excursion under off normal conditions.

The objective of this paper is to describe and discuss the experiments carried out to study the exothermic reactions between U_3Si , U_3Si_2 and U_6Fe and aluminium.

EXPERIMENTAL

Differential thermal analysis (DTA) was used to investigate the reactions quantitatively. The equipment was calibrated using metals with well known heat of fusion namely aluminium tin, lead, copper.

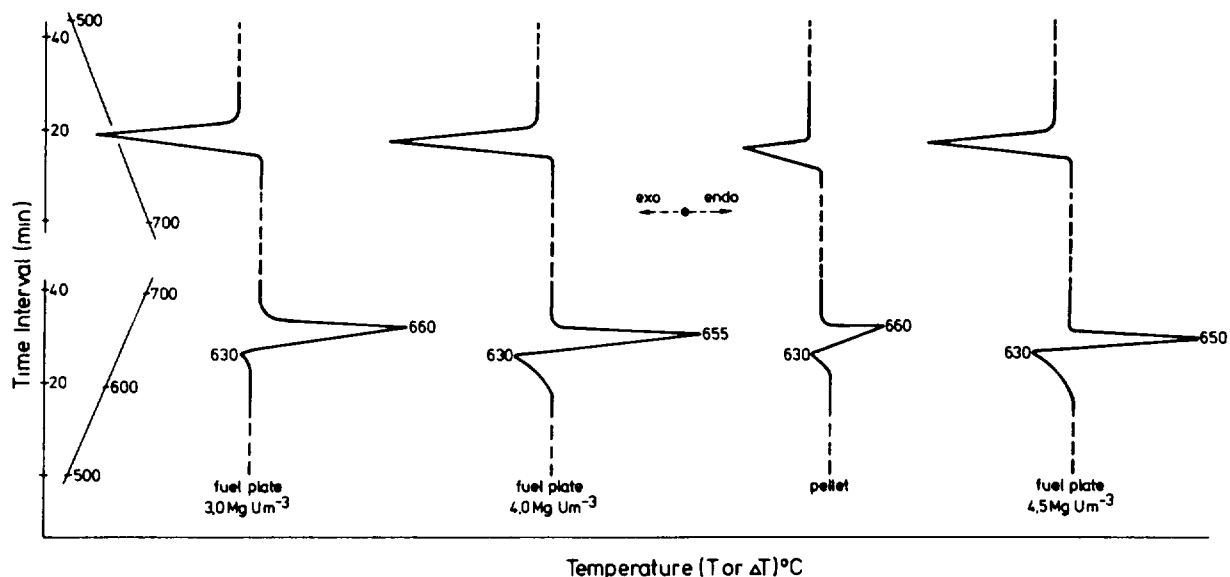


Fig. 1: Segments of DTA-thermograms of U_3Si_2 -Al dispersion fuel plates.

The experiments were carried out with samples punched out of miniature plates (particle size of the dispersant 63-90 μm) as well as with pellets of powder mixtures. The samples were heated in inert gas at a rate of 5 K/min up to 970 K; the heating and cooling runs being repeated up to 3 times.

U_3Si_2 -Al dispersions

Fig.1 shows segments of DTA-thermograms of U_3Si_2 -Al plate samples with U-densities in the meat of 3.0, 4.0 and 4.5 $Mg\ U m^{-3}$. It can be seen that in all cases during heating an exothermic reaction occurs at about 630°C. This reaction is in the vicinity of the endothermic melting of the excess aluminium. During the cooling cycle, an exothermic peak is observed which corresponds to the solidification of the excess Al-matrix/cladding. Repetition of the heating and cooling cycles does not show any additional changes except for the melting and solidification of the aluminium. X-ray diffraction analysis of the samples after DTA showed $U(Si,Al)_3$ to be the main product of the reaction. Fig.2 shows the microstructure of a typical sample of the fuel plate with a U-density of 4.0 $Mg\ U m^{-3}$ in the meat. The microstructure reveals the reacted particles of the original U_3Si_2 as well as the excess Al. A quantitative analysis of the reaction enthalpy gave the following values: 191 kJ/kg dispersant for 3.0 $Mg\ U m^{-3}$; 299 kJ/kg dispersant for 4.0 $Mg\ U m^{-3}$ and 285 kJ/kg dispersant for 4.5 $Mg\ U m^{-3}$.

U_3Si -Al dispersions

Fig.3 shows segments of DTA thermograms of U_3Si -Al plates samples with U-densities in the meat of 3.0, 4.0 and 6.0 $Mg\ U m^{-3}$ in the meat. It can be seen again that in all cases a more pronounced exothermic reaction occurs again at about 630°C in the vicinity of the endothermic melting of the Al-matrix and cladding. During the cooling cycle an exothermic reaction which corresponds to the solidification of the excess Al-matrix and cladding is observed. Repetition of the heating and cooling cycles also did not reveal additional changes except for the melting and solidification of the aluminium. X-ray diffraction analysis of the samples after the DTA showed again that $U(Si,Al)_3$ was the main product of the reaction. Fig.4 shows the microstructure of the fuel

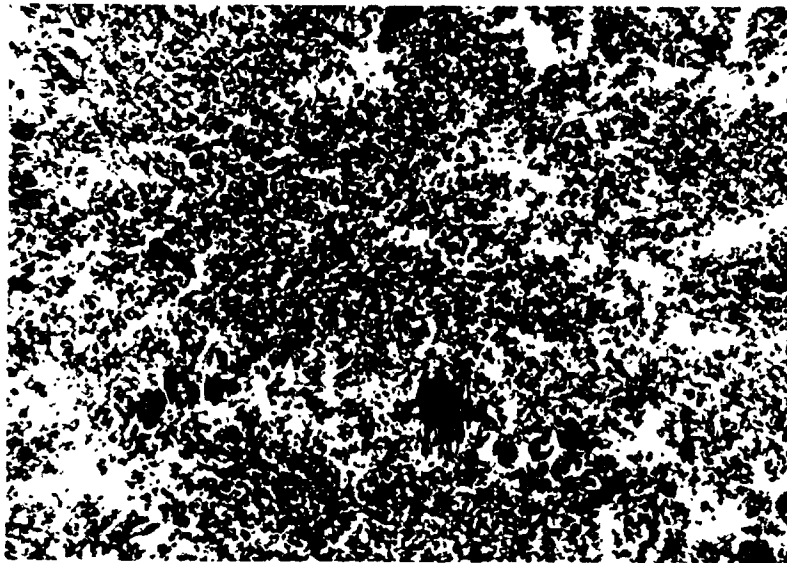


Fig. 2: Microstructure of U_3Si_2 -Al fuel plate sample (4.0 Mg U m^{-3}) after DTA.

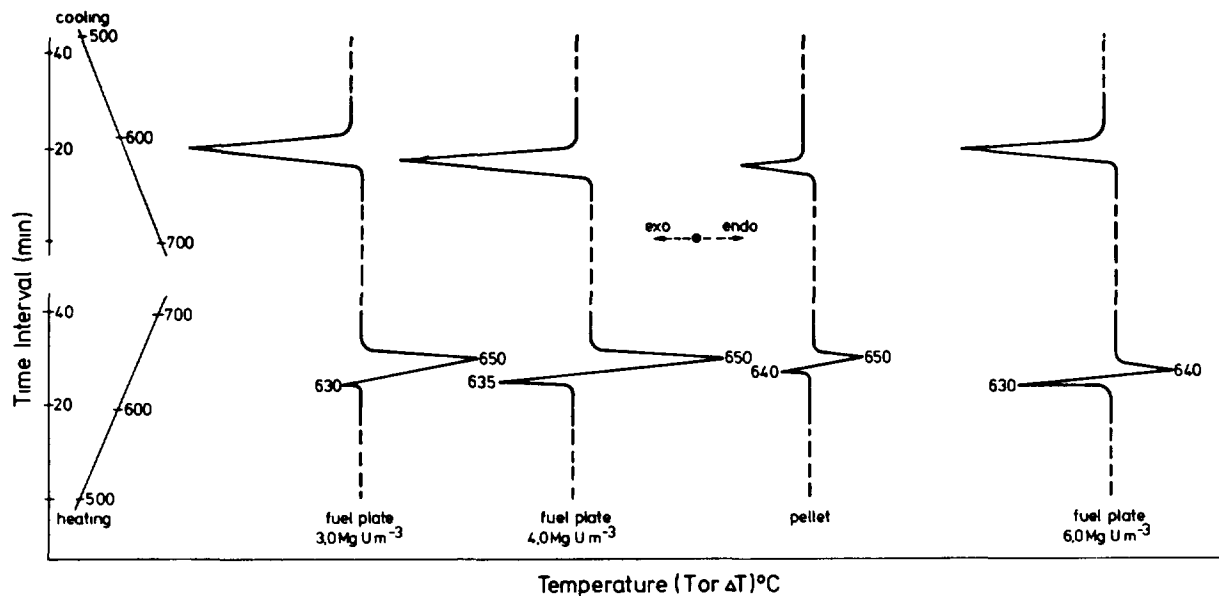


Fig. 3: Segments of DTA thermograms of U_3Si -Al dispersion fuel plates.

plates with 4.0 and 6.0 Mg U m^{-3} in the meat. They reveal that the original particles of U_3Si have reacted to form $U(Si,Al)_3$. The remaining aluminium can also be seen in the microstructure.

Quantitative evaluation of the reaction enthalpies gave the following results: 348 kJ/kg dispersant for 3.0 Mg U m^{-3} ; 289 kJ/kg dispersant for 4.0 Mg U m^{-3} and 304 kJ/kg dispersant for 6.0 Mg U m^{-3} .

U_6Fe -Al dispersions

Fig.5 shows segments of DTA thermograms of U_6Fe -Al fuel plates with U-densities of 4.0 , 6.0 and 7.0 Mg U m^{-3} in the meat. It can be seen that in all cases an exothermic reaction is observed at about 630°C during the heating

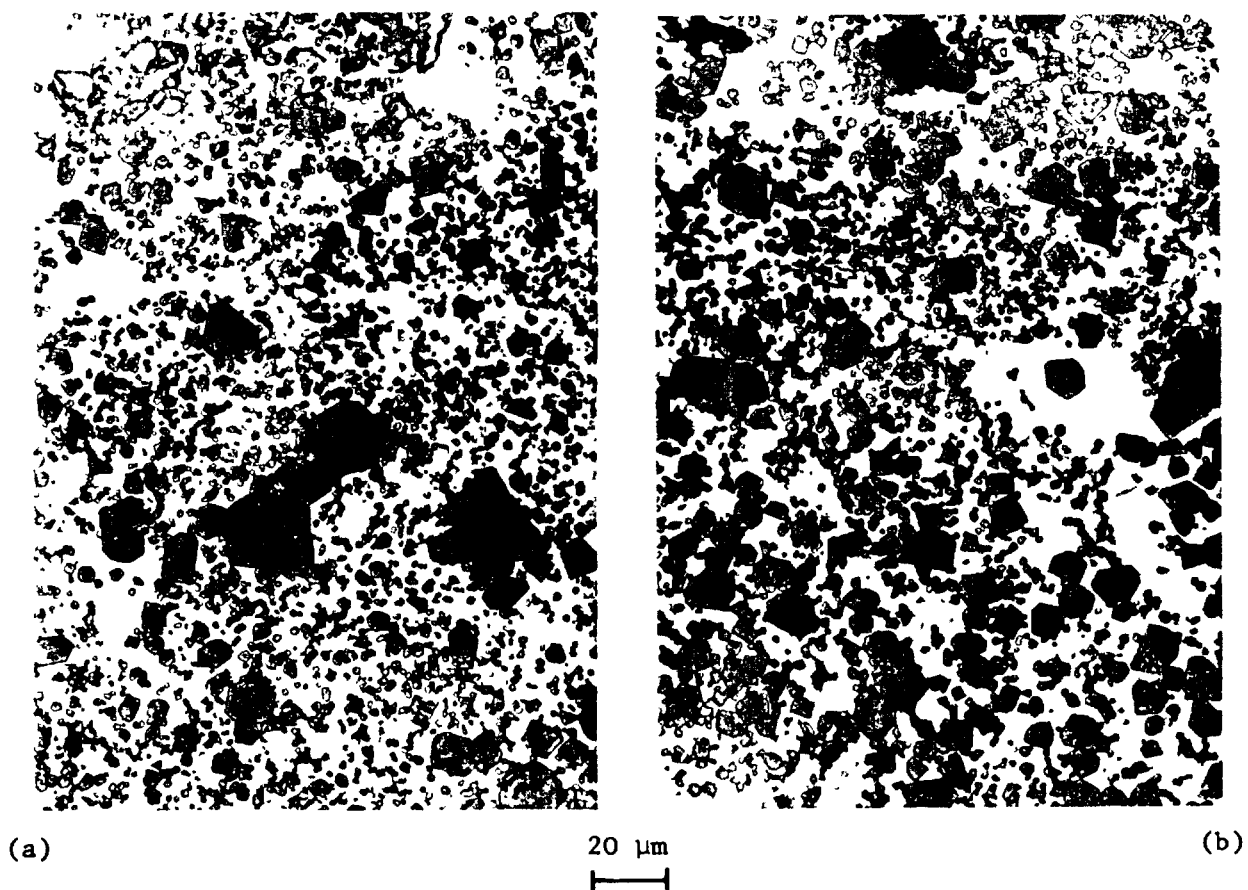


Fig. 4: Microstructures of $\text{U}_3\text{Si-Al}$ fuel plates [4.0 Mg U m^{-3} (a) and 6.0 Mg U m^{-3} (b)] after DTA.

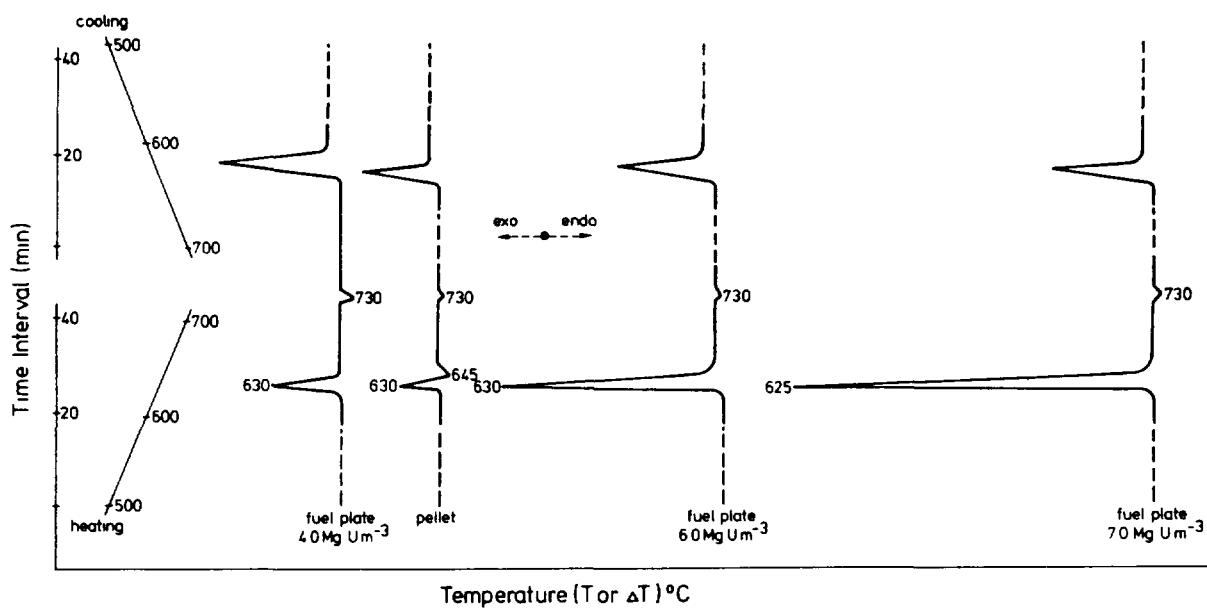


Fig. 5: Segments of DTA-thermograms of $\text{U}_6\text{Fe-Al}$ dispersion fuel plates.

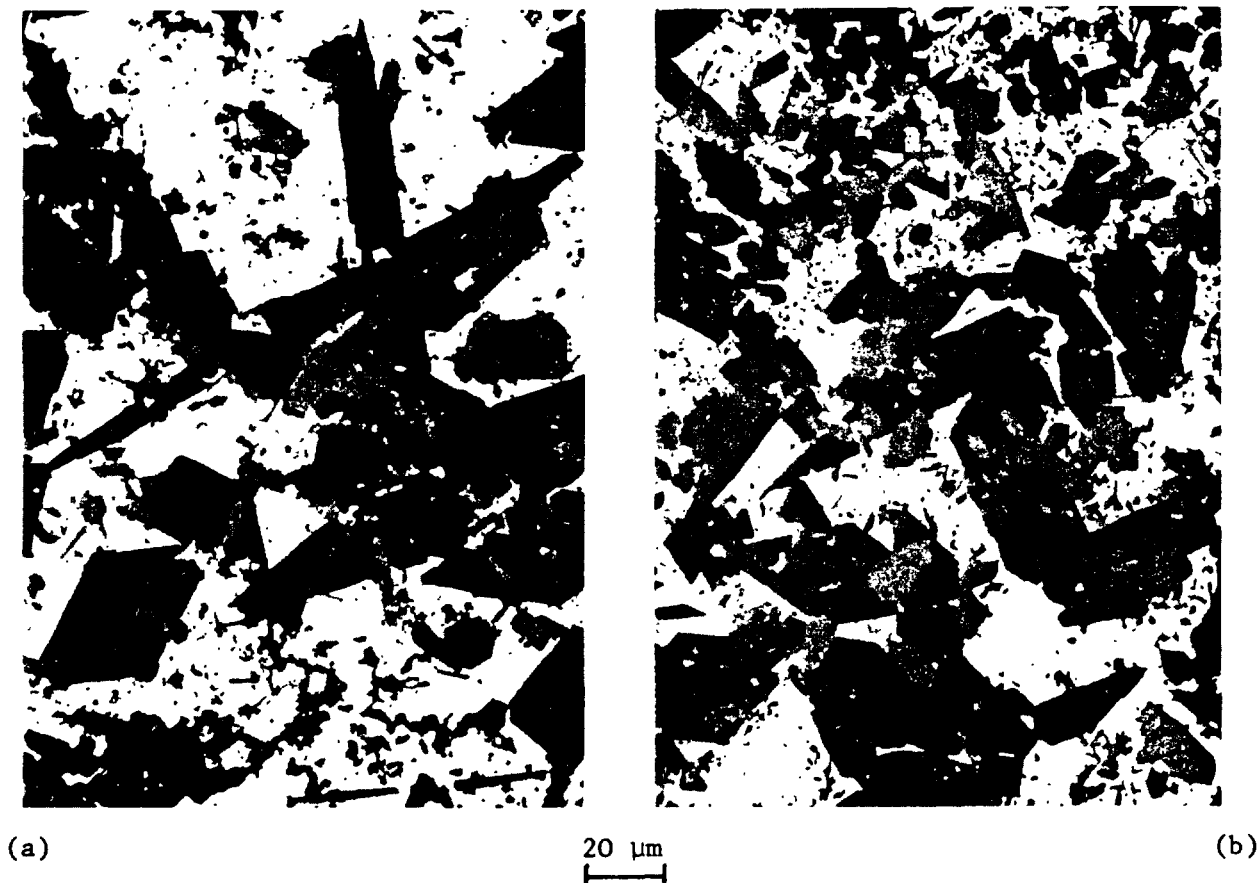


Fig. 6: Microstructures of U_6Fe -Al fuel plates [4.0 Mg U m^{-3} (a) and 7.0 Mg U m^{-3} (b)] after DTA.

cycle. In this case, the enthalpy of reaction is large enough to mask the endothermic melting of the Al-matrix and cladding. Another significant feature of these thermograms is that during the heating cycle, endothermic peaks at about 730°C which can be attributed to the melting of UAl_4 , can be seen. During the cooling cycle, an exothermic peak is observed that corresponds to the solidification of the excess aluminium which was masked during the heating cycle. X-ray diffraction analysis of the samples after cooling showed that UAl_4 , probably with Fe in solution was the main product of the reaction.

The microstructures of the fuel plates with 4.0 and 7.0 Mg U m^{-3} are shown in Fig. 6. They reveal that the original particles of U_6Fe have reacted forming UAl_4 . The remaining parts of the Al-matrix are also visible in the microstructure. Quantitative evaluation of the reaction enthalpies gave the following results: 320 kJ/kg dispersant for 4.0 Mg U m^{-3} ; 360 kJ/kg dispersant for 6.0 Mg U m^{-3} and 445 kJ/kg dispersant for 7.0 Mg U m^{-3} .

Additional experiments with powder mixtures

The experiments with fuel plates described thus far show that the main reaction product in the case of the silicides is $\text{U}(\text{Si},\text{Al})_3$ and in the case of U_6Fe , UAl_4 . Therefore additional DTA experiments were carried out using powder mixtures. In these cases the pellets were prepared from stoichiometric amounts of U_3Si , U_3Si_2 , U_6Fe and Al required to form $\text{U}(\text{Si},\text{Al})_3$ or UAl_4 (77.4 wt.-% U_3Si , 80.2 wt.-% U_3Si_2 and 69.6 wt.-% U_6Fe). In order to study the effect of the particle size, two powder fractions were used namely $63\text{--}90 \mu\text{m}$ and $\leq 45 \mu\text{m}$. The results are shown in Fig. 7.

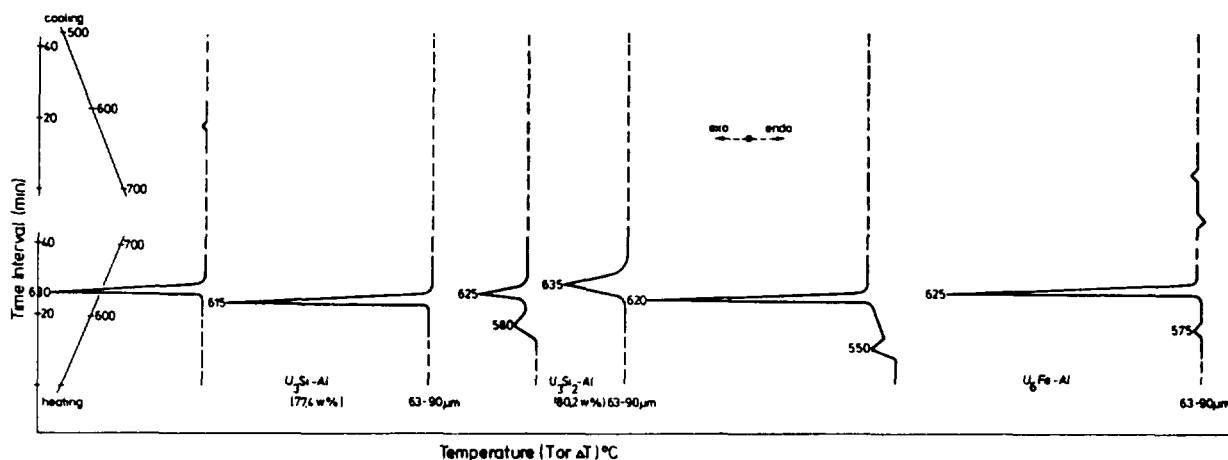


Fig. 7: Segments of DTA-thermograms of pellets of U_3Si -, U_3Si_2 - and U_6Fe -Al.

A comparison of these results with those of the fuel plates shows:

- In all cases no endothermic melting of the Al can be seen. It can thus be inferred that practically no excess aluminium remains after the reaction.
- In the case of the U_3Si -Al dispersions, there is small increase in the peak temperature when finer particles are used. It is hypothesised that the apparently unexpected effect could be related to the presence of larger quantities of U_3Si_2 in the finer powder fraction of U_3Si .
- In the case of the U_3Si_2 and U_6Fe powder mixtures additional exotherms are observed at lower temperatures ($580^\circ C$ for U_3Si ; $550-575^\circ C$ for U_6Fe) which probably can be attributed to the effect of size, distribution, as well as surface morphology of the particles.

Quantitative evaluation of the enthalpies of the reaction gave the following results: 210 kJ/kg U_3Si_2 and 265 kJ/kg U_3Si for the formation of $U(Si,Al)_3$ and 405 kJ/kg U_6Fe for the formation of UAl_4 .

SUMMARY AND CONCLUSIONS

Differential thermal analysis, metallography and X-ray diffraction were used to investigate the exothermic reactions in fuel plates and powder mixtures of U_3Si -, U_3Si_2 - and U_6Fe -Al dispersions. The experiments revealed that:

- On heating, U_3Si_2 -Al fuel plates show an exothermic reaction at about $630^\circ C$, followed by an endothermic melting of the unreacted aluminium. The reaction product is $U(Si,Al)_3$.
- On heating, U_3Si -Al fuel plates also show an exothermic reaction at about $630^\circ C$, followed by an endothermic melting of the unreacted aluminium. The reaction product is again $U(Si,Al)_3$.
- On heating, U_6Fe -Al fuel plates also show an exothermic reaction at about $630^\circ C$. The reaction product is UAl_4 , which shows an endothermic melting peak at $730^\circ C$.

- Quantitative analysis of the areas encompassed by these exotherms was used to estimate the enthalpy of reaction. The values obtained indicate that the enthalpy of reaction per unit weight of dispersant is lowest in the U_3Si_2 -Al system and highest in the U_6Fe -Al system. In addition, the experiments reveal that the heat is released over varying time intervals which are largest in the case of U_3Si_2 -Al and smaller in the case of U_3Si - and U_6Fe -Al.

REFERENCES

- /1/ S. Nazaré, "Investigations of Uraniumsilicide-based Dispersion Fuels for Use of Low Enrichment Uranium (LEU) in Research and Test Reactors", Report of the Kernforschungszentrum Karlsruhe, KfK 3372B, 1982
- /2/ S. Nazaré, "Low Enrichment Dispersion Fuels for Research and Test Reactors", Journal of Nuclear Materials, 124 (1984) 14-24
- /3/ A.E. Dwight, Argonne National Laboratory, Report ANL-82-14 (1982)
- /4/ S. Nazaré, Proc. of the Intern. Meeting on Research and Test Reactor Core Conversion from HEU to LEU Fuels, Argonne/Ill., CONF-821155, ANL-RERTR/TM4, p. 47
- /5/ G.L. Hofmann, L.A. Neimark, R.F. Mattas, *ibid*, p. 88
- /6/ G.L. Hofmann, L.A. Neimark, Proc. of the Intern. Meeting on Reduced Enrichment for Research and Test Reactors, 1983, Tokai, Japan, JAERI-M-84-073

Appendix I-4.4

DIFFERENTIAL THERMAL ANALYSIS AND METALLOGRAPHIC EXAMINATIONS OF U_3Si_2 POWDER AND U_3Si_2/Al (38 w/o) MINIPLATES

P. TOFT, A. JENSEN
Advanced Engineering Division,
Atlas-Danmark A/S,
Denmark

Abstract

The paper describes the thermodynamic and metallurgical behavior of U_3Si_2 powder and miniplates with regard to the following aspects:

- increasing temperatures up to $1400^{\circ}C$
- fuel plate stability
- formation of ternary intermetallic compounds
- growth of the formed ternary intermetallic crystals at increasing temperatures.

The miniplate core is $U_3Si_2/Al(38w/o)$ and the cladding is Al 6061.

The study concludes, that fuel plates will not remain stable under accident conditions. A fuel element will most likely melt down before a stable structure is established.

The work is performed under contract with RISØ National Laboratories, Denmark.

INTRODUCTION

The aim of the work is to examine the thermodynamic and metallurgical behavior of U_3Si_2 powder and U_3Si_2/Al (38w/o) miniplates at increasing temperatures.

The powder and miniplates were manufactured at Argonne National Laboratories, Chicago, USA.

EXPERIMENTS

DTA examinations (Differential thermal analysis)

Samples of U_3Si_2 powder and of U_3Si_2/Al (38w/o) miniplates are heated and cooled at the same rate ($20^{\circ}C/min$) in a DTA apparatus. The maximum heating temperature is $1400^{\circ}C$. The samples are heated in helium or in air. Solidification/liquidation temperatures, oxidation and phase transformations are registered on a plotter as endothermic and exothermic reactions.

Metallographic examinations

Metallographic examination is carried out on U_3Si_2/Al (38w/o) miniplates before and after heating in DTA. The composition of the intermetallic compounds are analysed by EDAX technique.

Preparation of samples

Two samples of U_3Si_2 powder weighing 700 mg each are mounted in Al_2O_3 crucibels. Samples of U_3Si_2/Al (38w/o) miniplates are cut to the following dimensions: 7 mm x 2 mm x 1.5 mm. The cutting surface of the core is during the DTA runs exposed to the ambient atmosphere. The samples are mounted in Al_2O_3 crucibels. As reference is used Al_2O_3 powder.

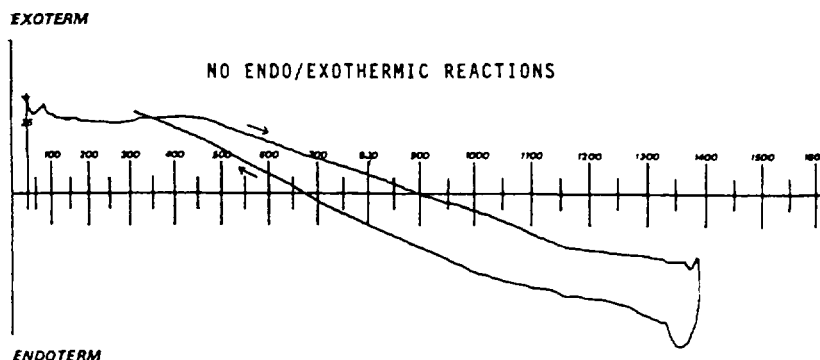
Treatment of samples (sample no.)

1. DTA on U_3Si_2 powder heated to $1400^{\circ}C$ in helium.
2. DTA on U_3Si_2 powder heated to $1400^{\circ}C$ in air.
3. Metallographic examination of the U_3Si_2/Al (38w/o) miniplate core before heated in DTA. EDAX analysis of phase compositions.
4. DTA on U_3Si_2/Al (38w/o) miniplate heated to $1400^{\circ}C$ in helium. Metallographic examination. EDAX analysis of phase compositions.
5. DTA on U_3Si_2/Al (38w/o) miniplate heated to $1400^{\circ}C$ in air.
6. DTA on cladding material Al 6061 heated to $1400^{\circ}C$ in air.
- 7,8,9 DTA on U_3Si_2/Al (38w/o) miniplate heated to $700^{\circ}C$, $900^{\circ}C$ and $1100^{\circ}C$ in helium. Metallographic examination. EDAX analysis of phase composition.

EVALUATION OF RESULTS

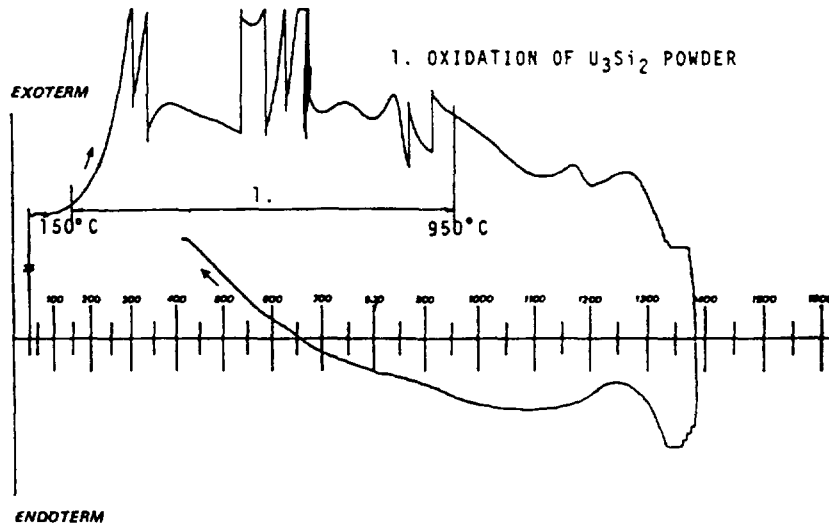
U_3Si_2 powder samples

SAMPLE 1: DTA ON U_3Si_2 POWDER HEATED TO $1400^{\circ}C$ IN HELIUM



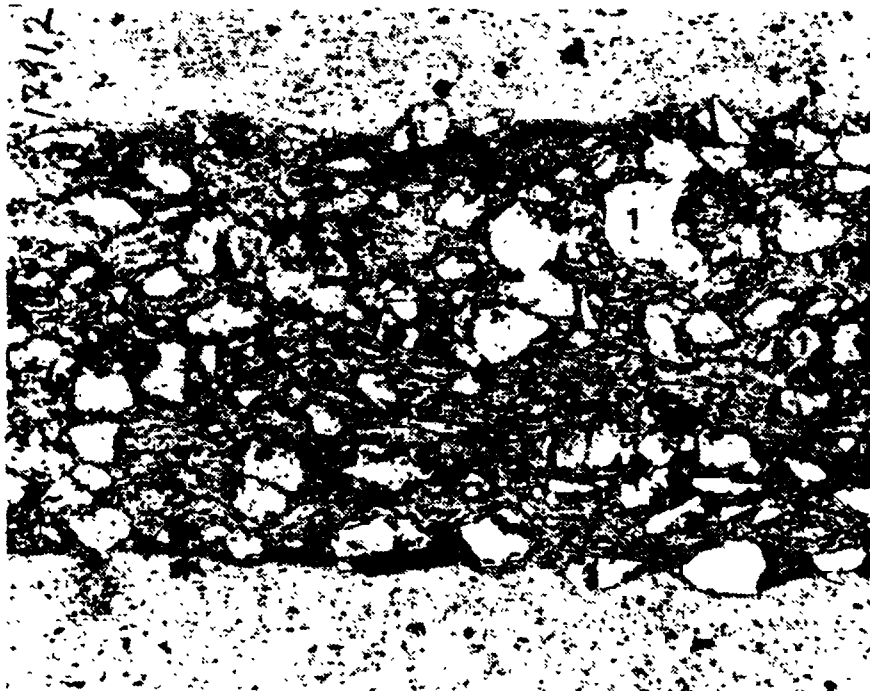
Sample 1: The U_3Si_2 powder is thermodynamic stable when heated in helium to $1400^{\circ}C$

SAMPLE 2: DTA ON U_3Si_2 POWDER HEATED TO 1400°C IN AIR



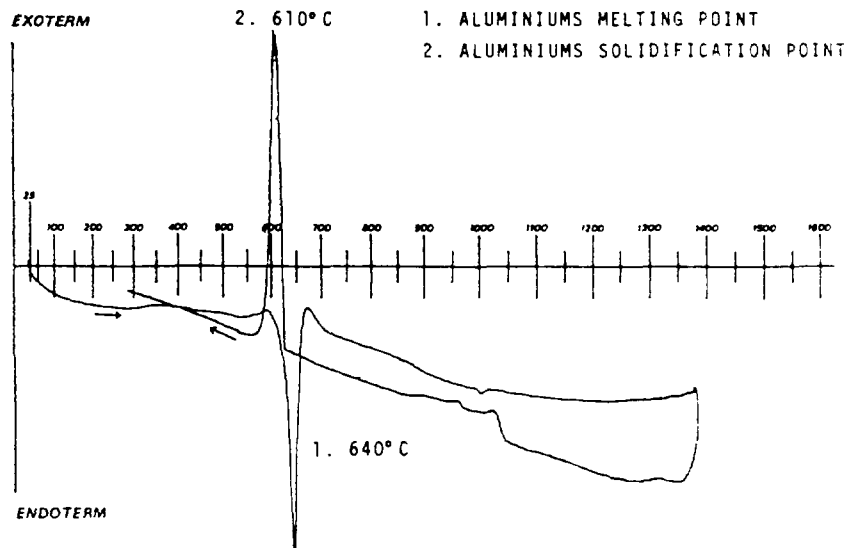
Sample 2: A powerfull exothermic reaction occurs in the temperature range 150-950°C caused by oxidation of the U_3Si_2 powder. The oxidation occurs mainly in to steps, at approx. 300°C and at approx. 630°C, both silicon and uranium oxides are probably formed.

U_3Si_2 /Al(38 w/o) miniplate samples

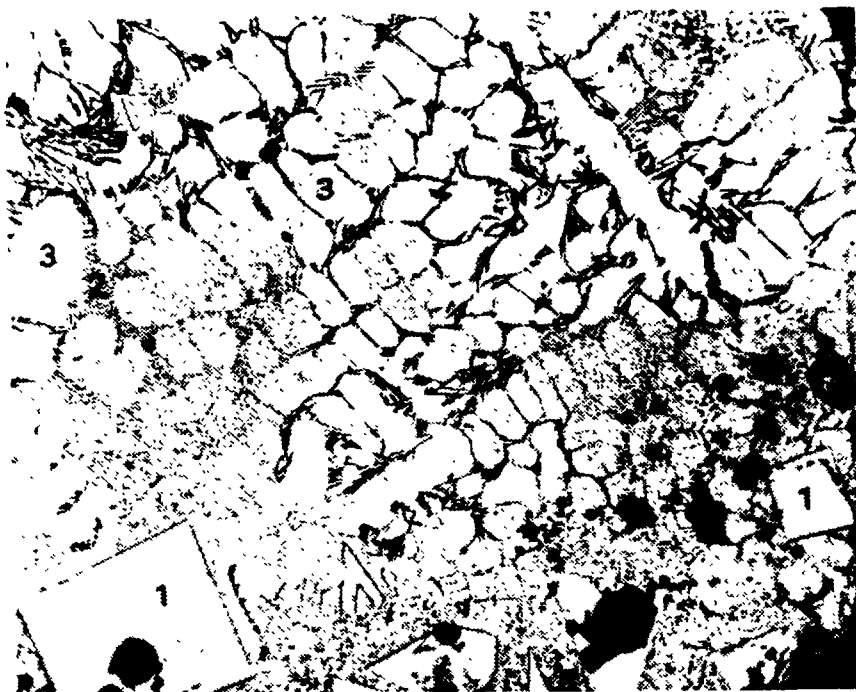


Micrograph 1 (x100)

Sample 3: The metallographic examination (micrograph 1) of the miniplate core before heating in DTA shows that the core material consists of U_3Si_2 (1) particles embedded in a pure aluminium matrix(2). The EDAX analysis gives the following composition: U_3Si_2 particles: U 90.3 w/o (52.2 a/o), Si 7.3 w/o (35.6 a/o). Matrix material: 99% Al.



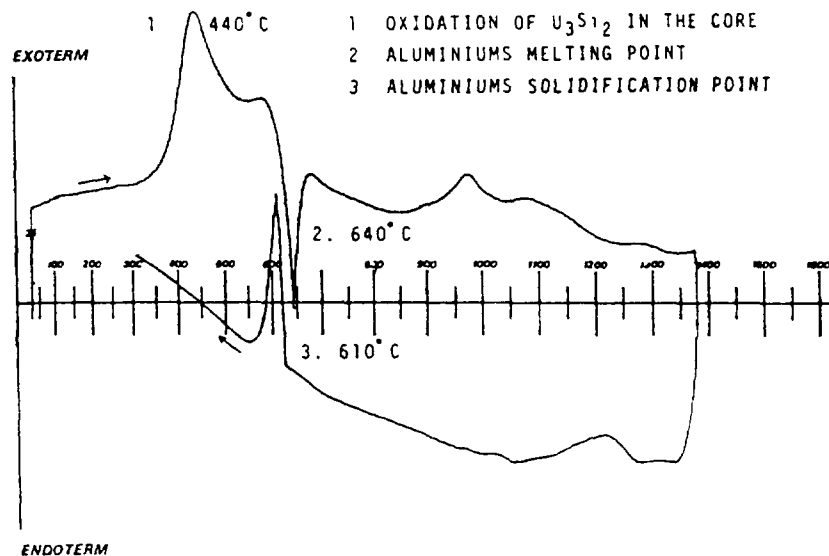
Sample 4: The endothermic (1) reaction is due to melting of both the cladding material and the matrix material in the core. The exothermic (2) reaction shows the solidification of the micro segreated aluminium. The metallographic examination of the sample shows that there is an reaction between U_3Si_2 and Al at or immediately above aluminiums melting point. The ternery intermetallic compound which is formed has according to EDAX analysis the following composition: U: 72.1 w/o (22.9 a/o), Si: 6.6 w/o (17.6 a/o), Al: 21.3 w/o (59.5 a/o).



Micrograph 2, 1400°C (x100)

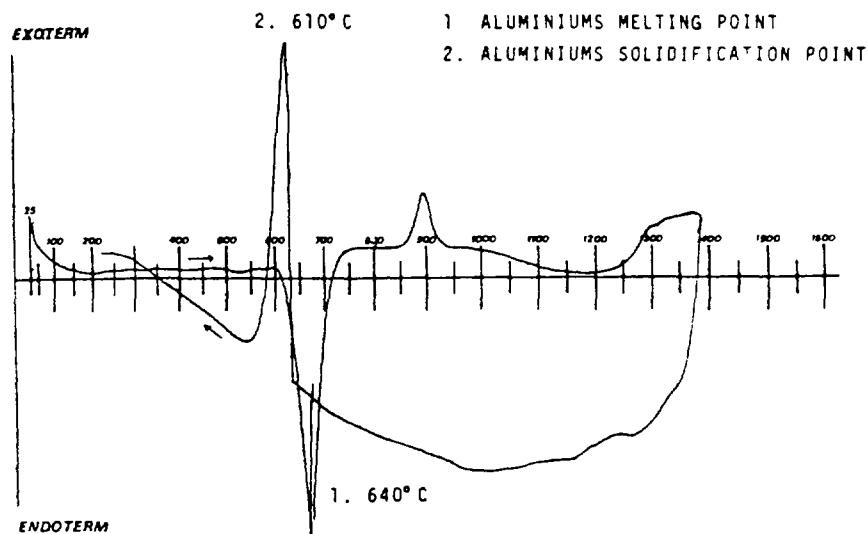
Micrograph 2 shows the ternary intermetallic compound as a big regular crystal (1). The micrograph shows also an eutectic phase (2) (fine and coarse laminated phase). This ternary phase consist probably of the above described ternary phase and micro segreated aluminium (3).

SAMPLE 5: DTA ON $U_3Si_2/Al(38w\%)$ MINIPLATE HEATED TO $1400^\circ C$ IN AIR

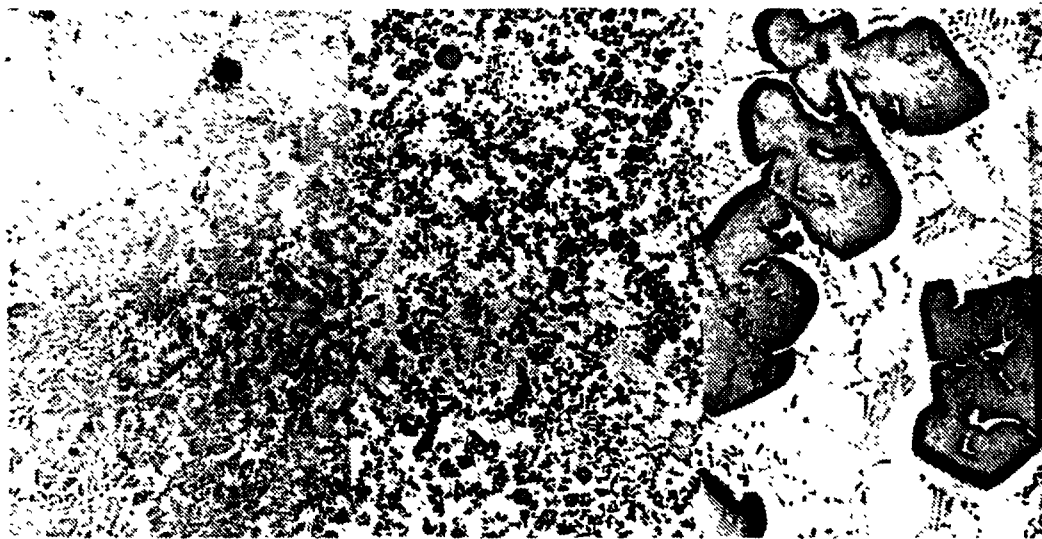


Sample 5: The exothermic reaction (1) at $440^\circ C$ is due to oxidation of the core surface (referring to the preparation of samples). The oxidation products is probably silicon oxides and uranium oxides.

SAMPLE 6 DTA ON CLADDING MATERIAL Al 6061 HEATED TO $1400^\circ C$ IN AIR



Sample 6: The oxidation of U_3Si_2 in the core is confirmed by the DTA examination of the cladding material Al 6061 who does not show any exothermic reactions before the melting point at $640^\circ C$.



x 100
Micrograph 3, 700°C

x 100
4, 900°C

x 100
5, 1100°C

Sample 7,8,9: In order to examine the formed ternary intermetallic crystals coalecens (growth to larger and fewer crystals) at increasing temperature, samples is heated to 700°C, 900°C and 1100°C in helium. The micrographs 3 and 4 shows a slow growht of the ternery crystals in the temperature range 640 to approx. 900°C. Micrograph 5 shows that there is a rapid growht after 900°C. Somewhere in the temp. range 900°C to 1100°C formes an eutectic phase consisting of the ternery intermetallic compound and micro segregated aluminium. This indicates that there is dissolved as mutch of the ternery compound in the melted aluminium that an eutectic composition is obtained. During cooling the eutectic phase is formed as a laminated phase.

CONCLUSION

Considering the metallographic examination and the results from the DTA runs, the following conclusion can be drawn.

U₃Si₂ powder

The U₃Si₂ powder is thermodynamic stable to 1400°C in helium. When heating in air there is a heavy oxidation in the temperature range 150-950°C. The oxidation products is probably silicon and uranium oxidation.

U₃Si₂/Al (38 w/o) miniplates

When heating in helium there is no exo/endothermic reactions below aluminiums melting point which could indicate any changes in the core and the cladding material. In or immediately above aluminiums melting point there is a reaction between U₃Si₂ and Al. The ternery

intermetallic compound which is formed has according to EDAX analysis the following composition: U: 72.1 w/o (22.9 a/o) Si: 6.6 w/o (17.6 a/o), Al: 21.3 w/o (59.5 - a/o). All the U Si in the core is transformed to the ternary intermetallic compound at this temperature (approx. 640°C). The stoichiometric composition once formed is fixed at increasing temperature. The ternary intermetallic phase is in the temperature range 640°C to approx. 900°C homogenously distributed in the form of crystals embedded in an aluminium matrix.

This concludes that the miniplate will not remain stable after aluminium's melting point. After 640°C there is a coalescence (growth to larger and fewer crystals) of the ternary crystals at increasing temperatures. During heating and during the growth process the crystals have a tendency to move towards the surface of the sample. This will result in an inhomogeneous distribution of ternary crystals in the aluminium matrix.

At temperatures above 900°C an eutectic phase is formed in the aluminium matrix. In order exactly to measure the ternary intermetallic composition, and when and how the eutectic phase is formed, further examinations are required. When heating in air there is a non-reversible exothermic reaction at approx. 440°C. This reaction is due to oxidation of the U_3Si_2 core surface.

ACKNOWLEDGMENTS

The authors are indebted to RISØ Metallurgical Department for the access to and the use of the department's equipment. Special thanks to Ole Olsen for preparing and photographing the metallographic specimens and to Kjeld Larsen for assistance with the differential thermal analysis. The assistance of Jan Borring in preparing the paper is gratefully acknowledged.

Appendix I-5

STRUCTURAL STABILITY

Appendix I-5.1

STRUCTURAL STABILITY OF PLATE-TYPE FUEL ELEMENTS USED IN US RESEARCH AND TEST REACTORS

ARGONNE NATIONAL LABORATORY
RERTR Program,
Argonne, Illinois,
United States of America

Abstract

Information is presented on the methods that have been used to design fuel elements for several research and test reactors in the U.S. The emphasis is on the methods of analysis and the tests used to ensure stability of the fuel elements under normal operating conditions of full flow and design power.

1. INTRODUCTION

The aluminum based fuel element of curved-plate design was a product of an Oak Ridge National Laboratory (ORNL) development program. These type elements were first utilized in 1950 to power the Bulk Shielding Reactor, a light water-cooled, moderated and reflected 1 MW pool-type reactor. The elements were next used in the Materials Testing Reactor (MTR), one of the first of the forced-circulation high power density testing and research reactors. Subsequent high power density tank-type reactor designs have used modified versions of the MTR-type element. Examples of some of these variations are the curved-plate serpentine elements used in the ATR, the flat-plate assemblies used in the ETR, the involute-type fuel design of the HFIR, and the concentric circular elements that were used in the CP-5 reactor. These are the exception, however, and the majority of the pool-type reactors in use in universities and research establishments around the world use plate-type elements similar to the MTR design.

Because of the differences in application, pool-type and tank-type research reactor fuel elements have some design differences. With pool-type elements in low power reactors the limiting condition normally is corrosion of aluminum. The most significant effect observed during examination of irradiated pool elements has been pitting and corrosion of the aluminum. This condition is attributed mainly to improper water quality control. With proper pH control, corrosion can be held in check.

The limiting factors in tank-type reactor fuel elements in high power reactors are reactivity lifetime and burn-up rate of the fissile U-235. Because of the high power densities, the lifetime of these fuel elements typically is from 3 to 6 weeks; therefore, there has been a trend toward increasing the loading of fissile material to increase fuel lifetime. In contrast to pool reactors, mechanical strength of the fuel element is also an

important factor. At the required high water velocities (typically ~ 10 m/sec), pressure differentials often develop across the plates which can cause permanent deformation. In order to increase the strength of fuel elements for application in high power density reactors, the original relatively soft 1100 aluminum alloy used in MTR-type assemblies has been replaced by much stronger aluminum alloys such as 6061. In addition, some of the early fabrication methods such as brazing and pinning of the fuel plates to the side plates has largely been supplanted by a roll swaging technique which has been found to give a superior finished element. Swaged joints also allow some slippage between the hot fuel plates and cooler fuel element side plates, thereby reducing thermal stresses in operation.

2. EXPERIENCE WITH FUEL FAILURES DURING REACTOR OPERATION

Failures of fuel plates in pool-type and tank-type research reactors, resulting in a release of fission products, have been relatively rare. The failures that have occurred in the U.S. fall into the following major categories:

1. Failure of cladding due to corrosion and/or pinhole manufacturing defects.
2. Fabrication deficiencies such as non-homogeneous fuel distribution, improper assembly of fuel plates to the side plates, defective brazing, etc.
3. Cooling starvation because of coolant channel blockage by foreign materials in reactor cooling system.
4. Thermal stresses and/or hydraulic pressure forces on fuel plates producing buckling.

Most of the reported instances of failures accompanied by fission product release fall in the first three categories, with blockage of coolant channels by foreign materials and fabrication deficiencies being predominate in the more serious incidents with high power density reactors.^{2,3,4}

The one reported instance of buckling failure of fuel plates due to stresses caused during operation by hydraulic pressure differentials and thermal gradients occurred in the MTR in 1954.⁵ For two years from reactor startup in 1952 to July of 1954, all the MTR fuel elements functioned as intended. Immediately prior to a fuel plate buckling failure in 1954, a number of changes were made to the original MTR fuel assembly design. These were:

1. The thickness of the fuel plates was reduced from 1.52 to 1.27 mm.
2. The thickness of the fuel side plates was reduced from 4.75 to 2.69 mm.
3. The number of fuel plates was increased from 18 to 19.
4. The fuel element fissile content was increased from 140 to 200 grams per assembly.
5. The opening in the lower fuel end box casting was decreased from 2400 to 2000 mm².

There were two effects of these changes:

1. The element was weakened by thinning the fuel and side plates.
2. The water pressure within the element was raised in comparison with the pressure outside as a result of restricting the flow of water through the lower end box. This change had the effect of increasing the lateral pressure differential across the outside concave plates from about 7 to 70 kPa. Furthermore, the thinning of the plates, as shown by subsequent tests, reduced the resistance to outward buckling from a capability to withstand about 160 kPa outward buckling from a capability to withstand about 169kPa differential to a value of only 60kPa.

The problem was corrected by taking the following remedial action:

1. The two outside fuel plates in the fuel element were increased in thickness from 1.27 to 1.65 mm.
2. The side plate thickness was increased from 2.69 to 3.00 mm.
3. The cross sectional area of the water exit channel in the lower box was restored to the original 2400 mm².

These changes reduced the lateral pressure differences to less than 34kPa and increased the resistance to buckling from about 60 to 160 kPa. There was no evidence that irradiation damage and accompanying changes in mechanical properties of the cladding and fuel alloy meat were responsible for the failure.

This early experience with the MTR is probably one reason why similar problems have not occurred in other high power density research and test reactors. Table 1 lists information on temperatures, flow velocities, and pressure drops for the five reactors currently operating in the U.S. which operate at power levels greater than 10 Mw and heat fluxes in excess of 150 W/cm². It is primarily this group of reactors, all having average flow velocities in excess of 9 m/s, where problems with fuel element structural stability due to thermal and hydraulic pressure stresses could be encountered. As shown, the ORR and the HFBR operate at conditions similar to the MTR and use a similar fuel element. Therefore, the extensive experience with MTR fuel elements under similar conditions has been adequate to assure satisfactory performance of the fuel elements for these reactors.

In going to the different fuel configurations, higher flow rates and considerably higher core pressure drops encountered in the ETR, ATR, and HFIR, MTR experience is no longer directly applicable, since the higher heat fluxes mean higher temperature differences and larger thermal stresses. Also, differences in channel thickness or configuration, which would not cause problems at lower flow rates and pressure drops, become significant and can cause problems at flow velocities in excess of 15 m/s and total core pressure drops greater than 0.7 mPa. Therefore, in order to assure performance of the fuel elements for these reactors, some stress analyses were usually performed for the fuel plates operating under the most severe conditions. The greatest reliance in proving the performance of these fuel elements prior to use in the reactor, however, was placed on an extensive series of flow and heating tests. The following sections describe some of the analytic and test procedures used in qualifying the ATR and ETR fuel elements.

Table 1. Fuel Operating Conditions in U.S. High Power Research and Test Reactors

	Advanced Test Reactor (ATR)	Engineering Test Reactor (ETR)	High Flux Isotope Reactor (HFIR)	Oak Ridge Research Reactor (ORR)	High Flux Beam Reactor (HFBR)	Materials Testing * Reactor (MTR)
Power Level (MW)	250	175	100	30	40	40
Average Power						
Per Assembly (kW)	6250	3200	NA	1200	1430	1500
Maximum Power						
Per Assembly (kW)	7500	4500	NA	1730	1960	2100
Maximum Fuel Plate Surface Temperature (°C)	168	204	304	122	168	154
Coolant Inlet Temperature (°C)	51.7	43.0	49.0	47.2	48.9	40.0
Coolant Exit Temperature (°C)	74.7	57.0	72.0	53.3	56.7	47.0
Heat Fluxes (W/cm ²)						
Average	185	130	245	52	120	110
Maximum	700	410	387	189	418	260
Plate Thickness (mm)	2.54, 1.27, 2.03	1.27	1.27	1.27	1.27	1.65, 1.27, 1.65
Flow Velocity (m/sec)						
Average	14.6	9.1	16.2	9.8	11.7	10.0
Maximum	18.3	10.4	16.2	11.6	12.4	12.2
Core Pressure Drop (MPa)	0.69	0.30	0.76	0.17	0.17	0.28

* Shutdown data included for comparison

3. STRESS ANALYSES OF FUEL PLATES

The following is a summary of the analytic approaches that have been used in estimating the stresses to be expected in reactor fuel elements during normal operation.

3.1 ATR Reactor

The ATR reactor core consists of 40 fuel elements arranged in a serpentine annulus configuration which provides 4 inner flux trap positions, four side flux trap positions and one center flux trap position.⁶ The individual fuel assemblies are 45° annular segments of a circle with an inner radius of 81 mm and an outer radius of 132 mm and contain 19 plates (Fig. 1). The overall length of the fuel plates is 1.26 m. The fuel plates are 1.27 mm thick overall with 0.38 mm cladding on each side of the fuel meat. The fuel meat is UAl_x dispersed in type-1100 aluminum (1.6-1.7 gU/cm³), and the cladding is type-6061 aluminum. As shown in Table A.5-1, the ATR has the highest power density of any U.S. research and test reactor, with a peak heat flux of 700 W/cm² and a core pressure drop of 0.7 mPa. It is currently operating on a 45 day fuel cycle with a peak fission density of 2.3×10^{21} fissions/cm³. Based on prior experience with the MTR and ETR reactors, it was recognized that operating under these conditions would require careful fuel element design and thorough testing.

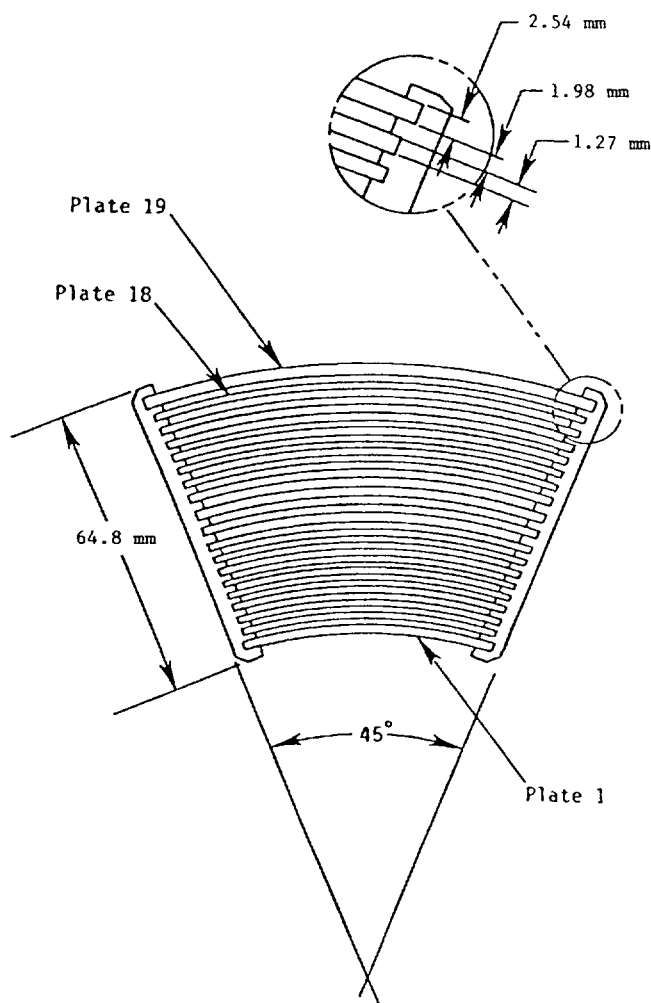


Figure 1 Cross Section of ATR Fuel Element

The original analysis done for the ATR fuel elements⁷ was basically a hand calculation method which considered only the two outermost fuel plates in a fuel assembly (plates 18 and 19) located in the highest power density region of the core. The assumptions used in these calculations were:

1. The fuel plates were considered to be homogeneous aluminum. That is, mechanical properties of the cladding were used for the whole plate, including the fuel meat.
2. The plate temperature difference was assumed to be one dimensional in the azimuthal direction.
3. The axial fuel plate elongation due to thermal expansion was assumed to be restrained only by the fuel element side plates.
4. Fuel plate failure was assumed to occur when the azimuthal stress reaches the yield strength in the plate center region.

In the ATR fuel, axial thermal stresses are produced in the fuel plate because its average operating temperature is about 110°C hotter than the assembly side plates. Furthermore, the neutron flux peaks at the outside edge of the fuel assembly, producing the highest power density and fuel temperatures in the plates close to where it joins the side plate, rather than the center.

Azimuthal stresses are generated in the fuel plate because of differences in channel flow characteristics as well as the temperature gradients. Differential hydraulic pressures are caused by differences in entrance and exit losses in adjacent channels of different thicknesses. The largest potential pressure differential occurs on the innermost plate (plate 1) or the outermost plate (plate 19) because an accumulation of manufacturing tolerances can create a large difference in channel thickness on the outside of these two plates. Plate 19 has a much larger radius and arc length than plate 1; therefore, bending stresses and transverse plate deflections will be much greater for plate 19. Since the maximum deviations in interior channel thicknesses are less than for the exterior coolant channels (channels 1 and 20) the potential pressure differences across the interior plates (2 to 18) are smaller than those for plates 1 and 19. The interior plates must be analyzed, however, since they are 1.27 mm thick, while plate 19 is 2.54 mm thick and plate 1 is 2.03 mm thick. Plate 18 has the largest arc length of the interior plates; consequently, it is potentially the critical interior plate with respect to azimuthal stress. The largest axial thermal stresses will also occur in plates 18 and 19 because they are hotter than the remaining plates and receive the same elongation restraint from the cooler side plates. Therefore, these two plates are the only ones that need be analyzed to define the limiting cases.⁷

The input pressure and temperature differentials for stress calculations were obtained for several different channel configurations using the MACABRE computer program, which was written specifically for ATR fuel element geometry. The calculated maximum fuel plate azimuthal stress of 2.19 mPa was found to occur at the exterior surface of plate 19 of the peak power element. This is well below the yield strength of type 6061-0 aluminum of 50.5 mPa at the plate surface temperature of 180°C. The calculated pressure differential across plate 19 was 30.6 kPa, toward channel 20. In performing these calculations it was found that only 9-36% (depending on the thickness) of the plate section modulus was provided by the fuel meat. Therefore, it was concluded that assuming the fuel meat had the same mechanical properties as the cladding introduced little error. The calculated axial thermal stresses exceeded the yield strength of the type 6061-0 aluminum over small regions for

the peak power element. However, since yielding occurs near the support (due to slipping in the swaged joint at the side plate) and tends to relieve these stresses, this was considered to be acceptable.⁷

Currently the two criteria used in the operation of the ATR reactor are: (1) the axial thermal stress should remain below the yield at the plate mid-point, although it may exceed yield near point of attachment to the side plate, and (2) the azimuthal stresses due to temperature and hydraulic forces should remain below the yield point. These have proven in practice to be satisfactory, as no failure due to buckling has occurred while operating within these constraints.

3.2 ETR Reactor

Fuel elements for the ETR consist of 19, 1.27 mm thick, flat plates 7.24 cm wide by approximately 90 cm long. The fuel meat is a UAl_x composite (0.95 g U/cm³) clad with 1100 ~ H12 aluminium. The fuel plates are assembled into the side plates by roll swaging; the spacing between plates is 2.74 mm. Like the ATR, the side plates of the fuel element are slotted to relieve pressure differentials between plates.

The analysis used to estimate whether or not the ETR fuel plates will buckle under normal reactor operation is somewhat different and less elaborate than that outlined above for the ATR. Basically the approach was to use the formula which describes the critical stress level in a flat plate prior to buckling based on classical plate theory.⁸ The analysis, which did not include consideration of hydraulic forces, established that the yield stress represented the critical stress for buckling. Therefore the approach used for the ETR plates is to limit the maximum compressive thermal stress computed at nominal operating temperatures, plus two standard deviations, to less than the lowest yield stress expected in irradiated fuel plates. The results showed that the fuel plates, with properties typical of irradiated fuel and operating at 204°C, can withstand a maximum average temperature differential of 55°C between the side plates and the fuel plates, and an approximately 22°C maximum temperature differential between the hottest fuel plate and the average of all other plates. It was stated that this method assures that ETR fuel plates will not exceed the buckling criterion, with 95% certainty. Furthermore, since the buckling criterion is conservative for a swaged joint construction, the probability of buckling is even smaller when using this approach.

The ETR has operated under conditions more severe than this a number of times with no apparent permanent plate deformations unless the fuel plates were mechanically pinned to the side plates. When a mechanical joint was made by pinning, which allows no relative motion between the fuel plates and the side plates, some fuel plate buckling did result. The ability of the fuel plate to slip in the swaged joint relieves the constraint which causes the buckling. The actual approach that has been used in operating the ETR is to keep the temperature in the hottest plate below that at which there have been problems with plate buckling, so heavy reliance is placed on reactor operating experience.⁹

4. FUEL ELEMENT PROOF TESTING

4.1 Hydraulic Flow Tests

As stated, the tolerance on coolant channel spacing of 2.0 mm is very critical in the ATR, not only because of heat transfer considerations,

but because of hydraulic pressure forces which can act on a fuel plate separating two coolant channels which are of unequal width. The two external coolant channels, numbers 1 and 20 (Fig. A.5-1) are bounded on one side by fuel plates and either by the flux trap baffle (channel 20). The core components are arranged to give a nominal 2.74 mm channel 1 and 2.87 mm channel 20 thickness. However, because of the tolerances involved in positioning the assemblies in the fuel annulus, these external channels vary considerably. A statistical evaluation of the tolerances was performed and this indicated that channel 20, the more critical of the two external channels because of the greater unrestrained fuel plate span, had a 2σ maximum thickness of 4.44 mm. Therefore, to withstand the hydraulic forces developed across these two external fuel plates, the thickness of plate 1 was increased to 2.03 mm and plate 19 was increased to 2.54 mm.

Isothermal hydraulic tests of the first ATR fuel assemblies¹⁰ indicated that, even with the thicker outer fuel plates (1 and 19) and close fabrication tolerances, lateral pressures between coolant channels were excessive.

These pressures were relieved by putting slots in the fuel assembly side plates at various locations. The slots allow the coolant to flow between channels and partially equalize pressures. An extensive series of pre-operational out-of-pile flow tests with the fuel assemblies modified in this fashion indicated that the maximum hydraulic pressure force occurred across plate 19 (between channels 19 and 20) approximately 86 cm above the lower edge of the 126 cm long fuel plate.¹⁰ This pressure differential was 40 kPa at 115% flow and is well within the fuel plate's capability to withstand without buckling at operating temperatures.

Hydraulic flow tests still play a predominant role in assuring reliability of fuel elements in the ATR core. All new fuel elements are tested at 130% of flow at a temperature of 175°C before being placed in the reactor core. Similar procedures are followed for the ETR reactor.

4.2 Differential Thermal Expansion Tests

As part of the development program for the ATR fuel, tests were run to determine if the compressive thermal stresses, discussed above, resulting from temperature differences between the aluminium clad fuel plates and the cooler side plates would distort or ripple the fuel plates.¹¹ The fuel plates are about 1.2 m long and of various widths ranging from 5.6 to 10.2 cm. To simulate the stress condition across the width of a fuel plate, steel bars were clamped to the edges of the individual test plates. A bar material was selected with a thermal expansion coefficient sufficiently different from the aluminum fuel plate to cause a compressive stress in the restrained plate when heated in a furnace. Two different size plates were tested; plate 18 with a 13.3 cm radius of curvature and plate 2 with a 8.13 cm radius (see Fig. A.5-1). The fuel plates, restrained by the steel bars, were placed electrically heated furnaces, and surface displacement measurements were made at 150°, 205°, and 260°C. These measurements were taken at 2.5 cm increments along the length down the axial centerline, and at the two 1/4 point intervals halfway between the center and the edge of the plate.

The results of these tests showed that there was no rippling of the plates, but merely an increase in the overall end-to-end curvature of the plate over that which existed at room temperature. In contrast, a number of flat plates tested in a similar manner exhibited a distinct ripple pattern with a wave length approximately equal to the plate width and with a maximum peak-to-peak surface displacement of 3.0 mm. Thus, this series of tests gave

confidence that the prototype ATR fuel assembly would withstand the expected thermal stresses and that the curved plate design provided considerably greater stability than a flat plate.

5. FUEL BEHAVIOR OVER DURATION OF FUEL CYCLE

5.1 Irradiation Effects

Irradiation experience with aluminum clad, UAl_x -aluminum platelets and full size ATR fuel elements indicates that irradiation growth is essentially all in the thickness (1.27 mm) dimension.¹²

Post irradiation measurements with ATR fuel elements indicated that there was only a 0.51 to 0.76 mm increase in the length (126 cm) at volumetric increases of 3 to 5%. This is consistent with experience in other high power density research and test reactors in that there have been no particular problems with irradiation induced volumetric or dimensional changes causing structural instability in the fuel plates. In spite of relatively large volume increases up to 6%, the measurements of fuel plates after irradiation have shown insignificant increases in length and width; all the increase has been in the thickness dimension. This has been explained by the fact that the clad material has a higher strength than the fuel meat in the length and width directions. Therefore the fuel meat flows plastically at operating temperatures when its compressive yield stress is reached, well below the tension yield stress of the cladding. The cladding, however, produces very little restraint in the thickness direction, and plastic flow of the fuel meat occurs in this direction.¹²

5.2 Buildup of Oxide Film on Fuel Plates

At the beginning of the ATR fuel cycle, the fuel plates heat up to a temperature 150-200°C while the side plates, heated by gamma absorption, operate at approximately 100°C. As discussed above, this temperature differential results in a compressive loading on the fuel plates which creates a potential for buckling. During prolonged irradiation in the reactor, the relatively hot fuel plate cladding reacts with the primary coolant to produce a hydrated aluminum oxide layer on the plate.¹³ This layer, which acts as a thermal insulator, causes the maximum plate temperature and thermal stress to initially increase over the fuel cycle life. Eventually the decreased power generation due to increased fuel burnup in high power regions overrides the corrosion layer effect, causing a peaking of the temperature at some point in time over the fuel cycle. Actual experience over the 700-900 hour ATR fuel cycle duration has shown that the oxide film is self-limiting in thickness, such that a maximum thickness of approximately 13-25 μm occurs after about 400 hours¹⁴. The overall effect of this film buildup is combination with increased fuel burnup is that the maximum fuel temperature increases from about 180°C to approximately 215°C. Because peak heat fluxes are 700 W/cm^2 , and the thermal conductivity of the oxide layer is only 0.022 $\text{W}/\text{cm}^\circ\text{C}$, the buildup of the oxide layer is an important parameter in determining the peak thermal stresses in the ATR fuel plates during operation. This same phenomenon occurs in the ETR reactor.

REFERENCES

1. R. J. Beaver and J. E. Cunningham, "Recent Developments in Aluminum-Base Fuel Elements for Research Reactors," Paper No. 4, pg. 40, TID-7559 Part I, Proceedings of Fuel Element Conference at Gatlinburg, TN, May 14-16, 1958.
2. Westinghouse Staff Report on WTR Fuel Element Failure, April 3, 1960, WTR-49 (July 7, 1960).
3. F. R. Keller, "Fuel Element Flow Blockage in the Engineering Test Reactor," IDO-16780 (May 10, 1962).
4. R. A. Costner, Jr., "MTR Fission Break Incident," Nuclear Safety 4, 4 (1963).
5. M. H. Bartz, "Performance of Metals During Six Years Service in the MTR," P/1878 U.S.A., Proceedings of the Second International Conference on the Peaceful Uses of Atomic Energy, Geneva, 1958.
6. D. R. de Boisblanc and S. Cohen, "Safety Analysis Report, Advanced Test Reactor," IDO-17021 (April, 1965).
7. C. A. Moore, "Calculations of Pressure Induced and Thermal Stresses for Advanced Test Reactor Fuel elements," IN-1303 (August, 1969).
8. "Design Basis Analysis of ETR-Phase II," Tech. Specs. CI-123 (February, 1972).
9. J. L. Liebenthal, EG&G-INEL, personal communication.
10. M. L. Griebenow, "Isothermal Hydraulic Measurements in Fuel Elements in ATR Core," Idaho Nuclear Corp. (September, 1968).
11. R. E. Deville, "Differential Thermal Expansion Tests on Advanced Test Reactor Fuel Plates," IDO-24461 (October 15, 1963).
12. M. L. Griebenow, "ATR Extended Burnup Program," ANCR-1015, Aerojet Nuclear Co. (November, 1971).
13. M. L. Griebenow and G. H. Hanson, "ATR Core-1 Thermal-Hydraulics Tests Results," TR-727, INEL (September, 1976).
14. G. N. Fillmore, EG&G-INEL, personal communication.

Appendix I-5.2

HYDRAULIC TESTS ON DUMMY FUEL ELEMENTS FOR JAERI REACTORS

T. SATO, K. SIMIZU, K. KUROSAWA, M. BANBA,
S. YAMAGUCHI, J. TSUNODA

JRR-2 Section,
Japan Atomic Energy Research Institute

F. NAKAYAMA, Y. ITABASHI, H. KANEKAWA,
R. OYAMADA, M. SAITO, T. NAGAMATSUYA

JMTR Section,
Japan Atomic Energy Research Institute

Tokai-mura, Naka-gun, Ibaraki-ken,
Japan

Edited by K. Tsuchihashi

Abstract

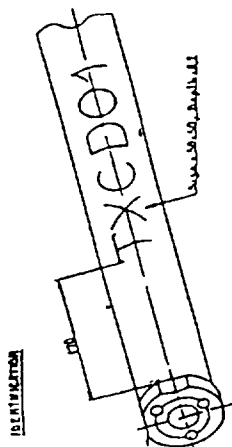
For the JRR-2 reactor and the JMTR reactor, dummy fuel elements using depleted uranium were fabricated and hydraulic tests were carried out for two purposes. One purpose was to confirm fabrication techniques and inspection methods in order to establish reasonable specifications for succeeding MEU fuel elements. The other purpose was to confirm the integrity of the fuel elements under normal and abnormal hydraulic conditions.

Along the RERT program, JAERI selected the steady and available solution to convert the cores of the JRR-2 and JMTR, although it did not yet meet the goal of the program. This is to use of MEU (45 % enriched) fuels with UAl_x dispersion type instead of current HEU (93 % enriched) fuels with U-Al alloy type. As the unique domestic fuel fabricator announced to retire from the supplier of research reactor fuels, the contracts had to be made between any of foreign fabricators. Consequently, not only the qualification of new type fuel but also the qualification of fabricator became the item of the licensing procedure.

For each reactor of the JRR-2 and the JMTR, the dummy fuel elements using depleted uranium were fabricated and the hydraulic tests were carried out for two purposes. One is to confirm fabrication technique and inspection methods resulting to the establishment of reasonable specifications for the succeeding MEU fuel elements. The other is to confirm the integrity against normal and abnormal hydraulic conditions.

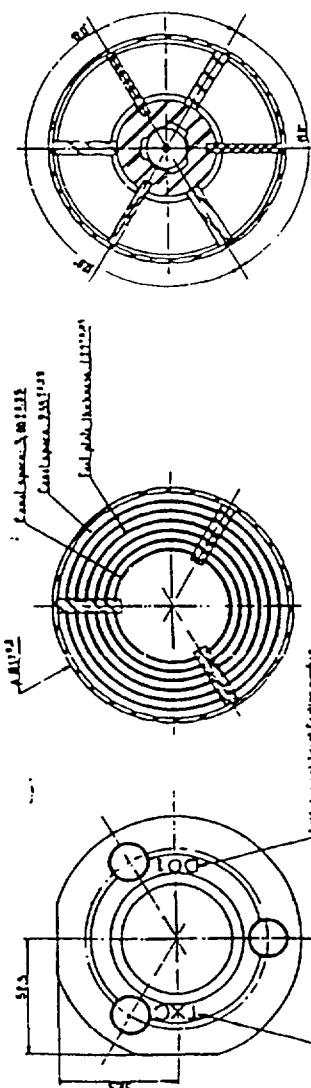
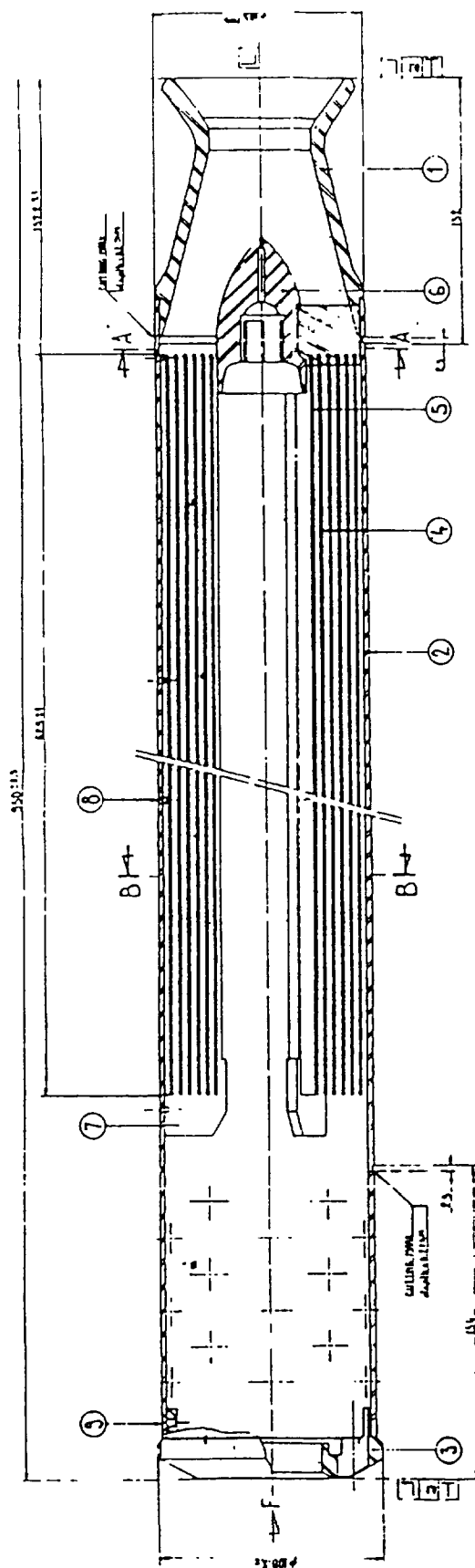
These tests were included in the activities in Phase B of the ANL-JAERI Joint Study on the RERT program.

This paper describes briefly the fabrications and the experiments.

[illegible]

III

- 1 - Mark "L" means perpendicular to the center line.
- 2 - Eccentricity of the fuel element shall be kept within 3 mm
- 3 - Fuel piece shall have suit. as confirmed with the fuel element manufacturer as necessary.
- 4 - 75 sharp edges shall be removed



11. Section

Fig. 1 Specification of manufacture

The JRR-2 is a 10 MW research reactor moderated and cooled by heavy water. The core has been operated by 17 MTR type and 7 cylindrical type fuel elements with 93 % EU arranged in hexagonal pitch.

In the MEU core we intend to use only the cylindrical elements to extend the cycle length by its larger reactivity worth and increase the capsule irradiation capability by utilizing the central channel of each element. In one cylindrical element, 15 fuel plates compose coaxial 5 cylindrical layers connected by 3 support plate. These layers are protected by an inner and an outer tubes. No change in geometry had been intended. It happened successively twice just after making the contract between JAERI and the CERCA in France for the fabrication of one dummy fuel element for hydraulic test. That is, we had breakage of the whole screws to fix the fuel support plates to the outer tube of a cylindrical element in the current core. It resulted in the floatage of the fuel plate group (support plates and fuel plates). It was concluded that the thermal stress due to the difference of temperature between the support plate and the outer tube broke the connecting screws.

Fabrication

By reflecting on the above defect, the supporting system of the dummy element was modified so as to fix all of lower ends of plate group and outer tubes to the lower adapter and release their upper ends for thermal expansion. The specifications for fabrication are shown in Fig. 1.

The following items were inspected at the site;

- (1) Material analyses and mechanical properties
- (2) U and U-Al analyses
- (3) Determination of UAl_3 - UAl_4 percentage
- (4) Uranium weight percentage in fuel core
- (5) Fuel core void content
- (6) Micrographs
- (7) Tensile test
- (8) Dimension of structural parts
- (9) Surface contamination

Results of the above inspections were satisfactory.

Hydraulic Tests

A diagram of measurement device constructed for this experiment is shown in Fig.2. Velocity was measured at each outlet fuel plate by a three-hole arrow head type yaw meter. An example of measured velocity profile is given in Fig. 3. Figure 4 shows a comparison of the measured and calculated velocity distributions. The calculation was made by solving hydro-dynamic equations in the fuel plates channel. The calculated profile agrees well with the measured one.

The endurance test was also performed during the continuous 3,000 hours under 1.3 times of the nominal flow. The visual inspection and the dimension measurement did not find any anomaly.

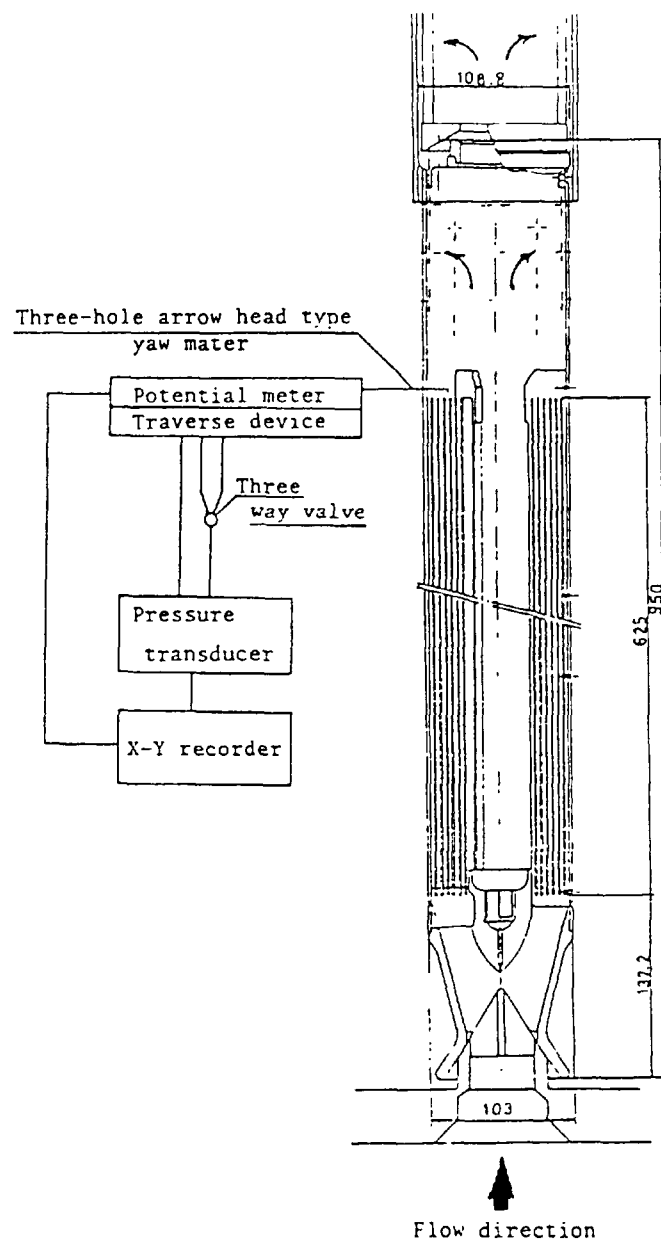


Fig.2 Diagram of measurement device

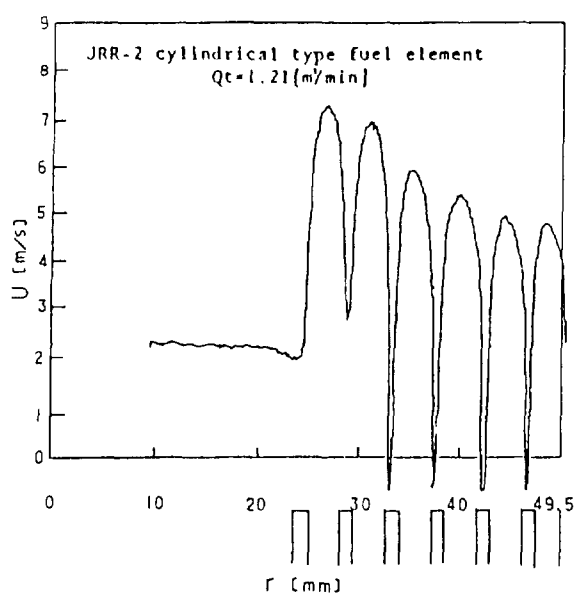


Fig.3 Measured velocity profile

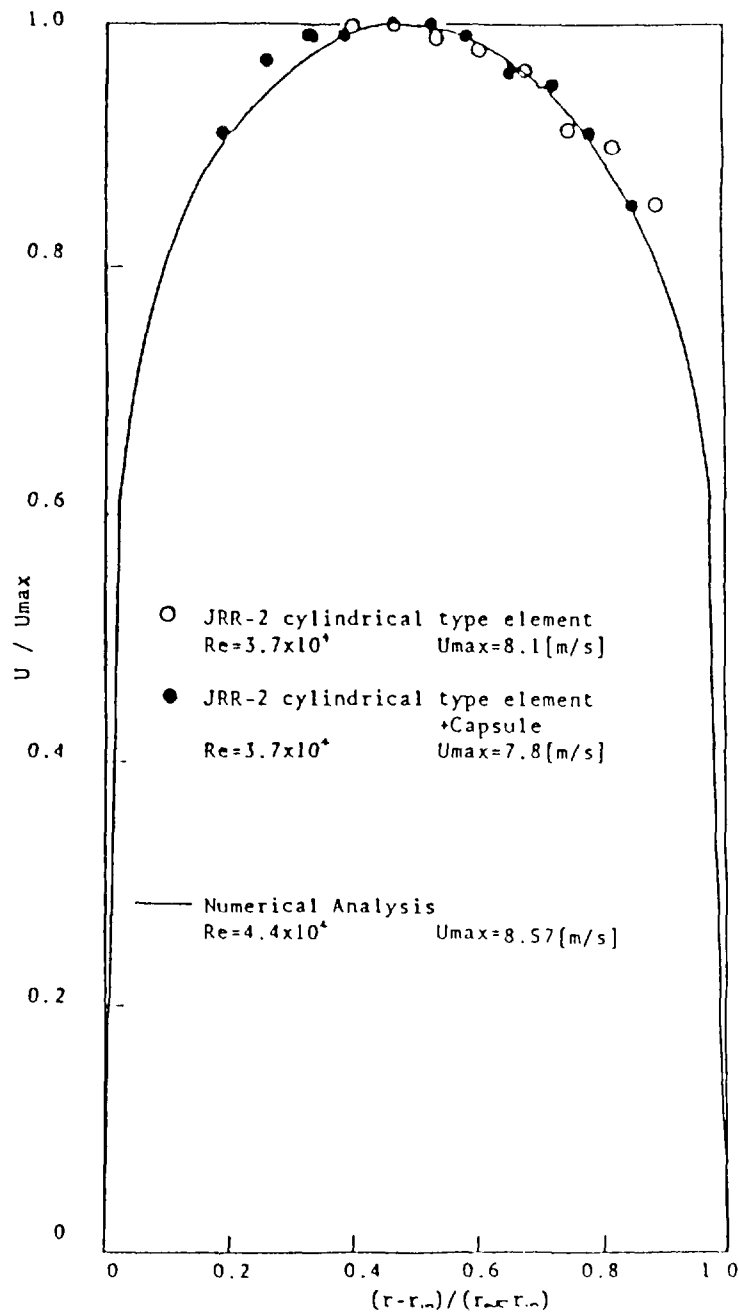


Fig.4 Measured and calculated velocity profiles

Vibration test was performed for possible combinations of the element and two kinds of irradiation capsules under several flow conditions. Results showed that the proper vibrations of the fuel plate group and the outer tube were different and no resonant vibration would occur under any flow condition.

The data obtained in these tests will be used as fundamental data for the SAR.

JMTR

The JMTR is a 50 MW MTR type reactor moderated and cooled by light water. Two standard fuel elements and one fuel follower with depleted uranium of 1.6 gU/cc were ordered to the NUKEM in FRG so that they might have the identical mechanical properties with those of the JMTR MEU (45%) fuels.

The hydraulic tests were designed to (1) measure the coolant velocity distribution between fuel plates, (2) confirm the strength of the standard fuel elements by exposing them in the hydraulic forces increased to 140 % of the nominal flow, (3) determine the critical velocity, and (4) confirm withstanding of the fuel follower in drop tests.

Specifications

No alteration in the dimensions of MEU elements from those of HEU was intended because it seemed impossible to complete this time-consuming optimization within the rather short period allowed. However, it became evident that minimum cladding thickness of MEU by powder metallurgical technique was thinner than that of HEU by alloying technique because uranium-aluminum grain in the dispersed fuel core projects into the aluminum cladding. To mitigate this problem, several efforts such as alteration of powder grain size and cladding materials were attempted, but the results were not improved yet. Consequently, the specifications for cladding and core thickness were changed as follows, after confirming that no problem would occur concerning the corrosion margin, the neutronics and the hot spot factor in the thermal hydraulics,

		Cladding Thickness			Core thickness		
HEU	nom	0.385 mm	min.	0.36 mm		0.50 ±	0.03 mm
MEU	ave.	0.36 mm	-	0.41 mm	ave	0.50 ±	0.03 mm
	min.	0.30 mm at projected point					

The cladding and core thickness were inspected in the following way; Three fuel plates were selected out of each roll batch, and from each plate three sections in the width direction and two sections in longitudinal direction were chosen as specimen. After abrasion of a section, cladding and fuel core thickness were measured by a microscope every 1 mm along the width of a plate, 60 mm, to evaluate the average value and to find projection points. This inspection was continued through the trials to improve the minimum cladding thickness. Totally, more than 45 sections were inspected.

Test Methods

The tests were conducted in the out-of pile single element hydraulic test loop. A sketch of the loop is shown in Fig. 1. The coolant velocity between fuel plates was measured with one set of arrow-head-type Pitot-tubes installed at the outlet of coolant channel. A sketch of the installed Pitot tubes is shown in Fig. 2.

Test Results

The results of the coolant velocity distribution measurement among the coolant channels of both standard and fuel-follower elements are

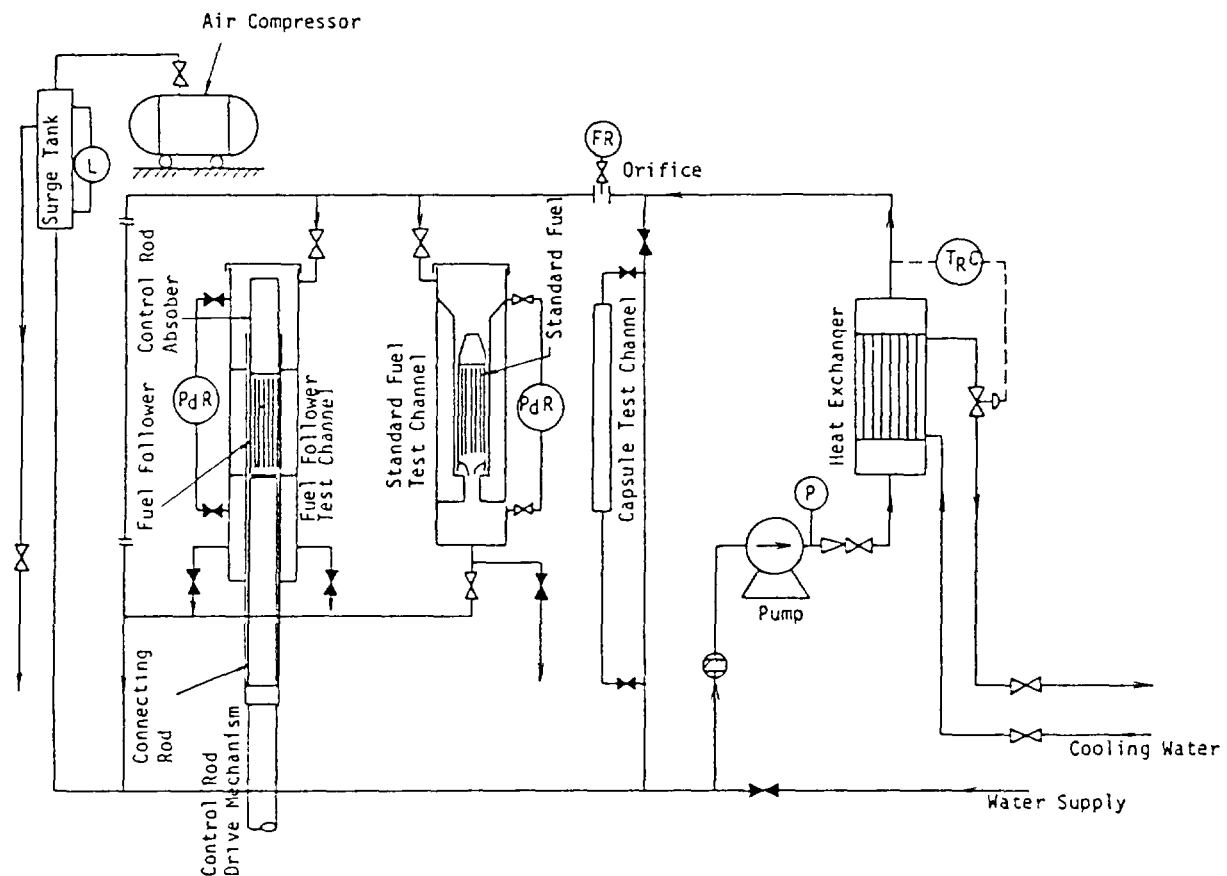


Fig.1 JMTR Hydraulic Test Loop.

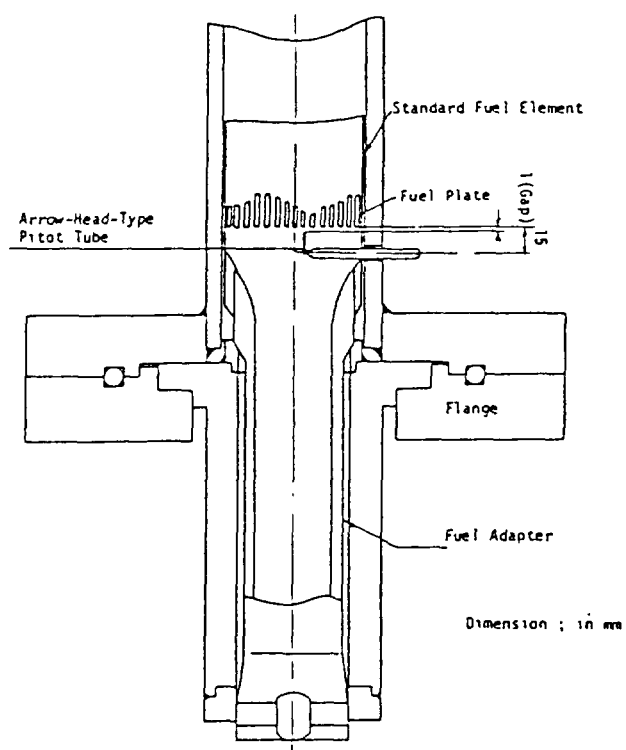


Fig.2 Installation of Pitoh Tube.

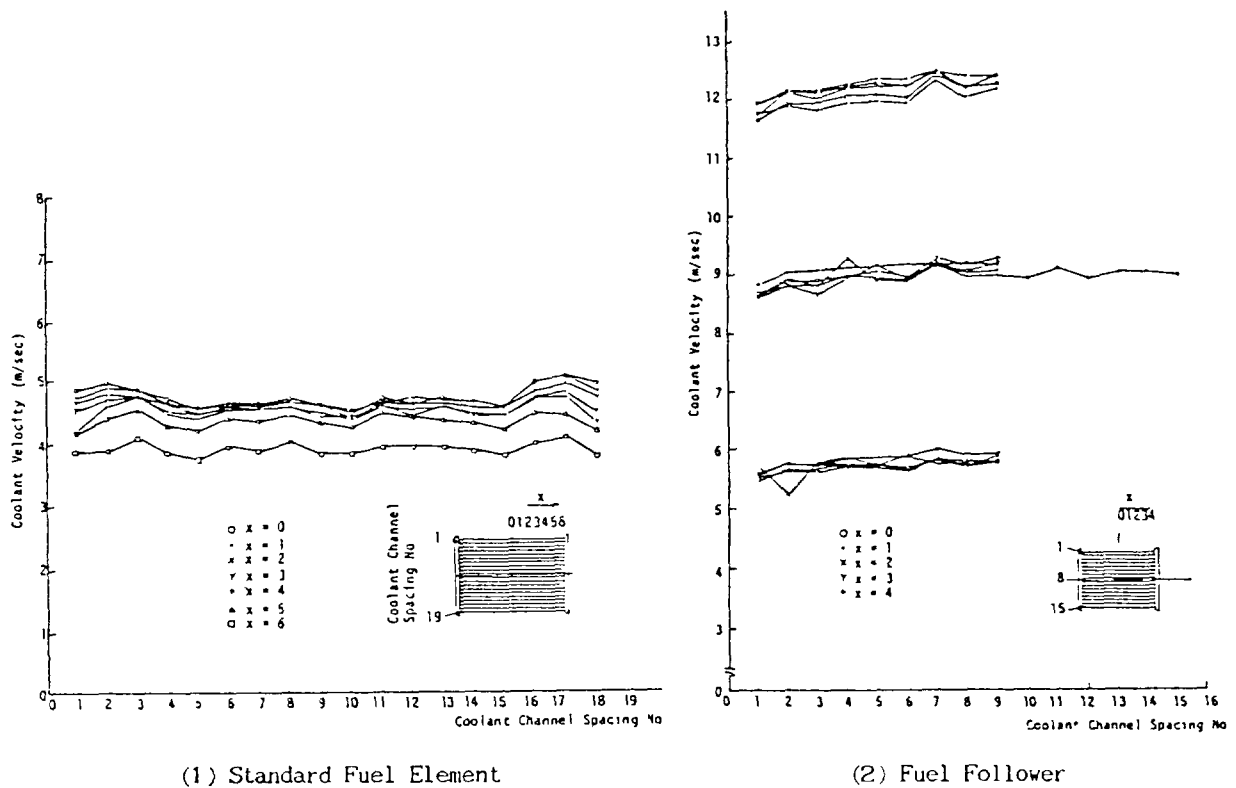


Fig 3 Coolant Velocity Distribution

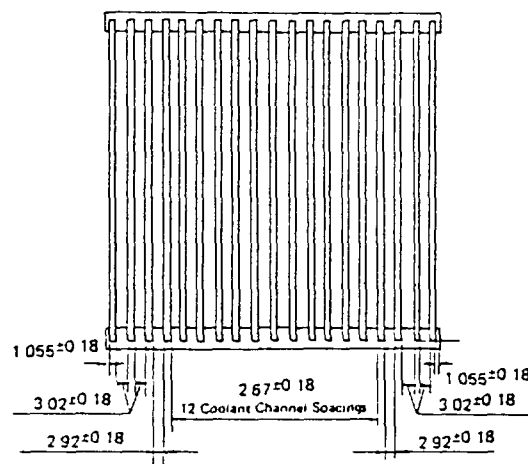


Fig 4 Coolant Channel Spacings

shown in Fig. 3. As shown in Fig. 4, the standard fuel element reveals good equalization in the coolant velocity distribution, because the coolant channel thickness are varied by layer to obtain uniform coolant velocity as shown in Fig. 4.

The standard fuel element was strong enough under the 6 hour test condition of 140% (14 m s^{-1}) of the average nominal velocity. This value was chosen so that this condition might cause the double value in pressure drop compared with the nominal flow.

The critical velocity for MEU fuel is estimated approximately 18 m/s on the assumption that fuel core has the same strength as the cladding material. The critical velocity is estimated conservatively to be approximately 15 m/s in disregard of the strength of fuel core, because the mechanical properties of fuel core were not clear. The results of the critical velocity test show that MEU fuel was withstanding against hydraulic force of at least 20 m/s which is the maximum velocity of the test system.

The drop-test for the dummy fuel-follower was repeated up to 100 times under the condition that the downward coolant flow was increased to 140% (14 m/s) of the nominal velocity. Further drop tests were performed up to 20 times each at 160 and 180% of nominal velocity (16 m/s and 18 m/s).

After all the tests, the fuel elements were visually inspected and their coolant channel spacings were measured with a strain gauge device. Both standard and fuel-follower elements were proved to be withstanding under the above hydraulic test conditions.

Conclusions for the JMTR elements

- (1) While the minimum cladding thickness for the dummy elements was specified to 0.30 mm, it seemed difficult to apply this standard to the MEU elements. It was decided to loosen the standard to 0.25 mm at projected points of UAl_x grains.
- (2) Integrity of dummy fuels was enough under the hydraulic test conditions which were more severe than will be encountered in the normal operation of the JMTR.

**'CAMEL' — FRENCH LEU FUEL FOR RESEARCH REACTORS
WITH EMPHASIS ON THE OSIRIS EXPERIENCE
OF CORE CONVERSION**

COMMISSARIAT A L'ENERGIE ATOMIQUE

Centre d'études nucléaires de Saclay,
Gif-sur-Yvette, France

Abstract

Key aspects of the design, development, and qualification of French LEU "Caramel" fuel are discussed. These aspects include descriptions of the fabrication steps, the quality control procedures that are employed in fuel fabrication, and the extensive qualification program to determine first the technological limits and then the safe and reliable operating ranges for this type of fuel.

Experience in utilizing "Caramel" fuel in the high performance OSIRIS reactor is emphasized. Necessary adaptations of the plant primary cooling circuit are described along with operating experience, changes in the experimental conditions, and possible application in other research reactors.

1. INTRODUCTION

One of the various activities carried out in France concerned with the design, fabrication and development of nuclear fuels was the development by the CEA of a plate type fuel (Caramel fuel). A Caramel fuel element is in the form of a plate consisting of two tight covering zircaloy sheets in which the UO_2 platelets are confined themselves within the network of a zircaloy grid. The plane geometry provides an effective means of overcoming the drawback of poor uranium oxide conductivity, and makes it possible to combine high specific power with low fuel temperature.

The different materials used in the Caramel type fuel assemblies i.e. UO_2 and Zr, are very well known after their extensive use in LWR's. Their physical properties, in pile behaviour, manufacturing features etc... are well mastered, and will therefore not be dealt with in this presentation.

The chief advantages of this fuel are the following :

- (1) It is a very low enriched fuel. It can be used in research reactors demanding high volumetric powers and neutron fluxes, with a required enrichment significantly lower than 20 % ^{235}U .

The difference between the densities of UO_2 matrix and U-Al, 10.3 and 1.6 g/cm³ respectively, leads to a higher uranium charge, making it possible to reduce the enrichment to between 3 and 10 %.

- (2) A second advantage of the Caramel fuel stems from its operating safety. Owing to its dispersion, any loss of tightness only puts a small amount of fissile material in contact with the coolant, thus limiting any contamination of the primary circuit.

Another safety factor is the operating temperature, which is considerably lower than the temperature at which fission gases are liberated.

The earliest research conducted at the CEA was directed towards applications in power, heat and naval propulsion reactors, and used thick (4 mm) Caramels owing to the low volumetric powers required.

The thin Caramels investigated since 1977 as part of the non-proliferation programme (INFCE) found their application in research reactors for which volumetric power levels are very high (mean value about 1700 W/cm³, maximum value 4300 W/cm³).

Thanks to the use of the low-enriched uranium Caramel fuel, the Commissariat à l'Energie Atomique proceeded to convert the core of the high-performance research reactor Osiris, at Saclay. The new Caramel fuel core has operated successfully since December 1979.

The Caramel type fuel takes advantage of the experience gained in LWR operation which alleviates most uncertainties and additional R and D effort, contrary to the use of less-known fuels like U-Al, U_3O_8 -Al or U_3Si -Al.

The following table summarizes the main characteristics of the reactors under-operation or in project (Thermos project) using Caramel type plate fuel elements.

Reactor	Power (MW)	Caramel thickness (mm)	Temperature of clad (°C)	Coolant pressure (bar)	Mean specific power (W/cm ³)	Maximum specific power (W/cm ³)
pool reactor (Osiris)	70	1,45	140	3	1 640	4 300
heat generator (Thermos)	100	2,25	160	11	275	1 070
ISIS	0,7	1,45	9,5	1,5	16	43

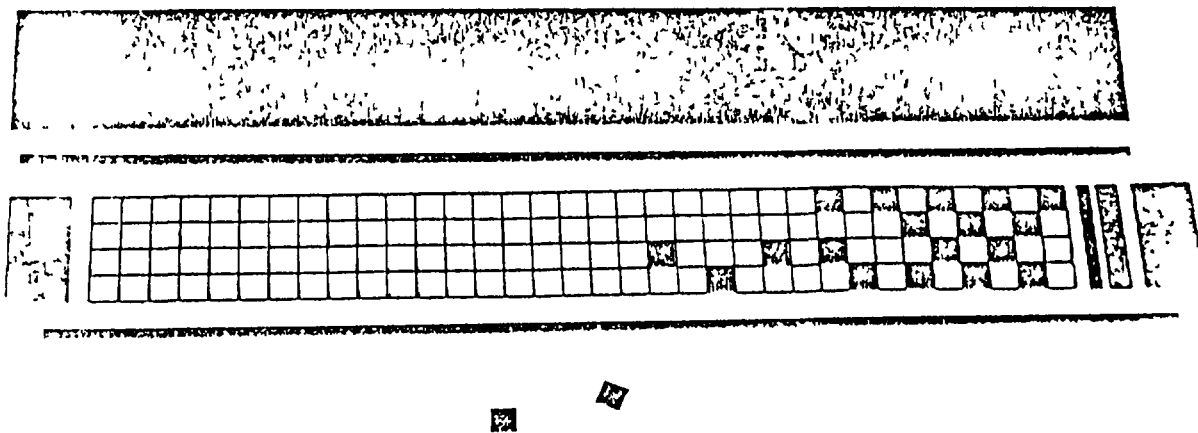


FIG 1 Components of a Caramel plate

2. DESCRIPTION

The Caramel type Osiris fuel element is in the form of a plate 700 mm long, 80 mm wide and 2,25 mm thick. Figure 1 shows the different components of a Caramel plate of the Osiris reactor. The sintered UO_2 fuel is in the form of a square-section parallelepiped measuring 17,1 x 17,1 mm and 1,45 mm thick. It is placed in a regular array within a square-pitched grid and confined between two zircaloy sheets. This assembly, fitted with zircaloy edge and end pieces, undergoes a series of welding operations designed to guarantee the perfect tightness of each UO_2 platelet to the exterior and to its neighbours.

Simultaneously, good contact is achieved between the oxide and the cladding. The fuel assemblies consist of several plates (14 or 17) in parallel position, held rigidly by slotted side-plates. They are equipped with a foot for water supply and a handling head.

The Caramel fuel is distinguished from the standard fuel pin by :

- . its plane geometry,
- . the absence of free volume,
- . good oxide/clad contact (no clearance)

The special features of the Caramel fuel impose specific operating conditions. Owing to the absence of voids (except for the open porosity of the fuel), the temperature of incipient fission gas evolution must never be exceeded. To achieve this condition, it is essential to guarantee excellent oxide/clad contact for the fuel element from the very beginning and to maintain this throughout its service life.

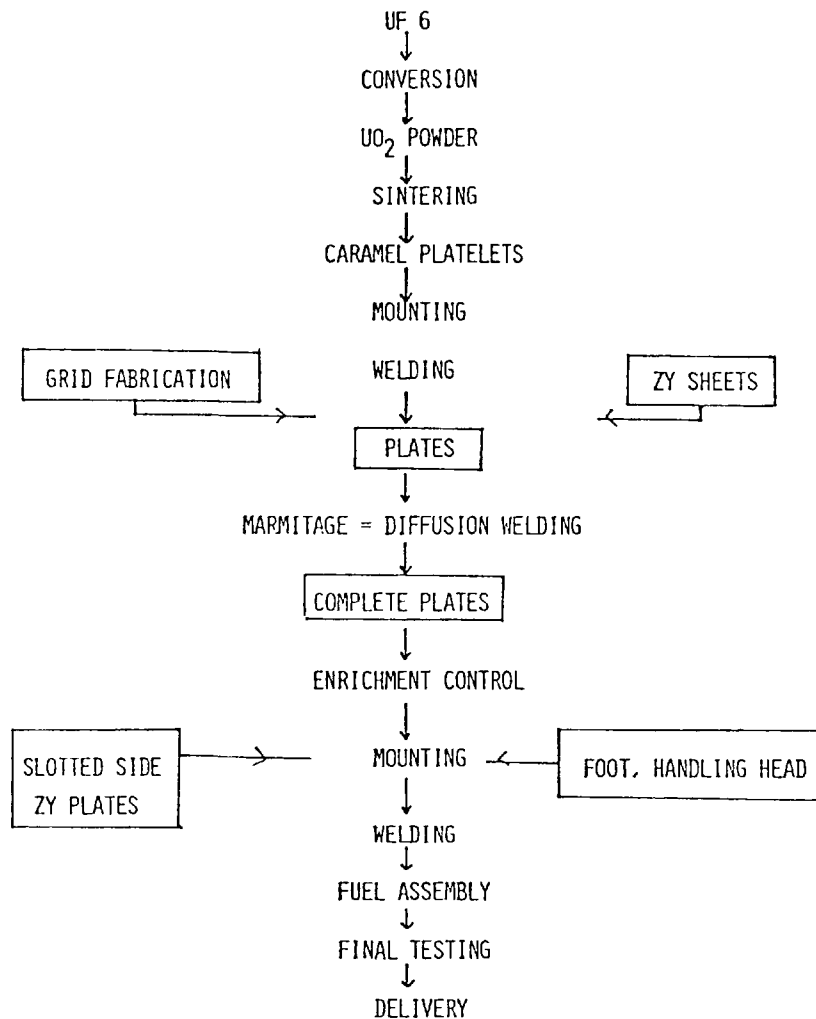


FIG. 2.

3. FABRICATION AND QUALITY CONTROL

3.1 Fabrication

The Caramel fuel is fabricated in workshops belonging to the CEA or its subsidiaries. Some components such as the zircaloy sheets, castings and machined parts are supplied by industry. The fabrication sequence is shown in Figure 2.

Fabrication is subdivided into the following phases :

3.1.1 Fabrication of oxide platelets (Caramels)

These platelets are fabricated by sintering UO₂ powder obtained by the wet method. The process employs the double normal cycle. The material is sintered under hydrogen at a temperature near 1600°C. The density of the sintered Caramel is equal to 94 % of the theoretical density.

It should be noted that the fabrication of Caramel fuels benefits from the experience gained in this area with PWR fuels.

Deposit of anti-diffusion barrier

Each Caramel is covered by a layer of chromium deposited by cathodic sputtering. This chromium performs the role of a barrier, by preventing the diffusion of oxygen into the zircaloy, that is liable to occur during the diffusion welding operation, also called "marmitage" (marmite = HP cooking pan) and described below.

3.1.2 Plate fabrication

The component parts of a plate are the following (figure 1) :

- . oxide platelets,
- . zircaloy grid obtained by welding zircaloy wires,
- . nickel foot that plays a role with respect to neutrons,
- . zircaloy side pieces,
- . zircaloy end pieces,
- . zircaloy sheet cladding.

The Caramels are placed within the grid cavities. The assembly including the grid with its Caramel load, the side pieces and end pieces is placed between two zircaloy sheets and welded tight. The plate closure operations are performed in the following order.

After resistance spot welding of the different parts, the sides are welded by a resistance seam welding unit.

The end pieces are then welded by electron bombardment welding that also places the plate under vacuum.

The closed plate is transferred to a diffusion welding enclosure and undergoes high temperature (greater than 900°C) and high pressure (≈ 1000 bar) treatment for four hours, also called "marmitage". This treatment guarantees the welding of all zircaloy components and especially between the grids and sheets, by ensuring the separation of each UO_2 platelet and good oxide/clad contact.

This marmitage treatment is followed by a control treatment under vacuum at 700°C.

The rough plates are then machined to the required dimensions. After undergoing the controls described in the next section, they are mounted on side plates. Electron bombardment welding is then used to join the Caramel plates and the side plates.

3.2 Quality control

All the materials and components are required to meet specifications.

Owing to its geometric characteristics and its operating conditions, the Caramel fuel must meet especially severe requirements, corresponding to specific control procedures.

These controls are carried out at all fabrication levels and include :

- . metrology of components and of the assembly (e.g. metrology of channels)
- . enrichment of each fuel platelet,
- . quality of the weld between metal components,
- . quality of oxide/clad contact.

These controls take place during fabrication as follows :

3.2.1 Controls in the fabrication of basic components

UO₂ platelet : metrology (length, width, thickness, density, visual appearance, chromium deposit inspection).

Tolerable surface defects have been defined on the basis of correlations between defect dimensions and the residual clad thickness after diffusion welding.

Zircaloy parts : metrology (surface condition after abrasion)

3.2.2 Controls applied to the finished plate

- . Visual appearance
- . Metrology
- . Checking of the absence of occluded gases, by heat treatment at 700°C under vacuum, with free-standing plates
- . Quality control of welds by micrography and corrosion test
- . Enrichment test

The enrichment test of Caramel plates consists in the determination of the charge of ²³⁵U per unit area by neutronometry. This check offers several advantages :

- . overall checking of various Caramel fabrication tolerances :
 - . enrichment,
 - . uranium content of UO₂
 - . density of UO₂ sinter
 - . Caramel thickness

- . possibility of systematic checking of all platelets making up a fuel plate
- . speed of control in comparison with traditional methods,
- . exact measurement of accounting for fabrication ranges,
- . control of a characteristic (charge of ^{235}U per unit area) of direct use for the calculation of reactor performance,
- . quality control of oxide/clad contact.

The quality of oxide/clad contact appears to be an important parameter in the design of the Caramel fuel. A thermal analysis method by infrared thermovision was developed for this purpose.

Actually it is not used, because the test performed at 800°C under vacuum serves to test the plates in conditions that are more severe than those of operation in a pool reactor. This test has proved highly satisfactory until now.

3.2.3 Control of finished assembly

- . Overall metrology of assembly (passage through a gauge)
- . Metrology of all channels
- . Check of surface pollution

Control procedures and final acceptance are carried out by an organization that is independent of the fuel manufacturer. In addition, a quality assurance system is implemented, covering design, fabrication and tests.

A preirradiation characterization report is written for each fuel assembly. All the data related to the assembly are included in this report :

Data about assembly components : origin, fabrication procedure, mechanical characteristics, measurements, weight, chemical analyses.

Measurement results for each plate.

Remarks after visual examination for each plate.

Results of enrichment control performed on each UO_2 platelet

Measurement results of all water subchannels (a recording is made of each platelet row)

A few examples of data recorded for each fuel assembly and contained in the characterization report are annexed at the end of this paper.

Fabrication experience

Considerable fabrication experience has been gained, because aside from fabrications for experimental irradiations, a large number of assemblies has been fabricated, as summarized below.

Reactor	Number of assemblies	Number of plates	Number of UO ₂ platelets	UO ₂ weight (kg)
PAT	16	576	101 952	1 497
CAP	4	44	13 728	192
OSIRIS	200	3 400	462 400	2 019
TOTAL	220	4 020	478 080	3 708

CAP - Prototype Advanced Boiler. PWR type reactor of a power of 100 MWth, located at Cadarache.

PAT - Land Based Prototype. PWR type reactor used as a prototype for naval propulsion, located at Cadarache.

At present, the fabrication shops have a total capacity of 200 Osiris - type assemblies per year.

4. QUALIFICATION OF CAMEL FUEL

An extensive programme involving experiments and qualification of the Caramel fuel has been undertaken and implemented in a broad range of specific powers and burnups. It was intended to determine initially the technological limits, and then the safe and reliable operating ranges for this type of fuel. This programme includes both parameter tests in irradiation test loops on specimens including a limited number of Caramels, and also irradiations of experimental assemblies carried out in the Osiris reactor and in the CAP and PAT prototype reactors.

The most important features of the programme are then exposed together with the main results obtained.

4.1 T I P programme

An exploratory programme was conducted during the 1965 to 1970 period with the EL 3 reactor at Saclay in order to define the technological limits of this fuel.

Seventeen test samples (containing 5 and 9 caramels) were irradiated at variable burnups and specific powers.

The specific power range explored ranged from 1000 to 3000 W/cm³.
The cladding temperature was between 280 and 340°C.

The results of these test showed that :

- it is possible to reach a burnup of 30000 MWD/T with specific powers as high as 3000 W/cm³ without any deterioration of the fuel. Above 30000 MWD/T, if this specific power is retained, there is a risk that the platelets will swell and release gas. This phenomenon does not necessarily lead to cladding failure.
- if, on the other hand, the specific power is reduced at this stage of the irradiation, a burnup as high as 50000 MWD/T can be achieved without significantly modifying the structure of the UO₂ platelets.

4.2 SILOE programme (1976)

In this programme, two irradiations were performed without any external pressure in the pool reactor Siloé at Grenoble. Two small assemblies, each containing a few samples, were irradiated.

The following irradiation conditions were employed :

Specific power	1060 W/cm ³	and	1500 W/cm ³
Irradiation period	245 days	!	202 days
Burnup	18300 MWD/T	!	25100 MWD/T
Temperature	100°C	!	100°C

Results obtained : Very good in-pile performance was obtained with the assemblies. Their appearance after irradiation was very satisfactory.

4.3 Irradiation programme in the Osiris reactor

As before, experimental test samples each containing few Caramels, were irradiated. The irradiations were carried out in the NaK loop at 300°C with an external pressure of 140 bars. Two series of irradiations were realized :

1973 - 1974 on 3 and 4 mm thick caramels

1975 - 1978 only on 4 mm thick caramels in order to define technological operating limits.

Specimens of the first series exhibited burnups exceeding 40000 MWD/T for the 3 mm thick caramels and 37500 MWD/T for the 4 mm thick caramels. The examinations carried out demonstrated that no gas had been released in the compartments and that the separators had performed very well.

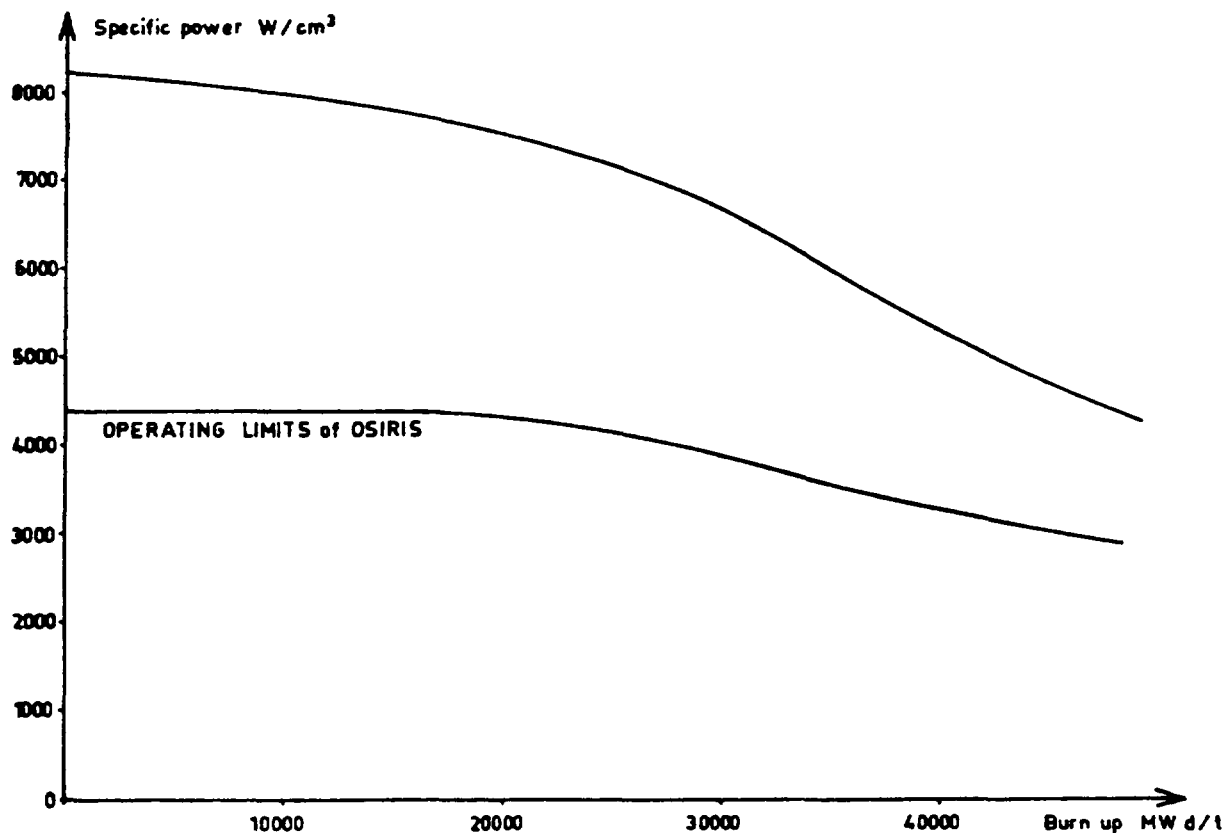


FIG. 3. Operating limits of 1.45 mm thick Caramel fuel meat.

The results obtained are related to :

- . thermal conductivity of uranium oxide as a function of burnup,
- . determination of the maximum normal service temperature,
- . maximum temperature of separators,
- . operating limits for the thicknesses of 3 and 4 mm.

Figure 3 shows an example of an operating limit for a 4 mm thick Caramel, up to a burnup of 50000 MWd/T . Since the maximum operating temperature of the fuel is known, it is possible to transpose these results to other Caramel geometries. Hence in the "equivalent" case of the Osiris reactor, maximum specific powers are greater than 5000 W/cm³, whereas the maximum operating specific powers of Osiris are about 4000 W/cm³ up to a burnup of 20000 MWd/T . They then decline to 2500 W/cm³ at the maximum burnup of 30000 MWd/T .

Other test irradiations, were performed in loops in the Osiris reactor : these include two irradiations of the Irène programme carried out in a pressurized water loop reproducing real cooling conditions ; in one of these irradiations used for safety studies, a leak detection signal was generated ; the depositing of corro-

sion products under low flow rate conditions was studied in the other irradiation.

Power cycling studies were performed on 4 mm thick caramels in samples having reached a burnup of 30000 MWD/T in the Osiris reactor before it was shut down in July 1978. These cycles were carried out under the following conditions :

uppermost part	1250 W/cm ³
lowest part	375 W/cm ³
withdrawal and descent velocity :	400 W.cm ⁻³ mn ⁻¹
number of cycles	3634

Finally, the start-up of the new core of Osiris was preceeded by the qualification of three precursor assemblies in the previous core ; these tests widely covered the range of operating conditions encountered with Osiris.

5. CARINE EXPERIMENT CARAMEL FUEL CLADDING FAILURE FOLLOWUP

To appraise the operational safety of such a fuel regarding risks of fission product or fissile material release into the reactor primary system, a cladding failure followup test has been carried out under conditions corresponding to OSIRIS operation and using a test loop independent of the EL 3 reactor.

This cell, located in the D₂O tank of EL 3, forms a heavy-water cooling system separate from the reactor cooling system. The possible pollution of heavy water is thus limited to that system.

A cladding burst detection device using delayed neutrons with ³He counters is installed in the system. This device is similar to that used in OSIRIS.

TEST CONDITIONS

The fuel element, manufactured by the same process as standard elements, comprised 32 UO₂ platelets enriched to 7 %.

The cladding defect is an $\sim 1\text{mm}^2$ circular hole. The fuel rating during irradiation was raised to 3050 W/cm³, cooling being ensured by heavy water circulating at 10 m/s. These conditions are very like those encountered in OSIRIS.

The fuel element was installed in an aluminium sleeve channeling water on both sides of the fuel plate to cool it.

The power released in the fuel was measured by establishing a heat balance. The cooling water temperatures were recorded by three thermocouples at the inlet and three triple thermocouples at the outlet to limit uncertainties arising from uniform temperatures in a cross section. The flow rate was measured by a calibrated turbine inserted in the system.

Cladding failure was detected by two parallel systems ; one uses a BF 3 counter normally operated on the EL 3 independent cell installation ; the other, of higher performance and used on OSIRIS, is fitted with an ^3He counter.

TEST RESULTS

The evolution of the signal showing the amount of delayed neutrons during irradiation is given in fig. 4. It should be noted that 3 pseudo-plateaus of activity are present at increasing levels. Their duration is of about 5 h for the first, 30 h for the second, and 3 h for the third. During the first two pseudo-plateaus, fission product wafts have given rise to activity peaks whose amplitude is near the average signal.

Between these pseudo-plateaus, the evolution of the signal is faster and faster, following an exponential law. The time to double the signal value, 30 h during the first phase of fast evolution, goes down to 3 h during the second phase.

After the third pseudo-plateau, severe activity variations due to fission product wafts are recorded, the average signal first increasing very rapidly, then stabilizing for about 1 h, 40 min.

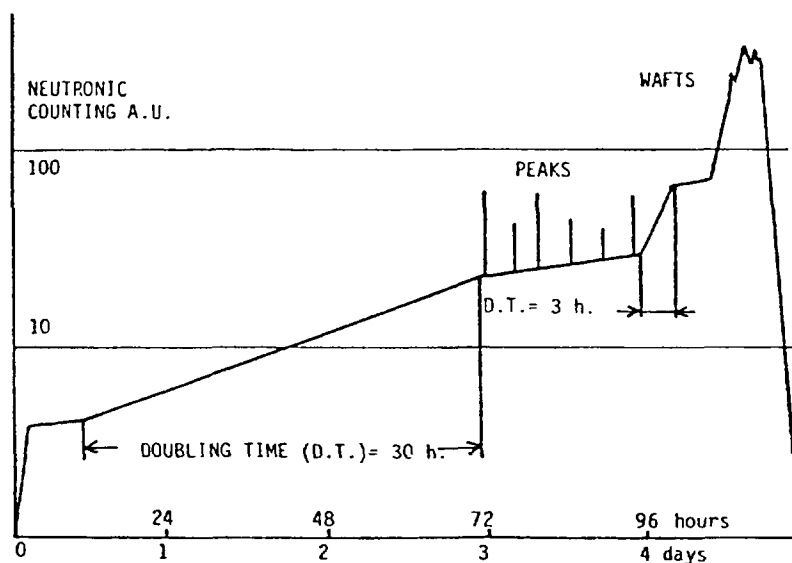


FIG. 4. CARINE — delayed neutron counting evolution during irradiation.

The delayed-neutron detection device used is completely representative of that installed in the OSIRIS reactor, which has allowed the time to determine when a cladding failure detection threshold is reached.

The results obtained show that this threshold is exceeded after the third pseudo-plateau and that irradiation still lasts for about 2 h in these conditions. Despite this fact, a very low level of activity of the radionuclides corresponding to fuel release was recorded.

The examinations carried out on the fuel after irradiation have shown that the hole previously drilled and the underlying fuel have not been spoiled significantly.

Moreover, the sequence of the experiment has proved the excellent behavior of the cladding failure detection system (CBD) installed on OSIRIS.

In conclusion the CARINE experiment has shown the excellent behavior of Carame fuel in the case of a cladding failure and the possibility of detecting a failure in Osiris before serious pollution occurs in the reactor systems.

6. THE OSIRIS EXPERIENCE

6.1 Adaptation of the plant

The OSIRIS reactor has been chosen for this experience of a LEU fuel in a research reactor because of its very high performances. The fuel is thus used in severe conditions which are going well beyond the needs of research reactors on the whole.

These severe conditions and the absence of margins except those necessary to the safety, with the U-Al HEU fuel mainly explain the necessity of the transformations of the core primary cooling circuit. It must indeed be remembered that this reactor was first designed for an operation at a rate of 50 MW ; the level of 70 MW was reached in 1968 only, after a small adaptation of the circulating pumps which were so driven to their limits.

The primary cooling system consisting of four groups of heat exchangers and pumps in parallel, each pump was associated with a heat exchanger. Three of these pumps were used simultaneously.

For the new fuel, the decrease of the number of plates of each fuel element (17 compared with 24 previously) had to be compensated by increasing the primary cooling flow rate to improve the removal conditions of the core power.

Because of the impossibility to increase the flow rate in each one of the exchangers, an adaptation of the main piping allows the connecting of the four exchangers to the outlet of each one of the four pumps. A main pipe connects the discharge of the pumps to the inlet of the heat exchangers. The pumps have been changed and their power increased. In this new situation the reactor is operated with three pumps and three heat exchangers.

The very works linked to the change of the fuel ran from the end of 1978 to August 1979. It was made use of a longer shutdown of the reactor for important maintenance works on the coatings of the storage capacities and of the decay tanks.

The other adaptations for the operation of the new oxide fuel were really lesser and limited to some strengthening of the structure of the dry storage tanks of the non irradiated fuels.

The modification of the cladding rupture detection system was already a project with U-Al fuel.

6.2 Changes in experimental conditions

For the experimental irradiations, the important parameters are the thermal and fast neutron fluxes levels. The gamma flux causes the liberation of additional heat energy which can be detrimental for the cooling. A certain quality of the neutron spectrum is aimed at for certain investigations of damage (better ratio of fast to thermal flux). We shall examine the irradiation conditions with the oxide fuel and compare them with the previous situation (U-Al).

The first calculations, then a serie of measuraments taken in ISIS out, at last, the experience of 18 month of OSIRIS operation provide us with an accurate idea of the changes in experimental conditions in OSIRIS.

6.2.1 The fast neutron flux ($E > 1$ MeV)

It was showed by the first calculations that the fast flux level was not modified with the new fuel if the core size was kept. This result has been verified from ISIS and OSIRIS. The loss in average fast flux level is indeed equal to the increase of the size of the core the number of fuel elements being passed from 39 to 44 because of the hydraulic and mechanical behavior of the reactor structures.

6.2.2 The thermal neutron flux

The very large absorption cross section of the new fuel, due to its high ^{235}U loading is reflected at an equivalent total power, by a

significant drop in thermal flux in the network (35 + 40 % for these experiments). The spectrum quality is however better (gain of about 40 % in the fast / thermal flux ratio) for experiments on damage on structure materials.

The drop in thermal flux in the network has no detrimental consequences on the experimental program, the network being exclusively used for its characteristics in fast fluxes.

The loss on the thermal flux in the periphery of the core is, on an average, of 15 %. But here also, it has to be taken into account the increase of the size of the core and of the number of available experimental location on the external grids.

6.2.3 Gamma heating

Gamma heating decreases in the network and this is an advantage for some experiments. In the network irradiation location

U-Al core : 10 to 15 Watt/g
oxide core : 4 to 8 Watt/g

6.3 State of the experience on OSIRIS

6.3.1 The reactor operation

The Osiris reactor was loaded with the new oxide LEU fuel in October 1979. A start-up test cycle took place in January/February 1980. From that time to July 1981, in addition of the start-up cycle, 12 cycles of roughly 4 weeks for each one took place. The total energy delivered by the reactor during this period is 21600 MWD at 70 MW.

The following table gives for each cycle, the ^{235}U loading in the beginning of the cycle the energy delivered by the reactor the number of EFPD of the cycle, the average burn-up of the unloaded fuel elements. It has to be pointed out that, for the first cycle, the average enrichment was only 6 % with fuel elements at 4,75 %, 5,62% and 7 %. The reloadings are done now with 7 % enriched fuel. At the end of 1982, this enrichment will be raised to 7,5 %

Each fuel element remains in the core for 5 or 6 cycles. At the end of each cycle it is proceeded to a partial refuelling and to a shuffling of the remaining fuels.

Cycle	²³⁵ U loading at the beginning of cycle	Energy delivered MWD	Number of EFPD	Average burn-up of the unloaded fuel element MWD/T
E ₀	20 733	1 542	22	4 970
E ₁	20 938	1 546	22,1	9 460
E ₂	21 586	1 813	25,9	16 460
E ₃	21 397	1 864	26,6	18 670
E ₄	21 164	1 670	23,9	20 090
E ₅	21 555	1 622	23,2	22 230
E ₆	21 817	1 650	23,6	24 370
E ₇	21 875	1 666	23,8	23 850
F ₁	21 482	1 732	24,7	24 300
F ₂	21 027	1 774	25,3	24 860
F ₃	21 408	1 938	27,7	24 960
F ₄	20 908	1 860	26,6	28 360
F ₅	20 480	994	13,7	27 455

6.3.2 Working conditions of the fuel and statistics

The working conditions of the fuel are very hard. Particularly, the average and maximum specific powers in the oxide are well beyond those met in PWR reactors or of those for almost all the research reactors throughout the world.

- average specific power in oxide : 1700 W/cm³ of UO₂
- maximum specific power in oxide : 4300 W/cm³ of UO₂

To make sure of the satisfactory behaviour of the fuel in the reactor, a programme of systematic non-destructive testing was undertaken. This involved testing the water channels, performed by a system of strain gauges, and a comparison with measurements taken after fabrication. It covered all the assemblies unloaded after the first six operating cycles, and half of the assemblies unloaded after the subsequent six cycles, making 90 assemblies in all.

This programme, currently under way, will be supplemented by destructive testing of one of the most irradiated assemblies, which has reached a burnup of 30000 MWD/T .

The overall measurements thus taken serve to provide a global estimate that is statistically representative of the changes in the characteristics and of the behaviour of the Osiris Caramel element under irradiation.

At the start-up with the oxide fuel, the licensing conditions allowed 20000 MWD/T average burn-up for a fuel element. This limit was raised to 25000 MWD/T in November 1980 and up to 30000 MWD/T in February 1981. These improvements were founded upon the good behavior of the fuel confirmed by the systematic non-destructive testings on unloaded irradiated elements. For the moment this average burn-up (30000 MWD/T) is not reached on the whole of the elements. It needs to raise the enrichment to 7,5 %.

Presently 63 elements have got an average burn-up above 20 000 MWD/T among, them, 26 have passed beyond 25000 MWD/T and 8 have reached an average burn-up between 28000 and 30000 MWD/T . It has to be pointed out that at an average burn-up of 30000 MWD/T corresponds to a maximum burn-up of 40000 to 43000 MWD/T for the most irradiated platelet

7. THE CASE OF OTHER RESEARCH REACTORS

The performance of the fuel in Osiris are high enough to cover all the possibilities of research reactors.

On the other hand, the adaptation of Osiris is not representative of the majority of the existing reactors, the power of which is of the order of the MW or a few MW. In those cases, the change of the fuel might be done without any important modification and with a shorter shut-down time than for Osiris. An exemple for a low power reactor is given by ISIS, the neutronic mock-up of OSIRIS, the power of which is limited to 700 KW. The change of the fuel has been realized without any modification of the core structures of the cooling circuit or of the control. The work has been limited to a strengthening of the structures of the storage racks. Its for the shut-down time, it was limited to the time necessary to the unloading of the old fuel, to the reloading with the new fuel and to the measurements of the core parameters for a safe operation (racks efficiency, power mapping, neutron flux). OSIRIS and ISIS are clearly situated at the two ends of the scale. Between the two, all the situations are possible and each case is a particular one.

Appendix I-7

URANIUM-ZIRCONIUM HYDRIDE TRIGA-LEU FUEL

GA TECHNOLOGIES, INC.
San Diego, California,
United States of America

Abstract

The development and testing of TRIGA-LEU fuel with up to 45 wt-% U is described. Topics that are discussed include properties of hydride fuels, the prompt negative temperature coefficient, pulse heating tests, fission product retention, and the limiting design basis parameter and values.

General specifications for Er-U-ZrH TRIGA-LEU fuel with 8.5 to 45 wt-% U and an outline of the inspections during manufacture of the fuel are also included.

1. INTRODUCTION

The development and use of U-ZrH_x fuels for the TRIGA reactor have been underway at GA since 1957. Over 6000 fuel elements of 7 distinct types have been fabricated for the 60 TRIGA research reactors which are under construction or have been placed in operation. The earliest of these has now passed 25 yrs of operation. U-ZrH fuel has exhibited unique safety features including a prompt negative temperature coefficient of reactivity, high fission product retentivity, chemical stability when quenched from high temperatures in water, and dimensional stability over large swings of temperature. The first TRIGA reactor to be exported was for the U.S. exhibit at the Second Geneva Conference on the Peaceful Uses of Atomic Energy in 1958.

The standard TRIGA fuel contains 8.5 wt-% uranium (20% enriched) as a fine metallic dispersion in a zirconium hydride matrix. The H/Zr ratio is nominally 1.6 (in the face-centered cubic delta phase). The equilibrium hydrogen dissociation pressure is governed by the composition and temperature. For ZrH_{1.6} the equilibrium hydrogen pressure is 1 atm at about 760°C. The single-phase, high-hydride composition eliminates the problems of density changes associated with phase changes and with thermal diffusion of the hydrogen. TRIGA fuel with 12 wt-% U has been proven through successful reactor operation for over a decade. Highly enriched versions of TRIGA

fuels (discontinued in 1979) contained up to about 3% erbium as a burnable poison to increase the core lifetime and contribute to the prompt negative temperature coefficient in the higher power (1 to 14 MW) TRIGA reactors. (Cores with steady-state power levels above 3 MW are not pulsing cores.) The calculated core lifetime with FLIP fuel in the 2-MW TRIGA is approximately 9 MW-yr. Over 25,000 pulses have been performed with the TRIGA fuel elements at GA, with fuel temperatures reaching peaks of about 1150°C.

TRIGA fuel was developed around the concept of inherent safety. A core composition was sought which had a large prompt negative temperature coefficient of reactivity such that if all the available excess reactivity were suddenly inserted into the core, the resulting fuel temperature would automatically cause the power excursion to terminate before any core damage resulted. Experiments then in progress demonstrated that zirconium hydride possesses a basic mechanism to produce the desired characteristic. Additional advantages were that ZrH has a good heat capacity, results in relatively small core sizes and high flux values due to the high hydrogen content, and could be used effectively in a rugged fuel element size.

In early 1976, GA undertook the development of fuels containing up to 45 wt-% uranium (3.7 gm U/cc) in order to allow the use of low enriched uranium (LEU) (under 20% enrichment) to replace the highly enriched fuels while maintaining long core life. The 45 wt-% fuel contains a relatively modest ~20 volume percent of uranium. These fuels were fabricated successfully, with the required hydrogen content and erbium loading. The structural features of the hydrided LEU fuel were similar to those of the well-proven 8.5 and 12 wt-% fuels, as shown by metallographic, electron microprobe analysis, and x-ray diffraction examination. The uniform distribution of the uranium on a macroscale and the distribution of the various phases were as expected from experience with the standard fuel. The high-U LEU fuels were subjected to thermal cycling, pulsing tests to 725°C, and water quench tests from 1200°C, which they survived successfully. The physical and thermal stability properties of the LEU fuels are acceptable. Very low release fractions of fission products were measured at normal operating temperatures, with the temperature dependent functions describing the fission product release rate for standard TRIGA fuel still remaining applicable to the TRIGA LEU fuel. Previous work on U-ZrH_x fuels during the SNAP reactor program had developed the technology up to 20 wt-% uranium and found no indication of this being a limit. Burnup of U-235 reached values of about 80% in SNAP program tests. Ongoing in-core tests at GA with 20 and 45 wt-%

fuel started in April 1978. These tests have been an unqualified success during pulsing and steady-state operation including over 2000 thermal cycles where the reactor has gone from shutdown to powers of 1 to 1.5 MW.

The final demonstration of the TRIGA LEU fuel is being performed by a full-scale, long-term fuel burnup test which is under way at the 30-MW Oak Ridge Research Reactor as part of the U.S. Department of Energy RERTR program managed by Argonne National Laboratory. A standard geometry 16-rod TRIGA LEU cluster containing uranium loadings of 20, 30, and 45 wt-% is being tested. The fuel rods are 12.95 mm O.D., clad with 4.06 mm Incoloy, and the fuel length is 559 mm.

The test objectives are to reach burnup values of 35, 40, and 50% of contained U-235 respectively in the fuels with 20, 30, and 45 wt-% uranium. The test began in December 1979 and these objectives have been successfully met in all but the 45 wt-% fuel and it should complete testing by the end of 1983.

The high-U LEU fuel was also subjected to water-quench safety tests by quenching from temperatures up to 1200°C. The results showed that this fuel also survives the quench tests with a benign response, with only minor cracking, volume shrinkage, loss of hydrogen, and surface oxidation.

The remaining evaluations included analytical assessments of the prompt negative temperature coefficient of reactivity and the core lifetime (Table 1). Nuclear design and analytical studies have shown that the prompt negative temperature coefficient for the 20 wt-% uranium fuel is essentially the same as that for standard fuel over the temperature range of interest (20° to 700°C) and greater than that for the FLIP fuel which it replaces. The prompt negative temperature coefficient for the more highly loaded LEU fuel shows a temperature dependence, whereas the coefficient is relatively constant for standard fuel. The value of the prompt negative temperature coefficient of reactivity is slightly lower for the 45 wt-% uranium fuel compared to the highly enriched fuel it replaces; however, it is still large and significantly higher than the prompt negative temperature coefficients for any other type of reactor fuel.

Inclusion of erbium burnable poison in the TRIGA LEU fuel has enabled core lifetimes of up to 7000 MWd to be predicted for the 45 wt-% fuel. It is emphasized that this is the core life to the time of initial refueling.

TABLE 1
CALCULATED BEGINNING OF LIFE PROMPT NEGATIVE
TEMPERATURE COEFFICIENT (α) AND CORE LIFETIME

TRIGA Fuel Type	Diameter (in.)	Length (in.)	Wt %		Uranium Enrichment (%)	$\times 10^{-5} = \alpha$ Average (23°-700°C)	Core Lifetime ^(a) (MWd)
			U	Er			
Standard	1.5	15	8.5	0.00	20	10	~100
LEU	1.5	15	20	0.50	20	11	1200
LEU	1.5	15	30	0.92	20	8	3000
FLIP	1.5	15	8.5	1.58	70	10	3500
10 MW	0.5	22	10	1.70	93	6	4800
10 MW-LEU	0.5	22	45	0.66	20	5	4000
14 MW	0.5	22	10	2.80	93	8	8000
14 MW-LEU	0.5	22	45	1.40	20	6	7000

^(a) Before initial reload.

For an equilibrium cycle core starting with 45 wt-% U fuel and removing fuel with 50% burnup of the contained uranium, the core life would be over 14000 MWd for the 14-MW core configuration.

2. PROPERTIES OF HYDRIDE FUELS

2.1. PHASE SYSTEMS

The ZrH and U-ZrH systems are essentially simple eutectoids containing at least four separate hydride phases in addition to the zirconium and uranium allotropes (Fig. 1). The hydride phases consist of the following:

1. Alpha phase: a low-temperature terminal solid solution of hydrogen in the hexagonal, close-packed, alpha zirconium lattice.
2. Beta phase: a solid solution of hydrogen dissolved in the high-temperature, body-centered cubic zirconium phase.
3. Delta phase: a face-centered cubic hydride phase. A delta-prime phase has also been reported, formed below 240°C from the delta phase.

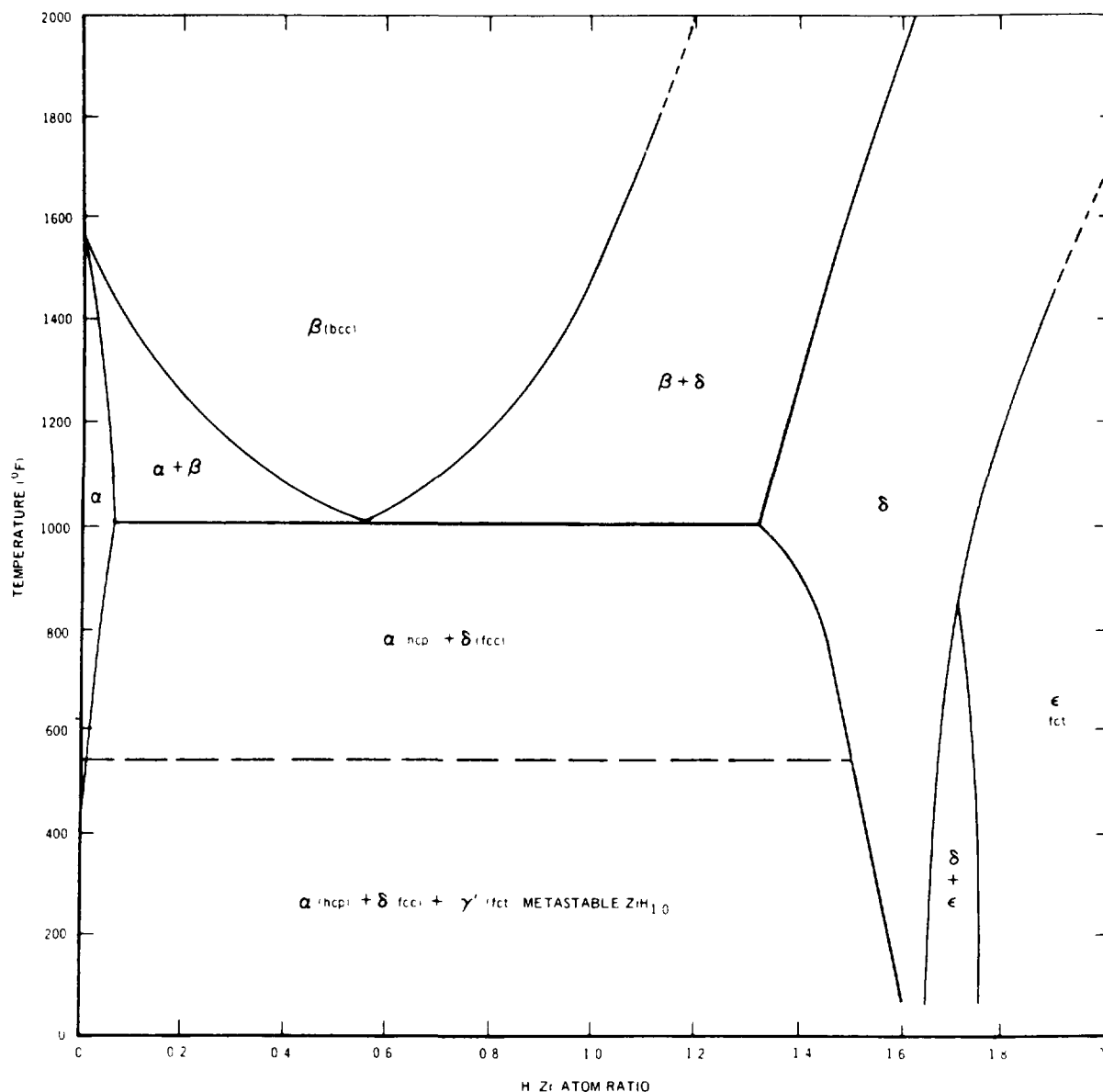


Fig. 1. Zirconium hydride phase diagram showing boundary determination

4. Epsilon phase: a face-centered tetragonal hydride phase with the ratio $c/a < 1$, extending beyond the delta phase to ZrH_2 . The epsilon phase is not a true equilibrium phase, and it appears as a banded, twin structure.

The effect of the uranium addition on the ZrH system is to shift all the phase boundaries of the ZrH diagram to slightly lower temperatures. For example, the eutectoid temperature is lowered from 547°C to 541°C. No new phases, and no uranium hydride have been detected.

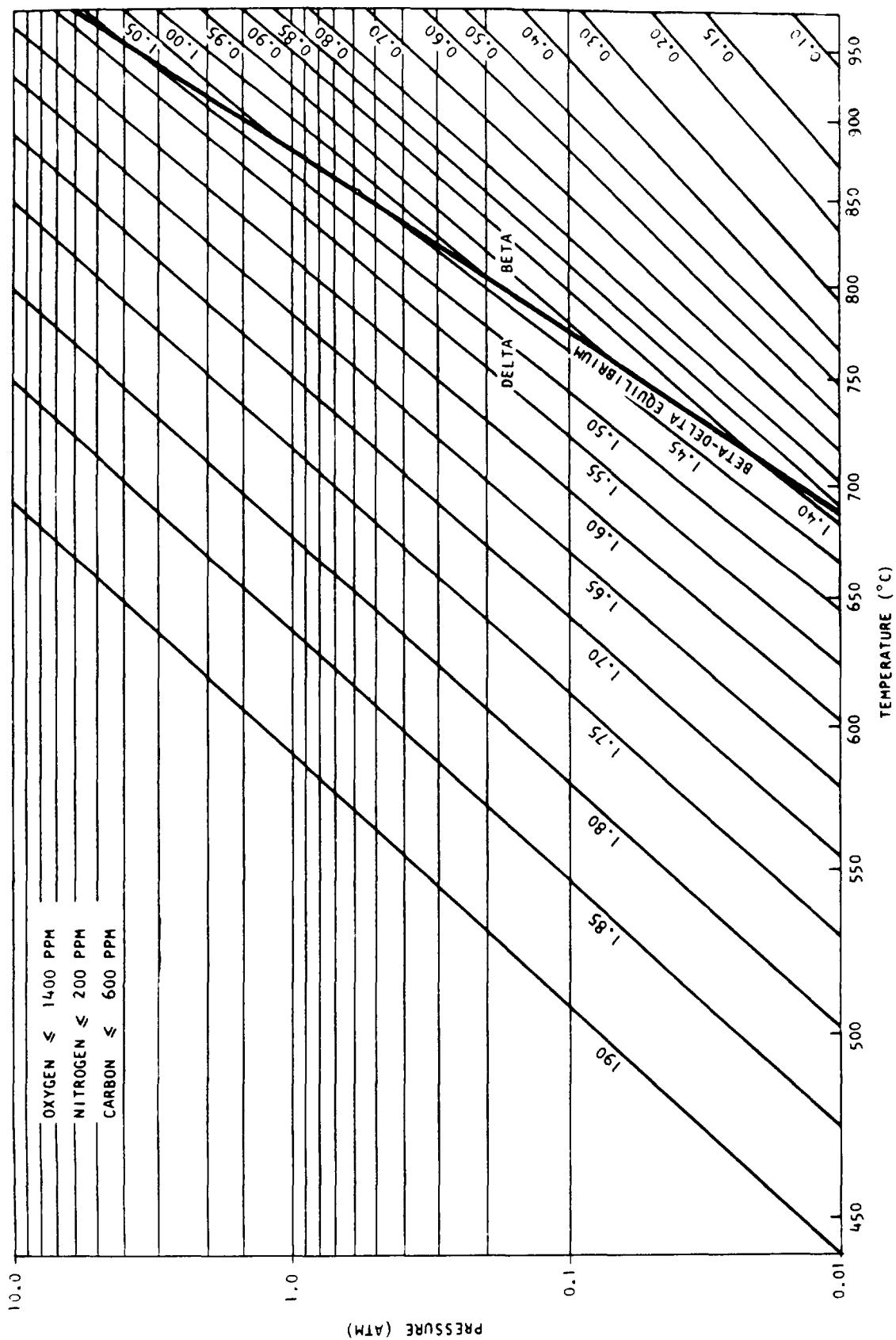


Fig. 2. Dissociation pressure isochores of zirconium hydride (expressed as H/Zr atom ratios)

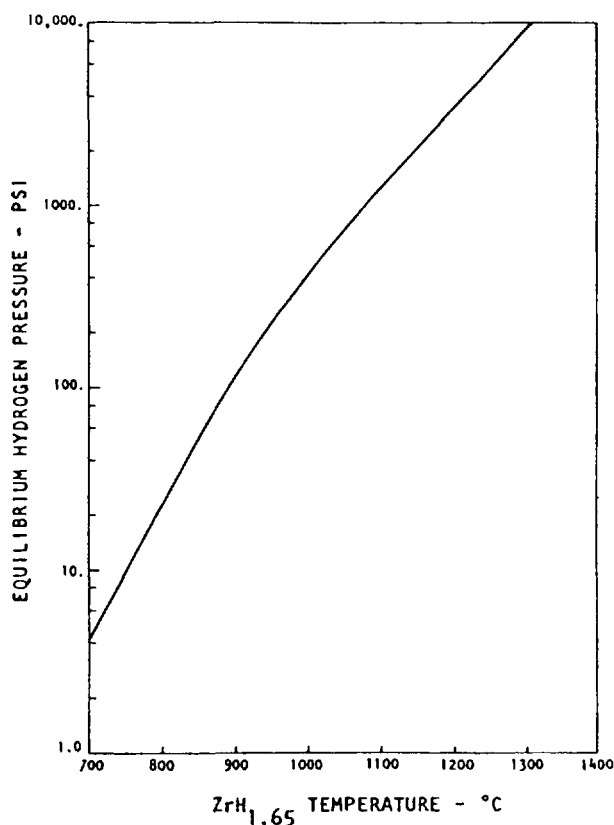


Fig. 3. Equilibrium hydrogen pressure over $\text{ZrH}_{1.65}$ versus temperature

2.2. DISSOCIATION PRESSURES

The hydrogen dissociation pressures of hydrides have been shown to be comparable in the alloys containing up to 75 wt-% U. The concentration of hydrogen is generally reported in terms of either weight percent or atoms of H/cm^3 of fuel (N_H). The equilibrium dissociation pressures in the ZrH system are given in Figs. 2 and 3. In the delta region, the dissociation pressure equilibria of the zirconium-hydrogen binary may be expressed in terms of composition and temperature by the relation

$$\log P = K_1 + (K_2 \times 10^3)/T \quad ,$$

where $K_1 = -3.8415 + 38.6433 X - 34.2639 X^2 + 9.2821 X^3$,

$K_2 = -31.2982 + 23.5741 X - 6.0280 X^2$,

P = pressure, atm,

T = temperature, K,

X = hydrogen-to-zirconium atom ratio.

The higher-hydride compositions ($H/Zr > 1.5$) are single-phase (delta or epsilon) and are not subject to thermal phase separation on thermal cycling. For a composition of about $ZrH_{1.6}$, the equilibrium hydrogen dissociation pressure is 1 atm at about $760^{\circ}C$. The absence of a second phase in the higher hydrides eliminates the problem of large volume changes associated with phase transformation at approximately $540^{\circ}C$ in the lower hydride compositions. Similarly, the absence of significant thermal diffusion of hydrogen in the higher hydrides precludes concomitant volume change and cracking. The clad material of stainless steel or nickel alloys will provide a satisfactory diffusion barrier to hydrogen at long-term (several years) sustained cladding temperatures below about $300^{\circ}C$.

2.3. HYDROGEN MIGRATION

Under nonisothermal conditions, hydrogen migrates to lower-temperature regions from higher-temperature regions. The equilibrium dissociation pressure obtained when the redistribution is complete is lower than the dissociation pressure before redistribution. The dimensional changes of rods resulting from hydrogen migration are of minor importance in the delta and epsilon phases.

2.4. HYDROGEN RETENTION

The rates of hydrogen loss through 250- μm -thick stainless steel cladding are low at cladding temperatures characteristic of TRIGA fuel elements. A 1% loss of hydrogen per year occurs at about $500^{\circ}C$ ($900^{\circ}F$) clad temperature.

2.5. DENSITY

The density of ZrH decreases with an increase in the hydrogen content. The density change is quite high up to the delta phase ($H/Zr = 1.5$) and then changes little with further increases in hydrogen. The bulk density of massively hydrided zirconium is reported to be about 2% lower than the x-ray density.

For hydrogen to zirconium ratios, x , of less than 1.6, the density of ZrH_x used for TRIGA design calculations is

$$\rho_{ZrH} = 1. / (0.1541 + 0.0145 X)$$

and for X greater than or equal to 1.6

$$\rho_{\text{ZrH}} = 1./((0.1706 + 0.0042 X) \quad .$$

The density of uranium-zirconium hydride is

$$\rho_{\text{UZrH}} = 1./(\text{w}_{\text{U}}/\rho_{\text{U}} + \text{w}_{\text{ZrH}}/\rho_{\text{ZrH}})$$

where w_{U} , w_{ZrH} = weight fraction of uranium and zirconium hydride respectively and ρ_{U} = uranium density (19.07 gm/cm³).

By combining the above formulae, and using $X = 1.6$, the following relationships are obtained for the uranium density and weight fraction in the U-ZrH_{1.6} alloy:

$$\rho_{\text{U(A)}} = \frac{\text{w}_{\text{U}}}{0.177 - 0.125 \text{w}_{\text{U}}} \quad ,$$

$$\text{w}_{\text{U}} = \frac{0.177\rho_{\text{U(A)}}}{1 + 0.125\rho_{\text{U(A)}}} \quad .$$

The relationship between the uranium density and the volume fraction of uranium in the alloy is given by:

$$\rho_{\text{U(A)}} = 19.07 \text{V}_{\text{f}}^{\text{U(A)}}$$

where $\text{V}_{\text{f}}^{\text{U(A)}}$ = volume fraction of uranium in the U-ZrH_{1.6} alloy.

2.6. THERMAL CONDUCTIVITY

Thermal conductivity measurements have been made over a range of temperatures. A problem in carrying out these measurements by conventional methods is the disturbing effect of hydrogen migration under the thermal gradients imposed on the specimens during the experiments. This has been minimized at GA by using a short-pulse heating technique to determine the thermal diffusivity and hence to permit calculation of the thermal conductivity. From the recent measurements at GA of thermal diffusivity coupled with the data on density and specific heat, the thermal conductivity of uranium-zirconium hydride with an H/Zr ratio of 1.6 is 0.042 ± 0.002 cal/sec-cm-°C and is insensitive both to the weight fraction of uranium and to the temperature.

2.7. HEAT CAPACITY

The heat content of zirconium hydride as a function of temperature and composition (ZrH_x) is approximated well by the following relationship:

$$\begin{aligned} (H-H_{25})_{\text{ZrH}_x} = & 0.03488 T^2 + [34.446 + 14.8071 (x - 1.65)]T \\ & - 882.95 - 370.18 (x - 1.65) \text{ J/mole} \end{aligned}$$

where T is in $^{\circ}\text{C}$.

The specific heat of $\text{ZrH}_{1.6}$ is

$$C_p = (0.06976 T + 33.706)/M \text{ J/g } ^{\circ}\text{C}$$

where M = the molecular weight of $\text{ZrH}_{1.6} = 92.83 \text{ g/mole}$.

The specific heat of uranium is

$$C_p = (1.305 \times 10^{-4} T + 0.1094) \text{ J/g } ^{\circ}\text{C}.$$

The specific heat of uranium-zirconium hydride is taken to be

$$C_{p(\text{UZrH})} = W(\text{U}) C_{p(\text{U})} + W(\text{ZrH}) C_{p(\text{ZrH})} \quad .$$

The volumetric specific heat of 8.5 wt-% U- $\text{ZrH}_{1.6}$ is calculated to be

$$C_p = 2.04 + 4.17 \times 10^{-3} T \text{ W-sec/cm}^3 \text{ } ^{\circ}\text{C (from } 0^{\circ}\text{C)} \quad .$$

2.8. CHEMICAL REACTIVITY

Zirconium hydride has a relatively low reactivity in water, steam, and air at temperatures up to about 600°C . Massive zirconium hydride has been heated in air for extended periods of time at temperatures up to 600°C with negligible loss of hydrogen. An oxide film forms which inhibits the loss of hydrogen.

The hydride fuel has excellent corrosion resistance in water. Bare fuel specimens have been subjected to a pressurized water environment at 570°F and 1230 psi during a 400 hr period in an autoclave. The average cor-

rosion rate was 350 mg/cm²-month weight gain, accompanied by a conversion of the surface layer of the hydride to an adherent oxide film. The maximum extent of corrosion penetration after 400 hr was less than 2 mils.

In the early phases of development of the TRIGA fuel, water-quench tests were carried out from elevated temperatures. Fuel rods (1-in. diam) were heated to 800°C and end-quenched to test for thermal shock and corrosion resistance. No deleterious effects were observed. Also, a 6-mm diam fuel rod was heated electrically to about 800°C and a rapid stream of water was sprayed on it; no significant reaction was observed. Small and large samples were heated to 900°C and quenched in water; the only effect observed was a slight surface discoloration. Finely divided U-ZrH powder was heated to 300°C and quenched in 80°C water; no reaction was observed. Later, these tests were extended to temperatures as high as 1200°C, in which tapered fuel rods were dropped into tapered aluminum cans in water. Although the samples cracked and lost hydrogen, no safety problem arose in these tests. Recently, the low-enriched TRIGA fuels have been subjected to water-quench safety tests at GA.

Quench tests were performed on 20%-enriched TRIGA fuel samples (45 wt-% uranium, 53 wt-% zirconium, 1 wt-% erbium, 1 wt-% hydrogen) to simulate cladding rupture and water ingress into the TRIGA reactor fuel rods during operation.

These results indicate satisfactory behavior of TRIGA fuel for temperatures to at least 1200°C. Under conditions where the clad temperature can approach the fuel temperature for several minutes (which may allow formation of eutectics with the clad), the results indicate satisfactory behavior to about 1050°C. This is still about 50° to 100°C higher than the temperature at which internal hydrogen pressure is expected to rupture the clad, should the clad temperature approach that of the fuel. It should be pointed out that thermocouples have performed well in instrumented TRIGA fuel elements at temperatures up to 650°C in long-term steady-state operations, and up to 1150°C in very short time pulse tests.

2.9. IRRADIATION EFFECTS

Most of the irradiation experience to date has been with the uranium-zirconium hydride fuels used in the SNAP (containing about 10 wt-% uranium)

and TRIGA reactors. The presence of uranium influences the radiation effects because of the damage resulting from fission recoils and fission gases. Some significant conclusions may be drawn from the results of these experiments. The uranium is present as a fine dispersal (about 1 μm diam) in the U-ZrH fuels, and hence the recoil damage is limited to small regions within the short (~ 10 μm) range of the fission recoils. The U-ZrH fuel exhibits high growth rate during initial operation, the so-called "offset" growth period, which has been ascribed to the vacancy-condensation type of growth phenomenon over the temperature range where voids are stable.

The swelling of the U-ZrH fuels at high burnups is governed by three basic mechanisms:

1. The accommodation of solid fission products resulting from fission of U-235. This growth is approximately 3% $\Delta V/V$ per metal atom % burnup. This mechanism is relatively temperature insensitive.
2. The agglomeration of fission gases at elevated temperatures (above 1300°F). This takes place by diffusion of the xenon and krypton to form gas bubbles.
3. A saturable cavity nucleation phenomenon which results from the nucleation and growth of irradiation-formed vacancies into voids over a certain range of temperatures where the voids are stable. The saturation of growth by this mechanism was termed offset swelling. It was deduced from the rapid decrease in fuel-to-cladding ΔT experienced during the early part of the irradiation. The saturation was reached in approximately 1500 hr.

The effect of fuel operating temperature (at offset) on fuel growth for a constant burnup rate (burnup per 10,000 hr) is shown in Fig. 4. The effect of burnup rate on fuel growth for a constant offset temperature is shown in Fig. 5. Note the decreased growth with higher burnup rates.

Burnups of up to about 0.52 total metal atom % (75% burnup of the U-235) have been attained in standard TRIGA fuel. The TRIGA LEU fuels contain 1.8, 2.9, and 4.8 metal atom % as U-235 for the fuels with 20, 30, and 45 wt-% U, respectively. Burnups of 35% and 40% of the contained uranium in 20 and 30 wt-% U fuels have been successfully completed in the Oak Ridge irradiation and the burnup of about 50% of the contained U in the fuel with 45 wt-% U should be completed by the end of 1983.

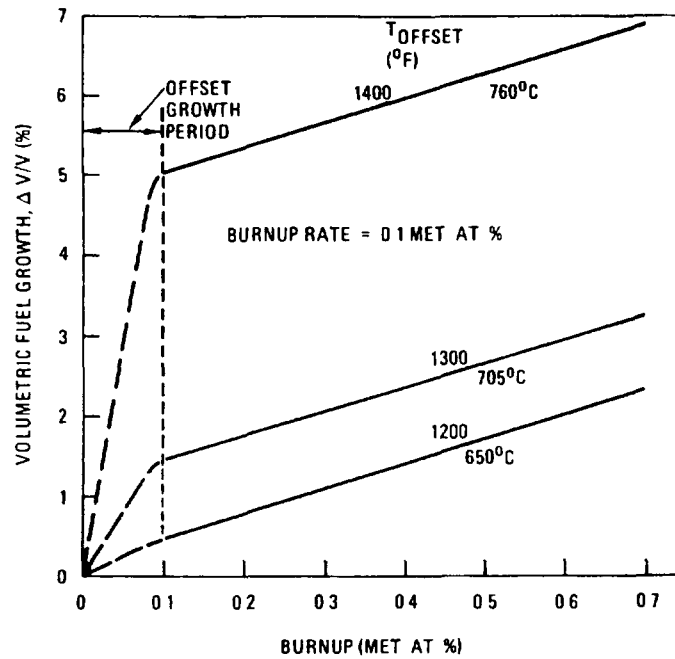


Fig. 4. U-ZrH volume increase versus burnup for different fuel operating temperatures

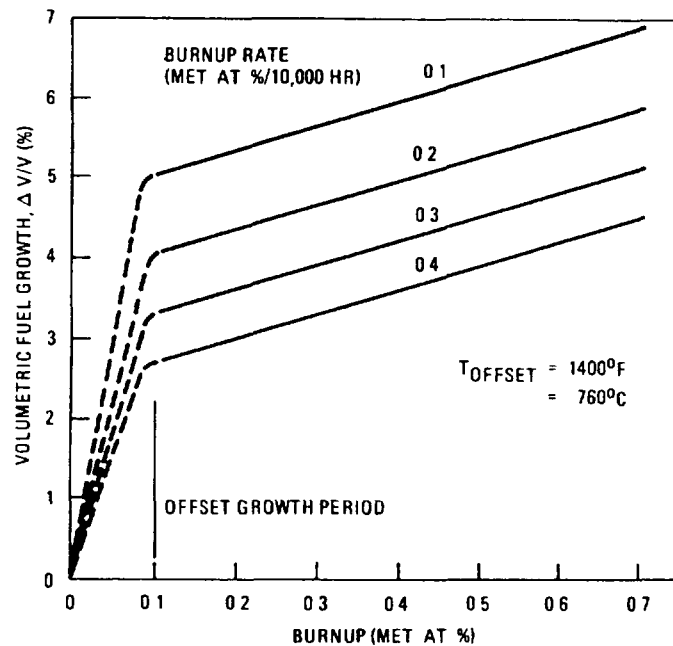


Fig. 5. U-ZrH volume increase versus burnup for different fuel burnup rates

2.10. ERBIUM ADDITIONS

All available evidence and extensive operating experience indicates that the addition of erbium to the U-ZrH introduces no deleterious effects to the fuel. Erbium has a high boiling point and a relatively low vapor

pressure so that it can be melted into the uranium-zirconium uniformly. The erbium is incorporated into the fuel during the melting process. All the analyses that have been made on the alloy show that the erbium is dispersed uniformly, much as is the uranium. Erbium is a metal and forms a metallic solution with the uranium-zirconium; thus there is no reason to believe that there will be any segregation of the erbium. Erbium forms a stable hydride (as stable as zirconium hydride) which also indicates that the erbium will remain uniformly dispersed through the alloy. Also, since neutron capture in erbium is an $n\text{-}\gamma$ reaction, there are no recoil products.

3. PROMPT NEGATIVE TEMPERATURE COEFFICIENT

The basic parameter which provides the greatest degree of safety in the operation of a TRIGA reactor system is the prompt negative temperature coefficient. This temperature coefficient (α) allows great freedom in steady-state operation, since the effect of accidental reactivity changes occurring from experimental devices in the core is minimized.

The prompt negative temperature coefficient for the TRIGA LEU core is based on the same core spectrum hardening characteristic that occurs in a standard* TRIGA core. The spectrum hardening is caused by heating of the fuel-moderator elements. The rise in temperature of the hydride increases the probability that a thermal neutron in the fuel element will gain energy from an excited state of an oscillating hydrogen atom in the lattice. As the neutrons gain energy from the ZrH, the thermal neutron spectrum in the fuel element shifts to a higher average energy (the spectrum is hardened), and the mean free path for neutrons in the element is increased appreciably. For a standard TRIGA element, the average chord length is comparable to a mean free path, and the probability of escape from the element before being captured is significantly increased as the fuel temperature is raised. In the water, the neutrons are rapidly rethermalized so that the capture and escape probabilities are relatively insensitive to the energy with which the neutron enters the water. The heating of the moderator mixed with the fuel in a standard TRIGA element thus causes the spectrum to harden more in the fuel than in the water. As a result, there is a temperature-dependent dis-

*A standard TRIGA core contains U-ZrH fuel with no erbium. The uranium enrichment is 20%, and the fuel element (rod) diameter is about 1.5 in. (3.8 cm) with a core water volume fraction of about 0.33.

advantage factor for the unit cell in which the ratio of absorptions in the fuel to total cell absorptions decreases as fuel element temperature is increased. This brings about a shift in the core neutron balance, giving a loss of reactivity.

In the TRIGA LEU fuel, the temperature-hardened spectrum is used to decrease reactivity through its interactions with a low-energy-resonance material. Thus, erbium, with its double resonance at ~ 0.5 eV, is used in the TRIGA LEU fuel as both a burnable poison and a material to enhance the prompt negative temperature coefficient. The ratio of the absorption probability to the neutron leakage probability is increased for TRIGA LEU fuel relative to the standard TRIGA fuel because the U-235 density in the fuel rod is greater and also because of the use of erbium. When the fuel-moderator material is heated, the neutron spectrum is hardened, and the neutrons have an increasing probability of being captured by the low-energy resonance in erbium. This increased parasitic absorption with temperature causes the reactivity to decrease as the fuel temperature increases. The neutron spectrum shift, pushing more of the thermal neutrons into the Er-167 resonance as the fuel temperature increases, is illustrated in Fig. 6, where cold and hot neutron spectra are plotted along with the energy-dependent absorption cross-section for Er-167. As with a standard TRIGA core, the temperature coefficient is prompt because the fuel is intimately mixed with a large portion of the moderator; thus, fuel and solid moderator temperatures rise simultaneously, producing the temperature-dependent spectrum shift.

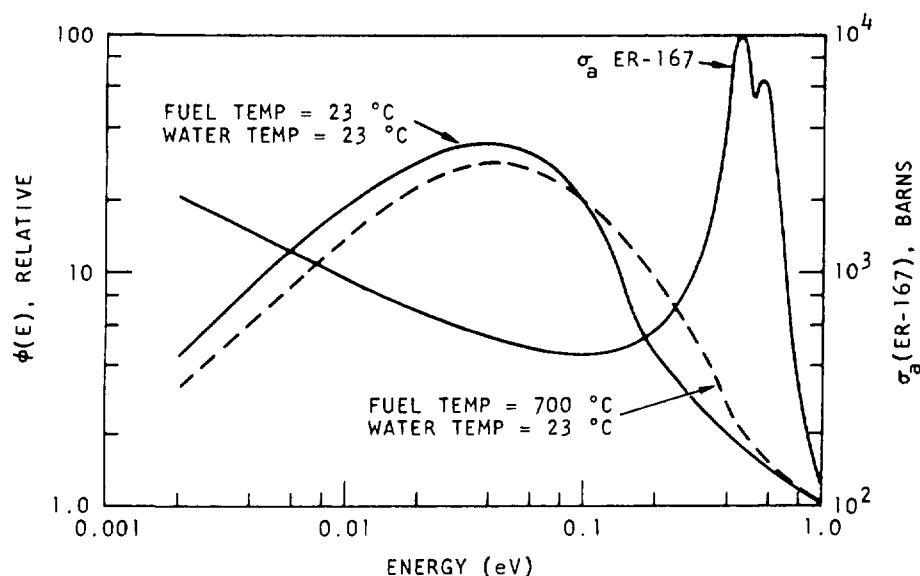


Fig. 6. Thermal neutron spectra versus fuel temperature relative to σ_a versus energy for Er-167

For the reasons just discussed, more than 50% of the temperature coefficient for a standard TRIGA core comes from the temperature-dependent disadvantage factor, or cell effect, and ~20% each come from Doppler broadening of the U-238 resonances and temperature-dependent leakage from the core. These effects produce a temperature coefficient of $\sim -10 \times 10^{-5}/^{\circ}\text{C}$, which is essentially constant with temperature. On the other hand, for a TRIGA LEU core, the effect of cell structure on the temperature coefficient is smaller. Over the temperature range 23° to 700°C, about 70% of the coefficient comes from temperature-dependent changes in the parasitic absorption within the core, and more than half of this effect is independent of the cell structure. Almost all the remaining part of the prompt negative temperature coefficient is contributed by Doppler broadening of the U-238 resonances. Over the temperature range 23° to 700°C, the temperature coefficient for the TRIGA LEU fuel with 20 wt-% U is about $1.07 \times 10^{-4}/^{\circ}\text{C}$, thus being somewhat greater than the value for standard TRIGA fuel. It is also temperature dependent.

4. PULSE HEATING

The U-ZrH fuel used in TRIGA reactors is capable of operation under conditions of transient experiments for delivery of high-intensity bursts of neutrons. For these experiments, done in reactors with steady-state power ratings of up to 3 MW, the reactor is equipped with a special control rod mechanism that provides a method of obtaining a step reactivity change of predetermined magnitude in the reactor. During the nuclear pulse, nearly all the energy is stored as thermal energy in the fuel material. This results in an almost instantaneous rise in the temperature of the fuel body. Fuel elements with 8.5 wt-% U have operated repeatedly in the advanced TRIGA prototype reactor (ATPR) to peak power levels of over 8000 MW providing a neutron fluence per pulse of about 10^{15} nvt.

The ATPR fuel elements have been subjected to thousands of pulses of 2000 MW and more. The nuclear safety stems from the large prompt negative temperature coefficient of reactivity of the uranium-zirconium hydride fuel-moderator material. The inherent prompt shutdown mechanism of TRIGA reactors has been demonstrated extensively during the tens of thousands of pulses conducted on TRIGA reactors. These tests involved step insertions of reactivity of up to $3\text{-}1/2\%$ $\delta k/k$. An in-pile test has been performed on fuel elements of a modified design (gapped) for high performance in the TRIGA

annular core pulse reactor (ACPR). As expected, there was satisfactory fuel body performance after 400 pulses at temperatures up to the design point of 1000°C. There was no evidence of interaction between the clad and the fuel. The transient gap pressure in the space between the fuel and the clad was measured during the pulse, and peak pressures were found to be less than 40 psia - well below the upper bound implied by the equilibrium pressure data. As testing at higher temperatures continued, there was some evidence that at hot-spot regions, where the temperature near the fuel surface reached about 1200°C, the fuel gradually swelled slightly over a large number of pulses under the influence of the hydrogen pressure in small bubbles that nucleated in the hot spots (~1200°C, U-ZrH_{1.65-1.70}) and formed a gray patch.

From the results of these tests, it can be concluded that U-ZrH fuel elements can be safely pulsed even to very high fuel temperatures. After more than 400 pulses to fuel temperatures over 1100°C, measurements showed that two of the five test elements exceeded the conservative dimensional tolerances. In the first 200 pulses, there was no external evidence of change in any of the five special test elements. The practical consequences of this are several-fold. First, small power reactors using U-ZrH fuel can safely sustain accidental power excursions to high fuel temperature. Second, and perhaps more significant, high-level pulsing reactors (fluence of 10¹⁵ nvt) can be operated with U-ZrH fuel with a reasonable fuel lifetime. For example, the annular core TRIGA reactor at JAERI (Japan) has operated since 1975, with over 1000 pulses of all sizes at fuel temperatures of up to 1000°C. Further, with regard to standard types of TRIGA research reactors, it is evident that present peak fuel temperatures are conservative.

5. FISSION PRODUCT RETENTION

A number of experiments have been performed to determine the extent to which fission products are retained by U-ZrH (TRIGA) fuel. Experiments on fuel with a uranium density of 0.5 g/cm³ (8.5 wt-% U) were conducted over a period of 11 yr and under a variety of conditions. Results prove that only a small fraction of the fission products are released, even in completely unclad U-ZrH fuel. The release fraction varies from 1.5 x 10⁻⁵ for an irradiation temperature of 350°C to ~10⁻² at 800°C.

The experiments show that there are two mechanisms involved in the release of fission products from U-ZrH fuel, each of which predominates over

a different temperature range. The first mechanism is that of fission fragment recoil into the gap between the fuel and clad. This effect predominates in fuel at temperatures up to $\sim 400^{\circ}\text{C}$; the recoil release rate is dependent on the fuel surface-to-volume ratio but is independent of fuel temperature. Above $\sim 400^{\circ}\text{C}$, the controlling mechanism for fission product release from U-ZrH fuel is a diffusion-like process, and the amount released is dependent on the fuel temperature, the fuel surface-to-volume ratio, the time of irradiation, and the isotope half-life.

The results of the U-ZrH experiments, and measurements by others of fission product release from Space Nuclear Auxiliary Power Program (SNAP) fuel, have been compared and found to be in good agreement.

The fractional release, ϕ , of fission product gases into the gap between fuel and clad from a full-size standard U-ZrH fuel element is given by:

$$\phi = 1.5 \times 10^{-5} + 3.6 \times 10^3 e^{-1.34 \times 104/T + 273} \quad ,$$

where T = fuel temperature, $^{\circ}\text{C}$.

This function is plotted in Fig. 7. The first term of this function is a constant for low-temperature release; the second term is the high-temperature portion.

The release fractions have all been normalized to a standard ratio of fuel-clad gap to fuel diameter, although individual measurements were made with different geometry.

The curve in Fig. 7 applies to a fuel element which has been irradiated for a time sufficiently long that all fission product activity is at equilibrium. Figure 7 shows that the measured values of fractional releases fall well below the curve. Therefore, for safety considerations, this curve gives conservative values for the high-temperature release from U-ZrH fuel.

The results of recent studies in the TRIGA reactor at GA on fission product release from fuel elements with high uranium loadings (up to 3.7 g U/cm^3 , 45 wt-% U) agree well with data just presented from similar experiments with lower U loadings. As was the case with the lower U loadings, the release was determined to be predominantly recoil controlled at temperatures

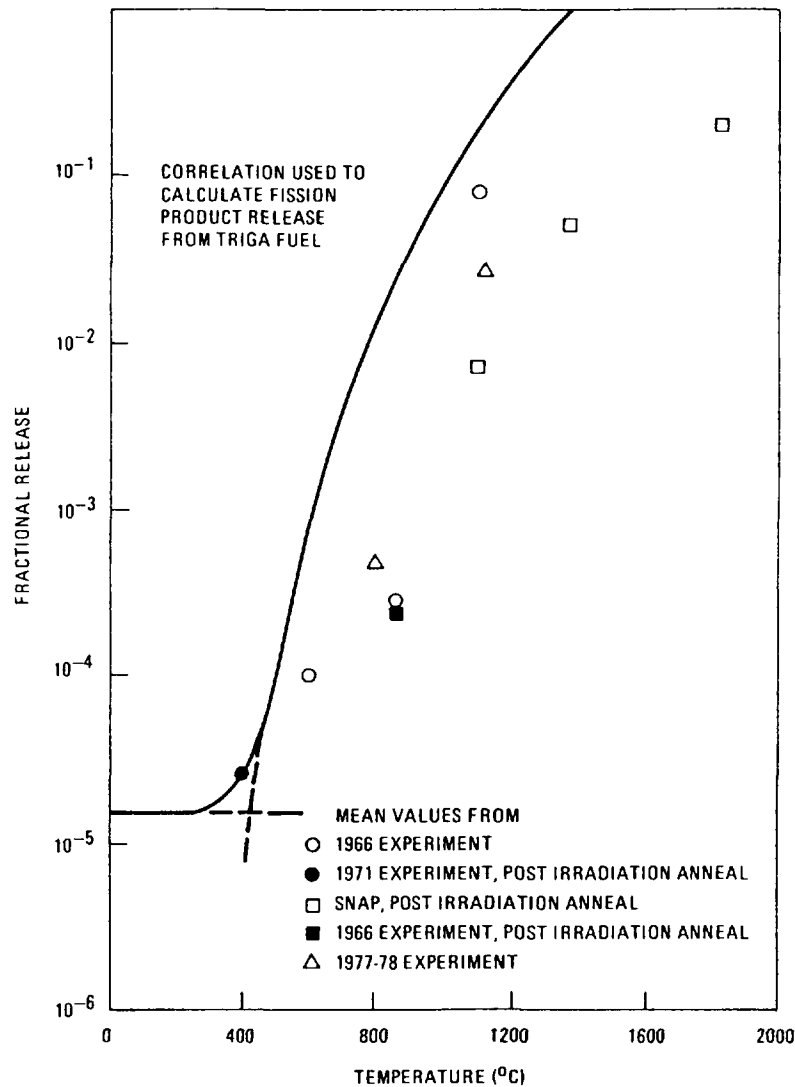


Fig. 7. Fractional release of gaseous fission products from U-ZrH fuel. Experimental values above 400°C corrected to infinite irradiation.

$\leq 400^\circ\text{C}$ and controlled by a migration or diffusion-like process above 400°C . Low-temperature release appears to be independent of uranium loadings, but the high-temperature release seems to decrease with increasing weight fractions of uranium. The correlation used to calculate the release of fission products from TRIGA fuel remains applicable for the high uranium loaded (TRIGA LEU) fuels as well as the 8.5 wt-% U-ZrH fuel for which it was originally derived. This correlation predicts higher fission product releases than measurements would indicate up to 1100°C . At normal TRIGA operating temperatures ($<750^\circ\text{C}$) there is a safety factor of approximately four between predicted and experimentally deduced values.

6. LIMITING DESIGN BASIS PARAMETER AND VALUES

Fuel-moderator temperature is the basic limit of TRIGA reactor operation. This limit stems from the out-gassing of hydrogen from the ZrH_x and the subsequent stress produced in the fuel element clad material. The strength of the clad as a function of temperature can set the upper limit on the fuel temperature. A fuel temperature safety limit of 1150°C for pulsing, stainless steel U-ZrH_{1.65} fuel is used as a design value to preclude the loss of clad integrity when the clad temperature is below 500°C . When clad temperatures can equal the fuel temperature, the fuel temperature limit is 950°C . There is also a steady-state operational fuel temperature design limit of 750°C based on consideration of irradiation- and fission-product-induced fuel growth and deformation. This is a time and temperature-dependent fuel growth as discussed earlier. A maximum temperature of 750°C has been used as the operational design basis temperature because resulting average fuel temperatures result in insignificant calculated fuel growth from temperature-dependent irradiation effects. (For ACPR fuel, where burnup is extremely low, the steady-state operational fuel temperature design criterion is 800°C .)

The dissociation pressure of the zirconium-hydrogen system is the principal contributor to the fuel element internal pressure at fuel temperatures above $\sim 800^\circ\text{C}$. Below $\sim 800^\circ\text{C}$, trapped air and fission product gases can be the major contributors to the internal pressure. At equilibrium condition, this pressure is a strong function not only of temperature but also of the ratio of hydrogen to zirconium atoms and the carbon content of the material. The current upper limit for the hydrogen-to-zirconium ratio is 1.65; the design value is 1.6. The carbon content is currently about 0.2% (2000 ppm). The equilibrium hydrogen pressure as a function of temperature for the fuel is shown in Fig. 3.

The equilibrium condition defined above never occurs, however, because the fuel is not a constant temperature over the whole volume. Consequently, the hydrogen pressures will be much lower than the equilibrium values calculated for the maximum temperature. As hydrogen is released from the hot fuel region, it is taken up in the cooler regions and the equilibrium that is obtained is characteristic of some temperature lower than the maximum. To evaluate this reduced pressure, diffusion theory is used to calculate the rate at which hydrogen is evolved and reabsorbed at the fuel surface. In the closed system considered here, the hydrogen not only diffuses into the

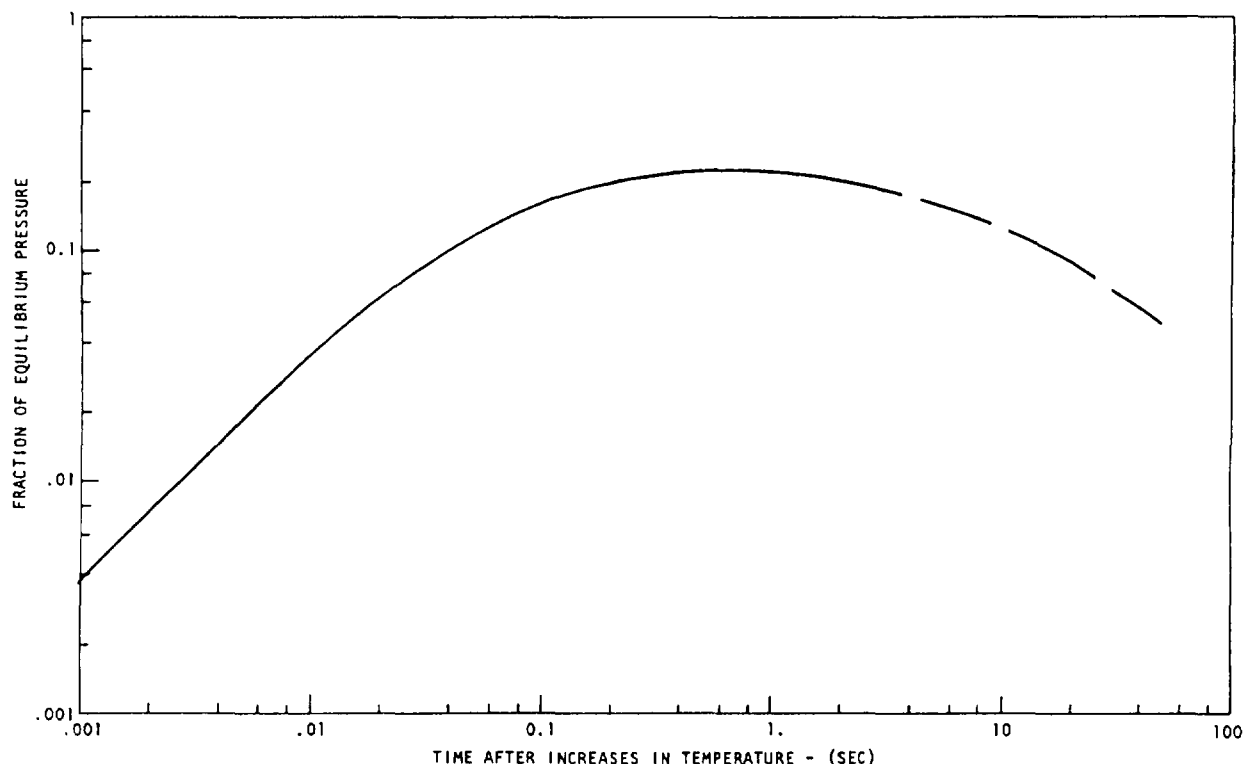


Fig. 8. Fuel element internal pressure versus time after a step increase in maximum fuel temperature

fuel/fuel clad gap, but also diffuses back into the fuel in the regions of lower fuel temperature. When the diffusion rates are equal, an equilibrium condition will exist.

In Fig. 8, the ratio of the fuel element internal pressure to the equilibrium hydrogen pressure is plotted as a function of time after a step increase in temperature. The maximum fuel temperature is 1150°C for which the equilibrium hydrogen pressure in $ZrH_{1.65}$ is 2080 psi. The calculation indicates, however, that the internal pressure increases for about 0.3 sec, when the pressure is ~420 psi, or ~20% of the equilibrium value. After this time, the pressure slowly decreases as the hydrogen continues to be redistributed along the length of the element from the hot regions to the cooler regions. Calculations were also made for step increases in power to the peak fuel temperatures of 1200° and 1350°C. Over this range, the time to the peak pressure and the fraction of the equilibrium pressure value achieved were approximately the same as for the 1150°C case. Thus, if the clad remains below ~138°C, the maximum internal pressure that would produce the yield stress in the clad is 1025 psi, and the corresponding equilibrium hydrogen pressure could be five times greater or ~5000 psi. This pressure corresponds to a maximum fuel temperature of ~1240°C in $ZrH_{1.65}$. Similarly,

the equilibrium hydrogen pressure could be 5×1840 or 9200 psi before the ultimate clad strength was reached corresponding to a fuel temperature of $\sim 1300^{\circ}\text{C}$.

The ultimate strength of the clad decreases slowly to about 57,000 psi at 500°C . Since the pressure is a strong function of fuel temperature, the fuel temperature to produce rupture decreases very slowly over this range, remaining at 1300°C for a clad temperature up to 300°C and decreasing to $\sim 1293^{\circ}\text{C}$ and 1282°C for clad temperatures of 400°C and 500°C respectively. For nongapped TRIGA pulsing fuel elements, the clad temperature during heat flow from a pulse is greater than the 138°C ACPR value but normally $< 500^{\circ}\text{C}$.

Measurements of hydrogen pressure in TRIGA fuel elements during steady-state operation have not been made. However, measurements have been made during transient operations and compared with the results of an analysis similar to that described here.

These measurements indicated that in a pulse in which the maximum temperature in the fuel was greater than 1000°C , the maximum pressure was only $\sim 6\%$ of the equilibrium value evaluated at the peak temperature. Calculations of the pressure resulting from such a pulse using the methods described above gave calculated pressure values above three times greater than the measured values.

An instantaneous increase in fuel temperature will produce the most severe pressure conditions. When a peak fuel temperature of 1150°C is reached by increasing the power over a finite period of time, the resulting pressure will be no greater than that for the step change in power analyzed above. As the temperature rise times become long compared with the diffusion time of hydrogen, the pressure will become increasingly less than for the case of a step change in power. The reason for this is that the pressure in the clad element results from the hot fuel dehydriding faster than the cooler fuel rehydrides (takes up the excess hydrogen to reach an equilibrium with the hydrogen over-pressure in the can). The slower the rise to peak temperature, the lower the pressure because of the additional time available for rehydriding.

The foregoing analysis gives a strong indication that the clad will not be ruptured if fuel temperatures are never greater than in the range of 1240°C to 1300°C , providing the clad temperature is less than 500°C . How-

ever, a conservative safety limit of 1150°C has been chosen for this condition. As a result, at this safety limit temperature the pressure is at least a factor of 5 (and up to a factor of 18) lower than would be necessary for clad failure. A factor of 5 is more than adequate to account for uncertainties in clad strength and manufacturing tolerances. The integrity of the clad has been demonstrated by TRIGA reactor pulse experiments to fuel temperatures $\geq 1150^{\circ}\text{C}$.

Under any condition in which the clad temperature increases above 500°C, such as during a loss-of-coolant accident or under film boiling conditions, the temperature safety limit must be decreased as the clad material loses much of its strength at elevated temperatures. To establish this limit, it is assumed that the fuel and the clad are at the same temperature. An analysis for this condition indicates that at a fuel and clad temperature of $\sim 950^{\circ}\text{C}$ the equilibrium hydrogen pressure produces a stress on the clad equal to its ultimate strength. There are no conceivable circumstances that could give rise to a situation in which the clad temperature was higher than the fuel.

The same argument about the redistribution of the hydrogen within the fuel presented earlier is valid for this case also. In addition, at elevated temperatures the clad becomes permeable to hydrogen. Thus, hydrogen not only will redistribute itself within the fuel to reduce the pressure, but also some hydrogen will escape from the system entirely.

The use of the ultimate strength of the clad material in the establishment of the safety limit under these conditions is justified because of the transient nature of such accidents.

7. GENERAL SPECIFICATIONS FOR ER-U-ZrH TRIGA LEU FUEL

Uranium content - 8.5, 12, 20, 30, 45 wt-% depending on fuel element model.

<u>Nominal (wt-%)</u>	<u>Range of Acceptance (wt-%)</u>
8.5	8.25 - 8.75
12	11.75 - 12.25
20	19.75 - 20.25
30	29.65 - 30.35
45	44.50 - 45.5

Uranium enrichment -	19.7 ± 0.2.							
Uranium homogeneity -	Manufacturing process produces homogenous distribution of uranium.							
Erbium -	Nominal range is 0.5 to 1.4 wt-% depending on fuel element model. Fuel with 8.5 wt-% U has no erbium. The range of acceptance (from the nominal value) is +5% to -10% for an element and +0% to -3% for a core.							
Erbium homogeneity -	Manufacturing process produces homogenous distribution of erbium.							
H/Zr ratio -	1.60 nominal (range 1.57 to 1.65).							
Cladding material -	304 stainless steel or Incoloy 800 depending on fuel element model (B + Cd ≤ 20 ppm).							
Thickness -	<table><tr><th><u>Nominal Element O.D. (in.)</u></th><th><u>Nominal Clad Thickness (in.)</u></th></tr><tr><td>1.5</td><td>0.020</td></tr><tr><td>0.5</td><td>0.016</td></tr></table>	<u>Nominal Element O.D. (in.)</u>	<u>Nominal Clad Thickness (in.)</u>	1.5	0.020	0.5	0.016	
<u>Nominal Element O.D. (in.)</u>	<u>Nominal Clad Thickness (in.)</u>							
1.5	0.020							
0.5	0.016							
Leak test -	A helium pressure leak test is performed where elements are subjected to helium pressure of 200 psig for 10 min and then put into a calibrated helium leak detector chamber.							
Dimensional inspection -	Elements are thoroughly checked for proper length, diameter (especially at welds), bow, and end-fitting straightness.							
Visual inspection of - cladding surface	Detailed inspection is performed for marred surfaces, porosity, or other faults which extend more than 0.001 in. below the surface; cracks of any type; and weld condition and appearance.							

8. OUTLINE OF INSPECTIONS DURING MANUFACTURE OF TRIGA FUEL

Title: INSPECTION OF TRIGA FUEL ELEMENTS

Doc. No. QDI 32-4	Issue A	Date	8/10/79	Page	of
-------------------	---------	------	---------	------	----

TABLE OF CONTENTS

	<u>Issue</u>
1.0 Scope	A
2.0 Release of Uranium for Fabrication	A
3.0 Sampling and Testing of Uranium Metal	A
4.0 Sampling and Testing of Zirconium Sponge	A
5.0 Sampling and Testing of Erbium Metal	A
6.0 Testing of Tubing Used as Cladding for Fuel Elements	A
7.0 Testing and Inspection of Graphite Plugs for Fuel Elements	A
8.0 Verification of Uranium, Erbium, and Zirconium Content in Casting (Melt) Charge	A
9.0 Sampling of Disks for Historical Purposes and Sampling for Percent Uranium and Percent Erbium from Each Casting After Zone Melting	A
10.0 Verification of Hydrogen-to-Zirconium Atom Ratio	A
11.0 Dimensional and Visual Inspection of Hydrided Melts	A
12.0 Witness of Element Assembly	A
13.0 Inspection of TRIGA Cladding Welds	A
14.0 Helium Backfill Check for Only 1/2 in. Diameter Fuel	A
15.0 Dimensional Inspection of Fuel Elements	A
16.0 Ferroxyl Test	A
17.0 Helium Pressure Leak Test of Fuel Elements	A
18.0 Overcheck of TRIGA Fuel Elements	A
19.0 Visual Inspection of Fuel and Control Rod Cladding Surfaces	A
20.0 Inspection and Witness of the Packaging of Completed Fuel Elements	A
21.0 TRIGA Special Element Test Procedure	A
22.0 Data Packages - When Requested	A
23.0 Calibration and Control of Measuring, Test and Inspection Devices	A

Appendix I-7.1

FINAL RESULTS FROM TRIGA LEU FUEL POST-IRRADIATION EXAMINATION AND EVALUATION FOLLOWING LONG TERM IRRADIATION TESTING IN THE ORR

G.B. WEST

GA Technologies, Inc.,
San Diego, California

M.T. SIMNAD

University of California,
San Diego, California

G.L. COPELAND

Oak Ridge National Laboratory,
Oak Ridge, Tennessee

United States of America

Abstract

The qualification testing of TRIGA-LEU (U-ZrH) fuels to high burnups in the ORR has been completed successfully over a 5-yr period. These fuels have included loadings of 20 wt %, 30 wt %, and 45 wt % uranium; 19.7% enriched. The irradiated fuel rods have been subjected to a comprehensive PIE following burnups of up to 64% of the U-235, exposures of 919 FPD and fast neutron fluences of 5×10^{21} n/cm². No limiting values were reached on fuel burnup. Fuel growth was as predicted. Evidence was shown of limited thermal migration of hydrogen. There was no pressure buildup inside the cladding. Fission product release from highly burned fuel doesn't appear to be significantly different from fresh fuel. The results have demonstrated that these fuels will retain their integrity to burnups well in excess of the design goals.

INTRODUCTION

As part of the testing of TRIGA (uranium zirconium-hydride, rodDED) low enriched uranium fuel, a 16-rod experimental cluster was irradiated in the Oak Ridge Research Reactor (ORR) between December 1979 and August 1984. This long-term fuel burnup test was part of the U.S. Department of Energy Reduced Enrichment Research and Test Reactor (RERTR) program managed by Argonne National Laboratory. A total of 19 U-ZrH fuel rods with three different fuel compositions were tested containing 20, 30, and 45 wt % uranium (19.7% enriched). The uranium density in the 45 wt % fuel is 3.7 gm/cm³. The test cluster operated incORE for 919 full power days. Some of the fuel test parameters are shown in Table 1.

In May 1982, after 575 full power days, the rods containing 20 and 30 wt % uranium were removed, having attained a burnup in the range of 50% of the contained uranium-235. Destructive examination of one rod each of the 20, 30, and 45 wt % fuel rods showed normal performance with no anomalies.

All post-irradiation examination (PIE) work described in this report was done at Oak Ridge National Laboratory. Irradiation of the 45 wt % rods was continued to the target burnup value of 50% and extended into the burnup range of 55% to 65% of the contained uranium-235, up to a test cluster exposure of 919 full power days. The burnup history of the 45 wt % rods is shown in Fig. 1.

A comprehensive PIE was performed on selected 45 wt % fuel rods from the ORR irradiation as the final step in the TRIGA LEU test program. The PIE included the following:

1. Gamma scan of rod 1086.
2. Diametral and bow measurements.
3. Burnup analysis on section from highest burnup region of rod 1086.
4. Measurement of pressure in and identification of gases from plenum inside fuel rod.
5. Physical testing of clad segments of rod 1086.
6. Performance of metallography on each type of fuel rod.

The metallography on rod 1086 indicated no major differences from the metallography which was previously performed on the 45 wt % fuel.

RESULTS

Limiting Values

No limiting values were reached on fuel burnup or irradiation effects in the U-ZrH-Incoloy-800 fuel-clad system nor were any indications evident that limiting values were being approached. This might well be expected since the U-ZrH fuel-moderator matrix with 45 wt % U contains only a modest 20 vol % U. It is felt that the fuel loading of the U-ZrH matrix could be significantly increased, likely into the 40 to 50 vol % range, and continue to demonstrate successful operation.

TABLE 1 TRIGA LEU FUEL ORR IN-PILE TEST PARAMETERS

	20 WT-% U	30 WT-% U	45 WT-% U
CONTAINED U-235 PER 22 IN FUEL ROD (GMI)	19	30	55
VOL-% U (19.7% ENRICHED)	7	11	20
MAX CALC ROD POWER GENERATION (KW)			
INITIAL CONFIGURATION	—	36	35
FULL CLUSTER CONFIGURATION	41	43	48
45 WT-% ONLY CONFIGURATION	—	—	55
TIME AT POWER (FPD)			
INITIAL CONFIG (DEC 79-NOV 80)	0	278	278
FULL CLUSTER CONFIG (MAY 81-MAY 82)	295	295	295
45 WT-% ONLY CONFIG (JULY 82-NOV 83)	0	0	328
45 WT-% ONLY CONFIG (AUG 84)	0	0	18
TARGET BURNUP OF U-235 (%)	35	40	50
FINAL BURNUP RANGE (%)	45-57	47-57	60-66

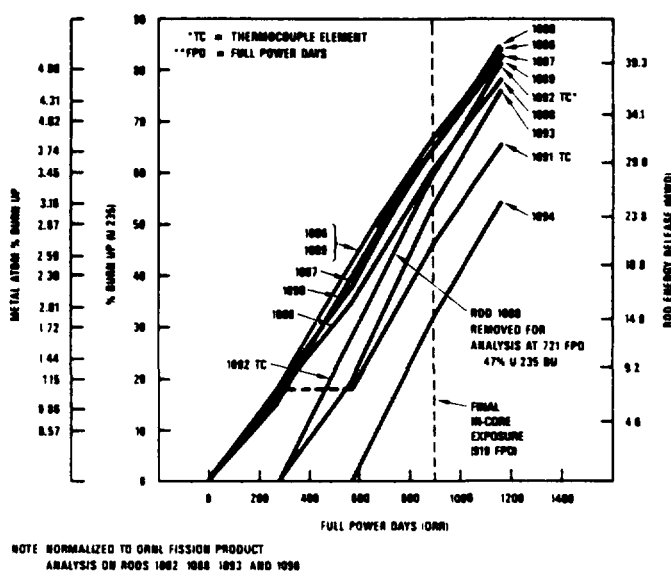


Fig. 1. Burnup versus full power days 45 wt % TRIGA LEU fuel in ORR

Diametral Fuel Growth and Cladding Ductility

The agreement between predicted and average measured fuel growth during burnup was very good, especially considering the ovalities and small inaccuracies of the measurements. It is concluded that the expected maximum average diametral growth was about 25 mils or about 4.6%, and the measured growth agreed with the predicted value within the accuracy of the measurements. Maximum ovalities were in the range of 20 to 30 mils. The Incoloy-800 clad yields during this growth, but maintains uniformity and very good ductility with end-of-life ductility estimated to be in the range of 10% to 20%. The good ductility was well demonstrated by the ring bend tests (Fig. 2) where several clad segments from a highly burned up fuel rod were compressed radially flat in a vice. The compressed rings experienced some spring-back on release, but no cracks were detected in the severely deformed areas.

RBT

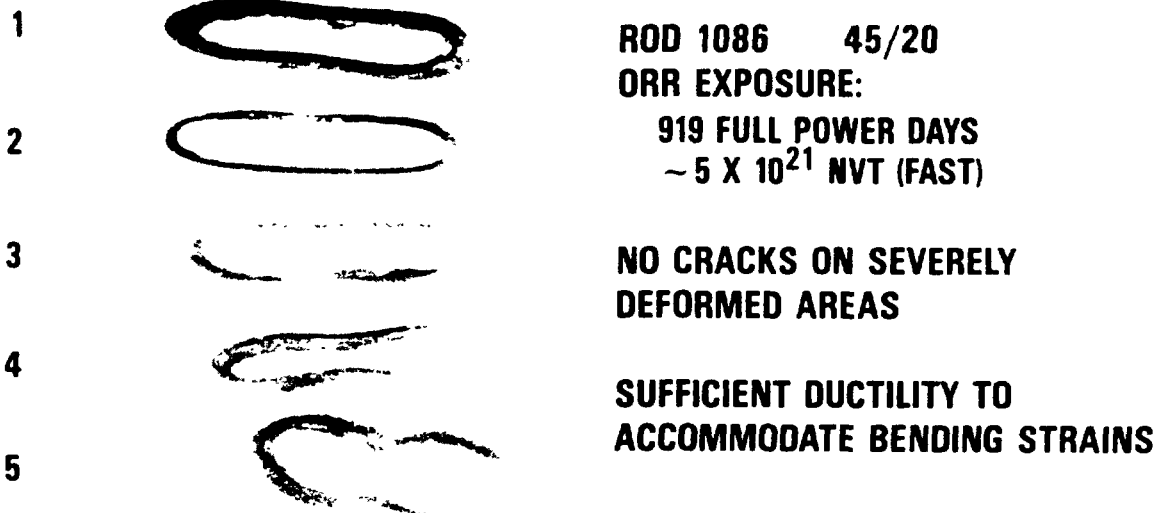


Fig. 2. Irradiated TRIGA LEU Incoloy 800 clad ring bend test results

Axial Length Changes

Measured axial length changes of the fuel rods ranged between 34 and 61 mils. These are small and acceptable values. This growth is not a direct measure of fuel growth, as there is a plenum region which can accommodate axial fuel growth, but rather is an important measure of fuel-clad interaction. Any serious ratcheting interaction between the fuel and clad would result in much larger fuel rod axial growth values than those encountered. The fuel rods were cycled through over 100 startup and shutdown cycles of the ORR. In addition, previous tests with several hundred power cycles have been performed in the TRIGA Mark F reactor at GA. The tests at GA also included

tests under pulsing conditions where reactivities of up to \$2.57 were inserted in 0.1 sec, pulsing the reactor power to over 2000 MW and the LEU fuel temperatures to over 600°C. No fuel ratcheting occurred. An important reason for the lack of any ratcheting between the fuel and clad is the good match between the thermal expansion properties of zirconium hydride fuel and Incoloy-800 clad as shown in Table 2.

TABLE 2
COMPARISON OF UZrH/ALLOY 800 AND
UO₂/ZIRCOLOY RADIAL EXPANSION

	EXPANSION COEFFICIENT [$\Delta L/L/^\circ C$]	AVERAGE TEMPERATURE ($^\circ C$)	RADIAL EXPANSION (MILS/0.5 IN. O.D. ROD)
U-ZrH	11×10^{-6}	450	1.2
INCOLOY	17×10^{-6}	160	0.7
UO ₂	11×10^{-6}	1200	3.3
ZIRCOLOY 2	5×10^{-6}	315	0.4

Measured Bow Values

The maximum measured bow of fuel rods removed from the constraints of the fuel cluster was 63 mils (1/16 in.). Most were less than 25 mils. These small values reflected the ease with which the individual fuel rods were removed from and reinserted into the fuel cluster many times over the duration of the irradiation. The spacers in the fuel cluster were designed for severe bending forces, but these results indicate that the bending forces resulting from fuel burnup are not large. It is pointed out, however, that the fuel rods were rotated 180 deg about four times during the irradiation as a crude, approximate means of balancing any bending forces due to fuel burnup.

Internal Pressure Buildup

There was no internal pressure buildup inside the fuel element cladding. Any fission gas release was insignificant from a pressure standpoint. The measured internal pressures were sub-atmospheric at the end of the irradiation because of absorption of oxygen and nitrogen by the zirconium fuel matrix from the partial pressure of air in the one atmosphere air-helium mixture inside the clad at the time of manufacture.

Metallographic Examinations

The metallographic examinations of the fuel rods indicate the presence of a dendritic structure, which is inherited from the solidification stage during the casting of the U-Zr rods. The zone-melting process that is used to densify the cast fuel rods gives rise to a dendritic structure. There is a large temperature range between the liquidus and solidus temperatures in the U-Zr phase diagram at the alloy compositions used. This results in microsegregation of the uranium within the dendritic structure. The average sizes of the microsegregated uranium vary from about 1 μm in 8.5 wt % U fuel to about 5 μm in the 45 wt % U fuel. This microsegregation has a beneficial effect on fission product release, measured during previous tests on TRIGA-LEU. The fission product release fraction is decreased by up to a factor of 100 at 1100°C for the 45 wt % U fuel with 5 μm uranium compared to 8.5 wt % U fuel with 1 μm uranium. The irradiated fuel rods also contain close arrays of micropores clustered at grain boundaries and dendrite/matrix phase interfaces. These pores are associated with fission gas bubbles and

etched solid fission products, which would be expected under long burnup conditions and do not have a harmful effect on fuel performance. Uranium would not be expected to migrate to any significant degree at temperatures characteristic of TRIGA fuel and there is no evidence of diffusion or migration of the uranium in even the most highly loaded and burned up fuel rods.

Hydrogen Migration

The metallographic studies of the irradiated fuel rods show evidence of limited but significant thermal migration of the hydrogen down the temperature gradients. The hydrogen migrates from the higher temperature central region towards the cooler surface regions of the fuel rods. The hydrogen migration reaches an equilibrium for any given temperature distribution. The time period necessary for this equilibrium to be reached and the variations in the hydrogen concentration depend upon the temperatures involved; the greater the temperature and temperature gradient, the faster the hydrogen moves. In any case the time to equilibrium would be relatively short compared to the irradiation time of this test and the hydrogen concentrations might vary by $\pm 10\%$ to 15% from their initial values. The hydrogen migration gives rise to four distinct annular regions (Fig. 3) with characteristic light and dark appearances and structural variations. However, the fuel rods are not significantly deformed by the redistribution of the hydrogen within the single gamma phase as strongly evidenced by their retention of dimensional and mechanical stability. These results reinforce conclusions reached through other operational results and fuel examination programs with U-ZrH fuel; namely that peak limit pulsing operations should not be performed with longer life fuel where equilibrium hydrogen redistribution has occurred. The increased H/Zr ratio at the outer radius of the fuel, coupled with high peak fuel temperatures which occur at the outer radius during a pulse, can cause excessive hydrogen pressures in the fuel matrix which can weaken and deform the fuel matrix and even cause excessive swelling and fuel element deformation. Pulse sizes should be modestly reduced in longer burning cores to account for the limited hydrogen redistribution.

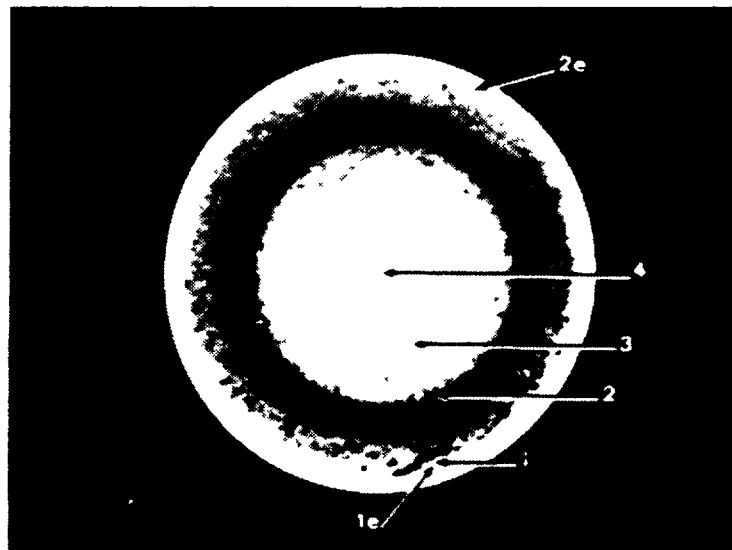


Fig. 3. Rod 1093, section met 2, macrograph showing locations of micrographs

Incoloy-800 Compatibility

The compatibility of the Incoloy-800 cladding with both the fuel and the coolant is excellent. A mechanical bond developed between the fuel and clad during the long term burnup swelling. No other type of fuel-clad bonding occurred. There is no evidence of corrosion by the coolant water after four

years of exposure in the ORR. The cladding i.d. shows no evidence of stress corrosion cracking by reaction with fission products or with the fuel. A thin ($\sim 5 \mu\text{m}$, $\sim 1\%$ of 16 mil clad thickness) layer in the i.d. of the cladding has been affected by fission recoil damage, as seen in the metallographic examination of the etched cladding (Fig. 4) adjacent to fuel. However, there are no cracks evident in the cladding i.d. or o.d., which confirms the excellent resistance of Incoloy-800 to stress corrosion cracking.



Fig. 4. Rod 1093, section met 2, location 2e

Damage to Fuel Rods

Two fuel rods were damaged to the point of releasing fission products after long exposure in the ORR. The cladding on one of the fuel rods suffered rapid fretting wear as a result of vibratory contact with a grid spacer in the fuel assembly. The vibration resulted from a change in the experiment configuration just prior to the failure. The other damaged rod failed as a result of water ingress through some defect in the cladding, which propagated through the cladding after the prolonged exposure to the operating stresses. In both cases it was the formation of steam inside the cladding, during a rise to power following reactor shutdown, that caused the highly localized rupture of the cladding and ejection of some fuel into the coolant water. In both cases, the damaged fuel rods showed only localized attack at the site of failure, with no propagation of the damage to the remainder of the fuel or cladding. Good clad ductility was evident. This confirmed the results of preirradiation corrosion tests which demonstrated the excellent corrosion resistance of the fuel. In the future, in order to further reduce the likelihood of using clad material which could contain defects, all clad for higher power reactors with forced flow cooling will be 100% ultrasonic tested.

Fission Product Release

Measured fission product release of stable xenon isotopic nuclei into the plenum of one of the fuel rods does not show the fission product release from highly burned up TRIGA-LEU fuel to be significantly different from the well documented and very low values for unirradiated and slightly burned up fuel, at least over the temperature range experienced during the ORR irradiation (25°C to 650°C). Table 3 gives the best estimate and upper and lower limits of fission product release. Figure 5 shows the measured temperature dependent fission product release fractions for unirradiated and slightly burned up TRIGA-LEU fuel. Averaging the release fraction over the calculated temperature distribution in a fuel rod gives a fission product release fraction of about 4×10^{-4} . Using temperatures for only the upper portion of the fuel rod gives a release fraction just somewhat below 1×10^{-4} .

Table 3
TRIGA-LEU Fission Product Release Fraction
for Highly Burned Up Fuel

Isotope	Measured Release Fraction Based on Various Source Assumptions		
	Entire Fuel Rod	Fraction Related To Top Surface Only (Upper Limit)	Upper-Most 1/2 in. Length of Fuel (Best Estimate)
Xe-131	7.1×10^{-6}	1.2×10^{-3}	3.1×10^{-4}
Xe-132	9.5×10^{-6}	1.7×10^{-3}	4.2×10^{-4}
Xe-134	8.9×10^{-6}	1.6×10^{-3}	3.9×10^{-4}
Xe-136	1.4×10^{-5}	2.5×10^{-3}	6.2×10^{-4}

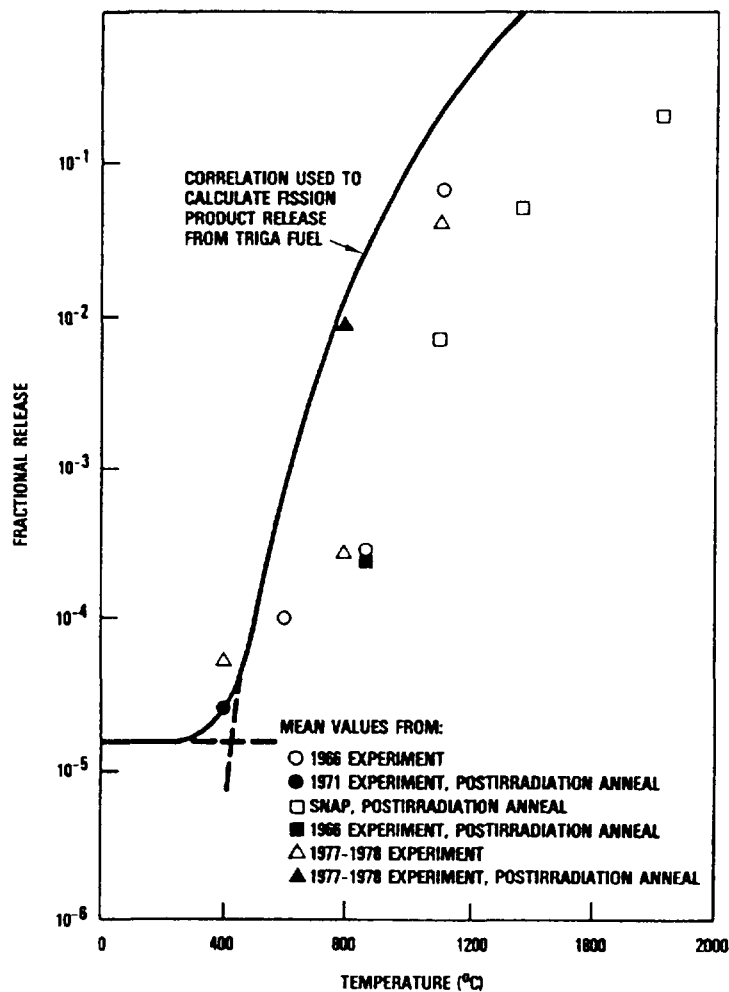


Fig. 5. Fractional release of gaseous fission products from unclad TRIGA fuel

CONCLUSIONS

The qualification testing of TRIGA-LEU fuels to high burnups, up to 64% of initially contained U-235, has been completed successfully over a 5-yr period. The burnups were well in excess of design goals. No limiting values were reached. The results have demonstrated the fuel material to be stable and retentive, even when exposed to water and steam. The Incoloy-800 clad has proven to be compatible and corrosion resistant, retaining its integrity with good ductility after long exposure.

Appendix J

IRRADIATION AND POST-IRRADIATION EXAMINATION (PIE) OF DISPERSION FUELS WITH HIGH URANIUM DENSITY

Abstract

Requirements on the reliability of LEU fuel are summarized from the point of view of a reactor operator and an outline of the philosophy and procedures that were utilized by the U.S. RERTR Program for non-destructive and destructive PIE of miniplates and full-size elements is described.

Extensive data are provided on the irradiation and post-irradiation examination of HEU and LEU dispersion fuels with high uranium density ($\geq 1.7 \text{ g/cm}^3$). Data includes burnup results, swelling and blister threshold temperature behavior, results of metallographic examinations, and fission product release behavior.

Appendix J-1

IRRADIATION AND PIE OF MTR HEU DISPERSION FUELS WITH URANIUM DENSITIES UP TO 1.7 g/cm³

Appendix J-1.1

PIE DATA FOR HEU (93%) ALUMINIDE AND OXIDE FUELS

ARGONNE NATIONAL LABORATORY
RERTR Program,
Argonne, Illinois,
United States of America

Abstract

Post-irradiation-examination data are summarized for HEU (93%) UAl_x-Al dispersion fuel with up to 1.7 g U/cm³ and for HEU (93%) U₃O₈-Al dispersion fuel with up to 1.2 g U/cm³.

HEU (93%) UAl_x-Al DISPERSION FUEL

Dispersions of UAl_x in aluminum have performed satisfactorily since 1967 with uranium densities up to about 1.7 g/cm³ in the Advanced Test Reactor (ATR) at the Idaho National Engineering Laboratory (INEL). The ATR core consists of 40 fuel elements, each with 975 g ²³⁵U (using 93% enriched uranium) contained in 19 fuel plates. The fuel meat thickness is 0.51 mm and the 6061-F aluminum clad varies between 0.38 and 1.0 mm. The active height of the plates is 1.21 m. The normal steady-state power level is 250 MW, and the peak (including hot channel factors) and the average surface heat fluxes are 870 and 185 W/cm², respectively.

The data and discussion in the following paragraphs on UAl_x-Al fuel are taken from Ref. 1, where additional information can be obtained.

As of 1980, over 1700 plate-type UAl_x-Al fuel elements have been operated in the ATR, ETR, and MTR test reactors at INEL in the past ten years. Of these elements, 48 were found to contain blistered fuel plates, nearly all during the first years of ATR operation. Investigations revealed that the blisters were associated with corrosion of thin cladding over the ends of the plate cores. Only small amounts of fission products were released to the coolant water since the growth of these blisters was a slow process. Consequently, the operation of the reactor was not interrupted.

The operating life of fuel elements in the ATR is determined by the burnup limit, which has been extended in steps to a fission density of 2.3×10^{21} fissions/cm³ of core. The irradiation performance data on which this burnup limit is based consist of post-irradiation measurements, both destructive and nondestructive, made on fuel elements and on sample fuel plates. Some of this data is presented here.

Swelling or growth of irradiated fuel plates results from the accumulation of solid and gaseous fission products and from chemical reactions that

Table 1 Growth and Swelling of UAl_x-Al Fuel Plate Cores for the ATR Reactor and for Test Samples.

Element and Sample Number	U atom/cm ³ (X10 ²¹)	Fission Density (X10 ²¹)	Irradiation Temperature (K)	Core Porosity (vol%)	Swelling $\left(\frac{\Delta V}{V} \%\right)$	Reference
Comp 3	2.48 ^c	0.75	423-473	10.5	1.4	17
Comp 4	3.32	1.0	423-473	14.0	0.3	17
Comp 9	2.48	0.75	423-473	10.5	1.0	17
584	3.40	0.68	423-473	4.6	0.6	18
587	3.40	1.52	423-473	4.6	5.1	18
621	3.65	1.18	423-473	4.1	2.5	18
622	3.65	0.80	423-473	6.2	1.0	18
623	3.65	1.13	423-473	4.5	2.5	18
625	3.65	0.48	423-473	4.5	1.5	18
169 11	3.38	2.16	373-473	8.4	4.7	19
169 12	3.39	2.27	373-473	8.4	5.9	19
169 19	2.65	1.84	373-473	6.6	4.7	19
169 36	3.34	2.35	373-473	7.9	6.4	19
169 37	3.34	2.38	373-473	7.8	6.0	19
169 38	3.39	2.34	373-473	7.0	7.4	19
169 39	3.35	2.23	423-473	7.5	5.7	19
XA8G	2.69	0.72	423-473	3.11	2.4 ^a	14
XA8G	3.39	0.99	423-473	3.11	2.9	14
XA20G	3.39	0.21	423-473	3.11	1.8	14
XA8G	2.69	0.40	423-473	3.11	2.2	14
XA8G	4.10	0.68	423-473	3.11	3.0 ^a	14
XA8G	3.39	0.54	423-473	3.11	1.7	14
XA8G	4.10	0.42	423-473	4.11	1.5	14
Fuel elements						
XA130K&A135K	4.25	2.0	423-473	5.94	6.3 ^a	19
169-4	4.22	2.46	423-473 ^b	11.6	2.0	19
169-5	4.20	2.69	423-473 ^b	12.0	4.7	19
XA20G	3.39	0.69	423-473	3.11	3.7 ^a	14

^aAverages of growth data on fuel elements where fission density is within 0.15×10^{21} fissions/cm³.

^bTemperature range is for fission densities between 1.2×10^{21} fissions/cm³ and value given

^c 1.0×10^{21} U atoms/cm³ corresponds to a uranium density of 0.39 g/cm³.

occur between the fuel and the matrix. The gaseous atoms (xenon and krypton) constitute ~15% of the fission products and are principally in solution in the microstructure. The solid fission product swelling would be expected to be proportional to the fission density less any volume accommodation from the fuel core porosity. The accommodation of solid fission products in the core porosity appears to be related to the core temperature and fission rate.

The swelling data²⁻⁵ from four fuel elements and sixteen samples are given in Table 1 and are plotted in Fig. 1. The empirical equation for 24 data points obtained by least-squares linear regression is

$$\frac{\Delta V}{V} \% = 2.6\% F / (10^{21} \text{ fissions/cm}^3 \text{ of core})$$

where F = fission density (fissions/cm³ of core). This equation indicates that swelling starts with fissioning. If burnup is defined as the fraction of original ²³⁵U atoms that are lost by fission or capture, the fission density can be expressed as

$$F \times 10^{-21} \text{ fissions/cm}^3 = 2.15 \epsilon \rho_U B$$

where ϵ = uranium enrichment
 ρ_U = uranium density, g/cm³
B = ²³⁵U fractional burnup

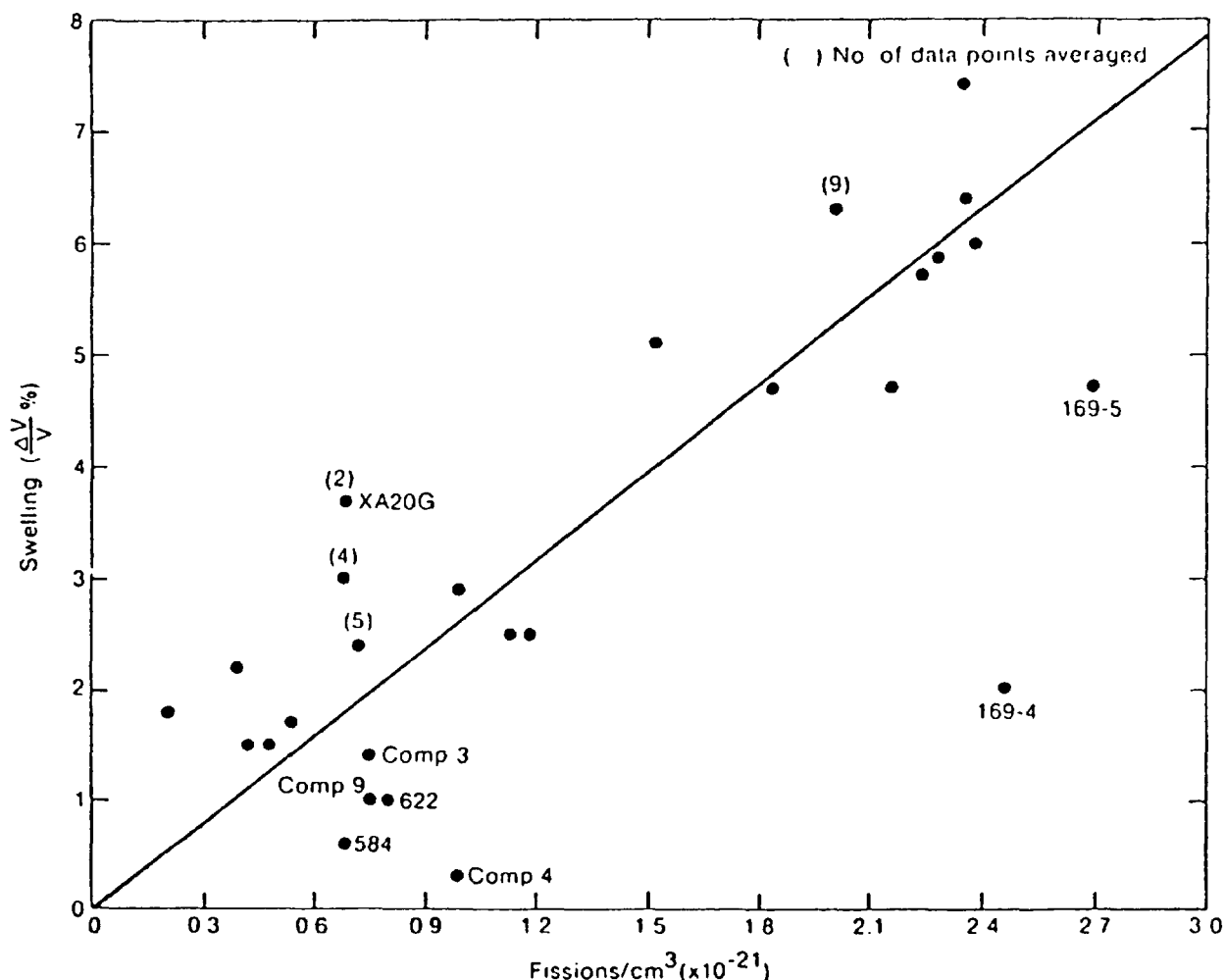


Figure 1 Swelling of Uranium Aluminide Fuel Plates as a Function of Fission Density (from Ref. 1).

Several parameters affect the scattering of the data in Fig. 1. These are: (1) irradiation temperature (however, the data have been selected to be in a narrow temperature range, 373-473 K), (2) fuel loading (U atoms/cm³), and (3) core porosity. The data in Fig. 1 and Table 1 indicate that increasing core porosity tends to reduce swelling. Three data points (169-4, 169-5, Comp 4), which have swelling values that lie well below the least squares linear regression curve in Fig. 1, correspond to samples with high initial porosity (>11.6%). Figure 2 shows a plot of core density and porosity of fuel plates with different uranium densities. At constant core density, the porosity increases with increasing uranium loading. It is probable that the factor which reduces the swelling at high fission densities is the pore volume, which accommodates the solid fission products during the slowing down process of the fission fragments. That is, the core behavior is plastic provided the temperature and fission density are high enough.

Postirradiation blister testing is commonly used as a criterion for predicting fuel element failure. The assumption is that the temperature at which breakaway swelling occurs is decreased as the concentration of the gaseous atoms (helium, xenon, krypton) increases and the pores or voids become filled. The criterion should be conservative since, under irradiation, gaseous atoms in bubbles undergo re-resolution from the slowing down process of the fission fragments.⁶⁻⁸ Although these re-resolution studies have been performed on UO₂ fuel,

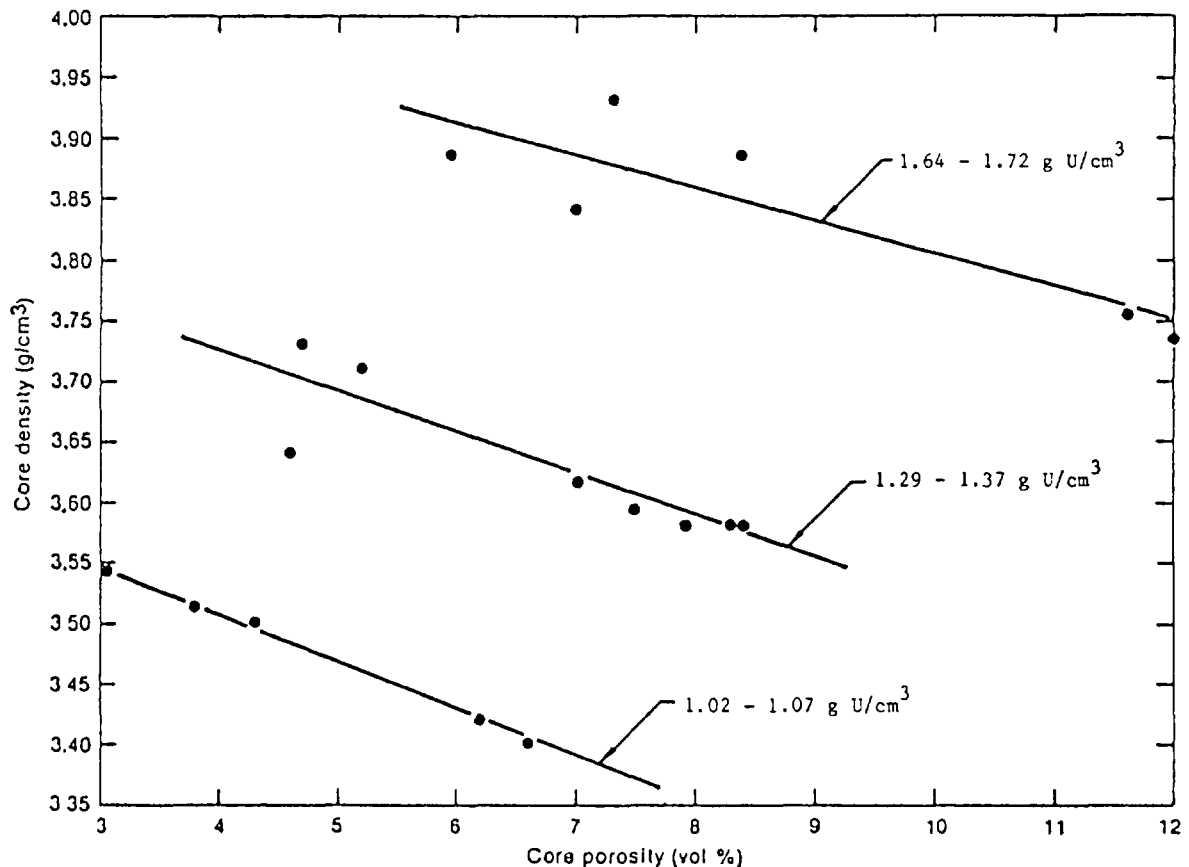


Fig. 2 Core Density and Porosity of Uranium Aluminide Fuel Plates with Different Fuel Loadings (from Reference 1).

the re-resolution mechanism will also apply for UAl_x -Al fuel, and the blister temperature in-reactor should be equal to or greater than in postirradiation tests.

The postirradiation blister temperatures are given in Table 2 and a least-squares regression analysis with proposed 2σ and 3σ limit curves is given in Fig. 3. The proposed limit curves are extended to a higher fission density at the minimum value of the polynomial. The polynomial is given as

$$T_B = 905 - 139.9 F + 44.8 F^2,$$

where F = fission density in units of 10^{21} fissions/cm³

T_B = blister temperature in K.

Thus, up to a fission density of 2.7×10^{21} fission/cm³, the potential for swelling from gaseous atoms as measured in a blister test is not strongly influenced by the burnup in uranium aluminide fuels. In addition, it is not physically realistic that the blister temperature would increase at fission densities beyond 1.5×10^{21} fissions/cm³. Hence, it is believed that the polynomial fit in the region beyond 1.5×10^{21} fissions/cm³ is due to the limited amount of data. The limiting curves for 2σ and 3σ were extended as horizontal lines from the minimum values in Fig. 3.

HEU (93%) U_3O_8 -Al DISPERSION FUEL

Although there is less experience with U_3O_8 dispersion-type fuel than with UAl_x dispersion-type fuel, the available irradiation data indicates

Table 2 Blister Temperatures for UAl_x-Al Fuel Elements for the ATR Reactor and for Test Samples.

Element	Sample Number	²³⁵ U atom/cm ³ (X10 ²¹)	Total U atom/cm ³ (X10 ²¹)	Burnup (%)	Fission Density [fiss/cm ³ of core (X10 ²¹)]	Temperature (K)
XA3G	2-21	2.50 ^a	2.69	37.0 ^b	0.98	755
	7-0	3.81	4.10	14.2	0.61	838
	7-7	3.81	4.10	18.8	0.79	838
	7-14	3.81	4.10	21.3	0.89	838
	7-21	3.81	4.10	21.3	0.89	838
	7-28	3.81	4.10	21.3	0.89	838
	7-35	3.81	4.10	18.0	0.75	838
	7-42	3.81	4.10	13.3	0.56	838
	15-25	3.81	4.10	33.3	1.40	810
	16-21	3.16	3.40	30.5	1.03	755
XA8G	7-T	3.81	4.10	6.7	~0.28	871
UAl _x 7F	11-T	3.81	4.10	6.7	~0.28	866
	11-B	3.81	4.10	6.7	~0.28	866
XA130K	0-7	3.96	4.26	13.2	0.56	---
	0-6	3.96	4.26	26.1	1.11	---
	0-5	3.96	4.26	39.7	1.69	767
	0-4	3.96	4.26	44.1	1.88	767
	0-3	3.96	4.26	46.2	1.97	800
	0-2	3.96	4.26	48.4	2.06	800
	0-1	3.96	4.26	49.8	2.12	---
XA135K	5-2	3.95	4.23	19.4	0.82	---
	5-3	3.95	4.23	31.3	1.32	797
	5-4	3.95	4.23	41.4	1.75	813
	5-5	3.95	4.23	44.9	1.90	813
	5-6	3.95	4.23	48.8	2.07	813
	5-7	3.95	4.23	51.4	2.17	813
	5-1	3.95	4.23	49.3	2.09	797
Sample	169-4	3.88	4.22	58.3	2.46	838
	169-5	3.86	4.20	64.0	2.69	838
	169-11	3.11	3.38	63.9	2.16	811
	169-12	3.11	3.39	67.0	2.27	838
	169-19	2.44	2.65	69.4	1.84	838
	169-36	3.11	3.34	70.4	2.35	838
	169-37	3.11	3.34	71.3	2.38	811
	169-38	3.14	3.39	69.0	2.34	811
	169-39	3.12	3.35	66.6	2.23	838

^a 1.0×10^{21} ²³⁵U atoms/cm³ corresponds to a uranium density of 0.42 g/cm³.

^b % burnup expressed as % of total uranium atoms burned.

that U₃O₈-Al fuel is capable of sustaining the requisite burnups for research and test reactors.

The HFIR reactor⁹ at ORNL uses U₃O₈-Al dispersion-type fuel which has a loading of about 1.2 g U/cm³ (40 wt% U₃O₈). The overall thickness of the plates (clad + fuel) is 1.27 mm, whereas the meat thickness varies from 0.25 to 0.76 mm. The fuel plates have an effective height of 508 mm. In the HFIR the average burnup of the fissile atoms is 31% (0.9×10^{21} fissions/cm³).¹⁰ To date, in HFIR, over 76,000 of these U₃O₈-Al dispersion-type fuel plates have been burned to the depletion limit of 1.9×10^{21} fissions/cm³ with no failures, although on two occasions fuel plates did develop suspected fission product leaks. In only one case, however, was the leak serious enough to require removal of the fuel element from the reactor. Post-irradiation destructive tests of selected fuel plates showed no evidence of blisters, cladding separation, or fuel meat cracking. In addition, some experimental plates have undergone burnups of up to 75% (2.1×10^{21} fissions/cm³) without failure or gross dimensional changes.¹¹

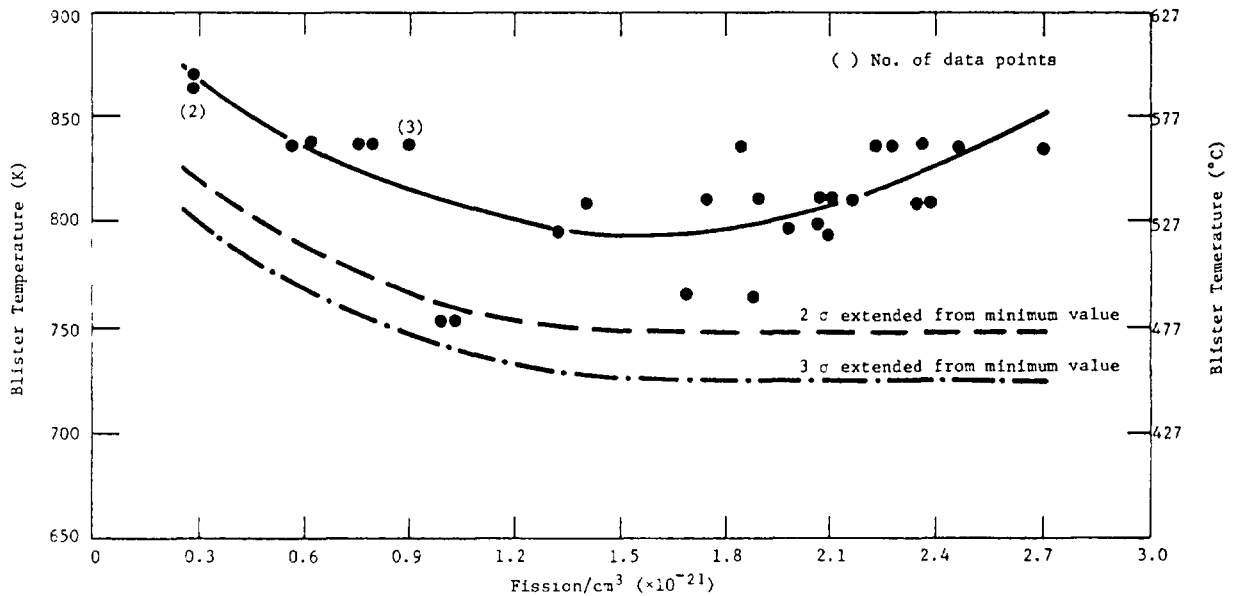


Figure 3 Blister Temperatures of Uranium Aluminide Fuel Plates as a Function of Fission Density. (Reference 1)

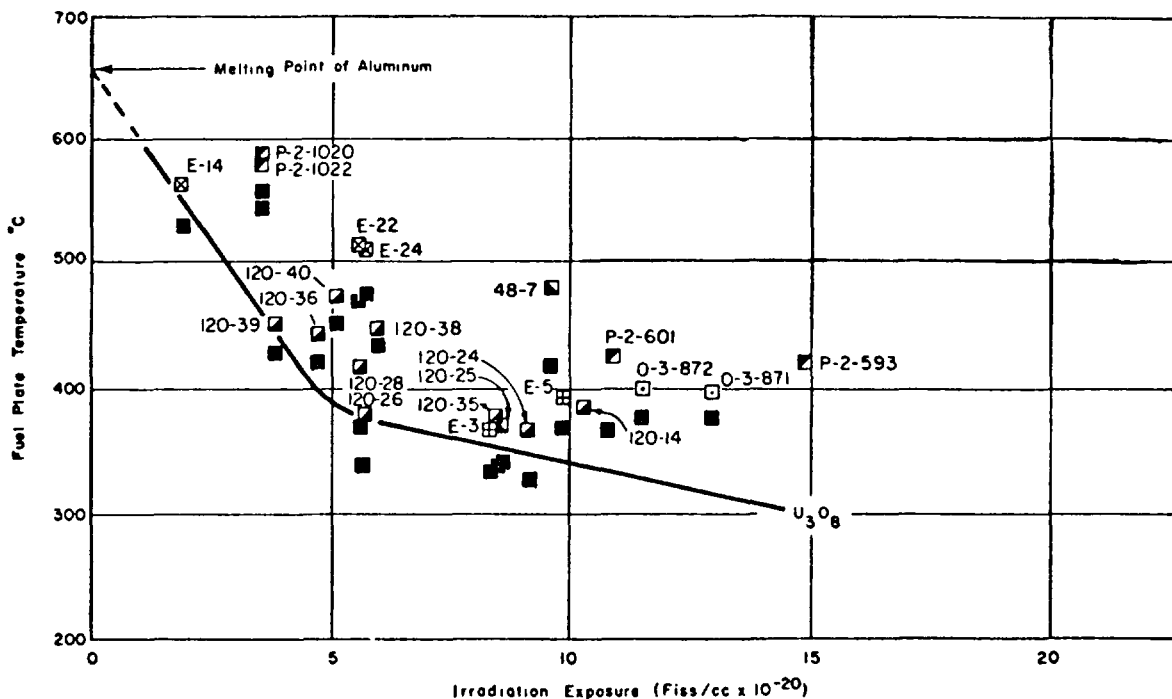


Fig. 4 Failure-no-failure Line for U_3O_8 -Al Dispersion Fuel. (Reference 12). Blistering is expected above the line, but not below. U_3O_8 loading varied from 22.3 to 41.6 wt.%.

Available data on postirradiation blister temperature testing of U_3O_8 -Al plate-type fuel are present in Figs. 4-6. The data shown in Fig. 4 were derived from tests on small, specially-fabricated, U_3O_8 -Al test samples. As shown in this figure, the blister temperature decreases sharply up to an irradiation level of 5×10^{20} fissions/cm³, but more slowly thereafter to an estimated temperature of 250°C at the highest burnup levels normally experienced with these fuels ($\sim 2.2 \times 10^{21}$ fissions/cm³).

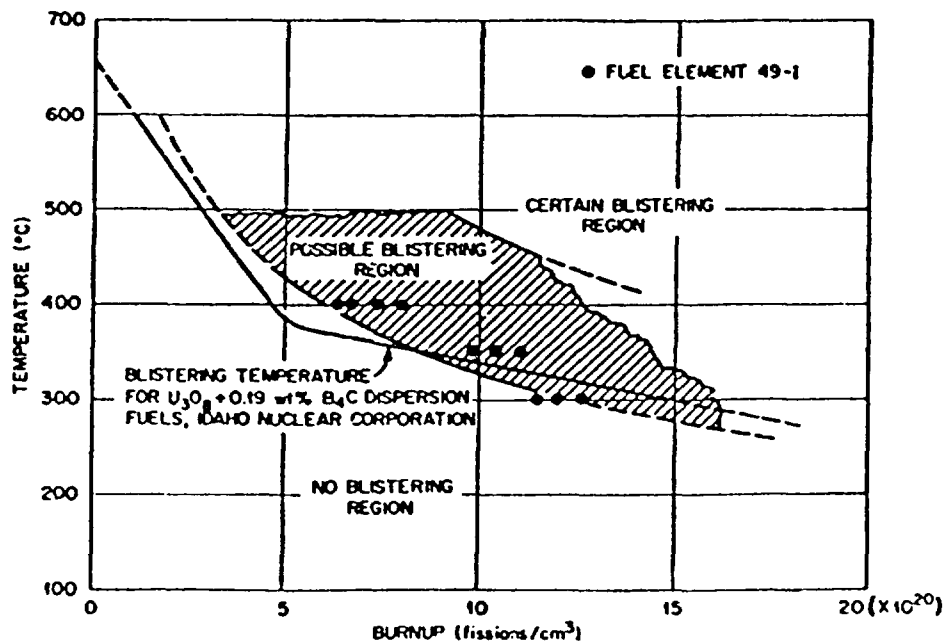


Fig. 5 Postirradiation Blistering Temperature of Inner HFIR Fuel plates (Reference 13). Idaho Nuclear Corporation results are from Marchbanks and Graber (Reference 14).

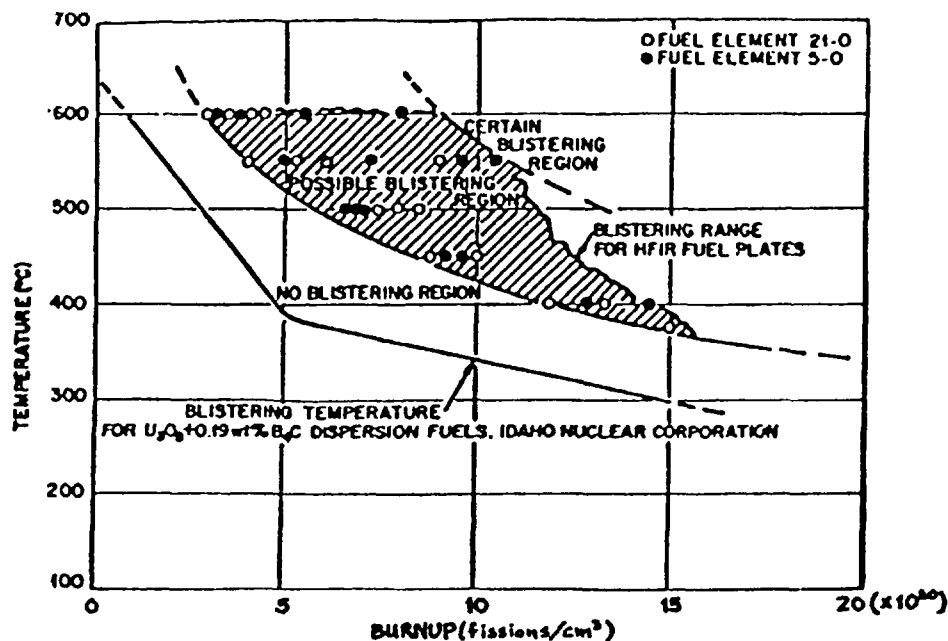


Fig. 6 Postirradiation Blistering Temperatures of Outer HFIR Fuel Plates (Reference 13). Idaho Nuclear Corporation results are from Marchbanks and Graber (Reference 14).

For purposes of comparison, the data in Fig. 4 are compared with the experience with a large number of HFIR fuel plates. These comparisons, which are presented in Figs. 5 and 6, show that the irradiation experience with the production run HFIR fuel has been better than that indicated by the small sample data. The solid line in Figs. 5 and 6 is the same line that represents the lower bound of the data in Fig. 4. Comparison of Figs. 5 and 6 shows that the higher loaded outer elements of the HFIR, which operate at a somewhat

higher temperature, exhibit more favorable (higher) blistering temperatures. This suggests that the fuel operating temperature is an important parameter in determining the post-irradiation blistering behavior.

Comparison of these data with those for uranium-aluminide fuel presented in Fig. 3 indicates that the blistering temperature for the U_3O_8 dispersion-type fuel at the higher burnup levels (1.5 to 2.0×10^{21}) is from 100 to $200^\circ C$ lower depending upon the irradiation temperature. Higher irradiation temperatures yield higher post-irradiation blistering temperatures.

REFERENCES

1. J. M. Beeston, R. R. Hobbins, G. W. Gibson, and W. C. Francis, "Development and Irradiation Performance of Uranium Aluminide Fuels in Test Reactors," Nuclear Technology 49, 136 (1980).
2. M. J. Graber, G. O. Hayner, R. R. Hobbins, and G. W. Gibson, "Performance Evaluation of Core II and III Advanced Test Reactor Fuel Elements," ANCR-1027, Aerojet Nuclear Company (1971).
3. M. J. Graber, G. W. Gibson, V. A. Walker, and W. C. Francis, "Results of ATR Sample Fuel Plate Irradiation Experiment," IDO-16958, Idaho Operation Office, Atomic Energy Commission (1964).
4. V. A. Walker, M. J. Graber, and G. W. Gibson, "ATR Fuel Materials Development Irradiation Results - Part II," IDO-17157, Idaho Operations Office, Atomic Energy Commission (1966).
5. Unpublished Internal Data, EG&G, Idaho, Inc.
6. A. D. Whapham, "Electron Microscope Observations of the Fission-Gas Bubble Distribution in UO_2 ," Nucl. Appl. 2, 123 (1966).
7. R. M. Cornell, M. V. Speight, and B. C. Masters, "The Role of Bubbles in Fission Gas Release from Uranium Dioxide," J. Nucl. Mater. 30, 170 (1969).
8. R. S. Nelson, "The Stability of Gas Bubbles in an Irradiation Environment," J. Nucl. Mater. 31, 153 (1969).
9. R. D. Cheverton, and T. M. Sims, "HFIR Core Nuclear Design," Oak Ridge National Laboratory Report ORNL-4621 (July 1971).
10. "Reactor Safety Evaluation of ORNL Proposal to Modify Fuel in ORR," Oak Ridge National Laboratory (Feb. 1977).
11. M. M. Martin, Oak Ridge National Laboratory, Oak Ridge, TN, personal communication (April 1978).
12. M. J. Graber and M. F. Marchbanks, "Blister Resistance of Various Aluminum Dispersion Fuel Systems," Idaho Nuclear Corporation Annual Progress Report on Reactor Fuels and Materials Development for FY 1967, IN-1121 (Feb. 1968), pp. 43-47.
13. A. E. Richt, R. W. Knight, and G. M. Adamson, Jr., "Postirradiation Examination and Evaluation of the Performance of HFIR Fuel Elements," Oak Ridge National Laboratory Report ORNL-4714 (Dec. 1971).
14. M. Marchbanks and M. J. Graber, "ORNL Versus Commercially Manufactured U_3O_8 ," Idaho Nuclear Corp. Annual Progress Report on Reactor Fuels and Materials Development for FY 1967, IN-1121 (Feb. 1968) pp. 37-39.

Appendix J-1.2

A STATISTICAL EVALUATION OF THE IRRADIATION PERFORMANCE OF HEU-BASED UAl_x -Al DISPERSION FUELS

S. GAHLERT, S. NAZARÉ
Kernforschungszentrum Karlsruhe GmbH,
Karlsruhe, Federal Republic of Germany

Abstract

A large body of data was generated during the development and testing of HEU (93%) UAl_x -Al fuel with U-densities up to 1.7 Mg U/m^3 . The data reveals a large scatter which can be expected not only from the parameter variation (metallurgical and testing) but also from the difficulties encountered in post-irradiation examinations.

This paper provides a statistical evaluation of the influence of various parameters such as fission density, burnup, fuel loading, boron content, and irradiation temperature on the two major performance criteria--namely swelling and blistering, and develops empirical equations capable of predicting the swelling and blistering behavior.

1. Introduction

UAl_x -Al dispersion fuel elements with U-densities up to about 1.7 Mg U m^{-3} have been in operation in various test reactors since almost 20 years. Because of its excellent performance under high flux and high burnup conditions UAl_x -Al can be considered to be a classical fuel for research and test reactors. During the development and testing, which was done mainly at INEL, ORNL and KfK, and subsequent operation, a large body of data was generated. The data reveals a large scatter which can be expected not only from the parameter variation (metallurgical and testing) but also from the difficulties encountered in post-irradiation examinations.

The objectives of this paper are:

- to statistically evaluate the influence of various parameters such as fission density, burnup, fuel loading, boron content, irradiation temperature, on the two major performance criteria - namely swelling and blistering;
- to develop empirical equations capable of predicting the swelling and blistering behaviour.

Wherever possible an attempt has been made to outline the relative importance of the individual parameters for the overall behaviour.

All plates considered in this paper were prepared by powder metallurgical techniques using the well known roll bonding method /3,9/. The fuel meat thickness of miniature as well as full size plates was typically 0.51 mm. The cladding thickness was generally 0.38 mm. Some full size plates had a thicker cladding up to 1.00 mm. Various commercial aluminum alloys were initially used as cladding materials (e.g. 6061, X8001, 1100, XAPO01, APM-768, MD101). The alloy 6061 is the now preferred cladding material.

An extensive irradiation testing program was carried out at INEL. Miniature plates were tested mainly in the ETR in a pressured water loop under maximum thermal neutron fluxes of $5.5 \cdot 10^{14} \text{ n cm}^{-2} \text{ s}^{-1}$ and heat fluxes of $7.6 \cdot 10^6 \text{ W m}^{-2}$ /12/. Irradiation temperatures were varied in a wide range from about 350 K to 550 K. Most full size elements were irradiated in the ATR, a high power reactor which allows very high thermal neutron fluxes up to $1 \cdot 10^{15} \text{ n cm}^{-2} \text{ s}^{-1}$ /6/. Miniature plates tested at ORNL were irradiated in the HFIR under a maximum thermal neutron flux of about $3.1 \cdot 10^{14} \text{ n cm}^{-2} \text{ s}^{-1}$ at temperatures between 320 and 370 K /5/. Irradiation testing at KfK was carried out in the FR 2 under maximum thermal neutron fluxes of $8.5 \cdot 10^{13} \text{ n cm}^{-2} \text{ s}^{-1}$ and maximum heat fluxes of $1 \cdot 10^6 \text{ W m}^{-2}$ /4/.

2. Swelling behaviour

Swelling is one of the main performance criteria for the evaluation of dispersion fuels. For the design and safe operation of the reactor, the dimensional stability under normal and off-normal conditions is very important. Multiple regression analysis was used to evaluate the effect of various irradiation parameters on swelling behaviour.

Table 1 summarizes the data of miniature plates used in the regression analysis.

It is well known that swelling depends on fission density. Discarding all other parameters and considering only fission density, the linear least square method yields the following equation:

$$\Delta V/V = -1.87 + (3.21 \cdot 10^{-27}) \cdot \text{FD} \quad (1)$$

with:

$\Delta V/V$ = swelling of the dispersion [%]

FD = fission density [$\text{fiss} \cdot \text{m}^{-3}$]

Table 1: Available data on swelling of miniature plates

Sample	UAl ₃ Content [wt%]	U-Loading [Mgm ⁻³]	Porosity [%]	Irradiation Temperature [K]	Fission Density [10 ²⁷ fiss m ⁻³]	Burnup ⁴ [%]	Swelling [%]	Reference
584	51.2	1.29	4.6	425	0.74	24.2	0.6	7
585		1.29	4.5	422	1.07	35.0	0.8	7
587		1.29	4.6	451	1.63	53.2	5.1	7
588		1.29	4.3	444	1.52	49.7	5.1	7
589		1.29	4.9	361	0.83	27.1	3.8	7
621	56.2	1.43	4.1	401	1.26	37.1	2.5	7
622		1.43	6.2	405	0.87	25.6	1.0	7
623		1.43	4.5	401	1.21	35.7	2.5	7
625		1.43	4.5	401	0.51	15.0	1.5	7
14-766	44.0 ¹	1.30	3.9	384	1.09	35.4	3.1	1
14-769	"	1.30	4.1	399	1.21	39.2	3.0	1
12-727	50.0	1.32	8.4	383	1.09	34.8	4.0	"
12-735		1.32	8.1	402	1.35	43.1	1.8	"
12-736		1.32	9.9	423	1.49	47.6	4.4	"
1-1003		1.32	11.7	505	0.33	10.6	-1.1	"
1-1005		1.32	10.1	526	0.62	19.9	-1.7	"
1-1007		1.32	11.3	511	0.58	18.5	-2.5	"
1-1046		1.32	10.4	498	0.30	9.6	-1.1	"
32-4	51.4	1.41	1.3	343	1.79	53.4	8.8	5
24-3	52.2	1.41	3.3	350	1.92	57.3	7.9	5
14-3	52.9	1.42	4.2	352	2.02	59.7	7.4	5
34-2	53.2	1.42	4.3	349	1.95	57.6	6.8	5
15-4	62.8	1.79	6.6	358	2.22	51.8	6.1	5
35-4	63.0	1.78	7.3	354	2.14	50.3	4.8	5
25-4	64.1	1.82	8.4	356	2.17	50.1	4.1	5
0-24-959	48.6 ²	1.36	2.5	438	1.69	52.0	6.7	5
0-24-964	48.6 ³	1.40	4.3	446	1.57	46.9	4.8	5
0-24-965	48.6 ³	1.40	4.3	433	1.77	52.9	6.0	5
I11-1848	43.9	1.10	10.9	483	0.41	15.7	-1.3	2
I11-1849	"	1.10	10.7	433	0.62	23.7	-1.4	"
I11-1850	"	1.10	11.2	403	0.63	24.1	-1.8	"
I69-1579	60.0	1.71	7.9	423	1.60	39.2	3.6	"
I69-1580	"	1.71	6.9	443	0.94	23.1	1.8	"
I70-1583	65.0	1.94	7.8	443	1.10	23.8	1.2	"
I70-1584	"	1.94	7.2	443	1.62	35.1	4.9	"
I71-1593	77.0	2.58	11.6	443	1.26	20.5	-1.9	"
I71-1594	"	2.58	13.2	423	2.39	39.0	1.1	"
I1-1800	51.0	1.35	9.8	473	0.98	30.5	1.5	"
I1-1811	"	1.35	6.6	473	1.03	32.0	1.5	"
I1-1826	"	1.35	7.8	473	1.01	31.4	2.5	"
I1-717	"	1.35	8.0	523	0.81	25.2	-0.8	"
I12-727	"	1.35	6.0	383	1.09	33.8	3.9	"
I1-1082	"	1.35	7.2	423	0.37	11.5	0.4	"
I1-1090	"	1.35	7.4	413	1.03	32.0	0.2	"
I1-1003	"	1.35	8.9	503	0.32	9.9	-1.1	"
I1-1005	"	1.35	7.5	523	0.62	19.2	-1.7	"
I1-1007	"	1.35	7.2	513	0.58	18.0	-2.4	"
I1-1046	"	1.35	7.5	498	0.30	9.3	-1.0	"
I1-1097	"	1.35	7.2	383	0.56	17.5	0.8	"
I1-1095	"	1.35	6.8	383	0.69	21.4	0.8	"
I1-1096	"	1.35	7.2	423	1.80	56.0	0.6	"
I6-682	46.0	1.17	4.1	398	0.58	20.8	1.7	"
I7-688	46.7	1.19	4.4	398	0.56	19.7	1.3	"
I11-709	43.9	1.10	3.5	423	1.51	57.6	2.3	"
I11-710	"	1.10	3.9	398	0.55	21.0	1.8	"
I23-1294	60.0	1.71	15.7	463	1.59	39.0	-4.2	"
I23-1296	"	1.71	13.5	443	1.62	39.7	-1.3	"
I23-1100	"	1.71	14.4	473	2.06	50.5	-1.9	"
I23-1105	"	1.71	13.1	473	1.41	34.6	-1.7	"
I19-1130	51.0	1.35	4.4	483	1.06	33.0	2.0	"
I34-1244	52.0	1.39	2.8	563	2.07	62.6	6.0	"
I34-1249	"	1.39	2.6	553	1.07	32.3	1.5	"
I34-1251	"	1.39	1.8	533	2.02	61.1	6.5	"
I1-587	51.0	1.35	4.7	473	1.62	50.3	5.1	"
I1-584	"	1.35	4.7	423	0.72	22.4	0.6	"
I1-585	"	1.35	4.5	443	1.07	33.2	0.8	"

1 UAl₃ 60 wt% UAl₂ and 40 wt% UAl₃ assumed

2 UAl₃ with 73.7 wt% U solid-state reacted

3 UAl₃ with 75.2 wt% U arc-cast

4 FIFA

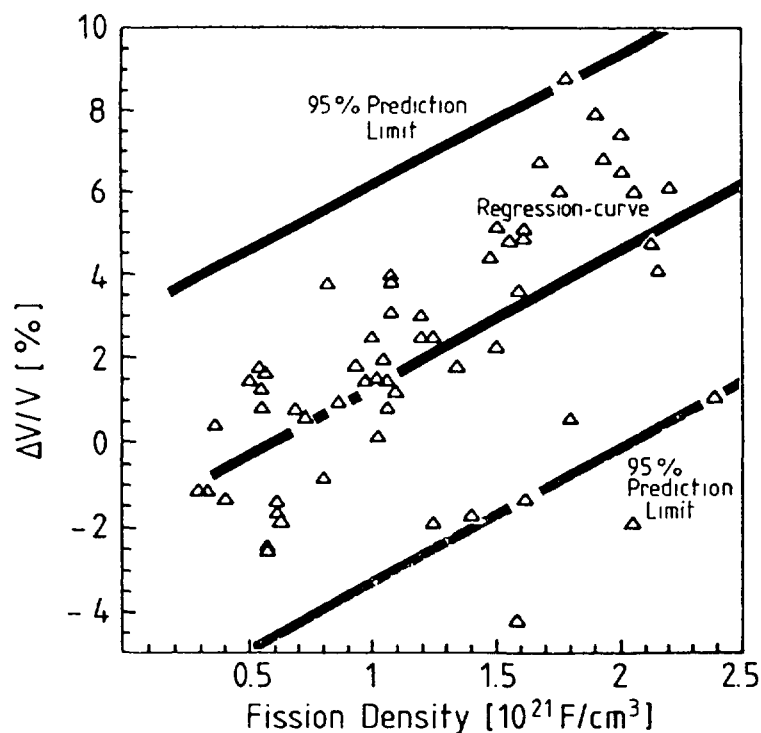


Fig. 1: Swelling of miniature plates as a function of fission density (comparison with regression analysis, equation 1)

In figure 1 the experimental data is compared with the regression line. Also shown are 95% prediction intervals for single observations (dashed lines). The fact that a number of plates showed shrinkage instead of swelling can only be explained by considering additionally the shrinkage of initial pores. A closer examination revealed, that this shrinkage occurred particularly at high porosities and at high irradiation temperatures. In fact, all the data points in the right lower part of the plot correspond to plates with high porosities and irradiation temperatures. As could be expected, the plate with the highest swelling (8.8%) also had a very low porosity (1.3%) and was irradiated at a low temperature (343 K).

The constant in the above equation (-1.87) has no physical meaning and is merely a consequence of the simple linear fit that cannot describe the complex shrinkage kinetics at low fission densities. The slope of 3.21 in equation 1 corresponds to a relative atomic volume increase of about 1.5 as compared to 3.04 theoretically predicted by Graber [11]. The fact that swelling is significantly lower than predicted theoretically is an indication that at least part of the solid and gaseous fission products is in solution in the lattice of the particle or in the recoil zone.

Naturally, a better fit can be obtained by discarding those data points that correspond to plates with high porosities (> 10%). The empirical equation is then given by:

$$\Delta V/V = -2.00 + (3.96 \cdot 10^{-27}) \cdot FD \quad (2)$$

The effect of porosity on swelling can be better described by considering porosity as an additional parameter in the regression analysis. The linear least squares fit obtained is given by:

$$\Delta V/V = 2.48 + (2.86 \cdot 10^{-27}) \cdot FD - 0.566 P \quad (3)$$

with:

P = initial core porosity [%].

The above equation yields a much higher coefficient of correlation (88.2%) as compared to equation 1 (61.95%). The equation also indicates that only part of the porosity available compensates the swelling by shrinkage during irradiation. In fact, microstructures of irradiated UAl_x -Al dispersions have usually revealed a rest porosity even after high burnup at high temperatures /10/.

There have been attempts in the past to take into account the effect of porosity merely by deducting it from swelling /5,9/. However, equation 3 indicates that this approach could lead to an underestimate of total swelling.

Including irradiation temperature as an additional parameter in the regression model gives the following equation:

$$\Delta V/V = 6.68 + (2.64 \cdot 10^{-27}) \cdot FD - 0.554 P - 0.00956 T \quad (4)$$

with:

T = irradiation temperature [K].

Equation 4 indicates that irradiation temperature has only a minor influence in comparison to fission density and porosity (the t-statistics being 8.71 for fission density, -10.27 for porosity and only 2.91 for temperature). Of course, equation 4 gives the best coefficient of correlation (89.7%).

It has been postulated, that swelling is influenced by fuel loading. However, the multiple regression analysis led to the conclusion that fuel loading does not effect swelling (t = 0.83). Nevertheless, fuel loading

Table 2: Available data on swelling of full size plates

Sample	UAl _x Content [wt%]	Porosity [%]	U-Loading [Mgm ⁻³]	Fission Density [10 ²⁷ fiss m ⁻³]	Burnup ³ [%]	Swelling [%]	Reference
XA8G1-2	42.7	3-11	1.05	0.30	12.0	1.8 ¹	6
XA8G1-42	"	"	"	0.62	24.8	2.5 ¹	"
XA8G2-2	"	"	"	0.30	12.0	1.8 ¹	"
XA8G2-10	"	"	"	0.75	30.0	2.3 ¹	"
XA8G2-14	"	"	"	0.89	35.6	2.8 ¹	"
XA8G2-31	"	"	"	0.86	34.4	0.4 ¹	"
XA8G2-35	"	"	"	0.74	29.6	3.9 ¹	"
XA8G2-43	"	"	"	0.43	17.2	2.2 ¹	"
XA8G4-18	50.6	"	1.32	1.06	33.7	2.9 ¹	"
XA8G4-6	"	"	1.32	0.58	18.4	1.7 ¹	"
XA8G8-2	57.6	"	1.60	0.26	6.8	1.7 ¹	"
XA8G8-26	"	"	"	0.91	23.9	6.4 ¹	"
XA8G8-30	"	"	"	0.86	22.6	3.0 ¹	"
XA8G8-34	"	"	"	0.78	20.5	2.4 ¹	"
XA8G8-38	"	"	"	0.63	16.5	1.8 ¹	"
XA8G8-42	"	"	"	0.45	11.8	1.5 ¹	"
XA20G4-2	50.6	"	1.32	0.60	19.0	0.4 ¹	"
XA20G4-18	"	"	"	0.85	27.0	4.3 ¹	"
XA20G4-34	"	"	"	0.63	20.0	3.0 ¹	"
XA20G4-42	"	"	"	0.23	7.3	1.8 ¹	"
XA130K	58.9	5.94	1.66	2.00	50.6	6.3 ²	9
XA135K	"	"	"	2.00	50.6	6.3 ²	9

1 estimated

2 averaged where fission density within $\pm 0.15 \cdot 10^{27}$ fiss m⁻³

3 FIFA

can have an indirect effect since high fuel loadings usually lead to high core porosities during fabrication. Also the particle size in the dispersion is not statistically significant ($t = -1.06$).

Table 2 summarizes the data of full size plates irradiated in the ATR at INEL. Since during the fuel development stage most of the irradiation testing is done using miniature plates the question arises whether full sizes plates compare favorably to miniature plates with regard to swelling behaviour. In figure 2 the data of full size plates are plotted together with the regression line and 95% prediction intervals based on miniature plates according to equation 2.

At first sight, swelling of full size plates appears to be slightly higher than swelling of miniature plates. In /6/ this is attributed to the fact that all these full size plates had very low core porosities. Taking porosity into account, the discrepancy can be fully accounted for using an average initial porosity of 2 to 4%. Thus swelling of full size and miniature plates is in good agreement.

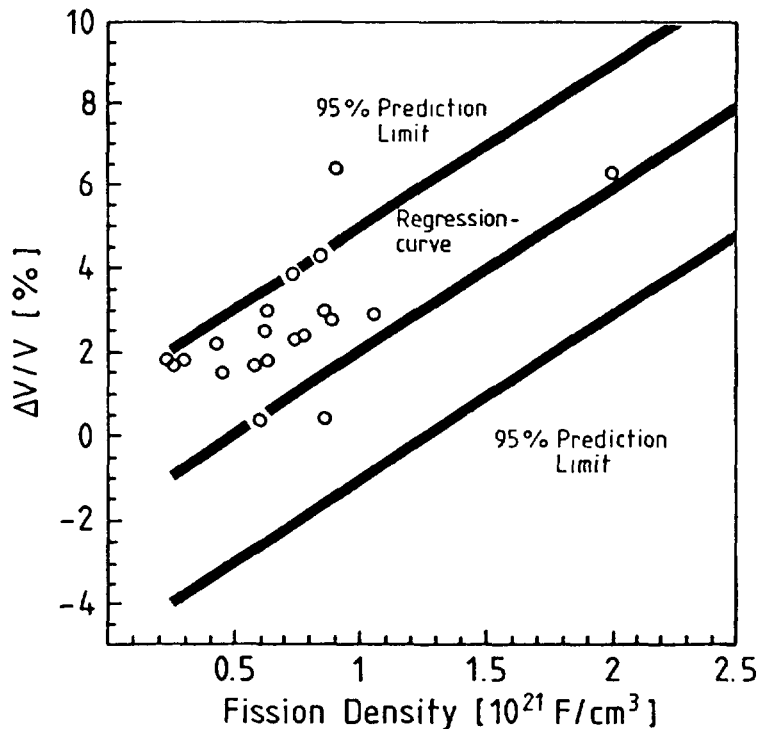


Fig. 2: Swelling of full size plates as a function of fission density (comparison with regression analyses of miniature plates, equation 2)

3. Blistering behaviour

Since under normal irradiation conditions an excessive swelling of the fuel generally does not occur, usually post-irradiation annealing tests (blister tests) are performed. The blister testing is carried out by annealing the plate at successively higher temperatures in steps of 30 K or 50 K (annealing time about 30-60 minutes) until blisters on the surface of the plates are visible. This so called "blister threshold temperature" gives an indication of the dimensional stability of the plate during short periods of overheating (off-normal conditions). However, it should be recognized that this test does not duplicate in-pile conditions. It is likely that these temperatures are conservative estimates of the operating limits because gaseous atoms undergo resolution under irradiation /9/. Table 3 shows the blister data of various miniature plates.

The effect of fission density, burnup, fuel loading, porosity, particle-size and B_4C -content on blister temperature was investigated using multiple regression. The analysis led to the conclusion that blister temperature depends mainly on fission density and B_4C -content. A linear fit gave

Table 3: Available data on blister threshold temperature of miniature plates

Sample	UAI ₁ Content [wt%]	U-Loading [Mgm ⁻³]	Porosity [%]	B ₂ C Content [wt%]	Fission Density [10 ²⁷ fiss m ⁻³]	Burnup ⁷ [%]	Blister Temperature [K]	Reference
I12-727	51.0	1.35	6.0	0.19	1.09	33.8	813 ³	2
I12-736	"	"	7.4	"	1.49	46.3	753 ³	"
I11-1003	"	"	8.9	"	0.32	9.9	863 ³	"
I11-1046	"	"	7.5	"	0.30	9.3	863 ³	"
I11-1097	"	"	7.2	"	0.56	17.5	813 ³	"
I11-1082	"	"	7.2	"	0.37	11.5	863 ³	"
I11-1090	"	"	7.4	"	1.03	32.0	813 ³	"
I11-1095	"	"	6.8	"	0.69	21.4	813 ³	"
I11-1096	"	"	7.2	"	1.80	56.0	813 ³	"
I6-682	46.0	1.17	4.1	"	0.58	20.8	863 ³	"
I11-709	43.9	1.10	3.5	—	1.51	57.6	863 ³	"
I12-737	51.0	1.35	6.1	0.19	0.84	26.1	753 ³	"
I34-1244	52.0	1.39	2.8	"	2.07	62.6	783 ³	"
I34-1249	"	1.39	2.6	"	1.07	32.3	843 ³	"
I34-1251	"	1.39	1.8	"	2.02	61.1	783 ³	"
I11-585	51.0	1.35	4.5	"	1.07	33.2	713 ³	"
I11-588	"	1.35	4.5	"	1.52	47.3	703 ³	"
I11-1848	43.9	1.10	10.9	—	0.41	15.7	873 ³	"
I11-1849	"	1.10	10.7	—	0.62	23.7	>873 ³	"
I11-1850	"	1.10	11.2	—	0.63	24.1	873 ³	"
I69-1579	60.0	1.71	7.9	—	1.60	39.2	873 ³	"
I69-1580	"	1.71	6.9	—	0.94	23.1	873 ³	"
I70-1583	65.0	1.94	7.8	—	1.10	23.8	873 ³	"
I70-1584	"	1.94	7.2	—	1.62	35.1	873 ³	"
I71-1593	77.0	2.58	11.6	—	1.26	20.5	873 ³	"
I71-1594	"	2.58	13.2	—	2.39	39.0	703 ³	"
I23-1294	60.0	1.71	15.7	0.19	1.59	39.0	753 ³	"
I23-1296	"	1.71	13.5	"	1.62	39.7	813 ³	"
I23-1100	"	1.71	14.4	"	2.06	50.5	723 ³	"
I23-1105	"	1.71	13.1	"	1.41	34.6	753 ³	"
I11-1800	51.0	1.35	9.8	"	0.98	30.5	753 ³	"
I11-1811	"	1.35	6.6	"	1.03	32.0	813 ³	"
I11-1826	"	1.35	7.8	"	1.01	31.4	643 ³	"
E-100	39.8	0.96	not available	"	0.12 ⁴	5.3	875 ^{2,4}	12
I13-30	50.1	1.32	"	"	0.51 ⁴	16.2	810 ^{3,4}	"
I13-12	"	1.32	"	"	0.77 ⁴	24.6	810 ^{3,4}	"
I13-13	"	1.32	"	"	0.95 ⁴	30.4	810 ^{3,4}	"
P20-1051	42.1	1.02	"	0.65	0.83 ⁴	34.3	780 ^{2,4}	"
P8-697	40.0	0.98	"	0.05	0.89 ⁴	38.4	810 ^{2,4}	"
I18-2	50.1	1.32	"	0.19	1.06 ⁴	33.8	810 ^{3,4}	"
E-90	39.8	0.96	"	"	0.94 ⁴	41.3	800 ^{4,5}	"
I13-4	50.1	1.32	"	"	2.00 ⁴	63.8	775 ^{1,4}	"
I13-7	"	1.32	"	"	2.03 ⁴	64.8	765 ^{4,6}	"
P24-1146	52.6	1.38	"	—	1.19 ⁴	36.4	825 ^{2,4}	"
I29-37	43.7	1.10	"	—	0.16 ⁴	6.2	913 ^{2,4}	"
I29-7	"	"	"	—	0.38 ⁴	14.6	898 ^{2,4}	"
I29-51	"	"	"	—	0.39 ⁴	15.0	897 ^{2,4}	"
I29-63	"	"	"	—	0.71 ⁴	27.3	878 ^{2,4}	"
I29-23	"	"	"	—	0.80 ⁴	30.8	861 ^{2,4}	"
I29-60	"	"	"	—	0.98 ⁴	37.7	846 ^{2,4}	"
I29-66	"	"	"	—	1.06 ⁴	40.8	843 ^{3,4}	"
I29-64	"	"	"	—	1.30 ⁴	50.0	862 ^{2,4}	"

1 10 K incrementals

2 30 K incrementals

3 50 K incrementals

4 data taken from plot therefore only approximations

5 last temperature before blistering T-90 K

6 last temperature before blistering T-190 K

7 FIFA

the best results (logarithmic, exponential and higher order models were also investigated). It could also be shown that blister temperature does not depend on fuel loading ($t = 0.09$) or particle size ($t = 0.16$). The influence of initial core porosity is only marginal ($t = -1.53$, a 5% increase of porosity leads to a decrease of blister temperature of only 15 K).

The linear least squares fit for blister temperature is given by:

$$T = 907 - (54.0 \cdot 10^{-27}) \cdot FD - 224 \cdot B \quad (5)$$

with

T = blister threshold temperature [K]

FD = fission density [$\text{fiss} \cdot \text{m}^{-3}$]

B = boron content [wt.% B_4C].

Both parameters, fission density as well as boron content, are highly significant ($t = -6.09$ and $t = -5.29$ respectively); the coefficient of correlation is 76.4%. Equation 5 shows that an addition of 0.19 wt.% B_4C leads to a decrease of blister temperature by about 45 K. Of course, this can be attributed to the formation of helium from boron. The decrease of blister temperature at higher fission densities shows that blister temperatures depend on fission gas concentration in the dispersion.

For the plates not containing B_4C , the blister threshold temperature is given by the equation:

$$T = 921 - (59.2 \cdot 10^{-27}) \cdot FD \quad (6)$$

Figure 3 shows the blister temperatures of all miniature plates with and without boron, as well as predicted blister temperatures for plates containing 0.19 wt.% B_4C according to equation 5 and for plates without boron according to equation 6. Also the corresponding lower 95% prediction limits for single observations are given.

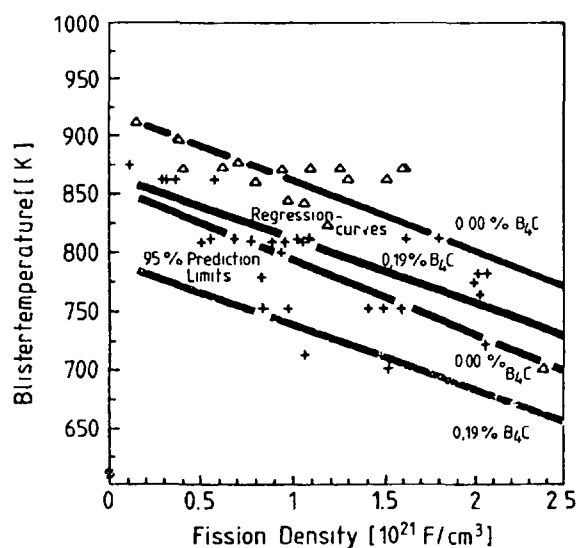


Fig. 3: Blister threshold temperature of miniature plates as a function of fusion density (comparison with regression analysis, equation 5 and 6)

The results of blister tests performed on full size plates are shown in table 4. In figure 4 the blister temperatures of full sizes plates are plotted against fission density. Also shown are the predicted blister temperatures based on miniature plates containing 0.19 wt.% B₄C according to equation 5 as well as the lower 95% prediction limit.

As can be seen from the plot, blister temperature of full size and miniature plates appear fully comparable.

4. Summary and Conclusions

The statistical evaluation of the irradiation data permits the following conclusions:

- Apart from the obvious influence of fission density, swelling is mainly related to porosity of the dispersion - higher porosity leads to lower swelling.

Table 4: Available data on blister threshold temperatures of full size plates

Sample	UAl _x Content [wt%]	U-Loading Mgm ⁻³	B ₄ C Content [wt%]	Fission Density [10 ²⁷ fiss m ⁻³]	Burnup ² [%]	Blister Temperature [K]	Reference
XA3G2-21	42.7	1.05	0.39	1.05	42.0	755	8
XA3G7-0	57.6	1.60	0.03	0.65	17.1	838	"
XA3G7-7	"	"	"	0.85	22.3	838	"
XA3G7-14	"	"	"	0.95	24.9	838	"
XA3G7-21	"	"	"	0.95	24.9	838	"
XA3G7-28	"	"	"	0.95	24.9	838	"
XA3G7-35	"	"	"	0.80	21.0	838	"
XA3G7-42	"	"	"	0.60	15.7	838	"
XA3G15-25	"	"	"	1.50	39.4	810	"
XA3G16-21	50.6	1.32	0.20	1.10	34.9	755	"
XA8G71d	57.6	1.60	0.03	0.30	7.9	>871	"
XA8G111d	"	"	"	0.30	7.9	>866	"
XA8G11b d	"	"	"	0.30	7.9	>866	"
XA130K0-5	59.0	1.66	not available	1.69	42.7	767	9
XA130K0-4	"	"	"	1.88	47.5	767	"
XA130K0-3	"	"	"	1.97	49.7	800	"
XA130K0-2	"	"	"	2.06	52.0	800	"
XA135K5-3	58.9	"	"	1.32	33.3	797	"
XA135K5-4	"	"	"	1.75	44.2	813	"
XA135K5-5	"	"	"	1.90	48.0	813	"
XA135L5-6	"	"	"	2.07	52.3	813	"
XA135K5-7	"	"	"	2.17	54.8	813	"
XA135K5-1	"	"	"	2.09	52.8	797	"
186E2-5	38.0	0.98	0.30	0.23 ¹	10.6	840 ¹	10 14
186E6-1	"	"	"	0.45 ¹	20.5	806 ¹	"
186E6-2	"	"	"	0.67 ¹	31.0	754 ¹	"
186E18-3	"	"	"	0.67 ¹	31.0	654 ¹	"
186E2-6	"	"	"	0.67 ¹	31.0	754 ¹	"
186E2-7	"	"	"	0.83 ¹	38.2	754 ¹	"
186E18-4	"	"	"	1.05 ¹	48.3	749 ¹	"

1 data taken from plot therefore only approximations

2 FIFA

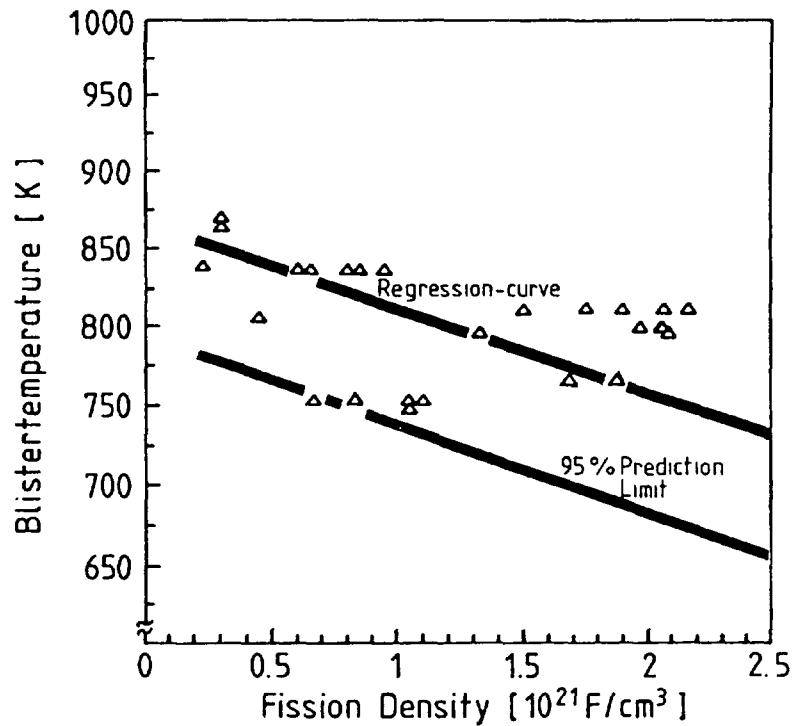


Fig. 4: Blister threshold temperature of full size plastes as a function of fission density (comparison with regression analysis miniature plates, eqn. 5)

- The effect of temperature on swelling appears to be an indirect one: sintering under irradiation is enhanced at higher temperatures and thus leads to a reduced net swelling.
- Although the uranium loading does not influence swelling per se, a reduction of swelling is observed at high uranium loadings. This can be attributed to the high porosity generally present in such dispersions.
- The blister temperature is mainly a function of fission density (additions of burnable poisons such as B_4C obviously reduce blister resistance).
- Porosity does not have a significant influence on blister behaviour.
- Blister threshold temperatures do not depend on uranium loading.
- Swelling and blistering behaviour of full size and miniature plates appear to be comparable.

References

- /1/ Francis W.C., Moen R.A. (eds.), IDO-17/218 (1966)
- /2/ Brugger R.M., Francis W.C. (eds.), IN-1437 (1970)
- /3/ Nazaré S., Ondracek G., Thümmeler F., J. Nucl. Mater. 56 (1975) 251
- /4/ Dienst W., Nazaré S., Thümmeler F., J. Nucl. Mater. 64 (1977) 1
- /5/ Martin M.M., Martin W.R., Richt A.E., ORNL-4856 (1973)
- /6/ Graber M.J. et al., ANCR-1027 (1971)
- /7/ Gibson G.W., Graber M.J., Walker V.A., IDO-17157 (1966)
- /8/ Griebenow M.L. (ed.), ANCR-1015 (1971)
- /9/ Beeston J.M. et al., Nucl. Technology 49 (1980) 136
- /10/ Gibson G.W., IN-1133 (1967)
- /11/ Francis W.C. (ed.), IDO-17154 (1965)
- /12/ Gibson G. W., Graber M.J. (eds.), IN-1131 (1967)
- /13/ Nazaré S, Ondracek G, Thümmeler F., KfK 1252 (1970)
- /14/ Covington E.D. (ed.), IN-1228 (1969)

Appendix J-1.3

IRRADIATION EXPERIMENTS

COMMISSARIAT A L'ENERGIE ATOMIQUE

Centre d'études nucléaires de Saclay,
Gif-sur-Yvette, France

Abstract

Irradiation experiments conducted in 1972-1973 in the OSIRIS reactor on fuel plates containing 93% enriched uranium are described. Eight plates contained UAl_3 -Al fuel with 35 wt% U (1.3 g U/cm^3) and 43 wt% U (1.7 g U/cm^3) and two plates contained U_3O_8 -Al fuel with 43 wt% U (1.7 g U/cm^3). The average burnup of the ^{235}U was 58.5% and the maximum burnup was 70%.

Results of the post-irradiation-examinations include data on dimensional measurements and metallographic examinations, the influence of grain size and the percentage of fines below 40 microns in the UAl_3 -Al plates with 35 wt% U, and the minimum temperature at which swelling appears with the occurrence of blisters after post-irradiation annealing. All of the tested plates behaved satisfactorily under irradiation.

In 1973, the trench CEA has inspected the OAZ-K-002 fuel-element after it had been irradiated in the OSIRIS reactor, as well as unirradiated fuel-plates of the same fabrication lot.

This element and the unirradiated fuel-plates had been fabricated by CERCA.

The examination tests purposes were the following :

- to compare the irradiation behaviour of plates containing 35 and 43 weight per cent of total uranium ;
- to observe the influence of grain size and percentage of particles below 40 microns ,
- to observe the behaviour of a U_3O_8 dispersion in Al matrix (43 w % total U)
- to determine the minimum temperature at which swelling appears with the occurrence of blisters after the post-irradiation annealing treatment.

The fuel-element OAZ-K-002 was geometrically identical to standard OSIRIS fuel-elements fabricated in 1971. It was consisting of 24 fuel-plates roll-swaged into 2 side-plates according to the standard technique.

The fuel-plates were of different kinds :

- UALx dispersion named "CERCA", containing 35 or 43 w % of 93 % enriched uranium
- UALx dispersion named "UAL3 dispersions" (in fact UAL4 + UAL3) containing 35 or 43 w % of 93 % enriched uranium
- U_3O_8 dispersion, in an aluminium matrix, containing 43 w % of 93 % enriched uranium.

The fuel-plates in position number 1-2 and 9 to 24 (35 w % of uranium) were geometrically identical to fuel-plates of standard elements : fuel-core thickness 0,51 mm, cladding thickness 0,38 mm.

The fuel-plates in position number 3 to 8 (43 w % uranium) contained a fuel-core 0,40 mm thick and cladding 0,44 mm thick.

Table I indicates the type of fuel contained in the different fuel-plates.

The following summary will be concerned with fuel-plates of the second type which corresponds, as far as the fabrication method is concerned, to the fuel-plates, for which a quotation has been sent by JAERI, and to the third type : U_3O_8 dispersions.

I - UNIRRADIATED FUEL-PLATES

I - 1. Micrographic examination :

For UAL3 dispersions, whatever the type of UALx dispersion (35 or 43 w % U, grain size 40-90 or 40-100 μ , percentage of particles below 40 μ : 25 or 50 %), the fuel metallurgical structure was comparable from one type to the other.

In all cases including U_3O_8 dispersions, the bonding between core and cladding was perfect.

I - 2. Dimensional measurements :

They have been performed on the samples punched out of the unirradiated fuel-plates according to fig. 1.

- Plate thickness :

The measurements carried out using a micrometer, are recorded in table II. Each value in this table was calculated by averaging 5 measurements.

TABLE I

DISPOSITION OF PLATES IN THE OAZ-K-002 TEST FUEL ELEMENT

Position inside the fuel-element	Plate id. number OAZ-K	Fuel composition
1 et 2	0006 0126	CERCA 35 w % U
3 et 4	0022 bis 003 bis	CERCA 35 w % U
5 et 6	0038 0039	UAl ₃ dispersion 43 w % U Grain size : same as HFR GRENOBLE
7 et 8	0043	U ₃ O ₈ dispersion 43 w % U
9 et 10	0054 0056	UAl ₃ dispersion 35 w % U Grain size : same as HFR GRENOBLE
11 et 12	0064 0069	UAl ₃ dispersion 35 w % U Grain size 40 - 100 μ 25 % fine powder (< 40 μ)
13 et 14	0077 0078	UAl ₃ dispersion 35 w % U Grain size 40 - 100 μ 50 % fine powder (< 40 μ)
15 à 24	0139 * 0147 * 0141 * 0142 * 0143 * 0144 * 0145 * 0146 * 0127 * 0001 bis	CERCA 35 w % U

* Plate with intentionally provoked US₃ type defects.

- Core and cladding thicknesses :

The measurements, under 100 times magnification, are recorded in table III. Each value was calculated by averaging 5 measurements performed every 3 mm.

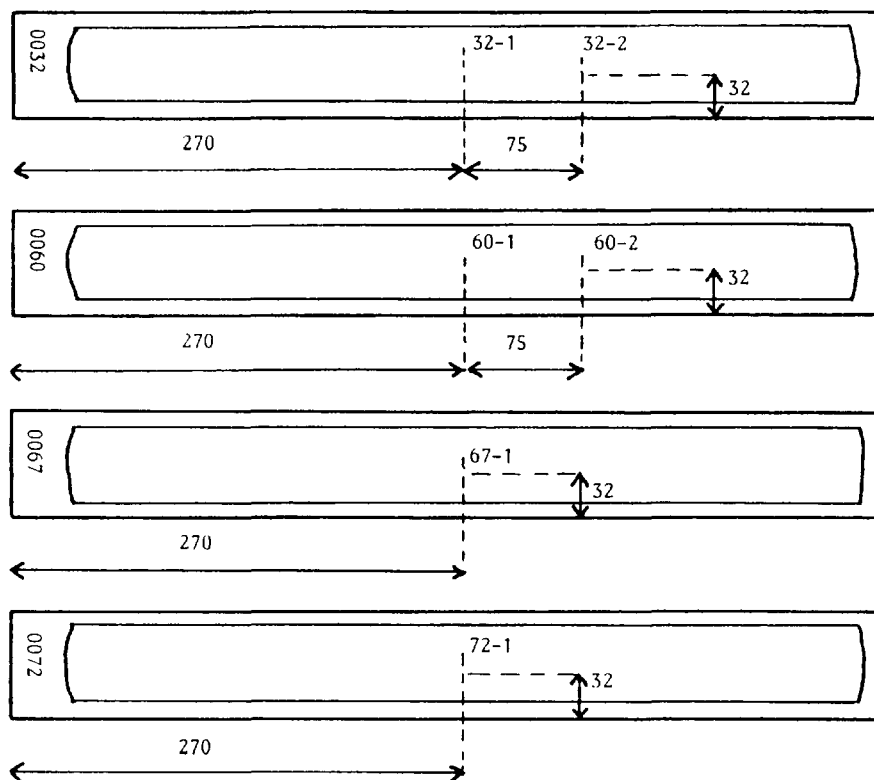


FIG. 1. Sampling on unirradiated fuel-plates for pre-irradiation micrographic examination.

TABLE II
PLATE THICKNESS BEFORE IRRADIATION

Measurements carried out on samples used for micrographic examination (mark 1 on sketch 2)

Plate : Id. number	Fuel composition	Cladding		Average of 5 measurements mm
		Frame	Cover	
0032	UAl ₃ dispersion 43 w % U Grain size : same as HFR GRENOBLE	AG 2	AG 2	1,275
0060	UAl ₃ dispersion 35 w % U Grain size 40 - 90 μ 25 % fine powder (< 40 μ)	AG 2	AG 2	1,290
0067	UAl ₃ dispersion 35 w % U Grain size 40 - 100 μ 25 % fine powder (< 40 μ)	AG 2	AG 2	1,280
0072	UAl ₃ dispersion 35 w % U Grain size 40 - 100 μ 50 % fine powder (< 40 μ)	AG 2	AG 2	1,280
0046	U ₃ O ₈ dispersion 43 w % U	AG 2	AG 2	1,290

TABLE III
MICROSCOPE MEASUREMENTS OF FUEL-CORE AND CLADDING BEFORE AND AFTER IRRADIATION - UNITS : MILLIMETRES

FUEL COMPOSITION (UAL dispersion) 3	Cladding		Fuel Core				Plate cover			
	Frame	Cover	Unirradiated plate		Irradiated plate		Unirradiated plate		Irradiated plate	
			Average	Min - Max	Average	Min - Max	Average	Min - Max	Average	Min - Max
35 w % U grain size : HFR Plates (unirradiated : 0060 number (irradiated : 0054	AG 2	AG 2	0,542	0,43-0,60	0,50	0,44-0,56	0,371	0,28-0,46	0,39	0,34-0,47
35 w % U grain size : 40 - 100 μ 25 % fine powder (< 40 μ) Plates (unirradiated : 0067 number (irradiated : 0069	AG 2	AG 2	0,488	0,42-0,57	0,523	0,44-0,594	0,396	0,30-0,45	0,376	0,321-0,445
35 w % U grain size : 40 - 100 μ 50 % fine powder (< 40 μ) Plates (unirradiated : 0072 (irradiated : 0077	AG 2	AG 2	0,498	0,44 - 0,58	0,54	0,49-0,584	0,392	0,31-0,46	0,37	0,306-0,42
43 w % U grain size : HFR Plates (unirradiated : 0032 number (irradiated : 0038	AG 2	AG 2	0,422	0,30-0,49	0,405	0,32-0,49	0,429	0,38-0,52	0,459	0,42-0,52
43 w % U Plates (unirradiated : 0046 number (irradiated : 0043	AG 2	AG 2	0,406	0,37-0,47	0,409	0,321-0,445	0,416	0,36-0,46	0,426	0,391-0,455

TABLE IV
 PLATE THICKNESS VARIATION AFTER IRRADIATION
 ELEMENT OAZ-K-002

FUEL CORE	Frame	Cover	Position inside element	N° plate OAZ K	Average before irradiation	After irradi. outside fuel- region cold end of the fuel-plate	Average after irradiation on fuel-region	Thickness variation outside fuel-region	Thickness variation on fuel-region
UAl ₃ dispersion 35 w % U	AG 2	AG 2	9 *	0054	1,28	1,30	1,33	+ 0,01	+ 0,05
Grain size : same as HFR			10	0056	1,28	1,33	1,33	+ 0,04	+ 0,05
Grenoble									
UAl ₃ dispersion 35 w % U			11	0064	1,27	1,31	1,31	+ 0,04	+ 0,04
Grain size : 40 - 100 μ	AG 2	AG 2							
25 % 40 u			12 *	0069	1,28	1,29	1,32	+ 0,01	+ 0,04
UAl ₃ dispersion 35 w % U			13 *	0077	1,28	1,30	1,33	+ 0,01	+ 0,05
Grain size 40 - 100 μ	AG 2	AG 2							
50 % 40 μ			14	0078	1,28	1,31	1,32	+ 0,02	+ 0,04
UAl ₃ dispersion 43 w % U			5 *	0038	1,26	1,27	1,30	+ 0,01	+ 0,04
Grain size : same as HFR	AG 2	AG2	6	0039	1,25	1,26	1,30	+ 0,01	+ 0,05
Grenoble									
U ₃ O ₈ dispersion			7 *	0043	1,28	1,31	1,32	+ 0,03	+ 0,04
43 w % U	AG 2	AG 2	8	0044	1,28	1,31	1,32	+ 0,03	+ 0,04

* Fuel-plate used for micrographic examination and blister test

II - IRRADIATION TEST

Characteristics of the OAZ-K-002 Fuel-element irradiation test :

- OSIRIS reactor working at 70 MW
- Inlet water temperature : 36 to 43° C
- Outlet water temperature : 48 to 55° C
- Average temperature of cladding at the inlet : \approx 60° C
- Average temperature of cladding at the outlet : \approx 75° C
- Percentage of total power (70 MW) per position in the core :
 - . position 21 : 1,80 - 2,10 %
 - . position 31 : 1,47 - 1,61 %
 - . position 37 : 1,40 - 1,62 %
- Irradiation of the element :
 - . introduction into the reactor core : January 27, 1972 Position 37
 - removal : burn-up : 3,5 % February 15, 1972
 - . reloading : March 16, 1972 Position 37
 - removal : burn-up 14,6 % May 8, 1972
 - . reloading : May 19, 1972 Position 37
 - removal : burn-up 19,2 % June 6, 1972
 - . reloading : October 9, 1972 Position 21
 - October 24, 1972 Position 31
 - Final removal from the reactor core : April 2, 1973
 - average burn-up 58,5 %
 - maximum burn-up 70 % in the center.
- Total irradiation exposure : 265 days
- Total irradiation test length : 430 days
- Storage time before inspection : 6 months

III - INSPECTION AFTER IRRADIATION

III - 1. Visual inspection of fuel-plates after disassembling :

Each one of the 24 plates has been inspected over its whole area using a periscope.

All the plates named "UAl₃ dispersions" and "U₃O₈ dispersions" were intact except for some microscopic corrosion pits, which were not severe, located on scratches, whatever the U content (35 or 43 W %), the kind of dispersed material (UAl₃ or U₃O₈) or the percentage of particles below 40 μ (25 or 50 %).

III - 2. Plate thickness measurements : (please refer to table IV)

Thickness measurements have been carried out in seven points regularly spaced along each fuel-plate axis, according to fig. 2.

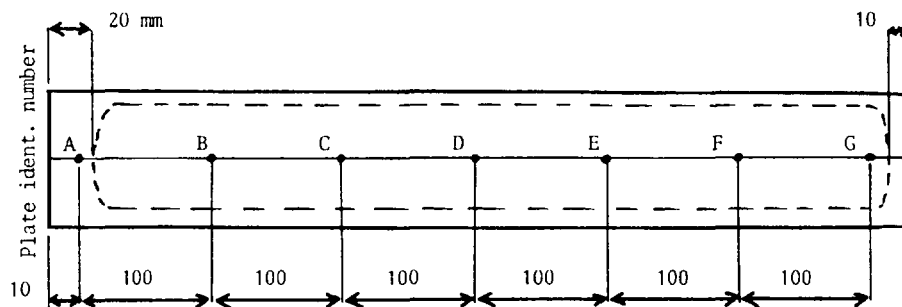


Plate thickness measurements have been carried out at the positions indicated on the sketch (7 measurements per plate)

The "A" position is located on the identification number side.

FIG. 2. Plate thickness measurement positions after irradiation.

These measurements show that thickness was practically uniform along each plate whereas flux and burn-up varied by a factor of 2 from the center to the ends, and temperature was raised by 15° C from the cold to the hot region of the plate.

As the different examinations have shown elsewhere, the bonding between core and cladding is good before and after irradiation. Since thickening due to oxidation is negligible (1-2 μ), it appears reasonable to say that the thickness increases of the fuel-plates are due to the fuel-cores swelling only. Thickness increases :

- UAl_3 dispersions, 35 w % U :
 - . grain size : 40-90 μ ; below 40 μ - 2 plates :
 - + 0,05 and + 0,05mm
 - (former HFR Grenoble specifications)
 - . grain size : 40-100 μ ; 25 % below 40 μ - 2 plates :
 - + 0,04 and + 0,04 mm
 - . grain size : 40-100 μ , 50 % below 40 μ - 2 plates :
 - + 0,04 and + 0,05 mm
- UAl_3 dispersions, 43 w % U :
 - . HFR Grenoble specifications (as above) : 2 plates :
 - + 0,04 and + 0,05 mm
- UAl 30g dispersions, 43 w % U :
 - . 2 plates
 - + 0,04 and + 0,04 mm

III - 3. Metallographic inspection :

III 3.1 Fuel-core :

- UAl_3 dispersions :

Due to irradiation, sintering has occurred ; only compact particles can now be observed

Traces, either of small porosities or of a secondary phase can be detected.

The aluminium matrix is not modified.

- U_3O_8 dispersions :

A marked difference can be observed between the dispersions before and after irradiation. Complete sintering of the U_3O_8 particles has occurred. Inside the U_3O_8 sintered particles, a secondary phase appears, a few porosities (which may also come from the removing of a reactive phase by polishing) also appear inside the sintered particles.

Around the particles, a reaction zone between the particles and the aluminium matrix can be observed. No decohesion can be detected in the matrix.

III 3.2. Dimensional measurements :

The cladding thickness is kept almost unmodified after irradiation, the corrosion effect being taken into account (cladding dissolving + layer of adherent oxide).

The Al_2O_3 layer on the cladding is continuous and quite constant in thickness : 5 to 8 μ .

The thickness of the fuel-core increases, which confirms measurements in paragraph III - 2.

III 3.3. Blister test :

This test consists in determining the minimum temperature at which the fission-products release leads to unacceptable swelling with occurrence of cladding blisters.

It is carried out on irradiated samples large enough in size (20 x 10 mm).

Blister test characteristics :

- three samples for each lot
- annealing time : 10 hours
- secondary vacuum
- temperatures
 - . for UAl_3 : 400 - 450 - 500 - 550° C
 - . for U_3O_8 : the same + 250 and 300° C

Since the results were very similar for the samples of a same lot of three, the examinations have been carried out on only one sample of each lot.

The following conclusions can be drawn from this test :

- the critical temperature leading to blistering is 500° C for UAl_3 dispersions and 300° C only for U_3O_8 dispersions.
- as far as external aspect and thickness variations are concerned there is no apparent difference between the different UAl_3 dispersion fuels (grain size, percentage of particles below 40 μ , U content).
- as far as microscopic aspect is concerned, microscope examination shows that :
 - . for UAl_3 dispersions :

The percentage of particles below 40 μ (25 or 50 %) as well as the U content (35 or 43 w %) do not modify the evolution of the core after the annealing treatment. In particular, dispersions containing 43 w % U behave as well as 35 w % U dispersions. Bonding between meat and cladding is good.

- . for U_3O_8 dispersions :

The fuel core is more cracked (inside the U_3O_8 particles as well as inside the Al matrix) than the fuel core of UAl_3 dispersions. Decohesions between matrix and particles are also larger and appear at lower temperature than in UAl_3 dispersions.

IV - DISCUSSION

Swelling measurements have been compared to American results (1) corresponding to irradiation conditions, uranium loadings and burn-up that were similar.

For the UAl_3 dispersions as well as for the U_3O_8 dispersions the results are very similar.

After irradiation, annealing temperatures leading to blister formation have been compared to these published by american authors (2). The results are in good agreement (fig. 3).

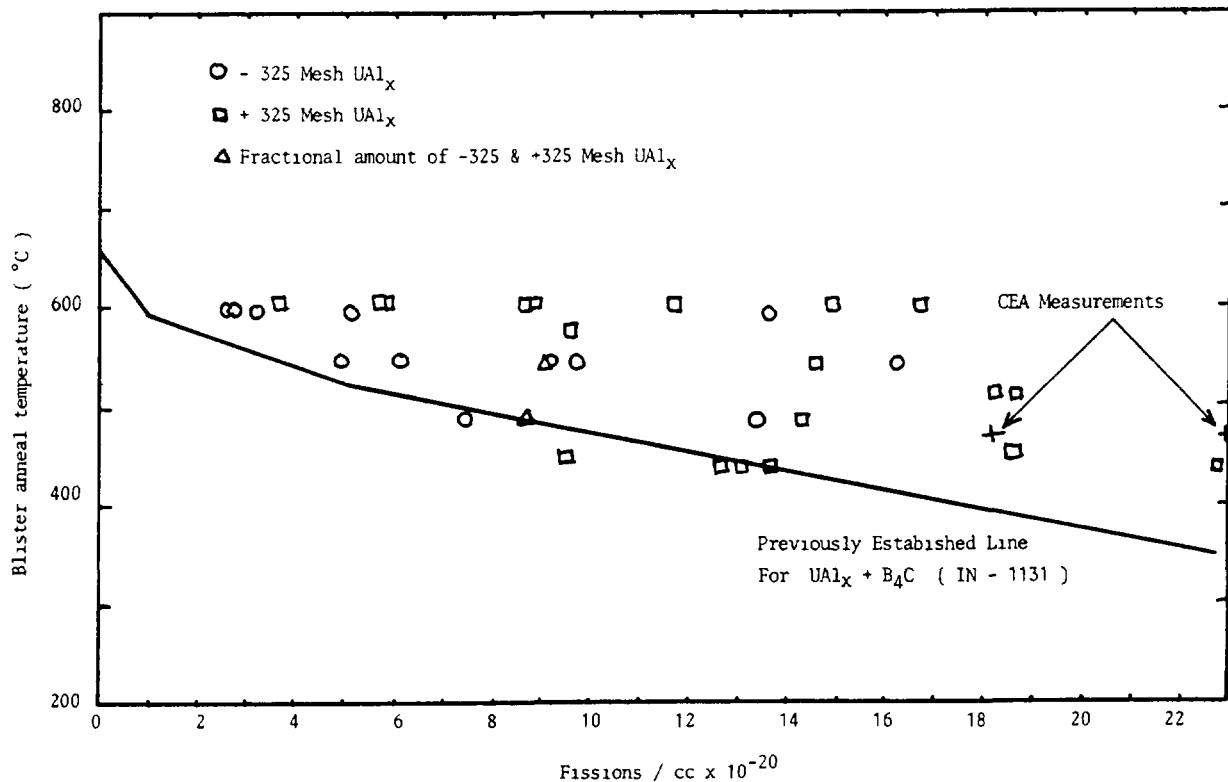


FIG. 3. Blister anneal temperatures for sample fuel plates fueled with - 325 mesh and + 325 mesh UAl_x compared to the previously established failure-no-failure line for $UAl_x + B_4C$.

- UAl_3 dispersions :

Measurements and inspection results, before and after annealing treatments show that, for the UAl_3 dispersions, the U content (35 or 43 w %), the burn-up (factor 2 from the fuel-plate center to the ends), the percentage of fine particles (25 or 50 %) do not play a great role as far as the behaviour under irradiation is concerned. In any case this behaviour is satisfactory. The fact that the percentage of fine particles has no influence is confirmed by american results (1).

- U_3O_8 dispersions :

U_3O_8 dispersions have also behaved satisfactorily ; but, in case of accidental temperature raise, the security margin is more narrow.

Whereas the reaction between U_3O_8 and the aluminium matrix does not occur below 450° C outside the reactor core, it is observed for interface temperatures of 100 - 150°C in swimming-pool reactor cores (1). Anyway, at these temperatures the reaction remains limited and can only be detected by metallographic inspection (see III 3.1).

Note : in all the cases, the maximum size of UAl_3 particles was 100 μ instead of 90 μ (corresponding to the former HFR Grenoble specifications).

V - CONCLUSION

- The fuel-plates of the irradiation-test OAZ-K-002 fuel-element have been examined after irradiation at an average burn-up of 58,5 % and maximum burn-up of 70 %.
- Under irradiation, the cores of the fuel-plates have behaved satisfactorily without any exception. No significant difference has appeared between fuel-plates whatever the fabrication procedure (CERCA or UAl_3 dispersion), the U content (35 or 43 w %), the kind of fuel (UAl_4 , $\text{UAl}_4 + \text{UAl}_3$, U_3O_8), the particle size (25 or 50 % of particles below 40 μ , the maximum size being 100 μ), and even the burn-up (40 to 70 %).
- After irradiation, microscopic inspection shows that the U_3O_8 dispersion cores where a surface reaction between U_3O_8 and Al takes place are more modified than the UAl_3 dispersion cores. In any case, these modifications are only of minor importance and are not able to influence the fuel-element behaviour in the reactor core.
- For all the types of fuel-plates, the bonding between cladding and core, and between frame and cladding was not damaged by irradiation.
- Blistering during the annealing treatment occurs :
 - . at 500°C for the UAl_3 dispersions, whatever the U content or the fabrication procedure
 - . at 300° C for the U_3O_8 dispersions.
- Following this irradiation test, the HFR Grenoble specifications concerning the powder have been modified as follows :
 - . the maximum content of fine particles (below 40 μ) has been raised from 25 to 50 %.
 - . the size-range of big particles has become 40-125 μ instead of 40-90 μ .

R E F E R E N C E S

- (1) Irradiation behavior of aluminium-base fuel dispersions
MM. MARTIN - A.E. RICHT - W.R. MARTIN
ONRL 4856 - Mai 1973
- (2) Metallurgy and materials science branch annual report FY 1970
Idaho Nuclear Corporation IN 1437
R.N. BRUGGER - W.C. FRANCIS

Appendix J-2

RELIABILITY OF LEU FUEL

W. KRULL

GKSS — Forschungszentrum Geesthacht GmbH,
Geesthacht, Federal Republic of Germany

Abstract

Requirements on the reliability of LEU fuel are summarized from the point of view of a German reactor operator and his independent experts.

From the view of a German reactor operator and his independent experts the demands on fuel reliability are /1/:

- a) The fabrication of the LEU fuel plates should be on a high quality standard. This includes, of course, quality control as before but as a good indication a minor number of unacceptable fuel plates, too.
- b) Irradiation of miniplates for getting esp. from post irradiation examination (PIE) detailed information about
 - corrosion behaviour
 - fission product release
 - swelling
 - limitations of relative burnup or fissions/cm³
(irradiation conditions should be well known e.g. thermal flux, burnup, power cycle, irradiation time, water quality)
- c) Stepwise examination of LEU fuel
 - ca. 10 miniplates irradiated up to max. burnup
 - PIE of these miniplates
 - >10% of the number of fuel elements of the reactor core (more than five fuel elements) up to max. burnup. Higher U-density and higher burnup values as those needed for the actual core conversion will be very helpful in the licensing procedure.
 - PIE of some fuel elements will be helpful
 - conversion of the whole core
- d) Of interest are fuel plate irradiation experiments from different manufacturers. But for the final core conversion there should be enough tested fuel plates or fuel elements from the chosen manufacturer. These tests can be performed in different reactors. But

it will be very helpful in the licensing procedure for the whole core conversion to have tests performed in the reactor under consideration.

- e) Guarantee for reprocessing the LEU fuel.

REFERENCE

- /1/ W. Krull: Remarks on the demands for the qualification of high density fuel, GKSS 84/E/40, 1984

Appendix J-3

POST-IRRADIATION EXAMINATIONS OF DISPERSION FUELS WITH REDUCED ENRICHEMENT

J.L. SNELGROVE
RERTR Program,
Argonne National Laboratory,
Argonne, Illinois,
United States of America

Abstract

This appendix outlines the philosophy and procedures that were utilized by the U.S. RERTR Program for non-destructive and destructive post-irradiation examination of miniplates and full-size elements utilizing low enriched (<20%) uranium fuels with high uranium densities.

Introduction

In order to attain its goal of providing the technical means for reducing the enrichment of uranium used in research and test reactor fuels, the U.S. Reduced Enrichment Research and Test Reactor (RERTR) Program has been active in the development and testing of high-density fuels. Irradiation testing has been performed on miniature fuel plates (miniplates) to establish fission-density limits as a function of uranium density for the various fuel types. Based upon successful results from the miniplates, full-size fuel elements of various fuel types, uranium densities, and designs were tested to demonstrate that full-size fuel plates fabricated under normal conditions by "commercial" fabricators behave as expected. The irradiations of full-size fuel elements provided both better statistics on fuel behavior than did the miniplates and a qualification of the participating fuel fabricators.

During the course of the irradiations, evidence of satisfactory fuel performance was obtained through periodic visual inspections and by periodic measurements of the water channel thicknesses. However, more detailed information was obtained during post-irradiation examinations (PIE's). The philosophy of the PIE's and an explanation of the various examinations performed are given below.

Philosophy

The purpose of the PIE's was to provide detailed information about the metallurgical behavior of the fuel during irradiation and about the anticipated behavior of the fuel following an accident in which the fuel is overheated but not melted. The data obtained had to be of sufficient quality and quantity to provide a sound basis for the licensing of these fuels. The philosophy of the PIE's under the RERTR Program was to obtain the primary data of fuel behavior from examinations of the miniplates and to obtain confirmatory data from examinations of the full-size elements. This implied much more extensive PIE's on the miniplates than on the full-size elements. In general, the miniplates embraced a wider range of uranium densities than did the full-size elements.

The major goals of the PIE's were: 1) to determine the amount of swelling as a function of uranium loading and burnup, 2) to determine the blister threshold temperature as a function of uranium loading and burnup, and 3) to ensure that there was no evidence of incipient failure in those fuel samples which appeared to be satisfactory. The extent of examinations of sectioned miniplates and full-sized plates was determined by what was observed during these and other examinations. It was anticipated that extensive examinations of plate sections would not be required for the uranium-aluminide and uranium-oxide fuels since they had been studied thoroughly at lower uranium densities. Much more detailed studies were made of the uranium-silicide fuels in order to fully characterize them. As stated previously, most of the metallurgical studies were performed using the miniplates. Only limited metallographic examinations for the full-size plates were made to confirm expected behavior unless anomalies were discovered during the nondestructive examinations.

Miniplate Examinations

Post-irradiation examinations of the RERTR Program miniplates were performed at Argonne National Laboratory and at Oak Ridge National Laboratory, depending upon the particular type of fuel being examined. The various types of examinations that were made are explained below.

1. Visual examination of module containing the miniplates. These examinations were made to determine if any abnormalities could be detected prior to removing plates from the module.
2. Visual examination of individual plates. During these examinations blisters or other unusual features were detected and photographed. Photographs were also made of typical miniplates.
3. Gamma scanning. The plates were scanned longitudinally and transversely to determine the distribution of one or more fission products. Typically, a long-lived isotope which was not expected to migrate, such as ^{137}Cs , was studied. Therefore, the relative distribution of fission products was the same as the relative distribution of fission events. These data were used to determine the relative fission densities in the various miniplates.
4. Dimensional measurements. The length, width, and thickness of each miniplate are measured to determine dimensional changes resulting from the irradiation. These data were of limited use in determining volume changes (swelling) of the miniplates due to relatively large uncertainties in the thickness measurements.
5. Weight and density measurements. The weight of the miniplates and their densities as determined by immersion techniques were used to accurately determine the volume changes of the miniplates.
6. Blister threshold temperature measurements. The threshold temperature for the formation of blisters was determined by the standard technique of heating the plate in a furnace to a specified temperature, holding at that temperature for approximately 30 minutes, and removing the plate for visual examination. The sequence was repeated for successive higher temperatures until blistering was observed. The threshold temperatures for other phenomena, such as significant fuel plate

warping, were also determined. Variations of the standard blister test technique were also employed when needed to more fully explain the observed phenomena.

7. Chemical or radiochemical burnup analysis. Samples of one or more miniplates from each batch were analyzed to determine the absolute burnup of ^{235}U . These data were used with gamma scanning data to assign absolute burnups (fission densities) to each miniplate.
8. Metallographic examination. Samples were removed from selected miniplates and examined metallographically to determine the swelling characteristics of individual fuel particles, chemical interactions of fuel and aluminum matrix, changes in bonding of cladding to fuel meat, changes in porosity, and the distribution of fission-gas bubbles.
9. Scanning electron microscopy. Samples from selected miniplates were examined with a scanning electron microscope to determine the distributions of fission-gas bubbles and other fission products in the fuel meat.
10. Electron microprobe analysis. An electron microprobe was used to study the distribution of fission products in the fuel meat.
11. Scanning Auger microscopy. A scanning Auger microscope was used to study the interaction layers in the fuel and aluminum matrix.
12. Gas release measurements. A miniplate was punctured under vacuum conditions at room temperature to determine the amount of gas released from the plate. The interconnected void volume of the fuel core was determined by backfilling with gas under standard conditions.
13. Measurement of fission-product release as a function of temperature. Using a series of temperature steps as was done for blister threshold temperature determination, the threshold temperature for the release of fission products and the amounts of fission products released as a function of temperature above threshold were determined.

The examinations listed in Nos. 1 through 8 and No. 13 were performed on all of the types of fuel being developed by the RERTR Program. The examinations listed in Nos. 9 through 11 were performed primarily on samples from the uranium-silicide miniplates that were examined at Argonne National Laboratory. The gas release measurements (No. 12) were made at Oak Ridge National Laboratory on selected $\text{U}_3\text{O}_8\text{-Al}$ miniplates.

Full-Size Element Examinations

Post-irradiation examinations of full-size fuel elements irradiated under the RERTR Program were performed at Argonne National Laboratory, Oak Ridge National Laboratory, The Netherlands Energy Research Foundation (Petten), and the Saclay Nuclear Research Centre (France), depending upon where the fuel elements were irradiated. The following examination steps for elements irradiated in the ORR illustrate the types of examinations made on each fuel element.

Nondestructive PIE

1. Visual Inspection

Purpose: To observe general appearance and photograph.

- a. Observe general external appearance.
- b. Note any unusual features.
- c. Photograph element exterior with close-ups of unusual features.
- d. Photograph through channels with element backlighted.

2. External Dimensions

Purpose: To determine dimensional changes during irradiation.

- a. Measure major external dimensions (length, width, depth).
- b. Determine amount of warp, twist, or bow.

3. Gamma Scanning of Fuel Element

Purpose: To determine relative longitudinal burnup (fission product) distribution for entire element and to determine relative burnup from element to element.

- a. Scan using Ge(Li) detector and multichannel analyzer for fission-product peaks in the energy range 100 to 1400 keV, including ^{106}Ru and ^{137}Cs .
- b. Scan longitudinally in 1.0-in. increments along centerline of element.

4. Measure Channel Gaps

Purpose: To detect unusual amounts of plate swelling or warping.

- a. Remove end fittings.
- b. Measure channel gaps on both sides of comb.

Destructive (Full) PIE

1. - 4. Same as above

5. Dismantling of Element

Purpose: To prepare plates for individual examination.

- a. Separate individual fuel plates from side plates.

6. Visual Inspection of Plates

Purpose: To detect blisters or other unusual features.

- a. Observe general external appearance of each plate and note any unusual features.
- b. Photograph typical plates (2 or 3) and any areas of unusual features.

7. Thickness Measurements

Purpose: To provide data for estimation of plate swelling. Since measured thickness changes always overestimate the volume change (only the "high" points on the surface are measured), these measurements served mainly to show that no unexpected swelling had occurred.

- a. Measure thickness at ~24 points on plates Nos. 1, 5, 9, 13, 17, including at least two points outside the fuel meat zone.
- b. Measure thickness at conspicuous spots.

8. Gamma Scanning

Purpose: To determine relative longitudinal and transverse burnup (fission product) distributions.

- a. Perform analog scan longitudinally along centerline for all plates, for both integral above 0.5 MeV and ^{137}Cs .
- b. Perform multichannel spectrum measurements along centerline at peak, as determined from analog scan, at 6 in. below peak, and at 10 in. above peak for plates Nos. 1, 5, 9, 13, and 17.
- c. Perform analog scan transversely at peak of longitudinal scan, at 6 in. below peak, and at 10 in. above peak for plates Nos. 1 and 9, for both integral above 0.5 MeV and ^{137}Cs .

9. Blister Testing

Purpose: To determine the threshold temperature for the formation of blisters. The threshold temperature was measured by the standard technique of heating the entire plate in a furnace to a specified temperature, holding at that temperature for approximately 30 minutes and removing the plate for visual examination. The sequence was repeated for successively higher temperatures until blistering was observed.

- a. Blister test two plates (Nos. 2 and 8).
- b. If results are not consistent, test also plate No. 18.

10. Metallography

Purpose: To confirm that the behavior of the fuel is as expected, based upon previous examinations of miniplates.

- a. Obtain two sections (high and low burnup) from the plate (other than No. 1) showing the highest burnup.
- b. Perform optical metallographic examination.

11. Burnup Analysis

Purpose: To determine the absolute number of fissions (burnup). These data were used with gamma scanning data to assign absolute burnups to each element.

- a. Obtain burnup samples from high- and low-burnup regions of plate sectioned for metallography.
- b. Determine burnup by ^{148}Nd method.

As was stated in the section on Philosophy, the examinations of full-size elements and fuel plates removed from them were intended to be confirmatory in nature; therefore, they were much less detailed than the corresponding examinations on the miniplates. Of course, any anomalies detected were fully investigated.

Appendix J-4
IRRADIATION AND PIE OF TEST PLATES, RODS,
AND FULL SIZED ELEMENTS

Appendix J-4.1

THE OAK RIDGE RESEARCH REACTOR

Appendix J-4.1.1

MINIPLATE IRRADIATIONS IN THE OAK RIDGE RESEARCH REACTOR

OAK RIDGE NATIONAL LABORATORY
Oak Ridge, Tennessee

ARGONNE NATIONAL LABORATORY
Argonne, Illinois

United States of America

Abstract

The miniplate irradiation program was designed to screen a large number of possible LEU fuel types for use in research and test reactors. Two hundred and forty-four miniplates fabricated by ANL, CNEA, EG&G Idaho, NUKEM, and ORNL were irradiated in the Oak Ridge Research Reactor (ORR). Eleven types of fuel were tested: U_3Si_2 , $U_3Si_{1.5}$, U_3Si , USi , U_3SiCu , U_3SiAl , U_3O_8 , UAl_x , UAl_2 , U_6Fe , and $U_6Mn_{1.3}$. The samples included a wide range (0.2% - 93%) of enrichments and uranium densities up to 8 Mg/m³. Most of the miniplates were irradiated beyond the 50% burnup level that is typical for research reactor fuel. Some were irradiated beyond 90% burnup of the contained ^{235}U . Extensive post-irradiation-examinations were performed. These examinations included measurement of swelling, blister threshold temperatures, fission product release temperatures, and metallurgical analyses.

1. INTRODUCTION

Since its inception in 1978, the U.S. Reduced Enrichment Research and Test Reactor (RERTR) Program has pursued the development of high density dispersion fuels as one method of making feasible the conversion of research and test reactors from the use of highly enriched uranium (HEU) to low enriched uranium (LEU) fuel. This program required irradiation of various fuel types to normal burnup levels and beyond, and examination to determine the effects of the irradiation. The irradiation program was conducted at the Oak Ridge Research Reactor (ORR), and the post-irradiation examinations took place at ORNL and at ANL. Both miniature plates (miniplates) and complete fuel elements were irradiated.

The miniplate irradiation program was designed to screen many different types of reduced enrichment fuel that might be suitable for use in research reactors. Miniplates with various fuel loadings were placed into a holder (module) which was in turn loaded into one of the regular fuel element positions in the ORR. Up to sixty miniplates contained in

five modules could be irradiated in a single fuel element position. The miniplates were irradiated until the desired burnup had been achieved, or until examination showed a failure of some type.

In the ORR program^{1,2}, some 244 miniplates of various candidate fuel materials were irradiated in the special irradiation test facility, designated as High-Uranium-Loaded Fuel Element Development (HFED). The miniplates were manufactured by ANL, Comision Nacional de Energía Atomica of Argentina (CNEA), EG&G Idaho, Inc., NUKEM GmbH, Hanau, Federal Republic of Germany (NUKEM) and ORNL.

The program required development of a number of pieces of hardware. These included the modules for holding twelve miniplates, and the module holder which could hold five modules. When properly loaded, the HFED assembly was loaded into a fuel element location within the reactor for irradiation. A poolside station was installed in the ORR pool to permit examination after irradiation. A channel gap measuring device (CGMD), obtained from EG&G Idaho, Inc., allowed the gaps between plates in the modules to be measured accurately.

During each of the reactor refueling shutdowns, gap measurements were made in each of the coolant channels in the HFED. Miniplates showing any significant swelling were removed for further testing and examination, and to prevent a serious fuel failure while in the reactor core.

After reaching the designated burnup level, or when swelling was detected, the miniplates were removed from the holders and stored in the ORR pool until they could be examined further. Most of the post-irradiation examination was performed at ORNL and ANL, but a number of plates were shipped to the Savannah River Laboratory for reprocessing tests. These tests and examinations formed the basis for the decision to proceed with U_3Si_2 fuel as the most likely successful material for the LEU program.

To ensure that the miniplates could be safely irradiated in the ORR facility, specifications were developed to control the manufacture and inspection of the plates. This Specification is included in this appendix as Attachment A.

It was necessary to ship many of the irradiated miniplates from ORNL for post-irradiation examination. These shipments had to conform to the various regulations controlling shipments of irradiated fuel. A small computer code to determine the remaining uranium content of the plates, the curie level and the heat load of the shipment was developed¹ at ORNL. This code, titled HFEDSHIP.BAS, is reproduced in Attachment B.

2. MINIPLATE IRRADIATION PROGRAM

The objectives of this irradiation program were to screen LEU fuel materials to determine their suitability for replacing the HEU materials currently in use and to provide a database of fuel characteristics leading to the development of full-sized LEU fuel elements for full-core reactor tests and operation. (A review of research reactor fuels as of 1982 can be found in Ref. 3.) To accomplish these objectives, miniplates were irradiated in a core positions in the ORR with peak neutron fluxes of $\sim 1.96 \times 10^{18}$ neutrons $m^{-2} s^{-1}$. Burnups of up to 2.2×10^{27} fission/ m^3 of fuel core volume were reached. At intervals during irradiation, measurements

were made to detect fuel swelling. After reaching the desired burnup level, or upon detection of fuel swelling, the plates were removed from the reactor, stored for cooling, and ultimately shipped to a hot cell for post-irradiation examination.

Table 1 lists the fuel types and the fabricators of the miniplates, along with the number of each type of miniplate, the uranium density in the fuel meat (g U/cm^3) and the uranium enrichment.

3. TEST FACILITY AND EQUIPMENT^{1,2}

3.1 Miniplate Design

The fuel plates used in the fuel elements for most research and test reactors consist of a fuel core of "meat" in aluminum alloy cladding. For the purposes of this experiment, a fuel-plate design was developed that had fuel meat and plate thicknesses typical of those used in existing reactors and that fit within an ORR fuel element core space. The width and length was much greater than its thickness to provide prototypical conditions with regard to constraint of the fuel meat by cladding and frame.

These conditions were met with a miniplate 114.3 mm long by 50.8 mm wide and either 1.27 or 1.52 mm thick, as shown in Fig. 1. The fuel meat could be up to 109 mm long by 46 mm wide. Fabrication of developmental fuel plates at ORNL and ANL has been previously reported.^{4,5}

A miniplate specification (see Attachment A) was prepared to match existing aluminum-clad, fuel-plate manufacturing techniques as far as practicable. Originally, the specification required a 0-temper condition of the cladding of the finished miniplate to ensure uniformity of cladding constraint conditions as produced by different fabricators. It was later determined that cladding temper did not play a major factor in miniplate performance, and this requirement was abandoned in favor of more nearly simulating commercial fuel-plate manufacturing techniques.

3.2 Experiment Design

The irradiation test facility, designated HFED, was designed to fit into a core position of the ORR,⁶ a 30-MW water-moderated reactor. The HFED experiment operated in various core positions at different times throughout the irradiation test period.

The HFED was designed to accommodate 60 miniplates at one time. The plates were contained in five modules; each module was originally designed to hold 12 miniplates, 6 of an overall thickness of 1.27 mm and 6 of an overall thickness of 1.52 mm. A second series of modules was built to hold 8 thin and 4 thick miniplates. A detailed view of a typical module with miniplates installed is shown in Fig. 2. The miniplates were held in position by their respective slots in the side plates, and by a hafnium (Hf) grid located in the bottom of each module. The Hf grids not only retained the miniplates but also served as neutron absorbers to depress the power peaks that otherwise would occur at the ends of the plates because of higher fuel loading caused by dogboning and/or neutron flux peaking caused by the water gaps between the ends of each module. (Dogboning is fuel core thickening that may occur near the ends of a fuel plate as a consequence of fabrication methods.) The modules were designed to provide a 2.54-mm-wide water coolant channel between each plate.

Table 1. Miniplates That Were Irradiated in the ORR.

Fuel Type	Fabri- cator	Enrich- ment	g U/cm ³	No. of Plates
U ₃ Si ₂	ANL	93.0	1.7	2
		40.1	3.9-4.0	2
			5.0-5.2	3
		19.8	3.7-3.8	4
			4.9-5.2	13
			5.6-5.7	7
	CNEA	0.2	4.7	2
U ₃ Si _{1.5}	ANL	40.0	3.8-3.9	2
		19.8	5.0-5.2	3
			5.8-6.0	2
U ₃ Si	ANL	92.6	2.0	2
		40.0	4.5	2
			5.9-6.4	4
		19.8-19.9	4.8	11
			5.6-5.7	4
			6.0-6.2	7
			6.3-6.5	5
			6.9-7.2	5
		0.22	6.1-6.2	2
	CNEA	19.8	4.8	1
			5.2	2
			6.1	1
	NUKEM	19.4	6.9	6
USi	ANL	40.1	3.8-3.9	3
		19.8	3.8-3.9	4
		0.2	3.7-3.8	3
U ₃ SiCu	ANL	40.0	3.8-4.1	3
			5.3	2
			5.9-6.1	3
			6.8-7.0	4
U ₃ SiAl	ANL	19.5-19.9	4.5-4.7	14
			5.6-5.9	7
			6.1-6.4	9
			6.9-7.0	6

Subtotal = 156

Table 1 (cont'd)

Fuel Type	Fabri- cator	Enrich- ment	g U/cm ³	No. of Plates
U ₃ O ₈	CNEA	19.7	2.5	2
			2.9-3.1	3
			3.5-3.6	3
	NUKEM	39.7 27.3 20.4	2.4	2
			2.3	2
			3.1	2
			3.1	2
	ORNL	93.2 45.0 19.5	0.7	1
			2.5-2.8	2
			3.1	3
			2.4-2.5	5
			2.8	11
			3.1	9
Aluminides				
UAl _x	CNEA	45.0 20.2	1.5	1
			2.3-2.5	5
	EG&G	40.2	1.9-2.0	4
			2.2-2.3	4
		19.9	1.9-2.0	3
			2.3	1
	NUKEM	39.8 27.1	2.1-2.2	2
			2.1	2
UAl ₂	ANL	44.8	3.0	2
	CNEA	19.8	3.0-3.1	5
Others				
U ₆ Fe	ANL	19.8 0.22	7.0	1
			7.8-8.0	3
			7.0-7.1	2
U ₃ Mn _{1.3}	ANL	40.0 19.8	6.2-6.3	3
			6.9-7.0	3

Subtotal = 88

TOTAL = 244

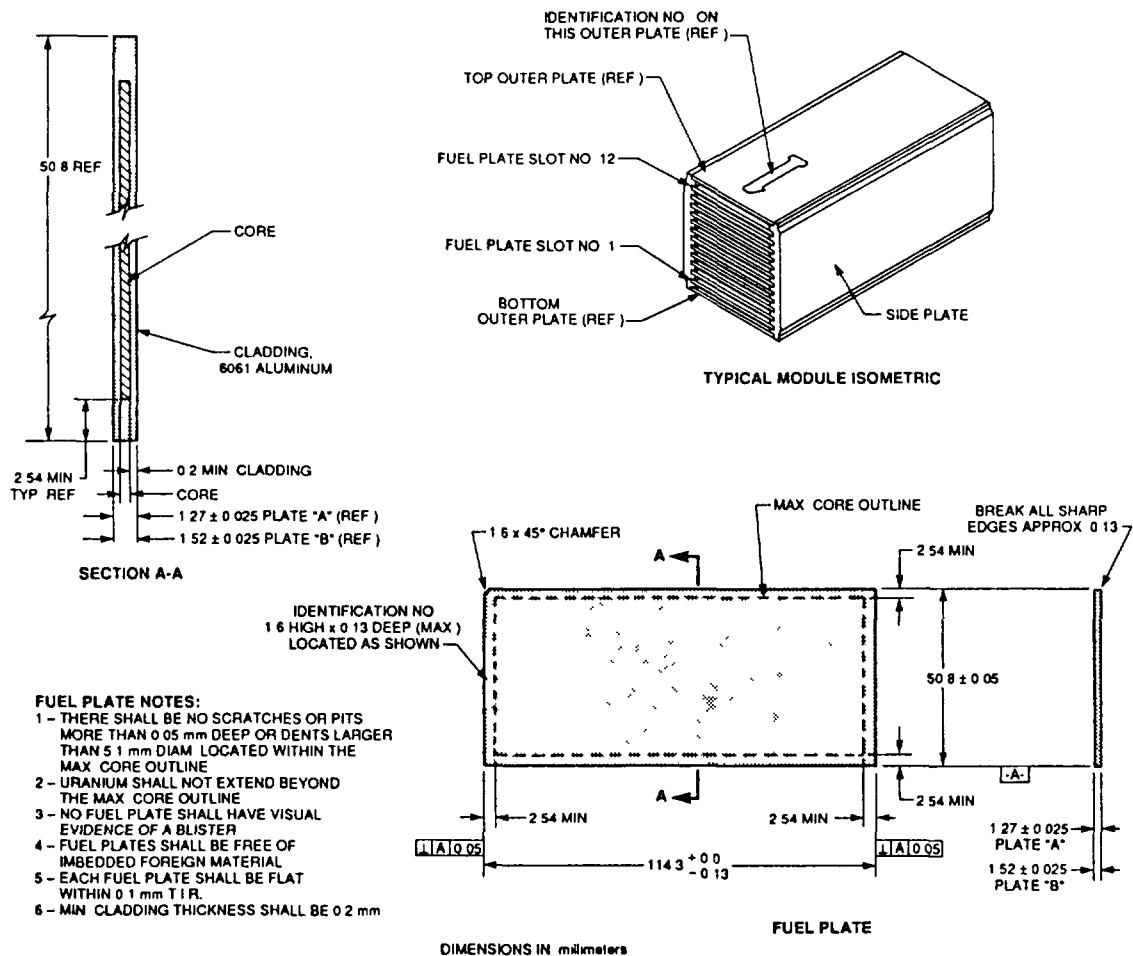


Fig. 1. HFED Irradiation Experiment Miniplate and Module Details.

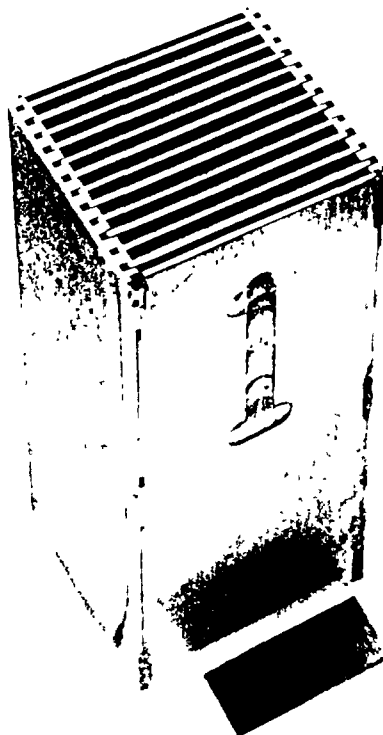


Fig. 2. Closeup view of a module with typical installation of miniplates. Note electron-beam welds along edges and widened slots along top edge to aid in miniplate insertion.

The five modules, stacked one above another, were held within a module holder sized to fit within an ORR core piece. The loaded assembly with selected modules, was placed in an ORR core position for irradiation. A photograph showing an exploded view of the HFED experiment and its various parts is presented in Fig. 3.

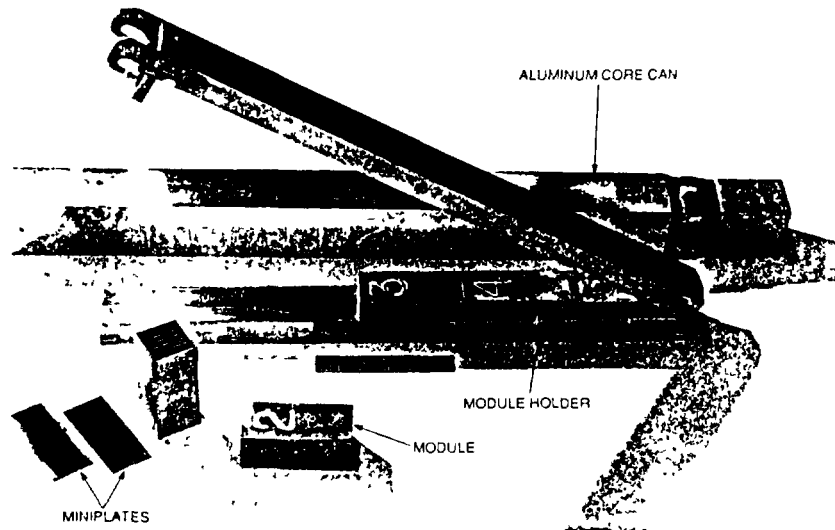


Fig. 3. Exploded view of the HFED miniplate irradiation experiment showing, from top to bottom, (1) ORR core piece, (2) module holder with three modules installed, (3) two typical miniplates and modules 1 and 2.

The reactor coolant water flowed downward through each channel in all five modules in series. Plates in the same plane through all five modules were of the same thickness, thus ensuring that each coolant channel had a constant dimension from top to bottom of the experiment assembly. A complete description of the design and initial operation of the HFED experiment can be found in Ref. 2.

3.3 Poolside Station and Metrology

An underwater examination facility was installed in the ORR pool to permit examination of the modules and fuel plates during the irradiation period. Fixtures to hold the experiment and the disassembled components were fastened to the facility. Special handling tools permitted opening the module holder and removing the modules, removing single plates, and reassembling the experiment.

The modules and fuel plates were examined visually as they were disassembled on the poolside station. The channel gaps between the fuel plates were also measured between most cycles while the reactor was being refueled. A probe, supplied by EG&G Idaho, Inc., incorporating two ultrasonic transducers and the necessary electronics, was inserted down through each of the channels. The elevation of the probe and the width of the channel were measured over the entire length of the five modules and recorded automatically.

4. CONDUCT OF EXPERIMENTS¹

4.1 Module Management

The Operations Division of ORNL had the responsibility to see that the acceptable operating limits for this experiment were not exceeded. To meet these requirements, they conducted extensive thermal-hydraulic calculations for the various materials proposed for irradiation. These calculations were confirmed with out-of-reactor flow tests and various flux measurements made in the ORNL Pool Critical Assembly. Measurements were made to compare the HFED assembly with a standard ORR fuel element and to determine the effects of the hafnium grid and the water spaces within the HFED assembly. The flux level for each module could be adjusted by selecting its position in the module holder, and by properly choosing the core position for the HFED. This permitted modules to be irradiated to the desired burnup levels. Of course, indications of swelling prompted the removal of some of the miniplates before reaching their burnup goals.

The initial series of miniplate irradiations in ORR began on July 18, 1980, and ended on June 13, 1983. There were 132 miniplates in 12 modules irradiated in this series. This series included miniplates manufactured by ANL, CNEA, EG&G Idaho, Inc., NUKEM, and ORNL. They were fueled with UAl_2 , UAl_x , U_3O_8 , U_3Si , and U_3Si_2 with enrichments from 20% to 93% ^{235}U , and fuel densities up to 7.16 Mg/m^3 .

The second series of irradiations began March 30, 1984 and ended January 30, 1987. In this series 112 miniplates were contained in 13 modules. Some modules included plates that had been irradiated earlier. This series included plates manufactured by ANL, CNEA, and NUKEM. They were fueled with USi , U_3Si_2 , $U_3Si_{1.5}$, U_3Si , U_3SiCu , UAl_2 , U_6Fe , and $U_6Mn_{1.3}$. Enrichments of from 0.2% (depleted) to 93% with fuel densities up to 8.0 Mg/m^3 were used in the process.

Between the fuel cycles, the experiment was removed from the core and placed in the poolside station for channel gap measurements. This measurement provided a means to detect swelling and possible incipient failure of the miniplates. During the irradiation program, some swelling and pillowing was detected, and the suspected plates were removed for hot cell examination. (Pillowing is gross swelling characterized by large-scale, fission-gas-driven separations within the fuel meat or at the meat/clad interface. The plate resembles a pillow after swelling.)

During the course of its irradiation, each miniplate experienced many thermal cycles owing to normal startups and shutdowns and power set backs required by other experiments. Fuel meat centerline temperatures are estimated to have been between 75 and 125°C during irradiation.

4.2 Results from Channel Gap Measurements

During the experiment, 86 sets of channel gap measurements were made. Each set of measurements resulted in 22 X-Y plots showing the gap and elevation of the probe as it passed through both the north and south sides of each of the 11 accessible channels. Typical X-Y plots of three adjacent slots are shown in Fig. 4. Careful analysis of all plots from run-to-run was necessary to distinguish bowing from swelling. Bowing could be discerned by gap narrowing on one side and equivalent enlargement of the gap on the opposite side of the plate. True swelling was detected by narrowing of the gap on both sides of a plate.

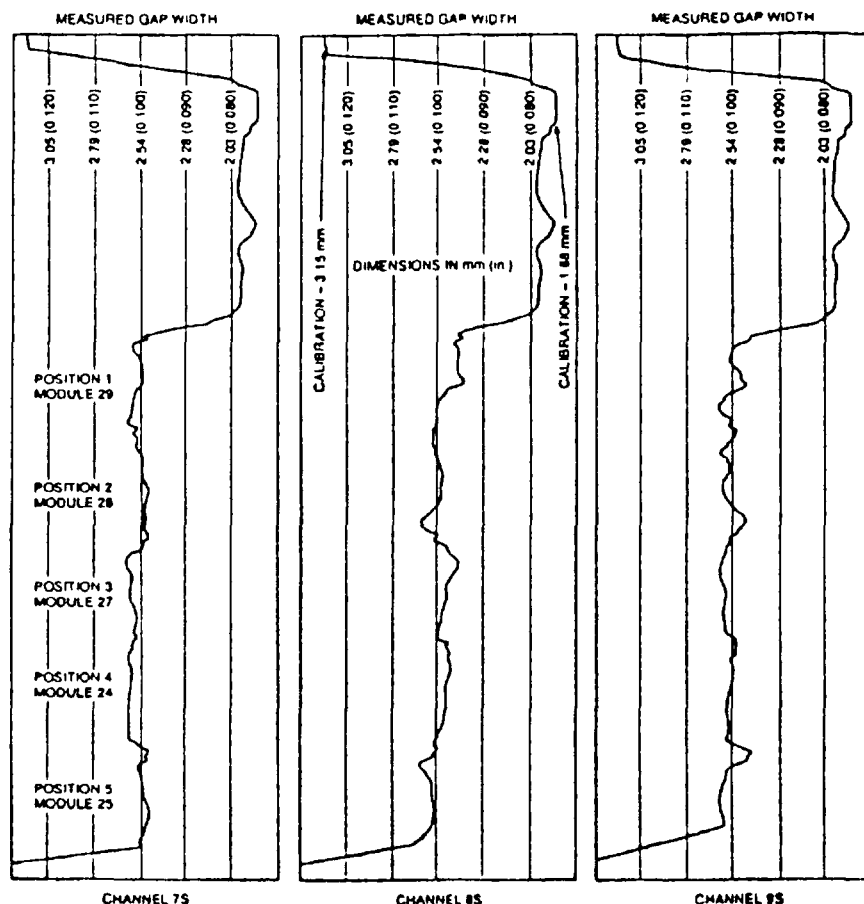


Fig. 4. Typical X-Y plots from channel gap measurements of three adjacent slots.

The CGMD proved to be very useful and provided important information regarding miniplate status during the irradiation period. The use of ultrasonic crystal detectors with the associated electronics and readout devices was successful in determining swelling of irradiated nuclear fuel plates.

5. TEST RESULTS

5.1 General

After irradiation and following suitable periods of cooling, the miniplates were subjected to an extensive series of postirradiation examinations (PIE). The key examinations were thickness and volume measurements to assess the swelling of the fuel meat, metallography to assess the condition of the fuel meat, and blister threshold temperature measurements. Gamma scans were performed to provide fission density profiles and plate-to-plate fission density normalization, and uranium and plutonium isotopic analyses of selected samples were performed to provide absolute burnup information. As described in Appendix G of Ref. 7, calculated ^{235}U fission fractions were used to convert ^{235}U fission densities to the total fission densities reported below. Fission product release studies were made on several of the miniplates.

5.2 Fuel Data and Microstructure

Fuel meat swelling data obtained from immersion density measurements and data from blister-threshold temperature measurements on the miniplates are summarized in Table 2.

UAl_x Fuel: Eleven plates contained medium-enriched uranium (MEU, 40-45%) with uranium densities ranging between 1.5 and 2.3 g/cm³. Nine plates contained LEU(≤20%) and two plates contained uranium with an enrichment of ~27%. The latter eleven plates had uranium densities ranging between 1.9 and 2.5 g/cm³. For all of these plates, swelling⁸⁻¹¹ of the fuel meat ranged between -0.3 and 4.3% for fission densities between 0.8×10^{21} and 1.8×10^{21} fissions/cm³. Two of the MEU plates were fabricated with 100% fine (≤44 μm) fuel particles. These plates showed the lowest net swelling even though their fission densities were 1.5×10^{21} fissions/cm³, probably because of a high initial void content of the fuel meat. All swelling data are consistent with similar data measured for HEU UAl_x fuel over the same range of fission densities (see Appendices J-1.1 and J-1.2 and Ref. 12).

Blister-threshold temperature tests^{8,11,13} on LEU and MEU miniplates with UAl_x fuel are consistent with blister-threshold temperatures in the range of 550 - 565°C. Metallographic examinations⁸ of sections of one LEU and two MEU (including a high fines) miniplates showed each plate to be in excellent condition. There were no indications of actual or incipient failures. A photomicrograph of a section from the MEU miniplate with the highest fission density is shown in Fig. 5. The few large voids seen may be remnants of the voids initially in the fuel meat. No other gas bubbles are evident in the fuel particles.

Based upon all of the results obtained, UAl_x appears to be an extremely well-behaved fuel for LEU and MEU applications requiring uranium densities of up to 2.5 g/cm³.

UAl₂ Fuel: Five LEU miniplates with 3.0 - 3.1 g U/cm³ and two miniplates with 45% enriched fuel and 3.0 g U/cm³ were irradiated in the ORR. Data¹⁴ on fuel meat swelling and blister-threshold temperature measurements are shown in Table 2.

U₃O₈ Fuel: A total of 47 miniplates containing U₃O₈ fuel were irradiated in the ORR. Selected data on the miniplate characteristics are shown in Table 1 and are summarized below. Data on the irradiations and post-irradiation-examinations have been published in Refs. 9-11, and 14-17.

U₃O₈-Al Miniplates Irradiated in the ORR.

Enrichment, %	Number of Miniplates	U Density, Range, g/cm ³
19 - 20	35	2.4 - 3.6
27	4	2.3 - 3.1
40 - 45	7	2.4 - 3.1
93	1	0.7

19-27% Enrichment Range: As shown in Table 2, miniplates in the 19-27% enrichment range showed either shrinkage or moderate swelling for fission densities between 0.8 and 1.6×10^{21} fissions/cm³. The higher-loaded plates with more as-fabricated void volume densified slightly while the lower-loaded plates began to swell. This result is in agreement with previous work which showed that fabrication voids are effective in accommodating irradiation swelling.¹⁸

Table 2. Summary of Swelling and Blister Threshold Temperature Data for High-Density Dispersion Fuels Irradiated in the ORR (From PIE of Miniature Fuel Plates).

Fuel Type	Fabricator*	Density Range, Mg/m ³		Enrichment	No. of Plates	Fission Density Range, 10 ²⁷ /m ³		Swelling Range, % $\Delta V/V_m$		Blister-Threshold Temperature, °C
		Low	High			Low	High	Low	High	
UAL _x	C	1.47		45.1	1	1.3		4.3		-
UAL _x	E	1.88	1.95	40.2	4	1.1	1.5	-0.3	0.6	550-565
UAL _x	E,N	2.13	2.31	39.8-40.2	6	1.3	1.8	1.9	3.4	550-561
UAL _x	E	1.88	1.99	19.9	3	0.8	0.9	0.7	2.9	>550
UAL _x	E,N,C	2.14	2.33	19.9-27.3	6	1.0	1.1	-1.7	4.0	>550
UAL _x	C	2.48	2.52	20.2	2	1.1		-3.9	-3.3	550
UAL ₂	C	2.99	3.09	19.8	5	1.3		-7.2	-2.7	475-500
U ₃ O ₈	O,N	2.40	2.46	39.7-45.0	3	1.7	2.0	2.9	9.7	470
U ₃ O ₈	O	2.77		45.0	1	2.3		p ⁺		-
U ₃ O ₈	O	3.10		45.0	3	2.1	2.5	11.2	p ⁺	-
U ₃ O ₈	O,N,C	2.30	2.48	19.5-27.3	9	0.8	1.1	0.0	2.0	490->550
U ₃ O ₈	O	2.76	2.79	19.5	11	0.9	1.2	-0.7	1.3	>550
U ₃ O ₈	O,N,C	2.91	3.13	19.5-27.3	16	1.0	1.6	-3.8	12.6	478-550
U ₃ O ₈	C	3.49	3.58	19.7	3	1.5		-5.4	-3.4	450
U ₃ Si ₂	A	1.66		93.0	2	1.4	2.1	4.9	11.6	-
U ₃ Si ₂	A	3.94	3.95	40.1	2	1.5	2.4	0.7	10.6	-
U ₃ Si ₂	A	4.95		40.1	1	1.4		~0		-
U ₃ Si ₂	A	5.13	5.18	40.1	2	1.6		-2.1	-1.1	-
U ₃ Si ₂	A	3.72	3.76	19.9	4	1.6	1.8	3.7	7.0	530
U ₃ Si ₂	C	4.81	4.88	19.7	6	1.7	1.8	1.5	2.8	525
U ₃ Si ₂	A	4.92	4.99	19.8	4	1.2	1.3	0.2	0.8	-
U ₃ Si ₂	A	5.1	5.2	19.8	5	1.0	2.3	0.0	4.6	-
U ₃ Si ₂	A	5.60	5.67	19.8	7	2.2	2.5	0.1	2.7	515
U ₃ Si	A	1.98	1.99	92.6	2	1.7	2.1	8.8	9.7	-
U ₃ Si	A	4.5		40.1	2	1.9	2.3	7.3	10.3	-
U ₃ Si	A	5.91		40.1	1	1.4		1.5		-
U ₃ Si	A	6.23	6.40	40.1	3	2.4	2.5	9.6	39.6	-
U ₃ Si	A	4.79	4.83	19.9	5	0.7		~0		510
U ₃ Si	A,C	4.77	4.81	19.9	7	1.7	2.1	5.2	12.0	500->550
U ₃ Si	C	5.18	5.20	19.8	2	2.2		10.3	11.4	500
U ₃ Si	A	5.65	5.72	19.9	4	1.9		0.4	6.8	525
U ₃ Si	A,C	6.05	6.16	19.8-19.9	5	1.5	2.6	0.8	20.4	-
U ₃ Si	A	6.23	6.33	19.8	4	2.4	2.5	25.4	38.8	-
U ₃ Si	N	6.89	6.93	19.4	6	2.5		13.3	21.7	-
U ₃ Si	A	6.92	7.13	19.8-19.9	5	1.4	2.6	1.7	44.3	-

*Fabricators: ANL, EG&G Idaho, ORNL, NUKEM, CNEA.

⁺Indicates that plates "pillowed" during irradiation.

The blister threshold temperatures for these plates are not substantially different than the 375 - 600°C temperatures historically experienced for highly-enriched low-loaded plates.¹⁹ Figure 6 is a photomicrograph¹⁵ of a section of an LEU plate containing 75 wt% U₃O₈ (3.1 g U/cm³) in the fuel meat. This plate had been blister-tested to 500°C. The meat is essentially a mixture of reaction products with islands of unreacted aluminum remaining. In the two plates examined after blister-testing the blisters occurred at the meat/cladding interface.

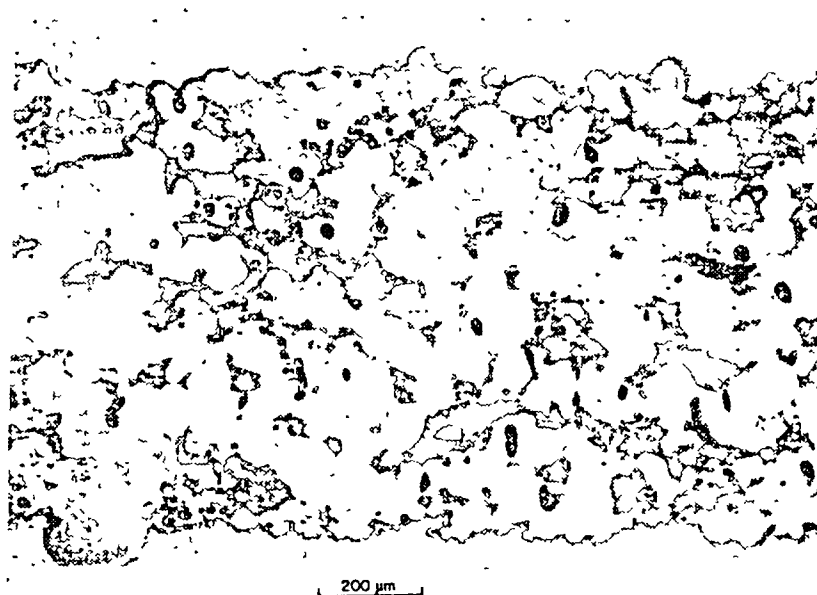


Fig. 5. Longitudinal Section⁸ of 2.3 Mg/m³ UAl_x Miniplate E-117 after Irradiation to 1.8×10^{27} Fissions/m³. (ORNL Photo R-78319)

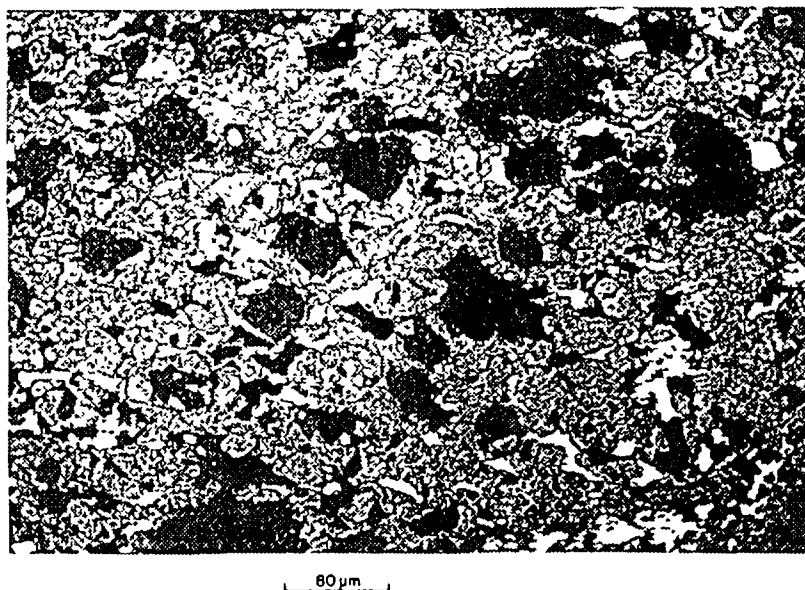


Fig 6. Micrograph¹⁵ of 75 wt%, 20%-enriched U₃O₈ Miniplate O-55-3 after Blister Annealing to 500°C Showing That the Meat Is Essentially Completely Reacted Except for Islands of Aluminum.

The data in Table 2, along with data contained in Appendix J-4.1.2 on full-sized fuel elements containing U₃O₈ fuel indicate that U₃O₈ appears to be a well-behaved fuel for LEU(<20%) applications requiring uranium densities up to 3.2 g U/cm³. It is worthwhile noting that the highest fission density attainable in LEU fuel plates with a uranium density of 3.2 g/cm³ is about 1.7×10^{21} fissions/cm³ (including non-²³⁵U fissions).

40-45% Enrichment Range: Three of the U₃O₈ miniplates with enrichments in the 40-45% range had "pillowed" out¹⁵ during irradiation in the ORR. Two

plates had a uranium density of 3.1 g/cm^3 and an estimated burnup of 2.3×10^{21} fissions/cm³. The third plate which "pillowed" had a uranium density of 2.8 g/cm^3 and an estimated burnup of 2.1×10^{21} fissions/cm³. Three other plates with uranium densities between 2.4 and 2.5 g/cm^3 and fission densities between 1.7 and 2.0×10^{21} fissions/cm³ showed no signs of abnormal swelling behavior or abnormal blister-threshold temperature behavior.

As a result, U_3O_8 fuel is **not recommended** for use with enrichments >20 and uranium densities which could yield fission densities $>1.7 \times 10^{21}$ fissions/cm³.

93% Enrichment Range: One miniplate was irradiated which contained 93% enriched uranium and a uranium density of 0.7 g/cm^3 . This plate was typical of the HEU U_3O_8 fuel used in full-sized ORR elements and was irradiated to provide a comparison with previous irradiation tests¹⁸. The swelling data for this plate at an estimated fission density of 1.1×10^{21} fissions/cm³ (~76% ^{235}U burnup) was consistent with previous measurements and no further testing was done.

Silicide Fuels: A total of 156 miniplates containing silicide fuels were irradiated in the ORR. Selected data on the miniplate characteristics are shown in Table 1 and are summarized below. Data on the irradiations and post-irradiation-examinations have been published in Refs. 8,11,14, 17, and 20-31.

Silicide Miniplates Irradiated in the ORR.

Enrichment, %	Number of Miniplates	U Density, Range, g/cm ³
U_3Si_2		
19 - 20	30	3.7 - 5.7
40	5	3.9 - 5.2
93	2	1.7
0.2	2	4.7
$\text{U}_3\text{Si}_{1.5}$		
19 - 20	5	5.0 - 6.0
40	2	3.8 - 3.9
U_3Si		
19 - 20	42	4.8 - 7.2
40	6	4.5 - 6.0
93	2	2.0
0.2	2	6.1 - 6.2
USi		
20	4	3.8 - 3.9
40	3	3.8 - 3.9
0.2	3	3.7 - 3.8
U_3SiCu		
40	12	3.8 - 7.0
U_3SiAl		
19 - 20	36	4.5 - 7.0

The net swelling of the fuel meat or fuel plate is usually of most interest to reactor operators. Fuel meat swelling data are shown in Table 2. However, fuel meat and fuel plate swelling can be calculated if the swelling behavior of the fuel particles is known. The fuel meat volume of

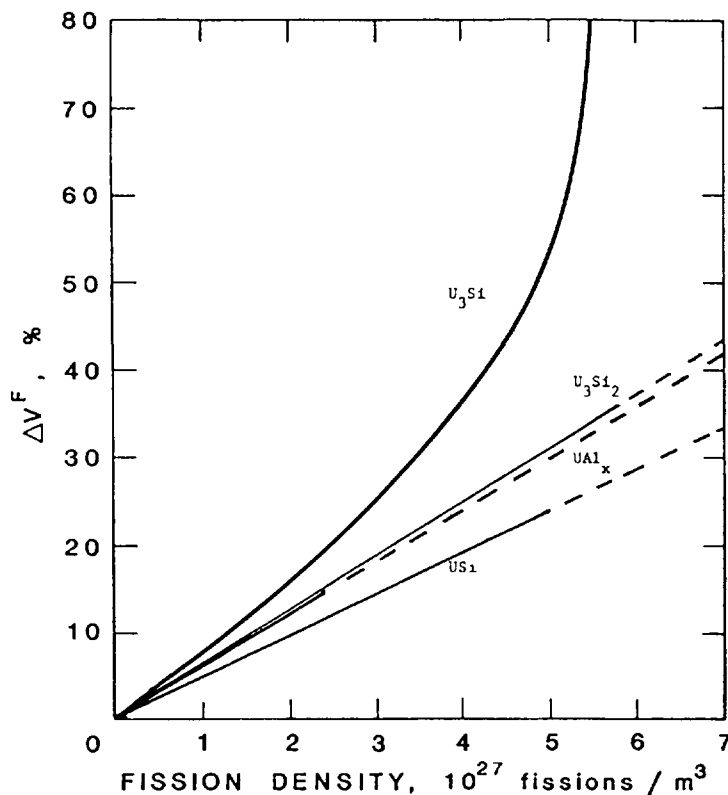


Fig. 7. Swelling of Uranium Silicide and UAl_x Fuel Particles vs. Fission Density in the Particle. Dashed Lines Indicate Fission Densities Not Attainable in LEU Fuel.

an unirradiated fuel plate is occupied by the fuel particles, the aluminum matrix, and pores created when matrix aluminum does not flow around all fuel particles and into the cracks produced in fuel particles during the rolling of the plate. Such pores can occupy from approximately 4% to greater than 12% of the volume of high-density fuel meats. During the early stages of irradiation, irradiation-induced sintering results in some consolidation of the pores, and the volume of the fuel meat can actually decrease. As the fuel particles begin to swell from the buildup of solid and gaseous fission products, the pores begin to be filled. The fuel meat exhibits a net positive volume change only after the volume of the fuel particles has increased by approximately the amount of the original pore volume. Since the amount of as-fabricated porosity is influenced by many factors³², the effect of the porosity must be removed to ascertain the swelling behavior of the fuel itself.

Thus, a clear picture of the swelling behavior of the various uranium silicides can be obtained by calculating the swelling of the fuel particles themselves, assuming that the as-fabricated porosity has been completely filled. The general trends of these data²⁷ and, for comparison, data for UAl_x ,¹² are shown in Fig. 7. The swelling of UAl_x , USi , and U_3Si_2 fuel particles is very stable, being a linear function of the fission density to fission densities well beyond those which can be achieved in LEU fuel (2.4 , 5.0 , and 5.8×10^{27} f/m³ in the fuel particles of UAl_x , USi , and U_3Si_2 , respectively). On the other hand, U_3Si fuel particles in highly loaded fuel plates exhibit an unstable behavior, called breakaway swelling, for fission densities greater than $\sim 4.5 \times 10^{27}$ f/m³ ($\sim 65\%$ ^{235}U burnup for LEU). The swelling rates per unit fission density of U_3Si_2 and UAl_x fuel particles are the same within the accuracy of the data. The slopes of the linear swelling curves are 4.8%, 6.0%, and 6.2% per 10^{27} f/m³ for USi , UAl_x , and

U_3Si_2 , respectively. These data were derived for 40 vol% loadings of USi , 28 to 36 vol% loadings of UAl_x , and 45 to 59 vol% loadings of U_3Si_2 . The UAl_x was fully enriched, and the uranium silicides were low enriched. The data of Table 3²⁷ indicate that the slope of the U_3Si_2 swelling curve may be marginally lower for lower fuel volume loadings. Given the fuel particle swelling rate, the fuel volume fraction, and the as-fabricated porosity, the meat swelling for a given fission density can be reliably predicted.

An example of the meat microstructure of a U_3Si_2 miniplate after >90% burnup is shown in Fig. 8. Some of the noteworthy features in this optical micrograph are the absence of fission gas bubbles and the fact that all of the as-fabricated porosity has been consumed by fuel particle swelling. Fuel-aluminum interaction was limited to a narrow zone around the U_3Si_2 particles with a thickness about equal to the range of fission product recoils in aluminum. Examination of fractured fuel particles using a scanning electron microscope (SEM) reveals a gas bubble morphology typical of pure U_3Si_2 , as shown in Fig. 9. The very uniform distribution of small gas bubbles that show no tendency to interlink is the reason for the stable swelling behavior of U_3Si_2 .

The microstructural changes in U_3Si miniplates resulting from irradiation to high burnups are quite different, as shown in Fig. 10. Fission gas bubbles are clearly visible in the optical micrograph. The bubble morphology, more clearly shown in the SEM images in Fig. 11, reveals a basic difference in fission gas behavior between U_3Si and U_3Si_2 . The fission gas bubbles in U_3Si are not uniformly distributed and vary widely in size. The large bubbles are growing rapidly and interlinking, resulting in a much larger fuel swelling rate than that of U_3Si_2 . The fuel in the full-sized U_3Si_2 plates exhibits characteristics of both U_3Si_2 and U_3Si .

The post irradiation blister threshold temperature has been used traditionally as an indicator of the relative failure resistance of plate-type dispersion fuels. The U_3Si_2 (and U_3Si) miniplates blistered at temperatures in the range of 515 to 530 C, except for very highly loaded U_3Si miniplates which, at the threshold of breakaway swelling, blistered at 450 to 475 C. The blister threshold temperature appears to be insensitive both to burnup and to fuel volume loading. These temperatures are at least as high as those measured for highly enriched UAl_x and U_3O_8 dispersion fuels in use today.^{12,19}

Other Fuels: $\text{U}_3\text{SiCu-Al}$ fuel contained a small ternary addition of Cu to the fuel particles in order to determine whether this Cu addition would suppress the swelling behavior of U_3Si fuel. Since it did not, this fuel was not pursued beyond the miniplate screening stage.

Miniplates containing $\text{U}_6\text{Fe-Al}$ fuel³³ and $\text{U}_3\text{SiAl-Al}$ fuel^{34,8} exhibited excessive swelling upon irradiation in the ORR and were also not pursued beyond the miniplate screening stage.

5.3 Fission Product Release

Over the years several studies of fission product release from plate-type reactor fuels have been performed, first for plates with U-Al alloy meat and later for plates with UAl_x and U_3O_8 dispersion meats. Results of these experiments have been summarized in Refs. 3 and 35. As part of the development of high-density fuels under the RERT Program, fission product

Table 3. U_3Si_2 Miniplate Swelling Data Summary

Plate No.*	U Dens., Mg/m ³	Fuel Vol. Fraction, %	Fuel Meat Porosity, %	²³⁵ U Burnup, %	Fuel Meat Fission Dens., 10 ²⁷ /m ³	Fuel Particle Fission Dens., 10 ²⁷ /m ³	Fuel Meat Swelling, Vol%	Fuel Particle Swelling, Vol%
A32	3.8	33.3	4.5	90	1.6	4.8	3.8	25
A34	3.8	33.4	4.3	90	1.6	4.8	4.1	25
A36	3.8	33.3	4.5	90	1.6	4.8	4.3	26
				96	1.8	5.5	7.1	35
A46	3.7	33.1	5.2	90	1.6	4.8	3.7	27
				96	1.8	5.5	6.8	36
A100	5.2	46.2	8.5	42	1.0	2.1	0.0	≤18
A85	5.0	45.4	10.3	79	1.8	4.2	1.6	26
A99	5.2	45.9	9.1	79	1.9	4.2	2.0	24
A87	5.1	45.6	9.8	85	2.1	4.6	3.3	29
A88	5.2	45.8	9.5	85	2.1	4.6	2.6	26
A89	5.6	49.8	13.4	85	2.3	4.6	0.9	29
A90	5.6	49.9	13.3	85	2.3	4.6	0.2	27
A91	5.6	49.7	13.5	85	2.3	4.6	0.1	27
A92	5.6	50.0	12.9	85	2.3	4.6	1.5	29
A93	5.6	50.0	13.0	85	2.3	4.6	0.4	26
A94	5.7	50.4	12.4	85	2.3	4.6	2.9	30
A123M	4.0	35.1	4.2	42	1.5	4.2	0.7	≤14
A124M	3.9	35.0	4.3	69	2.5	7.1	11.6	45
A125M	5.1	45.6	11.8	39	1.8	3.9	2.1	30
A126M	5.2	46.0	11.0	39	1.8	3.9	1.1	26
A121H	1.7	14.7	0.8	41	1.4	9.3	4.9	38
A122H	1.7	14.7	0.8	69	2.3	15.7	11.6	84

*All plates LEU except those with plate number ending in M (MEU) or H (HEU).

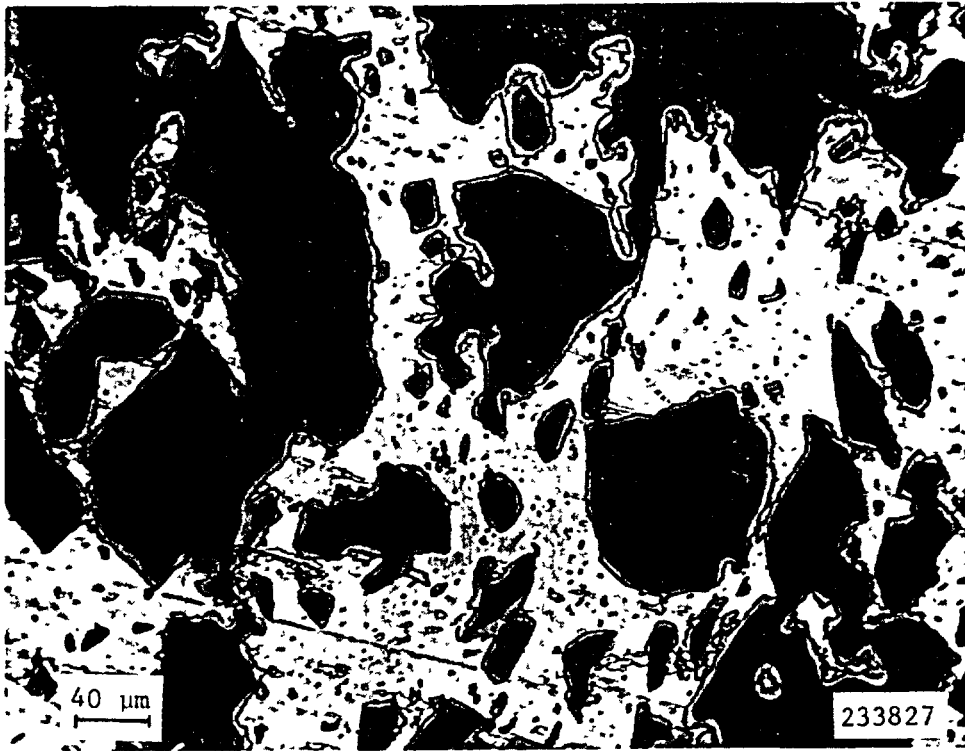


Fig. 8. Meat Microstructure of U_3Si_2 Miniplate After 90% Burnup (Bu).

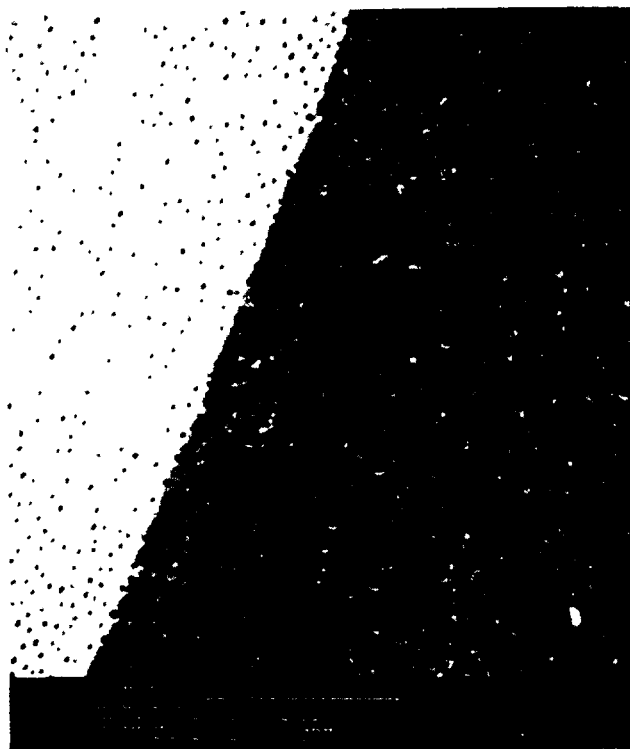


Fig. 9. Fission Gas Bubble Morphology in U_3Si_2 After 90% Bu.

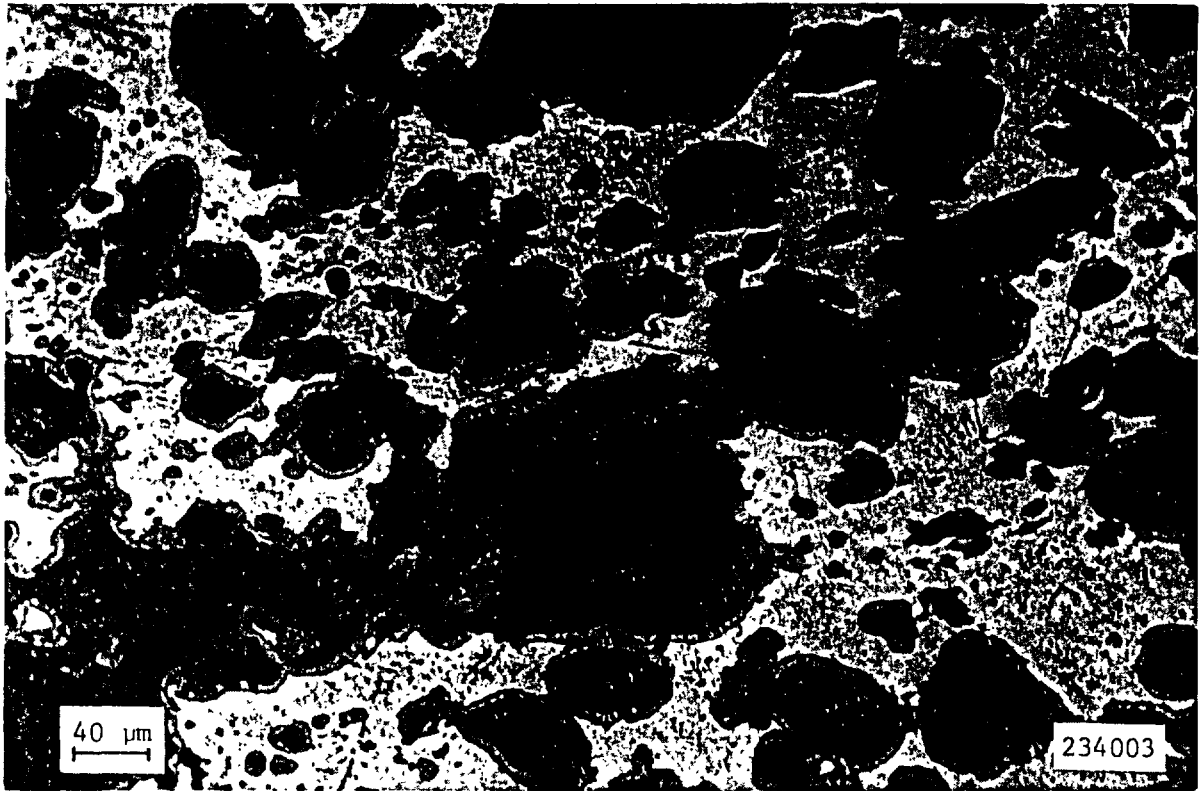


Fig. 10. Meat Microstructure of U_3Si Miniplate After 90% Bu.

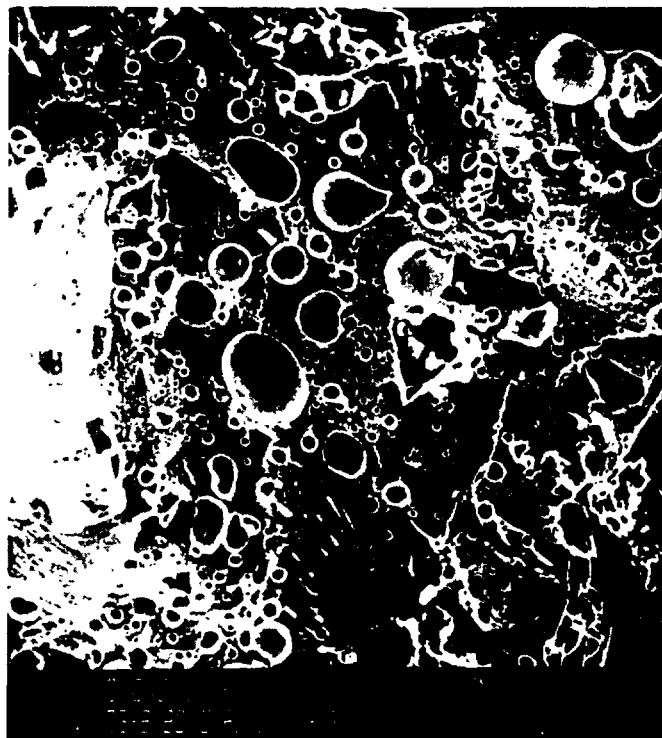


Fig. 11. Fission Gas Bubble Morphology in U_3Si After 90% Bu.

release measurements of limited scope have been performed. Detailed data on these measurements are provided in Appendix J-5. A brief summary of the main conclusions is given below.

Measurements using UAl_x miniplates were performed at ORNL in collaboration with the Kyoto University Research Reactor Institute primarily to determine the threshold temperature for fission product release and to measure release rates above that temperature.¹³ These tests showed that the first significant release of gaseous fission products occurred when the fuel plate blistered. Another significant release occurred at about the solidus temperature of the cladding, and a third significant release occurred at about the UAl_4 -Al eutectic temperature.

Similar measurements, using the same equipment, were made using U_3O_8 and U_3Si miniplates, with similar results.³⁶ The first release of gaseous fission products was detected when the plates blistered, at 500°C for the U_3O_8 plates. Essentially all of the gaseous fission products had been released by the end of the test at 650°C. From the amounts of Cs detected in the traps and from visual observations of deposits on the sample holder following the 650°C test, it was determined that much more Cs was released from the U_3Si plate than from the U_3O_8 plate.

Release/Born (R/B) ratio data of fission products for U-Al alloy, UAl_x -Al, and U_3Si_2 -Al fuels were measured³⁷ by JAERI in order to assess the integrity of uranium silicide fuel in the safety assessment for LEU conversion of the JMTR reactor. The results showed that the release rate of Iodine-131 at 700 °C for silicide and aluminide fuel are lower than the U-Al alloy fuel by approximately a factor of three. The release of rare gases in silicide and aluminide fuels are almost 100%, similar to alloy fuel.

REFERENCES

1. R. L. Senn, *Summary Report on the HFED Miniplate Irradiations for the RERTR Program*, ORNL-6539, Martin Marietta Energy Systems, Oak Ridge National Laboratory, April 1989
2. R. L. Senn and M. M. Martin, *Irradiation Testing of Miniature Fuel Plates for the RERTR Program*, Union Carbide Corp. Nuclear Div., Oak Ridge Natl. Lab., ORNL/TM-7761, July 1981.
3. D. Stahl, *Fuels for Research and Test Reactors, Status Review: July 1982*, Argonne National Laboratory Report ANL-83-5, 37-39, December 1982.
4. G. L. Copeland and M. M. Martin, *Fabrication of High-Uranium-Loaded U_3O_8 -Al Developmental Fuel Plates*, ORNL-TM-7607, Union Carbide Corp. Nuclear Div., Oak Ridge Natl. Lab., December 1980.
5. R. F. Domagala, T. C. Wiencek and H. R. Thresh, *U-Si and U-Si-Al Dispersion Fuel Alloy Development for Research and Test Reactors*, Nucl. Tech. 62, 353-60 (1983).
6. T. P. Hamrick and J. H. Swanks, *The Oak Ridge Research Reactor - A Functional Description*, ORNL-4169, Union Carbide Corp. Nuclear Div., Oak Ridge Nat. Lab., September 1968.

7. G. L. Copeland, R. W. Hobbs, G. L. Hofman, and J. L. Snelgrove, *Performance of Low-Enriched U_3Si_2 -Aluminum Dispersion Fuel Elements in the Oak Ridge Research Reactor*, Argonne National Laboratory Report ANL/RERTR/TM-10, October 1987.
8. J. L. Snelgrove, R. F. Domagala, T. C. Weincek, and G. L. Copeland, *Fuel Development Activities of the U.S. RERTR Program*, Proc. International Meeting on Reduced Enrichment for Research and Test Reactors, Tokai, Japan, October 24-27, 1983, JAERI-M 84-073, May 1984.
9. E. Perez, C. Kohut, D. Giorsetti, G. Copeland, and J. Snelgrove, *Irradiation Performance on CNEA UAl_x and U_3O_8 Miniplates*, Proc. International Meeting on Reduced Enrichment for Research and Test Reactors, Tokai, Japan, October 24-27, 1983, JAERI-M 84-073, May 1984.
10. M. F. Hrovat and H. W. Hassel, *Recent Status of Development and Irradiation Performance for Plate Type Fuel Elements with Reduced ^{235}U Enrichment at NUKEM*, Proc. International Meeting on Reduced Enrichment for Research and Test Reactors, Tokai, Japan, October 24-27, 1983, JAERI-M 84-073, May 1984.
11. J. L. Snelgrove, *RERTR Program Fuel Testing and Demonstration - An Update*, Proc. 1984 International Meeting on Reduced Enrichment for Research and Test Reactors, Argonne, Illinois, October 15-18, 1984, ANL/RERTR/TM-6 (CONF-8410173), July 1985.
12. J. M. Beeston, R. R. Hobbins, G. W. Gibson, and W. C. Francis, *Development and Irradiation Performance of Uranium Aluminide Fuels in Test Reactors*, Nucl. Tech. 49, 136-149, June 1980.
13. T. Shibata, T. Tamai, M. Hayashi, J. C. Posey, and J. L. Snelgrove, *Release of Fission Products from Irradiated Aluminide Fuel at High Temperatures*, Nucl. Sci. and Eng. 87, 405-417, 1984.
14. J. Gómez, R. Morando, E. E. Pérez and D. R. Giorsetti, CNEA; G. L. Copeland, ORNL; G. L. Hofman and J. L. Snelgrove, ANL, *Postirradiation Examination of High-U-Loaded Low-Enriched U_3O_8 , UAl_2 , and U_3Si Test Fuel Plates*, Proc. 1984 International Meeting on Reduced Enrichment for Research and Test Reactors, Argonne, Illinois, October 15-18, 1984, ANL/RERTR/TM-6 (CONF-8410173), May 1988.
15. G. L. Copeland and J. L. Snelgrove, *Examination of Irradiated High-U-Loaded U_3O_8 -Al Fuel Plates*, Proc. International Meeting on Research and Test Reactor Core Conversions from HEU to LEU Fuels, Argonne, Illinois, November 8-10, 1982, ANL/RERTR/TM-4 (CONF-821155), September 1983.
16. G.L. Hofman, G.L. Copeland, and J.E. Sanecki, *Microscopic Investigation into the Irradiation Behavior of U_3O_8 -Al Dispersion Fuel*, Nucl. Tech. 72, 338-44 (1986).
17. G. L. Hofman, *Crystal Structure Stability and Fission Gas Swelling in Intermetallic Uranium Compounds*, J. Nucl. Mat. 140, 256-63 (1986).
18. M. M. Martin, A. E. Richt, and W. R. Martin, *Irradiation Behavior of Aluminum-Base Fuel Dispersions*, ORNL-4856 (May 1973).

19. A. E. Richt, R. W. Knight, and G. M. Adamson, Jr., *Postirradiation Examination and Evaluation of the Performance of HFIR Fuel Elements*, Oak Ridge National Laboratory Report ORNL-4714, December 1971.
20. G. L. Hofman and L. Neimark, *Irradiation Behavior of Uranium-Silicide Dispersion Fuels*, Proc. International Meeting on Reduced Enrichment for Research and Test Reactors, Tokai, Japan, October 24-27, 1983, JAERI-M 84-073, May 1984.
21. G. L. Hofman and L. A. Neimark, *Postirradiation Analysis of Uranium-Silicide Dispersion Fuels*, Proc. 1984 International Meeting on Reduced Enrichment for Research and Test Reactors, Argonne, Illinois, October 15-18, 1984, ANL/RERTR/TM-6 (CONF-8410173), May 1988.
22. J.L. Snelgrove, G. L. Hofman, and G. L. Copeland, *Irradiation Performance of Reduced Enrichment Fuels Tested under the U.S. RERTR Program*, Reduced Enrichment for Research and Test Reactors - Proceedings of an International Meeting, Petten, The Netherlands, October 14-16, 1985, D. Reidel Publ. Co., 1986.
23. G. L. Hofman, L. A. Neimark, ANL and F. L. Olquin, ININ, *The Effect of Fabrication Variables on the Irradiation Performance of Uranium Silicide Dispersion Fuel Plates*, Proc. 1986 International Meeting on Reduced Enrichment for Research and Test Reactors, Gatlinburg, Tennessee, November 3-6, 1986, ANL/RERTR/TM-9 (CONF-861185), May 1988.
24. J. L. Snelgrove, *RERTR Program Fuel Development and Testing -- the Past Year and the Next*, Proc. 1986 International Meeting on Reduced Enrichment for Research and Test Reactors, Gatlinburg, Tennessee, November 3-6, 1986, ANL/RERTR/TM-9 (CONF-861185), May 1988.
25. J. L. Snelgrove, *Qualification Status of LEU Fuels*, Proc. 1987 International Meeting on Reduced Enrichment for Research and Test Reactors (RERTR), Buenos Aires, Argentina, September 28-October 2, 1987 (to be published).
26. G. L. Hofman, *Prospects for Stableigh Density Dispersion Fuels*, Proc. 1987 International Meeting on Reduced Enrichment for Research and Test Reactors (RERTR), Buenos Aires, Argentina, September 28-October 2, 1987 (to be published).
27. J. L. Snelgrove, R. F. Domagala, G. L. Hofman, T. C. Wiencek, G. L. Copeland, R. W. Hobbs, and R. L. Senn, *The Use of U_3Si_2 Dispersed in Aluminum in Plate-Type Fuel Elements for Research and Test Reactors*, Argonne National Laboratory Report ANL/RERTR/TM-11, October 1987.
28. G. L. Hofman, *Some Recent Observations on the Irradiation Behavior of Uranium Silicide Dispersion Fuel*, Proc. 1988 International Meeting on Reduced Enrichment for Research and Test Reactors, San Diego, California, September 19-22, 1988, ANL/RERTR/TM-13 (to be published).
29. J. Rest, G. L. Hofman, and R.C. Birtcher, *The Effect of Crystal Structure Stability on Swelling in Intermetallic Uranium Compounds*, Proc. 1988 International Meeting on Reduced Enrichment for Research and Test Reactors, San Diego, California, September 19-22, 1988, ANL/RERTR/TM-13 (to be published).

30. G. L. Hofman, A. Marajofsky, and C Kohut, *Irradiation Behavior of the CNEA's Experimental Uranium Silicide Dispersion Fuel Plates*, Proc. 1988 International Meeting on Reduced Enrichment for Research and Test Reactors, San Diego, California, September 19-22, 1988, ANL/RERTR/TM-13 (to be published).
31. G. L. Hofman and W-S. Ryu, *Detailed Analysis of Uranium Silicide Dispersion Fuel Swelling*, Proc. 1989 International Meeting on Reduced Enrichment for Research and Test Reactors, Berlin, Federal Republic of Germany, September 19-22, 1989 (to be published).
32. T. C. Weincek, *A Study of the Effect of Fabrication Variables on the Quality of Fuel Plates*, Proc. 1986 International Meeting on Reduced Enrichment for Research and Test Reactors, Gatlinburg, Tennessee, November 3-6, 1986, ANL/RERTR/TM-9 (CONF-861185), May 1988.
33. G. L. Hofman, R. F. Domagala, and G. L. Copeland, *Irradiation Behavior of Low-Enriched U₆Fe-AlI Dispersion Fuel Elements*, J. Nucl. Mat. 150, 238-43 (1987).
34. G. L. Hofman, L. A. Neimark, and R. F. Mattas, *Irradiation Behavior of Experimental Miniature Uranium Silicide Fuel Plates*, Proc. Intl. Mtg. on Research and Test Reactor Core Conversions from HEU to LEU Fuels, Argonne, Illinois, November 8-10, 1982, Argonne National Laboratory Report ANL/RERTR/TM-4 (CONF-821155), 117-133, September 1983.
35. R. E. Woodley, *The Release of Fission Products from Irradiated SRP Fuels at Elevated Temperature*, Hanford Engineering Development Laboratory Report HEDL-7598, June 1986.
36. J. C. Posey, *Release of Fission Products from Miniature Fuel Plates at Elevated Temperatures*, Proc. Intl. Mtg. on Research and Test Reactor Core Conversions from HEU to LEU Fuels, Argonne, Illinois, November 8-10, 1982, Argonne National Laboratory Report ANL/RERTR/TM-4 (CONF-821155), 117-133, September 1983.
37. M. Saito, Y. Futamura, H. Nakata, H. Ando, F. Sakurai, N. Aoka, A Sakakura, M. Ugajin, and E. Shirai, *Further Data of Silicide Fuel for the LEU Conversion of JMTR*, IAEA International Symposium on Research Reactor Safety, Operations and Modifications, Chalk River, Ontario, Canada, 23-27 October 1989, IAEA-SM-310/59P.

ATTACHMENT A

Reproduced from
ORNL-6539 (Ref. 1)

Document No: Q-11821-ET-002-S-0
Issue Date: January 31, 1980
Revision: 0

FUEL PLATE SPECIFICATION

for

RERTR IRRADIATION TESTS

located at

OAK RIDGE RESEARCH REACTOR

BUILDING 3042, ORNL

OAK RIDGE, TENNESSEE

ENGINEERING TECHNOLOGY DIVISION

OAK RIDGE NATIONAL LABORATORY

PREPARED BY

Ronald L. Linn
Project Engineer

Jan. 17/1980
Date

APPROVALS

J. Miller
QA Coordinator

1/21/80
Date

L. E. MacPherson
Section Head

1/21/80
Date

M. M. Martin
Program Manager

1/30/80
Date

DISTRIBUTION

H. C. Austin
R. J. Beaver
C. D. Cagle
W. R. Casto
J. A. Conlin
G. L. Copeland
R. F. Domagala, ANL
T. P. Hamrick
R. E. MacPherson
R. F. Mattas, ANL
M. M. Martin
C. A. Mills (2)
F. H. Neill (4)
D. G. Newton, EG&G
R. A. Schmidt
S. L. Seiffert, EG&G
R. L. Senn
M. Sims
D. Stahl, ANL
V. W. Storchok, EG&G
H. E. Trammell

FUEL PLATES FOR RERTR IRRADIATION TEST

1.0 Scope

This specification applies to Reduced-Enrichment Research and Test Reactor (RERTR) fuel plates suitable for irradiation in the Oak Ridge Research Reactor (ORR). These aluminum-base dispersion-type plates presently include (1) the high uranium content U_3O_8 -bearing miniplates being developed and fabricated at ORNL, (2) the high uranium content UAl_x -bearing miniplates being developed and fabricated at EG&G Idaho, Inc., and (3) the very high uranium content U_3Si - and $(U_3Si + Al)$ -bearing miniplates being developed and fabricated at ANL.

2.0 UCC-ND Drawings

ORR-HFED Experiment Plate Details	X3E-11821-0105-B
ORR-HFED Experiment Assembly	X3E-11821-0101-A

3.0 Materials

3.1 All materials that compose the cored region of the miniplates shall conform to the requirements of this document and the specifications of the cognizant organization (e.g., ORNL will specify the core materials within the U_3O_8 -bearing miniplates).

3.2 Cover plate and frame cladding shall conform to Standard Specification for Aluminum-Alloy Sheet and Plate, ANSI/ASTM Designation B209-77, for alloy 6061 and Alclad 6061.

4.0 Fuel Plate Requirements

4.1 The fuel plates shall be rolled by a combination of, first, hot rolling, and second, cold rolling at room temperature to a reduction in thickness of at least 10% to insure uniform cladding properties among fabricators.

4.2 After completion of hot rolling and before cold rolling, the fuel plates shall be annealed for 60 ± 10 min at $485 \pm 20^\circ C$. After cooling to room temperature, both sides of every fuel plate shall be visually examined for blisters. Visual detection of one or more blisters that would remain in the finally-sized fuel plate shall be cause for rejection.

4.3 After completion of cold rolling, the fuel plates shall be heat-treated at $485 \pm 20^\circ\text{C}$ for 60 ± 10 min followed by a cooling at a rate of $\leq 28^\circ\text{C/hr}$ to $\leq 260^\circ\text{C}$. After further cooling to room temperature, both sides of every fuel plate shall be visually examined for blisters. Visual detection of one or more blisters that would remain in the finally-sized fuel plates shall be cause for rejection.

4.4 Fuel plate, core, and cladding dimensions shall conform to UCC-ND Drawing X3E11821-0105-A.

4.5 Within the maximum core outline of UCC-ND Drawing X3E11821-0105-A and for any 4-mm to 2-mm-diam spot, the U^{235} surface density, in g/m^2 of core surface area, shall be ≤ 290 for fuel plates to be irradiated in Modules 3, 4, and 5 (see UCC-ND Drawing X3E11821-0101-A for module numbering scheme); and ≤ 500 for fuel plates to be irradiated in Modules 1 and 2.

4.6 The interfaces between the cover plates and frames of the fuel plates shall be metallurgically bonded. Grains that have grown across these interfaces for a minimum of 50% of the interfacial length constitute acceptable bonding.

4.7 The surfaces of the fuel plates shall be free from all foreign matter including moisture, dirt, oil, organic compounds, scale, paint, ink, graphite, all solders, silver, lead, mercury, thorium, chlorine, and fluorine.

4.8 The exterior surfaces of the fuel plates shall be free from uranium after fabrication. A final pickling treatment, which shall be performed before packaging for shipment to ORNL, of submerging the fuel plates in 45 vol% HNO_3 -55 vol% H_2O solution for 2 to 4 minutes at room temperature followed by rinsing in either demineralized or distilled water meets the intent of this requirement.

4.9 The fuel plates shall be identified as shown on UCC-ND Drawing X3E-11821-0105-A. Serial numbers of 0-001 through 0-999, E-001 through E-999, and A-001 through A-999 are permitted, respectively, for fuel plates supplied by ORNL, EG&G Idaho, Inc., and ANL.

5.0 Inspection

The fuel plate fabricator shall be responsible for inspection and certification of the achievement of requirements set forth in paragraphs 3 and 4 above and in paragraph 6 below.

6.0 Quality Assurance Documentation

6.1 The preirradiation data package for the fuel plates shall include the following items:

- (1) dimensional inspection reports (including an estimation of minimum clad thickness) for each plate;
- (2) radiographs of each plate; and
- (3) results from determination of the meat attributes including a tabulation of (a) plate number, (b) weight of plate, (c) weight of meat, (d) elemental composition of the meat, (e) ^{235}U enrichment (wt %), and (f) total ^{235}U loading.

6.2 Certified copies of inspection and test records to assure compliance with this specification and the preirradiation data package shall be supplied to R. L. Senn, Bldg. 9201-3, MS-5, P. O. Box "Y", Oak Ridge, Tennessee 37830.

7.0 Shipping

7.1 Storage of the fuel plates and final assembly of the HFED experiment will be conducted in Building 3012, ORNL. The fuel plate fabricators shall provide shipping containers and shall have full responsibility for the fuel plates while in transit to the site designated below. A duplicate copy of the tabulation of 6.1 (3) shall be included in the shipping container with the plates.

7.2 Fuel plate fabricators shall ship the fuel plates by acceptable means to the Oak Ridge National Laboratory, Building 3012, Oak Ridge, Tennessee 37830, Attention: H. C. Austin, Bldg. 3037 for M. M. Martin, Bldg. 4508, ORNL.

7.3 Accountability shall be transferred to facility F.Z.C., H. C. Austin, Bldg. 3037, ORNL.

Table 4.2. Listing for HFEDSHIP.BAS

```

10 LPRINT "*****"
20 LPRINT
30 LPRINT "  HFEDSHIP.BAS, A BASIC PROGRAM TO CALCULATE HEAT LOAD AND CURIE
40 LPRINT "  LEVEL OF IRRADIATED HFED MINIPLATES AS OF PRESENT DATE.
50 LPRINT "  TO RUN, LIST 100-300 AND ENTER DATA AS INSTRUCTED.
60 LPRINT
70 LPRINT "          R. L. SENN                      MAY 5, 1986
80 LPRINT
90 LPRINT "*****"
100 PRINT
110 'E$ = MODULE NO. OR PLATE-MODULE NO.
120 'F$ = TODAY'S DATE
130 'A = TIME OUT OF REACTOR, DAYS
140 'B = TIME IN REACTOR, DAYS
150 'C = GRAMS 235-U
160 'D = ESTIMATED FRACTIONAL U-235 BURNUP
170 'Z = SUMMING DEVICE (ENTER 1, OR 0 IF LAST CASE).
180 'P = WATTS/GRAM 235-U REMAINING
190 'TO RUN, TYPE DATA STATEMENTS BEGINNING WITH 510 WITH SEVEN (7)
200 'ENTRIES PER CASE, AS FOLLOWS:
210 ' 510 DATA A, B, C, D, E$, F$, Z
220 READ A, B, C, D, E$, F$, Z
230 P = 5.9*7.4*((A^-.2)-((A+B)^-.2))
240 G = P*C*(1-D)
250 SUM = SUM +G: H = G*240
270 NSUM = NSUM + H: LPRINT
290 PRINT "HEAT LOAD + CURIE LEVEL FOR "E$"      AS OF "F$
300 LPRINT"HEAT LOAD + CURIE LEVEL FOR "E$"      AS OF "F$:LPRINT
320 PRINT "TIME IN REACTOR =" B "FULL POWER DAYS"
330 LPRINT"TIME IN REACTOR =" B "FULL POWER DAYS"
340 PRINT "COOLING TIME =" A "DAYS"
350 LPRINT"COOLING TIME =" A "DAYS"
360 PRINT "TOTAL ORIGINAL 235-U=" C "GRAMS"
370 LPRINT "TOTAL ORIGINAL 235-U=" C "GRAMS"
380 PRINT "ESTIMATED FRACTIONAL 235-U BURNUP =" D
390 LPRINT "ESTIMATED FRACTIONAL 235-U BURNUP =" D
400 PRINT "REMAINING 235-U =" C*(1-D)
410 LPRINT "REMAINING 235-U =" C*(1-D) "GRAMS"
420 PRINT:LPRINT
430 PRINT "POWER/GM 235-U =" P:LPRINT "POWER/GM 235-U =" P
440 PRINT:LPRINT
450 PRINT "TOTAL HEAT LOAD =" G "WATTS","CURIE LEVEL =" H
460 LPRINT "TOTAL HEAT LOAD =" G "WATTS","CURIE LEVEL =" H
470 LPRINT
500 IF Z = 0 GOTO 590
510 DATA 249,252.68,15.163,.88,"MOD. 27",6/01/87,1
520 DATA 194,272.3,25.814,.84,"MOD. 30",6/01/87,1
530 DATA 194,234.65,20.497,.70,"MOD. 31",6/01/87,1
540 DATA 123,146.89,28.835,.30,"MOD. 33",6/01/87,1
550 DATA 123,321.55,7.660,.70,"PLATES A-114,-115",6/01/87,1
555 DATA 123,147,21.108,.40,"MOD. 34",6/01/87,1
560 DATA 123,401.62,9.995,.92,"PLATES A-87,-89,-90,-93",6/01/87,0
570 LPRINT:PRINT
580 GOTO 220
590 LPRINT:PRINT
600 PRINT "      TOTAL HEAT LOAD FOR ABOVE SHIPMENT=" SUM "WATTS"
610 LPRINT "      TOTAL HEAT LOAD FOR ABOVE SHIPMENT=" SUM "WATTS"
620 PRINT "      TOTAL RADIATION FOR ABOVE SHIPMENT=" NSUM "CURIES"
630 LPRINT "      TOTAL RADIATION FOR ABOVE SHIPMENT=" NSUM "CURIES"
640 END

```

Table 4.3. Output from HFEDSHIP.BAS for typical shipment

HFEDSHIP.BAS, A BASIC PROGRAM TO CALCULATE HEAT LOAD AND CURIE
LEVEL OF IRRADIATED HFED MINIPLATES AS OF PRESENT DATE.
TO RUN, LIST 100-300 AND ENTER DATA AS INSTRUCTED.

R. L. SENN

MAY 5, 1986

HEAT LOAD + CURIE LEVEL FOR MOD. 27 AS OF 6/01/87

TIME IN REACTOR = 252.68 FULL POWER DAYS
COOLING TIME = 249 DAYS
TOTAL ORIGINAL 235-U= 15.163 GRAMS
ESTIMATED FRACTIONAL 235-U BURNUP = .88
REMAINING 235-U = 1.81956 GRAMS

POWER/GM 235-U = 1.893304

TOTAL HEAT LOAD = 3.444981 WATTS CURIE LEVEL = 826.7954

HEAT LOAD + CURIE LEVEL FOR MOD. 30 AS OF 6/01/87

TIME IN REACTOR = 272.3 FULL POWER DAYS
COOLING TIME = 194 DAYS
TOTAL ORIGINAL 235-U= 25.814 GRAMS
ESTIMATED FRACTIONAL 235-U BURNUP = .84
REMAINING 235-U = 4.130241 GRAMS

POWER/GM 235-U = 2.449113

TOTAL HEAT LOAD = 10.11543 WATTS CURIE LEVEL = 2427.702

HEAT LOAD + CURIE LEVEL FOR MOD. 31 AS OF 6/01/87

TIME IN REACTOR = 234.65 FULL POWER DAYS
COOLING TIME = 194 DAYS
TOTAL ORIGINAL 235-U= 20.497 GRAMS
ESTIMATED FRACTIONAL 235-U BURNUP = .7
REMAINING 235-U = 6.149101 GRAMS

POWER/GM 235-U = 2.232195

TOTAL HEAT LOAD = 13.72599 WATTS CURIE LEVEL = 3294.238

HEAT LOAD + CURIE LEVEL FOR MOD. 33 AS OF 6/01/87

TIME IN REACTOR = 146.89 FULL POWER DAYS
COOLING TIME = 123 DAYS
TOTAL ORIGINAL 235-U= 28.835 GRAMS
ESTIMATED FRACTIONAL 235-U BURNUP = .3
REMAINING 235-U = 20.1845 GRAMS

POWER/GM 235-U = 2.425384

TOTAL HEAT LOAD = 48.95515 WATTS CURIE LEVEL = 11749.24

Table 4.3 (continued)

HEAT LOAD + CURIE LEVEL FOR PLATES A-114,-115 AS OF 6/01/87

TIME IN REACTOR = 321.55 FULL POWER DAYS
 COOLING TIME = 123 DAYS
 TOTAL ORIGINAL 235-U= 7.66 GRAMS
 ESTIMATED FRACTIONAL 235-U BURNUP = .7
 REMAINING 235-U = 2.298 GRAMS

POWER/GM 235-U = 3.779093

TOTAL HEAT LOAD = 8.684356 WATTS CURIE LEVEL = 2084.245

HEAT LOAD + CURIE LEVEL FOR MOD. 34 AS OF 6/01/87

TIME IN REACTOR = 147 FULL POWER DAYS
 COOLING TIME = 123 DAYS
 TOTAL ORIGINAL 235-U= 21.108 GRAMS
 ESTIMATED FRACTIONAL 235-U BURNUP = .4
 REMAINING 235-U = 12.6648 GRAMS

POWER/GM 235-U = 2.426544

TOTAL HEAT LOAD = 30.7317 WATTS CURIE LEVEL = 7375.608

HEAT LOAD + CURIE LEVEL FOR PLATES A-87,-89,-90,-93 AS OF 6/01/87

TIME IN REACTOR = 401.62 FULL POWER DAYS
 COOLING TIME = 123 DAYS
 TOTAL ORIGINAL 235-U= 9.995 GRAMS
 ESTIMATED FRACTIONAL 235-U BURNUP = .92
 REMAINING 235-U = .7995998 GRAMS

POWER/GM 235-U = 4.199284

TOTAL HEAT LOAD = 3.357747 WATTS CURIE LEVEL = 805.8592

TOTAL HEAT LOAD FOR ABOVE SHIPMENT= 119.0154 WATTS
 TOTAL RADIATION FOR ABOVE SHIPMENT= 28563.68 CURIES

Appendix J-4.1.2

FULL-SIZED ELEMENT IRRADIATIONS IN THE OAK RIDGE RESEARCH REACTOR

OAK RIDGE NATIONAL LABORATORY
Oak Ridge, Tennessee

ARGONNE NATIONAL LABORATORY
Argonne, Illinois

United States of America

Abstract

Twenty-one full-size test elements were irradiated in the ORR between 1981 and 1985 as part of the RERTR Program. The purpose of these irradiations was to confirm that the data obtained from the miniplate irradiations was applicable to complete elements. Table 1 lists the key characteristics of these elements: element number, fuel type, enrichment, initial uranium density and fissile loading, percentage ^{235}U depletion, and the date at which each irradiation was completed. This appendix consists of three papers that provide the main results of the irradiations and post-irradiation examinations.

CONTENTS

Part I

G.L. Copeland, G.L. Hofman, and J.L. Snelgrove, "Irradiation Performance of Low-Enriched Uranium Fuel Elements", Proc. 1984 International Meeting on Reduced Enrichment for Research and Test Reactors, October 15-18, 1984, Argonne, Illinois, ANL/RERTR/TM-6, CONF-8410173 (July 1985), pp. 152-166.

Part II

G.L. Copeland and J.L. Snelgrove, "Performance of Low-Enriched Uranium Aluminide-Aluminum Thick-Plate Fuel Elements in the Oak Ridge Research Reactor," paper excerpted from a draft of ANL/RERTR/TM-16, "Performance of Reduced Enrichment $\text{UAl}_x\text{-Al}$ and $\text{U}_3\text{O}_8\text{-Al}$ Fuel Elements in the Oak Ridge Research Reactor," by G.L. Copeland and J.L. Snelgrove (to be published).

Part III

G.L. Copeland, G.L. Hofman, and J.L. Snelgrove, "Examination of $\text{U}_3\text{Si}_2\text{-Al}$ Fuel Elements from the Oak Ridge Research Reactor", Proc. 1986 International Meeting on Reduced Enrichment for Research and Test Reactors, November 3-6, 1986, Gatlinburg, Tennessee, ANL/RERTR/TM-9, CONF-861185 (May 1988), pp. 211-221.

Following successful irradiation testing of the six U_3Si_2 fuel elements described in Part III, a whole-core demonstration of the U_3Si_2 fuel was conducted in the ORR between 1985 and 1987 to provide both reactor physics data and proof that commercially fabricated elements would perform well.

The fuel elements for the demonstration were fabricated by CERCA, NUKEM, and Babcock & Wilcox and were essentially identical with the test elements. The HEU-LEU transition phase of ORR demonstration is described in Volume 5, Appendix M-4.

Table 1. Full-Sized Fuel Elements Irradiated in the ORR.

Element No. ^a	Fuel Type	No. of Plates	Enrichment %	Initial U density Mg/m ³	Initial ²³⁵ U g	²³⁵ U Depletion %	Date Irrad. Complete
T291X	U ₃ O ₈	19	45.0	1.7	280	56 ^b	10/31/81
T292X	U ₃ O ₈	19	45.0	1.7	280	70 ^c	4/16/82
T293X	U ₃ O ₈	19	45.0	1.7	280	55 ^b	10/11/82
T294X	U ₃ O ₈	19	45.0	1.7	280	58 ^b	6/22/82
NLE451	UAl _x	19	44.9	1.7	284	75 ^c	10/11/82
NLE452	UAl _x	19	44.9	1.7	284	59 ^b	6/11/82
CLE451	UAl _x	19	44.9	1.7	282	71 ^c	11/18/82
CLE452	UAl _x	19	44.9	1.7	282	56 ^b	4/16/82
CLE453	UAl _x	19	44.9	1.7	284	75 ^b	9/15/83
NLE201	U ₃ O ₈	13	19.6	2.3	340	77 ^b	1/20/85
NLE202	U ₃ O ₈	13	19.6	2.3	340	58 ^b	5/30/85
CLE201	UAl _x	13	19.8	2.1	312	51	5/30/85
CLE202	UAl _x	13	19.8	2.3	336	71	1/20/85
CLE203	U ₃ O ₈	18	19.7	3.2	326	74 ^b	4/22/84
CLE204	U ₃ O ₈	18	19.7	3.2	326	54 ^c	9/29/83
NSI201	U ₃ Si ₂	19	19.7	4.8	340	35	1/14/83
NSI202	U ₃ Si ₂	19	19.7	4.8	340	82	8/14/84
CSI201	U ₃ Si ₂	19	19.8	4.8	339	52	10/13/83
CSI202	U ₃ Si ₂	19	19.8	4.8	339	82	8/14/84
BSI201	U ₃ Si ₂	19	19.8	4.8	339	54	4/22/84
BSI202	U ₃ Si ₂	19	19.8	4.8	339	77	12/19/84

^aFirst letter in element no. designates fabricator: Babcock & Wilcox (B), CERCA (C), NUKEM (N), or Texas Instruments (T).

^bEstimated burnup.

^cBased on preliminary evaluations of measurements.

Appendix J-4.1.2

Part I

IRRADIATION PERFORMANCE OF LOW-ENRICHED URANIUM FUEL ELEMENTS*

G.L. COPELAND

Oak Ridge National Laboratory,
Oak Ridge, Tennessee

G.L. HOFMAN, J.L. SNELGROVE

Argonne National Laboratory,
Argonne, Illinois

United States of America

Abstract

The status of the testing and evaluation of full-sized experimental low- and medium-enriched uranium fuel elements in the Oak Ridge Research Reactor is presented. Medium-enriched elements containing oxide and aluminide have been completely evaluated at burnups up to 75%. A low-enriched U_3Si_2 element has been evaluated at 41% burnup. Other silicide and oxide elements have completed irradiation satisfactorily to burnups of 75% and are now being evaluated. All results to date confirm the expected good performance of these elements in the medium power research reactor environment.

INTRODUCTION

This paper presents the results of irradiation of experimental medium- and low-enriched uranium fuel elements in the Oak Ridge Research Reactor (ORR). The purpose of the test irradiations is to confirm the expected good performance of these elements in a medium power research reactor to burnups in excess of that normally achieved in routine operation. This expectation of good performance is based on miniplate irradiations at even higher fuel concentrations and burnups.¹⁻⁵ Nine medium-enriched and 12 low-enriched elements have been produced by commercial fuel fabricators and irradiated in the ORR. Five elements remain in the reactor while the others have satisfactorily completed irradiation and have been evaluated or are now awaiting postirradiation examination (PIE).

ELEMENT DESCRIPTION

The experimental elements were designed to replace a standard ORR element. The standard element is a box type containing 19 curved plates and a total of 285 g of ^{235}U (highly enriched). The nominal plate thickness is

*Research sponsored by the Reduced Enrichment for Research and Test Reactors Program, U.S. Department of Energy, under contract DE-AC05-85OR21400 with Martin Marietta Energy Systems, Inc., and Argonne National Laboratory, operated by The University of Chicago, under contract W-31-109-Eng-38.

Table 1. Status of full-sized fuel elements irradiated in the ORR
(October 1984)

Element No. ^a	Fuel type	No. of plates	Enrichment %	Initial U density Mg/m ³	Initial ²³⁵ U g	²³⁵ U Depletion %	Remarks
T291X	U ₃ O ₈	19	45.0	1.7	280	56	PIE completed
T292X	U ₃ O ₈	19	45.0	1.7	280	72(70) ^b	PIE completed
T293X	U ₃ O ₈	19	45.0	1.7	280	55	Irrad. completed, no PIE
T294X	U ₃ O ₈	19	45.0	1.7	280	58	Irrad. completed, no PIE
NLE451	UAl _x	19	44.9	1.7	284	73(75) ^b	PIE completed
NLE452	UAl _x	19	44.9	1.7	284	59	PIE completed
CLE451	UAl _x	19	44.9	1.7	282	76(71) ^b	PIE completed
CLE452	UAl _x	19	44.9	1.7	282	56	PIE completed
CLE453	UAl _x	19	44.9	1.7	284	75	PIE in progress
NLE201	U ₃ O ₈	13	19.6	2.3	340	64	In ORR
NLE202	U ₃ O ₈	13	19.6	2.3	340	9	In ORR
CLE201	UAl _x	13	19.8	2.1	312	7	In ORR
CLE202	UAl _x	13	19.8	2.3	336	65	In ORR
CLE203	U ₃ O ₈	18	19.7	3.2	326	74	Irrad. completed 4/22/84
CLE204	U ₃ O ₈	18	19.7	3.2	326	57	PIE in progress
NSI201	U ₃ Si ₂	19	19.7	4.8	340	49(41) ^b	PIE completed
NSI202	U ₃ Si ₂	19	19.7	4.8	340	82	Irrad. completed 8/14/84
CSI201	U ₃ Si ₂	19	19.8	4.8	339	56	PIE in progress
CSI202	U ₃ Si ₂	19	19.8	4.8	339	82	Irrad. completed 8/14/84
BSI201	U ₃ Si ₂	19	19.8	4.8	339	55	Irrad. completed 4/22/84
BSI202	U ₃ Si ₂	19	19.8	4.8	339	76	In ORR

^aFirst letter in element no. designates fabricator: Babcock & Wilcox (B), CERCA (C), NUKEM (N), or Texas Instruments (T).

^bDepletion in parentheses based upon preliminary evaluations of measurements.

1.27-mm (0.050-in.) with a 0.51-mm (0.020-in.) fuel meat. The experimental elements are similar except for the 18 plate and 13 (flat) plate elements which have thicker meats and plates. The elements have been treated routinely for fuel shuffling except for the 13 plate elements which were restricted to low-flux positions early in life to meet heat-flux restrictions of the reactor. The water channels of the elements were periodically measured during reactor shutdowns. No abnormal changes were found on any of the elements.

A description of the elements and their current status is in Table 1. The elements contain U_3O_8 , U_3Al_x ($x \approx 3$), or U_3Si_2 dispersed in aluminum. The fuel fabricators were Texas Instruments (TI) and Babcock and Wilcox (B&W) in the United States, Compagnie pour l'Etude et la Realisation de Combustible Atomiques (CERCA) in France, and NUKEM in the Federal Republic of Germany. At least two elements of each type were irradiated, one of which was intended for normal burnup of about 50% depletion of ^{235}U and one of which was intended to achieve a burnup of 75% (substantially higher than would be achieved in normal reactor operation).

POSTIRRADIATION EXAMINATION PROCEDURES

Postirradiation examinations of the plate-type fuel elements irradiated in the ORR are conducted in the High-Radiation Level Examination Laboratory (HIREL) at ORNL, with the exception of metallography of uranium-silicide specimens, which is performed at the Argonne National Laboratory (ANL). Since the full-sized element irradiations are meant to be confirmatory in nature and not to provide basic irradiation-behavior data for the fuel, the emphasis of the PIEs is on checking the dimensional stability of the element and plates, on measuring blister-threshold temperatures and burnup levels, and on performing limited metallography. A summary of the PIE steps for a typical element is included in the Appendix. In some cases, such as for a first-of-a-kind element, more samples might be taken for certain steps, as for example plate thickness measurements. If any unusual or unexpected features are noted, more extensive examinations are performed as needed. In general, a nondestructive PIE is performed on the normal burnup element of a pair and a destructive (full) PIE is performed on the high burnup element. In some cases, a full PIE is performed on the normal burnup element.

As shown in Table 1, PIEs of six MEU elements and one LEU U_3Si_2 element have been completed. Nine other elements have completed irradiation with no apparent problems. Postirradiation examination is in progress on three of these, four are cooling prior to PIE, and no PIE is planned for the two additional TI elements.

RESULTS

Postirradiation examination results to date show completely satisfactory performance for all the elements.

Element Visual and Dimensional Inspection

A careful visual examination of each element has revealed no abnormal features. The elements appear to be essentially as-fabricated with the exception of the normal corrosion film and scuff marks from handling.

Measurements for length, width, thickness, twist, and bow reveal no significant changes. The elements are within the original fabrication specification envelope.

Channel Spacing Measurements

Each water channel was measured in two locations for the full length of the element. These measurements showed the channels to meet the minimum fabrication specification in each case. The channel spacings were very uniform with the exception of one channel in NLE-451 which opened up near one end. This apparently did not occur during irradiation since the adjacent channels were uniform.

Plate Visual Inspection

After removing the plates from the full-PIE elements, they were visually examined for defects. The plates were bowed and warped to some extent after removing from the element. The plates appeared to be in excellent condition with a uniform corrosion film over the meat and no apparent blisters, unusual swelling, or other defects.

Plate Thickness Measurements

Selected plates from each element were measured in 24 locations for thickness change. The accuracy of measurement for these plates is not sufficient for swelling data due to the curvature, warping, bowing, and lack of accurate preirradiation measurements. The thickness measurements showed uniformly varying swelling up to about 50 μm as a maximum with one exception. One area of one plate showed thickness changes up to 150 μm over a small area, which later proved to be erroneous measurements. This was a central plate from element CLE-451. Metallography of this area showed the plate to be of normal thickness with no unusual features in the microstructure which could have resulted in abnormal swelling.

Blister Annealing

Blister annealing of selected plates from each full-PIE element was accomplished by heating the plates singly in a tube furnace. The furnace was able to maintain a uniform maximum-temperature zone about 7-in. long in the maximum-burnup region of the plate. Temperatures decreased toward the ends of the plate by up to 10°C. The plates were sequentially heated for 30 min at 400, 450, 475, 500, 525, and 550°C or until blisters were observed. The plates, their maximum heating temperature, and the type blisters observed are listed in Table 2.

These data show that the blister threshold temperature of these high-loaded, low-enriched fuels is not significantly different from the low-loaded, highly-enriched fuels currently in use.

Metallography

The highest burnup plate (other than a side plate) based on gamma scanning was selected from each full-PIE element for metallographic examination. Metallographic sections were taken from the peak-burnup and low-burnup areas

Table 2. Results of blister anneals of full-sized plates from various fuel elements

Element no.	Plate position	Plate no.	Maximum temperature, °C	Description of blisters ^a
T292X	2	12-2-4	500	Many blisters over 15 in. of plate, both sides, typical PI
T292X	8	12-2-8	483	Small, typical PI, over ~10 in. of plate, both sides
NLE451	2	ORR-044	550	Small, typical PI, over about 7 in. of plate, both sides
NLE451	8	ORR-050	550	None
CLE451	2	OMIU-34	550	Very small blisters over non-fuel zone, both ends of plate, no blisters over fuel
CLE451	8	OMIU-40	550	Very small blisters similar to above over nonfuel zone but less noticeable, no blisters over fuel
NSI201	2	ORR-092	550	None
NSI201	8	ORR-100	550	None
NSI201	19	ORR-144	550	None

^aTypical PI — typical of postirradiation blisters observed previously in low-volume fraction fuels (i.e., appear to be discrete blisters between meat and cladding with no "pillowing").

of these plates (adjacent to the burnup analysis sample). Representative microstructures from the peak burnup areas of each fuel are shown in Figs. 1 through 6. In general, the microstructures are as expected from previous miniplate irradiations and reveal no abnormal conditions. The plates appear to be in excellent condition.

CONCLUSION

Postirradiation evaluation to date of medium- and low-enriched uranium elements from the ORR confirm their expected satisfactory performance in this medium powered research reactor. Medium-enriched elements containing oxide and aluminide fuel have been completely evaluated at up to 75% burnup. A low-enriched element containing U_3Si_2 has been completely evaluated at about 41% burnup. Low-enriched elements of U_3Si_2 and oxide have satisfactorily completed irradiation up to 75% burnup and are now awaiting complete evaluation.

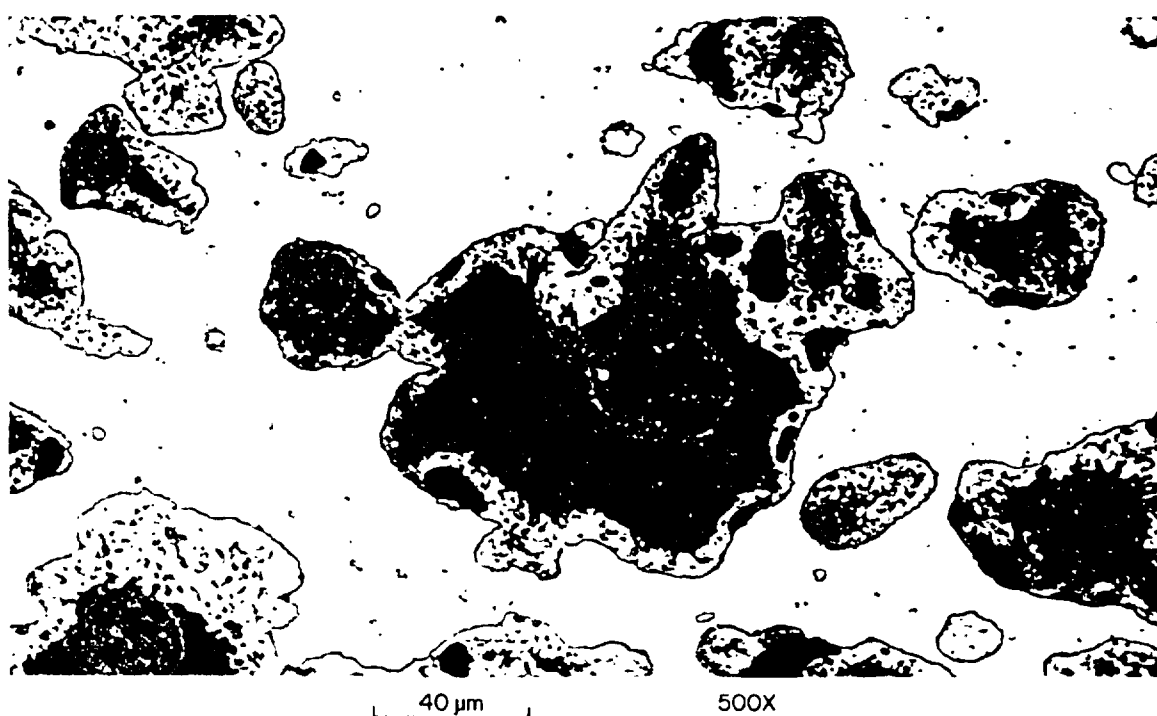
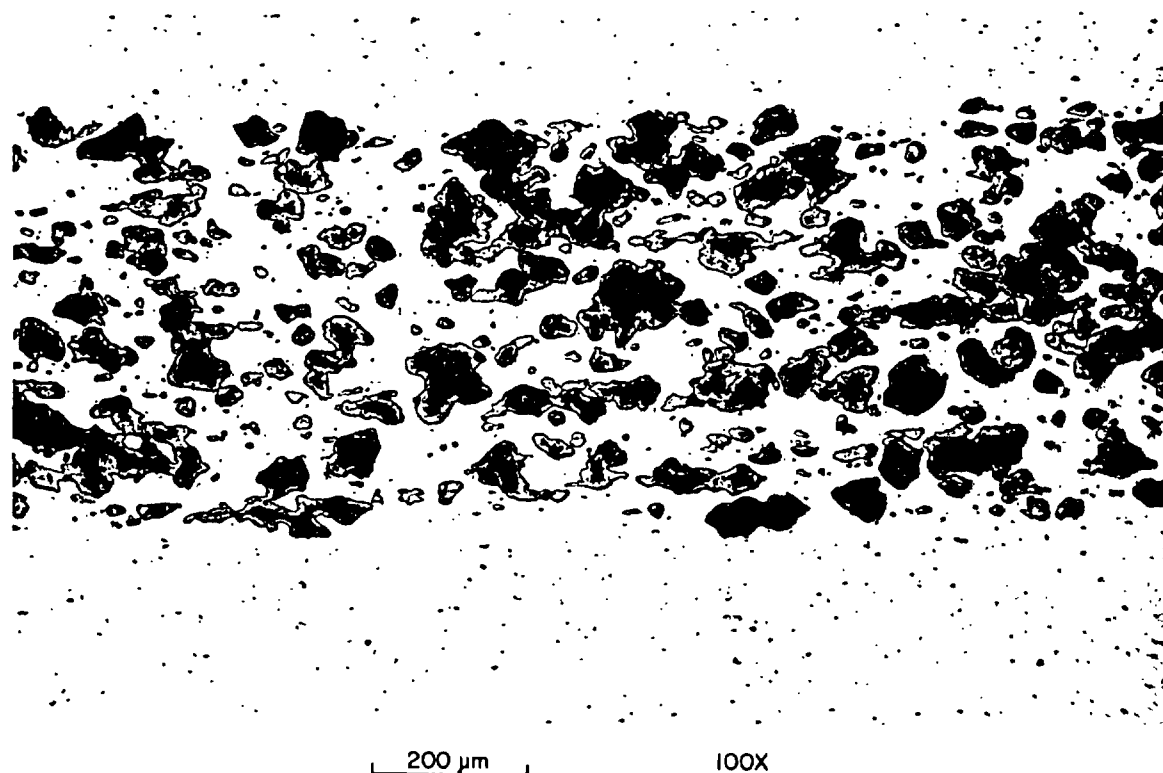
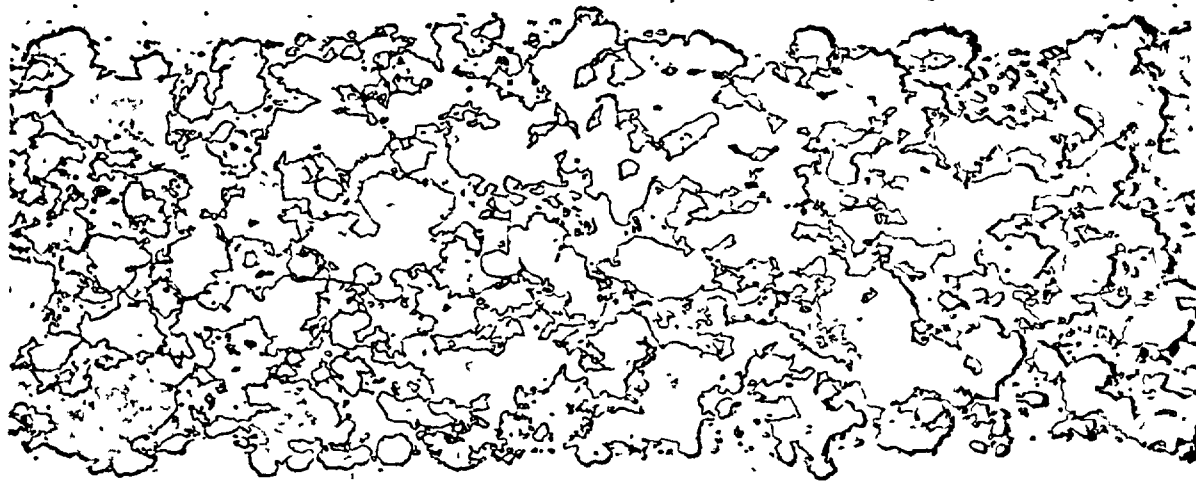


Fig. 1. Microstructure of MEU oxide plate from element T292X, plate 7, peak-burnup region, 86%. (R78807 top, R78808 bottom).



200 μ m

100X



40 μ m

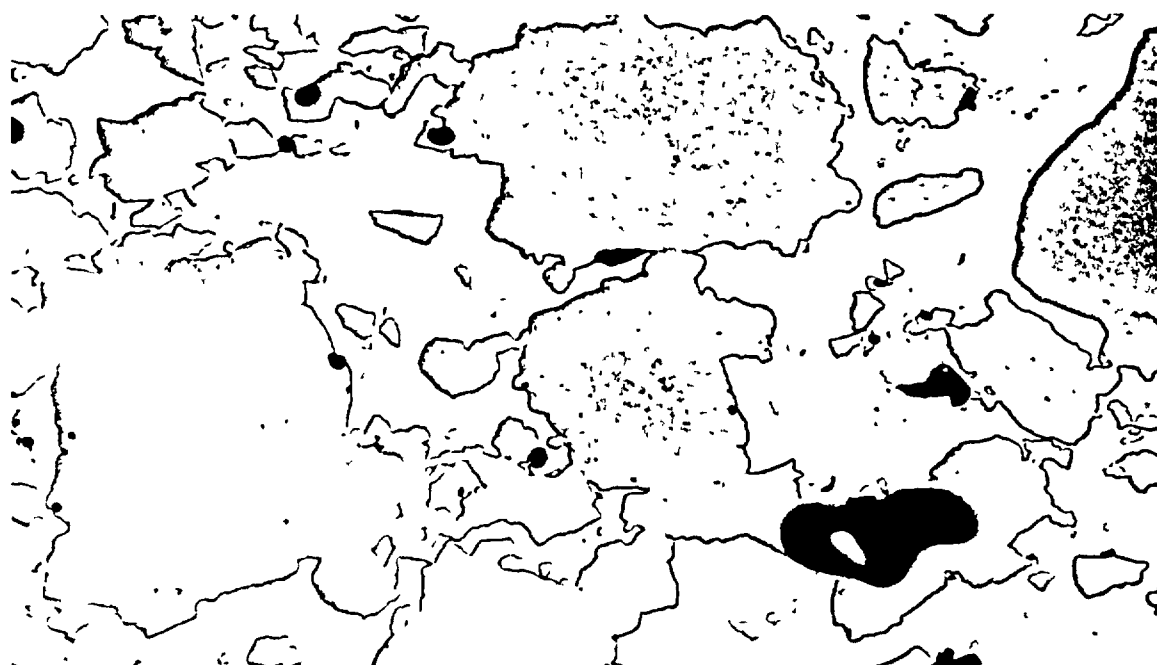
500X

Fig. 2. Microstructure of MEU aluminide plate from element CLE-451, plate 17, peak-burnup region, 87%. (R78795 top, R78795 bottom).



200 μ m

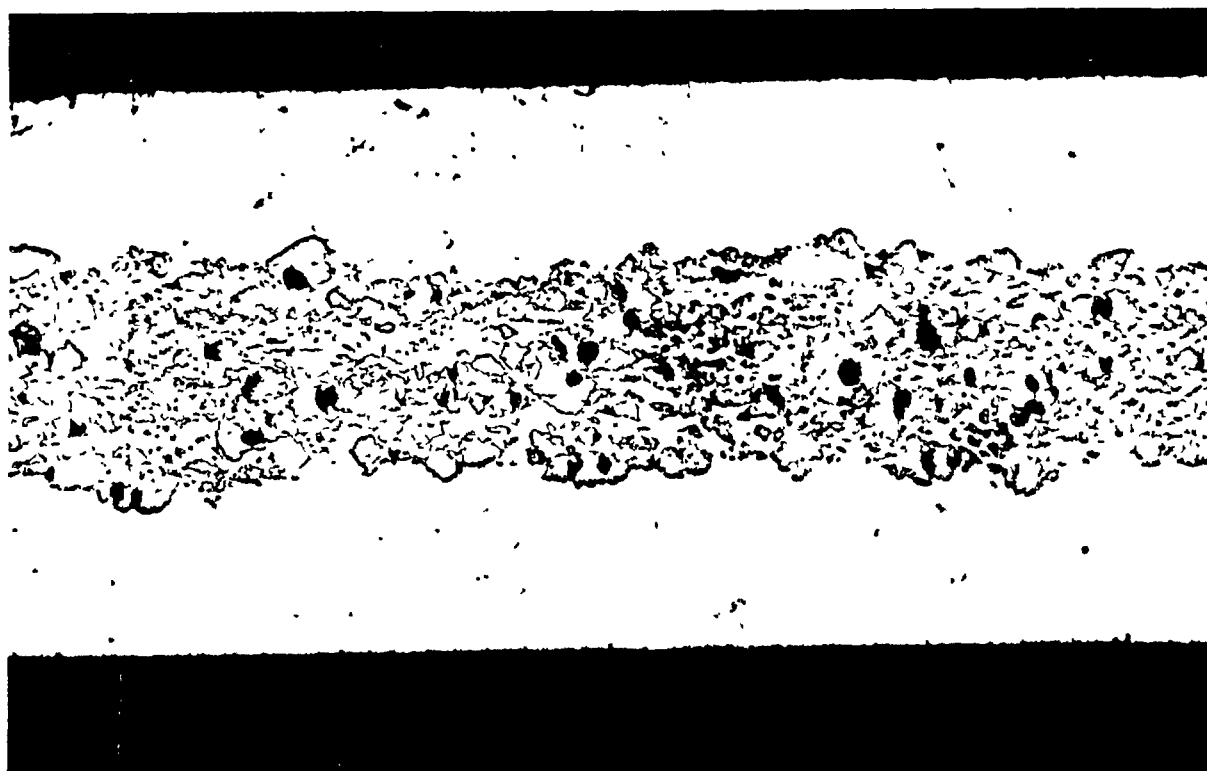
100X



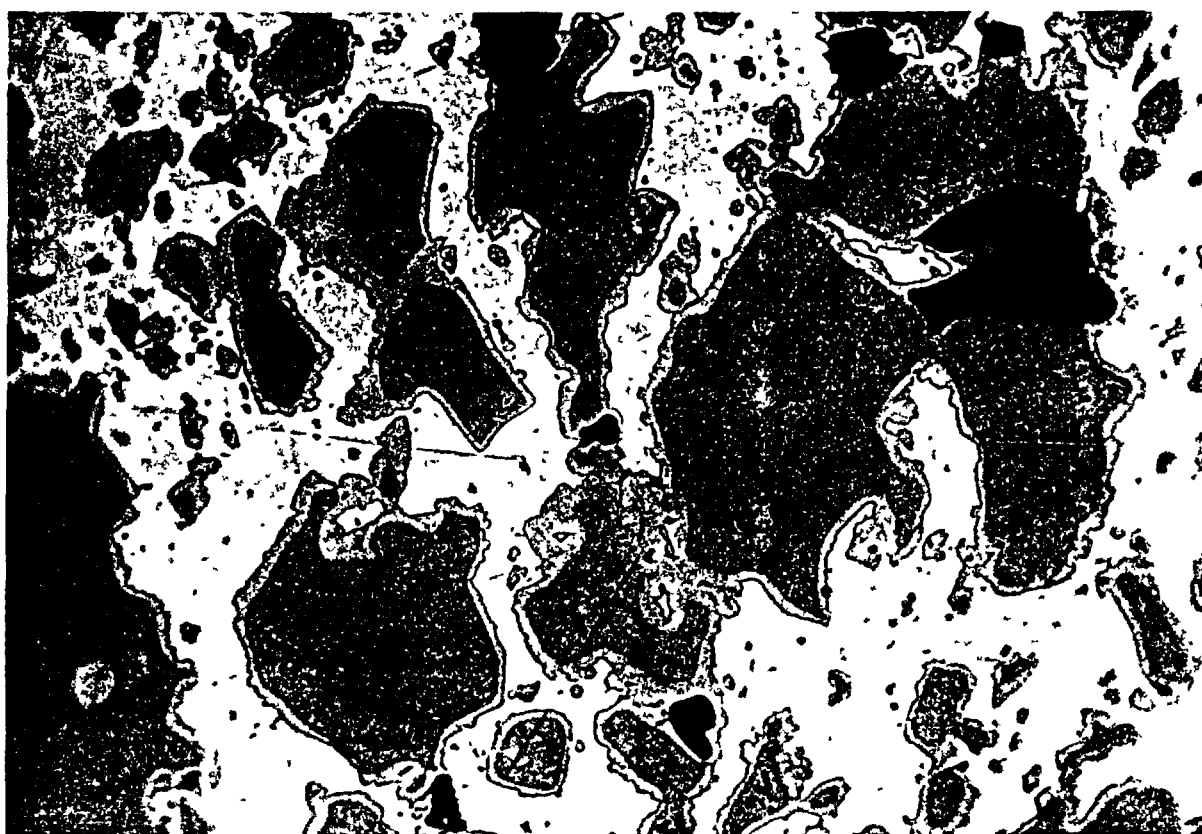
40 μ m

500X

Fig. 3. Microstructure of MEU aluminide plate from element NLE-451, plate 9, peak-burnup region, 91%. (R78801 top, R78802 bottom).



50X



500X

Fig. 4. Microstructure of LEU U₃Si₂ plate from element NSI-201, peak-burning region, 50%. The large voids are remnants of as-fabricated porosity. Reaction zones and absence of gas bubbles are similar to mini-plates.

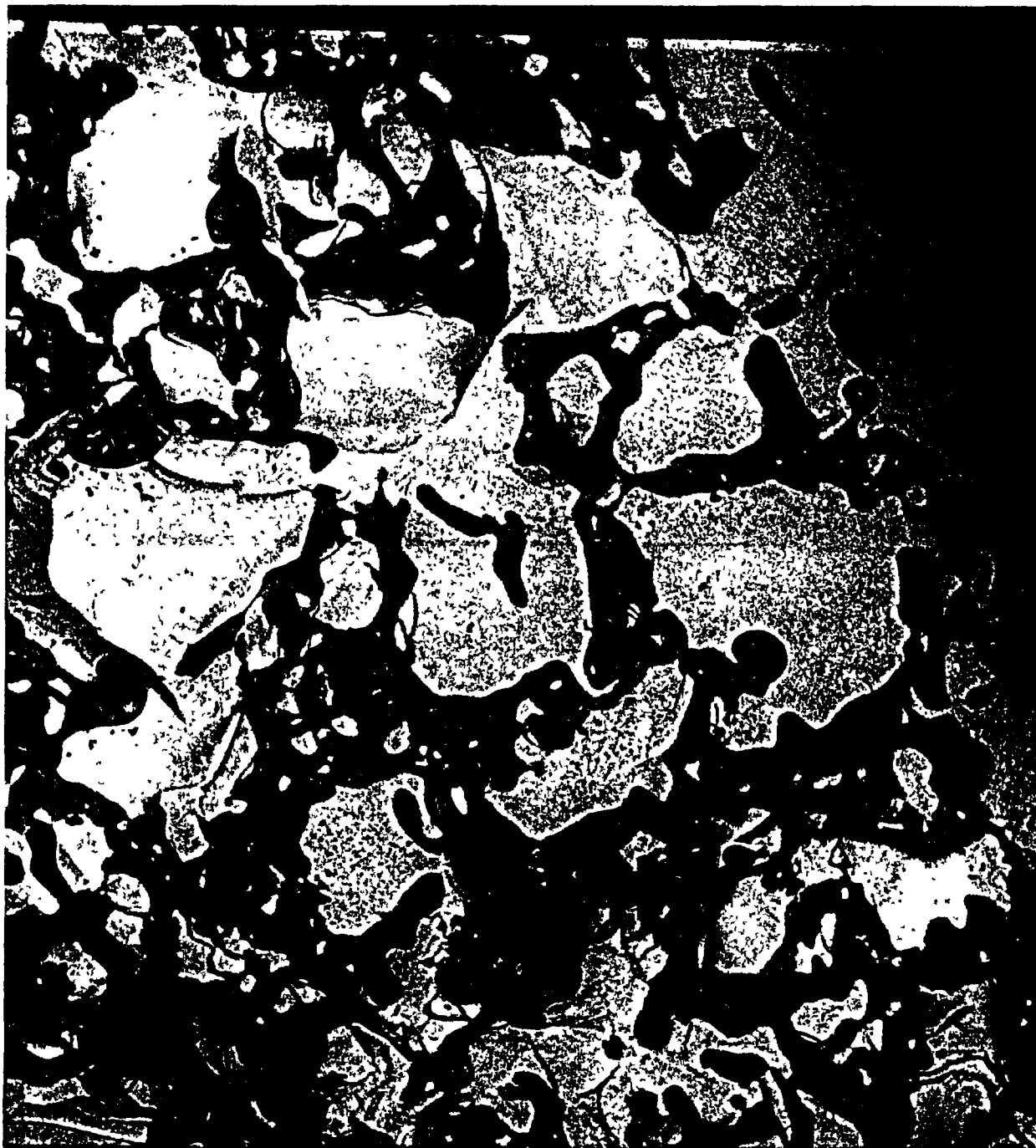


Fig. 5. Scanning Electron Micrograph of U_3Si_2 from element NSI-201 at $\sim 50\%$ ^{235}U depletion (using backscattered electrons). The dark area is aluminum, grey area is reaction zone, and the lighter area is the fuel particle. Note the presence of small stable gas bubbles in some grains and the lack of bubbles in other grains.



Fig. 6. Scanning Electron Micrograph of U_3Si_2 from element NSI-201 at $\sim 50\%$ burnup showing a grain with a distribution small uniform and stable gas bubbles. These observations are consistent with those from miniplate evaluations.

REFERENCES

1. G. L. Copeland and J. L. Snelgrove, "Examination of Irradiated High-U-Loaded U_3O_8 -Al Fuel Plates," in Proceedings of the International Meeting on Research and Test Reactor Core Conversions from HEU to LEU Fuels, Argonne, Illinois, November 8-10, 1982, ANL/RERTR/TM-4, CONF-821155 (September 1983), pp. 79-87.
2. G. L. Hofman and L. A. Neimark, "Irradiation Behavior of Uranium-Silicide Dispersion Fuels," in Proceedings of the International Meeting on Reduced Enrichment for Research and Test Reactors, 24-27 October 1983, Tokai, Japan, JAERI-M 84-073 (May 1984), pp. 43-53.
3. E. E. Perez, C. A. Kohut, D. R. Giorsetti, G. L. Copeland, and J. L. Snelgrove, "Irradiation Performance of CNEA UAl_x and U_3O_8 Miniplates," in Proceedings of the International Meeting on Reduced Enrichment for Research and Test Reactors, 24-27 October 1983, Tokai, Japan, JAERI-M 84-073 (May 1984), pp. 67-76.
4. M. F. Hrovat and H. W. Hassel, "Recent Status of Development and Irradiation Performance for Plate Type Fuel Elements with Reduced ^{235}U Enrichment at NUKEM," in Proceedings of the International Meeting on Reduced Enrichment for Research and Test Reactors, 24-27 October 1983, Tokai, Japan, JAERI-M 84-073 (May 1984), pp. 95-99.
5. J. L. Snelgrove, R. F. Domagala, T. C. Wiencek, and G. L. Copeland, "Fuel Development Activities of the U.S. RERTR Program," in Proceedings of the International Meeting on Reduced Enrichment for Research and Test Reactors, 24-27 October 1983, Tokai, Japan, JAERI-M 84-073 (May 1984), pp. 34-42.

Appendix J-4.1.2

Part II

PERFORMANCE OF LOW-ENRICHED URANIUM ALUMINIDE-ALUMINUM THICK-PLATE FUEL ELEMENTS IN THE OAK RIDGE RESEARCH REACTOR

G.L. COPELAND

Oak Ridge National Laboratory,
Oak Ridge, Tennessee

J.L. SNELGROVE

Argonne National Laboratory,
Argonne, Illinois

United States of America

Abstract

Two high-density, low-enriched, thick-plate UAl_x -Al dispersion fuel elements, fabricated by CERCA, have been tested in the Oak Ridge Research Reactor (ORR). The fuel meat was nominally 1.5 mm thick, and the uranium density in the fuel meat was 2.1 Mg/m^3 in one element and 2.3 Mg/m^3 in the other. The elements were irradiated in several core positions. The lower-density element was irradiated to approximately normal ORR burnup (50 to 56% ^{235}U depletion), and the higher-density element was irradiated to an average burnup of 72%, well above the burnups normally achieved in research and test reactors. Peak burnups over 97% were achieved.

Following suitable cooling periods, the elements were subjected to a series of nondestructive and destructive (higher-density element only) examinations, including visual inspection and dimensional measurements, channel gap thickness measurements, gamma scans, plate thickness measurements, blister threshold temperature tests, metallography, and isotopic burnup analyses. Externally, the elements were essentially unchanged from their as-fabricated condition. The behavior of the fuel was found to be entirely consistent with that expected on the basis of results of previous tests using miniature fuel plates. The plates showed small, uniform thickness changes, ranging up to $100 \mu\text{m}$ in regions of ~97% burnup. No blisters formed over the fuel meat during postirradiation anneals, even at 575°C .

It is concluded that high-density low-enriched UAl_x -Al dispersion fuel elements with fuel meat thicknesses up to 1.5 mm will perform at least as well in research and test reactors with up to medium power density as the high-enriched UAl_x -Al dispersion fuel elements currently being used in many reactors.

1. INTRODUCTION

Since its inception in 1978, the U. S. Reduced Enrichment Research and Test Reactor (RERTR) Program¹ has pursued the development of high-density dispersion fuels as one means of making feasible the conversion of research and test reactors from the use of highly enriched uranium (HEU) fuel to the use of low-enriched uranium (LEU) fuel. At that time the highest density fuels in common use in plate-type research reactor fuel elements were dispersions of uranium aluminide (UAl_x) and uranium oxide (U_3O_8) in aluminum

with uranium densities in the fuel meat of 1.7 and 1.3 Mg/m³, respectively. These two types of dispersion fuels have now been developed and tested for LEU applications up to their practical fabrication limits--2.4 Mg U/m³ for UAl_x and 3.2 Mg U/m³ for U₃O₈.² In addition, dispersions of uranium silicide (U₃Si₂) in aluminum has been developed and tested up to about 5.2 Mg U/m³.^{3,4}

Before the success of the high-density fuels was assured, a parallel concept for increasing the uranium content of fuel elements was pursued--increasing the volume fraction of fuel in the element by using fuel plates with much thicker fuel meat (~1.5 mm instead of ~0.5 mm) while decreasing the number of plates to maintain an adequate coolant channel thickness. In this way conversion of reactors with low to moderate power densities would have been possible with UAl_x or U₃O₈. Irradiation testing of elements of this type containing UAl_x and U₃O₈ was conducted in the Oak Ridge Research Reactor (ORR) and in the High Flux Reactor (HFR) at Petten, The Netherlands.⁵ However, the unqualified success of the U₃Si₂ dispersion fuel has eliminated the need for such large increases in fuel meat thickness. Nevertheless, irradiation of the four thick-plate UAl_x elements provided a demonstration of the good performance of highly loaded, low-enriched, aluminide dispersion fuel.

The two UAl_x elements irradiated in the ORR, their irradiation histories, and the results of their detailed postirradiation examination are described and discussed in this report.

2. DESCRIPTION OF FUEL ELEMENTS

2.1 General Description

The standard box-type ORR element contains 19 curved plates, each nominally 1.27 mm thick with 0.51-mm-thick meat and 0.38-mm-thick cladding. The standard ORR high-enriched U₃O₈ element contained 285 g of ²³⁵U (0.85 Mg U/m³, 12 vol% U₃O₈) while the low-enriched U₃Si₂ element with the same geometry contained 340 g of ²³⁵U (4.75 Mg U/m³, 42.1 vol% U₃Si₂). The low-enriched UAl_x elements discussed in this report contained 312 and 336 g of ²³⁵U. The additional uranium loading was achieved by increasing the volume loading of fuel in the meat and by increasing the meat thickness and decreasing the number of plates (giving a coolant channel thickness only slightly less than the 2.95-mm nominal of the standard element). The nominal meat thickness was 1.50 mm with 0.43-mm-thick cladding, giving a total plate thickness of 2.36 mm. The rigidity of these thick plates was great enough to provide stability without curving so they were left flat. Outer plates of unfueled aluminum were used to adapt the flat-plate element to the curved-plate ORR geometry. A cross-section of the element is shown in Fig. 1.

The uranium densities of the meat in these elements were 2.1 and 2.3 Mg U/m³ (~45 and 50 vol% UAl_x), which are near the upper limit of fabricability for UAl_x fuels (~2.4 Mg U/m³ for x=3). The lower- and higher-density elements were identified as CLE-201 and CLE-202, respectively.

2.2 Specifications

The elements were fabricated by CERCA (Compagnie pour l'Étude et la Réalisation de Combustibles Atomiques, Romans-sur-Isère, France) using specifications developed by them and approved by ANL/ORNL. The materials

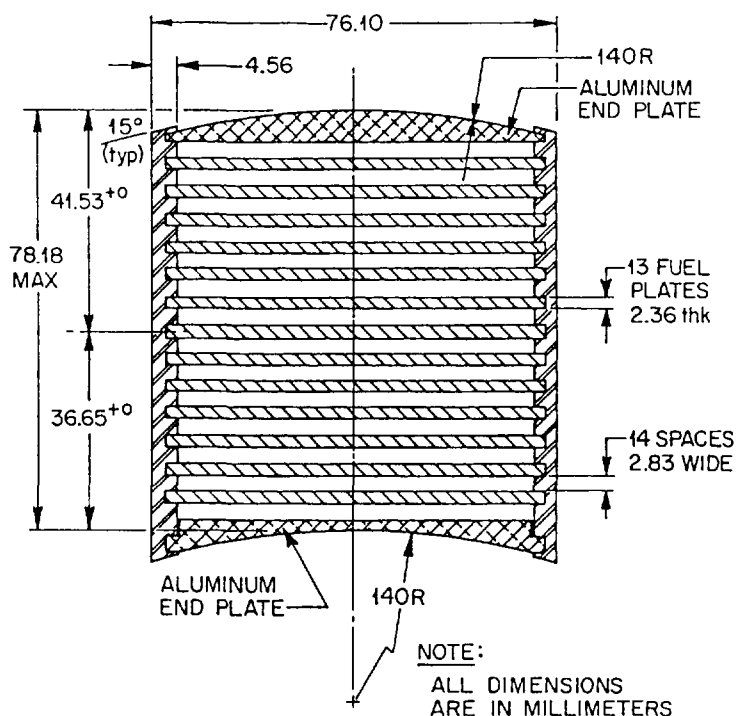


Fig. 1. Cross Section of 13-Flat-Thick-Plate ORR Test Element.

and fabrication and inspection procedures were essentially those used by CERCA in their standard production. The materials used in the test elements are listed in Table I. The composition and properties of the aluminum alloys used in the elements are listed in Table II.

The fuel plate specifications for the ORR HEU elements required a minimum cladding thickness of 0.33 mm. Surface defects with depths up to 0.13 mm were allowed, leaving a minimum of 0.20 mm of cladding over the fuel meat at any point. These specifications were retained for the UAl_x elements and were met with no apparent difficulty, probably because of the extra 0.05 mm of cladding.

Related to the high volume loading of fuel in the meat is an increased number of fuel particles at the surface of the fuel compact and, consequently, an increased probability for fuel particles to become dislodged and spread into nominally fuel-free zones during the rolling process. This phenomenon, referred to as fuel flaking or fuel out of zone, is identified by the occurrence of white spots on an X radiograph of the fuel plate. Although the specifications did not specifically address this problem, it was known to exist from previous development work, and ORNL used realistic criteria in judging the acceptability of plates with fuel out of zone. Since the amount of fission energy liberated in these relatively isolated particles is so small as to preclude any cooling problems, the only concern is the isolation of the fission products. In general, it was required that no particle be within 0.5 mm of the edges or ends of the plates. As discussed in Section 5.4, small blisters which formed during postirradiation annealing tests are believed to be associated with some of these out-of-zone particles. The formation of such blisters after out-of-pile annealing verifies that the fission products were retained within or near these particles during irradiation.

Table I. Materials Used in UAl_x Test Elements.

Part Name	Material
Fuel Plate	
Frame	AG 3 NE ^a /AG 5 NE ^b
Cover	AG 3 NE
Fuel Core	
Fuel	UAl_x
Matrix	A5 NE
Adapter Plate	AG 3 NE
Side Plate	AG 3 NE
End Adapter	356 Al ^c
Welding Wire	AG 3 NE

^aCLE-201^bCLE-202^cSupplied by ORNL/ANL

2.3 As-Fabricated Attributes

Three lots of UAl_x powder were used in the fabrication of plates for these elements. The compositions of these powders are listed in Table III. All of the powder was required to pass through a 150- μ m-mesh sieve, and up to 25 wt% was allowed to pass through a 44- μ m-mesh sieve.

A variable which influences the plate thickness change, or swelling, during irradiation is the void content of the as-fabricated plates. The void content depends on the fuel particle size, fuel volume fraction, and meat thickness (and probably on other properties as well). The void content was not determined for these plates. However, based on the amount residual porosity in the irradiated fuel and on our knowledge of porosities in other UAl_x and U_3Si_2 plates, we estimate that the as-fabricated porosity was of the order of 8 to 10%.

3. IRRADIATION HISTORY

Because the ^{235}U was contained in considerably fewer fuel plates than in a standard element, it was necessary to begin their irradiations in low-flux positions in order to remain within heat flux limits. Consequently,

Table II. Properties of Aluminum Alloys Specified for ORR LEU
 UAl_x Fuel Elements and of Similar U.S. Alloys.

Alloy ^a	AG 3 NE	AG 5 NE	5056 ^d	6061	6061-T6
Composition, wt% ^b					
Al ^c	96.8	94.2	94.8	97.6	97.6
Mg	2.75	5.15	5.0	1.0	1.0
Si	0.13	0.13	<0.3	0.6	0.6
Cu	0.004	<0.005	<0.1	0.28	0.28
Cr	0.01	0.11	0.12	0.2	0.2
Mn	0.06	0.10	0.12	<0.15	<0.15
Fe	0.26	0.28	---	---	---
Tensile Strength, MPa	235	~290 ^e	290	124	310
Yield Strength, MPa	127	~150 ^e	152	55	276
Hardness (HB)	42	~65 ^e	65	30	95
Thermal Conductivity, W/m·K	130	~120 ^e	120	180	167
Heat Capacity, J/kg·K	~900 ^e	~900 ^e	904	896	896
Solidus Temperature, °C	~605 ^e	~570 ^e	568	582	582
Liquidus Temperature, °C	650	~640 ^e	638	652	652

^aAll properties are for O-temper anneal unless listed otherwise.

^bActual value for AG 3 NE and AG 5 NE; average value of composition limit range for other alloys.

^cTypical Al contents are provided for comparison purposes only. The specification is for Al to constitute the remainder after accounting for additions and impurities.

^dFor reference; 6061 used in standard ORR HEU elements.

^eEstimate based on properties of similar U.S. alloys.

element powers and fuel meat power densities were lower than for other LEU elements irradiated in the ORR. The irradiation histories of the two elements are summarized in Table IV. The higher density element (CLE-202) was actually irradiated first; its good behavior allowed the irradiation of CLE-201 to begin in a higher-flux position. Element CLE-201 was irradiated to approximately the normal burnup for ORR elements, while CLE-202 was irradiated to a burnup higher than would likely be achieved in any application. The burnup of element CLE-201 was not measured, and its burnup was estimated from results of ORR fuel management calculations by multiplying the ORR-estimated burnup (175 g ²³⁵U, or 56%) by the ratio of the measured value to the ORR-estimated value of burnup for element CLE-202 (0.908).

The two basic core configurations employed during the irradiations are shown in Fig. 2. At various times experiments were replaced with Al filler pieces or with fuel elements. Although these UAl_x elements were not cycled through the core in a normal pattern, they did experience irradiation in a variety of core positions.

Table III. UAl_x Powder Compositions and Impurities.

Major Constituent, wt%	UAl_x Powder Lot No.			Specified Value
	24	30 ^a	32	
U	71.55	70.20	71.05	69.0 ± 3.0
Al	NA ^b	NA ^b	NA ^b	Remainder
Impurity, µg/g				
B	<5	<5	<5	5 max
C	165	136	174	3000 max
Cd	<2.5	<2.5	<2.5	10 max
H	45	65	55	200 max
N	<50	135	210	500 max
O	1560	2610	2310	7500 max
U Isotopic Content, % of Total U				
²³⁴ U	0.151	0.153	0.153	0.50 max
²³⁵ U	19.840	19.809	19.789	19.75 ± 0.2
²³⁶ U	0.219	0.216	0.213	1.00 max
²³⁸ U	79.970	79.822	79.845	Remainder

^aThe destructively analyzed plate 020V2034 contained UAl_x from Lot No. 30.

^bNot analyzed.

The detailed irradiation histories of the elements and their final burnups have been used to estimate average powers during each cycle. This analysis yielded peak cycle-averaged powers of ~0.75 and ~0.65 MW for elements CLE-201 and CLE-202, respectively. Using an effective heat transfer area of 1.07 m² (8% greater than the fuel meat area), maximum element-averaged heat fluxes of ~0.7 and ~0.6 MW/m² were calculated for CLE-201 and CLE-202, respectively. Table V gives estimated temperature drops from the center of the fuel meat to the bulk coolant for the two elements during their maximum-power cycles. A power-peaking factor of 2.0 was used, based on measured fluxes and on calculations for a fresh element. The peak heat flux listed in Table V is likely to be an overestimate, however, since the peak element power occurred after some burnup had been achieved, lowering the power-peaking factor. It is estimated that peak fuel centerline temperatures were between 120 and 140°C, assuming a bulk coolant temperature of 53°C.

Table IV. Irradiation History Summary for UAl_x Test Elements.

Core Position	Irradiation Time, fpd	
	CLE-201	CLE-202
A-9		40.02
B-2		84.34
B-9		131.56
C-6		152.04
A-2	82.72	
A-8	88.92	
D-8	39.36	
Total	211.00	407.96
Begin Irrad.	09/06/84	12/18/82
End Irrad.	05/30/85	01/20/85
Total No. of Cycles	17	32
Ave. Burnup, % ²³⁵ U	51 ^a	71 ^b
Ave. Burnup, ^c MWd	128	195
Ave. Power, MW	0.61	0.48

^aBased on ORR fuel management estimate normalized to measured value for element CLE-202, as explained in the text.

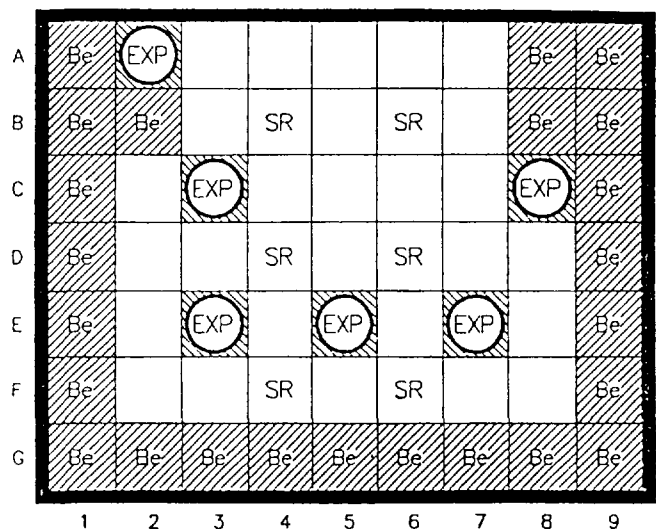
^bBased on gamma scanning and isotopic analysis.

^cBased on the following calculated ²³⁵U burnup rate correlation:

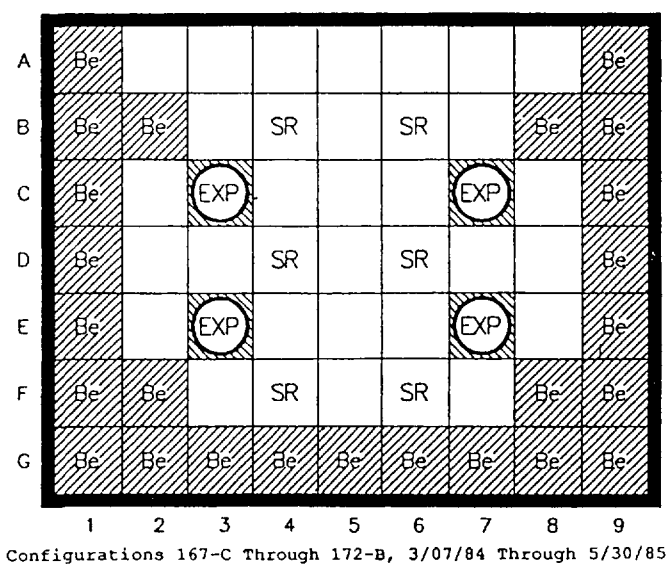
$$\text{Burnup rate (g/MWd)} = 1.2608 - 0.0004103 \cdot \text{Burnup (MWd)}.$$

4. POSTIRRADIATION EXAMINATION OF ELEMENTS

During November 1985 the two UAl_x elements, along with others, were transported to the ORNL High-Radiation-Level Examination Laboratory (HRLEL). The high-burnup element, CLE-202, was given a complete non-destructive and destructive examination, while the low-burnup element, CLE-201, was given only a nondestructive examination. The nondestructive portion consisted of visual examination, dimensional inspection, gamma



Configurations 163-E Through 167-A, 12/18/82 Through 2/23/84



Configurations 167-C Through 172-B, 3/07/84 Through 5/30/85

Fig. 2. Basic Core Configurations During Irradiation of UAl_x Elements.

scanning, and coolant channel measurements. Following this, element CLE-202 was dismantled and the plates were visually inspected. Selected plates were measured for thickness and gamma scanned. Two plates from the element were tested for blister threshold temperature, and one plate was sectioned for microstructural and burnup analyses.

4.1 Visual Examination

The elements were examined visually through the cell windows and through the Kollmorgan periscope. Both of the elements appeared to be in excellent condition. With the exception of the oxide film and some handling scratches the elements appeared to be as fabricated. Looking through the coolant channels with backlighting showed the channels to be uniform with no evidence of plate swelling or distortion. No abnormal conditions were observed.

Table V. Estimated Average and Peak Fuel Temperature Drops.

	Thickness, mm	Thermal Conductivity, W/m·K	
Fuel Meat (CLE-201)	0.74 ^a	40 ^b	
Fuel Meat (CLE-202)	0.74 ^a	25 ^b	
Cladding	0.43	130 ^c	
Boehmite Layer	0 - 0.025	2.25	

Temperature Drops, °C				
	CLE-201		CLE-202	
	Average	Peak	Average	Peak
	(0.70 MW/m ²)	(1.40 MW/m ²)	(0.60 MW/m ²)	(1.20 MW/m ²)
Fuel Meat	13.0	25.9	17.8	35.5
Cladding	2.3	4.6	2.0	4.0
Boehmite 25 µm thick	7.8	15.6	6.7	13.3
Water Film ^d	20.6	41.2	17.6	35.2
Total Minimum (no Boehmite)	35.9	71.6	37.4	74.7
Maximum	43.7	87.2	44.1	88.0

^aHalf-thickness.

^bBased on assumption that U₃Si₂ data is valid for UAl_x. See R. K. Williams, R. S. Graves, R. F. Domagala, and T. C. Wiencek, "Thermal Conductivities of U₃Si and U₃Si-Al Dispersion Fuels," Proc. 19th International Conference on Thermal Conductivity, Cookeville, Tennessee, USA, October 21-23, 1985, Thermal Conductivity, Vol. 19, Ed. D. W. Yarbrough, Plenum Pub. Corp. (1988).

^cSee Table II.

^dFilm coefficient calculated using the Dittus-Boelter correlation for a bulk water temperature of 53.3°C.

4.2 Dimensional Inspection

The width (between side plate outer surfaces) and stack height (between adapter plate curved surfaces) of each element were measured at the front, center, and back at six axial locations. The measurements were made by moving the element to given x-y coordinates between opposing dial micrometers and comparing the readings to a standard. By comparing readings from the upper and lower micrometers, bow or twist could be detected. The length of each element was determined by comparison to a standard using a fixture and a dial indicator. No unusual bow, twist, or swelling was

Table VI. Results of Dimensional Inspection of Irradiated Elements.

	Width,		Stack Height,		Length,	
	mm	in.	mm	in.	mm	in.
Fabrication Limit						
Maximum	76.10	2.996	78.18	3.078	975.1	38.390
Minimum	75.84	2.986	77.67	3.058	973.5	38.328
Element No.						
CLE-201	76.01 75.87	2.9925 2.9871	78.66 77.90	3.0969 3.0668	974.4	38.362
CLE-202	75.95 75.79	2.9903 2.9839	78.74 78.00	3.1000 3.0710	976.1	38.429

observed for any of the elements. A summary of the dimensional measurements is given in Table VI. The width of CLE-202 was slightly less than the fabrication limit at two points near the bottom of the element, and the stack heights for both elements were slightly greater than the fabrication limit at most points. Also, the length of CLE-202 was measured to be greater than the as-fabricated value.

4.3 Gamma Scanning of Elements

The elements were passed in front of a collimator (1.6-mm-diam x 432-mm-long), and analog profiles of gamma intensity versus axial position were obtained, using a NaI detector, for integrated energies greater than 0.5 Mev and for a narrow energy band containing the ^{137}Cs peak at about 0.67 Mev. One spectrum covering the full energy band of fission product gamma rays was obtained with a Ge(Li) detector in order to identify the fission products contributing to the integral data. The burnup profiles indicated by the scans were similar to those of other test elements with similar burnup (see, for example, Appendix D of Ref. 3). These data were not used to evaluate the element-averaged burnup and will not be discussed further.

4.4 Coolant Channel Measurements

Following removal of the end boxes from the elements, the coolant channel thicknesses were measured midway between the side plates along the entire length of the channel. The measuring technique was based on capacitances between the plates and the probe. These data show that the channels exceed the as-fabricated minimum dimension of 0.104 in. No comparable preirradiation data are available to determine changes during irradiation. However, the uniformity of the channels indicates that no excessive swelling or warping of the plates occurred.

5. EXAMINATION OF FUEL PLATES

All of the fuel plates were removed from element CLE-202 individually by cutting through the side plates into the coolant channels with a milling

machine. The strips of aluminum clinging to the fuel plate were then pulled off easily without damaging the plate.

5.1 Visual Inspection of Plates

The first examination of the plates following removal from the element was verification of the plate numbers and a thorough visual inspection. The plates exhibited some warping and bowing after removal from the element. This is typical of all plates from irradiated elements. All of the plates from the element appeared to be in good condition with no evidence of blisters, excessive swelling, or any other unusual condition.

5.2 Plate Thickness Measurements

Plate thickness was determined by positioning the plate between opposing dial micrometers at the desired point of measurement and comparing the reading to a standard. The indicator tip for the top surface was a 1/4-in. (6.35-mm)-diam flat and for the bottom surface was a 1/8-in. (3.18-mm)-diam ball. Measurements were made along tracks at the center of the plate and near each edge. The accuracy of the measurements was greatest along the center track due to more reproducible alignment; therefore, these data were used to estimate plate swelling. No attempt was made to remove the oxide film from the plates so this is included in the plate thickness. Near the end of the examinations, a new device which measures the capacitance of the air gap between two probes and the plate and compares that to a standard became available to measure the plate thickness. This device was used to confirm the thicknesses of several plates.

Five plates from the element (CLE-202) were selected for measurement. Plate thickness increases were determined from the thicknesses measured at each position by subtracting the plate thickness measured outside the fuel zone, near the end of the plate. This method at least partially corrects for the oxide film buildup, since the normalization region also has an oxide film, though probably not as thick as one as in the fuel zone, where heat fluxes are higher. Measurements made by CERCA were used to determine the amount of thickness difference between unfueled and fueled positions prior to irradiation. The average thickness changes of the five plates were 1.6 mils (41 μm) near the low-burnup position and 1.9 mils (48 μm) near the peak burnup position. These values correspond to 2.7 and 3.2% of the meat thickness. The data indicate considerable variation from plate to plate; however, the largest individual measurement would correspond to a swelling of only 7%, which should cause no concern. Because of uncertainties in the "correction" for the oxide film and because mechanical measuring devices always measure between "high" points on the surfaces, the measured thickness increases are upper limits on the actual increase. Since virtually all volume swelling in plate-type fuel occurs in the thickness direction, the measured thickness increases also represent upper limits on the actual meat volume swelling.

5.3 Plate Gamma Scanning and Burnup Analysis

Five plates from the element (including the one which was analyzed later for burnup) were selected for determination of the burnup profile along the length by gamma scanning. Each of these plates was passed in front of a collimator (0.51-mm-high \times 25.4-mm-wide \times 432-mm-long), and profiles of gamma intensity versus axial position were obtained, using a NaI detector, for integrated energies greater than 0.5 Mev and for energies corresponding to the ^{137}Cs peak at about 0.67 Mev. A full energy spectrum was obtained using a Ge(Li) detector at the peak burnup point of each of the thirteen plates of the element. The average-to-maximum ratio from the

profile (NaI) measurements and the average area (Ge(Li)) of the ^{137}Cs peaks at the maximum-burnup position of each plate were correlated with the analyzed burnup at the maximum-burnup point of one plate to obtain the average burnup of the element.

The burnup estimated by the ORR fuel management algorithm was about 10% higher than the average obtained from the above analysis, consistent with experience with other test elements. Note that the average burnup of element CLE-202 was intentionally pushed well beyond the approximately 50% normally achieved in reactors using this type of fuel. This resulted in a peak burnup of over 97% for the outer plate in position 1, based on the measured burnup for the plate in position 13 and the ratio the ^{137}Cs gamma intensities (Ge(Li)) at the peaks of the two plates. Accounting for non- ^{235}U fissions, the fission density in element CLE-202 ranged between $\sim 0.5 \times 10^{27}$ and 1.1×10^{27} f/m³.

5.4 Blister Threshold Testing

A method which has been used historically to compare the relative irradiation performance of dispersion plate-type research reactor fuels, especially under abnormally high operating temperatures, is their resistance to blistering during postirradiation annealing. This "blister threshold test" is performed by sequentially heating the plate (or portions thereof) to higher and higher temperatures and visually examining the plate after each heating for evidence of blisters. Two plates (from positions 2 and 6) of the element were blister threshold tested. The entire plate was heated to preclude the possibility of fission gas diffusing out of the plate rather than causing blisters at these relatively high volume fractions of fuel. The plates were held at the following temperatures for 30 minutes, removed from the furnace and cooled and examined, then heated to the next higher temperature (or removed from testing if blistering was observed): 400, 450, 475, 500, 525, 550, and 575°C. This corresponds closely to the testing done previously on highly enriched, low-volume-fraction oxide and aluminide fuels for which the current fuels are being considered as replacements. Typical blister threshold temperatures for the highly enriched uranium aluminide fuels in use today range from 480 to >565°C.⁶ Helium gas from the $^{10}\text{B}(n,\alpha)$ reaction in many of the ATR-type samples listed in Ref. 6 is believed to be responsible for some blister temperatures being lower than 550°C. Hofman⁷ found that the presence of ^{10}B in the fuel meat of uranium silicide dispersion fuel plates resulted in lowering of the blister threshold temperature by $\sim 100^\circ\text{C}$.

No typical postirradiation blisters (small isolated blisters between the meat and the cladding) were found on the two plates even after the 575°C heating. However, small blisters formed near the ends of both plates over the non-fueled regions. These small blisters started during the 450°C heating for the position-2 plate and during the 475°C heating for the position-6 plate. The appearance of these blisters is illustrated in Fig. 3. Blisters such as this have been previously found⁸ to be due to fuel flaking (individual particles of fuel between the frame and cladding in the nonfuel zone at the end of the plate). More recently it has been established⁷ that blisters tend to form first where fuel particles have been oxidized (for instance, during preheating before the first hot-rolling pass). It is highly likely that the fuel flakes near the ends of these UAl_x plates had been oxidized during fabrication. This flaking did not appear to effect the performance of the fuel during irradiation.

We conclude that the blister threshold temperature for the low-enriched, higher-loaded aluminide fuels is about the same as for the high-

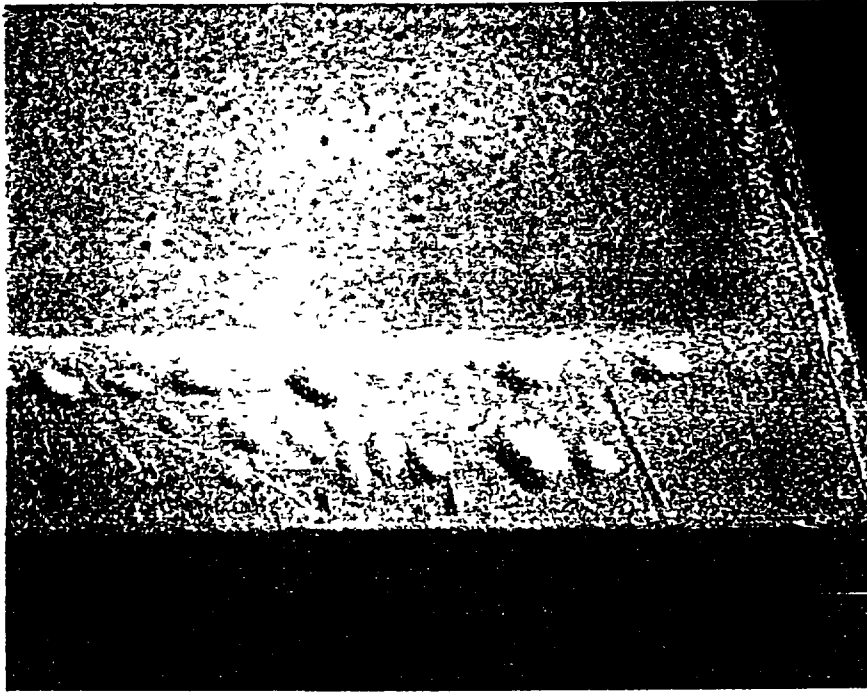


Fig. 3. Blisters over Nonfuel Region of Plate 020V2040, Element CLE-202, After Annealing at 475°C. (R79723)

enriched, lower-loaded aluminide fuels they are proposed to replace. From this testing we infer that the probability for a fuel plate to blister over the fuel zone in-reactor will not be increased by switching to these higher-density, low-enriched UAl_x fuels.

5.5 Metallography

Plate 020V2034 (the bottom fuel plate, position 13) from element CLE-202 was sectioned for destructive examination. The burnup analysis sections were taken from the minimum and maximum burnup areas of the plate as determined by the gamma scan profile. Metallography sections were located immediately adjacent to the burnup analysis sections.

The metallography sections were prepared for viewing (transverse to the length direction of the plate) using conventional techniques. The section was mounted in epoxy, ground on progressively finer silicon carbide paper through 600 grit, then vibratorily polished. The vibratory polishing was a three step process. The first and second steps were on a Texmet* cloth with a water medium and 3- μ m and 1- μ m diamond paste, respectively. The final polish was on Microcloth* with a thick water slurry of Magomet* for 12 minutes.

The microstructure at the top of the plate where the burnup level is 53.5% is shown in Figs. 4 and 5. The fuel (darker gray area) is now the continuous phase after its volume growth both by swelling and reaction with the aluminum matrix (UAl_3 transforms to UAl_4). The aluminum phase remaining is discontinuous and is seen as the lighter gray constituent. The black areas are voids (now probably containing some fission gas) which are remnants of the voids introduced during fabrication. The microstructure

*Texmet, Microcloth, and Magomet are trademarks of Buehler, Ltd.

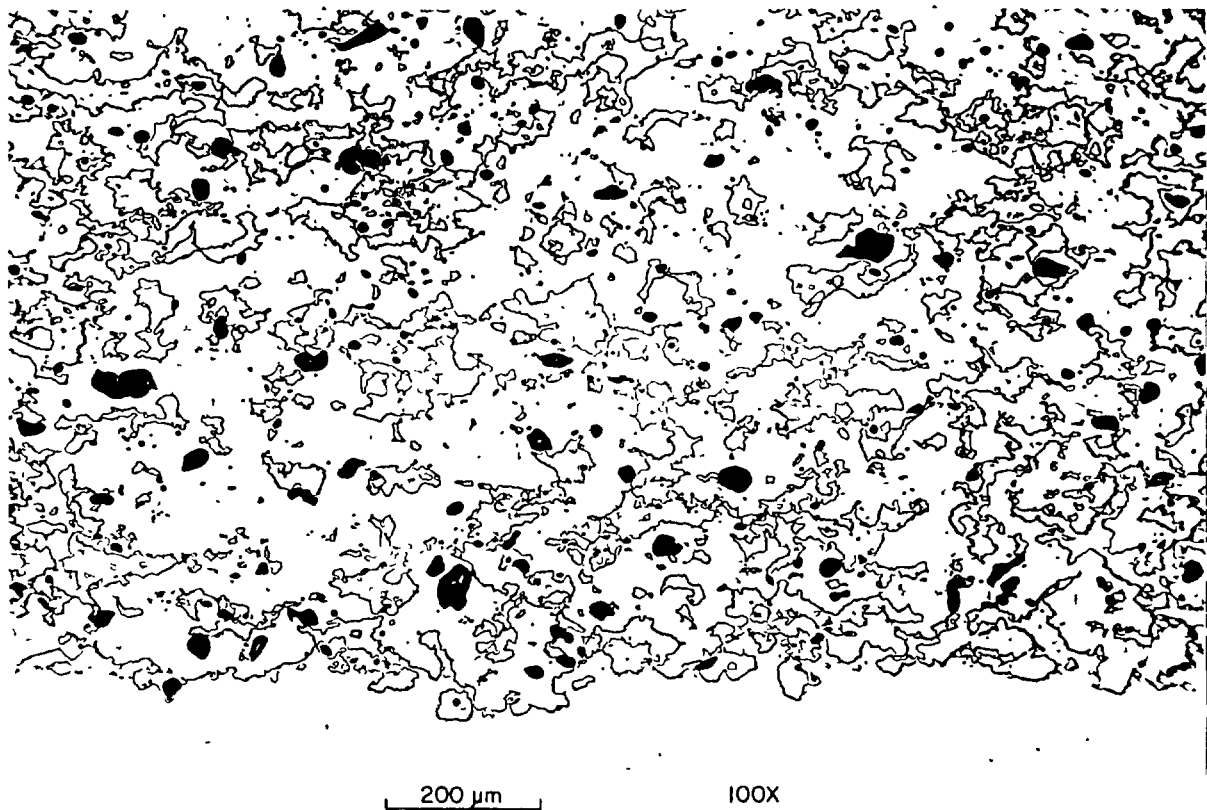


Fig. 4. Meat Microstructure at Top of Plate 020V2034, Element CLE-202, Where Burnup is 53.5%. (R79948)

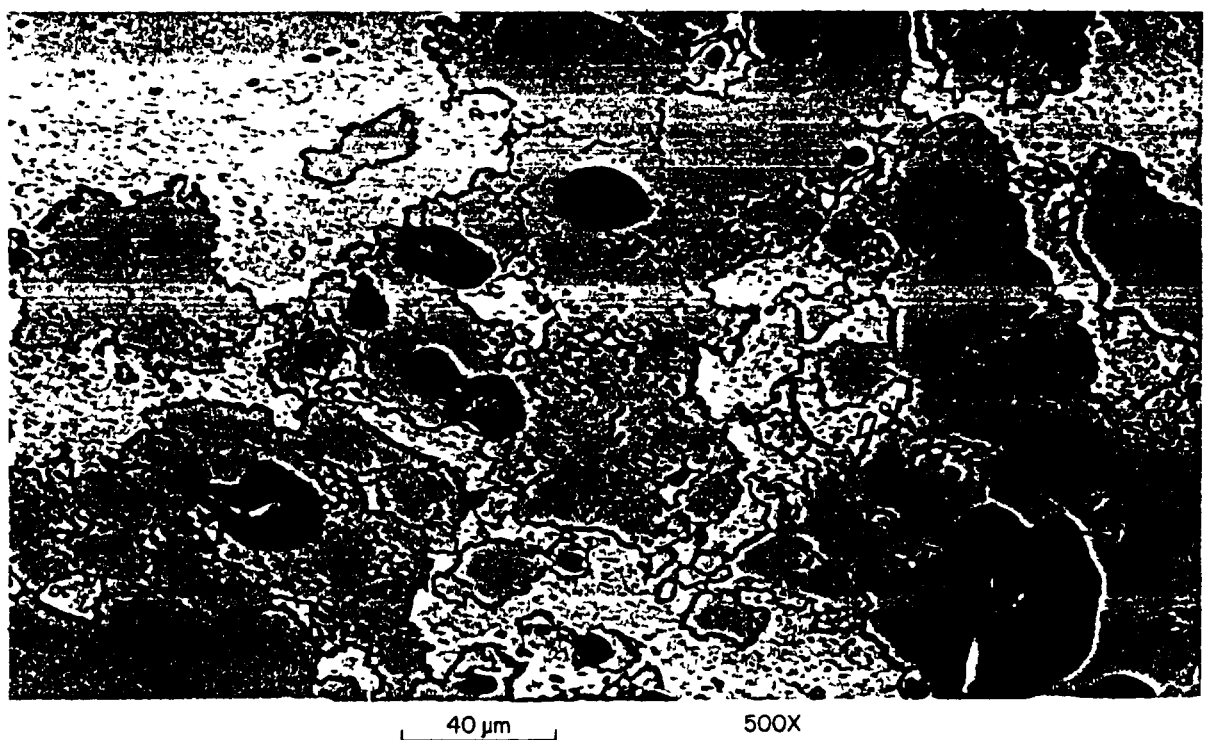


Fig. 5. Detail of Fig. 4. (R79949)

from the peak burnup area of the plate (94.9% depletion of ^{235}U) is shown in Figs. 6 and 7. The constituents are the same as in the lower burnup region, and, as expected, there are lower fractions of both voids and aluminum. The microstructural examination revealed the plate to be in excellent condition with no cracks, interactions with the cladding, or any evidence of impending instability.

Two features noted during the metallographic examinations require comment. The first of these, shown in Fig. 8, is probably an area of oxidized fuel at the meat-cladding interface. It is relatively common to find such localized areas of oxidized fuel at the meat-cladding interface in highly loaded UAl_x or U_3Si_2 dispersion fuel plates. The second feature is a series of inclusions in the cladding, shown in Figs. 9 and 10, which, of course, are not related to the fuel. Neither of these anomalies adversely affected the performance of the plate, and neither was studied further.

6. DISCUSSION OF RESULTS

The postirradiation examination of these low-enriched UAl_x fuel elements revealed the excellent behavior expected from previous miniplate tests.^{9,10} The elements appeared to be essentially as-fabricated after irradiation. The dimensional examination, visual examination, coolant channel measurements, and destructive examinations revealed no significant abnormalities nor any evidence of undesirable behavior. In general, the microstructures are as expected from previous miniplate irradiations and reveal no abnormal conditions. Qualitatively, the microstructures agree with the thickness measurements. The top of the plate (No. 020V2034), with ~4% measured thickness increase, shows more residual porosity than the high burnup region, with ~6% measured thickness increase. The minor dimensional changes observed after irradiation of the elements are insignificant to their performance. The plates remained flat with no observable warping (while constrained within the element), and the coolant channels remained uniform.

7. CONCLUSION

Evaluation of low-enriched UAl_x fuel elements containing thick flat plates after irradiation in the ORR confirms their expected satisfactory performance. The fuel meats of the plates were loaded to 2.1 and 2.3 Mg U/m^3 . Peak burnups ranged to above 97%--far above that expected from normal reactor operation. The elements were essentially as-fabricated, both dimensionally and visually. The plates showed small, uniform thickness changes. Blister threshold temperatures were above those typical of current fuels. Both elements showed completely satisfactory performance.

It is concluded that high-density low-enriched UAl_x -Al dispersion fuel elements with fuel meat thicknesses up to 1.5 mm will perform at least as well in research and test reactors with up to medium power density as the high-enriched UAl_x -Al dispersion fuel elements currently being used in many reactors.

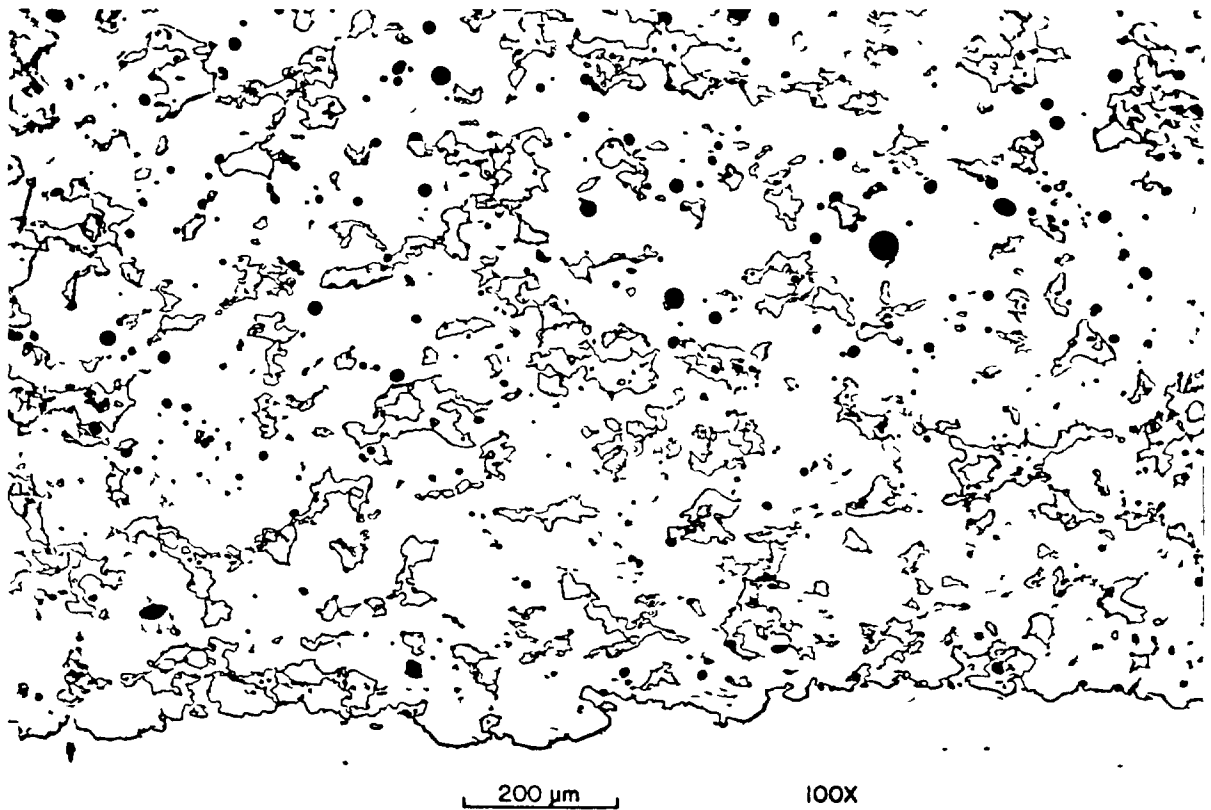


Fig. 6. Meat Microstructure at Peak Burnup Region of Plate 020V2034, Element CLE-202, Where Burnup is 94.9%. (R79952)

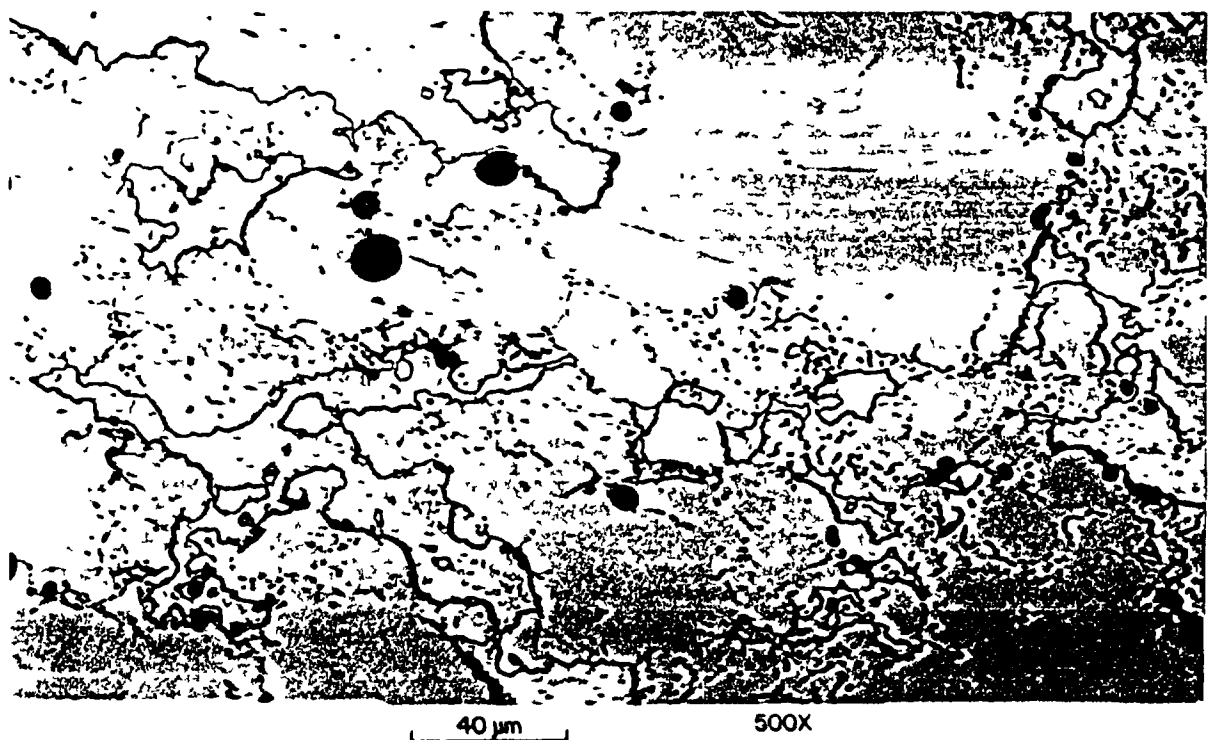


Fig. 7. Detail of Fig. 6. (R79953)

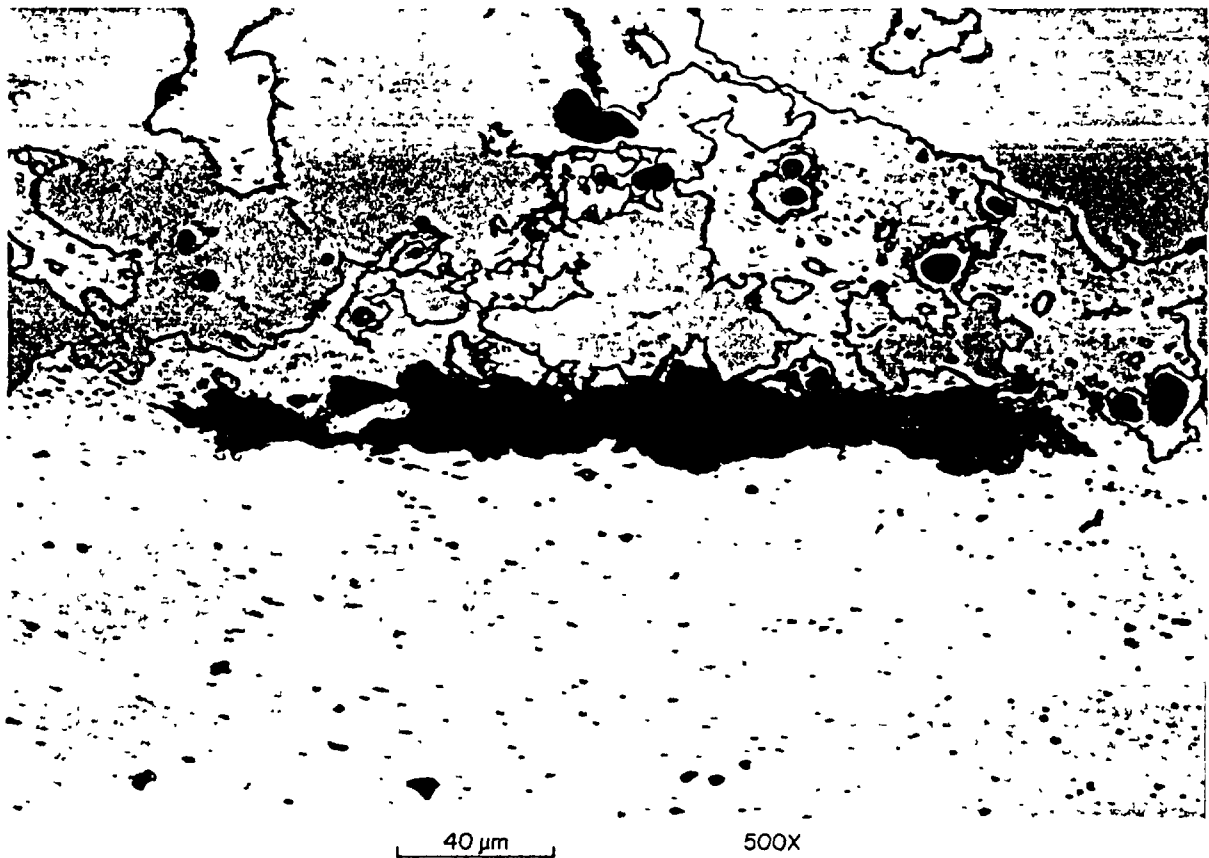


Fig. 8. Area of Probable Oxidation of UAl_x at Meat-Cladding Interface in Peak Burnup Section of Plate 020V2034, Element CLE-202. (R79954)

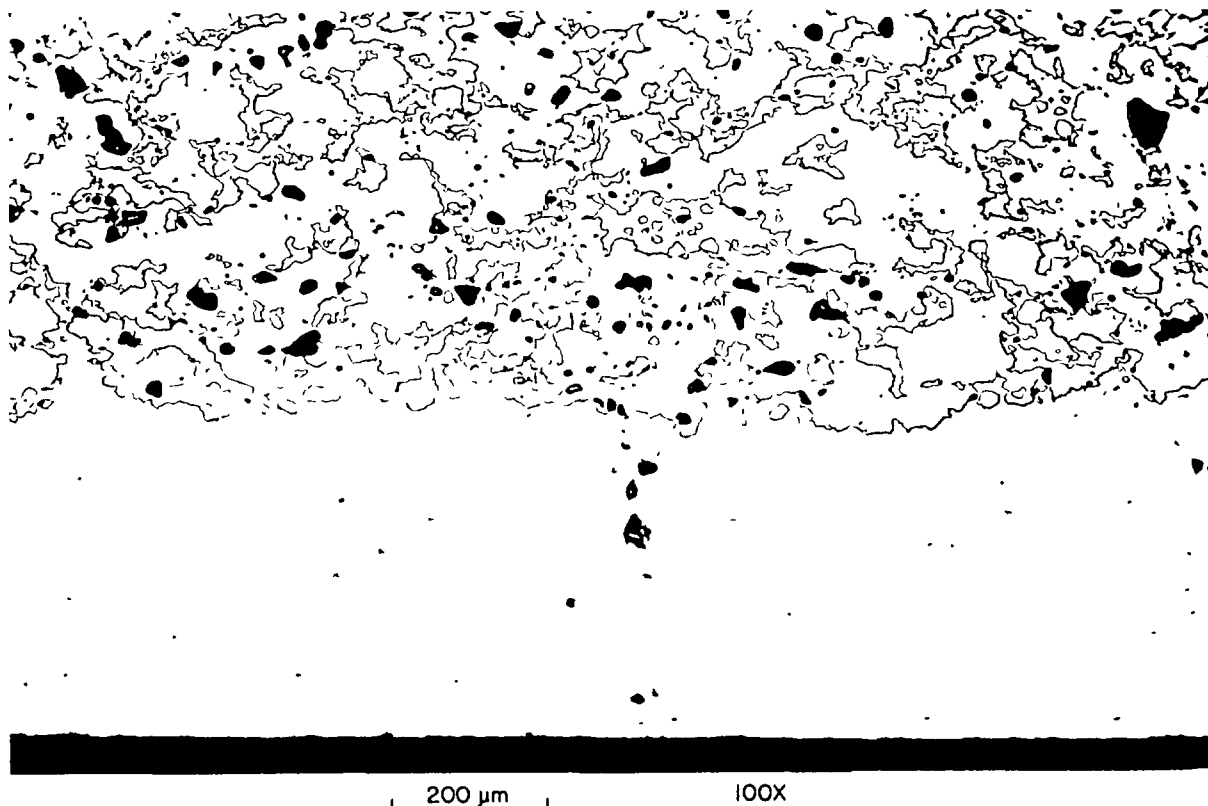


Fig. 9. Inclusion in Cladding in Section from Top of Plate 020V2034, Element CLE-202. (R79950)

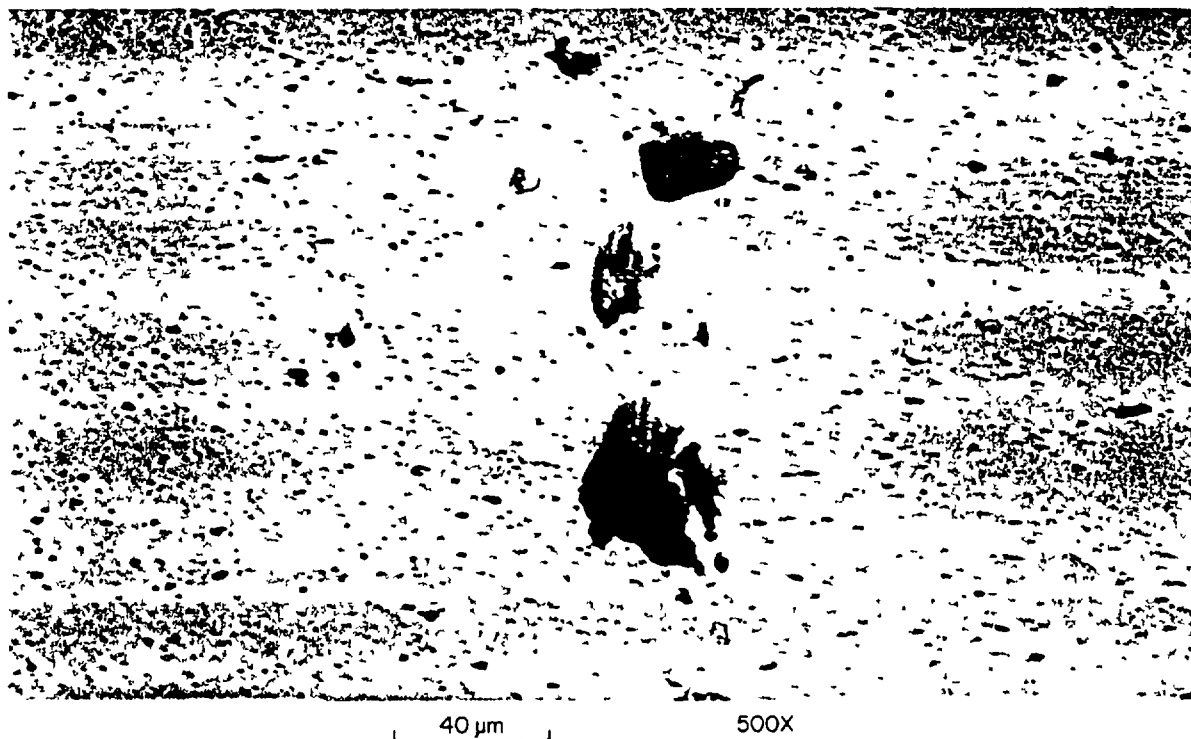


Fig. 10. Detail of Fig. 9. (R79951)

ACKNOWLEDGMENTS

Many persons made important contributions to the work reported here in the years involved in planning and performing the work and analyzing the results. The authors especially acknowledge the contributions of personnel associated with the ORR and the HRLEL at ORNL. Particular thanks are extended to R. W. Hobbs for his assistance in obtaining safety approval for the irradiations, to E. D. Clemmer for assistance during the irradiations, and to L. G. Shrader for assistance in following the progress of the hot cell examinations.

REFERENCES

1. A. Travelli, "Current Status of the RERTR Program," Proc. Int. Mtg. on Development, Fabrication and Application of Reduced Enrichment Fuels for Research and Test Reactors, Argonne Illinois, November 12-14, 1980, Argonne National Laboratory Report ANL/RERTR/TM-3 (CONF-801144), pp. 3-13 (1983).
2. J. L. Snelgrove, G. L. Hofman, and G. L. Copeland, "Irradiation Performance of Reduced-Enrichment Fuels Tested Under the U.S. RERTR Program," Reduced Enrichment for Research and Test Reactors--Proceedings of an International Meeting, Petten, The Netherlands, October 14-16, 1985, P. von der Hardt and A. Travelli, Eds., D. Reidel Publishing Company, Dordrecht, pp. 59-68 (1986).
3. G. L. Copeland, R. W. Hobbs, G. L. Hofman, and J. L. Snelgrove, "Performance of Low-Enriched U_3Si_2 -Aluminum Dispersion Fuel Elements in the Oak Ridge Research Reactor," Argonne National Laboratory Report ANL/RERTR/TM-10 (October 1987)

4. J. L. Snelgrove, R. F. Domagala, G. L. Hofman, T. C. Wiencek, G. L. Copeland, R. W. Hobbs, and R. L. Senn, "The Use of U_3Si_2 Dispersed in Aluminum in Plate-Type Fuel Elements for Research and Test Reactors," Argonne National Laboratory Report ANL/RERTR/TM-11 (October 1987).
5. H. Pruimboom, E. Lijbrink, K. van Otterdijk, and R. J. Swanenburg de Veye, "Status Report on the Irradiation Testing and Post-Irradiation Examination of Low-Enriched U_3O_8 -Al and UAl_x -Al Fuel Elements by the Netherlands Energy Research Foundation (ECN)," Proc. Int. Mtg. on Reduced Enrichment for Research and Test Reactors, 24-27 October, 1983, Tokai, Japan, Japan Atomic Energy Research Institute Report JAERI-M 84-073, pp. 148-202 (May 1984).
6. J. M. Beeston, R. R. Hobbins, G. W. Gibson, and W. C. Francis, "Development and Irradiation Performance of Uranium Aluminide Fuels in Test Reactors," Nucl. Tech. 49, 136-149 (June 1980).
7. G. L. Hofman, "Some Recent Observations on the Irradiation Behavior of Uranium Silicide Dispersion Fuel," Proc. 1988 Int. Mtg. on Reduced Enrichment for Research and Test Reactors, September 19-22, 1988, San Diego, California, Argonne National Laboratory Report ANL/RERTR/TM-13 (CONF 8809221), in press.
8. G. L. Copeland, G. L. Hofman, and J. L. Snelgrove, "Irradiation Performance of Low-Enriched Fuel Elements," Proc. 1984 Int. Mtg. on Reduced Enrichment for Research and Test Reactors, October 15-18, 1984, Argonne, Illinois, Argonne National Laboratory Report ANL/RERTR/TM-6 (CONF-8410173), pp. 152-166.
9. J. L. Snelgrove, R. F. Domagala, T. C. Wiencek, and G. L. Copeland, "Fuel Development Activities of the U.S. RERTR Program," Proc. Int. Mtg. on Reduced Enrichment for Research and Test Reactors, 24-27 October, 1983, Tokai, Japan, Japan Atomic Energy Research Institute Report JAERI-M 84-073, pp. 34-42 (May 1984).
10. E. Pérez, C. Kohut, D. Giorsetti, G. Copeland, and J. Snelgrove, "Irradiation Performance on CNEA UAl_x and U_3O_8 Miniplates," Proc. Int. Mtg. on Reduced Enrichment for Research and Test Reactors, 24-27 October, 1983, Tokai, Japan, Japan Atomic Energy Research Institute Report JAERI-M 84-073, pp. 67-76 (May 1984).

Appendix J-4.1.2
Part III

**EXAMINATION OF U_3Si_2 -Al FUEL ELEMENTS
FROM THE OAK RIDGE RESEARCH REACTOR**

G.L. COPELAND
Oak Ridge National Laboratory,
Oak Ridge, Tennessee

G.L. HOFMAN, J.L. SNELGROVE
Argonne National Laboratory,
Argonne, Illinois

United States of America

Abstract

The results of postirradiation examination of low-enriched U_3Si_2 fuel elements from the Oak Ridge Research Reactor are presented. The elements replaced standard highly-enriched elements and were handled routinely except that the burnup of three of the elements was extended beyond normal limits--up to about 98% peak. The elements were manufactured by commercial fuel suppliers. The performance of all elements was completely satisfactory.

INTRODUCTION

This paper presents the results of the irradiation of low-enriched U_3Si_2 fuel elements in the Oak Ridge Research Reactor (ORR). The purpose of the test irradiations was to confirm the expected good performance of these elements in a medium-powered research reactor under typical operating conditions to burnups in excess of those normally achieved. This expectation of good performance was based on miniplate irradiations at even higher fuel concentrations and burnups.^{1 3} Six experimental elements, two from each of the commercial manufacturers of U_3Si_2 fuel, were irradiated. One element from each manufacturer was irradiated to normal burnup (~50% average) and one was irradiated well beyond this point (~75% average). Postirradiation examination (PIE) of the six elements has been completed with completely satisfactory results for all.

ELEMENT DESCRIPTION

The experimental elements were designed to replace a standard ORR element. The box-type standard element contains 19 curved fuel plates and a total of 285 g of ^{235}U (highly enriched) as U_3O_8 dispersed in aluminum. The nominal plate thickness is 1.27 mm (0.050 in.) with a 0.51-mm (0.020-in.) fuel meat. The experimental elements were physically identical but contained a total of 340 g of ^{235}U (19.7 to 19.8% enriched) as U_3Si_2 dispersed in aluminum.

The additional ^{235}U more than compensates the neutronic poisoning of the additional ^{238}U . This loading requires 4.8 Mg/m^3 of uranium in the fuel meat (about 43 vol% U_3Si_2). Two elements were fabricated by each of three commercial research reactor fuel element suppliers. The fuel fabricators were Babcock and Wilcox in the United States, Compagnie pour l'Etude et la Realisation de Combustibles Atomiques (CERCA) in France, and NUKEM in the Federal Republic of Germany. The elements have been treated routinely for fuel shuffling. One of the elements from each manufacturer was irradiated to ~50% depletion of the originally contained ^{235}U (normal burnup), and one was irradiated to a burnup of ~75% (substantially higher than would be achieved in normal reactor operation).

POSTIRRADIATION EXAMINATION PROCEDURES

Postirradiation examinations of these elements were conducted at the High-Radiation-Level Examination Laboratory (HRLEL) at ORNL with the exceptions of scanning electron microscopy and some metallography, which were performed at Argonne National Laboratory. Since the irradiations of full-sized elements are meant to be confirmatory in nature rather than to provide basic irradiation behavior data for the fuel, the emphasis of the PIE is on checking the dimensional stability of the element and plates, on measuring the blister-threshold temperatures and burnup levels, and on performing limited metallography. A summary of the PIE steps has been published previously.⁴ Each of these elements was given a full destructive examination.

RESULTS

Postirradiation results confirm the completely satisfactory performance of all elements.

Element Visual and Dimensional Inspection

A careful visual examination of each element revealed no abnormal features. The elements appeared to be essentially as-fabricated with the exception of the normal corrosion film and scuff marks from handling. Measurements for length, width, crown height, twist, and bow revealed no significant changes. The element dimensions were essentially within the original fabrication specification envelope.

Channel Spacing Measurements

Each water channel was measured in two locations for the full length of the element. These measurements showed the channels to meet the minimum fabrication specification in each case. The channels were generally uniform with no abnormalities noted.

Plate Visual Inspection

After removing the plates from the elements, they were given a careful visual examination. The plates were bowed and warped to some extent after their removal from the element. The plates appeared to be in excellent condition with a uniform corrosion film over the meat and no apparent blisters, unusual swelling, or other defects.

Plate Thickness Measurements and Burnup Analysis

Selected plates from each element were measured in 24 locations for thickness change. In order to approximately account for effects of plate curvature on the thickness measurement and for the buildup of the oxide layer on the plate surfaces, thickness changes were computed relative to the plate thickness measured outside of the fuel zone, rather than relative to preirradiation measurements on flat plates. Due to warping, bowing, and other local surface irregularities, volumetric swellings of the fuel meat calculated from thickness changes are always larger than the actual volumetric swelling. This fact must be kept in mind if one should compare the swelling of these plates to the accurately measured swelling of similar miniplates. Average thickness increases (based on five plates) are shown in Table 1 and indicate uniform, low swelling for all elements. The data are separated into the low burnup region (the top two inches of the fuel zone) and the peak burnup region (about ten inches from the bottom of the fuel zone) and show the effect of burnup. The ^{235}U burnup (depletion) was determined at the peak and minimum points of one plate using ^{235}U isotopic ratios measured before and after irradiation by mass spectrometry and calculated correction factors to account for the buildup or depletion of the other uranium isotopes. The burnup data listed in Table 1 were obtained by averaging the ^{137}Cs gamma scan counts for the appropriate plate regions or for all of the plates and normalizing to the measured peak burnup.

The plate thickness changes also correlate with the amount of preirradiation voids (i.e., the onset of swelling is delayed by fabrication-induced porosity) and with the phases present (as discussed below in the metallography section). No unusual swelling was detected, indicating that there were no blisters or other indications of the onset of rapid swelling.

Table 1. Average Thickness Increase and Burnup

Element No.	Low Burnup Region			Peak Burnup Region			Element Average Burnup (%)
	Burnup (%)	Thickness Increase (mils)	Thickness Increase (μm)	Burnup (%)	Thickness Increase (mils)	Thickness Increase (μm)	
BSI-201	28	0.0	0	69	1.5	38	54
BSI-202	53	0.0	0	97	1.8	46	77
CSI-201	32	0.1	3	66	1.7	43	52
CSI-202	55	0.9	23	98	4.4	112	82
NSI-201	19	0.7	18	46	1.0	25	35
NSI-202	53	1.2	30	98	4.1	104	82

Blister Annealing

Blister annealing of selected plates from each element was accomplished by heating the plates singly in a tube furnace. The furnace was able to maintain a uniform maximum-temperature zone about seven inches long in the maximum burnup region of the plate. Temperatures decreased toward the ends of the plate by up to 10°C . The plates were sequentially heated for 30 minutes at 400, 450, 475, 500, 525, 550, and 575°C or until blisters were observed. The plates were cooled and visually examined for blisters between each heating cycle. The plates, their maximum heating temperature (blister threshold temperature), and the type of blisters observed are listed in Table 2.

These data show that the blister threshold temperature of these high-loaded, low-enriched silicide fuels is significantly higher than the minimum values for the low-loaded, highly-enriched fuels currently in use.

Table 2. Results of Blister Anneals of Full-Sized Plates

Element No.	Plate Position in Element	Plate No.	Maximum Temperature (°C)	Description of Blisters ^a
BSI-201	3	S-3-211-13	575	None
	8	S-3-210-23	575	Typical PI
BSI-202	3	S-3-213-15	550	Typical PI
	8	S-3-212-19	550	Typical PI
CSI-201	4	OSIIW065	550	Typical PI
	8	OSIIW054	550	Typical PI
CSI-202	3	OSIIW044	550	Typical PI ^b
	8	CSIIW026	550	Typical PI ^c
NSI-201	2	ORR-092	550	None
	8	ORR-100	550	None
	19	ORR-144	550	None
NSI-202	3	ORR-114	550	Typical PI
	9	ORR-123	550	Typical PI

^aTypical PI—typical of postirradiation blisters observed previously in low-volume-fraction fuels (i.e., appear to be discrete blisters between meat and cladding with no "pillowing").

^bSmall blisters off of fuel formed at 500°C.

^cSmall blisters off of fuel formed at 525°C.

Metallography

The inner plate with the highest burnup, based on gamma scanning, was selected from each element for metallographic examination. Metallographic sections were taken from the peak-burnup and low-burnup areas of these plates (adjacent to the burnup analysis sample). Representative microstructures from the low- and peak-burnup regions of each high-burnup element are shown in Figs. 1 through 6. The burnups listed in the figure captions are those measured for the adjacent samples. In general, the microstructures are as expected from previous miniplate irradiations and reveal no abnormal conditions. Qualitatively, the microstructures agree with the thickness measurements. No, or very little, swelling was measured for the areas showing fabrication porosity remaining. Plates containing more of the U_3Si phase (CSI's and NSI's) showed more areas with beginning formation of large gas bubbles and more thickness change. The plates which contained some free U as fabricated and less U_3Si (BSI's) showed fewer areas with large bubbles forming and less thickness change. The free U apparently converts to UAl_x during fabrication and/or irradiation and retains the gas. Overall, the plates appear to be in excellent condition.

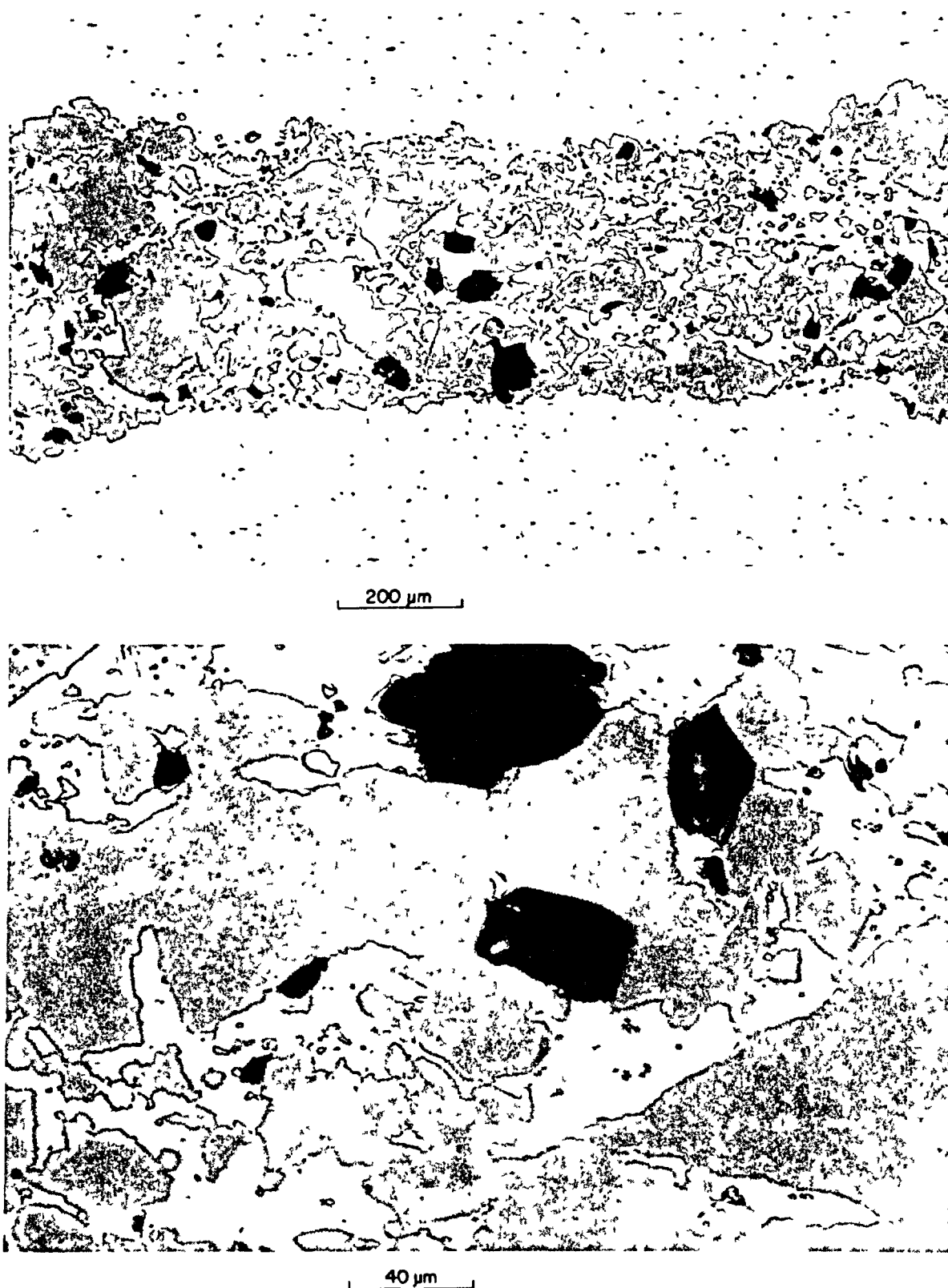


Fig. 1. Microstructure of BSI-202 at 51% burnup showing fabrication porosity remaining and small gas bubbles. (R79963 top and R79964 bottom).

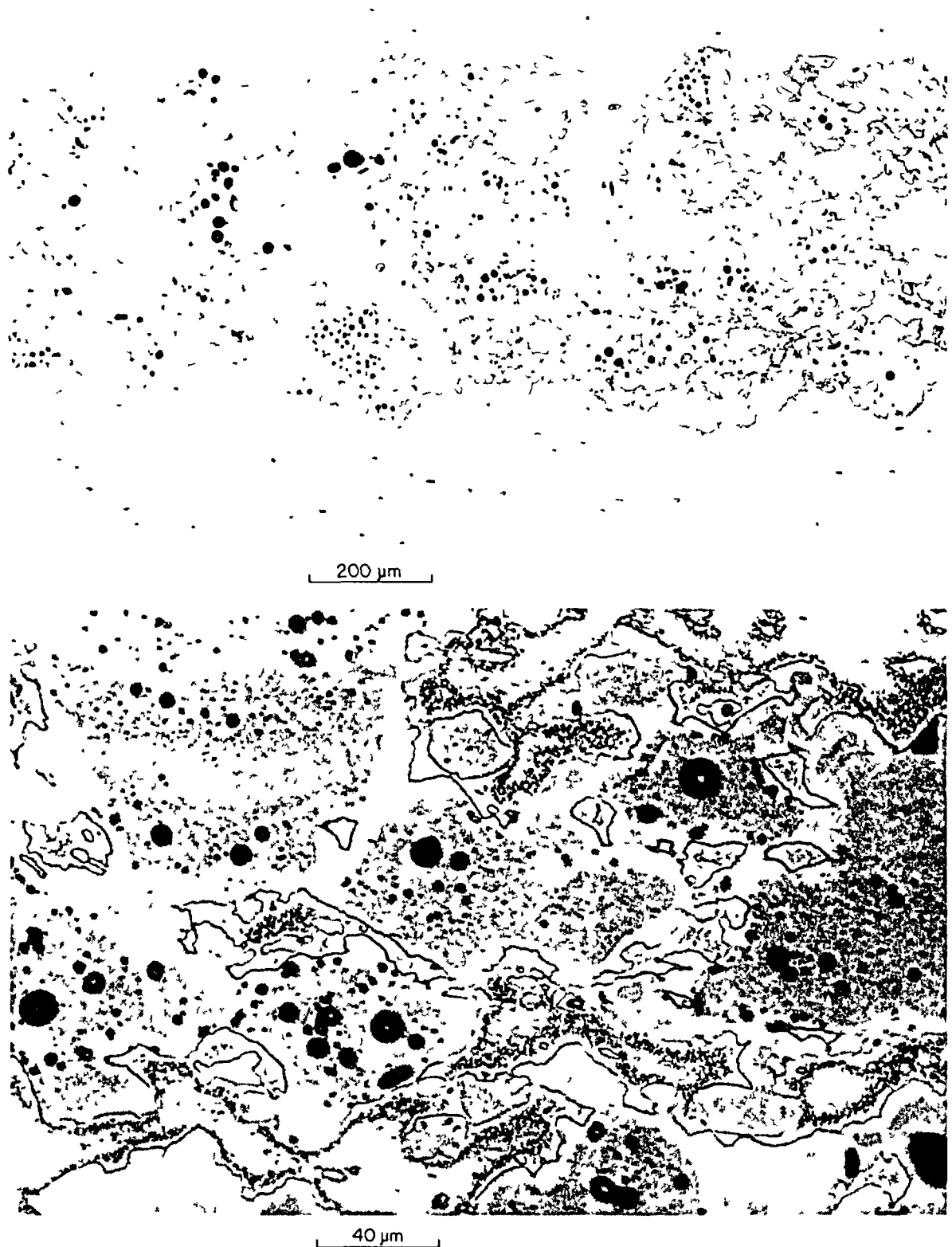


Fig. 2. Microstructure of BSI-202 at 97% burnup showing no fabrication porosity and beginning formation of large gas bubbles in some areas. (R79965 top and R79966 bottom).

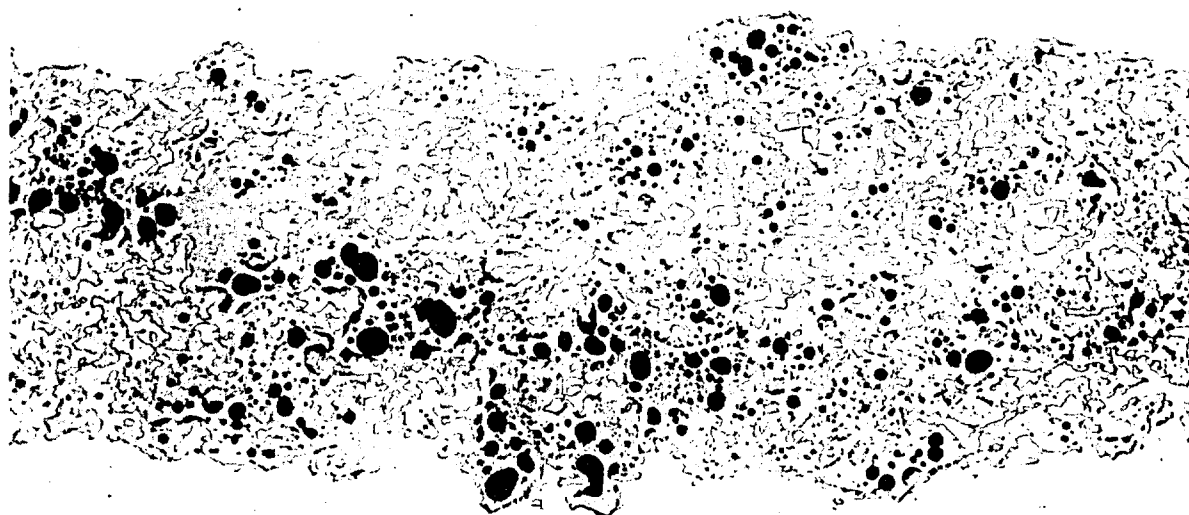


200 μm

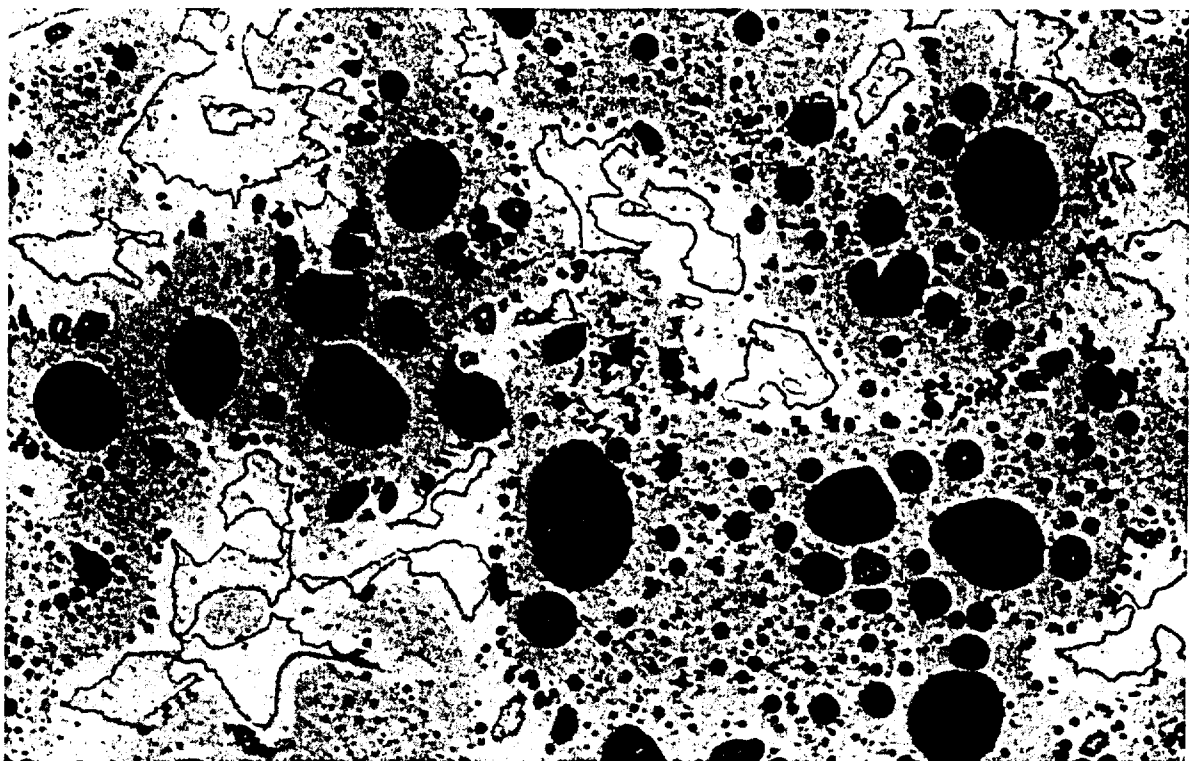


40 μm

Fig. 3. Microstructure of CSI-202 at 55% burnup showing no fabrication porosity and small gas bubbles. (R79955 top and R79956 bottom).



200 μm



40 μm

Fig. 4. Microstructure of CSI-202 at 97% burnup showing no fabrication porosity and early stage of linking of gas bubbles in some areas. (R79957 top and R79958 bottom).



200 μm

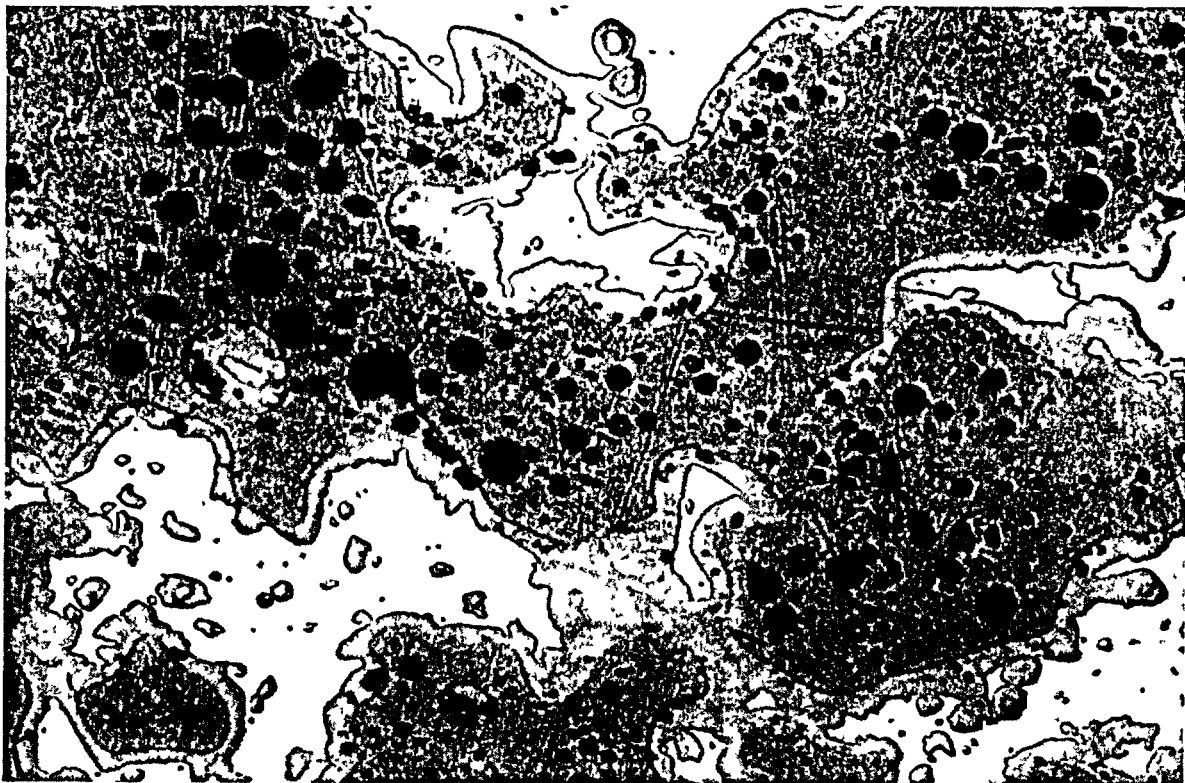


40 μm

Fig. 5. Microstructure of NSI-202 at 54% burnup showing fabrication porosity remaining and small gas bubbles. (R79559 top and R79558 bottom).



200 μm



40 μm

Fig. 6. Microstructure of NSI-202 at 96% burnup showing no fabrication porosity remaining and formation of large gas bubbles. (R79564 top and R79565 bottom).

CONCLUSION

Postirradiation evaluation of low-enriched U_3Si_2 fuel elements from the ORR confirmed their expected satisfactory performance in this medium-powered research reactor. Peak burnups ranged up to 98%—far above that expected from normal reactor operation. The elements were essentially as-fabricated, both dimensionally and visually. The plates showed small, uniform thickness changes. Blister threshold temperatures were above those typical of current fuels. Both elements from each manufacturer showed completely satisfactory performance.

REFERENCES

1. G. L. Hofman and L. A. Neimark, "Irradiation Behavior of Uranium-Silicide Dispersion Fuels," Proceedings of the International Meeting of Reduced Enrichment for Research and Test Reactors, 24-27 October 1983, Tokai, Japan, JAERI-M 84-073, pp.43-53 (May 1984).
2. J. L. Snelgrove, G. L. Hofman, and G. L. Copeland, "Irradiation Performance of Reduced-Enrichment Fuels Tested Under the U. S. RERTR Program," Reduced Enrichment for Research and Test Reactors, Proceedings of an International Meeting, Petten, The Netherlands, October 14-16, 1985, P. von der Hardt and A. Travelli, Eds., D. Reidel, Dordrecht, pp. 59-68 (1986).
3. G. L. Hofman and L. A. Neimark, "Postirradiation Analysis of Experimental Uranium-Silicide Dispersion Fuel Plates," Proceedings of the 1984 International Meeting on Reduced Enrichment for Research and Test Reactors, Argonne, Illinois, October 15-18, 1984, ANL/RERTR/TM-6, CONF-8410173, pp. 75-85, (July 1985).
4. G. L. Copeland, G. L. Hofman, and J. L. Snelgrove, "Irradiation Performance of Low-Enriched Uranium Fuel Elements," Proceedings of the 1984 International Meeting on Reduced Enrichment for Research and Test Reactors, Argonne, Illinois, October 15-18, 1984, ANL/RERTR/TM-6, CONF-8410173, pp. 152-166, (July 1985).

LEU AND MEU FUEL TESTING IN CEA REACTORS

C. BAAS*, M. BARNIER**, J.P. BEYLOT**,
P. MARTEL*, F. MERCHIE*

*Centre d'études nucléaires de Grenoble,
Commissariat à l'énergie atomique,
Grenoble

**Centre d'études nucléaires de Saclay,
Commissariat à l'énergie atomique,
Gif-sur-Yvette

France

Abstract

The progress achieved in the qualification of LEU and MEU fuels in the SILOE reactor and LEU fuel in the OSIRIS reactor is presented. This program, which began in the SILOE reactor in 1980 involves irradiation of a complete UAl element with 45% enriched uranium and 2.2 g U/cm^3 , full-sized plates with LEU U_3Si and U_3Si_2 fuels, and complete elements with LEU loadings of 6.0 g U/cm^3 with U_3Si and 5.2 g U/cm^3 with U_3Si_2 . Periodical examinations were carried out during irradiation, in particular plate thickness and water channel width measurements. Finally, the characteristics and status of a mixed $\text{U}_3\text{Si-U}_3\text{Si}_2$ element under irradiation in the OSIRIS reactor is presented.

1. GENERAL OUTLINES OF THE PROGRAM

Irradiation testing of LEU and MEU research reactor fuels began in the SILOE reactor in 1980 within the framework of agreements concluded between the CEA, ANL, and CERCA as part of the Reduced Enrichment Research and Test Reactor (RERTR) Program. Also as part of this program, irradiation testing of LEU silicide fuel began in the OSIRIS reactor in 1986.

The program is comprised of essentially three phases aimed at qualification of reduced enrichment fuels manufactured by CERCA.

The first phase, completed in 1983, involved irradiation in SILOE and post-irradiation-examination at Saclay of a complete fuel element containing UAl_x fuel with a uranium density of 2.2 g/cm^3 .

The second phase began in June 1982 and involved irradiation in SILOE of 4 U_3Si fuel plates with LEU densities of 5.5 g/cm^3 and 6.0 g/cm^3 using a special casing located in the reactor reflector. The intention was to examine the behaviour of these separate plates before irradiation testing of a complete fuel element. Similarly, 4 separate U_3Si_2 plates

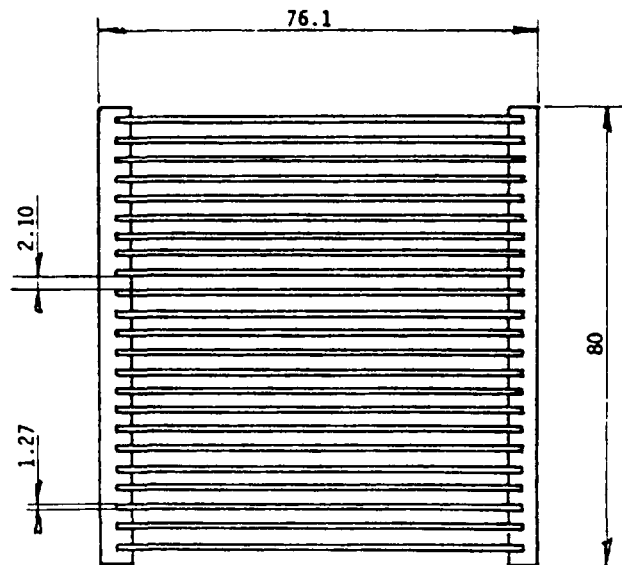


FIG. 1. Cross-section of standard 23-flat-plate fuel element for SILOE irradiation tests.

with LEU densities between 2.0 and 5.4 g/cm³ were also irradiated in the special casing.

In the third phase, complete LEU fuel elements containing 6.0 g/cm³ with U₃Si fuel and 5.2 g/cm³ with U₃Si₂ fuel were irradiated in the SILOE reactor. A standard HEU UAl element was also irradiated in SILOE for the purpose of comparing swelling behaviour. In order to keep the possibility of increasing the uranium density, necessary in certain cases, and to extend the knowledge of silicide-based fuels, a complete element containing a mixture of U₃Si and U₃Si₂ fuels with a density of 4.7 g/cm³ began irradiation in the OSIRIS reactor in 1986.

In all cases, various measurements were carried out during and after irradiation.

2. TESTING OF 45% ENRICHED UAl_x FUEL^(1,2)

2.1 CHARACTERISTICS OF THE ELEMENT TESTED

The geometry (Fig. 1) of the fuel element manufactured by CERCA was identical to the standard fuel element normally used with SILOE. The fuel element had a charge of 418.3 g of ²³⁵U and was made up of 23 plates (18.6 ± 0.37 g of ²³⁵U per plate). The fuel was UAl_x with 2.2 g U/cm³ and the uranium was 45% enriched.

Before the irradiation in the SILOE core was started, different measurements had been taken in order to complete the neutronic and thermo-hydraulic studies carried out previously, namely concerning the establishment of the safety file necessary to obtain the agreement of the safety authorities on the irradiation program:

- a) Hydraulic measurements: this measurement was taken on a hydraulic test loop in order to check the flowrate-pressure drop characteristic of the element.

b) Neutron Measurements:

• Reactivity Effect

At the start of irradiation, the element presented a gain in reactivity of + 50 pcm compared with a new standard element placed in the same position (53). After 6 months irradiation, a gain of + 70 pcm was again noted over an element with the same burn-up placed in the same position (22).

• Flux Measurements

These measurements were taken at low power and with miniature fission chambers (^{235}U coating for measurements with thermal neutrons, and ^{237}Np coating for measurements with fast neutrons).

The results obtained are presented in Figs. 2 and 3. These fluxes are quite comparable to those calculated elsewhere.

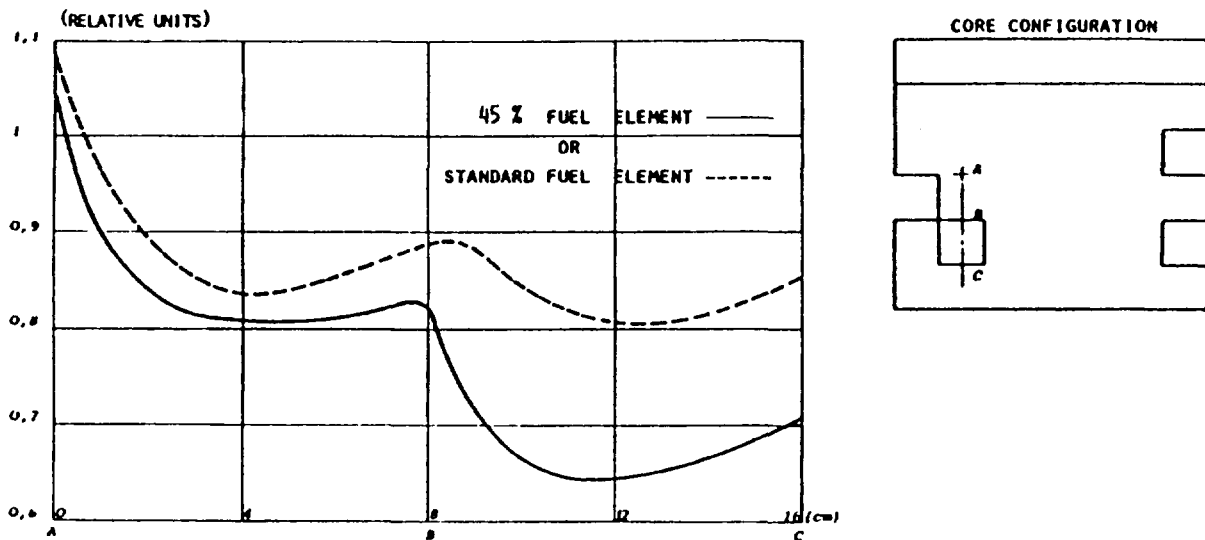


FIG. 2. Flux distribution measurement with miniature fission chamber (^{235}U).

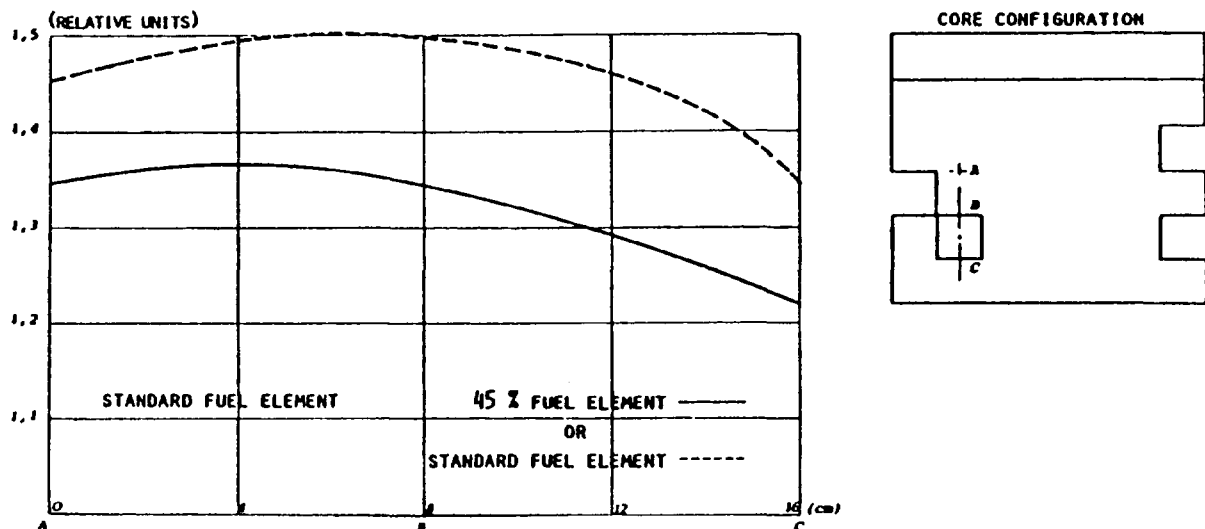


FIG. 3. Flux distribution measurement with miniature fission chamber (^{237}Np).

TABLE 1. IRRADIATION OF A 45% ENRICHED FUEL ELEMENT ($2\text{gU}_T/\text{cm}^3$)
Main irradiation data

Irradiation cycle	Position in core	BU _p (start of cycle) %	Corresponding weight U5 (g)	Mean Power dissipated (MW)	Counting rate DRG ¹ C ₁ [*] /C ₂ ^{**}	Energy released (MWJ)	Characteristics of reactor water during irradiation		Observations
							(MΩ/cm)	pH	
02/81	53	0	418.3	1.358	0.8	33.92	0.9	6	Visual examination outside pool before placing in reactor : No Comment Examination under water : No Comment " "
03/81	43	8.5	382.75	1.207	0.5	24	1.3	6.1	
04/81	64	17.3	345.9	1.400	1	24.96	1.45	6.1	
05/81	48	25	314	1.155	0.6	23.04	1.5	6.3	" "
06/81	67	31.9	285.9	0.77	1	15.68	1.6	6.4	" "
07/81	52	36.6	266.3	0.83	0.8	16.94	1.6	6.4	Examination in hot cell early Sept. 81 : No comment.
08/81	22	41.6	245.1	0.651	0.9	13.38	1.3	6.4	Examination under water : No comment
09/81	62	45.4	228.4	0.384	0.9	7.92	1.23	6.3	" "
10/81	64	47.8	218.5	0.441	1.3	9.00	1.3	6.2	At end of irradiation: BU 50.4% Residual MU _E : 207.25 g E total : 168.84 MW/D Examination in hot cell in Jan. 82: no comment

* Counting rate of element tested

** Mean counting rate of elements with residence times or BU similar to the element under consideration

¹DRG Failed Fuel Element Detection System

2.2 IRRADIATION CONDITIONS

The element for testing was placed in the SILOE reactor core on February 2, 1981 and its irradiation was terminated on November 26, 1981. The fuel element stayed in the core in different positions for 9 cycles. The main irradiation data are presented in Table 1.

Between the cycles, the fuel element was submitted to:

- a visual inspection under water or in the reactor hot cell
- a DRG test of the cladding (DRG: Fuel cladding failure detection system).

It is worth noting that from the results of the Failed Fuel Element Detection (DRG) test, carried out between each cycle, the behaviour of the element was ideal, since no fuel element failure was evidenced during irradiation. This good behaviour is confirmed moreover by the visual examinations performed each month (under water) and twice in a hot cell, in particular at the end of irradiation (January 1982).

The behaviour of the fuel element was excellent, and a final mean burn-up of 50.4% was reached.

2.3 POST-IRRADIATION-EXAMINATIONS (PIE)

The fuel element was loaded into a special transport cask and transferred to the hot laboratories of SACLAY (LECI*), in December 1982, in order to perform different non-destructive and destructive tests. The following operations were carried out:

- measuring the width of the 22 water channels between the fuel plates with special equipment allowing the exploration of 3 tracks in the axis of each channel. These measurements showed nothing particular.
- dismantling of the fuel element plate by plate.
- measuring the thickness of the plates longitudinally and transversely and comparing with the thickness measurements taken during fabrication, before assembling the plates. No significant difference was observed.
- metallographic examination of one plate presenting a high burn-up (57%). The photographs do not give any particular indications.

At the end of all these examinations, which terminated in June 1983, the plates were placed into a special support box and loaded into the transport cask to be transferred back into the SILOE reactor pool. Moreover, some of the plates were examined by spectrometry. All of the plates will be reprocessed.

Finally, it can be concluded that the behaviour of the fuel element proved excellent and that the UAl_x fuel with 2.2 g of total uranium per cubic centimeter ($E = 45\%$) is qualified to be used in research and test reactors.

*Laboratoire d'Examen des Combustibles Irradies (Irradiated Fuel Testing Hot Lab.) C.E.A. C.E.N. SACLAY, France

3. TESTING OF 19.75% ENRICHED URANIUM-SILICON FUEL (2-6)

The program up to October 1987 comprised irradiation of the following fuels, fabricated by CERCA, in the SILOE and OSIRIS reactors:

In SILOE:

- 4 separate U_3Si fuel plates
- 4 separate U_3Si_2 fuel plates
- 1 complete U_3Si fuel element
- 1 complete U_3Si_2 fuel element
- 1 complete HEU UAl fuel element

In OSIRIS:

- 1 complete $U_3Si-U_3Si_2$ fuel element

3.1 IRRADIATIONS IN THE SILOE REACTOR

3.1.1 Irradiation of Separate Fuel Plates (U_3Si and U_3Si_2)

The eight separate fuel plates had the same dimensions and thickness as the plates of the standard fuel elements for SILOE (Fig. 4).

U_3Si Fuel Plates		U_3Si_2 Fuel Plates	
g U/cm ³	g ²³⁵ U/Plate	g U/cm ³	g ²³⁵ U/Plate
5.5	20.2	2.0	7.4
5.5	20.2	3.7	13.6
6.0	21.2	5.2	19.1
6.0	21.2	5.4	19.9

The alloy used for the frame and cover of the fuel plates was an aluminum alloy containing 3% magnesium (alloy AG3 as per French standards).

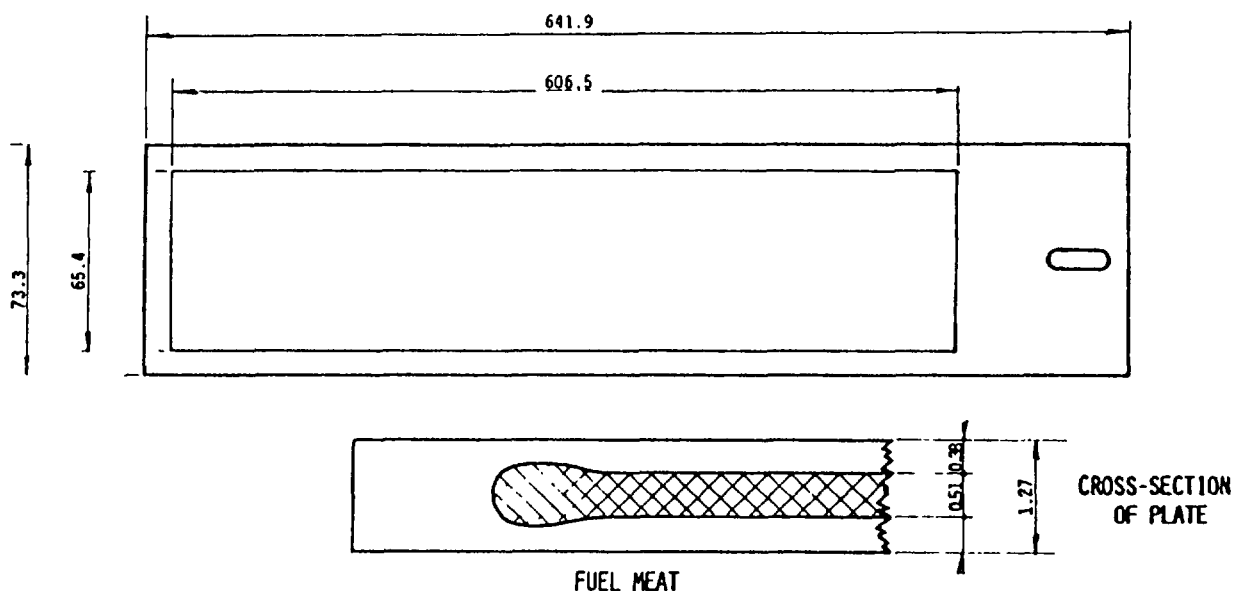


FIG. 4. Uranium-silicide plate for SILOE irradiation tests.

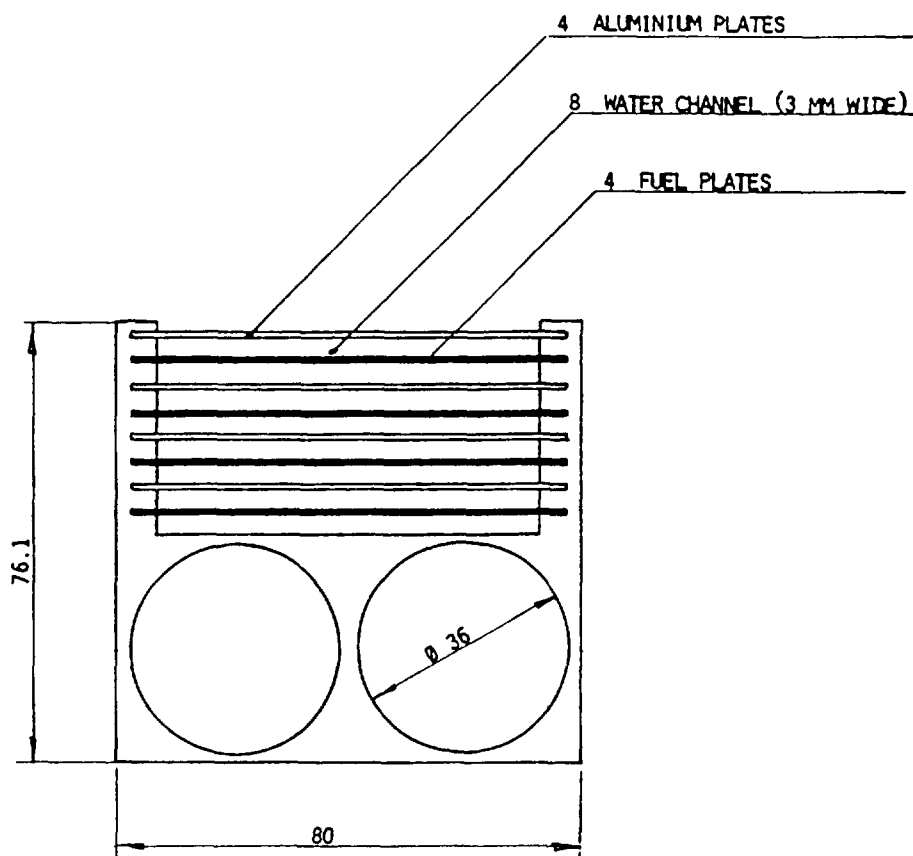


FIG. 5. Cross-section of the U_3Si plates holder.

Four fueled plates (either U_3Si or U_3Si_2) were placed in a special irradiation casing (shown in Fig. 5) located at the periphery of the core. Four other aluminum plates are roll-swaged in the sideplates of the casing. Two holes dia. 36 mm (on the rear end in relation to the reactor core) allow production of artificial elements, if required.

Each plate could be removed from the casing for examination at the end of each reactor operating cycle, i.e. after three weeks' irradiation. They were then examined visually under water and then placed on an immersed metrology bench to check fuel swelling under irradiation by measuring their thickness. The checks made also included cladding failure detection carried out before each new reactor operating cycle.

3.1.2 Irradiation of Complete Fuel Elements (U_3Si , U_3Si_2 and UAl)

The three complete fuel elements had the same geometry as a standard SILOE fuel element with 23 plates. The standard HEU UAl element was irradiated to compare the behaviour of U-Al alloys and silicides, from a swelling point of view.

Fuel Type	Complete Fuel Elements		
	Enr., %	g U/cm ³	g ²³⁵ U/Element
U_3Si	19.75	6.0	507
U_3Si_2	19.75	5.2	434
UAl	93	0.85	340

TABLE 2. LEU IRRADIATIONS IN SILOE

	Density gU _t /cm ³	Beginning of irradiation	End of irradiation	Number of scheduled cycles	Achieved cycles	Mean B U %	Thickness increase mm	Number of fission/cm ³
4 U ₃ Si plates	5,5 5,5 6 6	07/82	10/83 11/83 11/83 10/83		12	46 % (M) 53 % (M) 54 % (M) 43 % (M)	0,05 0,06 0,105 0,095	2,21.10 ²¹ 2,07.10 ²¹ 2,19.10 ²¹ 2,19.10 ²¹
4 U ₃ Si ₂ plates	2 3,7 5,2 5,4	07/84	31/01/86		15	78 % (M) 76 % (M) 75 % (M) 75 % (M)	0,035 0,045 0,045 0,055	8,80.10 ²⁰ 1,54.10 ²¹ 2,15.10 ²¹ 2,27.10 ²¹
U ₃ Si element (2 remov. plates)	6	10/84	10/10/85		9	52 % (M) 59 % (M)	0,070 0,095	1,76.10 ²¹ 2,06.10 ²¹
U ₃ Si ₂ element (2 remov. plates)	5,2	06/02/86		10	6	38 % (E)	0,01 0,015	1,1.10 ²¹ 1,1.10 ²¹
UAl element (2 remov. plates)	0,85	06/86		5	3	25 % (E)	0,02 0,02	5,5.10 ²⁰ 5,5.10 ²⁰

(M) = Measurement

(E) = Estimation

Each element had an interesting characteristic. Two of the plates of the fuel assembly were removable so that the same checks could be performed on both of these plates as those carried out on the plates irradiated separately in the special casing, i.e. visual examination and thickness measurements along five parallel tracks. In addition, the width of the water channels was checked using an eddy current device. Finally, cladding failure detection was performed at each intercycle on the element as a whole.

3.1.3 Results Obtained

U₃Si fuel (19.75%-enriched U)

The results obtained with U₃Si fuel in the plates irradiated in the casing and in the complete element are shown in Table 2 and in Figures 6 and 7.

It can be noted that the swelling becomes significant when the number of fissions exceeds 1.5×10^{21} per cm³. Below this value, it is difficult to account for what causes a plate thickness variation: swelling proper of the fuel or cladding oxidation. The swelling accelerates towards the end of the irradiation and for the highest number of fissions obtained, it can reach a value of 0.1 mm. This figure is however quite acceptable.

A clear variation of the swelling between the center and edge of the plate has been noted on all the plates examined, which confirms the relation between swelling and number of fissions, the burnup rate being higher at the center of the plates.

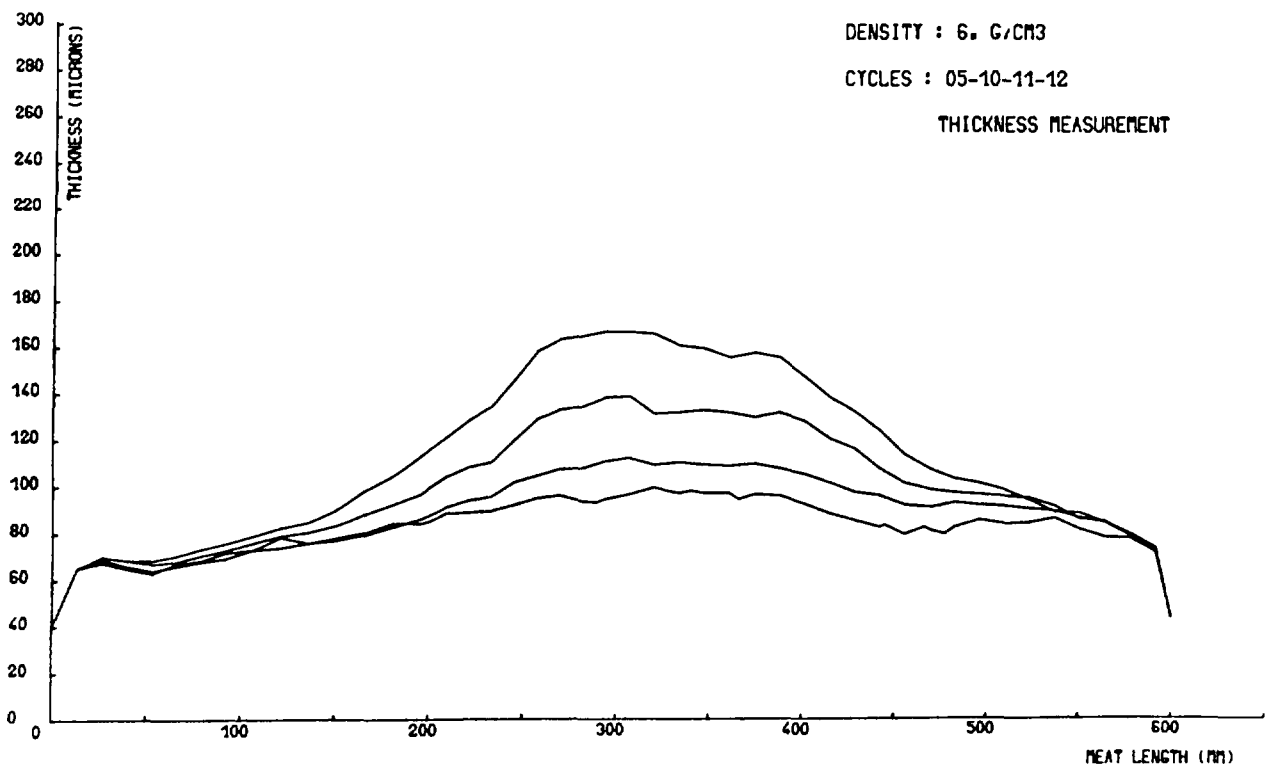


FIG. 6. Irradiation of U₃Si fuel plate.

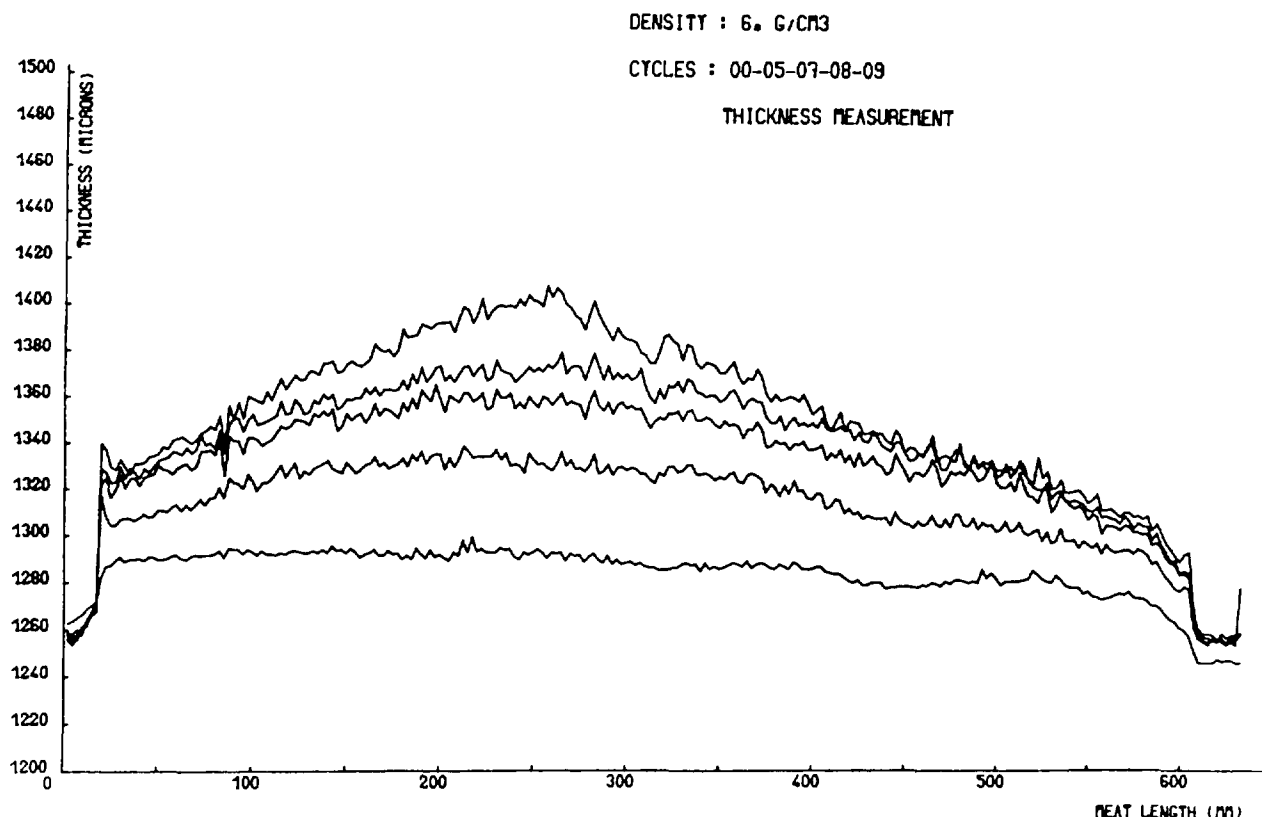


FIG. 7. Irradiation of U₃Si fuel element.

U₃Si₂ fuel (19.75%-enriched U)

The results obtained with U₃Si₂ fuel in the plates irradiated in the casing and in the complete element are shown in Table 2 and in Figures 8 and 9.

On these curves, it can be seen that the U₃Si₂ fuel presents a very small swelling, which leads to a less clear correlation between swelling and number of fissions than in the previous case. On the most heavily loaded plate (5.4 g/cm³), the number of fissions (estimated figure) is equal to $2.27 \times 10^{21} \text{ cm}^{-3}$, i.e. a value close to the physically possible maximum (approx. $2.7 \times 10^{21} \text{ cm}^{-3}$). The swellings observed are generally smaller by a factor 2 than those observed with the U₃Si.

Irradiation of a UAl element (93%-enriched U)

This irradiation involved a standard element normally used in the SILOE core, but two plates were not swaged so as to make them removable. This special feature enabled us to perform what had not been done up to now, swelling measurements of the UAl fuel used for over 20 years without any problem, so as to compare them with those carried out on the U₃Si and U₃Si₂ fuels. This irradiation program is now more than 50% completed and the results make it possible to forecast an identical behaviour to that of the U₃Si₂ fuel (Figure 10).

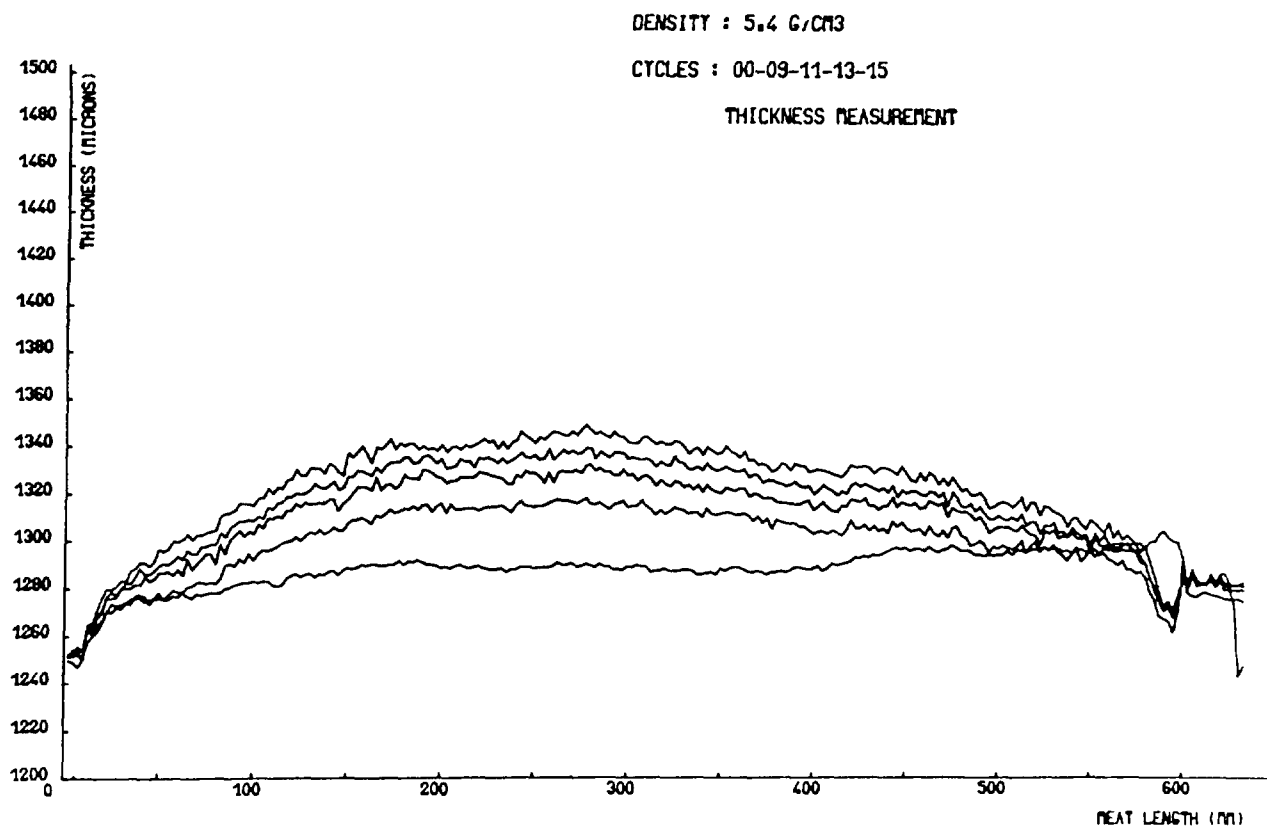


FIG. 8. Irradiation of U_3Si_2 fuel plate.

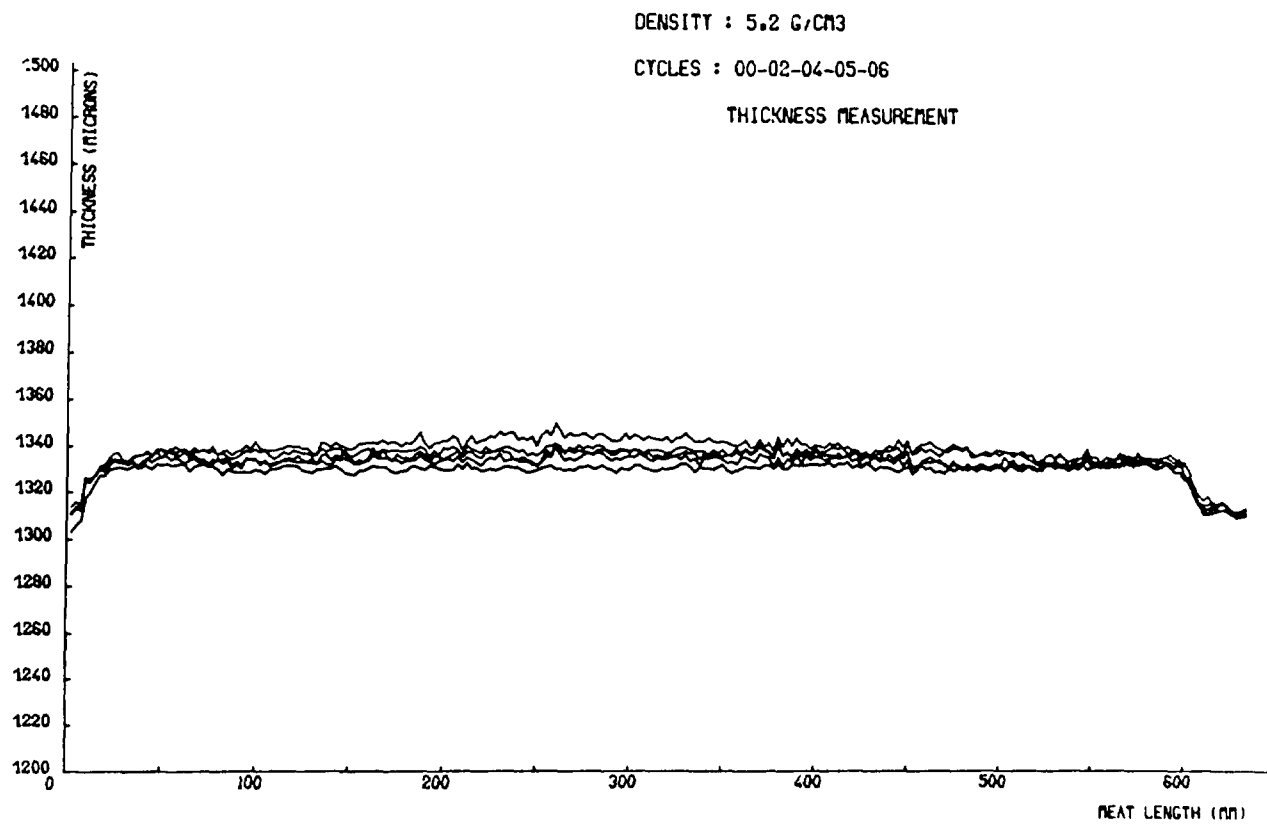


FIG. 9. Irradiation of U_3Si_2 fuel element.

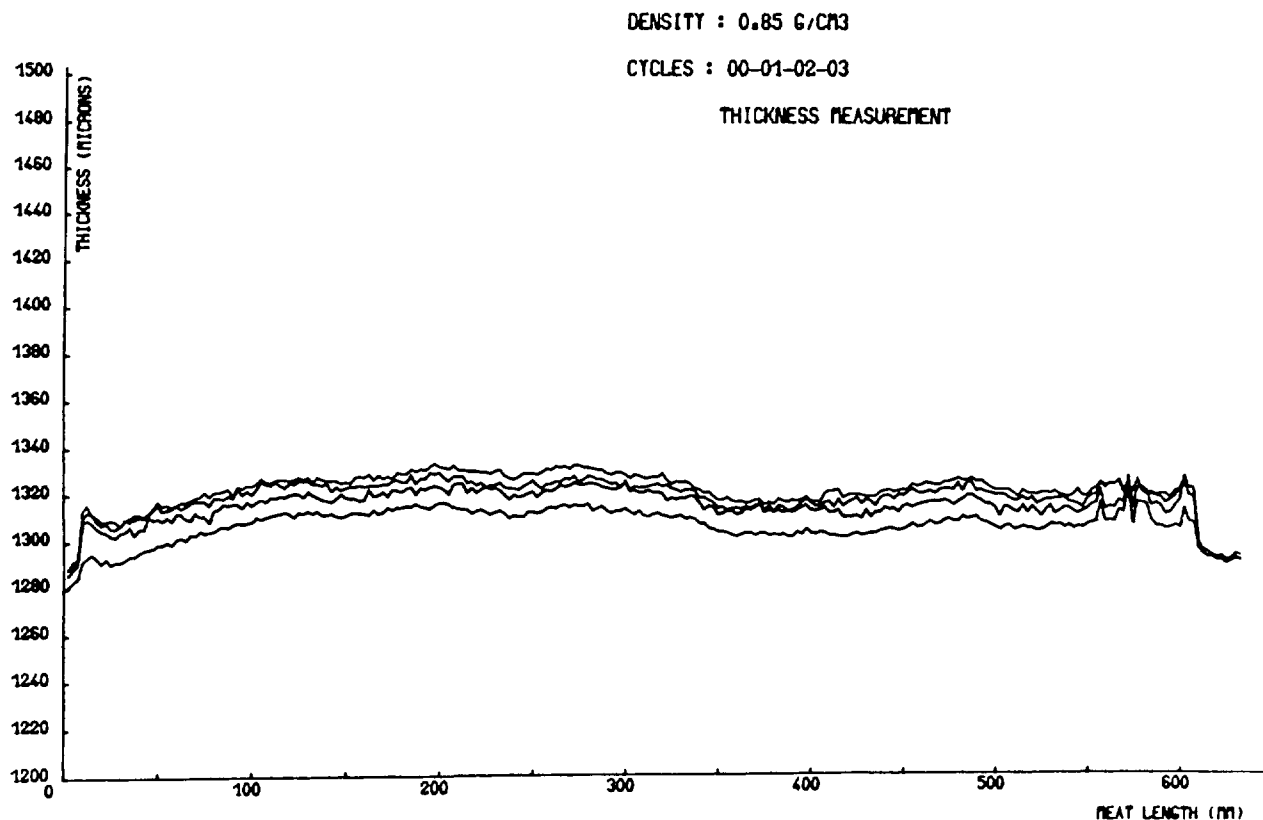


FIG. 10. Irradiation of UAI fuel element.

3.2 IRRADIATION IN THE OSIRIS REACTOR

Since January 1980, the OSIRIS reactor has been using the CAMEL low-enriched fuel which has proved fully satisfactory. However, it also appeared worthwhile carrying out irradiation of a fuel element manufactured from a silicon alloy in this reactor in order to collect as much data as possible on the behaviour of silicon-based fuels.

The fuel element was manufactured by CERCA and its irradiation began in November 1986. This element is similar in shape to the former UAI (93%) elements. Its main features are as follows:

- E = 19.70%
- d = 4.66 g/cm³
- number of plates = 21
- ²³⁵U weight/plate = 23.81 g

The density of uranium required to ensure normal reactor operation is equal to 4.66 g/cm³. This value could be obtained using a U₃Si₂ fuel which is now known to have a satisfactory behaviour. However, in order to keep the possibility of increasing the density, necessary in certain cases, and also to extend the knowledge of silicide-based fuels, we decided to use a fuel made up of a mixture of 30 wt% U₃Si and 70 wt% U₃Si₂ (U₃Si_{1.7}).

In September 1987, this element had reached an average burnup of 60% (maximum burnup of 72%), which represents approximately eight 21-day operating cycles of the OSIRIS reactor. Authorization has been obtained from the safety commission to continue irradiation of this element to an average burnup of 80%.

Before the element was inserted in the reactor, a channel measuring apparatus which had already been used elsewhere was fitted to this new element to achieve a zero point before irradiation and to enable the variations of the channel thickness measurements after each cycle to be followed.

4. CONCLUSION

All the qualification tests either in progress or scheduled in our reactors involve these silicon-based fuels. The results obtained up to now are satisfactory and enable more detailed studies to be carried out on the optimized performances which can be expected from complete cores made up of this type of fuel.

REFERENCES

1. F. Merchie, C. Baas, M. Ploujoux, "Qualification in the Reactor SILOE of Low Enriched Fuels for Research and Test Reactors," Proceedings of the International Meeting on Research and Test Reactor Core Conversions from HEU to LEU Fuels, November 8-10, 1982, Argonne, Illinois, USA, ANL/RERTR/TM-4, CONF-821155 (September 1983), pp. 242-253.
2. F. Merchie, C. Baas, and Mme M. Trotabas, "Progress Report on the Qualification in the Reactor SILOE of Low Enriched Fuels for Research and Test Reactors," Proceedings of the International Meeting on Reduced Enrichment for Research and Test Reactors, 24-27 October 1983, Tokai, Japan, JAERI-M 84-073 (May 1984), pp. 131-138.
3. F. Merchie, C. Baas, and P. Martel, "Irradiation Testing of LEU Fuels in the SILOE Reactor - Progress Report," Proceedings of the 1984 International Meeting on Reduced Enrichment for Research and Test Reactors, October 15-18, 1984, Argonne, Illinois, USA, ANL/RERTR/TM-6, CONF-8410173, pp. 146-151.
4. C. Baas, M. Barnier, J. P. Beylot, P. Martel, and F. Merchie, "Rapport D'Avancement sur la Reduction de l'Enrichissement du Combustible dans les Reacteurs Experimentaux du CEA," Proceedings of an International Meeting on Reduced Enrichment for Research and Test Reactors, October 14-16, 1985, Petten, The Netherlands, D. Reidel Publishing Company, Dordrecht, Holland (1986), pp. 49-57.
5. C. Baas, M. Barnier, J. P. Beylot, P. Martel, and F. Merchie, "Progress Report on LEU Fuel Testing in CEA Reactors," Proceedings of the 1986 International Meeting on Reduced Enrichment for Research and Test Reactors, November 3-6, 1986, Gatlinburg, Tennessee, USA, (to be published).
6. M. Barnier and J. P. Beylot, "OSIRIS, a MTR Adapted and Well Fitted to LEU Utilization - Qualification and Development," Proceedings of the International Meeting on Reduced Enrichment for Research and Test Reactors, 24-27 October 1983, Tokai, Japan, JAERI-M 84-073 (May 1984), pp. 256-267.
7. Y. Fanjas, "Silicide Fuel at CERCA - Status as of September 1987," Proceedings of the 1987 International Meeting on Reduced Enrichment for Research and Test Reactors, September 28 - October 2, 1987, Buenos Aires, Argentina (to be published).

Appendix J-4.3

FINAL REPORT ON THE IRRADIATION TESTING AND POST-IRRADIATION EXAMINATION OF LOW ENRICHED U_3O_8 -Al AND UAl_x -Al FUEL ELEMENTS BY THE NETHERLANDS ENERGY RESEARCH FOUNDATION (ECN)

H. PRUIMBOOM, E. LIJBRIJK, K.H. VAN OTTERDIJK,
R.J. SWANENBURG DE VEYE
Netherlands Energy Research Foundation,
Petten, Netherlands

Abstract

Within the framework of the RERTR-programme four low-enriched (20%) MTR-type fuel elements have been irradiated in the High Flux Reactor at Petten (The Netherlands) and subjected to post-irradiation examination. Two of the elements contain UAl_x -Al and two contain U_3O_8 -Al fuel. The test irradiation has been completed up to the target burn-up values of 50% and 75% respectively. An extensive surveillance programme carried out during the test period has confirmed the excellent in-reactor behaviour of both types. Post-irradiation examination of the test elements, comprising of dimensional measurements, burn-up determination, fuel metallography and blister testing, has confirmed the irradiation experiences. Good agreement between calculated and measured power and burn-up characteristics has been found. A survey of the test element characteristics, their irradiation history, the irradiation tests and the PIE results is given in this report.

1. INTRODUCTION

Four 20% enriched MTR-type fuel elements have been test irradiated in the 45 MW High Flux Reactor at Petten (The Netherlands) in the frame of an agreement between the Netherlands Energy Research Foundation (ECN), Argonne National Laboratory (ANL), NUKEM (F.R.G.) and CERCA (France). The purpose of the irradiation programme was to demonstrate the reliable and safe behaviour of high density UAl_x -Al and U_3O_8 -Al type fuel elements under application conditions which are typical for medium powered material testing reactors at ^{235}U burn-ups up to 75%. Further verification of this behaviour has been achieved by extensive Post Irradiation Examination (PIE).

All irradiations have been completed and the associated surveillance programmes, such as intermittent neutron dosimetry, plate deformation control and visual inspection have been rounded off. PIE has been completed on all four elements. The results will be reported in this report.

A detailed description of the test elements, of the irradiation characteristics and of the methods applied for inspection and characterization of the elements before and during irradiation is given in [1]. A summary of this information is given below.

2. THE PETTEN HIGH FLUX REACTOR

The High Flux Reactor (HFR) is part of the Joint Research Centre of the European Community at Petten (The Netherlands). It is a multi-purpose test reactor of the ORR-type and utilized for fundamental research,

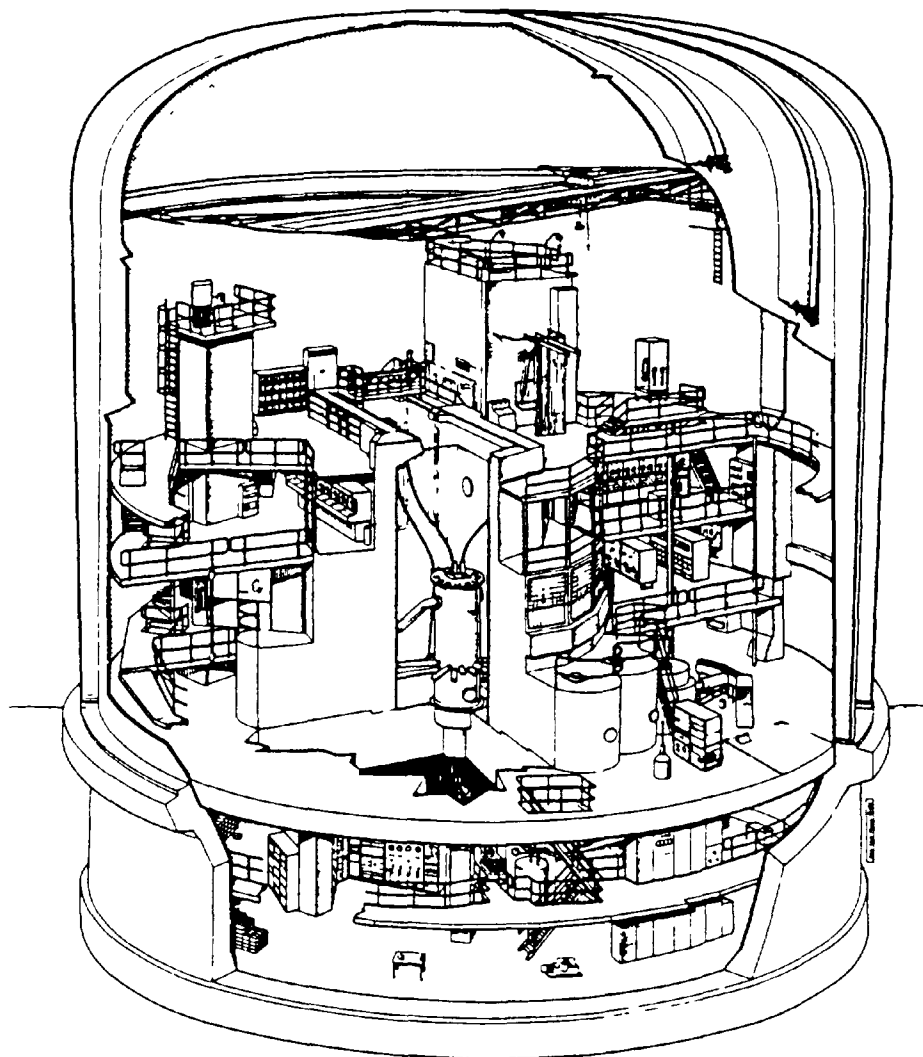


FIG. 1. Isometric drawing of HFR Petten.

reactor fuel and materials testing, safety experiments, radioisotope production and various non-destructive testing activities, such as neutron activation analysis and neutron radiography. It is water cooled and moderated, operates at a thermal power of 45 MW and has a nine-by-nine core configuration with 33 fuel elements, 6 control rods, 25 reflector elements and 17 irradiation experiment positions.

Figures 1 and 2 give an impression of reactor building and core lay-cut.

3. THE TEST ELEMENTS

All test elements contain 19.75% enriched uranium at a volume density in the meat of 2.1 g/cm^3 . Their design has been adapted to the existing configuration and dimensions of the HFR core, but some significant changes with respect to the standard HFR-HEU fuel elements had to be implemented in order to accommodate the required ^{235}U loading of 20 g per plate, to maintain thermohydraulic safety and to provide for the required irradiation characterization and surveillance measurements.

The changes comprise a.o.

- a) fuel meat thickness of 1.32 mm (instead of 0.51 mm) in order to achieve required ^{235}U loading

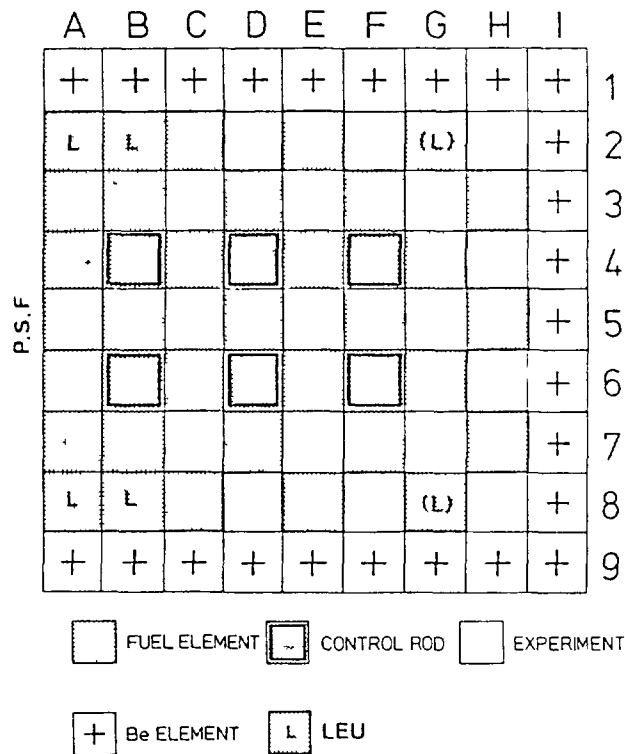


FIG. 2. Standard core loading pattern for the HFR Petten.

- b) 16 flat fuel plates (instead of 23 curved plates and non fuelled outer plates, in order to maintain required cooling channel widths
- c) square (instead of round) upper inlet sections in order to improve accessibility for cooling channel width measurements and neutron dosimetry
- d) longitudinal slots in outer plates in order to apply permanent and reloadable neutron fluence monitors.

In addition, one of each type test element has been provided with cadmium-wires (10 wires in each side plate, 0.5 mm diameter, 20µ aluminium clad) in order to test the effectiveness of cadmium as a burnable poison in comparison to the presently applied boron-absorber.

The materials specification for the test elements is given in Table 1. Figures 3 and 4 show various technical details.

4. IRRADIATION HISTORY

PFR core positions A2, A8, B2, P8, C2 and G2 (see fig. 2) were selected for the irradiations. Test element power in these positions ranged from 0.5 to 1.2 MW, which corresponds with maximum heat flux densities of 75 to 150 W/cm². In order to compensate for such power differences and for the flux gradients at the peripheral core positions the elements were periodically switched between the north and south position. The overall irradiation period for all four test elements extended from November 1981 to April 1983.

5. IRRADIATION SURVEILLANCE

5.1. Visual inspection

Each test element was subjected to careful visual observation after each irradiation cycle. No abnormalities have been observed.

TABLE 1. MATERIAL SPECIFICATIONS FOR LEU TEST ELEMENTS

	Type : LN-01-CD LN-02 U_3O_8 -Al (Nukem)	Type : LC-01-CD LC-02 $U Al_x$ -Al (Cerca)
<u>Fuel</u>		
Fuel meat composition	U_3O_8 -Al	$U Al_x$ -Al
Uranium - loading		
- per element	1660 \pm 35	1687 \pm 35 g
- per plate	104 \pm 2	105 \pm 2 g
- surface density	280 10^{-3}	280 10^{-3} g / cm ²
- volume density	2.1	2.1 g / cm ³
Enrichment	19.75 \pm 0.2 - 0.5	19.5
U-235 loading		
- per element	328 \pm 6	329 \pm 6 g
- per plate	20.5 \pm 0.4	20.6 \pm 0.4 g
- surface density	54.1 10^{-3}	54.2 10^{-3} g / cm ²
- volume density	0.41	0.41 g / cm ³
<u>Cadmium</u> - composition (1)	99.9%	99.9% pure grade
- nr. of wires	20	20
- diameter	0.05	0.05 cm
- weight per element	20.4	20.4 g
<u>Aluminium</u>		
- in meat	pure Al.	A 5 NE
- clad and frame	Al Mg 1 (or 2)	AG 2 NE (3 NE, 4 NE)
- side boxes and outside plates	Al Mg Si 7, F32	AG 3 NE
- end boxes	Gk Al Si 5 Mg	Cr-Al Si 5 Mg
- welding additure	Al Si 5 (or 12)	AG 3 NE

(1) Only in case of LN-01-CD and LC-01-CD.

5.2. Cooling channel width measurements

Measurements of the width of several preselected cooling channels have been taken on each test element at regular intervals during the irradiation. The measurements were taken by means of a specially developed ultrasonic scanning device with the following technical features:

- three (spring loaded) LS-sensors per cooling channel, providing three vertical scans with a resolution of 5 μ
- automatic recording of sensor position, signal and temperature
- very precise lateral positioning of the measuring device, allowing fast and easy access to the selected cooling channel
- special device for intermediate sensor recalibration.

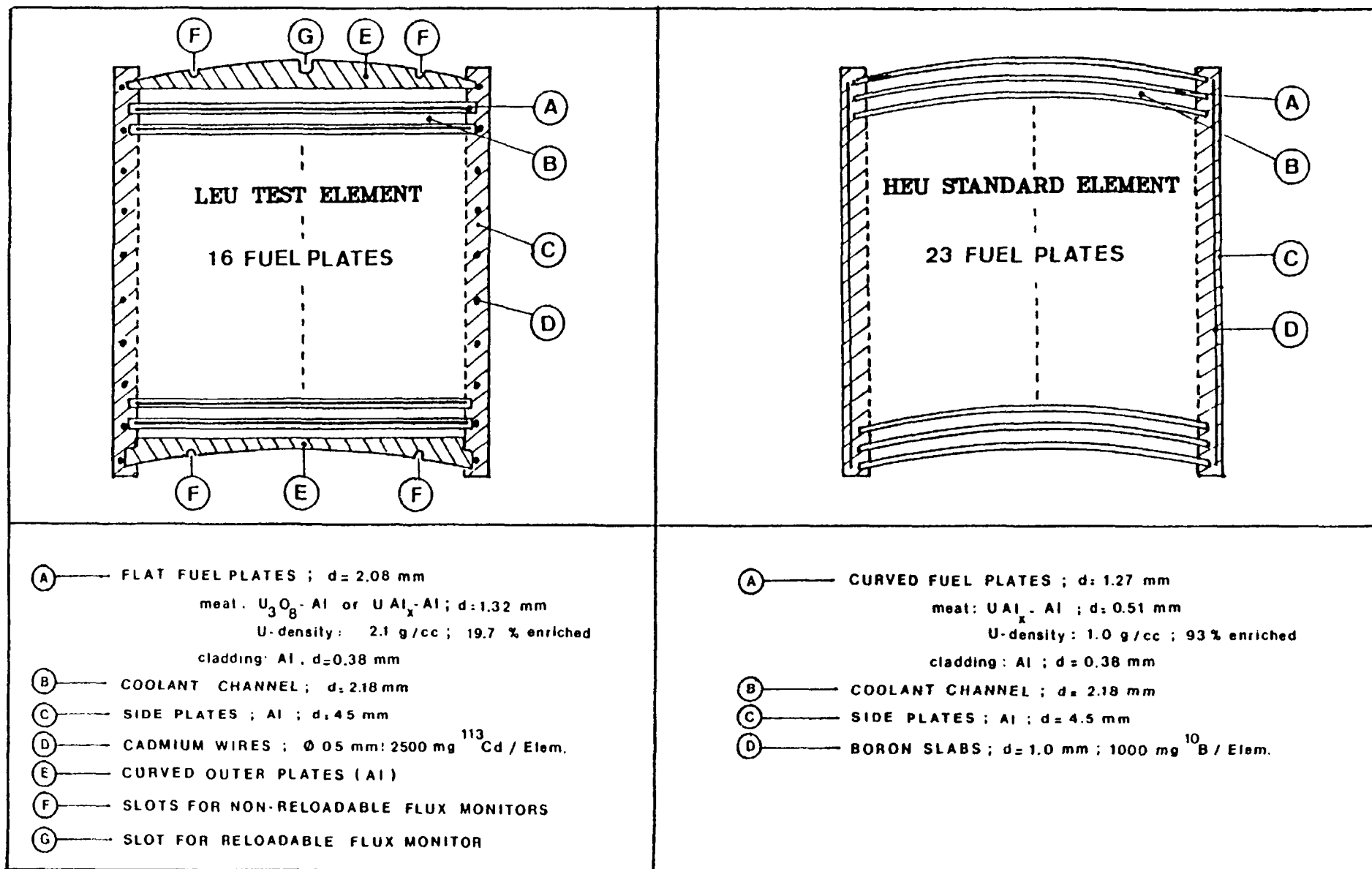


FIG. 3. Specifications of LEU test element and HEU standard element.

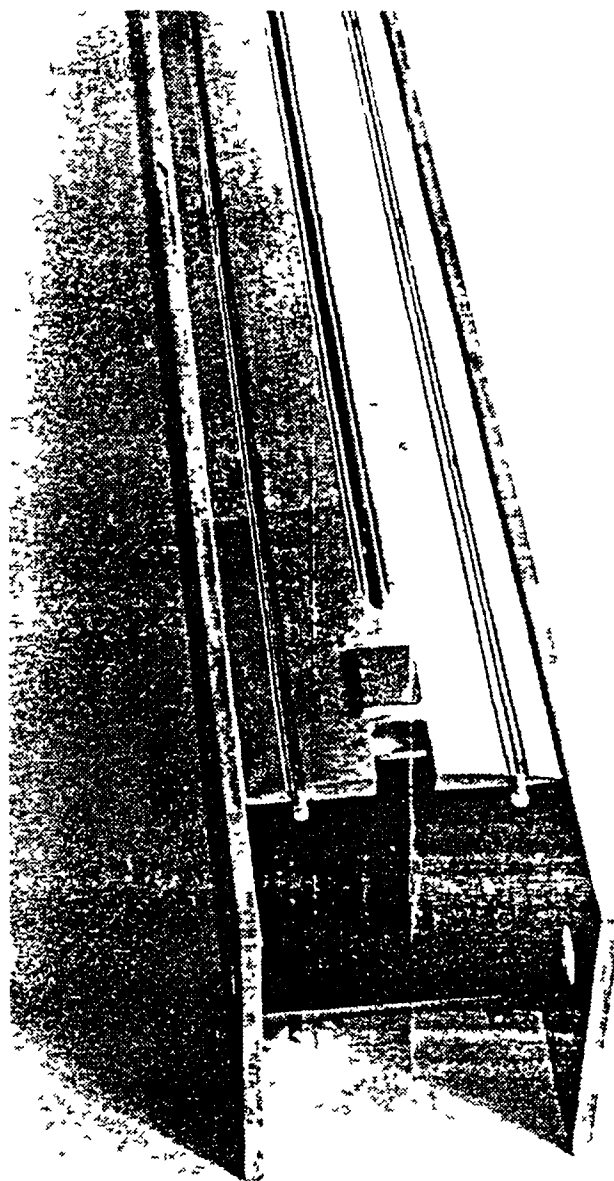


FIG 4 Inlet section of LEU test element

Figure 5 shows in detail the measuring sensors, more detailed technical information is given in [2].

Some typical channel width profiles are given in figures 6 and 7. Average cooling channel width values as a function of burn-up for all four test elements are shown in figure 8.

The general conclusion from these measurements is that no cooling channel width changes and thus no fuel plate deformations of any significance have occurred.

A detailed survey of the cooling channel width measuring procedures and results is given in [2].

5.3. Flux, fluence and power determination

Test fuel power, burn-up and isotopic composition during irradiation have been deduced from nuclear calculations and neutron dosimetry. The nuclear calculations were performed by means of a two dimensional diffusion code.

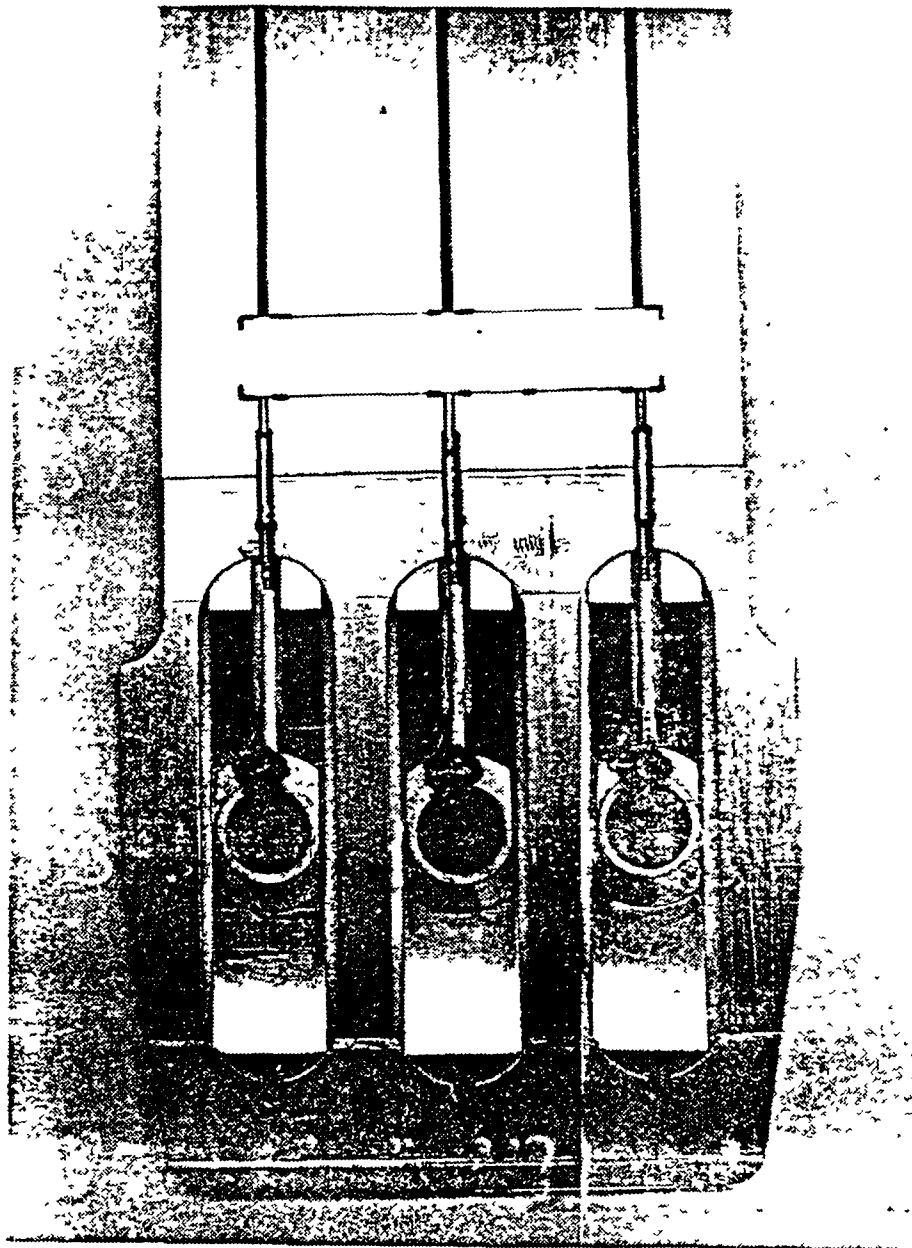


FIG. 5. Mounting configuration of ultrasonic sensors

For the test elements a representative calculation model consisting of a fuel region surrounded by two side plates and two outer plates has been defined.

For several ^{235}U and ^{113}Cd depletion values the nuclear data for this calculation model were determined and stored on a library file. For the actual $^{235}\text{U}/^{113}\text{Cd}$ combination a quadratic interpolation procedure was applied.

The depletion of the uranium contents of the LEU-elements was calculated accounting for burn-up chains of ^{235}U and ^{238}U . The calculations indicated that for a burn-up value of 75% the energy produced by ^{239}Pu and ^{241}Pu amounts to about 24% of the total power (see figure 10). The conversion ratio for the elements is about 0.17.

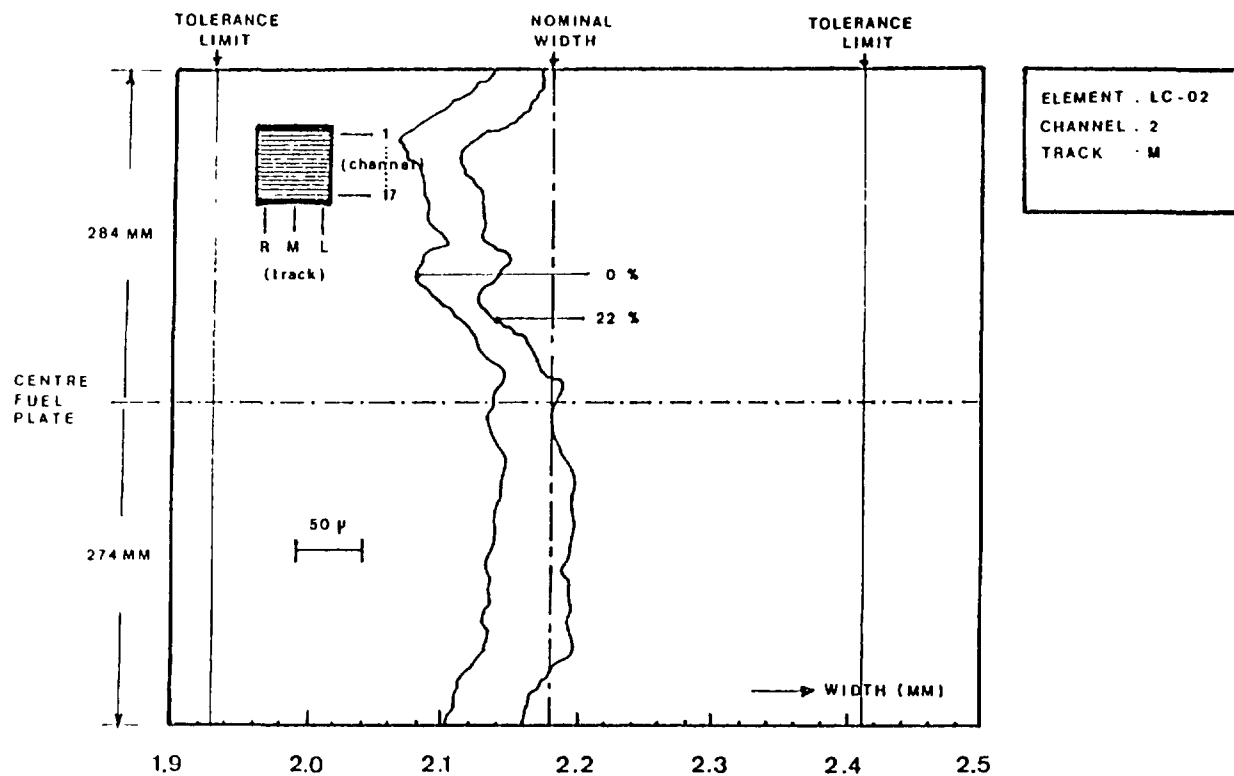


FIG. 6. Channel width as a function of height, with the burn-up as a parameter.

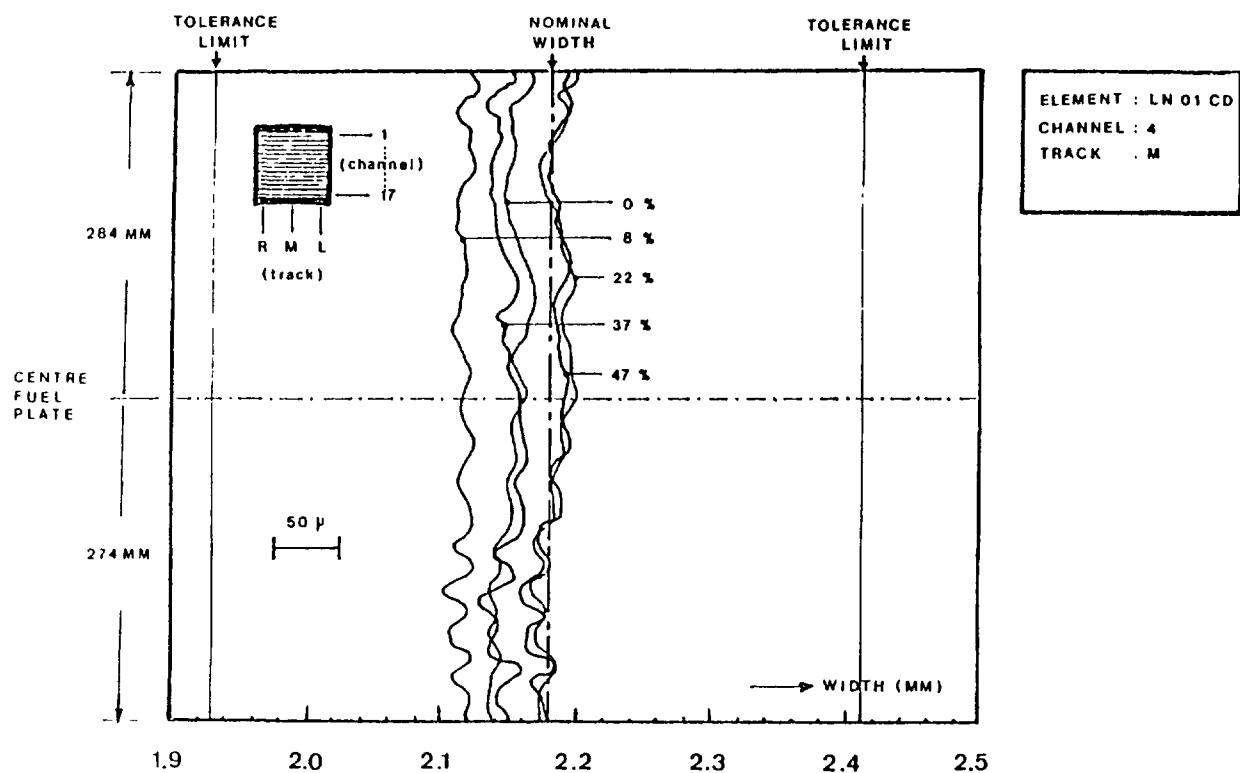


FIG. 7. Channel width as a function of height, with the burn-up as a parameter.

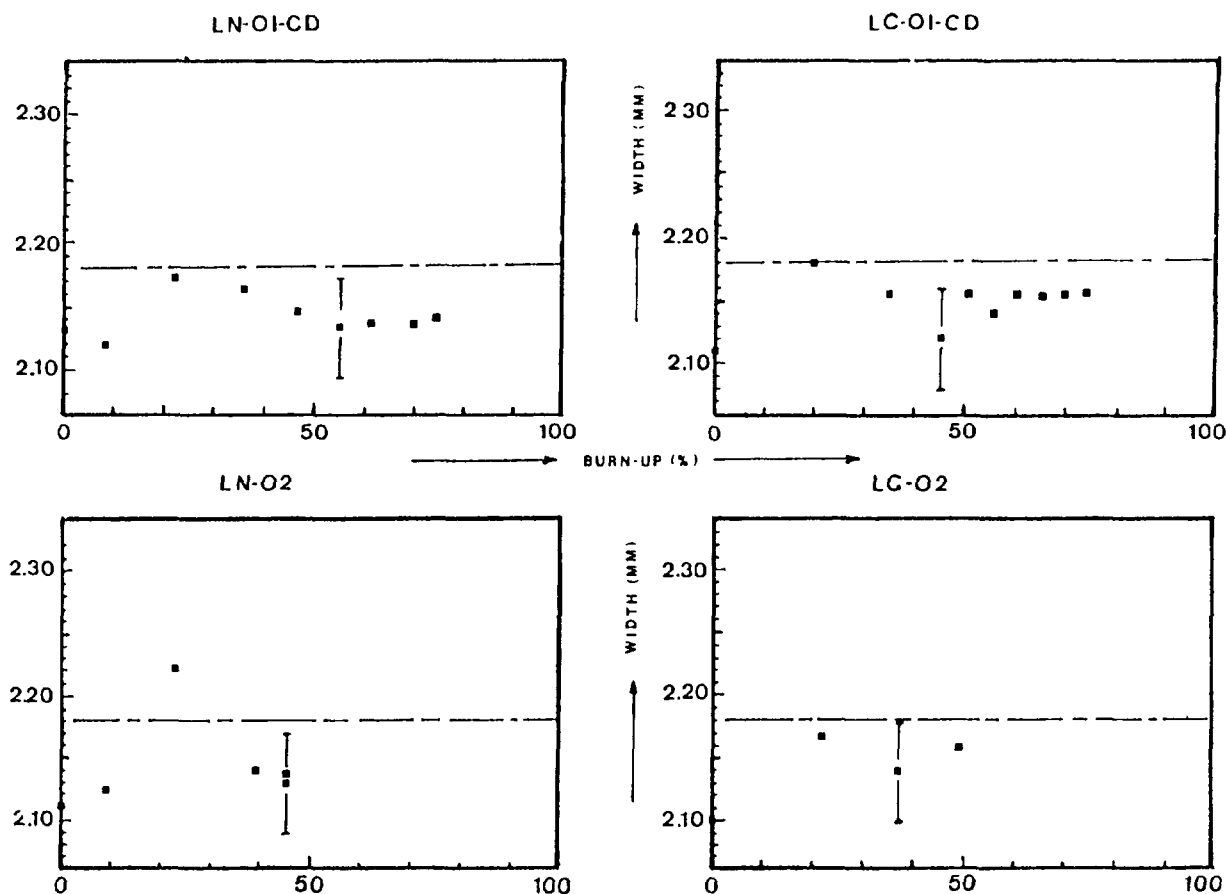


FIG. 8. Average coolant channel width as a function of burn-up.

For verification of the nuclear calculations extensive neutron dosimetry measurements were carried out, comprising

- application of four permanently installed fluence monitors in the outer plates of each test element (for overall burn-up verification)
- application of one reloadable fluence monitor in one of the outer plates, which was exchanged after each reactor cycle (for stepwise burn-up determination)
- application of up to 15 flux monitors devided over 5 cooling channels per element for flux distribution measurements at regular irradiation intervals.

From the detailed flux measurements some conclusions could be drawn :

- Especially in the LEU-elements without cadmium wires the radial flux and power gradients were somewhat (10 to 15%) higher than those in the ^{238}U -poisoned FFL elements. This is mainly caused by the ^{238}U resonance absorption, by the non fuel containing outer plates and by the absence of poison in the side plates.
- The presence of cadmium wires in the side plates of LEU-elements LN-OI-CD and LC-OI-CD, resulted in a minor reduction of above mentioned power peaking (5%).
- Power production values as derived from measured flux results and from calculations were in good agreement ($\pm 7\%$).

The results of the flux measurements over the total irradiation period are in good agreement with the results of gamma scanning and chemical burn-up analyses which are performed as part of the BNL programme.

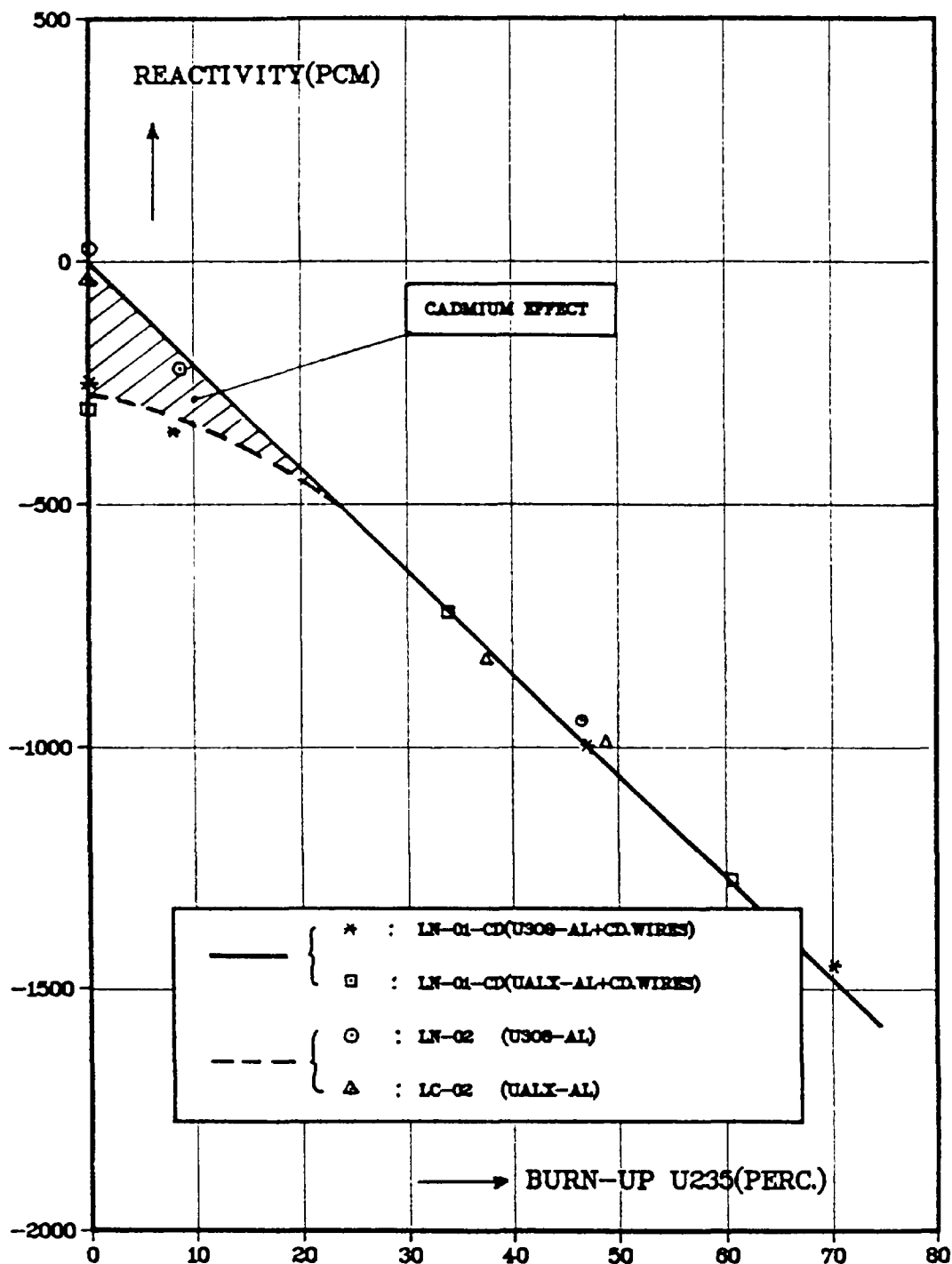


FIG. 9. Reactivity as a function of burn-up for LEU test elements as measured in position D5 of the HRF Petten.

5.4. Reactivity measurements

Periodical reactivity measurements have been performed for two reasons :

- determination of the reactivity of LEU-elements as a function of burn-up.
- determination of effectiveness of cadmium as a burnable poison.

The measurements have been performed by comparing the reactivity of the LEU-elements with that of a fresh HEU-element containing 404 ^{235}U and 1000 mg ^{10}B . Central core position D5 was selected for this purpose. It appeared that the reactivity value for the fresh LEU-elements without cadmium wires (LN-02 and LC-02) is equal to that of the fresh HEU-element.

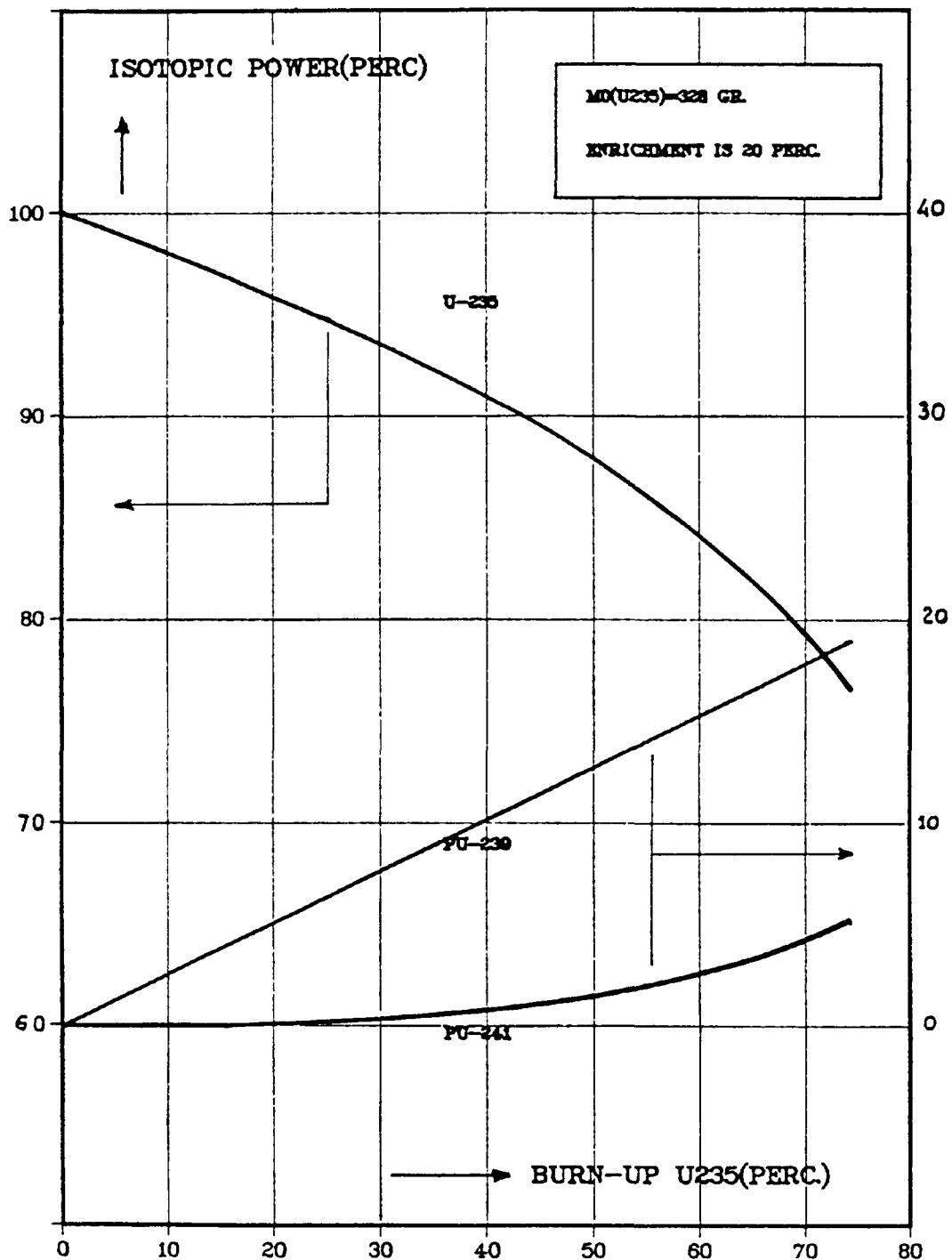


FIG. 10. Power production per fissile isotope in LEU test elements as a function of burn-up.

The initial effect of the cadmium wires in the LEU-elements (LN-01-CD - LC-01-CD) was measured to be -300 pcm. Measurements at increasing burn-up values indicated a reactivity development as shown in figure 9. In this curve the effects of samarium, xenon and bulk fission products have been included.

Complete depletion of the cadmium wires is reached after some 23% burn-up of the LEU-elements. This burn-up figure corresponds with a thermal fluence of about $0.54 \cdot 10^{21} \text{ cm}^{-2}$. The reactivity decrease due to burn-up in core position D5 is about 6.5 pcm/gr ^{235}U .

6. POST-IRRADIATION EXAMINATION

6.1. PIE methods

The PIE-programme has been carried out to verify the following test element characteristics

- external appearance (corrosion effects, blisters, local deformations, cracks, etc.)
- fuel element and fuel plate dimensions
- burn-up and burn-up distribution
- isotopic content of fuel
- temperature required for blister formation
- metallurgical composition and structure of fuel zone.

Special measuring devices and auxiliary equipment have been developed for the dismantling, handling and examination activities, such as

- an electrically heated dummy element in order to determine the fuel plate temperatures which could be expected during PIE
- measuring devices for fuel plate thickness scanning and fuel element length, bow and twist determination
- cutting devices for fuel plate sampling and segmentation
- an electrically heated furnace for blister temperature determination
- a special fuel plate container for intermediate fuel plate storage adapted to post-PIE fuel disposal transport requirements.

In addition to these hardware developments the software required for execution and evaluation of the γ -scanning measurements had to be adapted.

The scanning and measuring pattern for the various examinations has been chosen such that precise comparisons with pre-irradiation characterization results would be possible.

PIE has been completed on each of the four test elements.

6.2. PIE results

6.2.1. External appearance of the test elements

Apart from some superficial scratches on the outer plates (probably caused by in-reactor handling) no damage or local deformations have been observed.

Temperature sensing strips were used by means of which the temperature predictions obtained by the electrical dummy element have been verified. Maximum fuel element temperature was 80°C.

6.2.2. Dimensional check of complete elements

By means of a special measuring device all essential external dimensions as well as bow and twist of the elements were determined and compared with pre-irradiation measured data. No irradiation-induced changes have been detected.

6.2.3. External appearance and dimensions of fuel plates

Dismantling of the 16 fuel plates was carried out by longitudinal milling of the side plates. For fuel plate storage and identification a special container has been made.

Fuel plate inspection revealed no abnormalities. Some temperature induced colouring of the fuel plates as well as some minor corrosion effects could be observed. Measurements of corrosion layer thickness and structure have not been carried out.

For fuel plate thickness measurements a device shown in figure 12 has been applied. It consists of two opposite spherical shaped sensors (one fixed and the other movable) with the fuel plate in between.

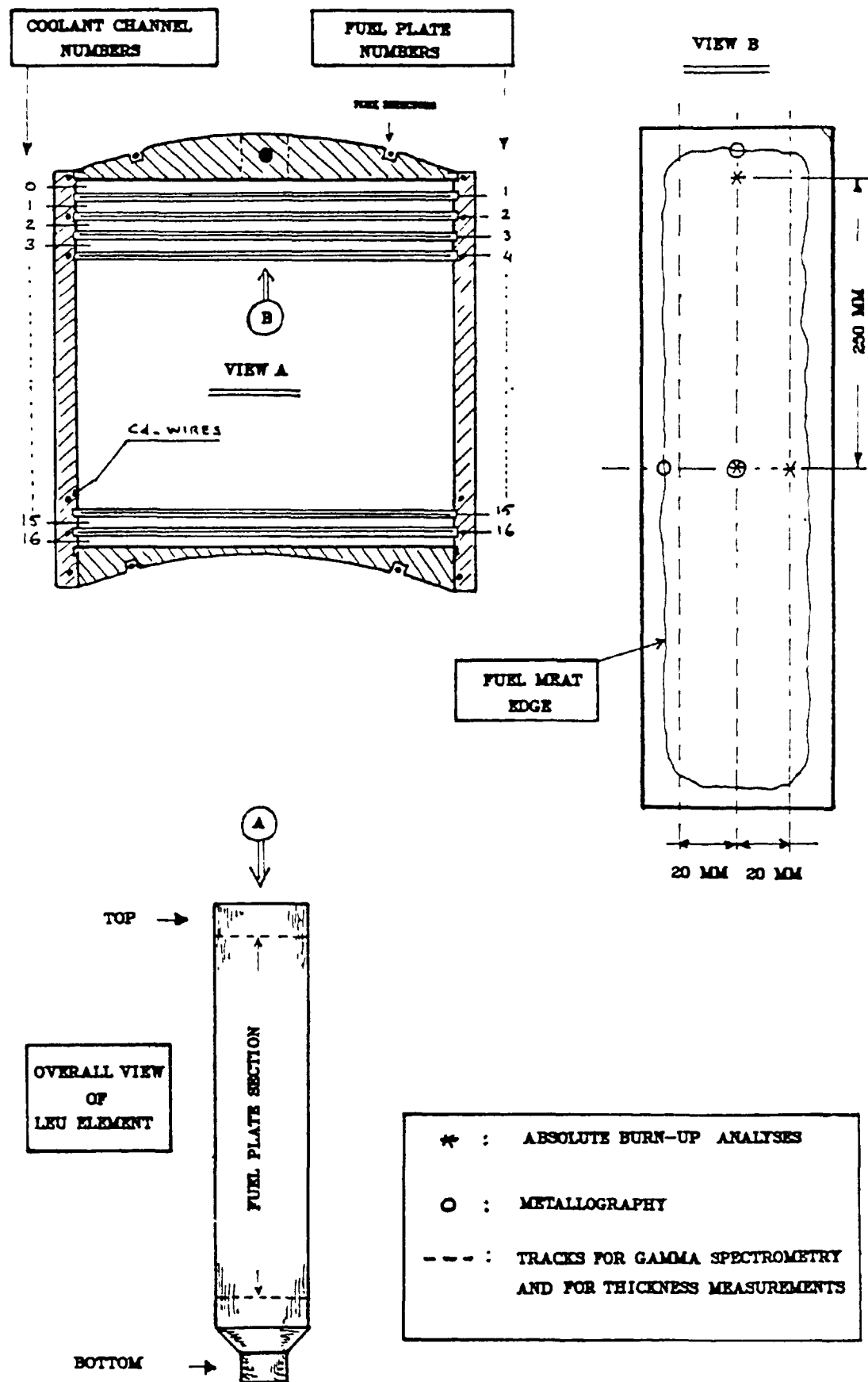


FIG. 11. Definition of plate and channel numbers and locations of measuring tracks and sampling.

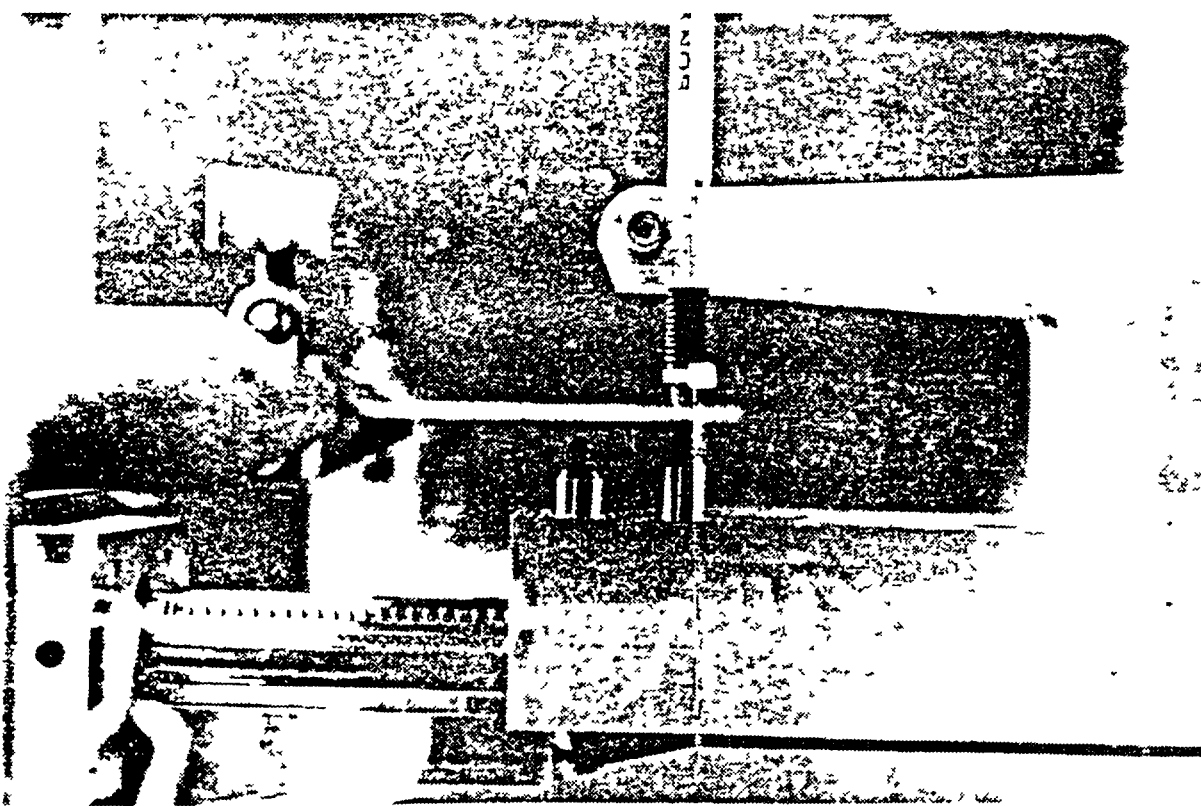
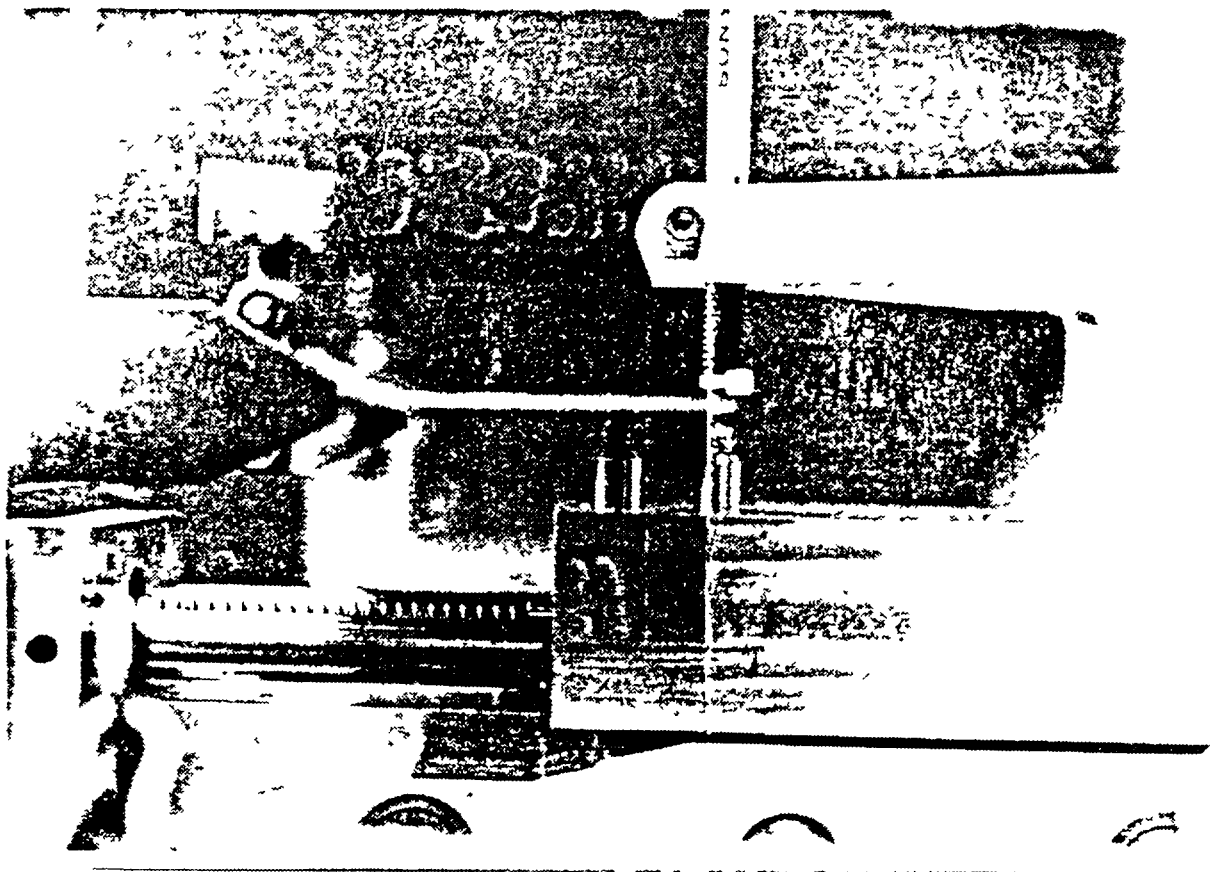


FIG 12 Detail of measuring device for plate thickness measurements

By moving the fuel plate the thickness profile is measured with the movable upper sensor (magnus scale principle). A thick cover is provided in order to guide the plate to the measuring position without damaging the two measuring sensors. Longitudinal as well as latitudinal tracks can be performed. The device was calibrated using steel calibres with various thicknesses in the range of interest.

In figure 13 and 14 the thickness profiles of the central fuel plates (no. 9) of two elements are presented. The profiles are rather smooth with some local spikes, probably caused by oxidation products.

Similar profiles for a fresh fuel plate are given in figure 15. They show no significant differences with those of the irradiated plates. Comparison of the measured thickness profiles of the irradiated plates with the plate width measurements made after fabrication yields only minor differences.

6.2.4. Gamma-scanning of fuel plates

For the determination of the relative burn-up distribution, the fission product activity in the LEU fuel plates was measured. Of each element five plates (1, 4, 8, 9.17 and 16) were selected. Three longitudinal scans and one latitudinal scan were performed per selected plate (see figure 11). The applied intervals for the axial scans and the latitudinal scan are 25 mm and 5 mm respectively. The measuring equipment consists of a fuel plate holder, provided with an accurate displacement mechanism, a collimator (2 x 2 mm opening), a Ge-Li detector, a 4096 channel spectrum analyser and a magnetic tape unit for data storage. Plotting and data evaluation is performed on an off-line computer (CYBER 75).

The following 9 long living fission products were measured:

Isotopes	Energy
Cs-137	661.6 keV
Ce-144	664.8 keV
Ce-144	125.5 keV
Ce/Pr-144	696.4 keV
Ce/Pr-144	2185.8 keV
Ru-103	497.1 keV
Ru-106	622.0 keV
Zr-95	724.2 keV
Nb-95	765.2 keV

The measured activity profiles are corrected for decay and for the influence of the dead time of the measuring circuit. Figures 16 and 17 show some Cs-137 activity profiles for the LEU-elements LN-02 and LC-02. The measurements show that the axial scans per element have very similar shapes ($\pm 2\%$). The measured profiles have been smoothed by the application of a fifth degree polynomial curve fitting procedure. From the Cs-137 profiles in figures 16 and 17 it can be concluded that the shape factors for the vertical and horizontal burn-up distribution are 1.25 and 1.20 respectively.

The maximum of the vertical burn-up distribution is located at about 10 cm below core mid height, which is in good agreement with the measured vertical thermal flux density distribution. From the measured distributions for burn-up and thermal flux density it can be derived that the spatial power distribution has been rather flat at the end of the irradiation period.

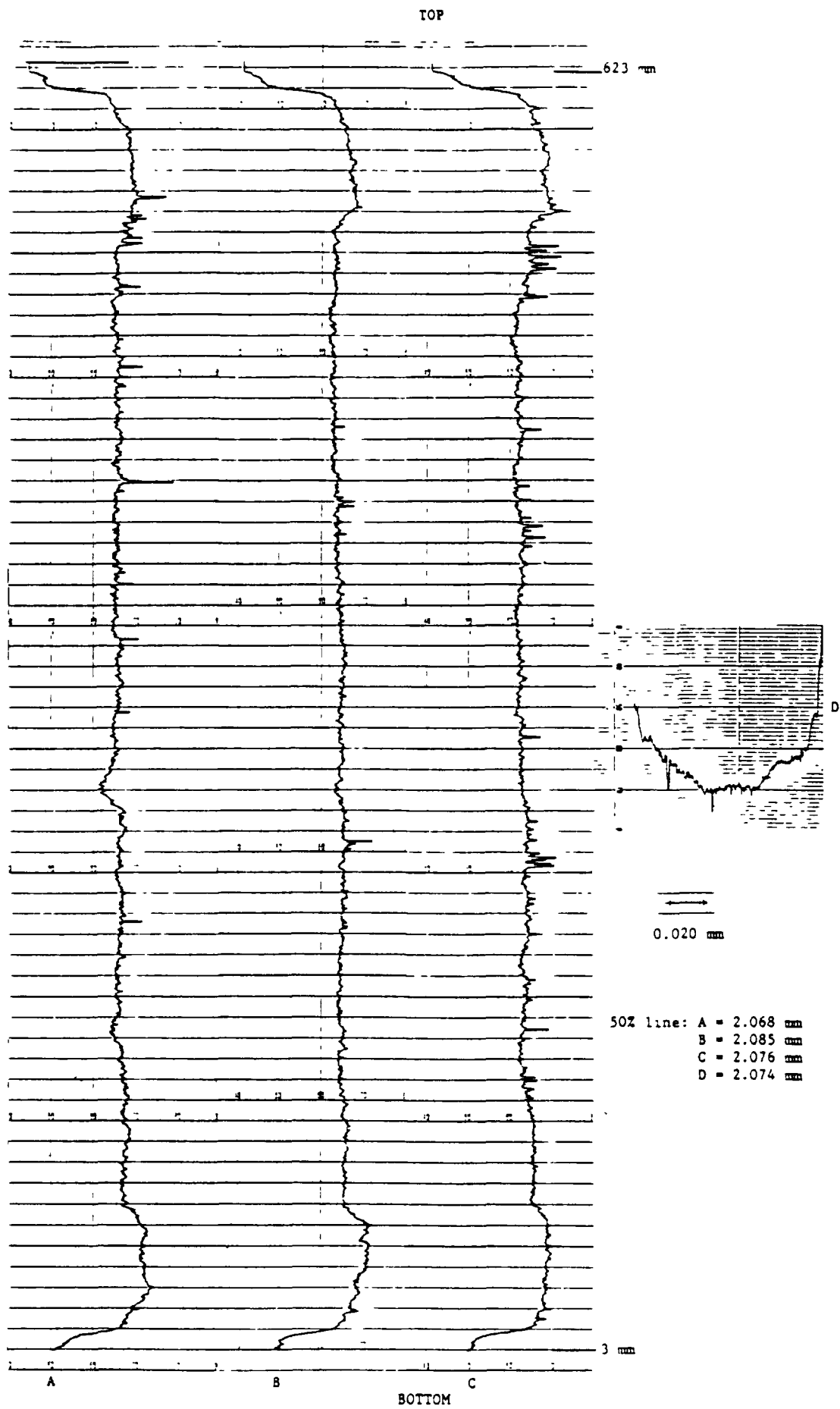


FIG. 13. Thickness profiles of LEU fuel plate (LN-02 plate 9 = YC 5374).

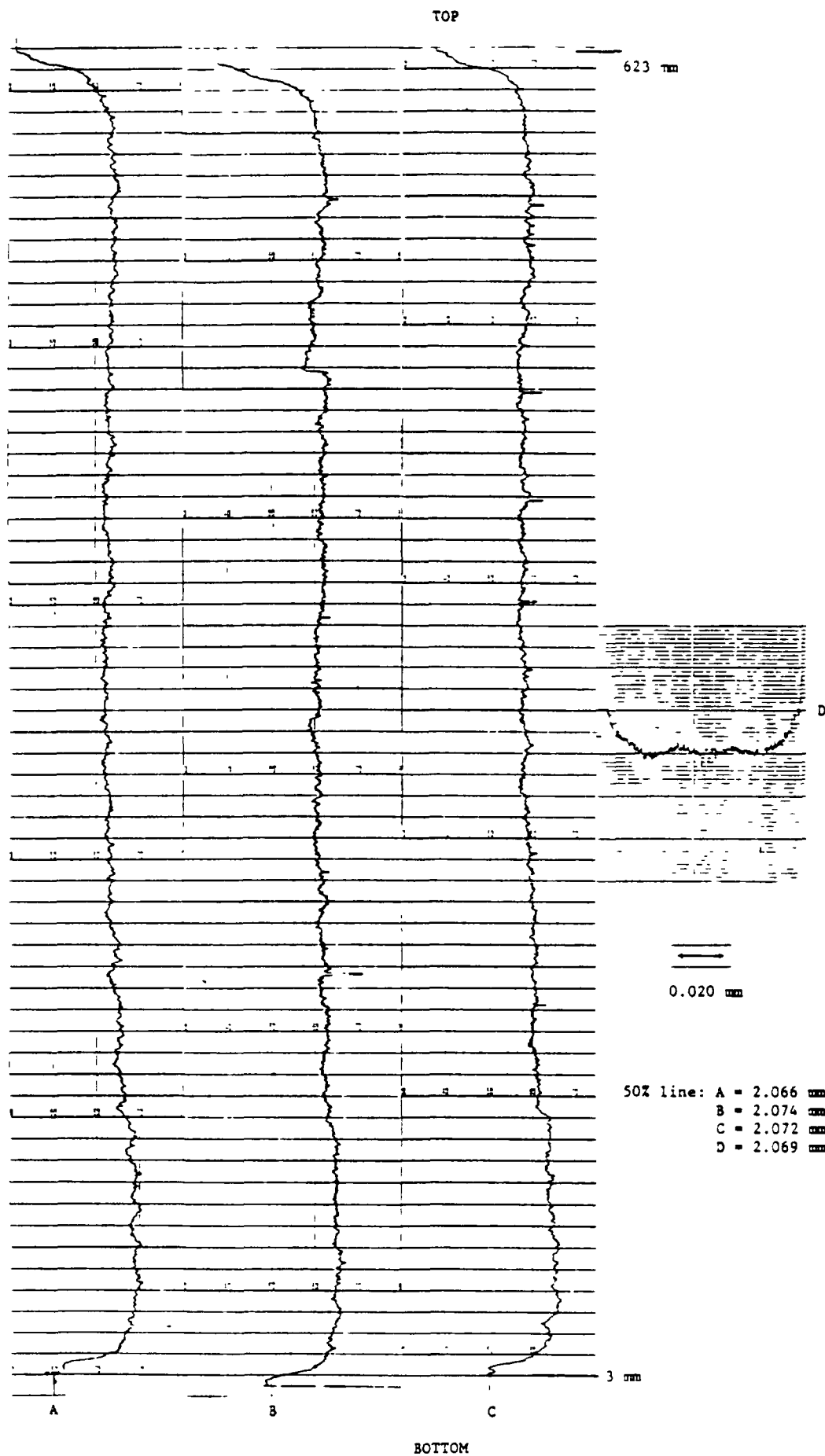


FIG. 15. Thickness profiles of unirradiated LEU fuel plate ($\text{U}_3\text{O}_8\text{-Al}$, plate YC5361).

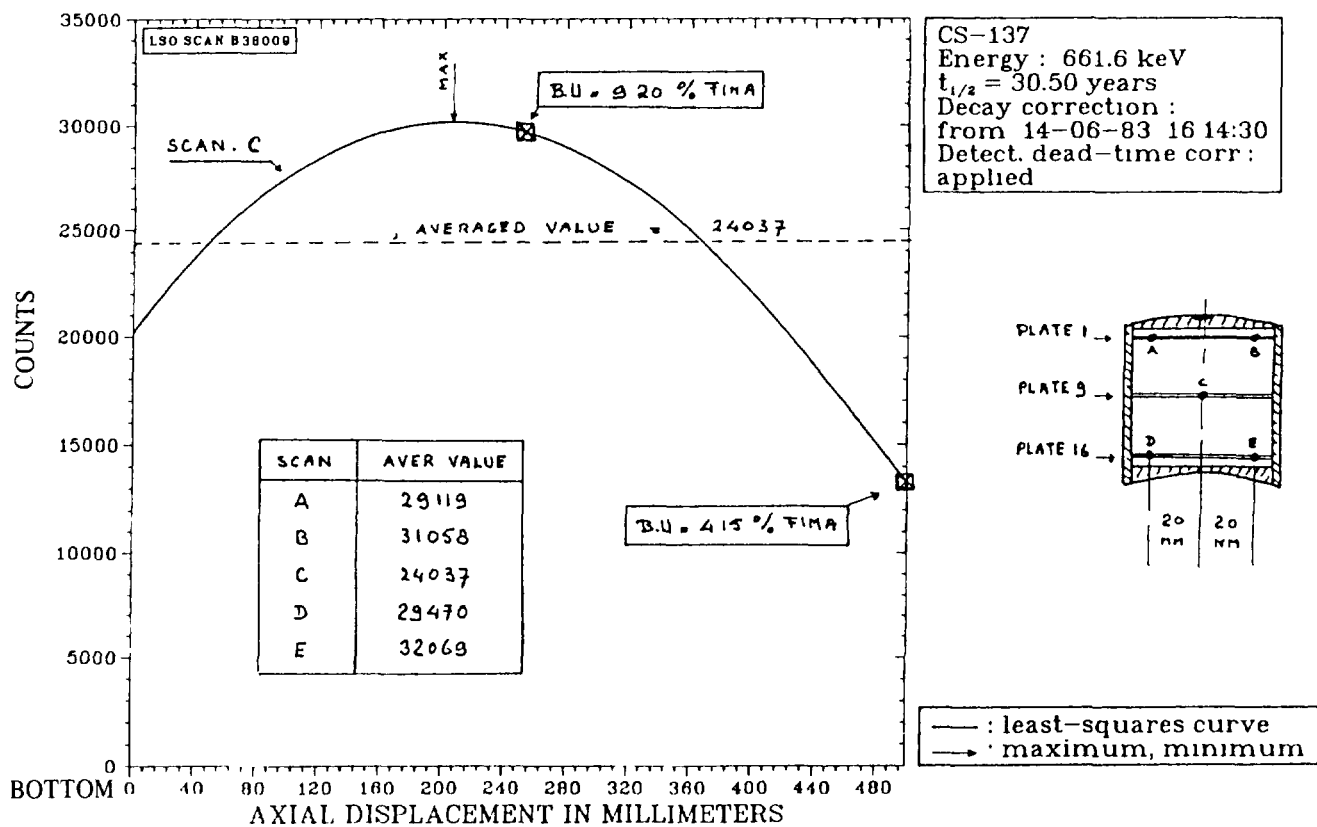


FIG. 16. Results of gamma spectrometry on LEU fuel plate 9 (YC5374) of LN-02.

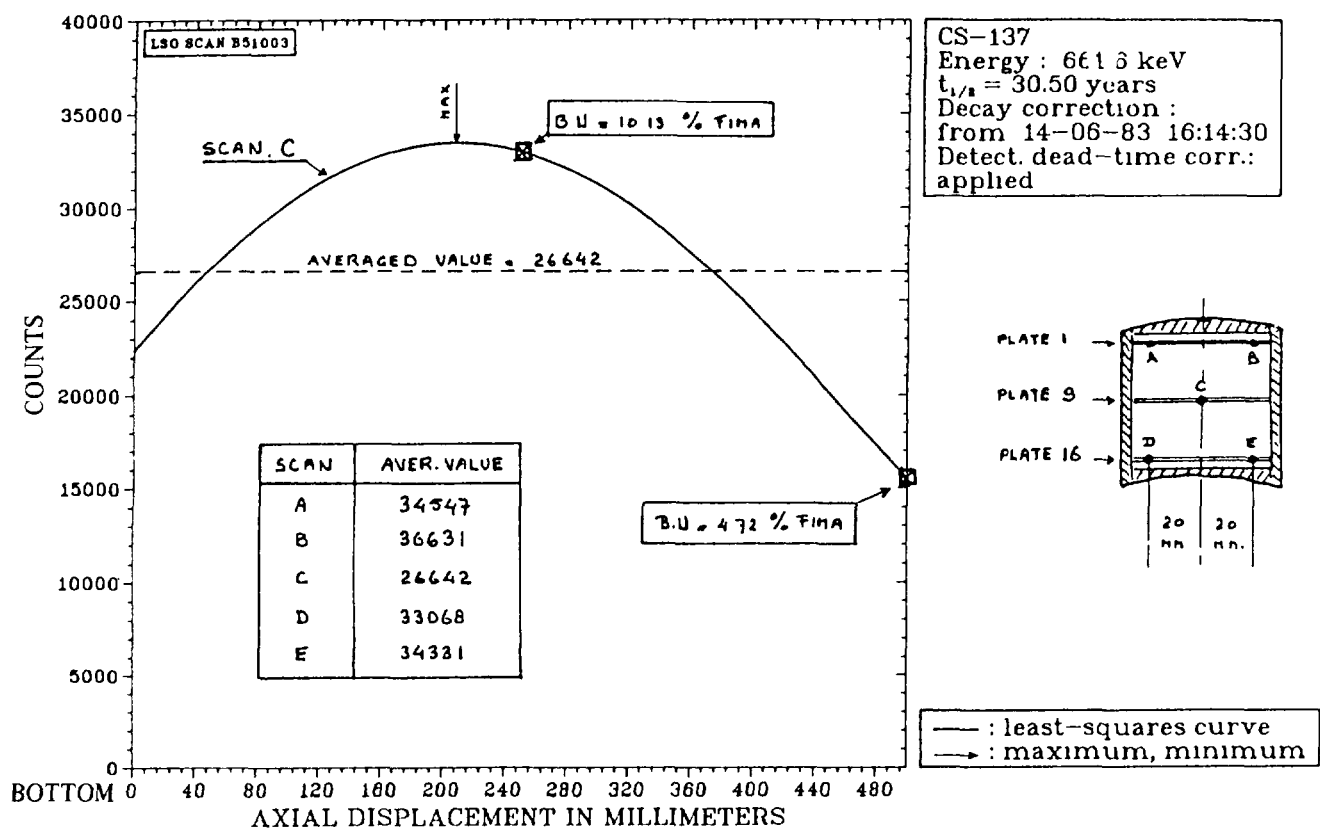


FIG. 17. Results of gamma spectrometry on LEU fuel plate 9 (H20-V2012) of LC-02.

TABLE 2. CALCULATED ISOTOPIC FUEL COMPOSITION OF LEU TEST ELEMENTS

Isotope	LN-02		LC-02	
	Mass (gr)		Mass (gr)	
	Initial	End of irr.	Initial	End of irr.
U-234	2.17	1.80	2.49	2.02
U-235	327.77	179.53	328.93	169.65
U-236	1.34	26.95	3.66	30.83
U-237	-	0.08	-	0.11
U-238	1339.25	1319.17	1329.95	1308.07
U-tot.	1670.53	1527.53	1665.03	1510.68
Pu-239	-	9.63	-	10.23
Pu-240	-	2.18	-	2.25
Pu-241	-	0.88	-	1.07
Pu-tot.	-	12.69	-	13.55
Np-237	-	0.75	-	1.03
Np-238	-	-	-	-
Np-239	-	0.46	-	0.45
Np-tot.	-	1.21	-	1.48
U-tot/Pu-tot	~	120.37	~	111.49

Isotope	LN-01-CD		LC-01-CD	
	Mass (gr)		Mass (gr)	
	Initial	End of irr.	Initial	End of irr.
U-234	2.17	1.45	2.50	1.68
U-235	327.81	86.37	329.81	90.02
U-236	1.34	41.05	3.67	42.89
U-237	-	0.17	-	0.15
U-238	1339.41	1297.61	1333.25	1291.86
U-tot.	1670.73	1426.65	1669.23	1426.61
Pu-239	-	10.79	-	11.09
Pu-240	-	3.81	-	3.84
Pu-241	-	2.72	-	2.69
Pu-tot.	-	17.42	-	17.62
Np-237	-	2.50	-	2.74
Np-238	-	0.01	-	0.01
Np-239	-	0.53	-	0.43
Np-tot.	-	3.04	-	3.18
U-tot/Pu-tot	~	81.90	~	80.96

6.2.5. Determination of absolute burn-up

The neodymium-148 method has been applied for burn-up determination of three samples (diameter 3 mm) taken from each of the two central fuel plates. The samples were acquired by means of a special punching device. Thermal ionization mass spectrometry was applied for determination of the isotopic composition of the samples, except for Pu-238 where alpha-spectrometry was utilized.

Results of burn-up and radioisotopic analysis are given in table 3. Absolute burn-up values for two plate locations have been indicated on the gamma-scan profiles given in the figures 16 and 17. Excellent agreement exists between the ratio of the measured burn-up values and the Cs-137 profile ($\pm 0.5\%$).

Good agreement ($\pm 5\%$) also exists between the measured values and the calculated composition of the relevant radioisotopes.

Table 2 gives a survey of the calculated element-averaged isotope composition of the fuel at the end of the irradiation.

6.2.6. Metallography

From plate no. 9 of each element three samples were prepared for metallographic examination of the fuel plate cross-section. The sampling plan included one longitudinal section in the center of the plate, one transverse section of the edge area at half the plate length and one longitudinal section of the TOF dogbone area about the plate centerline (see figure 18).

To offer a general impression of the structural condition of the fuel plate at this level of burn-up, some pictures of the longitudinal cross-section at the center of the plate are shown (see figure 19).

In the following a summary of the examination results for both fuel types is given.

U₃O₈ dispersed particles

Figure 20 shows the original condition of the as-fabricated fuel plates. It appears that the larger particles become heavily cracked by the rolling operations during plate fabrication. After sectioning, many fragments are free to drop out and actually do so during subsequent preparation stages. Some of the larger particles were so extensively fragmented that a nearly empty pocket remains, which accounts for the appearance of the large elongated cavities in figure 20. At 400x enlargement the particles are seen to contain a few small isolated sintering voids (figure 20).

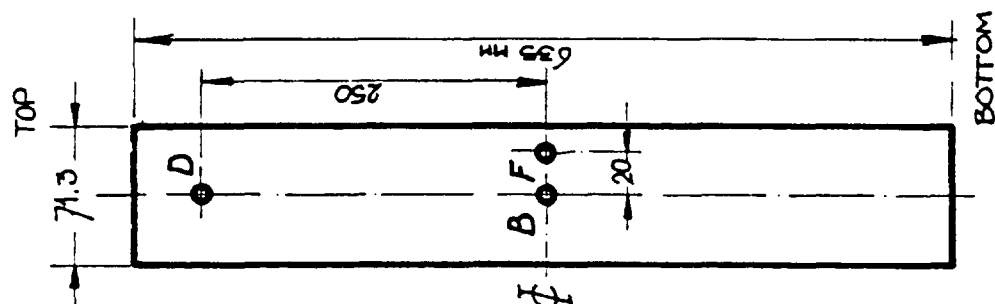
The micrographs picturing the morphology of U₃O₈ particles which were irradiated to a burn-up level of 45-50% (test element IN-02) reveal the existence of a secondary phase which allegedly results from a burn-up dependent reaction between U₃O₈ and the aluminium matrix. The reaction progresses from the periphery of the U₃O₈ particles inwards. The smallest particles are seen to be converted completely already. The reaction product is remarkably free of porosity, whereas in the remaining U₃O₈ a distinct category of small voids is developing during irradiation (see figure 21).

The appearance of the irradiated particles has changed in another sense, considering their original fragmented condition before irradiation. The cracks have disappeared completely and their replacement by a collection of large-size voids is indicative for considerable diffusional activity within the U₃O₈ during irradiation. Obviously the main cracks within the particles, as well as unbonded areas at the particle/matrix interface,

TABLE 3. RESULTS OF CHEMICAL BURNUP ANALYSES ON SAMPLES OF FUEL PLATE OF LEU TEST ELEMENTS

Burn-up parameter	LN-02; plate YC5374			LC-02; plate H20-V2012		
	sample identification			sample identification		
	B	D	F	B	D	F
Burn-up* (% FIMA)	9.2	4.15	10.16	10.23	4.72	10.93
U/pu ratio	87.5	168.8	85.2	81.9	151.5	81.7
U-composition (atomic fractions)	U-234	0.12	0.13	0.13	0.15	0.13
	U-235	10.98	15.82	10.08	15.31	9.18
	U-236	1.94	0.95	2.28	1.22	2.43
	U-238	86.97	83.11	87.51	83.33	88.26
Pu-composition (atomic fractions)	Pu-238	0.86	0.19	1.27	0.32	1.47
	Pu-239	74.77	88.44	72.23	86.83	70.35
	Pu-240	15.36	8.84	15.99	9.65	16.71
	Pu-241	7.73	2.40	8.83	3.01	9.44
	Pu-242	1.28	0.13	1.67	0.20	2.03

*) % FIMA = $\frac{F'}{U' + Pu' + F'}$ in which : F' = number of Nd-148 atoms
 U' = number of Uranium atoms
 Pu' = number of Plutonium atoms



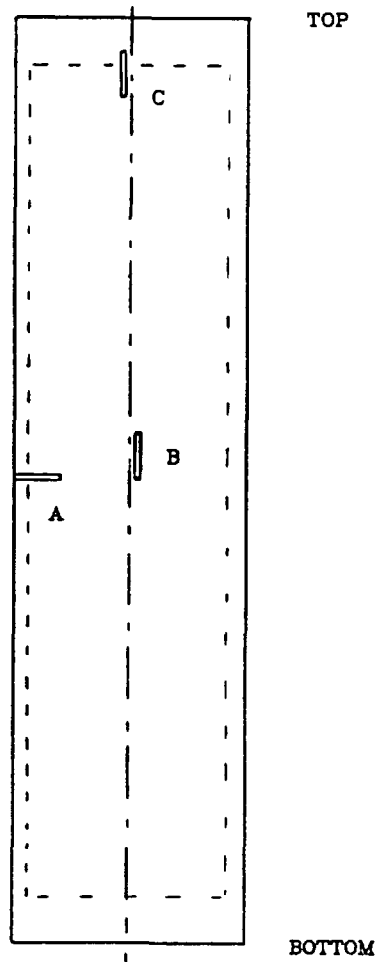


FIG. 18. Sampling plan for metallography.

have served as nucleation sites for the large voids. The relatively dense population of much smaller sized voids accounts for the accommodation of fission gas generated in the bulk U_3O_8 . The energy which is needed for the large-scale rearranging process during irradiation is readily supplied in situ by the fission reactions (see figure 22).

The pictures of the state of the U_3O_8 particles after 70-75% burn-up show only a moderate aggravation of the effects that were described above (see figure 23).

UAl_x dispersed particles

The original condition of the UAl_x particles before irradiation is shown by figure 24. This material also becomes cracked during rolling, but fragmentation is not as extensive as in the U_3O_8 particles.

The micrographs of the fuel section after irradiation to 45-50% burn-up (test element LC-02), show a similar healing effect on the rolling cracks as is observed in the U_3O_8 particles (see figure 25). Relative to the latter, the diffusion processes in UAl_x appear to be slower however. The pronounced directionality in the original rolling crack pattern is again well visible in figure 26, because of the still elongated appearance of the former crack openings. It is also obvious that fission gas retention in the crystal lattice is much higher in UAl_x than in U_3O_8 , considering the absence of small voids in the crystalline matrix and the

Text cont. on p. 360.

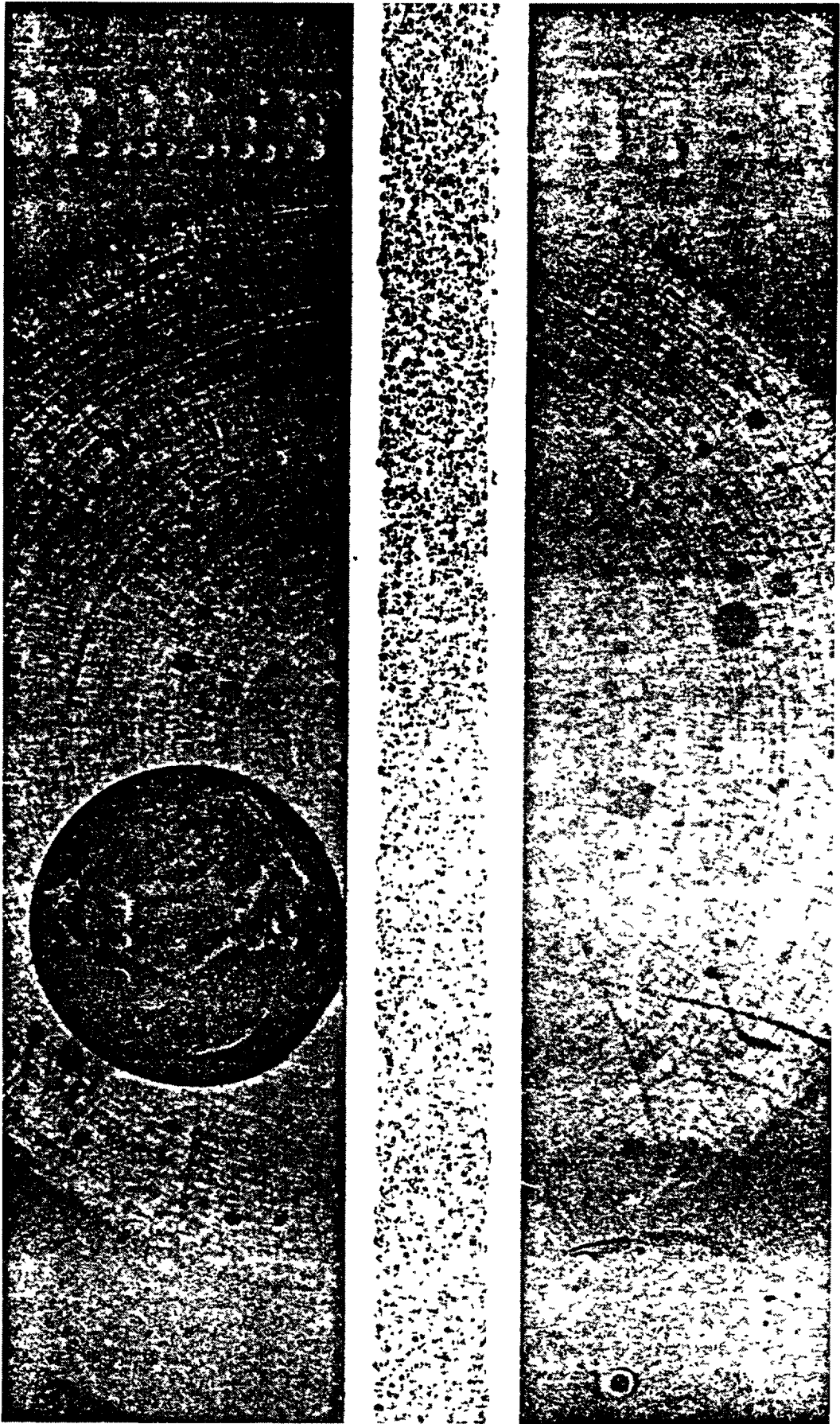


FIG 19 Macrograph of sample B of LN-02 (15x)

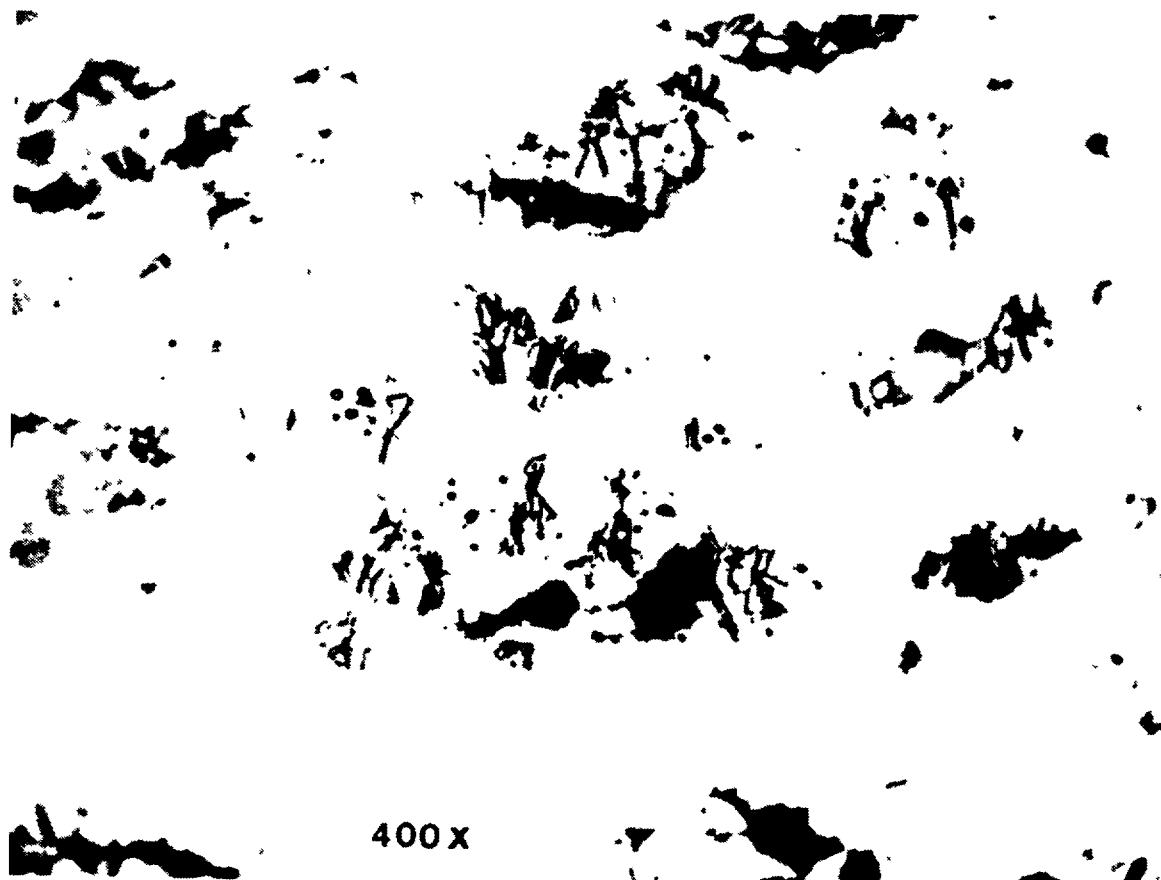
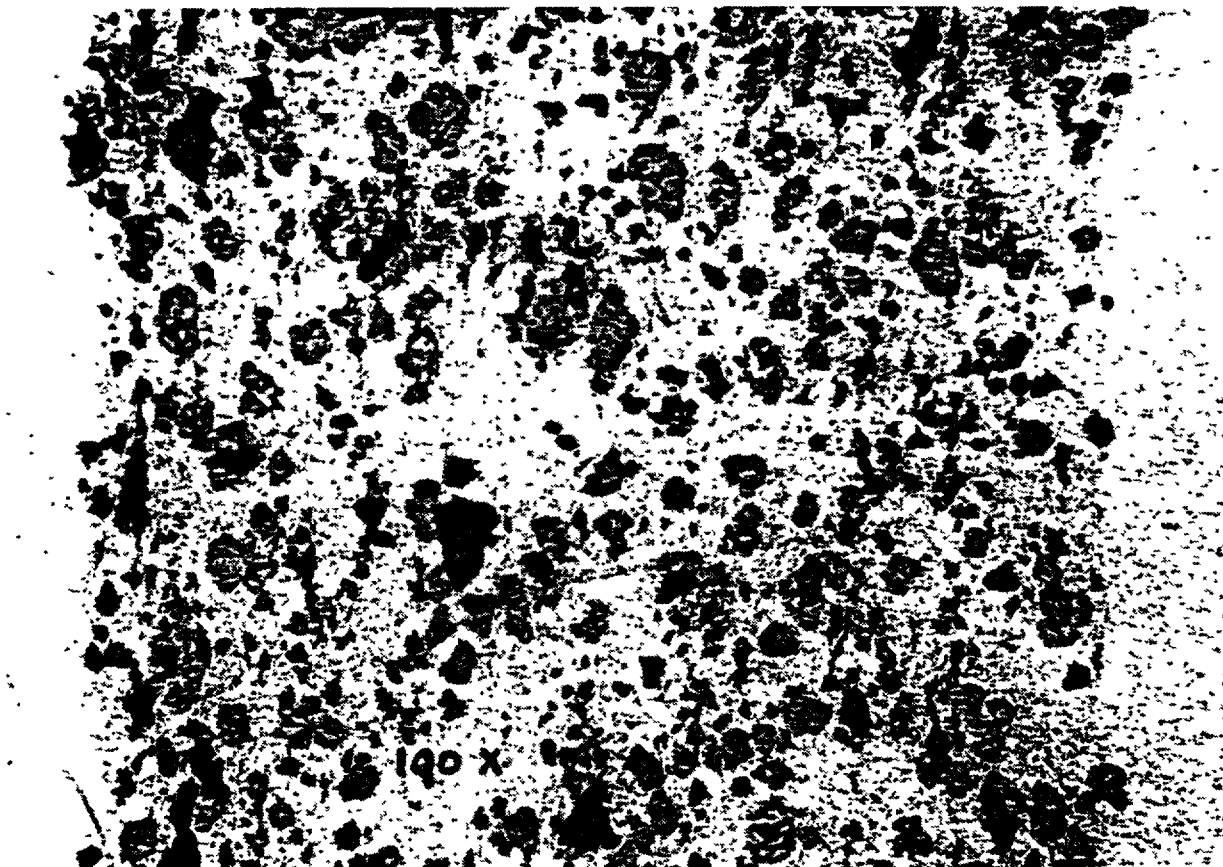


FIG. 20. Unirradiated $\text{U}_3\text{O}_8\text{-Al}$ (LN-02).

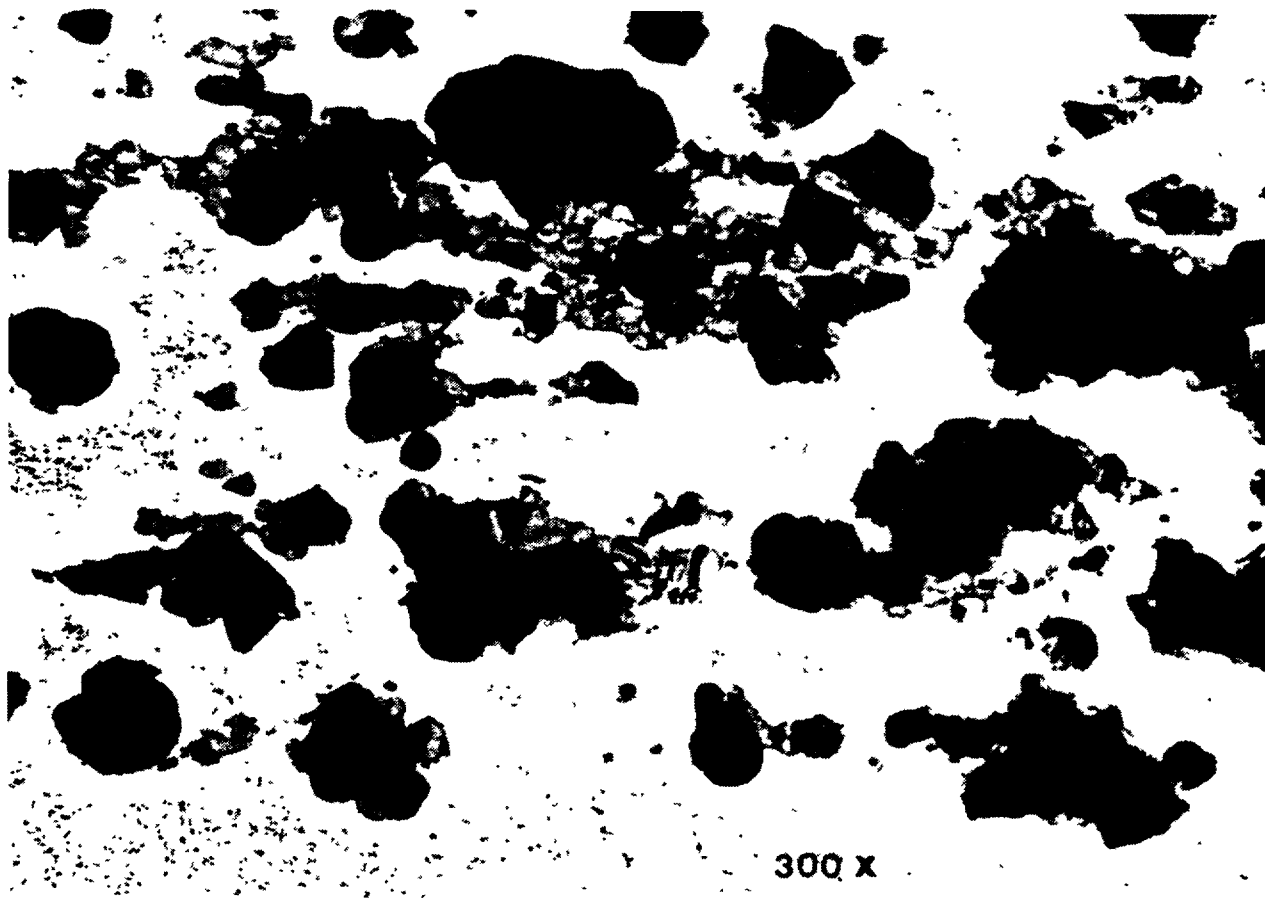
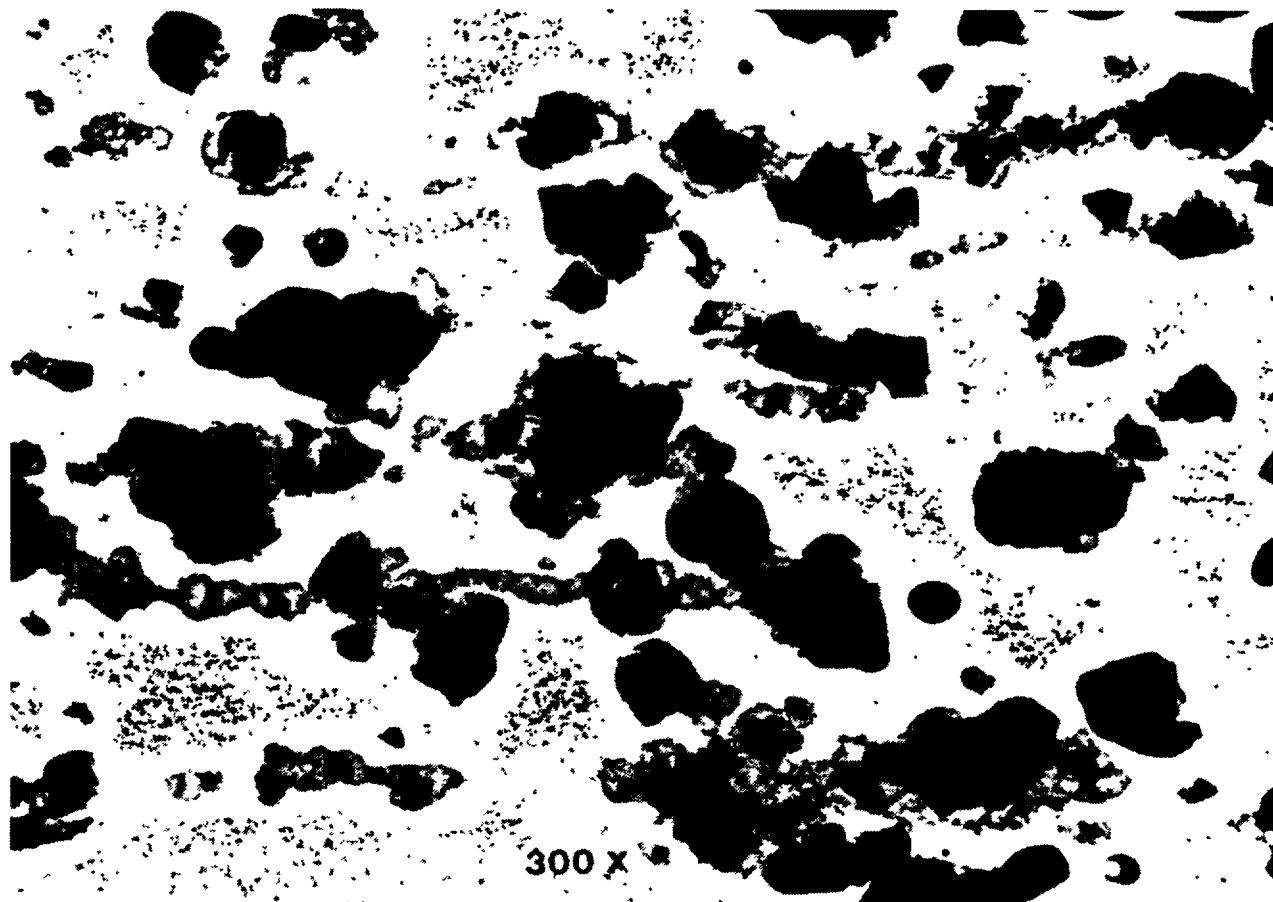


FIG. 21. Irradiated $\text{U}_3\text{O}_8\text{-Al}$ (LN-02, BU = 0.45).

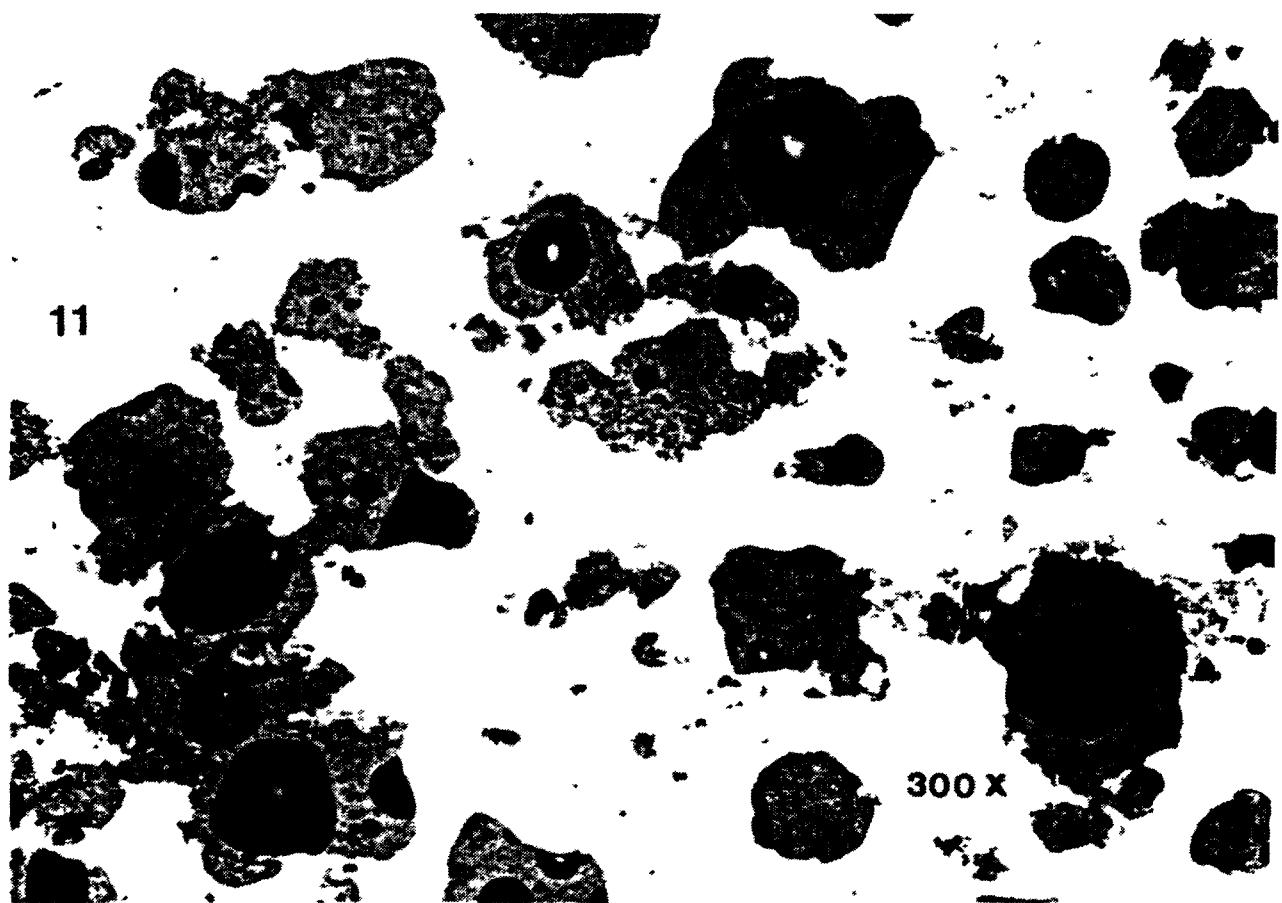
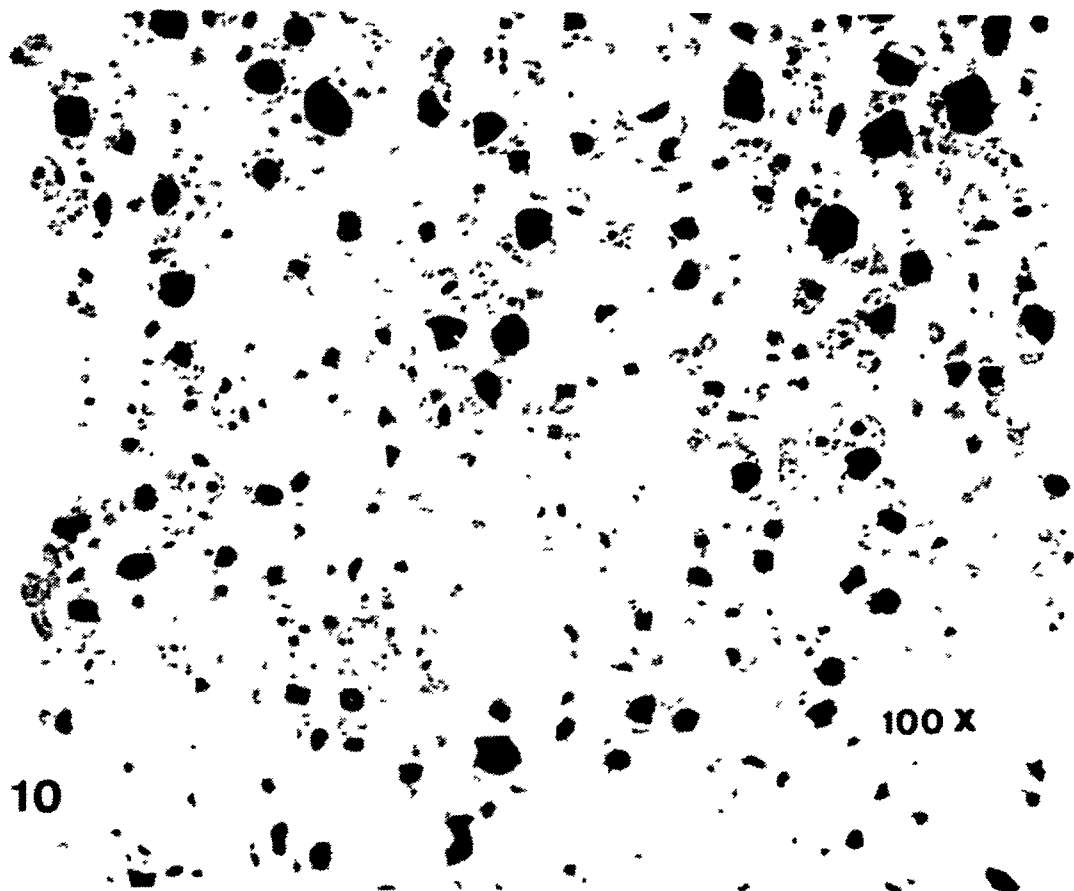


FIG 22 Irradiated $\text{U}_3\text{O}_8\text{-Al}$ (LN-02, BU = 0.45)

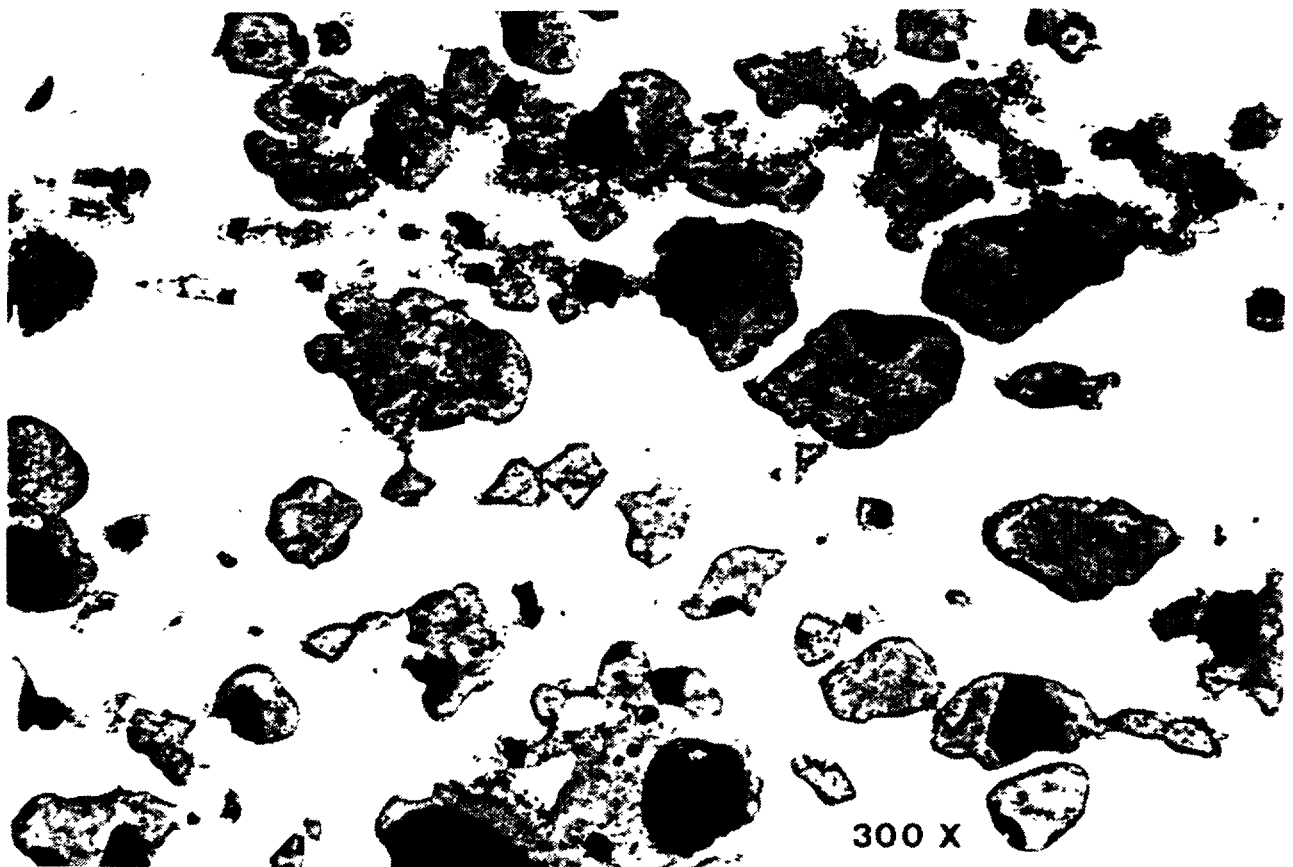
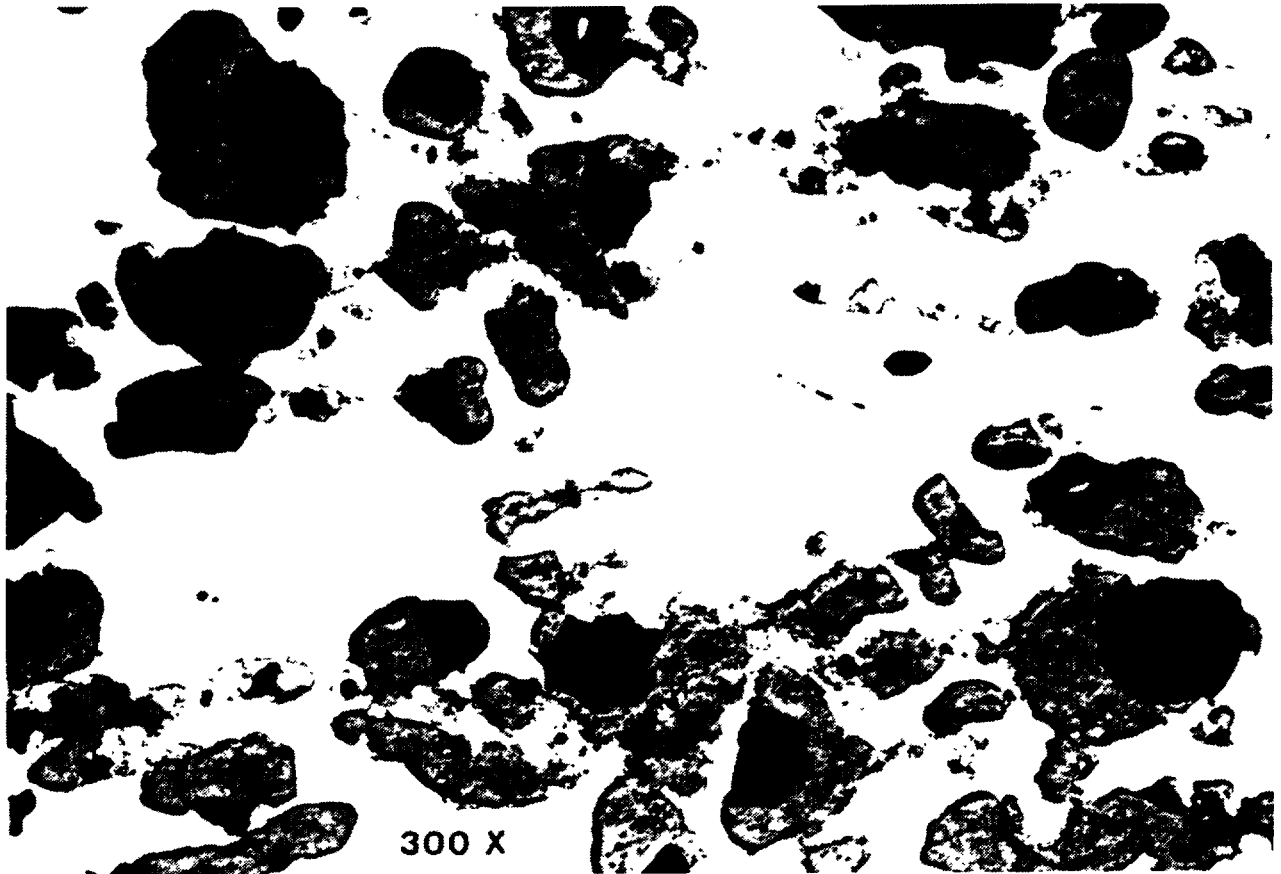


FIG. 23. Irradiated $\text{U}_3\text{O}_8\text{-Al}$ (LN-01-CD, BU = 0.74).



FIG. 24. Unirradiated $\text{UAl}_x\text{-Al}$ (LC-02).

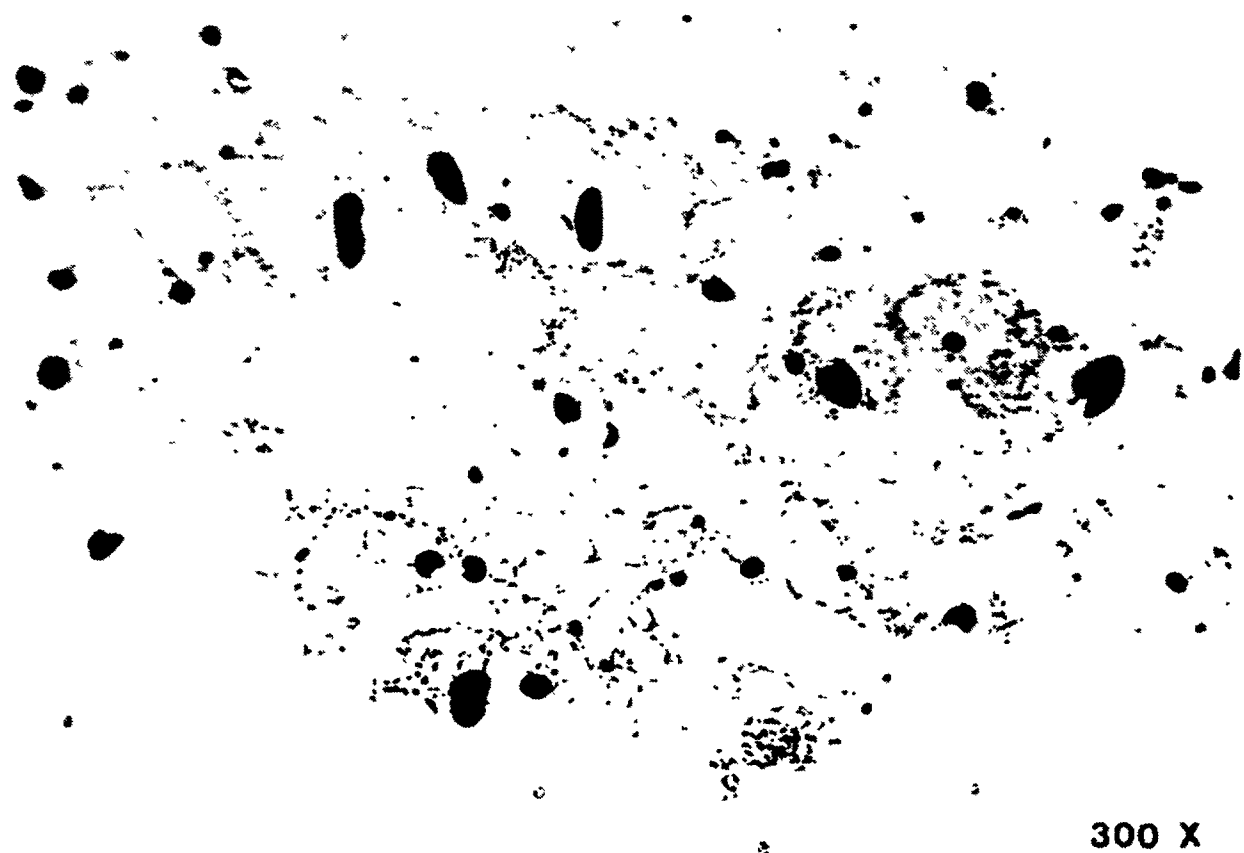


FIG. 25. Irradiated $\text{UAl}_x\text{-Al}$ (LC-02, $\text{BU} = 0.48$).

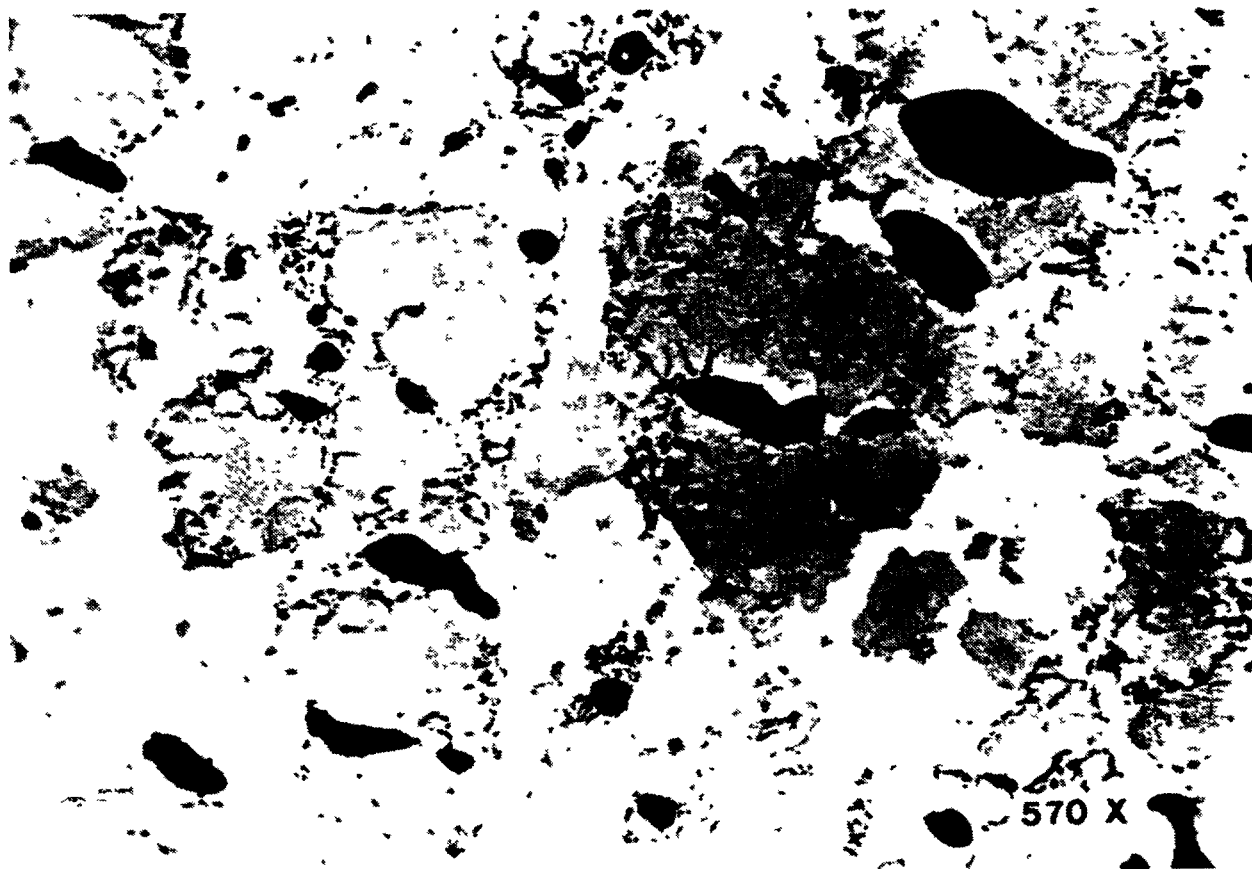


FIG 26 Irradiated UAl_x-Al (LC-02, BU = 0.48)

limited extent of their incidence in the grain boundaries (see figure 25). The practical reality of this was evident when samples for burn-up analysis were taken. For this purpose small diameter discs were cut from the fuel plates by means of a punch-and-die device. Whenever the U_3O_8 plates were punched, the hot-cell off-gas alarm was triggered systematically. Punching the UAl_x plates had no such effect.

During post-irradiation examination of UAl_x particulate material, one additional observation was made that may well be of secondary significance. In the dispersed fuel particles there is a more or less scattered occurrence of partial liquation at subgrain boundaries or other areas of lattice disorder, as illustrated by figure 26. As a matter of fact, during irradiation a secondary phase is formed that seems to agglomerate in the liquid state at the conditions which exist during reactor operation. It could be assumed that the mixture of U and Al with a growing fission product content, eventually attains a composition with a solidus temperature that is exceeded by the service temperature of the reactor fuel.

The morphological changes that are associated with the increase of the burn-up level to 70-75% (test element LC-01-Cd), again are characterized by an aggravation of the effects which have been observed at the intermediate burn-up level (see figure 27). The striking appearance of brittle cracks in the samples A and B of the particular fuel plate is a result of bending forces occurring during the disengagement of the fuel plate from the test element structure. The extreme hardness of the UAl_x particles, which is the reason for their apparent brittleness, is another indication of very nearly complete retention of fission gas atoms in the UAl_x crystal lattice, up to burn-up levels as high as 70-75%.

6.2.7. Blister tests

In order to investigate the tendency of irradiated fuel plates to develop blisters at elevated temperatures, a number of test plates were subjected to a heat treatment up to temperatures of 550°C.

For this purpose a special furnace was designed and manufactured. Principally this furnace consists of two electrically heated copper blocks with a 4 mm gap in between for insertion of the test plate. The heated section is supported by ceramic insulators and mounted in an aluminium containment. An accurate ($\pm 1^\circ\text{C}$) temperature measuring and control system is connected to the furnace. Additional provisions to measure and collect the released volatile fission products were available. The heat treatment of the test plates consists of a one step temperature increase from room temperature to 250°C, followed by steps of 50°C up to 550°C. Each temperature step in turn is followed by a holdtime of 30 minutes and subsequent visual inspection of the plate.

From the results of the blister tests it appeared that only the U_3O_8 -Al fuel plates with high burn-up (75%) develop blisters in the fuel meat zone above 525°C. These blisters are located at mid height near the fuel edge zone (see figure 28).

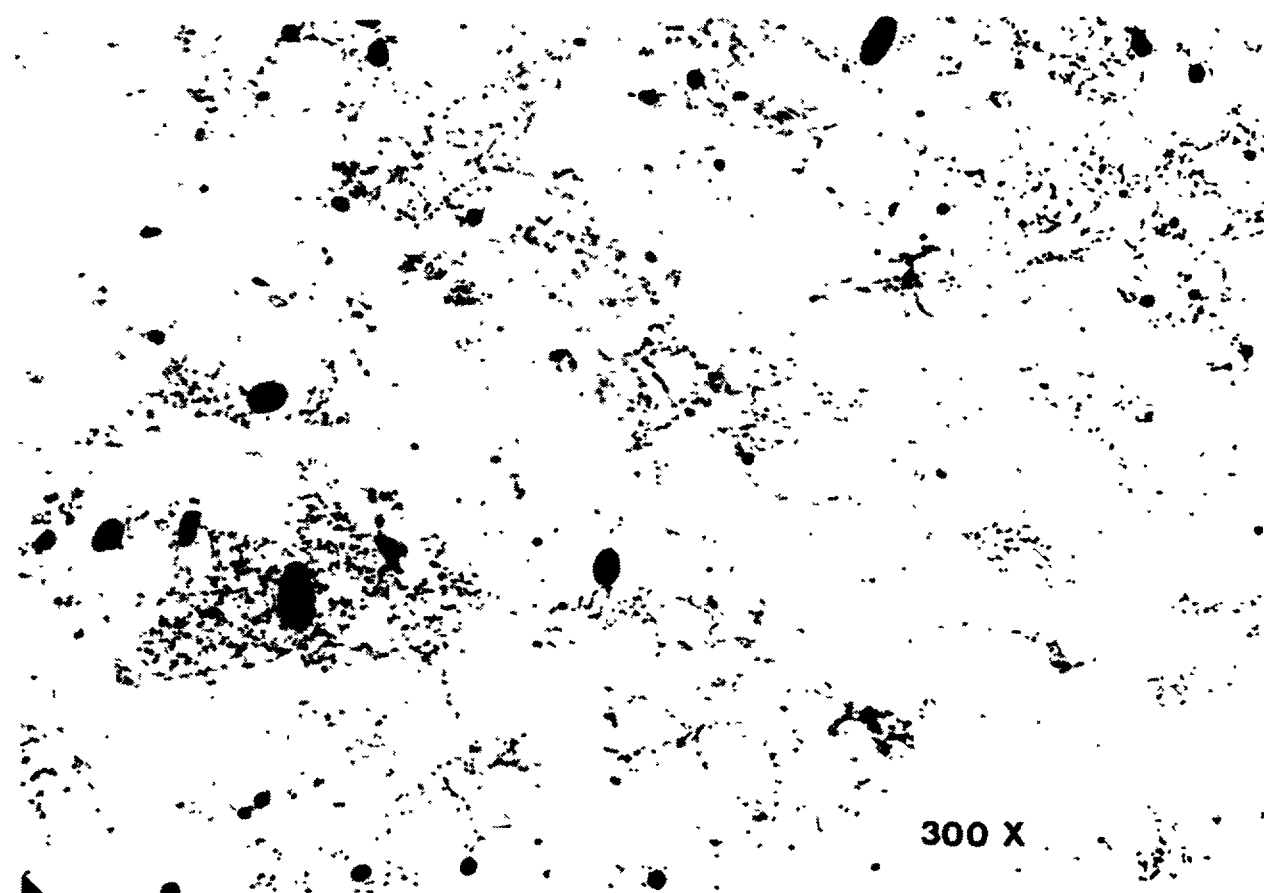
For the remaining test plates no blister formation in the meat zone was detected for temperatures up to 550°C.

Apart from the blistering in the meat zone some secondary observations were made :

- All the tested plates showed a discolouration on the surface of the Al-cladding in the meat zone, at temperatures of 475°C to 550°C (see figure 29).
- For all the plates a permanent length increase of about 5 mm was found after heating up to 550°C (see figure 30).
- The plates with the UAl_x -Al type fuel showed minor blister formation at the top and bottom of the plate, outside the fuel region (see figure 31).



300 X



300 X

FIG. 27. Irradiated $\text{UAl}_x\text{-Al}$ (LC-01-CD, BU = 0.73).



FIG 28. Blister formation on plate YC5355 (LN-O1-CD).

7. CONCLUSIONS AND FINAL OBSERVATIONS

From the practical experiences and measurements during irradiation and based on the results of post irradiation examinations of four LEU-assemblies having a burn-up of 50 to 75% the following main conclusions can be drawn :

- * All four test elements have shown excellent irradiation behaviour up to their target burn-up of 50% and 75% respectively.
- * From coolant channel width measurements no local or overall fuel plate deformation has been detected. This result has been confirmed by plate thickness measurements on the elements.

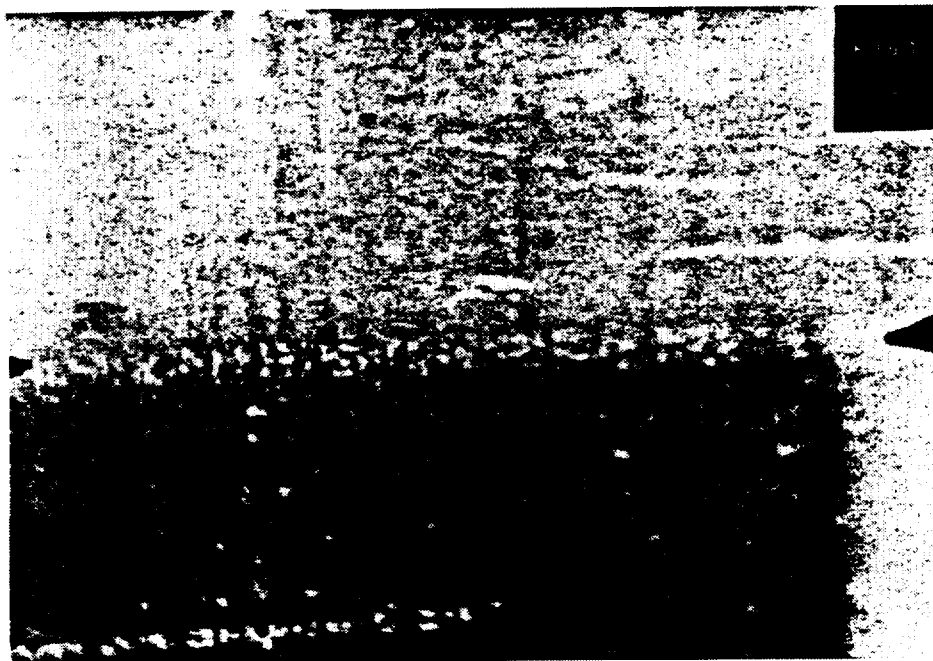


FIG. 29. Discolouration of the cladding surface.

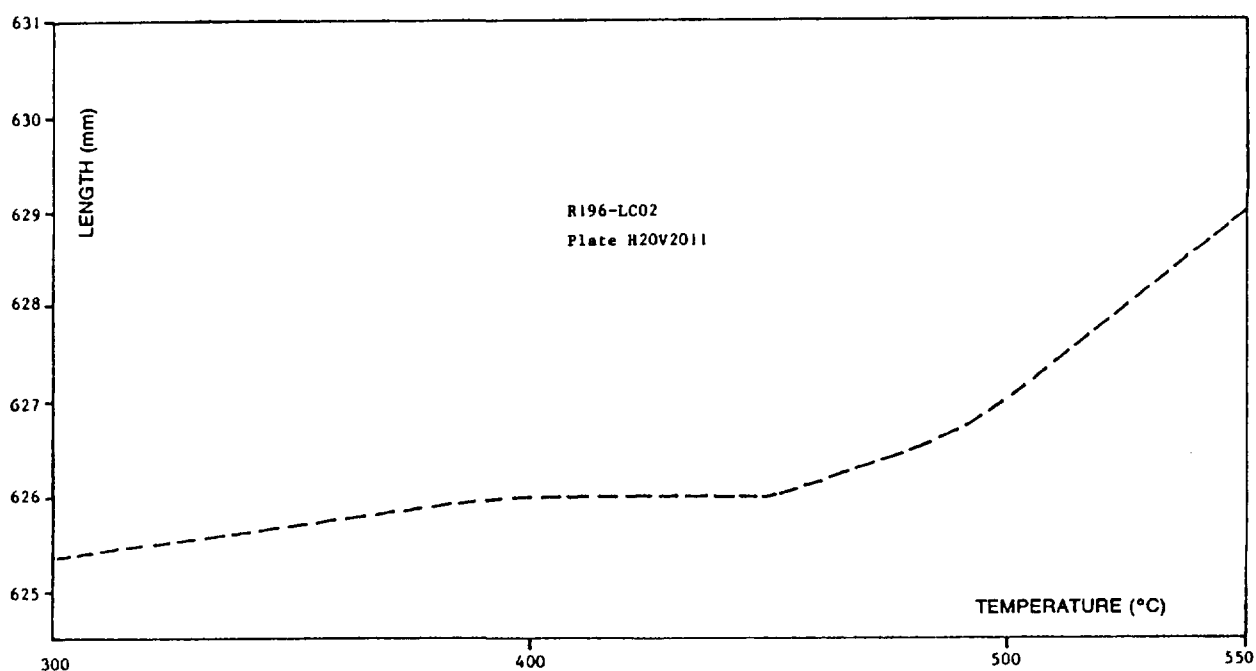


FIG. 30. Length increase of the test plate after heating.

- * From detailed flux measurements it was found that LEU test elements with non-fueled outer plates show distinct radial power peaking (20%) at the begin of irradiation. Application of cadmium poisoned side plates reduces this power peaking in E-W direction (5-10%).
 - * Reactivity measurements show that the depletion of cadmium wires ($d = 0.5 \text{ mm}$) is completed at a thermal neutron fluence of $0.5 \cdot 10^{21} \text{ cm}^{-2}$.
- For future application of cadmium as a burnable absorber in a LRU-EFR core the number of wires per side plate should be increased from 10 to



FIG 31 Minor blister formation outside the meat region

20. In that case the initial negative reactivity of the cadmium present in the first (6 x 500 pcm) and second (6 x 125 pcm) fuel zone will amount to 3750 pcm. At the end of cycle (26 days, 45 MW) about 750 pcm remains. In this way the ^{235}U burn-up effect will be compensated properly by the cadmium depletion. In comparison with ^{10}B , the application of cadmium will lead to a lower fuel inventory of the HFR-core.

- * Calculated and measured burn-up data are in good agreement ($\pm 5\%$).
- * The results of chemical burn-up analyses on fuel plate samples fit well with the burn-up distribution as measured with gamma-scanning ($\pm 5\%$).
- * At burn-up levels of 50% and 75% the calculated Pu-content amounts to 12.5 g and 17.5 g per element respectively.
- * At burn-up levels of 50% and 75% the calculated relative power production of plutonium in 20% enriched LEU-elements amounts to 13% and 24% respectively.
- * Metallography of U_3O_8 -Al fuel plates has indicated undisturbed bond integrity between fuel meat and cladding. Fabrication induced internal

- cracks have disappeared, whereas central cavities have formed within the fuel particles due to fission product diffusion and coalescing processes. An irradiation-induced U_3O_8 -Al reaction zone of low porosity has formed on the inner periphery of the fuel particles.
- * Metallography of UAl_x -Al fuel plates has equally shown good bond integrity. Certain irradiation-induced changes in the porosity structure have been observed.
 - * Metallography of U_3O_8 -Al fuel plates has indicated undisturbed bond integrity between fuel meat and cladding. Fabrication induced internal cracks have disappeared, whereas central cavities have formed within the fuel particles due to fission product diffusion and coalescing processes. A irradiation-induced U_3O_8 -Al reaction zone of low porosity has formed on the inner periphery of the fuel particles.
 - * Metallography of UAl_x -Al fuel plates has equally shown good bond integrity. Certain irradiation-induced changes in the porosity structure have been observed.
 - * Blister test on irradiated U_3O_8 -Al fuel plates with a burn-up of 75% have shown significant blister formation in the meat zone at mid height at 525°C (see figure 28). For lower burn-up levels (50%) no blisters have been detected for the same fuel type.
 - * As regards the UAl_x -Al plates no blister formation in the meat zone has been observed up to 550°C.
 - * During the blister tests a thermal expansion of the plates of 1% at 525°C was measured (see figure 30). Some of the plates had become somewhat warped after heating.
 - * For all the tested plates a clear discolouration of the plate surface in the meat region was observed at 500°C (see figure 29).
 - * The UAl_x plates show a minor blister development in the outer meat region at the top and bottom of the plate at 550°C (see figure 31).

REFERENCES

- [1] Pruimboom, H. and Swanenburg de Veye, R.J.
"Status report on the irradiation of LEU-test elements in the Petten High Flux Reactor"
- [2] Van Otterdijk, K.H.
Coolant channel measurements on irradiated LEU-elements (LOUISE-R196)
ECN-83-157
October 1983.
- [3] Dassel, G. and Bruggeling, F.J.
Gamma scan measurements on irradiated LEU test elements LC-02, LC-01-CD, LN-02 and LN-01-CD
ECN-85-044, ECN-85-045, ECN-85-042 and ECN-85-043
March 1985
- [4] Lijbrink, E.
Effects of fission process on the morphology of the uranium containing material component in reduced enrichment HFR test element fuel plates
ECN-85-002
October 1984
- [5] de Haan, K.W.
Visual inspection, dismantling and blister testing of irradiated LEU test elements LN02, LC02, LN01CD and LC01CD (LOUISE-R196)
ECN-84-141
September 1984

Appendix J-4.4

FULL SIZE ELEMENT IRRADIATIONS IN THE FRG-2

W. KRULL

GKSS — Forschungszentrum Geesthacht GmbH,
Geesthacht, Federal Republic of Germany

Abstract

Irradiation and post-irradiation-examination in the FRG-2 reactor of 5 test plates with LEU U_3Si_2 fuel and 21 full size elements with MEU UAl_x fuel, LEU U_3O_8 fuel, and LEU U_3Si_2 fuel are summarized. All test plates and fuel elements were irradiated to greater than 60% average burnup of the contained ^{235}U .

IRRADIATION AND PIE OF TEST PLATES IN THE FRG-2

Beginning March 1985 in an instrumented rig 5 U_3Si_2 -miniplates, $\rho = 4,75$ g U/cc, were irradiated to determine the influence of different grain size ratios on swelling. The content of fine grain ($\leq 40 \mu$) was up to 40 %. One of the 5 miniplates was instrumented with thermocouples. The following PIE's are being finished: visual inspection, dimensional and density measurements, gamma-scans, blister-tests and metallography. Burnup greater than 60%.

IRRADIATION OF FULL SIZE ELEMENTS IN THE FRG-2

The following fuel element performance tests are completed:

1. 10 fuel elements with 45 % up to 64 % enrichment UAl_x , $\rho = 1,41$ g U/cc reached a U-5 burnup up to 64 % in April 1984. Two of these fuel elements were instrumented with thermocouples. Continuous temperature measurements and loss of flow measurements were done. Reactivity values and micro neutronflux distributions were determined. No PIE's.
2. 7 fuel elements with 20 % enrichment, U_3O_8 , $\rho = 3,1$ g U/cc, Irradiations are finished. Burnup up to 66 %. No PIE's.
3. 4 fuel elements with 20 % enrichment U_3Si_2 , $\rho = 3,7$ g U/cc, Irradiations are finished. Burnup up to 68,5 %. No PIE's.

This information is summarized in the attached table.

CONVERSION OF FRG-REACTORS

78 fuel elements (U_3Si_2 , $\rho = 3,7$ g U/cc) are ordered and will be delivered in 1988 for the conversion of the FRG-1 and FRG-2 research reactors.

Table 1: Fuel Elements Qualification

	I	II	III	IV
Weight U-235 (g)	180	280	270	323
Weight U (g)	193, 200	622	1357	635
Enrichment (%)	90, 93	45	20	20
Meat material	UAl _x	UAl _x	U ₃ O ₈	U ₃ Si ₂
Density (g U/cc)	0,44 (0,45)	1,41	3,1	3,7
Canning material	AlMg1	AlMg1	AlMg2	AlMg2
Number		10	7	4
Average burnup (%)	45	≤ 64	≤ 66	≤ 65
Test status	present fuel	finished	finished	finished
Test finished	open	April 84	Autumn 86	Spring 87
Max peak burnup* 10 ²¹ fissions/cc (ex Pu)	0,66	1,01	0,88-1,00	1,20-1,24
Mean U-235 burnup* (%)	45	58,9-64,0	56,7-66,0	66,3-68,5

*) Fuel elements instrumented with thermocouples in the fuel plates have a burnup between 46,3 % and 60,6 %.

THE CONVERSION OF NRU FROM HEU TO LEU FUEL*

D.F. SEARS, M.D. ATFIELD, I.C. KENNEDY

Chalk River Nuclear Laboratories,
Atomic Energy of Canada Limited,
Chalk River, Ontario,
Canada

Abstract

The program at Chalk River Nuclear Laboratories (CRNL) to develop and test low-enriched uranium fuel (LEU, <20% U-235) is reviewed, and the status of the conversion of the NRU reactor from highly enriched uranium (HEU, 93% U-235) to LEU fuel is discussed. The replacement LEU fuels developed and tested at CRNL contain high-density uranium silicide particles dispersed in aluminum, in cylindrical rods. The silicides tested include U_3Si , $USiAl$, USi^*Al and U_3Si_2 (U-3.96 wt% Si; U-3.5 wt% Si-1.5 wt% Al; U-3.2 wt% Si-3 wt% Al; U-7.3 wt% Si, respectively). Fuel elements were fabricated with uranium loadings suitable for NRU, 3.15 gU/cm³, and for NRX, 4.5 gU/cm³, and were irradiated under normal fuel-operating conditions. Eight experimental irradiations involving 100 mini-elements and 84 full-length elements (7x12-element rods) were completed to qualify the LEU fuel and the fabrication technology. Post-irradiation examinations confirmed that the performance of the LEU fuel, and that of a medium-enrichment uranium (MEU, 45% U-235) alloy fuel tested as a back-up, was comparable to the HEU fuel. The uranium silicide dispersion fuel swelling was approximately linear up to burnups exceeding NRU's design terminal burnup (80 at%). NRU was partially converted to LEU fuel when the first 31 prototype fuel rods manufactured with the production equipment were installed in the reactor. The rods were loaded in NRU at a fueling rate of about two rods per week over the period 1988 September to December. This partial LEU core (one third of a full NRU core) has allowed the reactor engineers and physicists to evaluate the bulk effects of the LEU conversion on NRU operations. As expected, the irradiation is proceeding without incident.

1. INTRODUCTION

The NRU reactor at CRNL is a multipurpose, tank-type thermal research reactor, using D₂O moderator and coolant and highly enriched uranium (HEU, 93% U-235) U-Al alloy driver fuel. Various kinds of rod assemblies are suspended in the tank on a 7 1/4 in (19.7 mm) hexagonal lattice. The reactor produces radioisotopes, provides neutron beams for research, and has special facilities for testing metallurgical specimens and advanced power reactor fuels, and for performing fuel damage (blowdown) tests.

* Paper presented at the International Symposium on Research Reactor Safety, Operations and Modifications, Chalk River, Ontario, Canada, 23-27 October 1989 (AECL-9926, Vol. 3, Chalk River Nuclear Laboratories, Ontario (1990)).

The NRU reactor achieved criticality in 1957 and ran at 220 MW (Th) using driver fuel rods containing flat plates of natural uranium metal. It was converted to highly enriched, rod-type driver fuel in 1964, and currently runs at about 130 MW (Th). The linear-fissile loading of each 2.7 m long fuel element (twelve per rod) has risen from 0.3 g U-235/cm to the present 1.8 g U-235/cm. Roughly 90 of the 227 reactor sites are occupied by driver fuel, and these are taken to approximately 80% burnup in 11 months.

As part of an international effort to reduce the use of HEU, and the risk of nuclear proliferation, a development program was undertaken in 1980 to produce low enrichment uranium (LEU, <20% U-235) driver fuel for NRU. CRNL's progress has been reported at annual meetings sponsored by the U.S. Reduced Enrichment for Research and Test Reactors (RERTR) program [1-4]. The salient features of the LEU fuel development and testing program, and the current status of the NRU conversion program are reviewed in this paper. The LEU fuel burnup analysis has recently been completed using high-precision liquid chromatography, and where appropriate, the analyzed burnup values will be given.

2. FUEL DEVELOPMENT AND FABRICATION

The NRU fuel-rod design which consists of twelve elements, each containing an HEU-Al alloy core with finned aluminum cladding and aluminum end plugs (see Figure 1), has proven to be extremely durable and reliable. The geometry, dimensions and linear fissile loading of this 12-element fuel rod were maintained in the LEU conversion program for licensing simplicity. CRNL physics studies showed very little effect on reactor operations from using LEU driver rods, apart from the need to fuel 6 more reactor sites or reduce exit burnup by about 10%. The problem thus came down to the development of a replacement fuel with five times the HEU fuel uranium density, which would be stable to high burnup.

The replacement LEU fuel elements consist of a core, containing high-density uranium silicide particles dispersed in an aluminum matrix, with the same finned aluminum cladding and end plugs. The fuel is made by melting uranium and silicon in a high-frequency induction furnace. Cast billets are heat-treated to transform the as-cast structure to U_3Si , then the billets are reduced to powders via a series of comminution processes. Uranium silicide powder is mixed with aluminum powder and hot-extruded into cores. The finned aluminum cladding is extruded onto the cores in a semi-continuous process, with the cores acting as a floating mandrel. The cladding is welded to the end-plugs to hermetically seal the elements.

The high-density silicides tested were U_3Si , U_3Si alloyed with 1.5 wt% Al and 3 wt% Al, and U_3Si_2 (U-3.96 wt% Si; U-3.5 wt% Si-1.5 wt% Al; U-3.2 wt% Si-3 wt% Al, and U-7.3 wt% Si, respectively). Fuel elements were fabricated with uranium loadings suitable for NRU, 3.15 gU/cm³, and for NRX, 4.5 gU/cm³. Following the decision to shut down NRX, testing of NRX-type fuel was discontinued.

Industrial-scale fuel-production equipment has been installed in temporary facilities at CRNL, and is currently being used to manufacture prototype fuel rods to familiarize the operators with the manufacturing process, and to confirm that the production rate is high enough to meet CRNL's annual fuel requirements. To date, more than 90 kg of LEU has been processed into NRU rods (see section 4) and the production line is running satisfactorily. Most of the process variables and parameters established

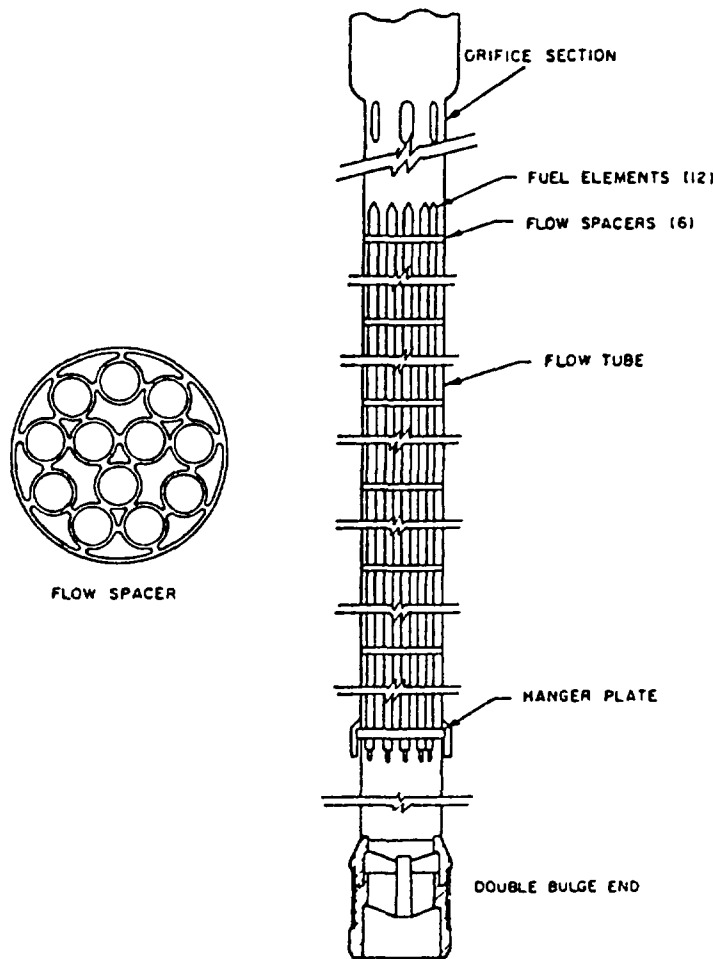


Fig. 1 NRU fuel rod.

during the development program have been used in the production line and no problems have resulted from scaling up.

A new building has been constructed for LEU fuel fabrication. The manufacturing equipment is scheduled for installation and re-commissioning in late 1989. It is anticipated that full-scale production of NRU LEU fuel will commence early in 1990 in the new building, and the first production fuel rods will be loaded into NRU later that year. NRU should be completely converted to LEU fuel within a year of the first production of LEU fuel rods in the new building.

3. LEU SILICIDE DISPERSION FUEL TESTING

3.1. Test Elements

The test vehicle for irradiating silicide dispersion fuel in most tests has been the mini-element. The mini-element fuel-core diameter (5.5 mm) and clad wall thickness (0.76 mm) are the same as in full-size NRU elements. Mini-elements are, however, only 184 mm long compared with 2.9 m for NRU elements. The mini-elements also resemble NRU elements in that they have six cooling fins at 60° intervals around the cladding, the fin width being 0.76 mm and fin height 0.96 mm. To date, approximately 100 mini-elements have been successfully irradiated to burnups in the range 56-93% U-235 depletion in the NRU and NRX reactors.

TABLE 1 Irradiation Program Status

EXPERIMENT	ELEMENTS	CORE MATERIAL	TEST OBJECTIVES	RESULTS	ANALYZED BURNUP (at%)
FZZ-905	8 4 4	Al-61.5% USiAl Al-21% U Al-37% U	Compare LEU dispersions (3.15 MgU/m ³) with U-Al alloys	LEU fuel performance comparable to MEU and HEU alloys	57
FZZ-909A	6 6	Al-72.4% USiAl Al-73.4% USi*Al	Test dispersions containing 4.5 MgU/m ³	Fuel swelling marginally above 1 vol% per 10 at% burnup	73
FZZ-909B	6 6	Al-61.5% USiAl Al-62.4% USi*Al	High burnup confirmation	Fuel swelling <1 vol% per 10 at% burnup and linear up to the terminal burnup	89
FZZ-910	8 8	Al-72.4% USiAl Al-73.4% USi*Al	Test dispersions with fines	Particle size needs to be controlled to minimum swelling	51
FZZ-911	4 8 4	Al-61.5% USiAl Al-62.4% USi*Al Al-61.5% USiAl	Drilled defects in cladding Fuel core surface imperfections	Corrosion resistance acceptable Surface defects have no detrimental effect Swelling 5.7 to 6.9 vol%	18-48 88
FZZ-913 ^a	36 48	Al-62.4% USi*Al Al-61.0% U ₃ Si	Full-size assembly irradiation	Both dispersions suitable for use in NRU. U ₃ Si chosen as reference	67-84
FZZ-915	6	Al-61.5% USiAl Al-72.4% USiAl Al-73.4% USi*Al	In-reactor corrosion of pre-irradiated dispersions	Prior irradiation enhances corrosion resistance	23-79
FZZ-918	16	Al-61.4% U ₃ Si	Define optimum particle size distributions	Swelling proportional to percentage of fines (5.8 to 6.8 vol% after 89 at% BU)	89
FZZ-921	12	Al-64% U ₃ Si ₂	Compare to U ₃ Si and evaluate effect of particle size	Behaviour similar to U Si dispersions but less swelling	

^a Full-length NRU 12-element assemblies

3.2. Irradiation Conditions

The LEU silicide dispersion fuels were irradiated in NRU. A medium-enrichment uranium (MEU, 45% U-235) fuel tested as a backup was irradiated in NRX. The mini-elements were irradiated in a fuel carriage made from an aluminum cylinder with four holes bored axially through it at 90° intervals. An aluminum liner containing a string of four mini-elements was inserted into each hole or flow channel. The mini-elements were located centrally in the flow channels by four-pronged anodized spiders located on the end spigots of the mini-elements. The assembly could be loaded in any of the normal driver fuel positions in NRU.

The mini-elements were irradiated at linear powers representative of a typical NRU driver fuel rod, ranging from 40 to 112 kW/m. The typical neutron flux was approximately 1.1×10^{18} n/m²/s, the heavy-water coolant flow approximately 7.28 L/s, and coolant velocity approximately 10.9 m/s. The coolant inlet temperature ranged between 30 to 37°C and the coolant outlet temperature between 40 to 45°C during the mini-element irradiations.

3.3. Mini-Element Test Results

The fuel test matrix is shown in Table 1. The detailed results were reported elsewhere [1-4], therefore only the salient features of the irradiations will be reported here.

3.3.1. Comparison of HEU-Al and LEU Silicide Dispersion Fuel Performance

In Exp-FZZ-905, mini-elements containing Al-21 wt% U alloy fuel (93% enriched U), Al-37 wt% U alloy fuel (45% enriched U) and Al-61.5 wt% USiAl (20% enriched U) silicide dispersion fuel, with 0.63 gU-235/cm³, the fissile loading suitable for use in NRU (and for the new MAPLE-X reactors), were irradiated to 57% U-235 burnup (analyzed). The elements were in excellent condition after irradiation; they appeared as they did in the as-fabricated condition except for a dull oxide layer on the cladding. Post-irradiation examinations (PIE) showed that the performance of the uranium silicide dispersion and the MEU alloy fuel was comparable to the HEU alloy fuel. All element diametral changes were less than 1.6% and length changes were within 0.2% after 57 at% burnup. As shown in Figure 2, the Al-HEU fuel microstructure remained essentially unchanged after irradiation but the LEU silicide particles reacted with the aluminum matrix material, forming a thin interfacial layer, probably UAl₃ with dissolved Si, around the fuel particles. Fission-gas bubbles ranging in size up to 5 μm were contained in the kernels of the fuel particles. Considerably less fission-gas bubbles were retained in the interfacial layers. Fuel-core swelling ranged between 3.4 to 4.5 vol% at the exit burnup. From the results it appears that all three materials swell at roughly the same rate, up to 57 at% burnup.

3.3.2. High-Burnup Confirmation

In the Exp-FZZ-909B irradiation, mini-elements containing the USiAl and USi*Al dispersions, with 3.15 gU/cm³, were irradiated up to 89 at% burnup (analyzed). Immersion density measurement indicated that the cores had swollen by 5.92-7.63 vol% after 77 at% burnup and by 6.57-7.76 vol% after 89 at% burnup, see Figure 3. These results showed swelling was approximately linear right up to 89 at% burnup, and confirmed that NRU-composition silicide dispersion fuels could exceed the design terminal burnup (80 at%) without exceeding the threshold of breakaway swelling.

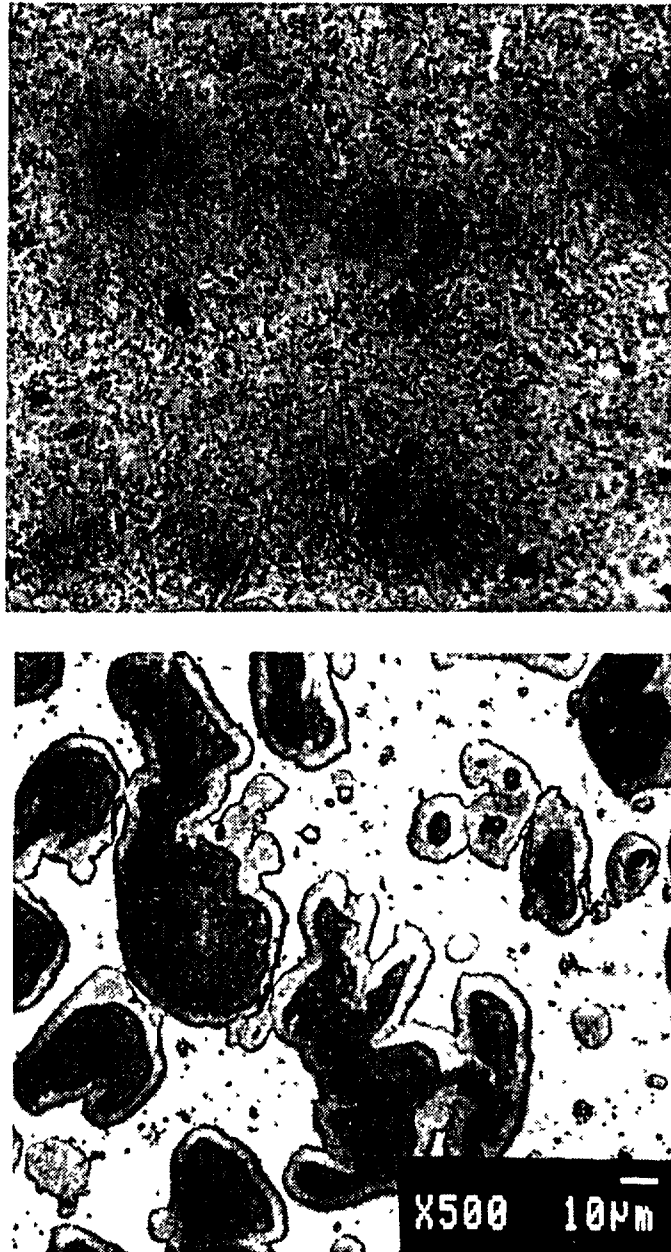


Fig. 2 Microstructure of: (a) Al-21 wt% U fuel after 57 at% burnup, UAl_4 - dark grey, Al - light grey; (b) Al-61.5 wt% USiAl after 57 at% burnup, U_3Si - dark grey, UAl_3 - light grey, Al - white.

PIE showed that both dispersions behaved similarly, i.e., the uranium silicide reacted with the aluminum matrix and fission-gas bubbles formed in the fuel particles. The interfacial layers were thinner near the fuel-core periphery and their edges were more sharply defined than at the fuel-core centre. The fission-gas bubbles were about the same diameter (up to $5\ \mu\text{m}$) in both locations but thicker interfacial layers and more particle coalescence had occurred at the fuel-core centre.

3.3.3. Dispersions with High U Loading and Fine Particles

In the FZZ-909A experiment, Al-USiAl and Al-USi*Al dispersions containing the higher loading required for NRX ($4.5\ \text{gU}/\text{cm}^3$) were tested. Fuel

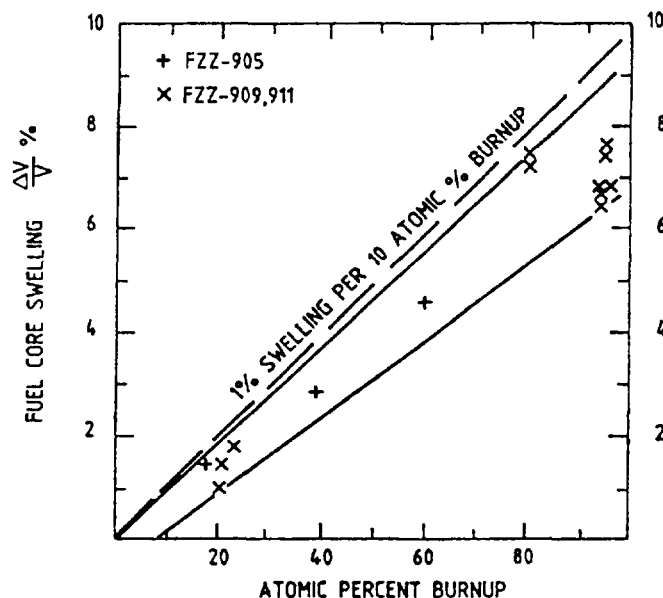


Fig. 3 Swelling of LEU fuel core containing Al-61.5 wt% USiAl and Al-62.4 wt% USi*Al.

performance was good and the materials behaved similar to the dispersions containing 3.15 gU/cm^3 ; however, swelling was marginally over 1 vol% per 10 at% burnup, at the terminal burnup of 74 at%.

In the Exp-FZZ-910 experiment, dispersions with a high loading of fine particles showed greater swelling compared to fuel with coarser particles at similar burnup. Mini-elements containing USiAl and USi*Al dispersions with fine particle-size distributions and 4.5 gU/cm^3 loading exceeded the swelling envelope of approximately 1 vol% per 10 at% burnup of the previous mini-element irradiations. The results suggest that particle size must be closely controlled to ensure good performance at high U loadings.

3.3.4. In-Reactor Corrosion

In-reactor corrosion behaviour of uranium silicide dispersion fuels has been investigated in the FZZ-911 and the FZZ-915 irradiations. The mini-elements contained Al-USiAl and Al-USi*Al, 3.15 gU/cm^3 . In the FZZ-911A experiment, four mini-elements had 1.2 mm diameter holes drilled in the cladding mid-section, and were irradiated in the linear power range 60-87 kW/m in NRU. The first and second mini-elements were removed from the reactor after reaching 19 and 32 at% burnup, respectively, and the remaining two after 48 at% burnup (analyzed).

Post-irradiated metallography and neutron radiography revealed that ellipsoidal cavities had developed beneath the holes in the cladding. The cavity size increased with increasing burnup. These cavities correspond to 1.1 mg and 3.2 mg of U-235 lost to the coolant after 19 and 32 at% burnup, respectively, and 9.8-48.0 mg U-235 after 48 at% burnup. These results indicate that the corrosion rate of the purposely defected fuel elements is acceptably low.

The FZZ-915 experiment was similar to the FZZ-911 experiment, except that the mini-elements were pre-irradiated to burnups in the range of 23 to 79 at% (analyzed) before the 1.2 mm diameter holes were drilled in the

cladding. These elements were further irradiated in the NRU reactor to evaluate the performance of the defective fuel, and during the additional 38 full-power days no increase in activity in the coolant above the normal background was detected. Neutron radiography and metallographic examinations revealed that the cavities were typically 0.7 mm deep by 1.3 mm across, i.e., only marginally larger than the original cavity made by the drill tip. These results indicate that the corrosion resistance of the LEU fuel is possibly increased by previous burnup.

3.3.5. Fuel-Core Surface Imperfections

The objective of the FZZ-911B experiment was to evaluate the performance of intact mini-elements having slight as-fabricated or deliberately introduced imperfections (machined grooves) in the core surface. However, the mini-elements contained the same fine particles that caused enhanced swelling in Exp-FZZ-910. Therefore, examinations were also carried out to determine the effects of the fine particle size on the core swelling when the loading is 3.15 gU/cm³.

Post-irradiation examinations revealed that the aluminum cladding had flowed into and filled the surface defects. More importantly, the core volume of the FZZ-911B mini-elements had only increased by approximately 4.9% after approximately 60 at% burnup compared with 7.0 to 17.5% swelling in the FZZ-910 cores at about the same burnup. Swelling was 7.1 vol% after 80 at% burnup. These results indicate that core surface defects had no detrimental effect on fuel performance, and fuel swelling was acceptable at the lower silicide loading required for NRU, even when fine particles were used.

3.3.6. Effect of Particle Size on Core Swelling

In the Exp-FZZ-918 experiment, 16 mini-elements containing Al-61.4 wt% uranium silicide were irradiated in NRU to help establish limits on the particle-size distribution to be used in the manufacturing specifications. The mini-elements were divided into 4 groups, each group containing progressively lower fractions of fines (particles less than 44 μ m in size).

Fuel swelling was linear with burnup, and to a first approximation proportional to the percentage of fines contained. After 89 at% burnup (analyzed) the mini-elements containing a high proportion of fines swelled by 6.6 to 6.8 vol% while the mini-element with a low fraction of fines swelled by 5.8 vol%.

3.3.7. AL-U₃Si₂ Dispersion Fuel

We have recently expanded the program to include U₃Si₂ dispersions to complement the U₃Si line. Twelve Al-U₃Si₂ mini-elements (3.15 gU/cm³) were fabricated with a variety of particle-size distributions and installed in NRU in 1988 June. The assembly was removed for interim post-irradiation examinations after reaching approximately 60 and 80 at% burnup, then it was returned to the reactor to continue the irradiation to 93 at% burnup. Metallographic examinations showed that the U₃Si₂ fuel behaved similarly to the U₃Si dispersions. An interfacial layer formed around the fuel particles, and fission-gas bubbles, ranging in diameter up to 10 μ m, could be seen in the fuel particles. The U₃Si₂ was not heat treated, and contained 4 wt% free uranium, the highest level expected from local non-uniformity in full-size castings. This appeared to have no detrimental effect on fuel performance. However, no swelling dependence on particle-

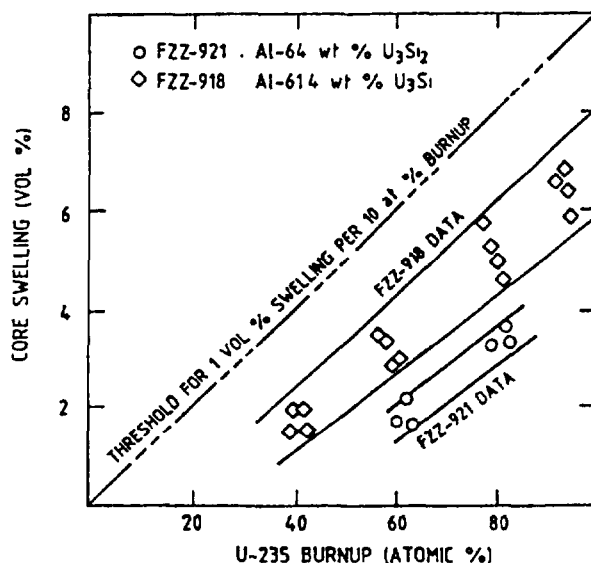


Fig. 4 Swelling of LEU fuel core containing Al-61 wt% U₃Si and Al-64 wt% U₃Si₂.

size distribution was observed, and the Al-U₃Si₂ dispersion fuel swelling was lower than Al-U₃Si at similar burnup. The results are shown in Figure 4, and are compared with data from Al-U₃Si mini-elements (Exp-FZZ-918).

3.4. Thermal Ramp Tests: Post-Irradiation Heating Tests

Thermal ramping tests were conducted in hot cells to determine the effects of temperature excursions on the dimensional stability and fission-product activity release from previously irradiated silicide dispersion fuel. Whole mini-elements and short segments of mini-elements with the fuel meat exposed were chosen, having fuel burnups of either 23 or 93 at%. Half the samples contained Al-61.5 w/o USiAl and half contained Al-62.4 w/o USi*Al.

The test conditions were: Argon gas flow rate - 1.66 mL/s; Heating rate - 0.2 and 0.4°C/s; Temperature - in the range 530 to 720°C; Holding time - temperature held constant ($\pm 4^\circ\text{C}$) for an hour.

In the thermal ramp tests, a whole mini-element irradiated to 93 at% burnup developed small localized blisters, some with pinhole cracks releasing fission products (⁸⁵Kr and ¹³⁷Cs) after 0.25 h at 530°C. This behaviour prevented gross pillowing or ballooning. A mini-element irradiated to 93 at% burnup and ramped to 640°C developed radial cracks, which tore the cladding and released fission products from the core. Even at this high temperature the element maintained considerable structural integrity. This behaviour is interpreted to mean that coolant channels would not become blocked even if the fuel was subjected to some hypothetical abnormal event with the potential to cause overheating of the core, e.g. 530°C compared with the normal operating maximum of 200°C.

3.5. Full-Size NRU Fuel Test Results

The excellent performance of mini-elements containing the USiAl and USi*Al dispersion fuel led naturally to the fabrication and testing of full-size, 12-element NRU fuel assemblies. In experiment FZZ-913, seven assemblies were irradiated in NRU, 3 containing Al-62.4 wt% USi*Al and 4 containing Al-61.0 wt% U₃Si (identified as FL-001 to FL-007). The LEU assemblies were installed in NRU during 1984, replacing the currently used HEU alloy

fuel in NRU, and were irradiated at typical driver-fuel operating conditions. The electrical conductivity of the coolant ranged between 0.25 and 0.7 $\mu\text{mho/cm}$ during irradiation. The pH was not routinely measured, but ranged between 5.5 and 7. The coolant inlet temperature ranged between 30-37°C and the outlet between 60-70°C. Inlet pressure was approximately 80 psi (579 KPa) and outlet approximately 30 psi (207 KPa). Each rod occupies an average of 5 core positions during its lifetime (~340 d residence time @ 70% efficiency) as it is moved from the outside of the core (low-flux site) to the centre (high-flux site) and back to the outside. Average element linear power ranged from 40-50 kW/m, with the maximum being approximately 80 kW/m.

Burnup analysis showed that the rods were irradiated to 67 to 84 at% burnup (peak). Visual examinations showed that the fuel elements were in good condition; they were identical in appearance to the HEU elements with the normal aluminum oxide layer coating the surface. Dimensional measurements indicated that elongation during irradiation was negligible; the USi*Al and the U₃Si dispersion fuel elements were within 0.5% of their original length.

Post-irradiation metallography revealed that, as expected, the full-length elements' high burnup behaviour was similar to that of the mini-elements. The fuel particles had reacted with the matrix aluminum forming the normal aluminide interfacial layer (UAl₃ with dissolved Si). The interfacial layer which formed around the U₃Si particles was considerably thinner than that in the USi*Al dispersion. Small fission-gas bubbles were contained in the kernels of the fuel particles and ranged in size up to 10 μm in diameter. Considerably fewer fission-gas bubbles had been retained in the interfacial layers.

Evidence of the axial burnup gradient was observed in the full-length elements. In the high-burnup sections (mid-length) more particle coalescence had occurred than at the lower burnup sections (ends). There was less evidence of particle coalescence in the U₃Si dispersion. However, there was no evidence of the linking-up of fission-gas bubbles in any of the fuels examined, indicating that the fuels were well away from the onset of breakaway swelling. Immersion-density swelling measurements could not be made on the full-length elements, so estimates based on the dimensional changes from the underwater and metallographic examinations have been calculated. Core diameter increases of up to 3% and 4% have been measured at the ends and at the middle of the fuel elements, respectively. These give conservative estimates of the core's swelling by less than 1 vol% per 10 at% burnup at the terminal burnup of 84 at%.

It is clear that the high-burnup performance of USi*Al and U₃Si dispersion fuel containing 3.15 gU/cm³--the loading required for the research reactors at CRNL--is acceptable. Factors contributing to the good performance were the suitable particle-size distribution and the superior restraint provided by the thick-walled cladding.

4. STATUS OF NRU CONVERSION

NRU was partially converted to LEU when the first 31 LEU fuel rods manufactured using industrial-scale equipment were installed during 1988 September to December. This partial (one third) LEU core allowed the reactor engineers and physicists to evaluate the bulk effects of LEU conversion on reactor operations. Table 2 shows the burnup profiles of selected Al-U₃Si dispersion fuel rods from the first campaign, as of 1989

TABLE 2

STATUS OF SELECT LEU FUEL IRRADIATIONS (AS OF 1989 JULY 31)

ROD ID	INSERTION DATE	REMOVAL DATE	INITIAL U-235 (g)	BURNUP (% U-235)	POWER Mwd
FL008	88 09 29	89 07 30	495.7	80	320.1
FL009	88 09 30	---	494.1	79	314.2
FL010	88 10 01	---	493.9	79	313.1
FL011	88 10 04	89 07 30	497.0	80	321.3
FL012	88 10 06	89 05 31	494.0	61	244.9
FL015	88 10 13	---	492.6	77	304.9
FL020	88 11 07	---	493.3	72	285.3
FL028	88 12 12	---	492.1	71	282.5
FL038	88 12 28	---	494.0	54	215.8

July. As expected, the irradiation is proceeding without incident and the reactor engineers have seen no difference in fuel-rod behaviour or handling compared to HEU fuel. In a given neutron flux the reactivity worth of the LEU rods is indistinguishable from HEU rods at comparable burnup. Bulk parameters such as coolant/moderator chemistry and overall reactivity have not changed perceptibly with the partial LEU core.

In 1989 July, the first of the rods reached their exit burnup. Two of these rods were cut apart in the NRU bays for PIE. Under-water visual examinations revealed clean, straight elements with only the light oxide coating on the cladding that is normally also seen on the HEU elements. No detailed metallographic examinations were planned since the rods behaved satisfactorily during irradiation, as expected. One of the elements which was inadvertently bent during handling demonstrated good ductility after full irradiation. By the end of 1989 all of the prototype LEU fuel rods will have completed their irradiation in NRU.

Fuel production in the new facility is expected to begin in 1990. It is expected that the full conversion of NRU will commence when a stable fuel production rate exceeding the fuel-usage rate is achieved. The projected date for this milestone is 1990 September.

5. CONCLUSIONS

1. Suitable LEU silicide dispersion fuels have been developed and tested at CRNL for the conversion of NRU from HEU to LEU. Under NRU fuel operating conditions, the fuels are stable up to burnups exceeding the design terminal burnup (80 at%).
2. NRU has been partially converted to LEU; 31 prototype LEU rods containing AL-61 wt% U₃Si fuel (one third of a NRU core) were installed during 1988 September to December. The irradiation is continuing without incident, as expected. Post-irradiation

examinations of the first rods to be discharged confirmed that the fuel achieved the design burnup in good condition.

3. Construction of a new fuel-fabrication facility is essentially completed and LEU fuel production is expected to begin in 1990. The complete conversion of NRU is expected to begin in 1990 September.

ACKNOWLEDGEMENTS

Many people, some of whom have since left CRNL, have contributed to the success of the LEU fuel development and conversion program. They are too numerous to properly acknowledge here. However, we would especially like to thank J.C. Wood, M.T. Foo, L.C. Berthiaume, L.N. Herbert, J.D. Schaefer, J.G. Goudreau, F.C. Iglesias, R.G. Barrand, J. Mitchell, J.R. Kelm, R.J. Chenier and the CRNL hot-cell metallography group, and E.J. McKee and the rod-shop group, for their contributions.

REFERENCES

- [1] J.C. Wood, M.T. Foo and L.C. Berthiaume, "The Development and Testing of Reduced Enrichment Fuels for Canadian Research Reactors", Proceedings of the International Meeting on Research and Test Reactor Core Conversions from HEU to LEU Fuels, Argonne, Illinois, 1982 November 8-10.
- [2] J.C. Wood, M.T. Foo, L.C. Berthiaume, L.N. Herbert and J.D. Schaefer, "Advances in the Manufacturing and Irradiation Testing of Reduced Enrichment Fuels for Canadian Research Reactors", Proceedings of the International Meeting on RERTR, Tokai, Japan, 1983 October 24-27.
- [3] D.F. Sears, L.C. Berthiaume and L.N. Herbert, "Fabrication and Irradiation Testing of Reduced Enrichment Fuels For Canadian Research Reactors", Proceedings of the International Meeting on RERTR, Gatlinburg, Tennessee, 1986 October.
- [4] J.W. Schreader, I.C. Kennedy and D.F. Sears, "Status of Canadian Low-Enriched Uranium Conversion Program", Proceedings of the International Meeting on RERTR, San Diego, California, USA, 1988 September 19-22.

Appendix J-4.6

DEVELOPMENT OF LOW ENRICHMENT MTR FUEL AT DOUNREAY

D. SINCLAIR

Dounreay Nuclear Power Development Establishment,
United Kingdom Atomic Energy Authority,
Thurso, Caithness,
United Kingdom

Abstract

Work up to October 1983 on the development of a manufacturing route for the manufacture of low enriched fuel at Dounreay concentrated on the roll-bonding method of plate manufacture. Both U-Al alloy and U_3O_8 -Al cermet elements at 45% enrichment have been irradiated and the fabrication of 20% enriched U_3O_8 -Al cermet elements is in hand.

INTRODUCTION (1-3)

The United Kingdom Atomic Energy Authority operate a MTR fuel fabrication plant, with a capacity of about 1,000 fuel elements per year, at Dounreay on the north coast of Scotland. The prime purpose of this plant is to manufacture fuel elements for the DIDO and PLUTO reactors at the Harwell research establishment and fuel element development has been concentrated on the requirements of these reactors with close co-operation between the two establishments.

In addition to the Harwell reactors Dounreay supplies fuel elements to various university reactors in the United Kingdom and a number of overseas customers, on a commercial basis.

Development work has been concentrated on the production of fuels with higher uranium loadings as a step towards "reduced enrichment" fuel production. Initial work successfully developed the traditional melting and casting route to produce fully satisfactory alloys, up to 35 w/o U/Al and later work has successfully produced fuel plates using the U_3O_8 /Al cermet route.

Irradiation of medium enriched (45% U-235) fuels to high burn-up has been carried out and post-irradiation examination has confirmed the acceptability of such fuels fabricated using both the conventional U-Al alloy technology and the U_3O_8 -Al cermet technology.

Plate fabrication trials using natural uranium in U_3O_8 -Al cermet cores have been completed satisfactorily and fuel elements with cermet cores containing uranium at low enrichment (20% U-235) are currently being manufactured for test irradiation.

FABRICATION METHODS

Two methods are currently (October 1983) in use at Dounreay for the routine fabrication of MTR fuel, both using U-Al alloy technology.

- i. the traditional roll-bonding method of producing fuel plates which can either be assembled directly into flat-plate fuel elements or preformed and electron-beam welded into fuel tubes for assembly into concentric-tube fuel elements, and
- ii. the co-extrusion of alloy inserts contained within aluminium sleeves to produce completely clad fuel tubes in a single operation. These tubes are then assembled into concentric-tube fuel elements.

PROGRESS TO DATE (October 1983) (3)

Medium Enriched Fuel (45% U-235)

To date, work has been concentrated on the roll-bonding method to permit the production of medium enriched fuel plates in both alloy and cermet forms.

A 45% enriched concentric-tube fuel element incorporating U-Al alloy cores with a uranium density of 1.1 g U/cm^3 has been irradiated (Table 1) to 52.3% burn-up and the post irradiation examination has been completed. The examination showed the surfaces of the fuel plates to be free of blisters and other gross defects. Both longitudinal and transverse micro-sections, taken from positions along the length of the fuel tube, showed the cladding and core to be clean and sound with good uniform dispersion of the intermetallic compounds UAl_3 and UAl_4 . Good metallurgical bonding between the cladding and fuel core had been maintained, and there was regular good axial alignment of the cladding and core with the cladding thickness within the original specified limits. Tapering and dog-boning at the core ends were slight.

A fuel tube, electron-beam welded from U_3O_8 -Al cermet core plates with a uranium density of 1.1 g U/cm^3 has been irradiated (Table 2) to 68% burn-up and post irradiation examination has been completed. Visual examinations of the irradiated tube showed it to be free from blisters or other gross defects. The irradiated tube was heated to 250°C and held for 15 minutes and then in 50°C steps to 500°C with an examination for blisters following each step. No blistering occurred at any stage of this test. Both longitudinal and transverse micro-sections, taken along the length of the plate, showed the thickness of the core and cladding to be uniform with good axial alignment of the core and cladding. Good metallurgical bonding between cladding and the core had been maintained. Cracks observed in the core in some specimens were later demonstrated to have formed during cutting operations carried out to obtain the metallographic samples. Variations in size and distribution of U_3O_8 particles in the core were as anticipated from pre-irradiation samples. Characteristic end effects - tapering and dog-boning - were typical and slight.

Two more 45% enriched fuel elements with U_3O_8 -Al cermet cores are currently undergoing irradiation; one in a 5 MW light water research reactor and the other in the 25 MW PLUTO research reactor at Harwell. Post irradiation results on the former will be available in about 18 months and on the latter by the middle of 1984.

TABLE 1

45% ENRICHED 'DIDO' TYPE FUEL ELEMENT (U-Al alloy - 1.1 g U/cm³)
IRRADIATION CONDITIONS

Reactor	= PLUTO (AERE HARWELL)
Average Burn-up	= 52.3% U-235 atoms
Total average thermal dose (average over whole element)	= 1.15×10^{21} n cm ⁻²
Total fast neutron dose (above 1 MeV) (at centre line of fuel)	= 4.4×10^{20} n cm ⁻²

TABLE 2

45% ENRICHED 'DIDO' TYPE FUEL TUBE (U₃O₈-Al cermet - 1.1 g U/cm³)
IRRADIATION CONDITIONS

Reactor	= PLUTO (AERE HARWELL)
Average Burn-up	= 68% U-235 atoms
Total average thermal dose (average over whole element)	= 1.4×10^{21} n. cm ⁻²
Total fast neutron dose (above 1 MeV) (at centre line of fuel)	= 5.2×10^{20} n.cm ⁻²

Work on the development of U₃O₈-Al cermet cored co-extruded fuels has been on a low priority. Some cermet thick wall inserts have been produced by isostatic pressing but to date these have not been dimensionally or structurally suitable for co-extrusion. Work will continue, applying experience gained in the work to date.

Low Enriched Fuel (< 20% U-235)

Development of fuel containing uranium of low enrichment has been restricted to the production of U₃O₈-Al cermet cored fuel plates which retain their standard external dimensions. Plate rolling trials have been carried out using natural uranium and these indicated that compacts of adequate handling strength with a uranium density of 3.0 g U/cm³ could be produced without binder at a compaction pressure of 30 tons/in² (463 MN/m²). This work is now being applied to the fabrication of five, 20% enriched, concentric fuel elements containing cores with a nominal uranium density of 2.9 g U/cm³. These elements will be irradiated in the Juelich reactor FRJ-2. An additional fuel element containing identical fuel plates is being fabricated for irradiation in the PLUTO reactor at Harwell, starting later this year.

REFERENCES

1. B. Hickey, "Note on Current Position Regarding the Development by the UKAEA of Reduced Enrichment Fuels for Research and Test Reactors," Proceedings of the International Meeting on Development, Fabrication and Application of Reduced Enrichment Fuels for Research and Test Reactors, Argonne, Illinois, November 12-14, 1980, ANL/RERTR/TM-3, CONF-801144 (August 1983), pp. 250-251.
2. P. Chare and D. Sinclair, "Development of Low Enriched MTR Fuel at Dounreay," IAEA Seminar on Research Reactor Operation and Use, Juelich, Federal Republic of Germany, 14-18 September 1981, IAEA-SR-77.
3. D. Sinclair, "Development of Low Enriched Fuel at Dounreay - Progress Report," Proceedings of the International Meeting on Reduced Enrichment for Research and Test Reactors, Tokai, Japan, 24-27 October 1983, JAERI-M 84-073 (May 1984), pp. 31-33.

Appendix J-4.7
Part I

IRRADIATION OF MEU AND LEU
TEST FUEL ELEMENTS IN DR 3

K. HAACK
Risø National Laboratory,
Roskilde, Denmark

Abstract

Irradiation of three MEU and three LEU fuel elements in the Danish reactor DR 3.

Thermal and fast neutron flux density scans of the core have been made and the results, related to the U235-content of each fuel element, are compared with the values from HEU fuel elements. The test elements were taken to burn-up percentages of 50-60%. Reactivity values of the test elements at charge and at discharge have been measured and the values are compared with those of HEU fuel elements.

1. INTRODUCTION

As a part of the current programme for evaluation of the feasibility of research reactor conversion to lower enriched fuel organized by IAEA, irradiations of medium enriched uranium (MEU) and low enriched uranium (LEU) test fuel elements have been carried out in reactor DR 3, Risø, Denmark.

The irradiation of the 3 MEU elements was finished in February 1983. The 3 LEU elements were irradiated in the same core positions and in continuation of the MEU element series. The LEU element irradiation test was finished September 1983.

The test fuel elements were geometrically identical to the remaining fuel elements in the core, which were 93% enriched cylindrical tube type (Mk 4) with an initial ^{235}U content of 150g (20 elements) and 120g (3 elements). During the test period 7-12 irradiation rigs and isotope production rigs were present in the core in some of the 50mm central irradiation holes of the fuel elements. All other fuel elements

contained flux scanning rigs. The 3 test elements contained flux scanning rigs all the time.

The reactor was operated at 10 MW thermal power in 4 weeks cycles with about 5 days shut-down in each cycle. The bulk heavy water temperature was 50-55°C.

2. SPECIFICATIONS

Table 1 shows the specifications for the MEU and LEU test elements, - with those of the present standard HEU fuel elements included for the sake of comparison.

As it is seen, the three types are nearly identical with respect to the outside geometrical dimensions. So the hydraulic parameters are nearly the same.

TABLE 1

Manufacturer	HV	HV	NUKEM
Enrichment %	93	45	19.75
Fuel meat type	UAl-alloy	UAl-alloy	U ₃ O ₈ -Al
Uranium density gcm ⁻³	0.57	1.18	2.7
U-235 content, g	150	150	180
Fuel meat thickness, mm	0.53	0.53	0.65
Cladding	99.5% Al	99.5% Al	99.5% Al
Cladding thickness, mm	0.47	0.47	min. 0.43
Fuel plate thickness, mm	1.47 [±] 0.02	1.47 [±] 0.02	1.51 [±] 0.05
Fuel plate length, mm	583 [±] 12	583 [±] 12	min. 590
Fuel plate width, mm	60.5 and 92.5	60.5 and 98.5	65.3-75.6-85.8-96.1
Fuel tube diameters:			
Tube no. 1, mm	63.85	63.85	63.8
Tube no. 2, mm	73.65	73.65	73.6
Tube no. 3, mm	83.45	83.45	83.4
Tube no. 4, mm	93.25	93.25	93.2
Cover tube, mm	103	103	102.6

Each type consists of four coaxial fuel tubes and an outer Al cover tube, fitted in 4 combs at top and bottom. In the centre is space for a 54mm o.d. experiment thimble.

The main differences between the types are the enrichment and the consequent meat density change. Furthermore, the NUKEM type differ with respect to

- meat material
- meat thickness
- ^{235}U content.

3. IRRADIATION SCHEDULE

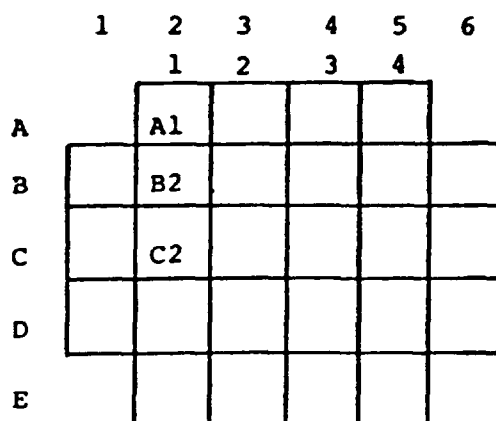


FIG. 1.

The MEU and LEU test elements were irradiated in the core positions A1, B2 and C2, see fig. 1. The MEU series were in the core from May 1982 to February 1983, followed by the LEU series which lasted until September 1983. The installation of each element was displaced one operation cycle (4 weeks) relative to

the preceding element in the same series, in order to be able to utilize the experience gained.

The burn-up percentages of the test elements at discharge were:

Element no.	1	2	3
MEU	52	58	57
LEU	55	51	57

4. NEUTRON FLUX DENSITY MEASUREMENTS

Thermal and fast flux scanings have been made in all core positions equipped with flux scan rigs, i.e. in 14-19 fuel elements including the 3 test elements, in each operation cycle. Co and Ni foils have been used, 8 with 10cm distance for each axial scanning in a fuel element.

The aim was to unveil possible flux differences between HEU, MEU and LEU fuel elements. The thermal neutron flux in a core position is mainly influenced by the ^{235}U -content in the fuel element and by the coarse control arm (CCA) angle. Thus, in order to obtain good comparisons between HEU and MEU fluxes, it is necessary to select flux scans with HEU and MEU fuel containing nearly the same ^{235}U amount and run with nearly the same CCA-angle. Obvious, these conditions are coinciding very rare, so that comparison would be based on a very few examples.

However, a more comprehensive utilization of all the measurement results in the MEU and LEU test elements can be made by plotting the fast/thermal flux ratio against the ^{235}U -content, a method described by Wright 1). As the power P in a fuel element is proportional to the fast flux ϕ_f and also proportional to the product of the ^{235}U -content $M_{\text{U}235}$ times the thermal flux ϕ_{th} :

$$P = K_1 \times \phi_f \qquad P = K_2 \times M_{\text{U}235} \times \phi_{\text{th}}$$

$$\text{he obtained } \frac{\phi_f}{\phi_{\text{th}}} = K_3 M_{\text{U}235} \qquad (1)$$

Thus the plot of equation (1) should be linear for specific fuel element types and flux scan rig types.

The method has been used earlier to unveil differences between various fuel element and rig types.

Fig. 2 and 3 show the flux measurement results from the MEU and LEU testings, respectively. The lower graphs show the measurements in the test elements, the upper ones show

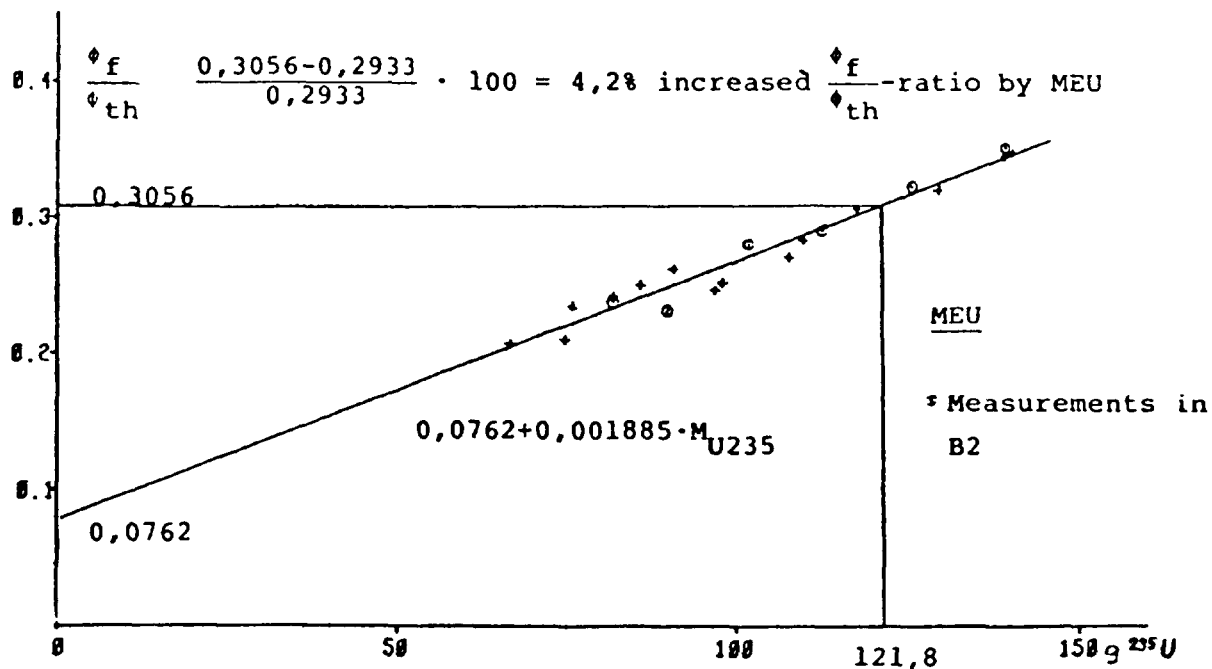
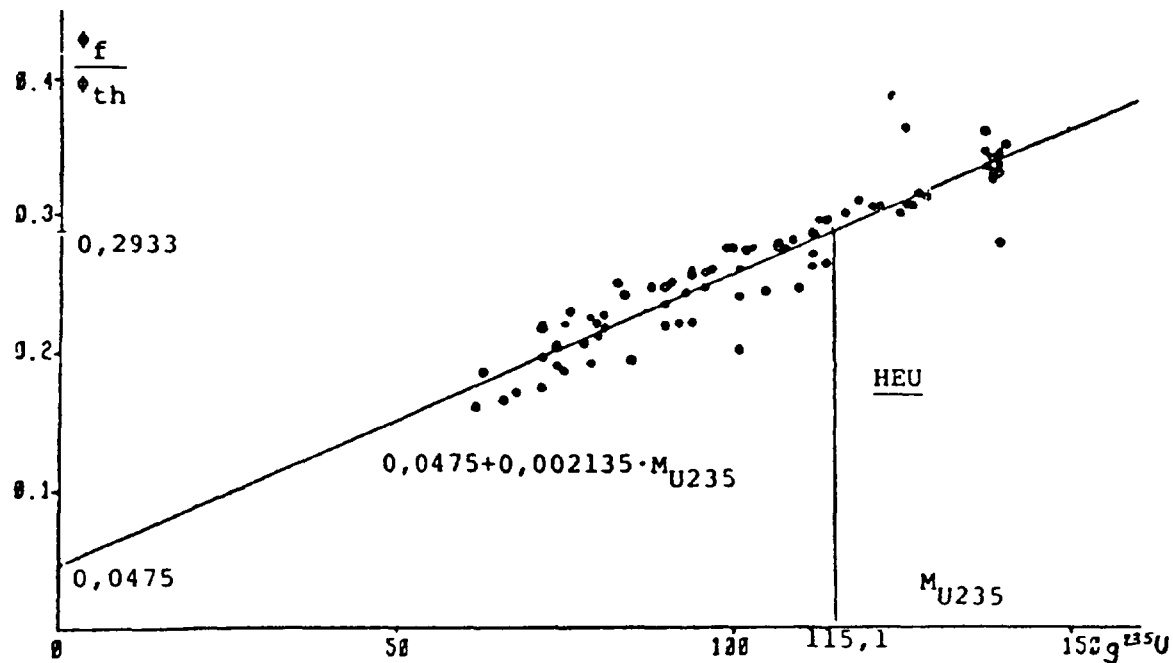


FIG. 2. Difference in fast/thermal flux ratio between HEU and MEU fuel elements.

those in the remaining HEU elements present in the core during the test element irradiation cycles.

The thermal flux value used in the flux ratio is the mean value of the axial thermal neutron flux distribution in the core section of the fuel element in question. The fast flux value used in the flux ratio is the maximum fast neutron flux, which is a good representative of the fast flux because

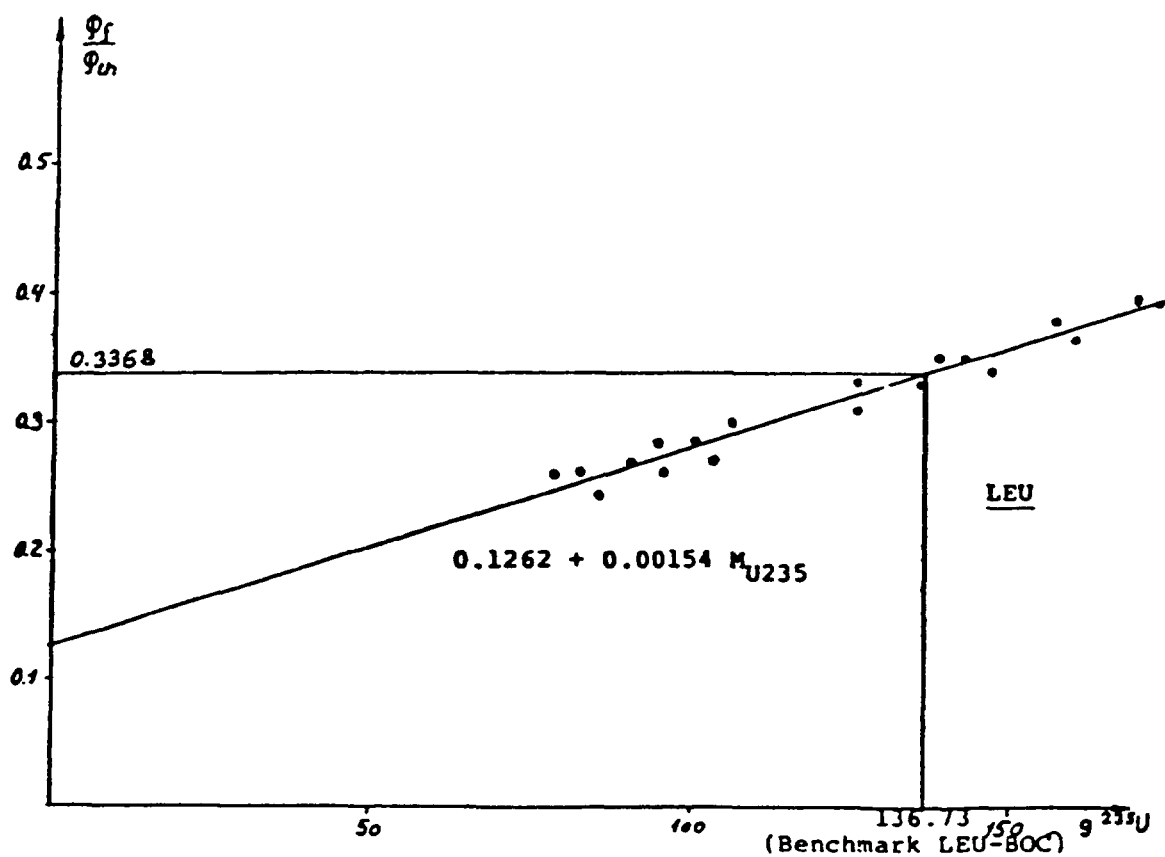
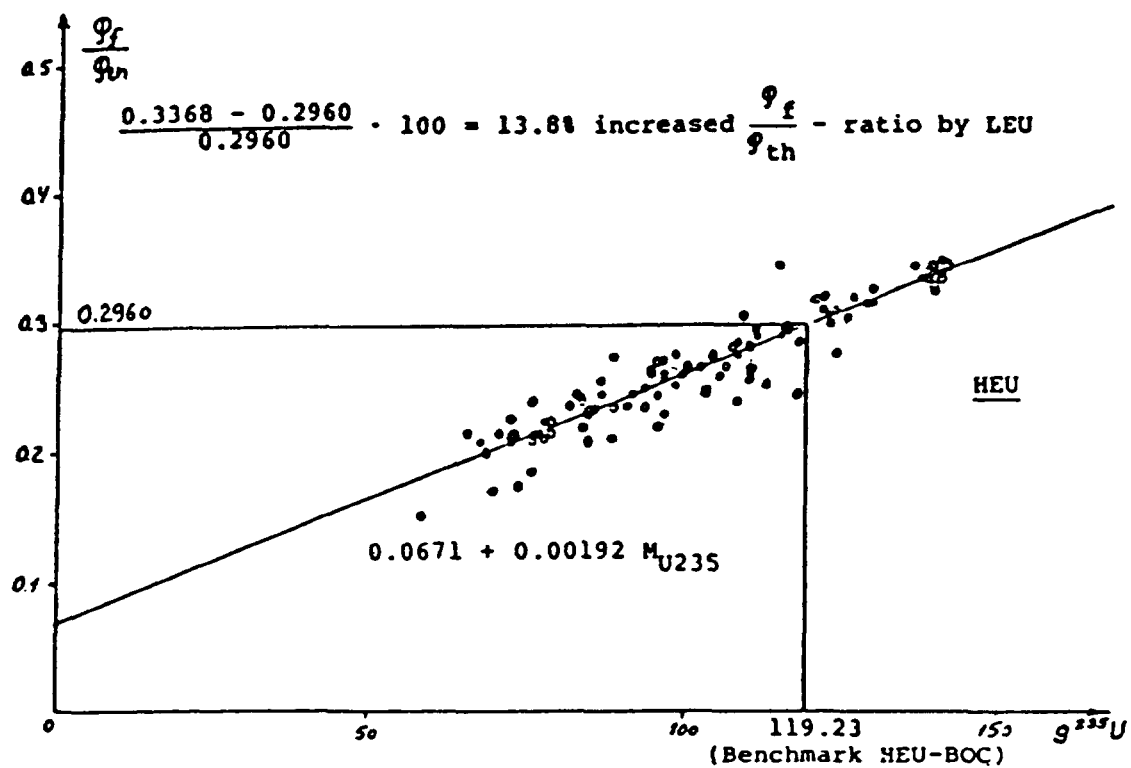


FIG. 3. Difference in fast/thermal flux ratio between HEU and LEU fuel elements.

the axial fast flux distribution is roughly rectangular shaped and rather insensitive of absorber movements and other changes in the core.

On figs. 2 and 3 also the regression lines belonging to the flux ratios are shown. By means of the line equations, good estimates of the expected flux ratio changes owing to conversion to MEU and LEU can be obtained.

Calculations on the DR 3 core conversions 2), 3), 4) show that the ^{235}U -content has to be increased by 6.7 g in the MEU core and 17.5 g in the LEU core. The flux ratio belonging to the mean ^{235}U -content of the HEU elements, 115.1 g (fig.2) is read on the regression line: 0.2933. The corresponding flux ratio read on the MEU regression line at a 6.7 g higher mean ^{235}U -content, 121.8 g, is: 0.3056.

The depreciation of the ϕ_f/ϕ_{th} -ratio is thus for MEU: 4.2%.

The corresponding depreciation for LEU can be obtained in a similar way: 13.8%.

5. REACTIVITY MEASUREMENTS

The reactivity change at the insertion and at the withdrawal of each MEU test element has been measured. The values are given in table 3 and compared to the expected values, which are based on statistics from several years of HEU fuel element changes.

The main differences concerning reactivity between HEU elements and those with lower enrichments are the bigger contents of ^{238}U and Pu in the lower enriched elements.

In table 3 the calculated Pu contents are added to the residual ^{235}U -content in order to get the total fissile content to be used as input to the calculation of the estimated reactivity changes at discharge of the elements. Consequently the deviations

TABLE 2. REACTIVITY ACCOUNT FOR LEU TEST FUEL ELEMENT CHANGES

LEU	Position	A1	B2	C2
<u>At loading:</u>				
Measured difference between 148g HEU and 180g LEU		+ 0.07% dk/k	+ 0.04% dk/k	+ 0.06% dk/k
Expected difference between 148g HEU and 180g HEU		+ 0.17% dk/k	+ 0.24% dk/k	+ 0.37% dk/k
Loss due to excess U238 in LEU (~750g)		0.10% dk/k	0.20% dk/k	0.31% dk/k
<u>At discharge:</u>				
Measured difference between discharged LEU and 148g HEU		+ 0.82% dk/k	+ 1.74% dk/k	+ 1.68% dk/k
Calculated U235 content in discharged LEU	82 g		78 g	73 g
Calculated Pu239 content in discharged LEU	5 g		5 g	5 g
Expected difference between similar ^{x)} HEU and new 148g HEU		+ 0.66% dk/k	1.04% dk/k	+ 1.31% dk/k
Gain by removing excess U238 in LEU (~745g)		0.16% dk/k	0.70% dk/k	0.37% dk/k

x) with the same fissionable content as the discharged LEU.

TABLE 3. REACTIVITY ACCOUNT FOR MEU TEST FUEL ELEMENT CHANGES

MEU	Position	A1	B2	C2
<u>At loading:</u>				
Fissile content of discharged HEU		123 g	81 g	70 g
Measured difference between discharged HEU and 147g MEU		+ 0.22% dk/k	+ 0.93% dk/k	+ 1.33% dk/k
Expected difference between discharged HEU and 147g HEU		+ 0.24% dk/k	+ 1.06% dk/k	+ 1.46% dk/k
Loss due to excess U238 in MEU (169g)		0.02% dk/k	0.13% dk/k	0.13% dk/k
<u>At discharge:</u>				
Measured difference between discharged MEU and 147g HEU		+ 0.73% dk/k	+ 1.46% dk/k	+ 1.71% dk/k
Calculated U235 content in discharged MEU		71 g	62 g	64 g
Calculated Pu239 content in discharged MEU		2 g	2 g	2 g
Expected difference between similar ^{x)} HEU and new 147g HEU		+ 0.81% dk/k	+ 1.33% dk/k	+ 1.54% dk/k
Gain by removing excess U238 in MEU (167g)		- 0.09% dk/k	0.13% dk/k	0.17% dk/k

x) with the same fissile content as the discharged MEU.

between measured and expected reactivity changes are mainly owing to the absorbing influence of the ^{238}U -contents.

At the loading of each LEU test element a new standard HEU element was previously installed in order to measure the very difference between a new 180g LEU U_3O_8 element and a new 150g HEU UAl-alloy element. The estimated reactivity changes have been calculated in this case using a special set of factors, valid for "new-to-new fuel element changes".

Except for the unusual high reactivity change measured at the discharge from B2, the losses due to excess ^{238}U at loading and at discharge agree fairly well. The expected increases of the reactivity worths of ^{238}U from A1 at the core edge over B2 to C2 (close to the core center) are also distinct.

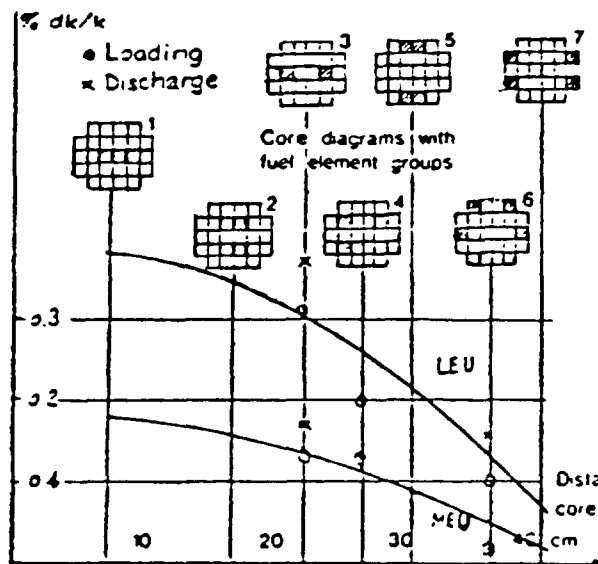


FIG. 4.

Rough estimates of the reactivity consumption due to ^{238}U in full MEU and LEU cores can be made by plotting the measured losses of reactivity owing to ^{238}U as a function of the distance of the fuel element from the core center, see fig. 4.

By reading the contributions from the remaining fuel elements on the regression curves, the total reactivity loss is found at 5.8% dk/k and 2.6% dk/k for the LEU and MEU core, respectively.

These reactivity losses can be compensated for by adding about 14g ^{235}U to each LEU-element and about 6g ^{235}U to each MEU-element.

6. POST IRRADIATION EXAMINATIONS

The routine procedure for preparing irradiated fuel elements for shipment to the reprocessing plant is to cut the fuel tubes outside the fuel meat section. By this operation the tubes separate and it is feasible to make a visual examination of the individual fuel tubes in the cutting pond, by means of bright light and using binoculars. It was intended to examine the fuel elements more thoroughly in the Hot Cell's if the visual inspection unveiled blisters or other irregularities.

The MEU fuel elements were found to be in perfect condition.

Post irradiation examinations on the LEU test elements have not yet been performed (Sep. 1983). They will be made when the elements have cooled about 3 months.

REFERENCES

1. S.B. Wright, Fast Neutron Fluxes in Mk III Fuel Elements in DIDO and PLUTO, AERE-M 864, Harwell, U.K., 1961.
2. J. Matos. Enrichment Reduction Calculations for the DIDO, DR 3 and JRR-2 Reactors, ANL (USA), Appendix A in "Research Reactor Core Conversion From the Use of Highly Enriched Uranium to the Use of Low Enriched Uranium Fuels", Guidebook Addendum, Heavy Water Research Reactors, IAEA, Wien, 1982.
3. C.F. Højerup. Enrichment Reduction Calculations for the DR 3 Reactor, Risø, Denmark, Appendix E to the Guidebook Addendum referred to above.
4. Benchmark Calculations, Appendix F to the Guidebook Addendum referred to above.
5. K.E. Beckurts, K. Wirtz, Neutron Physics, Springer Verlag, Berlin, 1964.

Appendix J-4.7

Part II

IRRADIATION IN DR 3 OF THREE DANISH MANUFACTURED LEU SILICIDE TEST FUEL ELEMENTS

RISØ NATIONAL LABORATORY
Roskilde, Denmark

Abstract

The 3 test fuel elements of the U_3Si_2 -Al type enriched to 19.75% with 180g ^{235}U was manufactured by ATLAS AED. The silicide powder was delivered by Babcock & Wilcox, USA. The elements were irradiated in DR 3 from August 1986 to April 1987 to burn-ups ranging from 51% to 57%. The elements performed perfect during the irradiation. The fuel tubes have been visually inspected for blisters and other irregularities after cutting in the pond. No defects were found. Later on thickness measurements of the fuel tube plates will be attempted and documentary photographing of the fuel tube surfaces will be undertaken.

SPECIFICATIONS:

The table below shows the specifications of the test elements and the present HEU elements, for comparison.

The outside geometrical dimensions are identical.

The fuel meat of the test element is 3.8% shorter and 0.8-2.7% narrower than that of the present fuel element. The reason is that it is necessary to have better clearance from the edges to the meat for the cermet fuel types.

IRRADIATION DATA:

In table 2 is given the relevant irradiation data, the burn-up of ^{235}U and the production of Pu.

Table 3 shows the irradiation positions in the core.

Table 1. Fuel element specifications

	Present element	Test element
Enrichment, %	93	19.75
Fuel meat	UAl-alloy	U ₃ Si ₂ -Al
Al	83.6 w/o	33.6 w/o
Powder composition	-	15-20% fine (<45µm)
Cladding	99.5% Al	AlMg1
U-density g/cm ³	0.55	3.35
²³⁵ U-content, g	150	180
<u>Fuel plates:</u>		
Meat thickness mm (mean)	0.55	0.55
Cladding thickness mm (mean)	0.46	0.46
Plate thickness mm	1.47 ± 0.02	1.47 ± 0.02
Plate length mm (mean)	583 ± 12	560 ± 12
Plate width mm (mean)	60.5 and 92.5	60.0 and 90.0 ± 1
<u>Fuel tubes:</u>		
Meat thickness mm (mean)	0.56	0.56
Wall thickness mm	1.50	1.50
Fuel length mm (mean)	600	577
Fuel tube length mm	660.4	660.4
Tube outer diameters mm		
1. tube	63.85	63.85
2. tube	73.65	73.65
3. tube	83.45	83.45
4. tube	93.25	93.25
Cover tube OD/ID	103/100	103/100
Channel width, mean, mm	3.40	3.40
Channel width, min., mm	3.12	3.12

Table 2. Irradiation data

Test element no.	007/18	008/18	009/18
Irradiation starts	11.july 1986	15.aug. 1986	12.sep. 1986
Core position	A1	B2	C3
Initial ²³⁵ U-content,g	180.9	180.8	180.9
End ²³⁵ U-content,g	78.1	88.2	80.2
End enrichment,%	9.82	10.93	10.05
Burn-up,%	57	51	56
End Pu-content,g	5.5	5.2	5.4
Irradiation stops	29.mar. 1987	1.mar. 1987	29.mar. 1987
No. of reactor cycles	9	7	7

Table 3. Test element core positions

	A1			
	B2			
	C2			

The remaining 23 core positions were loaded with HEU fuel elements with 150g and 120g (0-3 elements) ^{235}U . The mean burn-up of the HEU elements is close to 50% at the end of the irradiation.

REACTIVITY MEASUREMENTS:

The reactivity values of the test elements were measured relative to HEU fuel elements, at the time of insertion and at the time of withdrawal.

Earlier experience from reactivity measurements on three NUKEM 180g U_3O_8 -Al test elements ¹⁾ indicated that the reactivity value of a 180g LEU fuel element in a HEU-core equals that of a 150g HEU fuel element. This has been confirmed by DR 3/SIM calculations.

Therefore the estimations of the reactivity changes by insertion or withdrawal of the LEU test elements were calculated by subtracting 30g from the ^{235}U -content and multiply this reduced ^{235}U -content by the appropriate fuel worth factor.

Table 4 shows the results. It is seen that the measured and calculated values are in good accordance.

IRRADIATION PERFORMANCE:

The outlet temperatures have varied within $\pm 5^\circ\text{C}$ around the D_2O bulk temperature.

Table 4. Reactivity measurements at insertion
and withdrawal of the test elements

Position	S.D.No.	Element No.		Grms. U-235		Reactivity change	
		IN	OUT	IN	OUT	Measured %dk/k	Calculated %dk/k
A1	324	18/007	15/895	181	148	+0.09	+0.03
B2	325	18/008	15/898	181	148	+0.05	+0.05
C2	326	18/009	15/902	181	148	+0.05	+0.06
A1	332	18/007	15/922	87	148	-1.06	-1.00
B2	332	15/924	18/008	148	88	+1.46	+1.44
A1	333	15/925	18/007	148	76	+1.11	+1.10
C2	333	15/926	18/009	148	80	+1.84	+1.86

The small concentrations of fission products in the heavy water from surface contamination of the fuel elements have stayed at the normal level during the irradiation time of the test elements. The concentrations of impurities in the primary cooling water system are measured by γ -spectroscopy of samples from the system each reactor cycle.

This is an evidence that no fission product leak has occurred in the test elements.

The test elements have behaved perfect in all respects. No unusual occurrences have been observed.

POST IRRADIATION EXAMINATIONS:

The fuel tubes are separated by the routine cutting of used fuel elements. This enable a thorough inspection of the inside and outside surfaces of the fuel tubes. The tubes are placed vertically on the pond bottom with a bright lamp at the lower end. This arrangement makes it feasible to see even very small blisters, because the small angle scattering of the light is very sensitive to obliquities of the surface.

No blisters were seen. The surface of the tubes were light grey, but the alumina layer on element no. 8 seemed to be fragile and tended to fall off in flakes during handling in the cutting pond, leaving shiny areas of the Al-surface. The flakes were very thin, probably a few hundreds of a mm. It was not possible to recover a flake for examination, the flakes broke down to powder by touching. The element 18/008 had a temperature rise to about 230°C during a 1.5 hour stop of the air cooling through the internal storage block. It occurred in march 1987, before the two other test elements were taken to the storage block. This might be the reason why 18/008 appears different compared to the other two test elements.

The fission product content in the cutting pond has been very low, at the usual level, which is caused by surface contamination on the fuel elements.

Further examinations are planned but not yet undertaken:

- 1) Fuel tube wall thickness measurements spotwise in the area of highest power density.
- 2) Documentary photographing of the tube inside and outside surfaces against small angle scattering light, and photographing of eventual interesting surface areas.

REFERENCES

1. E. Nonbøl, Development of a Model for the Danish Research Reactor DR 3, Risø-RP-05-85, March 1985.
2. K. Haack, Irradiation of MEU and LEU Test Fuel Elements in DR 3, Proceedings of the International Meeting on Reduced Enrichment for Research and Test Reactors, 24-27 october 1983, Tokai, Japan, JAERI-M-84-073, May 1984.

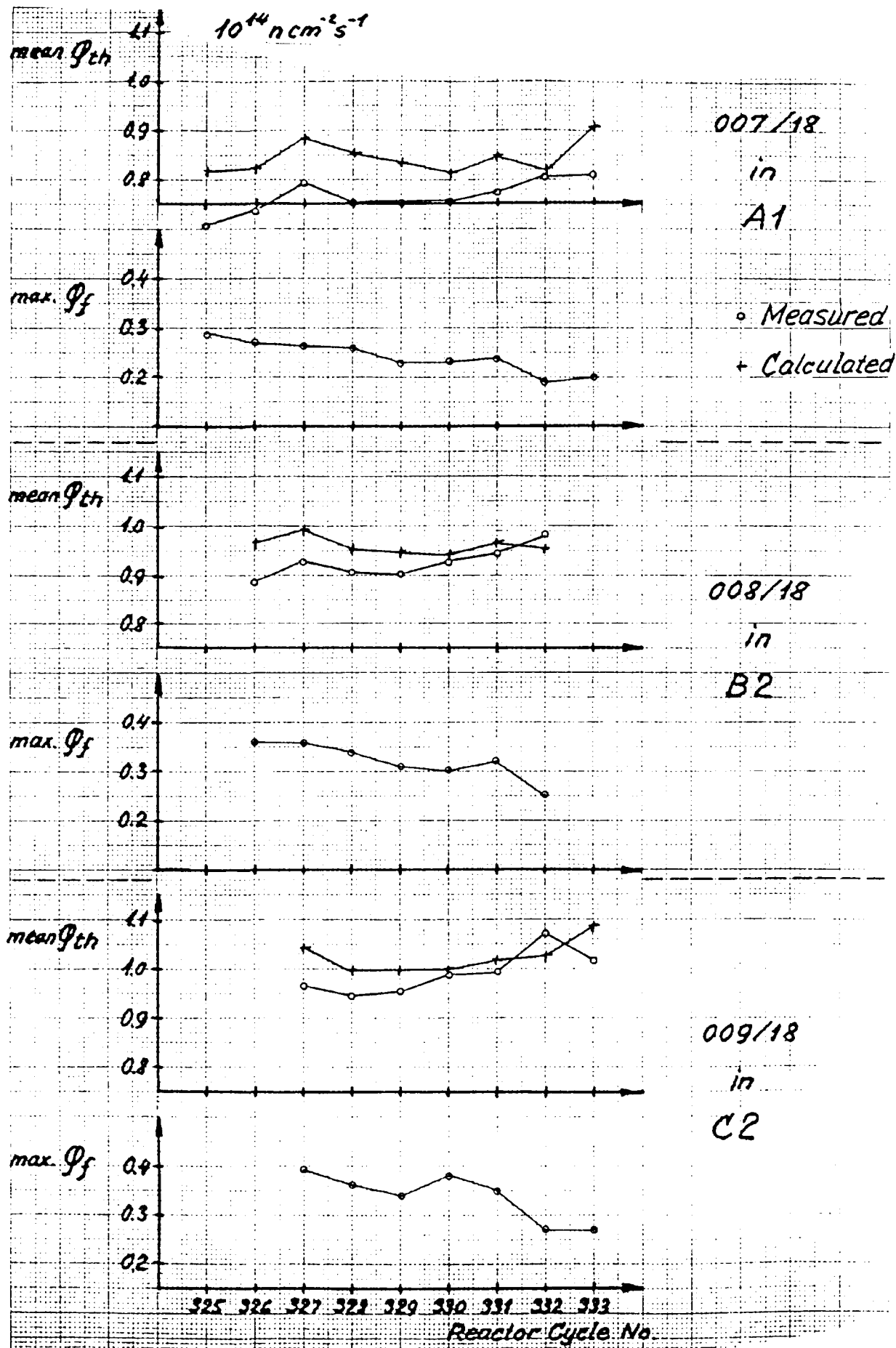
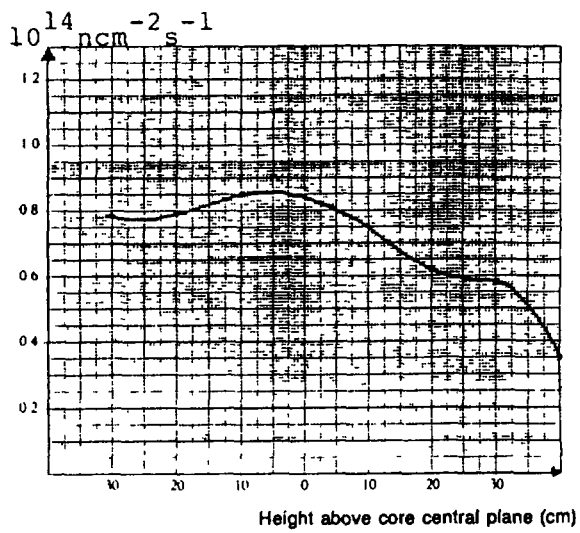
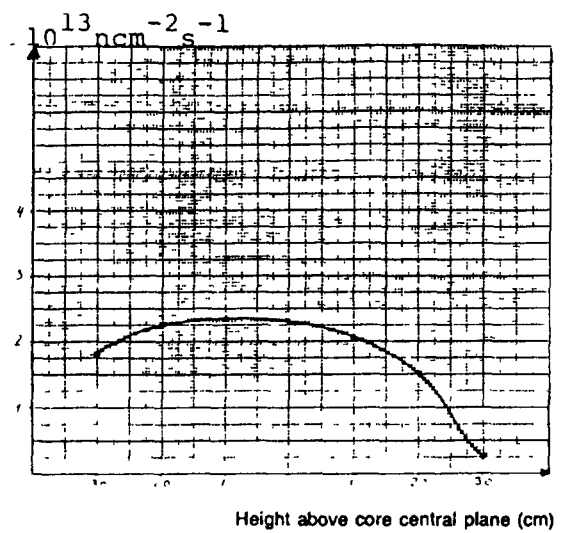


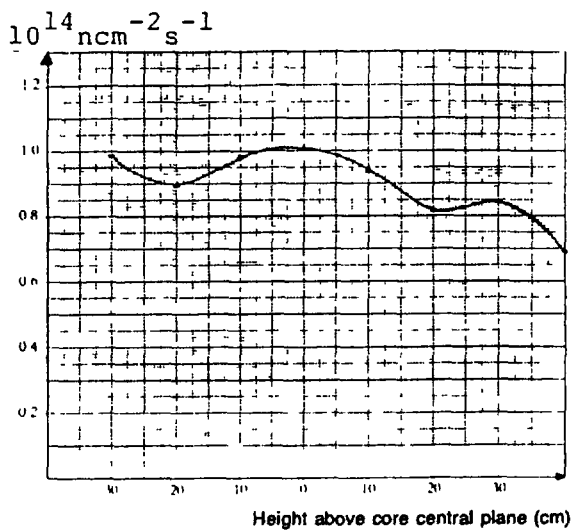
FIG. 1. Neutron flux densities in ATLAS test elements.



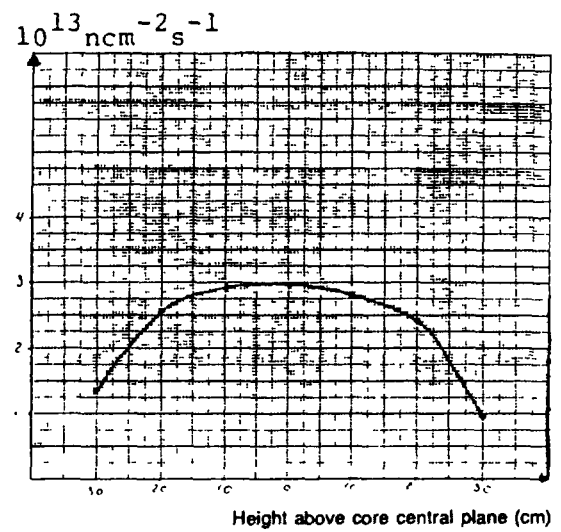
ϕ_{th} in A1. Cycle no. 330



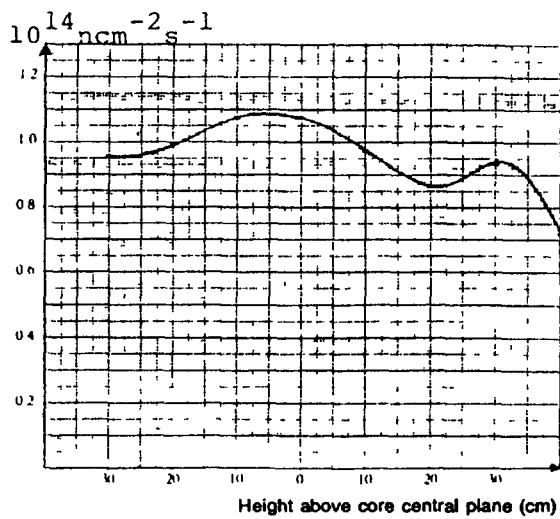
ϕ_f in A1. Cycle no. 329



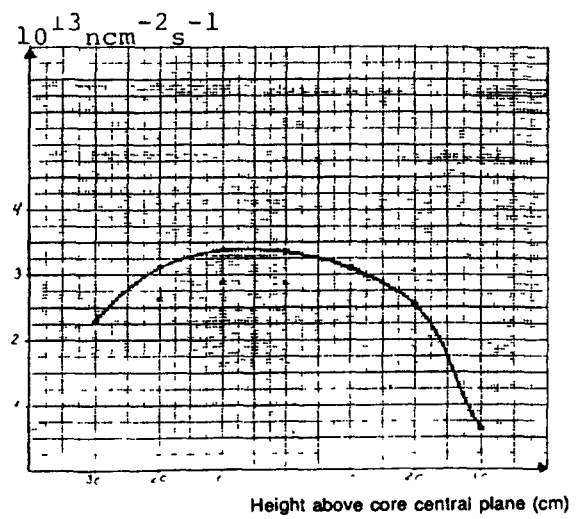
ϕ_{th} in B2. Cycle no. 330



ϕ_f in B2. Cycle no. 330.



ϕ_{th} in C2. Cycle no. 330



ϕ_f in C2. Cycle no. 330

FIG. 2. Axial neutron flux density distributions.

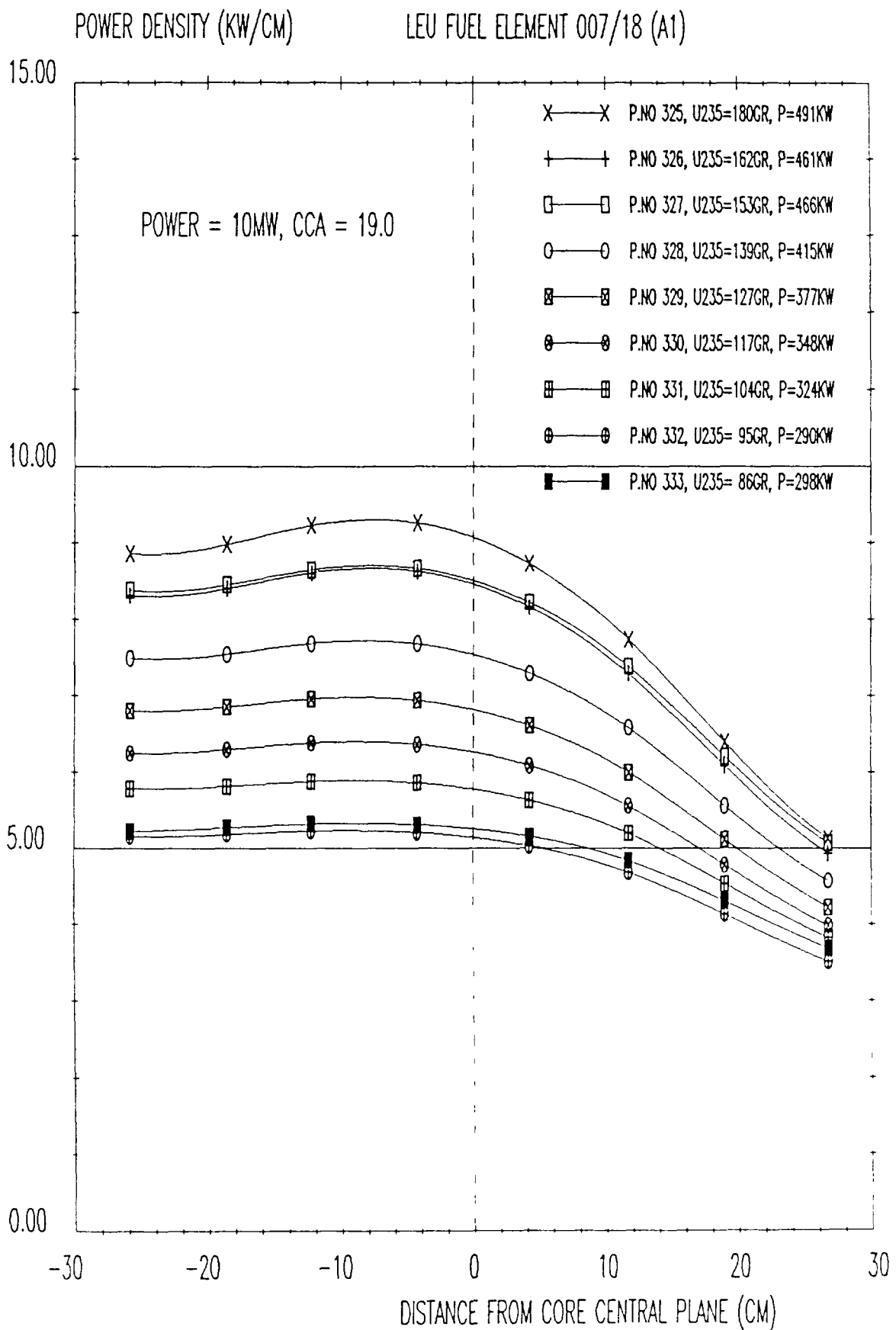


FIG. 3. Axial power density distributions through the in-core life of test element 007/18.

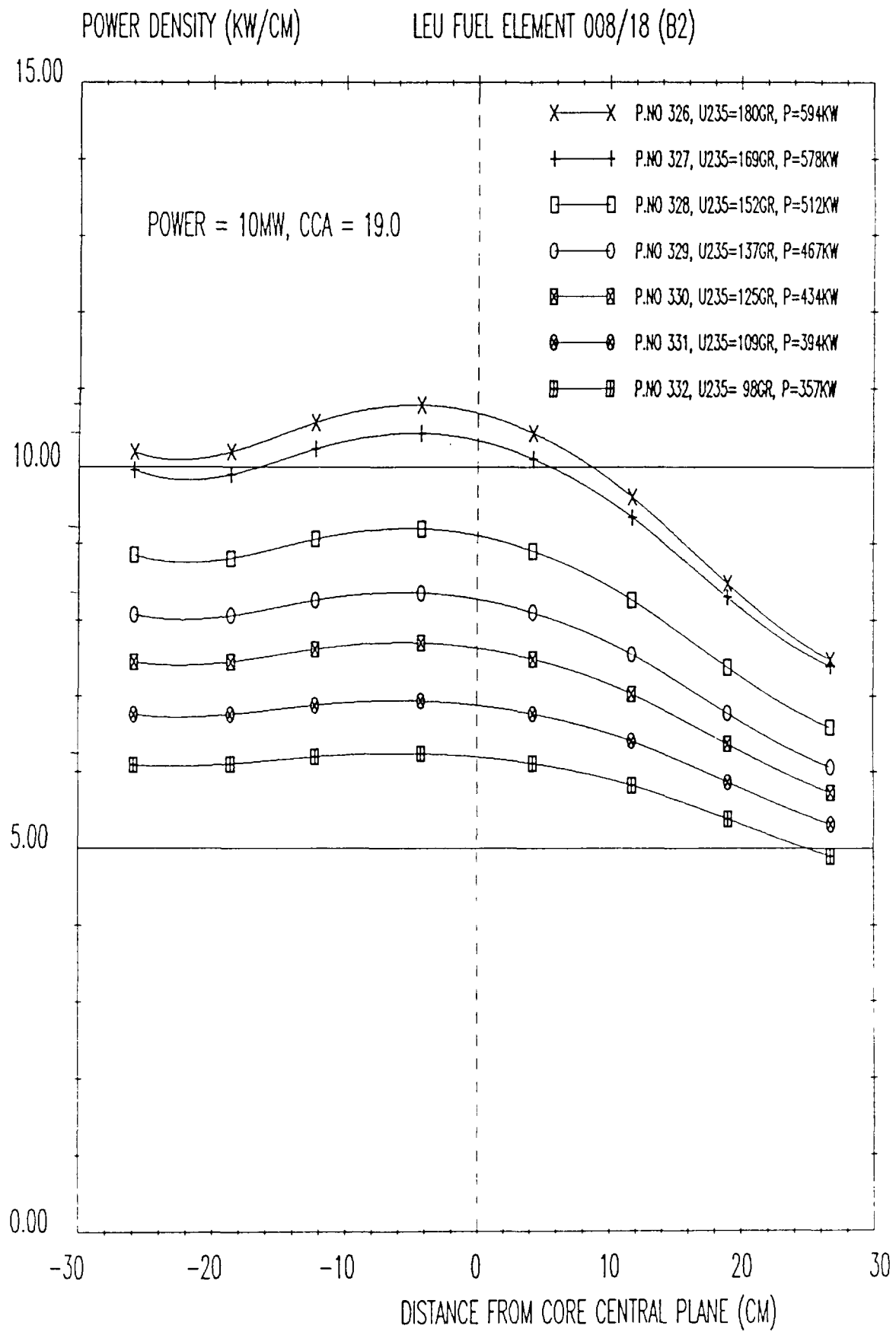


FIG. 4. Axial power density distributions through the in-core life of test element 008/18.

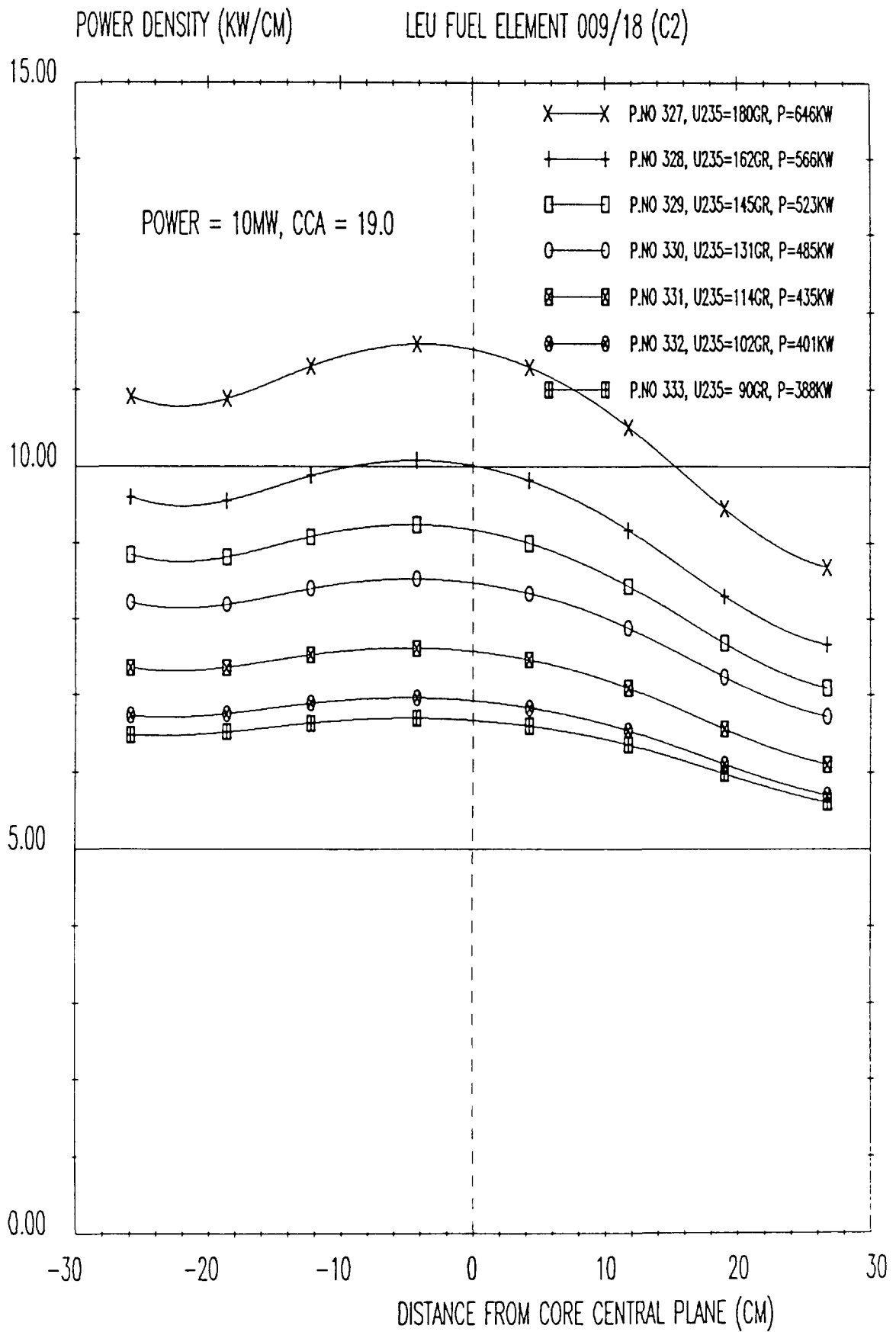


FIG. 5. Axial power density distributions through the in-core life of test element 009/18.

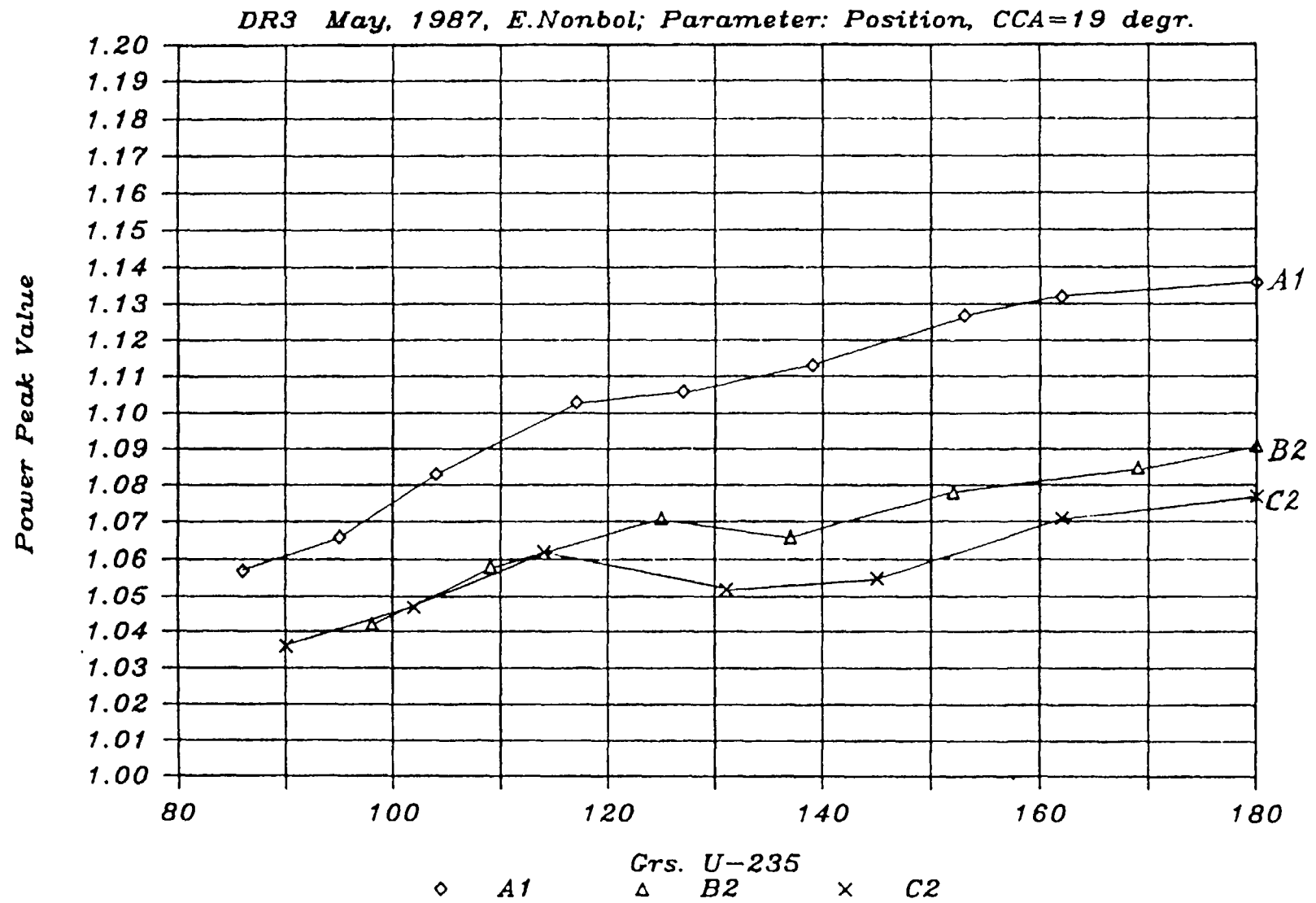


FIG. 6. Power peak values for LEU vs grs. ^{235}U .

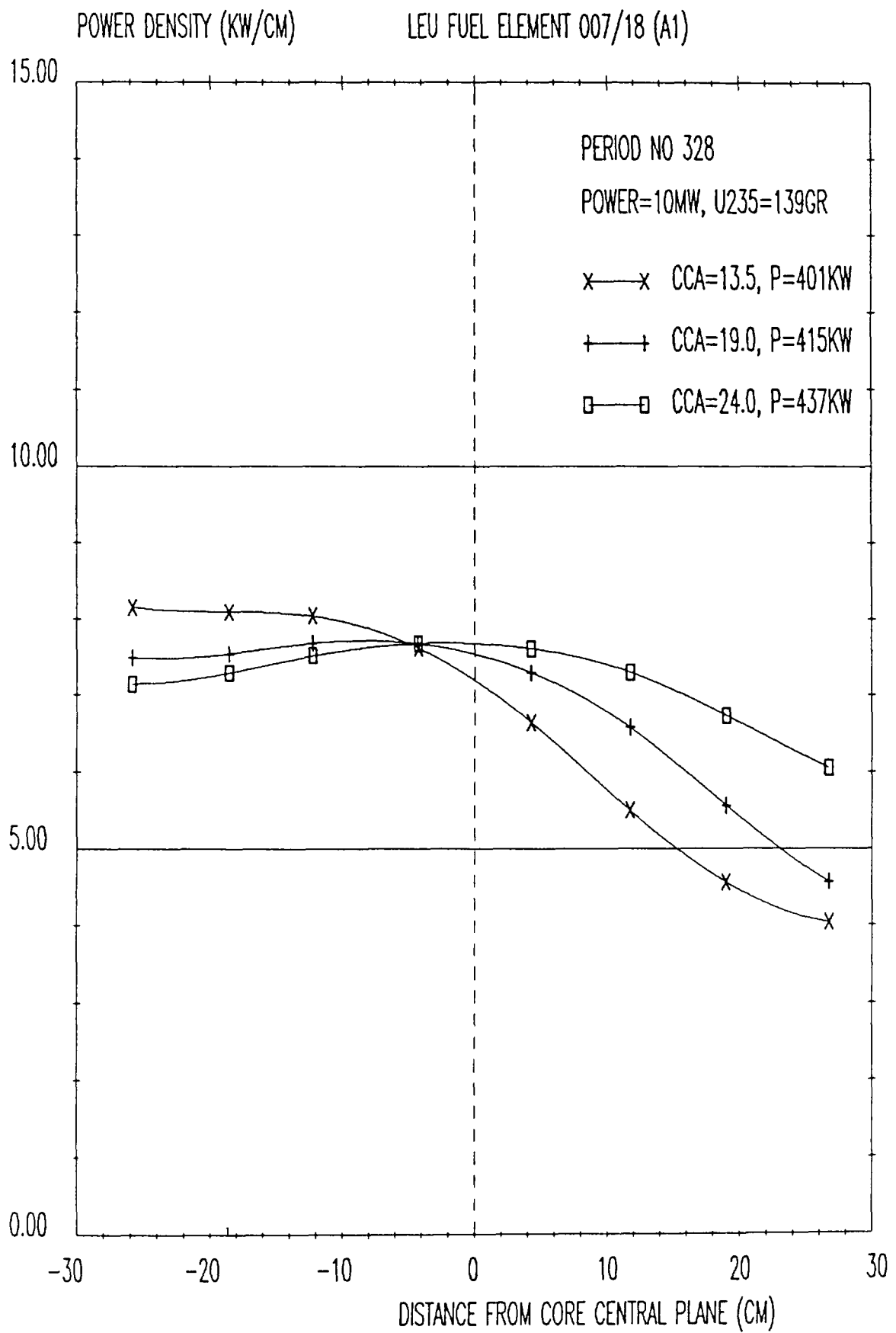


FIG. 7. Change of axial power density distribution through reactor cycle No. 328.

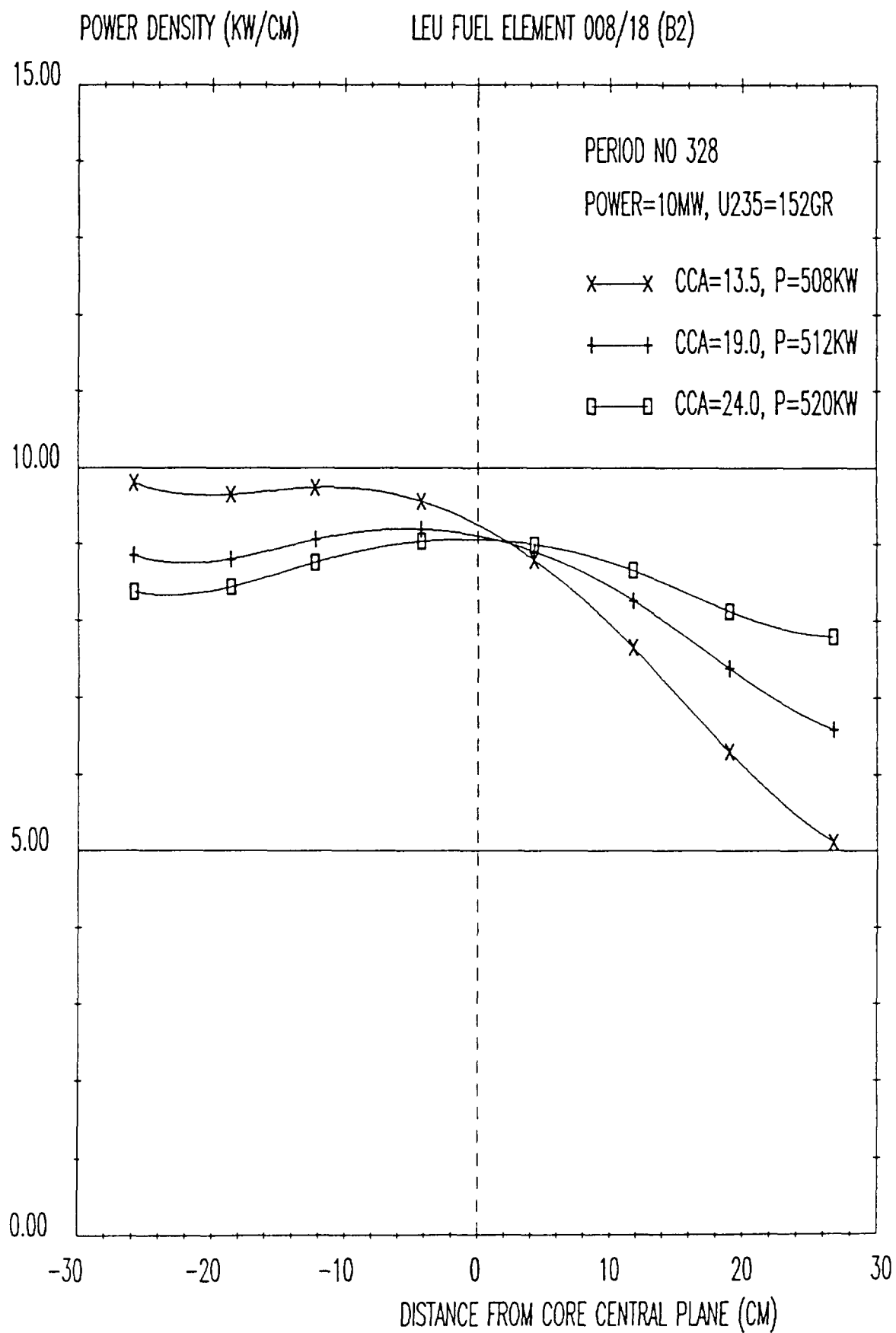


FIG. 8. Change of axial power density distribution through reactor cycle No. 328.

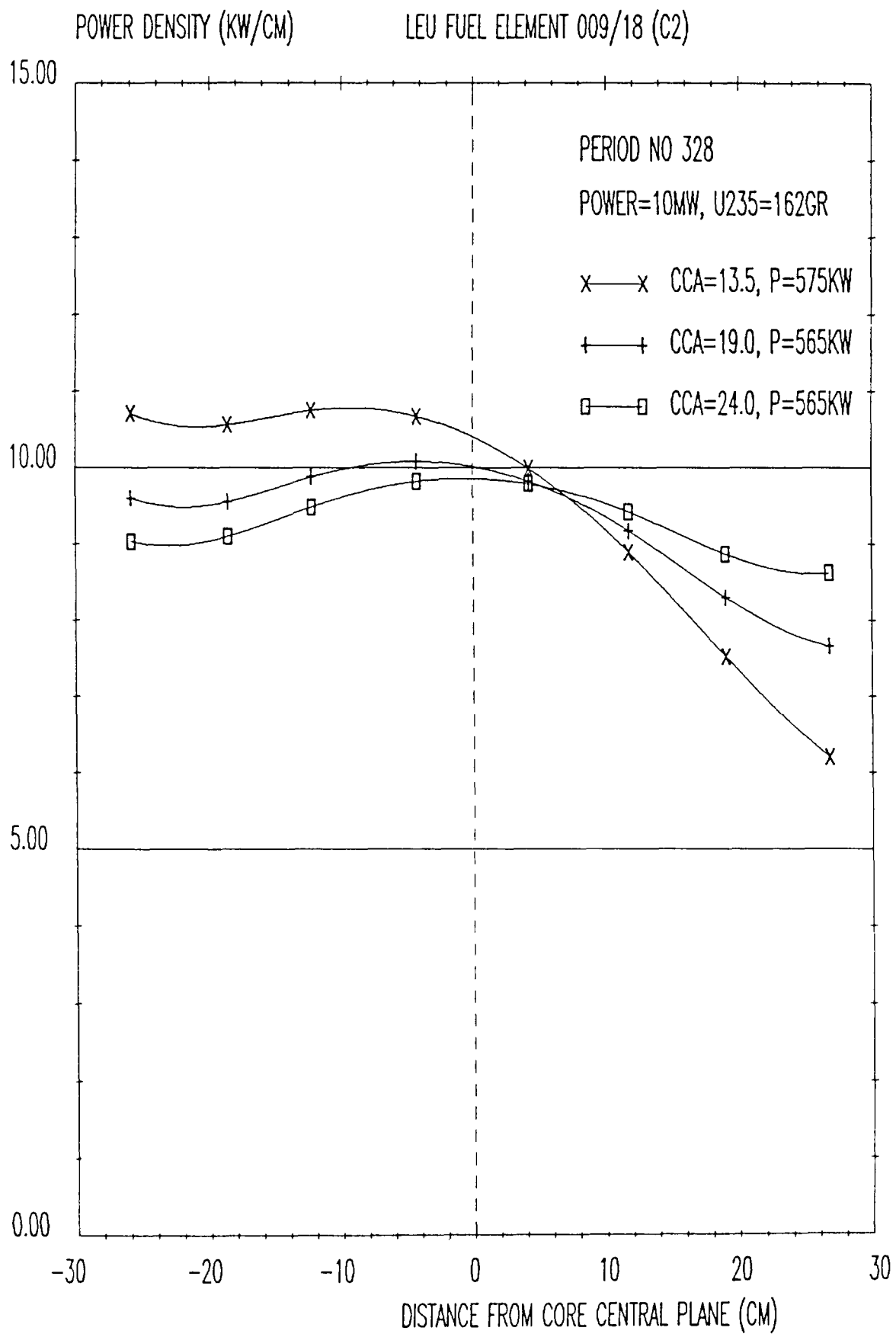


FIG. 9. Change of axial power density distribution through reactor cycle No. 328.

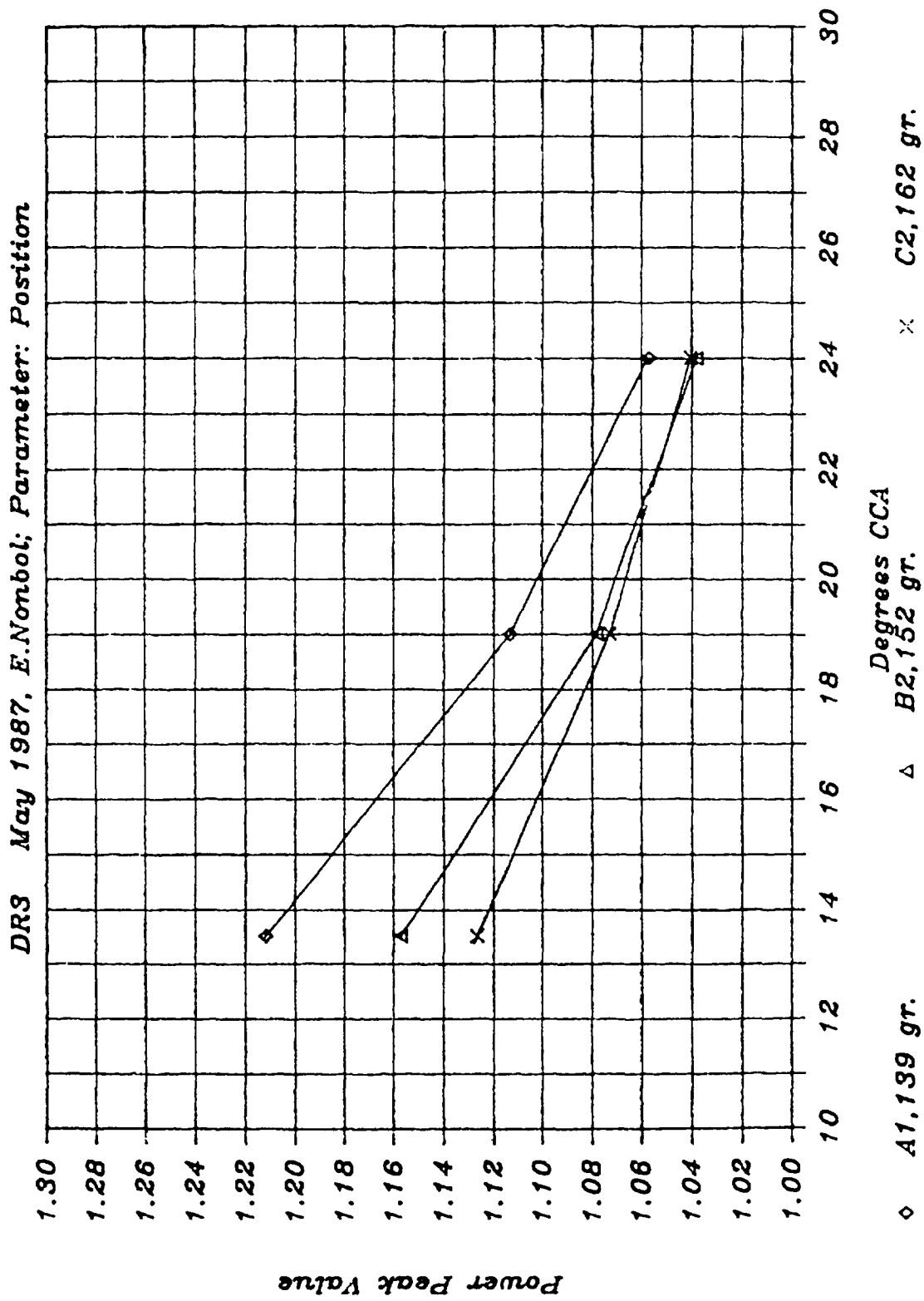


FIG. 10. Power peak values for LEU vs degrees CCA.

Appendix J-5

FISSION PRODUCT RELEASE

Appendix J-5.1

FISSION PRODUCT RELEASE FROM ALLOY, ALUMINIDE, OXIDE, AND SILICIDE FUELS

D. STAHL, J.L. SNELGROVE
RERTR Program,
Argonne National Laboratory,
Argonne, Illinois,
United States of America

1. INTRODUCTION

Information on the release of fission products from plate-type fuels is relatively scarce. Much of the early data is for uranium metal or UO_2 fuels;^{1,2} however, some data are available from the 1960s for uranium-aluminum alloy fuels and for UAl_x and U_3O_8 dispersion fuels. A renewed interest in plate- and tube-type fuels during the 1980s, partly as a consequence of the RERTR Program, has resulted in new fission product release measurements for U-Al alloy and UAl_x , U_3O_8 , and uranium silicide dispersion fuels. As discussed in the following paragraphs, the out-of-pile data for all types of aluminum-based plate-type fuel shows a consistent pattern, namely that major release of fission gases begins when the aluminum cladding blisters or begins to melt. Once having reached the melting point, however, the release of the noble gases is essentially complete in heating the fuel another 100°C. The volatile fission products are released more slowly as a function of temperature, and their release rates vary with fuel type.

Available data from reactor accidents indicate that, in cases where water coolant is present in the core when fuel melts, only the noble gases are released in any quantity. The iodines and less volatile fission products are effectively retained by the water.

2. PLATE-TYPE FUELS

2.1 Releases During Controlled Out-of-Pile Experiments

Fission product release studies were performed on U-Al alloy plate fuels at ORNL during the late 1950s and early 1960s^{2,3} and at HEDL during the mid-1980s^{4,5}. In the ORNL studies fuel plate samples were irradiated to trace (13.5 to 60.5 h of irradiation), 3.2 at.%, 9.0 at.%, and 23.6 at.% burnups, while the HEDL samples had been irradiated to ~52 wt% burnup. The fractional releases of the noble gases and iodine at a given temperature increased markedly between trace and 3.2% burnup and then remained approximately the same for the higher burnups. The tests at ORNL and at HEDL were conducted at several temperatures ranging between 700 and 1100°C and in inert gas, air, and steam atmospheres. Noble gas release was virtually 100% at the 700°C temperature in all atmospheres. Based on the results of a

study at INEL covering a wider temperature range,⁶ most of the fission gas is released from U-Al alloy fuel at about the 640°C eutectic temperature. At 700°C iodine release fractions were significantly lower for inert and steam atmospheres than for air, but at 900°C at least 90% of the iodine had been released in all atmospheres. The ORNL and HEDL data for cesium release are not in good agreement, with the HEDL measurements indicating larger releases. There is some indication in the ORNL data that the release fraction for cesium increases with increasing burnup; therefore, the much higher burnup of the HEDL samples might account for the higher releases measured there. The HEDL study also showed larger release fractions for tellurium than did the ORNL study. The release of ruthenium was small (<1%) over the entire temperature range (700°C-1085°C) tested at ORNL.

An irradiation program was carried out in the ETR and MTR on 1.27-cm-diameter high-density pellets of UAl_3 , UAl_4 , and 20 wt% U-Al alloy fuel (discussed above).^{6,7} After irradiation to a burnup of 18-35% of the ^{235}U , the pellets were subjected to slow heating (presumably under evacuated conditions) to permit the collection of fission products and the monitoring of noble gas release by counting ^{85}Kr . No activity release was found below 600°C. The UAl_4 released 28% of its fission gas at about 730°C, the UAl_4 peritectic temperature, with additional significant releases between 1165 and 1395°C. For UAl_3 , most fission gas was released at 1280°C, with an additional release occurring at about 1350°C, the UAl_3 peritectic temperature. In addition, it was noted that the major release of cesium occurred near 730°C for UAl_4 and 1350°C for UAl_3 .⁷ Smaller releases occurred at temperatures slightly above and below these peritectic temperatures. The rate of release of cesium was slower than that of the noble gases for UAl_4 and the U-Al alloy, but was as rapid as the noble gases for the UAl_3 ,⁶ probably because of the much higher release temperature for UAl_3 . These releases, however, are indicative of bulk fuel only. As discussed above for the U-Al alloy fuel and below for the dispersion fuels, however, the matrix plays a key role in the release of fission products from dispersion fuels.

One study was found in the literature⁸ which compares the fission gas release from two plates of UAl_3 -Al fuel ($\sim 1.3 - 1.4$ g U/cm³) and one plate of U_3O_8 -Al fuel (~ 1.3 g U/cm³). The burnup was 18-26% of the ^{235}U . The irradiated plates were heated under vacuum in Vycor tubes at 600°C, 630°C, then 675°C, each with a 30-minute hold. The temperature at which fission gases began to evolve was in a narrow temperature range between 575 and 600°C for both types of plates. No fission gases had been detected after heating the plates at 500°C for 40 minutes. Since the solidus temperature of type 6061 aluminum cladding is 582°C, it was inferred that fission gas release began at this temperature. The bulk of the fission gas was released by 630°C, with the UAl_3 fuel releasing gas at a faster rate and at a lower temperature than the U_3O_8 fuel. Fission product cesium was released from the fuels, but was deposited in copper tubing upstream from the gas collection reservoir. No cesium was found in the gas analysis.

Similar measurements on highly loaded (33 to 44 vol%) UAl_x , U_3O_8 , and U_3Si dispersion fuel plates were made during the RERTR Program.^{9,10} These measurements showed that the first significant release of fission gases occurred when the plates blistered. In the case of the U_3O_8 and U_3Si fuels, the blister temperatures were well below the cladding solidus temperature. Therefore, the threshold temperature for fission product release from a dispersion fuel plate is the lower of the blister temperature or the cladding solidus temperature. A second large release of fission gas occurred during the 650°C test for each fuel type. This release is assumed to be related to the reaction of the U_3O_8 or U_3Si with the aluminum matrix

and to the UAl_4 -Al eutectic. Although some data for iodine and cesium releases are reported, these data must not be used absolutely since the equipment was designed for accurate measurement of the noble gases only. On a qualitative basis, however, it was seen that cesium was released by the U_3Si sample much more readily than by the U_3O_8 sample.

At HEDL Woodley has measured the release of fission products from 0.9-g U/cm^3 U_3O_8 at the temperatures and in the atmospheres discussed above for the U-Al alloy.^{4,5} Again, most of the noble gases were released by a temperature of 700°C. Iodine release rates were somewhat lower than for the alloy fuel. Experiments are in progress in Japan to measure the fission product release fractions for UAl_x and U_3Si_2 dispersion fuels heated in dry air. Preliminary data^{11,12,13} for 20%-burned fuel show release rates similar to those measured at HEDL for U_3O_8 dispersion fuel, except for Cs release from the U_3Si_2 dispersion samples, which is considerably more rapid at the lower temperatures. With the exception of Cs release from U_3Si_2 , the release fractions for the UAl_x and U_3Si_2 dispersions are lower than those measured by Parker et al.² for U-Al alloy at comparable temperatures. Additional measurements using 70%-burnup fuel samples were scheduled to begin during January 1990.

A summary of some of the above data is presented in Fig. 1. The conclusion is that no fission products are released below the melting point of the cladding (582°C), unless the plate blisters first, and that essentially all of the fission gas is released by 675°C. As shown in the figure, fission products such as iodine are released more slowly than the noble gases.

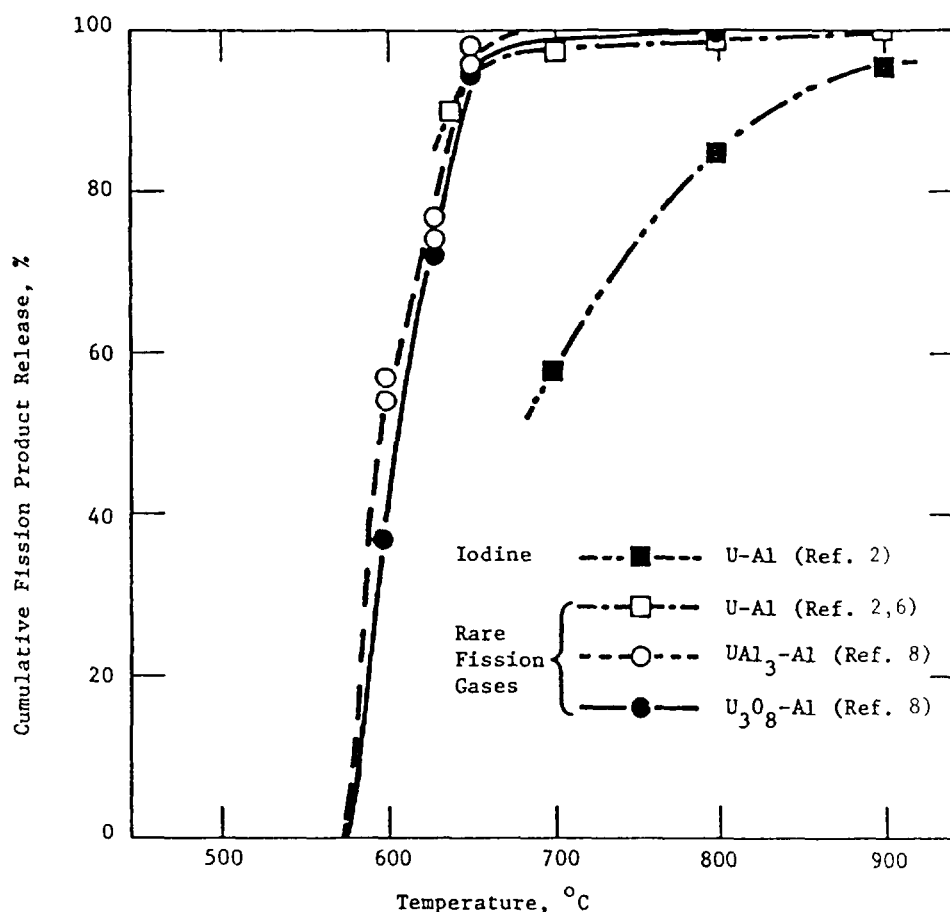


Figure 1 Fission Product Release from Plate-Type Fuels (Burnup = 20-25% of ^{235}U)

2.2 Releases During Reactor Accidents

The release of fission products during reactor accidents was also examined. Several accidents involved U-Al fuel which had undergone melting due to flow blockages caused by extraneous material. Partial melting of one subassembly occurred in each case and the fission products, except for the noble gases, were largely contained within the coolant water. Similar results were obtained as a result of a 30-MJ excursion of the ISIS reactor.¹⁴ Releases into the water and air were monitored and were found to be 0.06% and 0.001%, respectively, all significantly less than 1 Ci. Controlled overpower excursion tests at CABRI using a special control drive assembly produced significant (70%) melting of the control fuel plate with the release of 100% of the noble gas and <10% release of iodine and tellurium from the molten fuel.¹⁵ However, both these elements were retained in the water and only between 0.0005 and 0.005% was released to the reactor room.

More extensive damage and somewhat greater releases occurred in the SPERT-1 destructive test and the SL-1 accident.^{16,17} The nuclear energies and peak powers generated were 31 and 130 MJ, and 2.3×10^2 and 1.9×10^4 MW, respectively. In the SPERT-1 test, partial melting of all of the fuel plates occurred, and more than 50% of the plates were fully melted. Fission product release, mainly due to fission gases, was estimated to be about 0.7% of the total inventory. Iodine release to the atmosphere was estimated to be less than 0.01%. The reactor building was only moderately contaminated and re-entry occurred about four hours after the test. As a result of the SL-1 accident, the building was badly contaminated, with an extensive low-level deposition of ^{131}I . Total fission product release was estimated to be 5-10% of the total inventory, and release to the environment was estimated to be only about 0.01%. The iodine release to the environment was estimated to be less than 0.5%.

REFERENCES FOR FISSION PRODUCT RELEASE FROM RESEARCH REACTOR FUELS

1. G. W. Parker and C. J. Barton, "Fission Product Release," Chapter 18, Technology of Nuclear Reactor Safety, Volume 2, Thompson and Beckerley, Eds., MIT press, pp. 525-618, 1973.
2. G. W. Parker, G. E. Creek, C. J. Barton, W. J. Martin, and R. A. Lorenz, "Out-of-Pile Studies of Fission-Product Release from Overheated Reactor Fuels at ORNL, 1955-1965," Oak Ridge National Laboratory Report ORNL-3981, pp. 59-66, July 1967.
3. G. E. Creek, W. J. Martin, and G. W. Parker, "Experiments on the Release of Fission Products from Molten Reactor Fuels," Oak Ridge National Laboratory Report ORNL-2616, pp. 11-12, July 1959.
4. R. E. Woodley, "The Release of Fission Products from Irradiated SRP Fuels at Elevated Temperature: Data Report on the First Stage of the SRP Source Term Study," Hanford Engineering Development Laboratory Report HEDL-7598, June 1986.
5. R. E. Woodley, "The Release of Fission Products from Irradiated SRP Fuels at Elevated Temperatures: Data Report on the Second Stage of the SRP Source Term Study," Hanford Engineering Development Laboratory Report HEDL-7651, March 1987.

6. R. R. Hammer, L. L. Dickerson, and R. R. Hobbins, "Fission Product Release from Uranium Aluminide Fuels," in *Metallurgy and Materials Science Branch Annual Report—Fiscal Year 1970*, W. C. Francis, Ed., IN-1437, pp. 27-34, November 1970.
7. M. J. Graber and G. W. Gibson, "Bulk UAl_x Fuel Irradiations," in *Reactor Engineering branch Annual Report—Fiscal Year 1969*, IN-1335, pp. 47-49, November 1969.
8. M. J. Graber, M. Zukor, and G. W. Gibson, "Fission Gas Release from Fuel Plate Meltdown," Annual Progress Report on Reactor Fuels and Materials Development for FY 1966, IDO-17218, pp. 52-58, November 1966.
9. T. Shibata, T. Tamai, M. Hayashi, J. C. Posey, and J. L. Snelgrove, "Release of Fission Products from Irradiated Aluminide Fuel at Elevated Temperatures," *Nucl. Sci. and Eng.* **87**, 405-417, 1984.
10. J. C. Posey, "Release of Fission Products from Miniature Fuel Plates at Elevated Temperatures," Proc. Int. Mtg. on Research and Test Reactor Core Conversions from HEU to LEU Fuels, Argonne, Illinois, November 8-10, 1982, Argonne National Laboratory Report ANL/RERTR/TM-4 (CONF-821155), pp. 117-133, September 1983.
11. F. Sakurai, Y. Komori, J. Saito, B. Komukai, H. Ando, H. Nakata, A. Sakakura, S. Niiho, M. Saito, and Y. Futamura, "Progress in Safety Evaluation for the JMTR Core Conversion to LEU Fuel," Proc. 12th Int. Mtg. on Reduced Enrichment for Research and Test Reactors, Berlin Germany, September 10-14, 1989, in press.
12. M. Saito, Y. Futamura, H. Nakata, H. Ando, F. Sakurai, N. Ooka, A. Sakakura, M. Ugajin, and E. Shirai, "Further Data of Silicide Fuel for the LEU Conversion of JMTR," paper presented at the Int. Symp. on Research Reactor Safety, Operations and Modifications, Chalk River, Ontario, Canada, October 23-27, 1989.
13. Y. Komori, Japan Atomic Energy Research Institute, personal communication (November 1989).
14. P. Lebauleux, et al., "The Behavior of Fission Products Observed During the Operation of the C.E.N. Saclay Reactors," Congress on Diffusion of Fission Products, Saclay, Nov. 4-6, 1969, AAEC-LIB/Trans -615, Feb. 1977.
15. J. Dadillon, "Experimental Study of the Behavior of Fission Products in a Pool Reactor Accident," C.E.A. Bulletin d'Information Scientifiques et Techniques, 112, pp. 13-18, 1967.
16. R. W. Miller, A. Sola, and R. K. McCardell, "Report of the SPERT 1 Destructive Test Program on an Aluminum, Plate-type, Water-Moderated Reactor, IDO-16883, June 1964.
17. T. J. Thompson, "Accidents and Destructive Tests," Chapter 11, *The Technology of Nuclear Reactor Safety*, Volume 1, Thompson and Beckerley, Editors, MIT Press, pp. 608-708, 1973.

**RELEASE OF FISSION PRODUCTS FROM IRRADIATED
ALUMINIDE FUEL AT HIGH TEMPERATURES***

(Abstract)

T. SHIBATA, T. TAMAI, M. HAYASHI

Research Reactor Institute,
Kyoto University,
Osaka, Japan

J.C. POSEY

Oak Ridge National Laboratory,
Oak Ridge, Tennessee,
United States of America

J.L. SNELGROVE

Argonne National Laboratory,
Argonne, Illinois,
United States of America

Irradiated uranium-aluminide fuel plates of 40% ^{235}U enrichment were heated for the determination of the amounts of fission products released at temperatures up to and higher than the melting point of the fuel cladding material. The release of fission products from the fuel plate at temperatures below 500°C was negligible. Three stages of fission product release were observed. The first rapid release was observed at ~561°C along with blistering of the plates. The next release, which occurred at 585°C, might have been caused by melting of the Type 6061 aluminum alloy. The last release of fission product gases occurred at 650°C, which probably corresponds to the eutectic temperature of the uranium-aluminum alloy.

The released material was mostly xenon, and small amounts of iodine and cesium were observed.

* The full text of this paper was published in Nuclear Science and Engineering, 87, 405-417 (1984).

Appendix J-5.3

RELEASE OF FISSION PRODUCTS FROM MINIATURE FUEL PLATES AT ELEVATED TEMPERATURE

J.C. POSEY

Oak Ridge National Laboratory,
Oak Ridge, Tennessee,
United States of America

Abstract

Three miniature fuel plates were tested at progressively higher temperatures. A U_3Si plated blistered and released fission gases at 500°C . Two U_3O_8 filled plates blistered and released fission gases at 550°C .

INTRODUCTION

The Reduced Enrichment Research and Test Reactors (RERTR) program requires the development of fuel plates of reduced ^{235}U enrichment but high total uranium content. The low ^{235}U enrichment reduces the danger of bomb use.

This report describes an experimental investigation of plate damage and failure at elevated temperature. This work was done in September 1982 at Oak Ridge National Laboratory. Miniature fuel plates were tested at progressively higher temperatures. Warping blister formation and the escape of fission products were observed and the temperatures at which they occurred were determined.

PROCEDURE

Three miniature fuel plates from a group irradiated in the Oak Ridge Research Reactor were tested. This group of plates have been described by Senn and Martin.¹ The plates were rectangular, 115 mm long and 50 mm wide. They consisted of a layer of an uranium compound sandwiched between sheets of aluminum alloy (6061). Details of the three plates used in this work are given in Table 1.

Table 1. Miniature fuel plates

Plate number	Nominal thickness		Fissile bearing compound	Uranium density kg/m ³	²³⁵ U enrichment wt %	Total ²³⁵ U loading mg
	μm	inches				
A-19	1270	0.050	U ₃ Si	4814	19.88	2081
O-50-1	1270	0.050	U ₃ O ₈	2759	19.47	1154
O-58-8	1524	0.060	U ₃ O ₈	3102	19.47	1663

The plates had been removed from the reactor on May 24, 1982. The tests described in this report were carried out during the period of Aug. 26 to Sept. 10, 1982. Consequently, nearly all of the ¹³³Xe and ¹³¹I had decayed and they could not be used effectively as indicators of a breach of the containment of the fission products within the plate. The escape of ⁸⁵Kr was used as an indicator of containment failure.

Figure 1 is a flow sheet of the equipment used in this work. The fuel plate was contained in a quartz tube in the furnace. Helium gas flowed over the plate and then through a sample tray containing activated charcoal at liquid nitrogen temperature. Any ⁸⁵Kr escaping from the

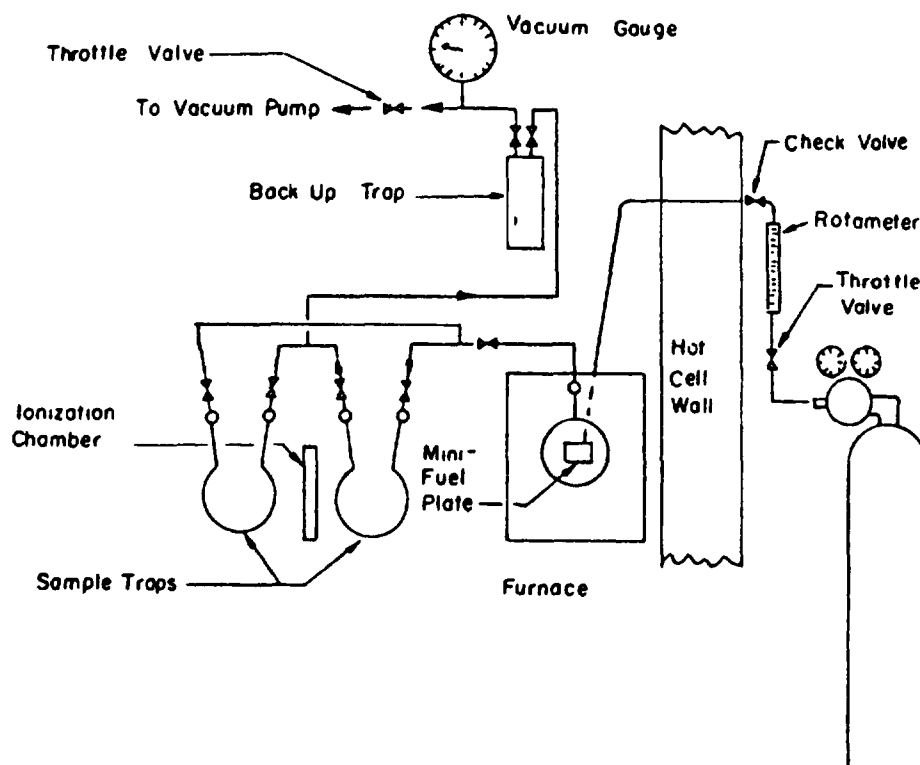


FIG. 1. Flow sheet.

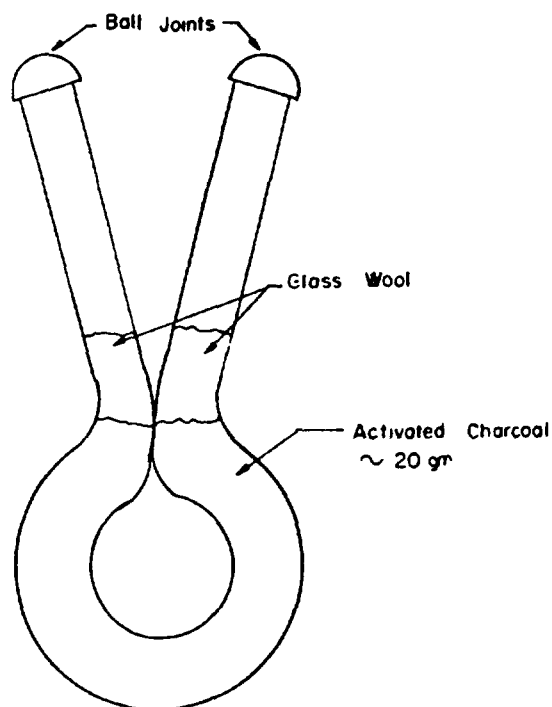


FIG. 2. Sample trap.

plate accumulated in this tray. The flow could be diverted through an alternate trap of the same type. The gas flow then passed through a second larger charcoal trap, followed by a throttle valve and a vacuum pump. The sample trap removed any volatile fission products from the gas stream. The back up trap was present as a safety precaution to trap any ^{131}I that might pass the sample trap.

The helium flow and pressure were controlled by two throttle valves, one located in the helium inlet line outside of the hot cell, the other located in the hot cell just before the vacuum pump. The flow was held at 100 ± 20 cc/min; the pressure was very slightly below atmospheric.

The sample traps (Fig. 2) were designed to lay flat on the crystal cover of a GeLi counter. This allowed an efficient geometry for counting.

An ionization chamber was mounted on the outside of the vacuum flask that held the sample trap. The trapping of a large amount of radioactive material could be detected by this instrument. This method had been very effective in detecting ^{133}Xe released by fresh fuel plates but was found to be ineffective in detecting ^{85}Kr in the amounts involved.

The furnace was heated by a nichrome resistance coil. The temperature was regulated by a proportional controller. The heated zone of the furnace was 7 in. long and 3 in. in diameter. Line of sight gamma radiation from the intensely radioactive fuel plate to the sample trap ionization chamber was blocked by 2 in. of lead brick. The rest of the furnace was covered with 1/4 in. sheet lead. This absorbed much of the low energy gamma radiation which is especially prone to back scatter.

A quartz tube (Fig. 3) fit inside the furnace. Two chromel-alumel thermocouples, sheathed in stainless steel entered the back of the tube through a small quartz tube. The helium gas entered through the same tube. The other end of the tube terminated in a large ground quartz ball joint. The tube was connected through this joint to the sample collection system.

The fuel plate was held in a quartz sample holder (Fig. 4). The fuel plate lay in this holder in a slanted position. As the holder slid into the quartz tube the slanted surface of the plate contacted a thermocouple causing it to bend up slightly. This assured that the

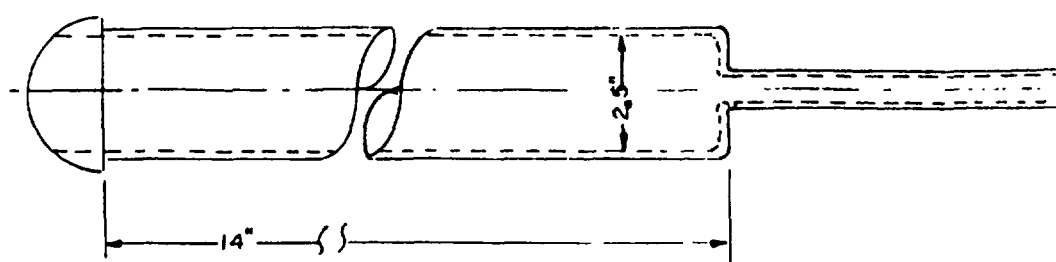


FIG. 3. Furnace tube.

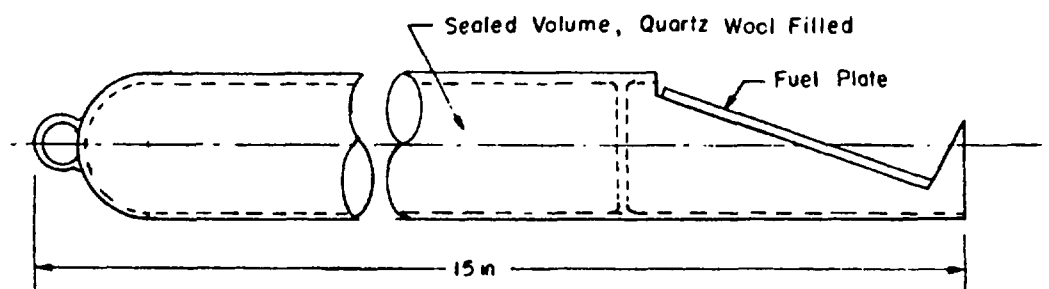


FIG. 4. Sample holder.

thermocouple junction was in contact with the plate. The temperature was recorded by a single point recorder. The recorder could be read to 2°F. A second thermocouple was bent upward so that its junction contacted the inner surface of the quartz tube. This thermocouple was connected to the proportional controller.

Each plate was tested in the following manner.

1. The plate was examined visually and photographed. Its thickness was measured in six places by means of a micrometer.
2. The plate was mounted in the sample holder which was placed in the furnace tube. The tube was then connected to the sample collection system.
3. The flow of helium was started and the sample trap was cooled to liquid nitrogen temperature.
4. The furnace was heated to the operating temperature which was maintained for 30 min.
5. The furnace was allowed to cool.
6. After the furnace had cooled to approximately 100°C below operating temperature, the helium flow was diverted through the alternate trap and the loaded trap was allowed to warm to room temperature. The adsorbed helium was allowed to escape through the down stream stopcock which was allowed to remain open.
7. The trap was then removed from the manifold and its openings were capped. It was then removed from the hot cell and its outer surface was washed. Its radioactive content was then measured using the Geli counter. Counting times of up to 16 h were used to measure very low levels of activity.
8. After the plate had cooled to ~250°C it was removed from the furnace, inspected, and the thickness measured. Photographs were made when blisters appeared. The thickness measurements were discontinued after warping or blistering became severe. Plate A-19 was not cooled or removed from the furnace after the tests at 600°C and 650°C and plate O-58-8 was not removed after the 650°C test.

RESULTS AND DISCUSSION

The principal results of these tests are given in Tables 2 and 3. The U_3Si filled plate, A-19, warped, swelled, blistered, and released krypton during the 500°C test. A photograph of these blisters is shown in Fig. 5. They were small and located along the edge of the meat area. The amount of krypton released at 500°C was <0.1% of the total released from this plate. Largest releases occurred at 565°C and 650°C.

The oxide filled plates showed some warping and swelling at 500°C and 525°C. At 550°C large blisters formed and large releases of krypton occurred. These blisters are shown in Figs. 6 and 7. A second test was made at 550°C using plate O-58-8. Only a small amount of krypton left the plate. This indicates that the release was not a continuing process. The greatest release of krypton took place during the 650°C test.

The results of the thickness measurements are given in Tables 4, 5, and 6. The positions at which these measurements were made are identified by the position number. The numbers were assigned starting at a corner identified by a small chamfer. Numbers 1, 2, and 3 are

Table 2. Effects of temperature on U_3Si filled plate
Plate A-19

Temperature of test, °C	Results
300	None
400	None
450	None
475	Darkening at edge of meat area
500	Blisters along edge of meat area, swelling, and warping. 0.33 mCi of ^{85}Kr in trap
515	More swelling, 21 mCi of ^{85}Kr trapped
530	33 mCi of ^{85}Kr trapped
565	110 mCi of ^{85}Kr trapped
600	10 mCi of ^{85}Kr trapped
650	240 mCi of ^{85}Kr trapped
700	15 mCi of 85 trapped

Table 3. Effects of temperature on U_3O_8 filled
miniature fuel plates
Plates O-50-1 and O-58-8

Temperature of test, °C	Plate number	Results
300	O-58-8	None
400	O-58-8	None
425	O-50-1	Meat area light grey, outer area dark grey
450	O-58-8	Meat area light grey, outer area dary grey
475	O-50-1	Meat area light grey, outer area dark grey
500	O-58-8	Reveral — meat area is now darker, slight warping and swelling
525	O-50-1	Warping and swelling
550	O-50-1	Large blisters, 59 mCi of ^{85}Kr
1st 550 ^a	O-58-8	Large blisters, 52 mCi of ^{85}Kr
2nd 550 ^b	O-58-8	1.2 mCi of ^{85}Kr
600	O-58-8	0.1 mCi of ^{85}Kr
650	O-58-8	150 mCi of ^{85}Kr
700	O-58-8	0.9 mCi of ^{85}Kr

^aTwo tests were made at 550°C to determine whether or not krypton
release continued at this temperature.



FIG. 5. Plate A-19 after 500°C test.

in line along the plate about 3/4 in. in from the edge. They were
approximately 1 1/8 in., 2 1/4 in., and 3 3/8 in. from the end of the
plate. Numbers 4, 5, and 6 were in a similar row 3/4 in. from the
other edge of the plate.

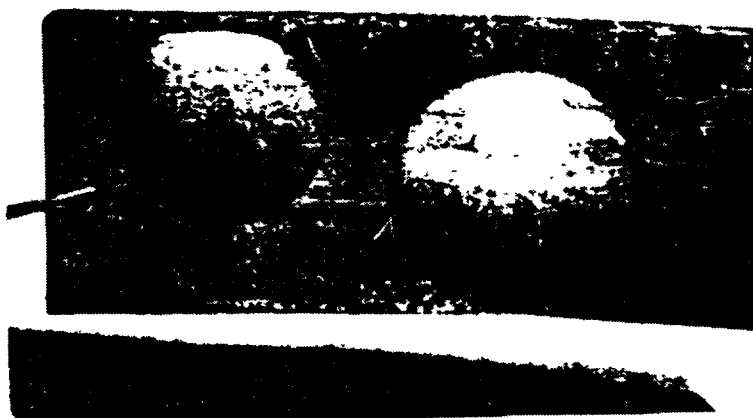


FIG. 6. Plate O-58-8 after 550°C test.



FIG. 7. Plate O-58-8 after 550°C test.

The U_3Si filled plate A-19 showed swelling in the 500°C test; blistering and krypton release occurred in the same test. The U_3O_8 filled plate O-58-8 showed some swelling at 500°C; blistering and krypton release were not observed until the 550°C test. Plate O-50-1 showed no swelling at 475°C but did at 525°C. It was not tested at 500°C.

Both ^{134}Cs and ^{137}Cs were found in the traps after the tests at the higher temperatures. These data are given in Table 7. These quantities are indicative of the relative amounts of cesium volatilizing from the plates but are in no sense quantitative measurements to the total amounts. Most of the cesium would be deposited on surfaces before reaching the traps because of either condensation or reaction.

Much more cesium was found in the trap after the tests of the silicide filled plate than was found after the tests of the oxide filled

Table 4. Swelling of plate A-19, U_3Si filled

Temperature of test, °C	Thickness of plate, in.					
	Position 1	Position 2	Position 3	Position 4	Position 5	Position 6
Initial	0.0533	0.0535	0.0542	0.0535	0.0537	0.0555
300	0.0530	0.0533	0.0536	0.0535	0.0532	0.0539
400	0.0536	0.0533	0.0539	0.0533	0.0532	0.0567
450	0.0532	0.0534	0.0535	0.0532	0.0535	0.0551
475	0.0534	0.0536	0.0538	0.0533	0.0533	0.0550
500	0.0627	0.0563	0.0542	0.0532	0.0598	0.0595
515	0.0619	0.0588	0.0551	0.0531	0.0710	0.0758

Table 5. Swelling of plate O-50-1, U_3O_8 filled

Temperature of test, °C	Thickness of plate, in.					
	Position 1	Position 2	Position 3	Position 4	Position 5	Position 6
Initial	0.0510	0.0511	0.0513	0.0510	0.0513	0.0514
425	0.0509	0.0509	0.0509	0.0509	0.0510	0.0510
475	0.0512	0.0514	0.0510	0.0513	0.0515	0.0514
525	0.0518	0.0540	0.0584	0.0597	0.0585	0.0515

Table 6. Swelling of plate O-58-8, U_3O_8 filled

Temperature of test, °C	Thickness of plate, in.					
	Position 1	Position 2	Position 3	Position 4	Position 5	Position 6
Initial	0.0610	0.0612	0.0612	0.0615	0.0618	0.0615
300	0.0614	0.0613	0.0612	0.0613	0.0613	0.0617
400	0.0610	0.0610	0.0613	0.0613	0.0615	0.0614
450	0.0604	0.0610	0.0610	0.0620	0.0613	0.0614
500	0.0606	0.0642	0.0643	0.0689	0.0673	0.0616

plate. The cesium apparently was in a more volatile form in the silicide filled plate. The alternate trap was used in the 650°C test of plate A-19 and in the 700°C test of plate O-58-8. This trap was at a greater distance from the furnace than was the usual sample trap. Consequently, the line losses of cesium were greater than in cases of the other samples.

Table 7. Cesium found in traps after tests

Plate	Temperature °C	¹³⁴ Cs, mCi	¹³⁷ Cs, mCi
A-19	565	71	41
A-19	600	0.20	0.13
A-19	650	415	251
A-19	700	1300	793
O-58-8	550	0.003	0.002
O-58-8	600	0.0004	0.0003
O-58-8	650	2.2	1.2
O-58-8	700	0.34	0.21

The presence of surface deposits of cesium in the system was verified by surface smears made using Q-tips. One smear was taken from plate O-58-8 after the 600°C test at the sight of a small crack at the edge of a blister. Another was taken from the plate holder near the plate after the same test. A third was taken from plate A-19 after the 565°C test. All Q-tips gave survey meter readings of >10 R. Gamma scans showed the presence of only ¹³⁴Cs and ¹³⁷Cs.

Film deposits were observed on the sample holder after the 700°C melt down of plate A-19. These deposits were analyzed by spark source mass spectrometry. The results are given in Table 8. The concentrations are relative with cesium equal to 100. Sample 1 was taken at a point just down stream with respect to helium flow, from the plate. Sample 2 was taken from a cooler zone farther down stream. The isotopic composition of the cesium was 44%, ¹³³Cs; 4%, ¹³⁴Cs; 4%, ¹³⁵Cs; and 48%, ¹³⁷Cs. The iodine was 11%, ¹²⁷I and 89%, ¹²⁹I. The isotopic composition of the cadmium was that of fission product cadmium.

Plate O-58-8 has been turned over to the analytical division for analysis. When the results are received the exact degree of burn-up can be calculated.

SUMMARY

Three miniature fuel plates were tested at progressively higher temperatures. A U₃Si filled plate blistered, warped, and released ⁸⁵Kr

Table 8. Composition of deposits

Element	Relative concentration	
	Sample 1	Sample 2
Ag	2	0
Al	5	50
B	0.3	1
Ca	0.3	5
Cd	0	1500
Cr	2	0.5
Cs	100	100
Cu	0	10
Fe	10	30
I	0	10
K	1	5
Mg	150	3
Na	3	1
Pb	0	6
Rb	25	40
Si	10	25
Ti	25	2
Zn	1	20

at 500°C. Two U_3O_8 filled plates blistered and released ^{85}Kr at 550°C. At temperatures in the range of 565°C to 700°C appreciable ^{134}Cs and ^{137}Cs left the plates. The cesium losses from the silicide filled plate were greater than those from the oxide filled plate.

REFERENCE

1. R. L. Senn and M. M. Martin, Irradiation Testing of Miniature Fuel Plates for the RERTR Program, ORNL/TM-7761, July 1981.

**FURTHER DATA OF SILICIDE FUEL
FOR THE LEU CONVERSION OF JMTR***

M. SAITO, Y. FUTAMURA, H. NAKATA,
H. ANDO, F. SAKURAI, N. OOKA,
A. SAKAKURA, M. UGAJIN, E. SHIRAI
Oarai Research Establishment,
Japan Atomic Energy Research Institute,
Oarai-machi, Ibaraki-ken,
Japan

Abstract

Data of silicide fuel for the safety assessment of the JMTR LEU fuel conversion are being measured. The data include release of fission products, thermal properties, behaviors under accident condition and metallurgical characters. Methods of the experiments are discussed. Results of fission products release at high temperature are described. The release of iodine from the silicide fuel considerably lower than the U-Al alloy fuel.

1. INTRODUCTION

The Japan Materials Testing Reactor (JMTR) is a 50-MW, tank-type reactor and its core conversion from highly enriched uranium fuel to aluminide medium enriched uranium (MEU) fuel was carried out in 1986. The effort to convert the core to silicide low enriched uranium (LEU) fuel continues, which is a final goal.

In the silicide core, the U-235 content is increased to extend the operation cycle length and burnable absorber is introduced to reduce the reactivity swing during the cycle. Neutronic calculations are continued for the LEU-fueled cores. Safety analysis is also to be conducted by more stringent method and criteria than previous ones. Therefore, more detailed data such as temperature-dependent property data, R/B ratio (R: release, B: born) of fission products (FPs) etc. are necessary in order to assess integrity of the uranium silicide fuel in the safety assessment. These data are also required by the authorities concerned because there is no data for the uranium silicide fuel.

2. SAFETY REVIEW FOR LEU FUEL USE

The guideline of safety assessment in the application for the license of the reactor installation is being all over revised based on LWR-base criteria. In the present safety analysis for the MEU-fueled core, the anticipated operational transients (AOT) are included in the postulated accidents (PA), and no safety criteria for PA are set up.

* Paper presented at the International Symposium on Research Reactor Safety, Operations and Modifications, Chalk River, Ontario, Canada, 23-27 October 1989 (AECL-9926, Vol. 1, Chalk River Nuclear Laboratories, Ontario (1990)).

Table 1 Representative AOT and PA to be revised

-
- * Uncontrolled positive reactivity insertion by reactivity control system from low power start up condition.
 - * Uncontrolled positive reactivity insertion by reactivity control system at rated power.
 - * Positive reactivity insertion by sudden temperature drop of the primary coolant.
 - * Single and multiple reactor coolant pump trips.
 - * Pressure drop of the primary coolant.
 - * Loss of A-C power.
 - * Core channel flow blockage.
 - * Reactor coolant pump shaft seizure.
 - * Loss-of-coolant accidents resulting from the postulated primary coolant pipe break.
-

In the revised application, the safety criteria will be set up as follows ;

Safety criteria for AOT

The core must be kept so as to be able to revert to the normal operational condition without damage when AOT occurs.

Safety criteria for this ;

- * Minimum departure from nucleate boiling ratio ≥ 1.5 .
- * Fuel core maximum temperature \leq Blister threshold temperature (400°C).
- * No significant deformation of fuel plate.
- * Pressure loaded to the primary coolant system $\leq 1.1 \times$ Maximum operational pressure (1.8 MPa).

Safety criteria for PA

- * The reactor core must be covered by water in any cases.
- * The reactor core must not be led to significant damage, and can be cooled enough.
- * Pressure loaded to the primary coolant system $\leq 1.2 \times$ Maximum operational pressure (1.8 MPa).
- * No significant risk of radiation doses to the public.

Representative AOT and PA being discussed are listed in Table 1.

Integrity of the fuel must be kept even in case of AOT. Therefore, temperature-dependent property data up to 400 °C are necessary for the fuel meat, because the maximum temperature allowed in connection with the blister-threshold temperature is 400°C in case of AOT. In addition, measurement of R/B ratio of FPs of uranium silicide fuel at high temperature is underway for assessing radiological consequences of PA and hypothetical accident. Extensive experiments for reactivity initiated accident behavior by using Nuclear Safety Research Reactor (NSRR), a pulse reactor at JAERI and basic studies on compatibility of U_xSi_y particle and aluminum matrix, FP release mechanism, etc. are scheduled to obtain the JAERI's original data of the new silicide fuel.

The LEU conversion program of JMTR is shown in Fig. 1. Full core demonstration will be started in 1993.

3. MEASUREMENT OF R/B RATIOS OF FP

3.1 Objectives

R/B ratio data of FPs used in accident analysis in safety review for the JMTR core conversion from HEU to MEU fuel are based on the data measured at Oak Ridge National Laboratory using U-Al alloy fuel.

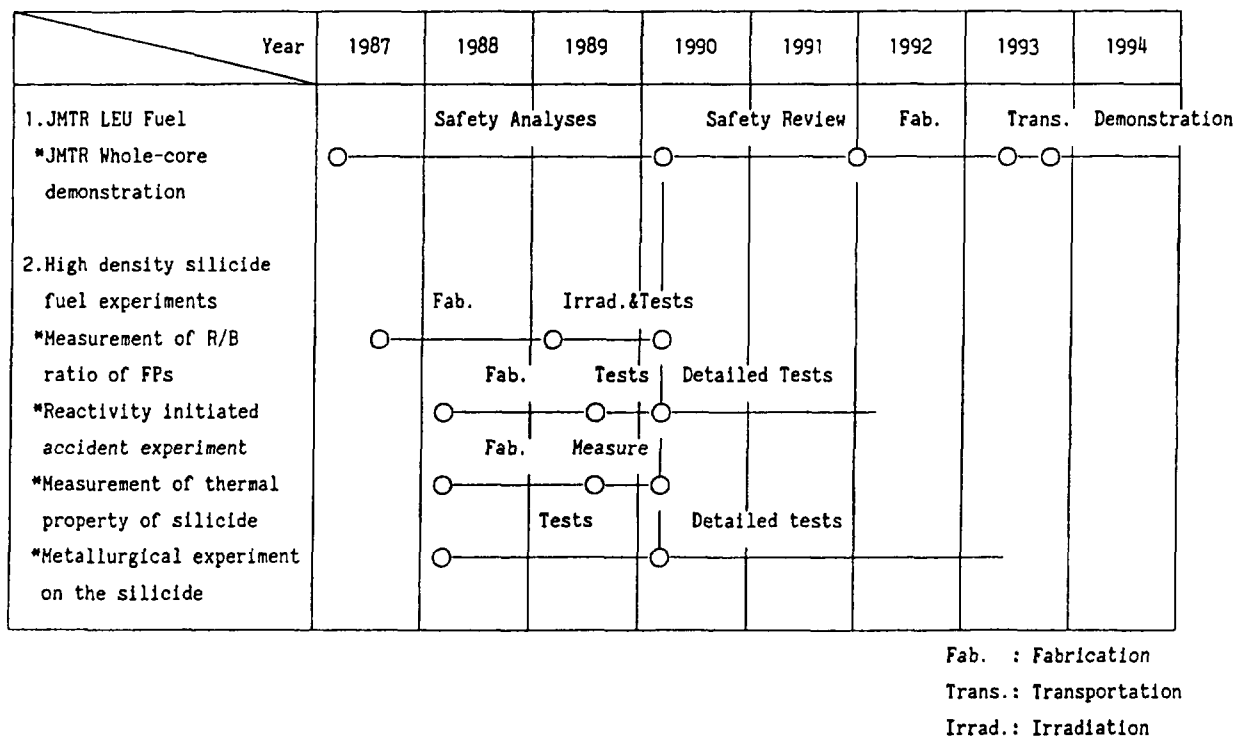


Fig. 1 JMTR LEU Core Conversion Program

Although R/B ratio of FPs of the uranium silicide fuel is believed to have better retention performance against FP leakage than the U-Al alloy, we planned to measure the data to provide a wide data base. Such stance is also necessary to convince the competent authority.

Since flow blockage is through to be the most possible and expansible accident in the JMTR, it is assumed to be the cause of both severe and hypothetical accident. And, 10% and 100% of the core are assumed to be melted in the case of former and the latter, respectively. As a general rule, 100% of core melt assumption is required in the hypothetical accident analysis for the most safety side like the light water power reactor.

In the meanwhile, important FPs for the accident analysis are rare gas and iodine, and R/B ratio of 100% for rare gas and of 60% for elemental iodine have been used. The R/B ratio of iodine was the data of U-Al alloy at 700°C which is approximately the melting temperature of the fuel plate. Therefore, it is necessary to measure the data of dispersion fuel, especially UAl_2 -Al and U_3Si_2 -Al dispersion fuel.

3.2 Methods of experiment

The shape of the specimen is shown in Fig. 2. Three kinds of specimen were chosen for the experiment as shown in Table 2. Burnup levels of the mini-plate fuel were chosen as about 20% and 70%. The burnup of the specimen stated in this report is 20% as shown in Table 3.

The FP release experiment was carried out in a hot cell at JMTR. A schematic of the equipments used in the experiment is shown in Fig. 3. An infrared furnace was used for heating the specimen. The specimen was placed on a sample holder in a quartz tube, as shown in Fig. 3.

Dry air was flowed over the specimen and then through multi-layer filters and sample traps cooled by dry ice. These experiments were conducted at 600, 700, 800, 900, 1000 and 1100 °C. After holding at each temperature for 60 min, the furnace was cooled. Then, the multi-layer filters, the sample traps, the connecting tubes, the sample holder and so on were removed and placed on a Ge detector for the measurement of the gamma-ray activities of the released FPs.

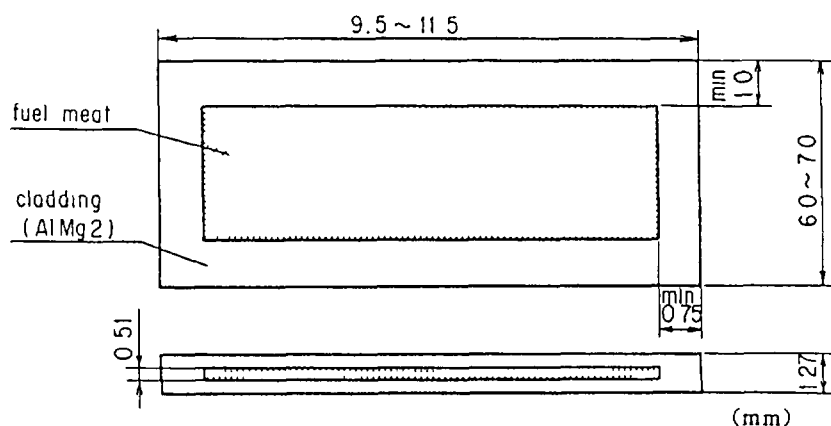


Fig. 2 Test specimen for the FP release experiment
which was cut from the irradiated mini-plate

Table 2 Description of fuel meat in the test specimen

specimen I.D.	composition of dispersion fuel meat	enrichment (²³⁵ U:%)	uranium density (g/ cm ³)	²³⁵ U (mg)
A-12	(UAl ₃ (70%), UAl ₄ (30%))-Al	44.99	1.6	8.16
B-11	((U ₃ Si ₂ (90%), USi(10%))-Al	19.80	4.8	8.96
C-05	((U ₃ Si(50%), U ₃ Si ₂ (50%))-Al	19.76	4.8	8.89

Table 3 Irradiation conditions of the test specimen

specimen I.D.	thermal neutron flux (n/cm ² .s)	irradiation time (day)	burnup	
			(%)	(fiss./cc)
A-12	2.66×10^{14}	22.1	22.1	3.5×10^{21}
B-11	2.62×10^{14}	22.1	21.6	4.4×10^{21}
C-05	2.75×10^{14}	22.1	22.6	4.7×10^{21}

3.3 Results

The relative release of Iodine-131 for silicide and aluminide dispersion fuel are shown in Figure 4. The results of U-Al alloy fuel are also shown in the figure. The release rate of iodine at 700 °C for silicide and aluminide fuel are lower than the U-Al alloy fuel by approximately a factor of 3, as shown in the figure. The results for rare gases and solid FPs are obtained. The release of rare gases are almost 100% similar to the alloy fuel.

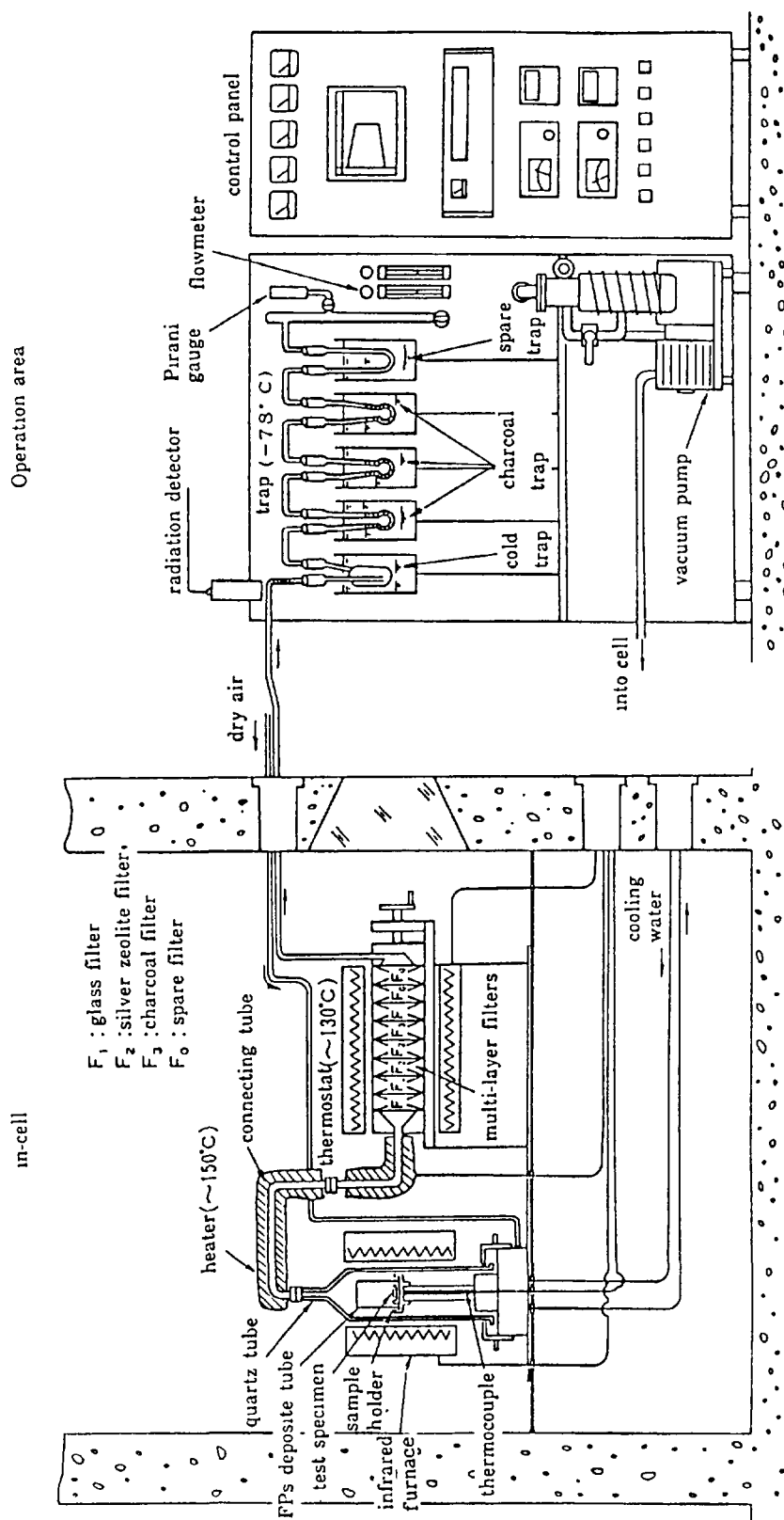


Fig. 3 Equipments for the FP release and collection system

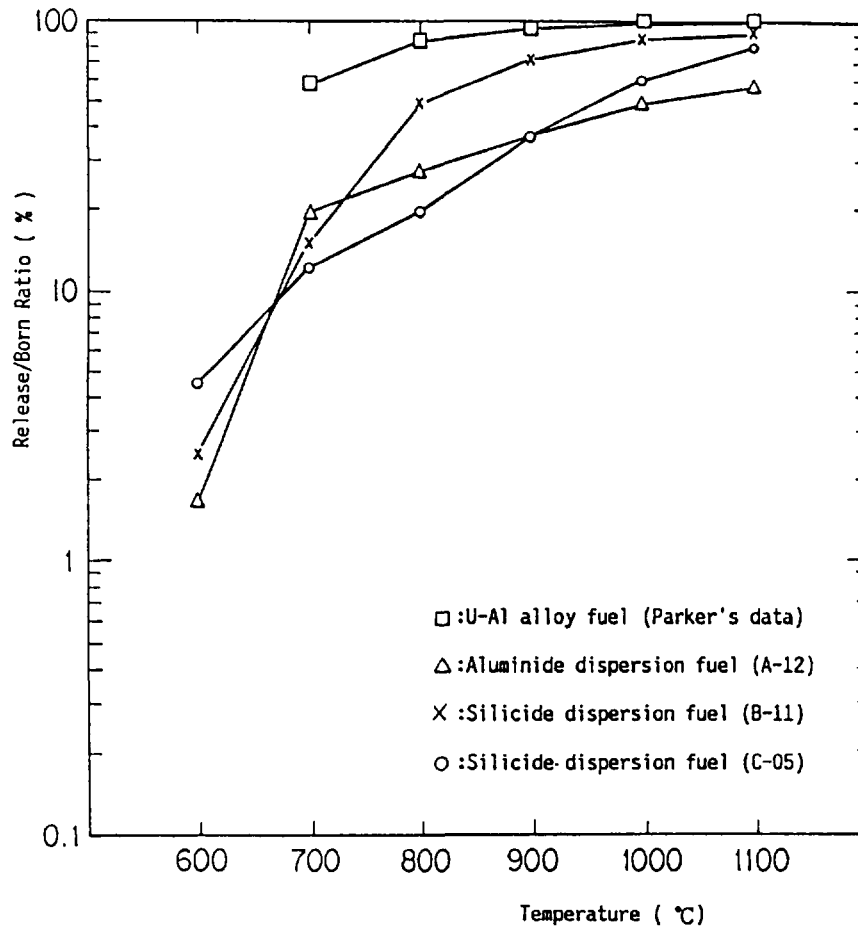


Fig. 4 Cumulative amount of ^{131}I released from silicide and aluminide fuel. Values of U-Al alloy also are shown.

4. MEASUREMENT OF THERMAL PROPERTIES OF THE SILICIDE

For the safety analysis, the thermal conductivity of silicide fuel are necessary to conform the integrity of the fuel up to the temperature which appears in anticipated operational transients.

The thermal conductivity(k) of the silicide fuel is calculated as the product of thermal diffusivity(α), heat capacity(C_p) and density(ρ). Thermal diffusivity is measured by the Laser Flash Meathod. A short-duration pulse of thermal energy from a laser is added on one side of the slab specimen as shown in Fig. 5 and allowed to propagate through the specimen. The thermal response of the opposite face of the specimen is monitored as a function of time(Fig. 6). Thermal diffusivity is then calculated in relation to the time and specimen thickness by following formula;

$$\alpha = A \cdot \frac{L^2}{t_{1/2}}$$

where α : thermal diffusivity
 L : thickness of specimen
 $t_{1/2}$: time to reach the half of temperature rise
 A : constant.

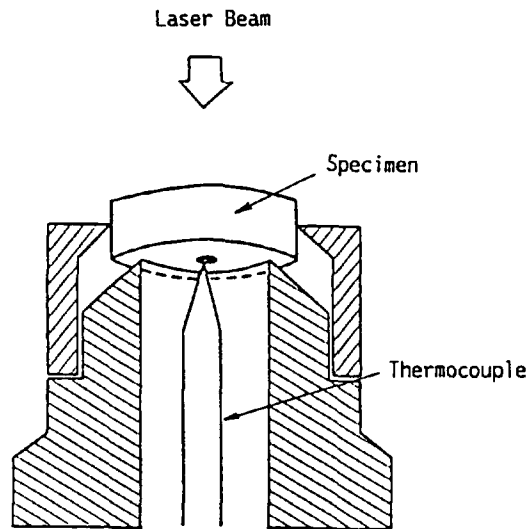


Fig. 5 A schematic of the thermal conductivity measuring system.

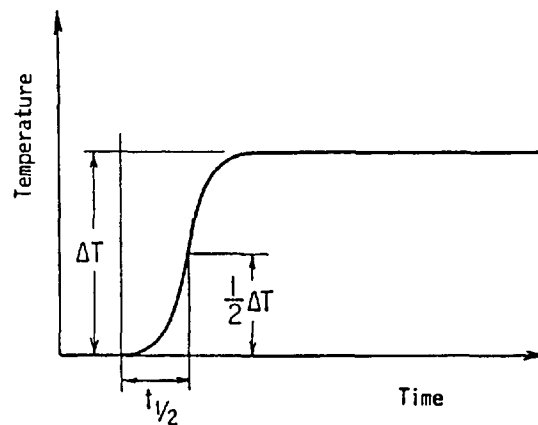


Fig. 6 Thermal response of the specimen from laser energy.

Heat capacity is also measured by this method using following formula;

$$C_p = \frac{E}{\Delta T \cdot m}$$

where E : laser energy absorbed into specimen
 ΔT : temperature rise of specimen
 m : mass of specimen

Thermal diffusivity is converted to thermal conductivity as following ;

$$k = \alpha \cdot C_p \cdot \rho$$

The specimens were fabricated as a parameter of silicon contents, i.e., 7.4, 7.6, 7.9 w/o of silicon. The shape of the specimen is a disk (10 ϕ \times 3 t).

Thermal expansion coefficient of the silicide fuel also is measured by the differential dilatometry. The measurement of thermal properties is conducted from room temperature to 400°C.

5. EXPERIMENT OF FUEL BEHAVIOR UNDER REACTIVITY INITIATED ACCIDENT CONDITION

The experiment is concerned with determining the behaviors of uranium silicide fuel when it is subjected to short period power excursion resulting in high energy densities in the fuel. It is necessary for the safety assessment to clarify the difference of the behavior under the accident condition between the silicide and the aluminide, whose behavior have been made clear experimentally in the Transient Reactor Test Facility (TREAT).

The test specimens (mini-plates of silicide fuel) are encapsulated and irradiated at the Nuclear Safety Reactor (NSRR) in JAERI. Specifically, the following items will be studied;

- (1) Fuel element failure thresholds and failure mechanisms.
- (2) Heat transfer processes and physical characteristics bearing on failure mechanism.
- (3) Chemical reactions which can generate additional energy.
- (4) The pressure wave shock phenomena and water hammer resulting from thermal to mechanical energy conversion.
- (5) Type and amount of fuel dispersed and fission products released resulting from failure.

The fuel plate will be subjected to series of tests designed to determine the threshold of failure and also to tests at short periods which will cause complete destruction of the fuel plate. The safety assessment of NSRR experiment is underway. Design and fabrication of irradiation capsule and test specimen are scheduled in this year.

6. METALLURGICAL EXPERIMENTS ON THE SILICIDE

The experiment are aimed at understanding the metallurgical characters, irradiation behavior, fission products release with regard to the silicide materials for a basic research.

We consider that the system of uranium-silicon is incompletely understood despite of the many studies. The candidate composition of the silicide currently considered is U_3Si_2 , which, however, involve a slight amount of USi or U_2Si . U_3Si_2 and U_2Si react with aluminum matrix at relative high temperature around $500^\circ C$ for short time to form $U(Al, Si)_3$, which cause the thermal growth of the plate. We feel that USi would also react with the aluminum at the temperature. Therefore, important is that the detailed data on these reaction is obtained by our hands. The reactions mentioned above are studied out-of-pile. Under irradiated conditions, however, the reaction rate is supposedly changed from the unirradiated conditions due to, for instance, generation of fission products and acceleration of the diffusion coefficients. Therefore, it is necessary to establish the data base on the reaction kinetic under irradiation and unirradiation. For the purposes, we will perform irradiation experiments in JMTR where the temperature is well controlled.

The following experiments are conducted using silicide fuel material prepared in JAERI.

① Preparing test;

The uranium silicide alloy are produced in the shape of a button by melting uranium metal and elemental silicon in an arc furnace. Buttons are crushed to powder in a glovebox using a steel mortar and pestle. And fuel powder and aluminium powder are mixed in the desired proportions and formed under pressure into a powder-metallurgical compact.

② Phase transition and compatibility test;

Phase transition of the uranium silicide alloys with aluminium are investigated experimentally. Chemical stability of the uranium silicide fuel will be clarified through the experiments.

③ Irradiation test;

Irradiation of the uranium silicide fuel is conducted using a temperature-controlled capsule in JMTR. FP gas release behavior and chemical stability under irradiation will be clarified.

REFERENCES

- (1) PARKER, G.W., MARTIN, W.J., CREEK, G.E., LORENZ, R.A., Release of Fission Products on Out-of-pile Melting of Reactor Fuel, ORNL-3483, Oak Ridge Natl Lab. (1963).
- (2) SHIBATA, T., TAMAI, T., HAYASHI, M., POSEY, J.C., SNELGROVE, J.L., Release of Fission Products from Irradiated Aluminide Fuel at High Temperatures, Nucl. Sci. Eng. 87 (1984) 405.

Appendix K

EXAMPLES OF FUEL SPECIFICATIONS AND INSPECTION PROCEDURES

Abstract

Standardization of specifications and inspection procedures for LEU plate-type fuels are discussed and detailed examples of fuel specifications and inspection procedures are provided for several fuel element geometries and fuel types. Methodology for determination of cladding thickness is also described.

Appendix K-1

STANDARDIZATION OF SPECIFICATIONS AND INSPECTION PROCEDURES FOR LEU PLATE-TYPE RESEARCH REACTOR FUELS

W. KRULL

GKSS — Forschungszentrum Geesthacht GmbH,
Geesthacht, Federal Republic of Germany

Abstract

The subject of standardization of specifications and inspection procedures has become important as one means of limiting fuel cost increases inherent with conversions to LEU plate-type research reactor fuels. An edited version of a draft report of an IAEA Consultant's Group is presented here. It is concluded that specifications should be carefully reviewed when changing from HEU to LEU fuel in order to avoid perpetuating overly restrictive requirements. Tentative recommendations are given for a number of specification topics.

1. INTRODUCTION

1.1 Overview

Research reactors are beginning to operate with low-enriched, high-uranium-density fuels that have been developed as part of the international programme to convert research reactor cores from high-enriched uranium (HEU) to low-enriched uranium (LEU). Most of the necessary irradiation tests, as part of the fuel qualification test, are being performed, and many results and data from post-irradiation examinations (PIE) are becoming available. As fuel up to a uranium density of 4,8 g U/cc is or will be soon qualified, more research reactors will be converting to LEU. The decreasing availability of HEU fuel for research reactors mandates that reactor operators consider the conversion of their reactors to LEU.

The IAEA has published several documents /1-4/ related to research reactor core conversions. Annual international meetings have been held since 1978 and proceedings published /5-10/. The IAEA can provide technical assistance to reactor operators who wish to consider conversion of their reactors from the use of HEU fuel to the use of LEU fuels.

With the transition to high-density LEU fuel, fabrication costs of research reactor fuel elements have a tendency to increase because of two reasons. First, the needed amount of powder of the uranium compound increases by more than a factor of five. Second, fabrication requirements are in many cases nearer the fabrication limits. Therefore, it is important that efforts be undertaken to eliminate or reduce unnecessary requirements in the specifications or inspection procedures of research reactor fuel elements utilizing LEU.

An additional stimulus for standardizing specifications and inspection procedures at this time is provided by the fact that most LEU conversions will occur within a short time span and that nearly all of them will require preparation of new specifications and inspection procedures. In this sense, the LEU conversions offer an opportunity for improving the rationality and efficiency of the fuel fabrication and inspection processes.

This report focuses on the standardization of specifications and inspection processes of high-uranium-density LEU fuels for research reactors. However, in many cases the results can be extended directly also to other research reactor fuels.

1.2 Scope of the Report

This report is intended for the research reactor operator, research reactor fuel element fabricator, licensing authorities and the consultants or experts of the licensing authority or the operator, to be used as a manual or checklist for designing, ordering, fabricating, inspecting and licensing research reactor fuel elements. The considerations and decisions to be made must take into account the existing knowledge of the qualification status of the high-density, low-enriched-uranium fuel, design and safety demands, fabrication possibilities and economic questions.

It is believed that there are many reasons for the details of the existing specifications and inspection procedures for research reactor fuel elements:

- tradition
- others using the same specifications or the same fuel element
- proposals by the fabricators
- operation experience
- nuclear and thermodynamic design
- safety demands
- authority and/or consultants recommendations
- economic aspects

The goal of this report is to provide a more documented, rational and economic basis for the specifications and inspection procedures. This will be especially important for the new LEU fuels, because many of them will be using high volume fractions of the fuel particles in the fuel meat and will be close to the fabrication limits. The uranium density must be increased by a factor of 5,5 or even more if converting from HEU to LEU fuel.

While most of HEU fuels had around, or less than, 20 vol% fuel in the meat, with a maximum around 33 vol%, many LEU fuels will be close to 45 vol%, which is considered the present fabrication limit. With 45 vol%, the corresponding uranium densities are as follows:

UAl_x	$\rho = 2,1 \text{ g U/cc}$
U_3O_8	$\rho = 3,2 \text{ g U/cc}$
U_3Si_2	$\rho = 5,1 \text{ g U/cc}$
U_3Si	$\rho = 6,6 \text{ g U/cc}$

With increasing vol% of fuel the fabrication difficulties increase rapidly. These fabrication difficulties are related to: white spots, homogeneity, cladding thickness, dog boning, etc. For this reason fabrication costs for LEU fuel elements are at present by far higher than for HEU fuel elements if specifications are unchanged. To limit the number of refused or rejected fuel plates and/or fuel elements, efforts are undertaken to reduce specification

demands wherever it is possible and acceptable. It is hoped that this will limit the increase in LEU fuel fabrication costs to a reasonable amount without undue reduction in safety.

It should be emphasized that this report is intended to be used for general guidance and is not to be construed as requirements that the reactor operator, consultant or licensing authority must follow. The report is meant to assist the operator in developing his own specifications and inspection procedures for the fuel elements of his research reactor, taking all necessary considerations into account, including detailed discussion with the selected vendor.

This report complements the IAEA Guidebooks TECDOC-233 /1/, TECDOC-324 /2/, TECDOC-304 /3/ and the Guidebook /4/ that is expected to be published in 1986-1987. Therefore, in this report reference will often be made to Guidebooks as well as other more specialized references.

Chapter 2 gives a detailed discussion of many special specification subjects and informs the operator in some cases about general economic impacts of specification variations. Some inspection procedures of more general interest are discussed in Chapter 3.

2. SPECIFICATIONS

2.1 General

The fuel types considered for the fabrication of plate-type fuels with HEU and LEU are UAl_x , U_3O_8 , and U_xSi_y . Individual fuel vendors do not manufacture all fuel types with both HEU and LEU.

HEU as used here refers to 90% - 93% enrichment. In the case of U_xSi_y , HEU may be necessary if new reactor designs use the development potential of the high-density-uranium fuel. Such studies are underway. Since U_3O_8 and UAl_x may continue to be used by some reactors, e.g., U_3O_8 in HFIR, RP-10, MPR-30 and UAl_x for reactors with peak burnups $> 2 \times 10^{21}$ fissions/cc, the possible cost reduction from having only one production line may not be realized.

Taking further into account that the so-called "unique purpose" reactors /11/ shall use the lowest qualified enrichment together with the corresponding highest uranium density for their design, the future situation will be probably more complicated than the present one. It is possible that enrichments other than 19,75% and 90% - 93% will be in common use. Due to the above mentioned demand, a larger number of different intermediate enrichments may be in use for many years. This will reduce the proliferation risk but increase the fabrication cost.

One of the most important parameters for qualifying a fuel to certain limits of operation is the swelling behavior as a function of burnup. For U_xSi_y the swelling rate is influenced by the porosity, the volume ratio of U_3Si/U_3Si_2 and vol% of U_xSi_y in the fuel meat. Therefore, in some cases these values may need to be introduced into the specifications. There is absolutely no requirement to have these corresponding parameters specified if low-enriched UAl_x or U_3O_8 is used as meat material.

General information about different topics on the specifications of research reactor fuel elements can be found in the literature ranging from a

standard for quality control /12/, remarks on related topics /13,14/, to very special topics /15-17/ and examples /Vol. 4 in /4//.

It is not the intention to comment in detail on all parts of the specification since

- many parameters are more or less standardized
- other parameters have only a minor impact on fabrication cost and
- some parameters come from the design of the reactor.

Nevertheless, it is strongly recommended that specifications and inspection procedures be reviewed and unnecessary but restricting limitations be removed. This should be done before ordering the fuel elements for the conversion of the research reactor to LEU fuel.

2.2 Geometry

Most of the geometric conditions are fixed since, e.g., grid plate dimensions cannot be changed. Some geometric design values can be adjusted in some cases if this is within the design limitations. For this reason a few values are given which are used in most of the fuel element designs:

fuel meat thickness	: 0,51 mm, a few 0,76 mm
fuel meat width	: 60 mm and 62,8 mm
(influences the peaking factor)	
fuel meat length	: 600 mm, a few up to 800 mm
number of plates	: 23, some less
plate thickness	: 1,27 mm, a few thicker

2.3 Fuels

2.3.1 Fuel Composition

No comments are made regarding UAl_x and U_3O_8 . As mentioned in Chapter 2.1, the phase composition of the U_xSi_y fuel should be known. This can be determined with sufficient accuracy only by taking a large number of metallurgical cuts or powder samples. Therefore, the vendors are developing correlations which are believed to be satisfactory in most cases.

Metallurgical cuts and microscopic analysis are very expensive. They should be included in the specifications only if absolutely necessary for safety reasons. In most cases the correlations will be sufficient.

2.3.2 Particle Size Distribution

The particle size must be $<150 \mu m$. Up to 50 wt% of the fuel powder can have a particle size less than $40 \mu m$ (or $45 \mu m$, if non-metric standards are used). Other existing limitations in particle size and % of fines are believed not necessary based on results of PIE's (the existing specifications for UAl_x and U_3O_8 can be taken for U_xSi_y , too). However the maximum particle size and the distribution of particle sizes will influence other parameters, such as porosity and minimum cladding thickness. Therefore, a maximum particle size might be an advantage for some applications. For customers

interested in a maximum particle size of 125 μm for example, the vendors should be contacted to determine the relative cost increase per fuel element.

The control sieving must be carried out with a set of sieves of 40 μm or 45 μm , 150 μm and 180 μm . If all particles pass the sieve with 180 μm , it is allowed to have 1% of the fuel powder on the sieve of 150 μm .

2.3.3 Porosity

The built-in porosity in the fuel meat provides space to accommodate the initial swelling of the fuel particles. The amount of built-in porosity is dependent on the vendor, fabrication process and vol% of fuel in the meat. /8,10/ For the dependence of swelling rates on porosity, see /8,10/. In some critical applications of U_xSi_y , which can swell considerably due to the high fission density attainable, it may be desirable to specify the amount of built-in porosity in order to limit, for example, channel gap thickness changes during operation. Such a specification is not necessary for low-enriched UAl_x and U_3O_8 or, in most cases, for U_xSi_y .

2.3.4 Al-Powder

There are slight differences in the existing specifications which are believed to be of minor importance. Care should be taken in limiting the amount of poisoning impurities such as B, Cd, and Li. Other impurities can normally be varied over a greater range. The current specification limits should be used as a guideline for operators and fabricators. In order to avoid unwanted nuclear and metallurgical behavior, some limits should be specified. These considerations can be applied to the fuel powder, too.

2.3.5 U-Content of Fuel Plate

There is no problem with accuracy (ca. 2%). Total U-content cannot be standardized.

2.4 Fuel Plate

2.4.1 Homogeneity

With increasing vol% of fuel and uranium density, the present homogeneity limits will result in an increase in the number of rejected fuel plates. Homogeneity limits in the specifications may be a result of hot spot analyses and therefore part of the overall safety features. However, it may be worthwhile to discuss these limits with relevant authorities to determine whether adequate safety margins can be maintained with looser homogeneity limits so that fabrication cost can be reduced.

With the standard technique homogeneity deviations are determined over a plate surface area of 1 cm^2 . Smaller measuring areas will give, for physical reasons, greater variations. All commonly used measuring techniques are acceptable.

Design or safety limits on homogeneity are related to the plus tolerances of the homogeneity. The existing minus tolerances are not as critical. Greater minus deviations may be acceptable, therefore, but their control allows an insight into the overall quality of fuel plate fabrication.

Since homogeneity limits have a great impact on fabrication cost, the operator should obtain cost factors related to different homogeneity limits from the vendor in order to perform a proper cost-benefit analysis.

2.4.2 Plate Thickness

The tolerance on the overall plate thickness influences the minimum cladding thickness and therefore must be limited. Also, if there are tight demands on channel spacing, these cannot be achieved if the tolerance on the plate thickness is too large. For these reasons the tolerance of the plate thickness will be based on the minimum cladding thickness and the tolerance on channel spacing.

2.4.3 Minimum Cladding Thickness

A minimum cladding thickness is specified in order to protect against the release of fission products, especially after the cladding surface may have been subjected to corrosion.

Corrosion is influenced by many factors: cladding thickness, cladding material, surface treatment, copper or chlorine impurities, temperature, pH and conductivity of the water, water quality (e.g. Cu, Cl), lifetime of the fuel, overall operating conditions over years, etc. Some of these factors are or may be correlated. Typical types of corrosion occurring on plate-type fuel elements are pitting corrosion and uniform plate corrosion. Since fission product release from fuel elements will cause many problems, any type of corrosion must be minimized to avoid such difficulties.

The minimum cladding thickness can and will be different for different research reactors depending on various conditions of use (e.g., if the fuel lifetime is 3 weeks or 3 years). Any change of the minimum cladding thickness should be based on reported operating experience and documentation of the actual cladding thickness obtained for a specified minimum. One has to be sure that the reported operating experience is not the result of other factors but is related only to the specified values of minimum cladding thickness. The correlation between specified and actual minimum cladding thickness must be known. The first detailed measurements on this topic have been reported in /15/.

Historically the cladding thickness has been specified as $0,38 \pm 0,08$ mm in most cases. Due to higher density fuel with a larger vol% of fuel in the meat (more fuel particles), an increasing number of fuel particles have been found violating the 0,30 mm minimum cladding thickness. In order to reduce the rejection rate and the fabrication cost, fuel plates have been accepted with fuel particles in the region down to 0,25 mm (0,23 mm in some cases) and even to 0,20 mm for the HFIR. It is obvious that the acceptance of fuel plates with extremely low minimum cladding thickness will reduce the fabrication cost. The acceptable minimum is closely related to the overall long term operating conditions, the materials used and the fabrication technique. For this reason no general statement for the acceptable minimum cladding thickness can be given at present and may never be possible. Fission product release coming from pitting corrosion was found in the past even in cases where the minimum cladding thickness was 0,30 mm.

To enable the reactor operator to make the best decision for his reactor, the fuel fabricators should be contacted to determine relative prices for different minimum cladding thicknesses.

2.4.4 Cladding Material

Fabricators normally use aluminum cladding materials with specified additions and impurities following their national standards. In use have been: pure Al (99,5% Al), pure Al (99,85% Al), Al 1100, AlFeNi, and Mg-containing aluminum-alloys such as Al 6061, AG1NE, AG2NE, AG3NE, AlMg1, AlMg2, AlMg3. With increasing uranium density and increasing coolant flow velocity, weak Al-cladding materials cannot be used because bonding and cladding thickness difficulties may arise during the fabrication process and mechanical stability difficulties of the fuel plate may arise during operation. One advantage of the Mg-containing aluminum alloys is their increased corrosion resistance. For this reason it is recommended that Mg-containing Al-alloys be used if possible. However, in most cases all cladding materials in use are acceptable. In order to reduce cost, the fabricators should limit the number of different cladding materials in their fabrication lines to one or two.

Requirements on the acceptable impurities are the same as discussed for the fuel in Chapter 2.3.4. In some cases an increase of the boron content from 10 ppm to 30 ppm can be accepted since the ^{10}B will be totally consumed during the lifetime of the fuel.

2.4.5 Surface Defects

Significant surface defects may be caused by some lack of attention during the fabrication process or by removing foreign particles from the cladding. No foreign particles with unknown chemical composition can be accepted in the cladding. Surface defects must be limited in size and depth to avoid fission product leakage during the whole lifetime of the fuel element. To date there has been no report that surface defects and pitting corrosion are correlated. However, since there are other corrosion phenomena possible (plate type, potential effects) the depth of surface defects must be limited. The allowed depth should inversely follow the minimum cladding thickness. It is recommended that the difference between the two not be less than 125 μm ; otherwise, plates should be rejected. For example:

minimum cladding thickness	250 μm
maximum surface defects	125 μm .

In the dogboning zone, if there is evidence of dogboning in the plates, surface defects not deeper than 75 μm are acceptable. Outside the meat zone, defects up to 300 μm may be acceptable depending on the number of these defects and the prevalence and location of white spots (see Chapter 2.4.7).

2.4.6 Surface Treatment

The surface treatment selected may influence the corrosion behavior of the fuel plate. Therefore the surface must be absolutely free from Cl. In most cases only etching and cleaning with demineralized water is used and is sufficient. With an additional treatment with hot water (100°C) or steam, a corrosion resistant layer of stable Boehmite is produced, and the corrosion resistance is increased by more than a factor of 10. This additional treatment will increase the fuel element cost.

2.4.7 White Spots

With increasing uranium density and increasing vol% of fuel in the meat a significant number of so-called white spots have been detected on the x-ray films. These white spots are fuel particles located between the frame and the

cladding outside the specified meat zone. Limits on the location and clustering of the fuel particles are necessary for two reasons:

- to avoid fission product leaks
- to ensure the appropriate cooling of the plate even in zones where the plate is not cooled by turbulent flow.

At present it has not been established that there is a correlation between blisters outside the meat zone and fuel particles at these positions. If such a correlation is found, this will become important only for high burnup values. PIE's are going on and results will be reported.

The specification given below is recommended for the acceptance of white spots. This proposed specification avoids the measurement of the distance between the white spots and/or the necessity to calculate the overall area of the white spots. These measurements and/or calculations were found in the past to be totally impractical and extremely expensive.

- a) No particles (evidenced as white spots on the position radiograph) shall be within 0,4 mm of the edges or ends of the fuel plate.
- b) The maximum dimension of a stray particle shall be 0,5 mm. Touching particles shall be considered as a single particle for the purpose of determining the largest dimension.
- c) The maximum number of stray particles in any 20 mm² area located between the maximum core length or width and within 0,4 mm of the plate edge or end shall not be greater than ten (10).
- d) *) A stringer of fuel generated from the corners of the core ends is acceptable provided it comes no closer than 1,3 mm from the plate ends.
- e) No stray particles shall be allowed in the comb or identification areas.
- f) Stray particles found within 0,4 mm of the plate edge or end may be removed by filing. These handworked areas shall not be greater than 0,5 mm in depth.

2.4.8 Surface Contamination

There is no present need to change the commonly specified values (ca. 5-10 µg U/plate).

2.4.9 Burnable Poisons

Burnable poisons are in use for higher power research reactors. These burnable poisons can be in side plates or at the top or bottom of fuel plates. The present knowledge is that some care may be necessary if poison is mixed with fuel. Experiments are going on to determine the swelling behavior in these cases, especially for uranium silicide fuel.

2.5 Fuel Element

As stated in Chapter 2.2, no recommendations on most of the geometry factors can be given since they are specific to the overall design.

*Discussions on this point are continuing.

2.5.1 Channel Gap Spacing

The minimum channel gap is one of the parameters in the calculations for the hot channel, and for this reason the tolerances are included in the thermodynamic calculation and the safety report in most cases. But in general, since many reactors operate with large safety margins, the chosen tolerances should be rechecked, because fuel element fabrication cost is significantly influenced by the chosen tolerances and the inspection procedure.

In almost all cases only the minimum tolerance is of importance and controlled. Therefore, to specify a plus tolerance is unnecessary in most cases. The fuel fabricators should be contacted to obtain relative costs related to different requirements for tolerances and inspection procedure. When specifying channel gaps one has to consider the gap between neighboring fuel elements with the same care. The cooling conditions between neighboring fuel elements are not as good as within the fuel elements in many cases.

2.5.2 Burnup Warranty

Any burnup warranty must be discussed between operator and vendor and depends on too many conditions for a general recommendation.

3. INSPECTION PROCEDURES

The chosen inspection procedure depends on many different factors, such as

- license requirement
- consultants demands
- fabricator experience
- inspectors experience
- changed or unchanged fabrication process
- evidence of defects
- reactor design.

The inspection can be performed by the independent quality control department of the fabricator and/or independent expert and/or customer. The extent of inspection ranges between 100%, sampling (extended to 100% if a given percentage of values are found out of the specified ones) and 0%. The extent and percentage of inspection may limit the throughput of the fabrication and, therefore, may have a great impact on the fuel element fabrication cost. It is estimated that inspection cost ranges between 1/3 and 2/3 of the total fabrication cost, depending on the chosen procedure. It is strongly recommended that all inspectors be well trained and that the inspectors not reject plates or elements in all cases if the values are slightly outside the specified ones. The inspectors should use their experience to decide in such cases whether to recommend acceptance or rejection.

Since the chosen detailed inspection procedure is influenced by many different factors, recommendations could be developed only for some selected points.

3.1 Particle Size

See Chapter 2.3.2.

3.2 Bonding

The most effective quality check on bonding is the blister test. The chosen blister temperature depends on the selected cladding material and should be only slightly different from the hot rolling temperature. The temperature range is normally between 410°C and 500°C.

In addition to the blister test, the ultrasonic test* is in use. With this method, defects >2 mm ϕ can be detected. With high uranium density there are increasing difficulties near the ends and edges of the fuel core. The measurements need careful interpretation and the method should be separately discussed between the customer and the fabricator.

3.3 White Spots

See Chapter 2.4.7.

3.4 Radiographic Inspection

Fluoroscopy and/or x-ray film is in use. The selected method depends on the need for control and documentation. Care should be taken to cut the fuel plate symmetrically out of the rolled plate.

3.5 Surface Contamination

Smear test (sampling) and 100% control with α -counters are in use. Normally only background is detected. If there are positive measuring results, the rolling process should be inspected.

3.6 Channel Gap Spacing

Minimum check with go gauge only, or for extremely high requirements, registered measurements are in use. See Chapter 2.5.1.

4. CONCLUSION

The specifications currently used for HEU fuel should not be taken as ultimate demands when going to high-density LEU fuel. At that time, the specification demands should be carefully reviewed to use this possibility for reducing the fuel element fabrication cost. This review should include the most important safety margins, the existing operating experience and the operating conditions of the plant. The operator should discuss the specifications finally chosen in detail with the fabricator and licensing authority. Whether additional parties need to be involved depends on the special circumstances and the experience of the operator, of his experts and of his authority. The IAEA may be contacted for assistance.

*Excellent for discovering no bonding between Al-frame and cover plate.

REFERENCES

- /1/ Research Reactor Core conversions from the Use of Highly Enriched Uranium to the Use of Low Enriched Uranium Fuel, Guidebook, TECDOC-233, Vienna, 1980.
- /2/ Research Reactor Core Conversion from the Use of Highly Enriched Uranium to the Use of Low Enriched Uranium Fuels, Guidebook Addendum, Heavy Water Moderator Reactors, TECDOC-324, Vienna, 1985.
- /3/ Core Instrumentation and Pre-Operational Procedures for Core Conversion HEU to LEU, TECDOC-304, Vienna, 1984.
- /4/ Research Reactor Core Conversion from the Use of Highly Enriched Uranium to the Use of Low Enriched Uranium Fuels, Safety and Licensing Guidebook, Vol. 1 Summary, Vol. 2 Analyses, Vol. 3 Analytical Verification, Vol. 4 Fuels, Vol. 5 Operations, TECDOC- , Estimated date of publication 1986-1987.
- /5/ Proceedings of the International Meeting on Development, Fabrication and Application of Reduced Enrichment Fuels for Research and Test Reactors, Argonne, USA, 12-14 November 1980, ANL/RERTR/TM-3.
- /6/ Proceedings of the International Meeting on Research and Test Reactor Core Conversions from HEU to LEU Fuels, Argonne, USA, 8-10 November 1982, ANL/RERTR/TM-4.
- /7/ Proceedings of the International Meeting on Reduced Enrichment for Research and Test Reactors, 24-27 October 1983, Tokai, Japan, JAERI-M 84-073.
- /8/ Proceedings of the 1984 International Meeting on Reduced Enrichment for Research and Test Reactors, Argonne, USA, 15-18 October 1984, ANL/RERTR/TM-6.
- /9/ Proceedings of the International Meeting on Reduced Enrichment for Research and Test Reactors, Petten, Netherlands, 14-16 October 1985, D. Reidel Publishing Company, Dordrecht
- /10/ Proceedings of the International Meeting on Reduced Enrichment for Research and Test Reactors, Gatlinburg, USA 3-6 November 1986, ANL/RERTR/TM-9 (these proceedings).
- /11/ Limiting the Use of Highly Enriched Uranium in Domestically Licensed Research and Test Reactors, U.S. Fed. Reg. Vol. 51, No. 37, 25 February 1986.
- /12/ Quality control for plate-type uranium-aluminum fuel elements, ANS-15.2 (1974).
- /13/ W. Krull: Remarks on the Demands for the Qualification of High Density Fuel, GKSS 84/E/40 (1984).
- /14/ D. R. Harris, J. E. Matos, H. H. Young: Conversion and Standardization of University Reactor Fuels Using Low-Enrichment Uranium-Operations and Cost, in /9/.

- /15/ T. Görgenyi, H. Hutch: Determination of Cladding Thickness in Fuel Plates for Material Test and Research Reactors, IAEA-Seminar on Research Reactor Operation and Use, Jülich, September 1981.
- /16/ M. Neuberger, M. Müller, U. Schütt: Automatisch Kuhlspaltmessung mit Rechnerauswertung, Jahrestagung Kerntechnik, 8-10.4..86, Aachen
- /17/ W. H. Anderson, Jr.: Quality Assurance and Inspection Techniques in Use at Babcock and Wilcox, in /10/.

Appendix K-2

FUEL ELEMENTS WITH LEU UAl_x -AI FUEL FOR THE FORD NUCLEAR REACTOR

Appendix K-2.1

SPECIFICATIONS

ARGONNE NATIONAL LABORATORY
Argonne, Illinois

FORD NUCLEAR REACTOR/UNIVERSITY OF MICHIGAN
Ann Arbor, Michigan

United States of America

Abstract

As part of the U.S. RERTR Program, a full-core demonstration with LEU fuel began in December 1981 in the Ford Nuclear Reactor (FNR) at the University of Michigan. The LEU standard and control fuel elements were manufactured by CERCA and by NUKEM using specifications prepared by ANL. The ANL specifications were derived from those prepared by EG&G-Idaho for HEU fuel elements manufactured for the FNR by Atomics International.

Due to differences among fabricators in some of the normal manufacturing processes and materials, some of the specifications were negotiated by ANL and the University of Michigan with each manufacturer to arrive at mutually agreeable specifications.

The specifications agreed to with NUKEM are presented here as an illustration only. A similar set of specifications was agreed to with CERCA. In this example, materials, material numbers, document numbers and drawing numbers specific to a single fabricator have been deleted.

1.0 SCOPE

1.1 Description

This Specification details the materials, components, testing, inspection, and quality control requirements for the fabrication of standard and control Fuel Elements for the Ford Nuclear Reactor at the University of Michigan, Ann Arbor, Michigan.

1.2 Definitions

For the purpose of this Specification, the following terms are identified. (Capitalization shall denote the use of a defined term.)

1.2.1 Batch

A quantity of UAl_x produced in one operation.

1.2.2 Blend

To mix or mingle constituents of a Batch.

1.2.3 Certification

A document form signed and dated by the responsible authority of a pertinent function or activity, stating that a material or a component meets specified requirements.

1.2.4 Contractor

The primary vendor selected by Argonne National Laboratory to manufacture the product.

1.2.5 Development

A determination of processes, equipment, and parameters required to produce a product in compliance with this Specification.

1.2.6 Dogbone Area

Thickening of Fuel Core at ends of Fuel Plates. This occurs during rolling process.

1.2.7 Dummy Fuel Element

An element consisting of unfueled simulated Fuel Plates.

1.2.8 Failure

The condition arising when representative samples, which are the basis for process control and product acceptance, fail to meet the requirements of this Specification.

1.2.9 Fuel Core

The uranium-bearing region of each Fuel Plate.

1.2.10 Fuel Element

The bundle of Fuel Plates and hardware components, as defined in Section 3.0.

1.2.11 Fuel Plate

The Fuel Core complete with aluminum frame and cladding.

1.2.12 In-Process-Controls

Checks made during Production to assure that the manufacturing processes, equipment, and personnel are capable of producing a product meeting specified requirements.

1.2.13 Laboratory

Argonne National Laboratory (ANL).

1.2.14 Lot

A group of sequentially numbered pieces handled as a unit, or material traceable to common processing step. A Lot shall consist of a minimum of sixteen (16) Fuel Plates.

1.2.15 Manufacture(ing)

All fabrication, assembly, test, inspection, and quality control processes.

1.2.16 Production

The phase of the program, following qualification, during which the product is in Manufacture(ing).

1.2.17 Production-Quality-Control

The sampling plans, inspections, and tests required during Production to assure that the product is in compliance with this Specification.

1.2.18 Qualification

A demonstration that the manufacturing processes and equipment can produce a product in compliance with this Specification.

1.2.19 Rejection

Materials, parts, components, or assembly products which will not be accepted as part of the contract requirements of this program because of non-compliance with this Specification.

1.2.20 Requalification

A demonstration that a single or group of manufacturing processes, equipment, and personnel can produce a product in compliance with this Specification after the original Qualification has been completed.

Requalification is required for a change in material, process, or operator.

1.2.21 Specification

All parts and supplements of this document, its references, drawings, and standards.

1.2.22 Sub-tier Supplier

Any vendor selected by the Contractor to furnish materials, services, or manufactured parts for the products.

1.2.23 User

Ford Nuclear Reactor, University of Michigan.

2.0 APPLICABLE DOCUMENTS

This Specification was elaborated on the basis of the documents cited herein. In case of non-conformance, the latest revision of this Specification shall be valid.

2.1 Specification for Standard Ford Fuel Element Assembly

No. A0004-1000-SA.

2.2 Argonne National Laboratory Procedures

AQR-001 Quality Verification Program Requirements.

2.3 Drawings (ANL)

A0004-0002-DC University of Michigan Standard and Control Fuel Plate
A0004-0003-DC University of Michigan Standard and Control Fuel Element
Adaptor
A0004-0004-DC University of Michigan Standard Fuel Element Assembly
A0004-0005-DC University of Michigan Control Fuel Element Assembly

2.4 Supplemental Specifications

A0004-0114-SA Calibration Requirements
A0004-1005-SA Specification for Enriched U-Metal for UAl_x Reactor Fuel
Elements

2.5 Contractor Documents

Production and control shall be effected according to the documents of work (drawings, inspection scheme, specifications) stated in the appendix in conformance with the respective latest revision which is given in the list of documents.

3.0 TECHNICAL REQUIREMENTS

3.1 Product Requirements

The Standard Fuel Element, Part Number A0004-0004-DC, consists of N_s Fuel Plates, two (2) side plates, two (2) bail supports, one (1) bail, and one (1) adaptor. The Control Fuel Element, Part Number A0004-0005-DC, consists of N_c Fuel Plates, two (2) side plates, two (2) guide plates and one (1) adaptor. The Fuel Elements have Fuel Plates and control rod guide plates attached to the side plates by mechanical means; end adapters are attached to the fuel section by screws.

3.2 Fuel Plates

3.2.1 Fuel Loading

Each Fuel Plate shall contain M_p grams \pm 2% U-235 based upon final weight of the final compact and chemical and isotopic analysis of the constituents. Each loading of the Fuel Plates shall be recorded in grams to two (2) decimal places.

3.2.2 Fuel Homogeneity

Non-homogeneity of the surface density in g/cm^2 of U-235 shall not exceed \pm 30%-100% within the maximum and minimum limit lines of the meat area (zone 3) relative to the nominal value, \pm 30%-20% within the dog-boning area (zone 2), and \pm 20% in the nominal meat area (zone 1).

According to the determination in the inspection scheme, a defined quantity of Fuel Plates shall be continually examined by means of gamma absorption in a trace with a 25 mm^2 collimator (Round

window 5.6 mm diameter). The result shall be analogously recorded together with (+) standards. For calibration Al-step standards of equal absorption shall be used which represent the minimum, nominal, and maximum uranium content.

3.2.3 Core Configuration

The outline of the Fuel Core shall be within the largest and smallest areas as defined by the Fuel Core Drawing (Scheme), item 7.4, dimensions and their respective tolerances. Fuel flakes are allowed except within 0.38 mm of the edge and the ends of the fuel plates.

3.2.4 Internal Defects and Bond Integrity

A bond across the clad/frame and clad/Fuel Core interfaces is required. Internal defects shall be examined and evaluated as described in Paragraph 4.4.5.

3.2.5 Surface Finish and Defects

The finished Fuel Plates shall be free from pits, dents, scratches, and other areas of metal removed in excess of 0.13 mm deep, except in the Dogbone Area, within 38 mm from the end of the Fuel Core. In this area, such depressions shall be limited to 0.08 mm deep.

3.2.6 Cleanliness

The Contractor shall take all precautions necessary to maintain a high standard of cleanliness during fabrication to ensure that no foreign materials or corrosion products are present in the finished Fuel Plates and Elements. The finished Fuel Elements shall be completely free of dirt, scum, scale, graphite, grease, organic compounds, and other foreign matter inside and outside.

All metal chips, turnings, dusts, abrasives, weld spatter, scale, and other particles shall be removed without destroying the continuity of the surfaces.

All oil and grease shall be removed by the use of a degreasing agent approved by the Laboratory, and all surfaces, including all crevices shall be thoroughly rinsed with distilled water.

3.2.7 Identification

Each finished Fuel Plate shall be identified by a number stamped into the top 3 mm of the Fuel Plate, not in excess of 0.15 mm in depth. The identification number shall be on the convex surface of the Fuel Plate before forming. Positive identification must be maintained relative to the complete fabrication history, including the Plate Lot, Fuel Blend, basic material lots, heat or melt, manufacturing cycle, and quality control phases.

3.2.8 Storage

All fuel plates that have received final cleaning shall be contained in clean polyethylene bags while (1) awaiting final assembly, (2) being transferred into storage, or (3) being maintained in storage. Any Fuel Plate exposed to contamination shall be reinspected to the requirements of Paragraph 3.2.6. Fuel Plates shall not be exposed to any chlorine-containing material during storage.

3.3 Fuel Elements

3.3.1 Fuel Loading

Each Standard Fuel Element shall contain M_S grams $\pm 2\%$ U-235.
Each Control Fuel Element shall contain M_C grams $\pm 2\%$ U-235.
(Note: See Appendix of this Specification for values M_S and M_C).

3.3.2 Material

All material used or contained in the product shall comply with all the requirements of this Specification unless exempted by written document by the Laboratory.

3.3.3 Cleanliness

The standards of cleanliness required for the Fuel Plates by Paragraph 3.2.6 are also required for the Fuel Elements.

3.3.4 Assembly

The Fuel Plates shall be attached to the side plates by mechanical swaging. Fuel Plate identification numbers shall be on the bail end of the element.

3.3.5 Identification

Each Fuel Element shall have an identifying number such as MIXXX. The number shall be placed on the outside of the side plates as shown on the drawings and shall consist of 68 mm block characters cut 0.5 mm deep. The Fuel Elements shall be numbered serially. The Laboratory will provide consecutive serial numbers.

3.3.6 Storage

All Fuel Elements that have received final cleaning shall be sealed in clean polyethylene bags while (1) being transferred into storage, (2) being maintained in storage, or (3) being prepared for shipment or packaging. Any material exposed to contamination shall be reinspected according to the requirements of Paragraph 3.2.6. Fuel Elements shall not be exposed to any chlorine-containing material during storage.

3.4 Materials of Construction

Note: Contractors located outside the United States territory may substitute materials and standards comparable to those listed, after approval by the Laboratory.

3.4.1 Component Materials

The materials requirement for the components comprising the Fuel Element are specified in the Appendix, item 7.6 Materials.

3.4.1.1 Fuel Cores

The Fuel Core of the Fuel Plate shall be UAl_x inter-metallic powder dispersed in aluminum alloy powder. The UAl_x powder and the Al powder shall be produced according to the Contractor's specifications, after approval by the Laboratory. Two one gram samples of Blended UAl_x Batches used in producing Fuel Cores shall be obtained by the Contractor for the Laboratory

and held at the Contractor's plant for the Laboratory's use. During the course of the subcontract, any and all samples not called for and in the possession of the Contractor will be considered part of the Contractor's scrap.

3.4.1.2 Frames

The frames shall be Aluminum Plate Alloy as specified in the Appendix, item 7.6, unclad or clad on both sides with Alloy 1100. If clad, the thickness of Alloy 1100 on each side shall be as noted in Subparagraph 3.4.1.3. Maximum allowable boron content shall be 30 ppm.

3.4.1.3 Cover Plate

The fuel cladding (cover plate) shall be Aluminum Alloy as specified in the Appendix, item 7.6, unclad or clad on one side with Alloy 1100. Maximum allowable boron content shall be 30 ppm. If clad, each cover plate shall have an Alloy 1100 clad thickness no less than 3 percent and a nominal maximum of 6 percent of the total thickness of the composite plate, provided the three sigma limit does not exceed 7.5 percent.

Compliance with the clad thickness requirements may be accomplished by a Subcontractor-developed statistical sampling and analytical method approved by the Laboratory.

4.0 QUALITY CONTROL AND QUALITY ASSURANCE REQUIREMENTS

4.1 Records and Reports

4.1.1 Distribution of Reports (Prior to Fabrication)

The Contractor shall supply three (3) copies of the following data and records to the Laboratory prior to fabrication of the initial element for review and approval:

4.1.1.1 Contractor Drawings

All shop drawings of component parts of the Fuel Element and Fuel Element Assembly. Other current drawings initiated by Contractor shall be maintained and filed subject to the Laboratory's review.

4.1.1.2 Integrated Manufacturing and Inspection Test Plan

The Contractor shall prepare a sequential listing of the various manufacturing and test steps with approximate schedule dates necessary for the fabrications.

4.1.1.3 Procedure for Fuel Plate U-235 Content

A detailed description as to the manner by which the Contractor proposes to assign Fuel Plate U-235 content. Included in the description must be sampling, analytical, and quality control procedures and a statement as to the estimated absolute accuracy of the assigned Fuel Plate and Fuel Element U-235 content.

4.1.1.4 Manufacturing Procedures

All programs, processes, and procedures, and all changes and modifications thereto, to be used to Manufacture the product, as listed in Section 4.2.

4.1.1.5 Plate Fabrication and Qualification Records

All records required by Paragraph 4.3.1.

4.1.1.6 Element Fabrication Qualification Records

All records required by Paragraph 4.3.2.

4.1.1.7 In-Process Controls Procedures

Those procedures established to comply with the requirements of Paragraph 4.3.3.

4.1.2 Distribution of Reports (Prior to, or Concurrent with, Shipment)

Prior to, or concurrent with, the shipment of each Fuel Element the Contractor shall provide the Laboratory with three (3) copies of the items listed in Paragraph 4.1.2.1 through 4.1.2.10 (radiograph: one (1) copy).

The three (3) copies required include the one (1) copy of those items required to accompany shipment by Section 5.1.

4.1.2.1 Material Certification

Certification of all material compliance to the requirements of this Specification including any chemical and physical test results pertaining thereto.

4.1.2.2 Certification of Product Compliance

Certification of product compliance to the requirements of this Specification except, as the case may be, for previous Laboratory-approved deviations, such deviations to be detailed in the Certification. The Certification shall include any test data pertaining thereto not specifically listed in Subparagraphs 4.1.2.3 through 4.1.2.10.

4.1.2.3 Dimensional Inspection Reports

Inspection reports, including dimensional data, to the requirements of Paragraph 4.4.9.

4.1.2.4 Fuel Plate Uranium Data

Individual Fuel Plate uranium data as required to be reported by Paragraph 5.1.3.

4.1.2.5 Fuel Element Uranium Data

Individual Fuel Element uranium data as required to be reported by Paragraph 5.1.4.

4.1.2.6 Fuel Plate and Element Radiation Counts

Radiation count from each Fuel Plate and Fuel Element exterior, as required to be reported by Paragraph 5.1.5.

4.1.2.7 Pull Test Results

Results of pull tests as required to be reported by Paragraph 5.1.6.

4.1.2.8 Plate Radiographs

Plate radiographs to the requirements of Paragraphs 4.4.3 and 4.4.4.

4.1.2.9 Plate Section Photomicrographs

Plate section photomicrographs to the requirements of Paragraph 4.4.7.

4.1.2.10 Visual Inspection Reports and Data

Visual inspection reports and data to the requirements of Paragraph 4.4.6.

4.1.3 Distribution of Reports (as applicable)

Three (3) copies of the following reports are required by this Specification:

4.1.3.1 Reports

Up to three (3) interim reports detailing program progress against a previously submitted schedule shall be supplied by the Contractor to the Laboratory approximately bimonthly.

4.1.3.2 Failure Notification

During production, complete records shall be kept by the Contractor. In the event of a failure, the time, nature, description, corrective action taken, and proposed further corrective action shall be reported to the Laboratory within five (5) working days after such failure.

4.1.3.3 Requalification Records

The results and data from any requalification work, as required by Paragraph 4.3.4.

4.2 Manufacturing Procedures

All programs, processes, and procedures, and all changes and modifications thereto, to be used to Manufacture the product shall be submitted to the Laboratory prior to use for review and approval. These shall include:

4.2.1 Materials Specifications

Contractor's specifications for all materials listed in Section 3.4 and in the Appendix, item 7.6 (Materials).

4.2.2 Identification of Sub-tier Suppliers

This listing to include the addresses of all Sub-tier Suppliers.

4.2.3 Manufacturing Procedures

All fabrication, assembly, cleaning, surface treatment, handling and demonstration procedures.

4.2.3.1 The Fuel Plate fabrication procedure must include the provision that the Fuel Plates will be first hot-rolled, then cold-rolled. The final reduction of the Fuel Plate thickness shall be accomplished by cold-rolling. The final reduction shall be approximately 20 percent followed by annealing if required. Blister and ultrasonic testing of the Fuel Plate in accordance with Paragraph 4.4.5 may either precede or follow the cold-rolling step.

4.2.4 QA-QC Procedures

All test, inspection, production, and Quality Control procedures, including all non-destructive tests, and all standards and sample sectioning drawings.

4.2.5 In Process Controls Procedure

The In-Process Controls, sampling programs, and procedures.

4.2.6 Production Sampling Procedures

The Production-Quality-Control sampling program and procedures.

4.2.7 Repair Procedures

All repair programs and procedures.

4.2.8 Final Inspection Procedures

All final inspection, washing, packaging, storage, and shipping procedures.

4.3 Quality Assurance - Fuel Plate and Fuel Element

4.3.1 Plate Fabrication Qualification

Plate fabrication Qualification shall be based upon production by the Contractor of a minimum of two (2) Lots of Fuel Plates, using uranium of the specified enrichment in the form of UAl_x for the cores. All acceptable Fuel Plates may be used in Fuel Elements with the Laboratory's approval. Three (3) copies of records for the testing, inspection, and Qualification for the following items shall be submitted to the Laboratory, and the Laboratory's approval shall be obtained, prior to beginning Fuel Plate Production.

4.3.1.1 Uranium Distribution

Punchings from a minimum of one (1) randomly selected Fuel Plate per Lot during Qualification, shall be taken, and each punching shall be chemically analyzed for uranium to the requirements of Paragraph 3.2.2.

The number and location of the punchings from the Fuel Plate shall be fixed in the inspection scheme.

4.3.1.2 Uranium Content

A minimum of one (1) randomly selected Fuel Core per Lot during Qualification shall be destructively assayed for uranium to the requirements of Paragraph 3.2.1.

4.3.1.3 Clad-Core-Clad Dimensions

A minimum of one (1) randomly selected Fuel Plate per Lot during Qualification shall be used to make sections, and these sections evaluated to the requirements of the applicable drawings.

The number and location of the sections shall be fixed in the inspection scheme.

4.3.1.4 Internal Defects and Bond Integrity

All Fuel Plates produced for Qualification shall be evaluated to the requirements of Paragraph 3.2.4 by ultrasonic and blister testing of each Fuel Plate. Any indication of non-bond, voids, blisters, lamination, or other discontinuities in excess of 3 mm in any dimension, shall place the item in Failure. In addition, a bending test shall be made.

4.3.1.5 Core Configuration

All Fuel Plates produced for Qualification shall be evaluated to the requirements of Paragraph 3.2.3 by the procedure of Paragraph 4.4.4.

4.3.1.6 Surface Finish and Defects

All Fuel Plates produced for Qualification shall be evaluated to the requirements of Paragraph 3.2.5 by the procedure of Paragraph 4.4.6.

4.3.1.7 Cleanliness and Surface Contamination (Fuel)

All Fuel Plates produced for Qualification shall be evaluated to the requirements of Paragraph 3.2.6 by the procedure of Paragraph 4.4.8.

4.3.2 Element Fabrication Qualification

Element fabrication qualification shall be based upon the production of the test pieces listed below. Three (3) copies of records for the testing, inspection, and qualification for the following items shall be submitted to the Laboratory, and the Laboratory's approval shall be obtained, prior to beginning Fuel Element Production.

4.3.2.1 Mechanical Integrity

The Contractor shall assemble three (3) 60 mm long dummy sections of a Fuel Element. Each section shall be evaluated to the requirements of the procedure of Paragraph 4.4.10.

4.3.2.2 Dimensional

The Contractor shall fabricate a Dummy Fuel Element which shall be evaluated to the dimensional requirements of the drawings listed in Paragraph 2.1.4 of this Specification. The Dummy Fuel Element shall be shipped to the User for insertion tests in the reactor core. The Laboratory shall not authorize Production prior to completion of insertion tests by the User.

4.3.3 In-Process Controls

The Contractor shall establish a process control program whereby checks are made on Manufacturing processes, operational procedures, intermediate product characteristics, and equipment to demonstrate that process stability during Production is at least equal to that demonstrated during Qualification. These In-Process Controls shall include, but not necessarily be limited to, the following:

4.3.3.1 Evaluation of Fuel Plates with regard to the requirements of Paragraphs 3.2.2, 3.2.3, 3.2.5 and 3.2.6 by the procedures of Paragraphs 4.4.3, 4.4.4, 4.4.6 and 4.4.8, respectively.

4.3.3.2 Fabrication of 60 mm test specimens, using unfueled simulated plate sections, to the requirements of Paragraph 3.3.4, and pull tests by the procedures of Paragraph 4.4.10. Swaging of test specimens will be interspersed in the normal production process without previous adjustment of the operation. The extent of inspection shall be fixed in the inspection scheme.

4.3.4 Requalification

Unless otherwise approved by the Laboratory, Requalification shall be limited to swaging. Process Requalification shall meet the same requirements as the original Qualification. All Requalification work shall meet all the requirements of this Specification unless specifically exempted by the Laboratory. The Contractor shall notify the Laboratory of any intended Requalification work, and shall submit three (3) copies of the results and data therefrom. Production may be resumed when the Contractor has met all of the requirements of this section and received written approval from the Laboratory.

4.4 Test and Inspection Requirements

The following tests and inspections shall be performed by the Contractor to assure that the product quality is in accordance with the requirements of this Specification:

4.4.1 Materials

A "Certification of Chemical Analysis" or a certified Mill Test Report shall be supplied to the Laboratory for each lot of material used in the fabrication of Fuel Elements to establish compliance with the requirements of Paragraph 3.4.1. This certificate shall give the actual results of the chemical analysis for the material. The certification shall state the analytical method used in making the determinations for each chemical element or

compound reported and shall give the precision and accuracy of the method used. All materials shall be traceable to the Fuel Elements fabricated from these materials.

4.4.2 Fuel Loading

The requirements of Paragraph 3.2.1 for fuel loading shall be established in accordance with Paragraph 4.1.1.3 by the Contractor subject to the approval of the Laboratory.

4.4.3 Homogeneity

The requirements of Paragraph 3.2.2 on the homogeneity of the plates shall be met.

4.4.4 Fuel Core Configuration

Compliance with the Fuel Core Configuration requirements of Paragraph 3.2.3 shall be by visual inspection (X-ray filming and fluoroscopic examination). The extent of inspection shall be fixed in the inspection scheme. Visual radiograph inspections shall be performed without magnification on a light table.

4.4.5 Bond Integrity

Compliance with internal defects and bond integrity requirements of Paragraph 3.2.4 shall be established by ultrasonic examination of one (1) randomly chosen Fuel Plate per Production Lot and by performing a blister test on all Fuel Plates. The blister test shall be performed either before or after cold-rolling, by heating each plate to a temperature between 424°C and 546°C, holding at that temperature for a period of one hour. Any Fuel Plate exhibiting blisters or non-bonds exceeding 3 mm in any dimension shall be rejected. In addition, a bending test shall be made.

4.4.6 Surface Conditions and Defects

Compliance with surface conditions and defect requirements of Paragraph 3.2.5 and Paragraph 3.2.6 shall be established by visual inspection without magnification of the Fuel Plates and Elements. The extent of inspection shall be fixed in the inspection scheme.

4.4.7 Clad-Core-Clad Dimension

Compliance with the requirements of the applicable drawings with regard to clad-core-clad dimensions shall be established by Qualification and by examination of randomly selected Fuel Plates, which may have been rejected for reasons which do not affect clad and core dimensions. The Fuel Plate shall be sectioned, mounted for metallographic examination, polished and etched, and evaluated to the requirements of the applicable drawings. Photomicrographs shall be made of each section. The extent of inspection shall be fixed in the inspection scheme. Should failure occur, three (3) additional Fuel Plates shall be randomly selected from the 100 Fuel Plates last produced and examined in the same manner. Should failure occur in any of these samples, all 100 Fuel Plates shall be rejected.

4.4.8 Cleanliness

Fuel Plate and Element cleanliness requirements of Paragraph 3.2.6 and Paragraph 3.3.3 shall be established by visual inspection of

the Fuel Plates and Elements and by In-Process Controls. The surfaces of the Fuel Plates and the completed Fuel Elements shall be counted for radioactive contamination. The surface contamination shall be less than 54 micrograms uranium per square meter. The extent of inspection shall be fixed in the inspection scheme.

4.4.9 Dimensional Inspection

Compliance with all external dimensions of the Fuel Plates, the gap dimension of all coolant flow channels as measured in center section, and external dimensions of the Fuel Element shall be by inspection. All dimensions of this Specification shall apply at a temperature of $21^{\circ}\text{C} \pm 2.8^{\circ}\text{C}$. In addition, the fuel element assembly shall be tested for external dimensional adherence and for endfitting dimensions by use of two (2) functional fit gauges furnished by the User, to assure compatibility with the User's reactor core components. The extent of inspection shall be fixed in the inspection scheme.

4.4.10 Mechanical Integrity

Mechanical integrity shall be established by the Contractor by performing "pull tests" on the specimens required by Sub-paragraph 4.3.3.2. "Roll-swaged" joints between the Fuel Plates and side plates shall be able to withstand a load of not less than 27 N/mm of side plate joint. The extent of inspection shall be fixed in the inspection scheme.

4.5 Calibration Requirements

All Contractor's measuring and test equipment used for acceptance of materials or components to the requirements of this Specification shall meet Laboratory requirement A0001-0114-SA.

4.6 Nonconforming Items

The Contractor shall control nonconforming items per the requirements of Laboratory Procedure AQR-001.

5.0 PREPARATION FOR DELIVERY

5.1 Records

One (1) copy (except as noted) of the following data and records shall accompany the shipments:

- 5.1.1 Certification of product compliance to the requirements of this Specification including any test data pertaining thereto not specifically listed in Paragraphs 5.1.2 through 5.1.10.
- 5.1.2 Dimensional data as required by Paragraph 4.4.9.
- 5.1.3 Individual Fuel Plate uranium data including:
 - 5.1.3.1 Contractor's core compact data sheets
 - 5.1.3.2 Serial number with batch identification
 - 5.1.3.3 Uranium content

- 5.1.3.4 Fuel Plate core weight
- 5.1.3.5 U-235 enrichment
- 5.1.3.6 Total U-235 content
- 5.1.4 Individual Fuel Element uranium data including:
 - 5.1.4.1 Serial number of the Fuel Element
 - 5.1.4.2 Uranium content
 - 5.1.4.3 U-235 content
 - 5.1.4.4 Serial number of each Fuel Plate in the Fuel Element.
- 5.1.5 Radiation count from Fuel Plate and Fuel Element exterior, as required by Paragraph 4.4.8. The counting period, counter, background, efficiency, and type of counter used shall be reported.
- 5.1.6 Results of pull tests specified in Paragraph 4.4.10.
- 5.1.7 List of all applicable waivers and deviations for related Fuel Plates or Fuel Elements.
- 5.1.8 Radiographs as specified in Paragraphs 4.4.3 and 4.4.4.
- 5.1.9 Photomicrographs as specified in Paragraph 4.4.7.
- 5.1.10 Visual inspection reports and data as specified in Paragraph 4.4.6.
- 5.2 Packaging and Shipping
 - 5.2.1 The Contractor shall provide suitable shipping boxes for the Fuel Elements, in accordance with all U.S. Regulations.
 - 5.2.2 The Contractor shall load the Fuel Elements into the shipping boxes in sealed polyethylene bags in a clean dry condition, free from extraneous materials. The polyethylene shall be at least 0.15 mm thick.
 - 5.2.3 The Contractor shall take all necessary precautions during packing to prevent damage to the Fuel Elements during shipment. Each box shall be provided with a tamper-proof seal. Each box shall be loaded and shipping documents shall be prepared in accordance with all applicable regulations.

6.0 NOTES AND SUPPLEMENTAL INFORMATION

6.1 Compliance with Specifications

All materials, workmanship, and procedures shall be subject to inspection, examination, and test by the Laboratory, and to rejection by the Laboratory for non-compliance with the Specifications at any and all times during Manufacture, and at any and all places where such Manufacture is carried on. Final detailed inspection and acceptance or rejection (except for defects due to shipping damage) will be made by the Laboratory at the

Contrator's Plant. The Laboratory shall have the right to reject any one or more of the finished products for defects in workmanship, or defects in any of the materials comprising the finished product which otherwise fail to meet the Specification.

6.2 Deviations from Specifications

Notwithstanding other provisions of these Specifications, the Laboratory may, at its option, when requested in writing, waive certain minor deviations from requirements of the Specifications and drawings where the failure to meet any specific requirement either alone or in combination with other such failures will not, in the opinion of the Laboratory, significantly reduce the efficiency or performance of the assembly. Acceptance of a Fuel Element by the Laboratory with one or more such deviations from the Specifications shall not be construed to mean that the Laboratory approves or will approve similar deviations in Elements not yet delivered under the Contract.

6.3 Fuel Plate Sampling Procedures for Destructive Tests

The sampling procedure shall be fixed in the inspection scheme.

6.4 Distribution of Documents

The Laboratory shall receive three (3) copies of all documents (drawings, specifications, inspection scheme, reports, description, records, certificates, etc.).

6.5 Approval of Documents

The Laboratory shall approve of or comment on all documents (see Section 6.4) within two (2) weeks. The approved documents shall be at the manufacturer at least two (2) weeks before starting production or inspection.

7.0 APPENDIX

7.1 Scope and Specification of Quantities

This appendix specifies the number of Fuel Plates contained in a Standard Fuel Element (N_S), the number of Fuel Plates contained in a Control Fuel Element (N_C), the mass of U-235 contained in a Fuel Plate (M_P), the mass of U-235 contained in a Standard Fuel Element (M_S), and the mass of U-235 contained in a Control Fuel Element (M_C).

7.1.1 N_S : The number of Fuel Plates in a Standard Fuel Element shall be eighteen (18).

7.1.2 N_C : The number of Fuel Plates in a Control Fuel Element shall be nine (9).

7.1.3 M_P : The mass of U-235 contained in a Fuel Plate shall be 9.28 g \pm 2%.

7.1.4 M_S : The mass of U-235 contained in a Standard Fuel Element shall be 167.0 g \pm 2%.

7.1.5 M_C : The mass of U-235 contained in a Control Fuel Element shall be 83.5 g \pm 2%.

7.2 Drawing and Inspection Scheme Numbers for Standard Fuel Element and Control Fuel Element

See table on page 474.

7.3 U-235 Content, Surface Density, and Enrichment

U-235 Content

Standard Element	18 plates
	9.28 g \pm 2% U-235 per plate
	167.0 g \pm 2% U-235 per element
Control Element	9 plates
	9.28 g \pm 2% U-235 per plate
	83.5 g \pm 2% U-235 per element

U-235 Surface Density

Nominal Value	26.7 mg U-235/cm ²
Zone 1 nom. mg U-235/cm ²	\pm 20%
Zone 2 nom. mg U-235/cm ²	\pm 30%
	- 20%
Zone 3 nom. mg U-235/cm ²	\pm 30%
	- 100%

U-235 Enrichment: 19.75 + 0.2 wt%
- 0.5 wt%

7.4 Fuel Plate 19.75% U-235 (scheme)

See figure and table on page 475.

7.5 UAl_x Powder and Al Powder

UAl_x Powder: according to Contractor Specification No. X.

Al Powder: according to Contractor Specification No. X.

7.6 Materials for Standard Fuel Element and Control Fuel Element

See table on page 476.

7.7 List of Revisions

To be listed on final pages of this Appendix.

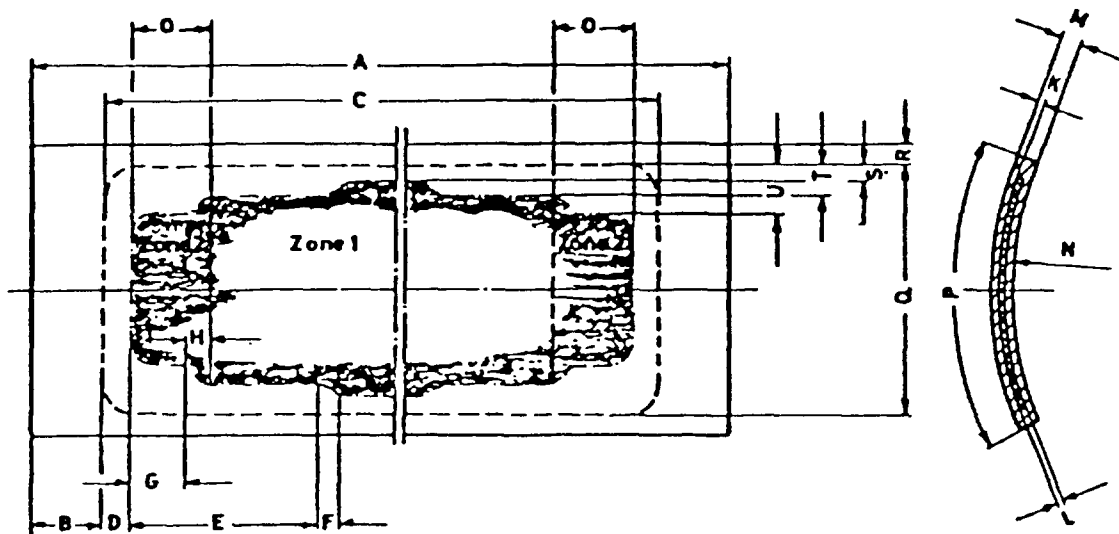
7.2 Drawing and Inspection Scheme Numbers for Standard Fuel Element and Control Fuel Element

<u>Standard Fuel Element (18 Plates)</u>		<u>Control Fuel Element (9 Plates)</u>	
<u>Drawing No.</u>	<u>Name</u>	<u>Drawing No.</u>	<u>Name</u>
X	Fuel Element	X	Fuel Element
X	List of Parts	X	List of Parts
X	Adaptor End	X	Adaptor End
X	Side Plate, Right	X	Side Plate, Right
X	Side Plate, Left	X	Side Plate, Left
X	Outer Fuel Plate	X	Outer Fuel Plate
X	Inner Fuel Plate	X	Inner Fuel Plate
X	Handle	X	Guide Plate
X	Bail Support		
<u>Inspection Scheme No.</u>	<u>Name</u>	<u>Inspection Scheme No.</u>	<u>Name</u>
X	Standard Fuel Element	X	Control Fuel Element

The revision index for the drawing and inspection scheme is shown in the List of Documents in the inspection scheme.

7.4 Fuel Plate 19.75% U-235 (scheme)

18 plates per Standard Element / 9 plates per Control Element



Outer Fuel Plate Drawing No: X

A	727	± 0.2
B	min.	58
C	max.	610
D	max.	19
E	max.	62
F	max.	6.5
G	max.	24
H	max.	6.5
K	min.	0.25
L	Ref.	0.76
M	1.52	± 0.05
N	Ref. R	140*
O	max.	38
P	69.4	± 0.10
Q	max.	63.50
R	min.	3.4
S	max.	4.7
T	max.	10.3
U	max.	15.9

Inner Fuel Plate Drawing No: X

A	625.5	± 0.2
B	min.	8
C	max.	610
D	max.	19
E	max.	62
F	max.	6.5
G	max.	24
H	max.	6.5
K	min.	0.25
L	Ref.	0.76
M	1.52	± 0.05
N	Ref. R	140*
O	max.	38
P	69.4	± 0.10
Q	max.	63.50
R	min.	3.4
S	max.	4.7
T	max.	10.3
U	max.	15.9

*The radius shall be 140 mm in the Fuel Element Assembly

7.6 Materials for Standard Fuel Element and Control Fuel ElementMaterials - Standard Fuel Element (18 plates)

<u>Drawing No.</u>	<u>Name</u>	<u>Material</u>	<u>Material No.</u>	<u>Specification</u>
X	Adaptor End	X	X	X
X	Side Plate, Right	X	X	X
X	Side Plate, Left	X	X	X
X	Outer Fuel Plate			
X	Inner Fuel Plate			
	Fuel Core	X		X
	Frame Sheet	X	X	X
	Cover Sheet	X	X	X
X	Handle	X	X	X
X	Bail Support	X	X	X
	Welding Wire	X	X	

Materials - Control Fuel Element (9 plates)

<u>Drawing No.</u>	<u>Name</u>	<u>Material</u>	<u>Material No.</u>	<u>Specification</u>
X	Adaptor End	X	X	X
X	Side Plate, Right	X	X	X
X	Side Plate, Left	X	X	X
X	Outer Fuel Plate			
X	Inner Fuel Plate			
	Fuel Core	X		X
	Frame Sheet	X	X	X
	Cover Sheet	X	X	X
X	Guide Plate	X	X	X
	Welding Wire	X	X	

Appendix K-2.2

INSPECTION SCHEME

ARGONNE NATIONAL LABORATORY

Argonne, Illinois

FORD NUCLEAR REACTOR/UNIVERSITY OF MICHIGAN

Ann Arbor, Michigan

United States of America

Abstract

As part of the U.S. RERTR Program, a full-core demonstration with LEU fuel began in December 1981 in the Ford Nuclear Reactor (FNR) at the University of Michigan. The LEU standard and control fuel elements were manufactured by CERCA and by NUKEM.

The inspection scheme for standard fuel elements that was agreed to with NUKEM is presented here as an illustration only. A similar inspection scheme was agreed to with CERCA. In this example, all document numbers, drawing numbers, and form numbers have been deleted or replaced with a generic identification.

INSPECTION SCHEME - SUMMARY

Specification

XXX

Drawings

XXX1 Standard Fuel Element
XXX2 Parts List
XXX3 End Adapter
XXX4 Side Plate, right
XXX5 Side Plate, left
XXX6 Outer Fuel Plate
XXX7 Inner Fuel Plate
XXX8 Handle
XXX9 Support Plate
XXX10 Roll Swagging Drawing

Note: The documents of work cited herein do not indicate the revision status. This status is given on the sheet "List of Documents."

Fuel enrichment with U-235	19.75 ± 0.2 $- 0.5$ wt.%
Number of plates in the fuel element	16 inner plates 2 outer plates
U-235 content per plate	$9.28 \text{ g} \pm 2\%$

U-235 content per fuel
element

167.0 g \pm 2%

Surface density of U-235

Nominal value of 26.7 mg U-235/cm²

Zone 1 nom. mg. U-235/cm² \pm 20%

Zone 2 nom. mg U-235/cm² $\begin{matrix} + 30\% \\ - 20\% \end{matrix}$

Zone 3 nom. mg U-235/cm² $\begin{matrix} + 30\% \\ - 100\% \end{matrix}$

Tests:

1. End adapter according to Test Sheet No. 1
2. Side plate according to Test Sheet No. 2
3. Fuel core according to Test Sheet No. 3
 - 3.1. UAl_x-powder according to Inspection Certificate Form A
4. Inner fuel plate according to Test Sheet No. 4
5. Outer fuel plate according to Test Sheet No. 5
 - 5.1 Sections according to Inspection Certificate Form B
 - 5.2 Contamination inspection according to Inspection Certificate Form C
 - 5.3 Plate Acceptance Record Form D
6. Fuel box
 - 6.1 The roll swagging stability side plate/fuel plate shall be examined by test specimens before starting roll swagging operations and after having finished ten (10) fuel boxes in each case (Pull Test Specimen Form E).
 - 6.2 Plate distance and dimension "x" shall be examined before assembly of the end adapter (Inspection Certificate Form F).
7. Fuel element test according to Inspection Certificate Form F
 - 7.1 Identification Form
 - 7.2 Contamination inspection

Acceptance records and Inspection Certificates according to DIN 50049 (3 each)
for:

- Certification that the fuel elements were manufactured and examined according to specification.
- Dimensional inspection of the fuel element (Form F).
- Fuel weight and fuel enrichment level (Form G).
- Pull tests of roll swagging specimens (Form H).
- U contamination inspection of the fuel plates and elements (Form C).
- X-ray films of the fuel plates (one copy).

- Testing of cladding and core thickness of fuel plates (Form B).
- Records on x-ray absorption inspection (check for homogeneity) of the fuel plates (one copy).
- Surface treatment of the fuel plates.
- Al powder used in the UAl_x -Al mixture.
- UAl_x powder used in the UAl_x -Al mixture.
- U metal used in the UAl_x .
- Semifinished products according to the parts list.
- Acceptance Record Sheet (Form I).

Test Equipment:

End Adapter Gauge (Form J)
 Calibration Steps (Form K)
 FNR Gauge 1
 FNR Gauge 4
 End Adapter Gauge (Form L)
 Measurement Bridge (Form M)

IDENTIFICATION FORM

Order No:

Contractor Order No:

Description:

.....

.....

The elements to be manufactured according to the
description above shall be identified as follows:

Element type:

Numbered from to

Element type:

Numbered from to

Element type:

Numbered from to

RANDOM SAMPLE PROCEDURE (RSP)

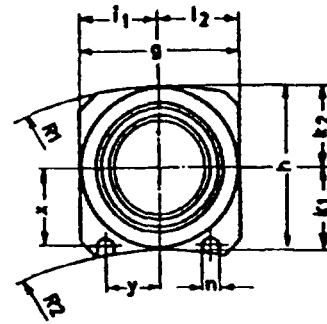
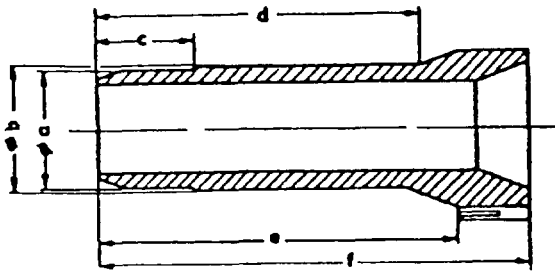
N	n	a	r
0 - 30	5	0	1
31 - 60	10	0	1
61 - 90	15	0	1
91 - 120	20	0	1

If the number of defective items found in a random sample of n items equals a , the related lot of N items shall be considered as good and shall be accepted. If the number of defective items found is equal to or greater than r , the entire lot of N items shall be examined.

N: lot size
n: random sample size
a: acceptance number
r: rejection number

TEST SHEET NO. 1, END ADAPTER

Drawing No. XXX3 Rev.

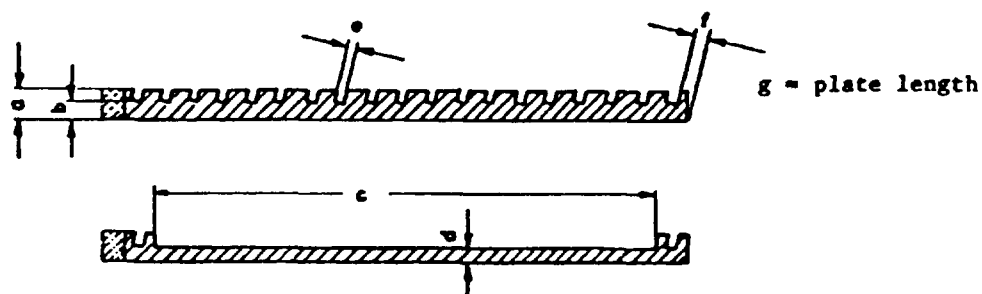


Dim.	Nominal, mm	Testing Equipment/ Test Specification	Testing Process	Test Sample Size, %	Tested By QC* P*
			Check all dimensions according to drawing	RSP	x
a	60 ± 0.25	micrometer	Measure diameter "a"	100	x
b	61 + 0.2 - 0.5	micrometer	Measure diameter "b"	100	x
c	30.5 ± 0.3	depth gauge	Measure dimension "c"	100	x
d	127 ± 0.5	depth gauge	Measure dimension "d"	100	x
e	146 ± 0.2	depth gauge	Measure dimension "e"	100	x
f	171 ± 0.3	depth gauge	Measure dimension "f"	100	x
g	69.84 - 0.1	micrometer	Measure dimension "g"	100	x
h	73.9 - 0.1	dial indicator	Measure dimension "h"	100	x
i1/i2	34.92 - 0.05	prism dial indicator	Measure dimension "i"	100	x
k1/k2	36.95 - 0.05	prism dial indicator	Measure dimension "k"	100	x
n	6.5 + 0.1	fitting piece 6.5 mm diameter	Check 2 arresting holes	100	x
x	34.04 ± 0.05	fitting gauge	Check position of the		
y	23.4 ± 0.05	(Form J)	two arresting holes	100	x
R1	R 140	radius gauge R 140 (concave)	Check radii visually	RSP	x
R2	R 140	radius gauge R 140 (convex)			
		visual	Check the surface for design according to drawing	100	x

*Tested by QC (QC), Production (P)

TEST SHEET NO. 2, STANDARD FUEL ELEMENT SIDE PLATE

Drawing No. XXX4 (Right) Rev.
XXX5 (Left)

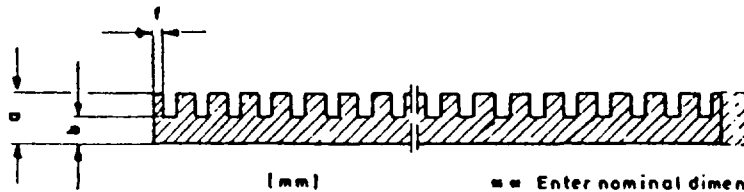


Dim.	Nominal, mm	Testing Equipment/ Test Specification	Testing Process	Test Sample Size, %	Tested By	
					QC*	P*
			Check all dimensions according to drawing.	RSP	x	
a	4.75 ± 0.1	micrometer	Measure thickness "a"+	100	x	
b	2.6 - 0.1	dial indicator measuring pin"J"	Measure dimension "b" (front, middle, back)+	RSP	x	
c	70 + 0.5	slide gauge	Measure dimension "c"	RSP	x	
d	2.4 - 0.5	micrometer	Measure dimension "d"	RSP	x	
e	1.65 + 0.05	measuring gauge of 1.65 mm	Check groove width "e"	RSP	x	
f	2.23 ± 0.2	device	Measure dimension "f"+ (front, middle, back)	RSP	x	
g	727 ± 0.2	slide gauge	Measure length "g"	RSP	x	
	max. 0.1	measuring plate sensor gauge	Establish maximum deflection on edge.+	100	x	

*Tested by QC (QC), Production (P)

+Record results on Record Form N.

RECORD FORM N, SIDE PLATES FOR MTR FUEL ELEMENTS



Order No:

Drawing No: Test Report No:

Identification:

Test Sheet No:

No.	a*	b	f	Length	Bow*	Surface	Compiled by the Workshop

*100% testing and recording

1 copy to the workshop

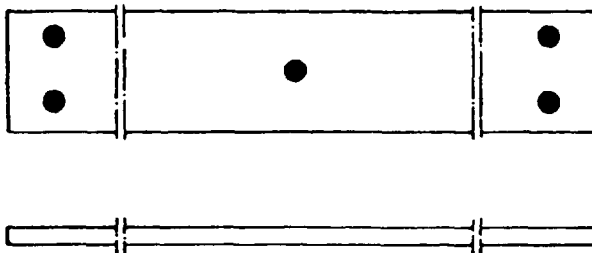
**Enter nominal dimensions (mm) according to drawing.

Inspector:

Date:

TEST SHEET NO. 3, FUEL CORE FOR FUEL PLATES

Drawing No: XXX6 Rev.
 XXX7



Dim.	Nominal, mm	Testing Equipment/ Test Specification	Testing Process	Test Sample Size, %	Tested By QC* P*
		balance analysis Doc. YYY	The U-235 content is determined by weighing each fuel core and multiplying this value by the analyzed value of the U and U-235 content.	100	x
		<u>Alternative:</u>			
		double counting apparatus Doc. YYY	Determine the U-235 content by measuring the 185 keV characteristic radiation.**	100	x
	see operational data sheet	micrometer	Measure thickness at 5 points (see sketch) and record mean value.	20	x
		x-ray film	Check for homogeneity and possible inclusions.	100	x
			Record fuel core No., fuel core weight, U content, and U-235 content (Form P).	100	x
		analysis	During qualification, an analysis of U and U-235 content of one fuel core per lot shall be made.		
			Two (2) samples of 1 gram each from the UAl _x powder intended for production of the fuel cores shall be obtained and kept.		

*Tested by QC (QC) Production (P)

**The possible application of this procedure for the enrichment level of 19.75% U-235 is still to be tested.

RECORD FORM P, FUEL CORE FOR FUEL PLATES

Key word: Order No: Enrichment of U-235%

batch No: UAl_x -Cermet ☐ U_3O_8 -Cermet ☐

No.	Core No.	Weight,g	U,g	U-235,g	Thickness*,mm	Plate No.	Element No.	Remarks
1								
2								
3								
4								
5								
6								
7								
8								
9								
10								
11								
12								
13								
14								
15								
16								
17								
18								
19								
20								
21								
22								
23								
24								
25								
26								
27								
28								
29								
30								

Corrections: Distribution:

Inspector:

.....

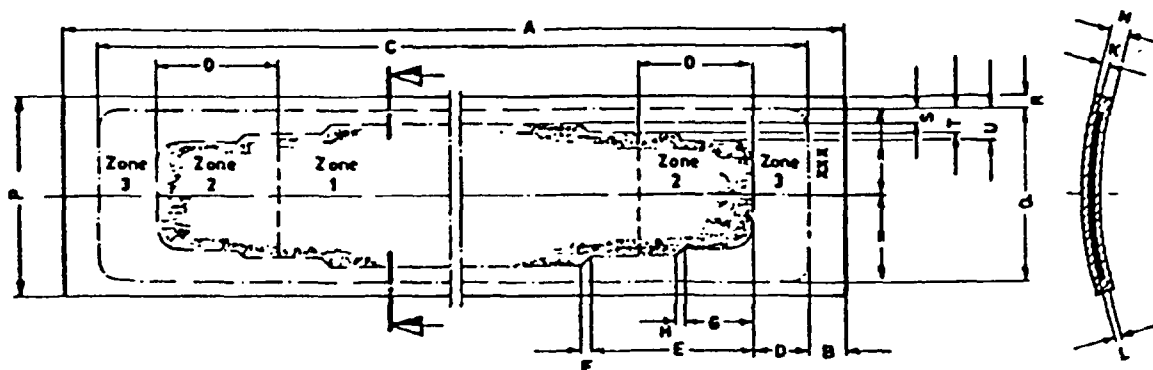
Date:

.....

.....

*Median of 5 tests

TEST SHEET NO. 4, INNER FUEL PLATE



Dim.	Nominal, mm	Testing Equipment/ Test Specification	Testing Process	Test Sample Size, %	Tested By	
					QC*	P*
<u>plate not bent:</u>						
	no blisters	anneal 1h at 424 - 546 °C DOC. YYY	visual inspection for bond defects (metallurgi- cal) after annealing	100		x
		x-ray screen and mask	radiograph and center	100		x
	Zone 1 ± 20%	x-ray unit calibration steps Form K	inspection of U distribu- tion by means of x-ray absorption	RSP		x
	Zone 2 + 30% - 20%		In this phase of qualifi- cation, one plate is sectioned and chemically analyzed. Sampling see Form Q (Appendix 1).			
	Zone 3 + 30% -100%					
	bond defects ≤3 mm diameter	US unit DOC. YYY	Check for perfect bond (metallurgical) between fuel and cladding material.	RSP		x
			during the qualification process	100		x
B	min. 8	x-ray film and	dimensional inspection			
R	min. 3.4	mask	of inner geometry	RSP		x
D	max. 19	Form R				
E	max. 62	DOC. YYY				
F	max. 6.5					
G	max. 24					
H	max. 6.5					
O	max. 38					
Q	max. 63.5					
U	max. 15.9					
T	max. 10.3					
S	max. 4.7					
C	max. 610					

*Tested by QC (QC), Production (P)

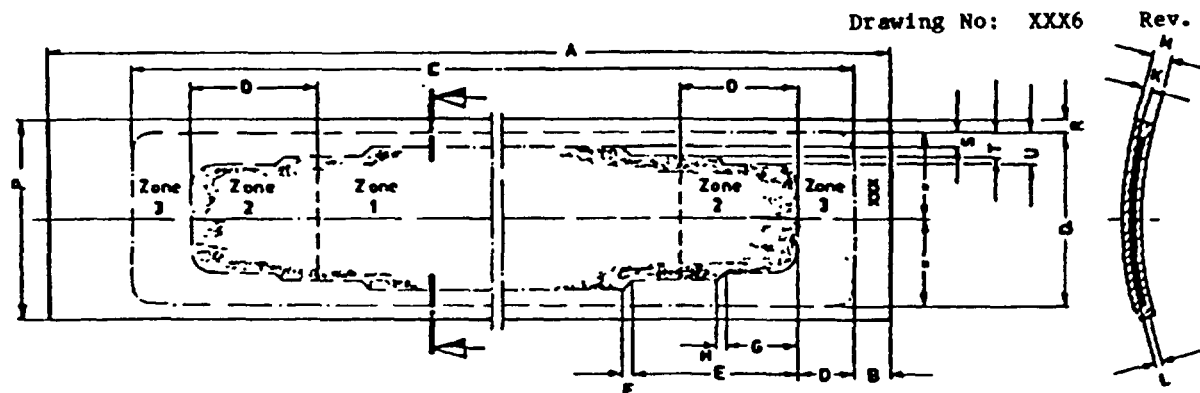
TEST SHEET NO. 4, INNER FUEL PLATE (Cont.)

Drawing No. XXX7 Rev.

Dim.	Nominal, mm	Testing Equipment/ Test Specification	Testing Process	Test Sample Size, %	Tested By	
					QC*	P*
A	625.5 ± 0.2	measuring device DOC. YYY	dimensional inspection of outer geometry	RSP	x	
P	69.4 ± 0.1					
M	1.52 ± 0.05					
K	min. 0.25	microscope	Examine cladding and meat thickness by means of sections.			
L	ref. 0.76		Together with the sec- tions, samples shall be obtained for the photo- micrographs (see Inspec- tion Certificate Form B).			
			Testing scope: during qualification, 1 plate per lot; then	1	x	
	no bond defects	clamping device DOC. YYY	bend test at plate sections	RSP	x	
	<u>plate bent:</u>					
	<5 µg U-235 per 929 cm ²	counting apparatus	contamination inspection One fuel plate per batch (100%, if 5 µm is exceeded).		x	
	allowable damage Zone 2 <0.08 mm other <0.13 mm deep	visual light section microscope DOC. YYY	Surface inspection If necessary, measure surface defects.	100	x	

*Tested by QC (QC), Production (P)

TEST SHEET NO. 5, OUTER FUEL PLATE



Dim.	Nominal, mm	Testing Equipment/ Test Specification	Testing Process	Test Sample Size, %	Tested By QC* P*
<u>plate not bent:</u>					
	no blisters	anneal 1h at 424 - 546 °C DOC. YYY	visual inspection for bond defects (metallurgi- cal) after annealing	100	x
		x-ray screen and mask	radiograph and center	100	x
	Zone 1 ± 20%	x-ray unit calibration steps Form K	inspection of U distribu- tion by means of x-ray absorption	RSP	x
	Zone 2 + 30% - 20%		In this phase of qualifi- cation, one plate is sectioned and chemically analyzed. Sampling see Form Q (Appendix 1).		
	Zone 3 + 30% -100%				
	bond defects ≤3 mm diameter	US unit DOC. YYY	Check for perfect bond (metallurgical) between fuel and cladding material.	RSP	x
			during the qualification process	100	x
B	min. 8	x-ray film and	dimensional inspection of		
R	min. 3.4	mask	inner geometry	RSP	x
D	max. 19	Form R			
E	max. 62	DOC. YYY**			
F	max. 6.5				
G	max. 24				
H	max. 6.5				
O	max. 38				
Q	max. 63.5				
U	max. 15.9				
T	max. 10.3				
S	max. 4.7				
C	max. 610				

**For the prototype fuel element,
these dimensions are tested by means
of a slide gauge.

*Tested by QC (QC), Production (P)

TEST SHEET NO. 5, OUTER FUEL PLATE (Cont.)

Drawing No. XXX6 Rev.

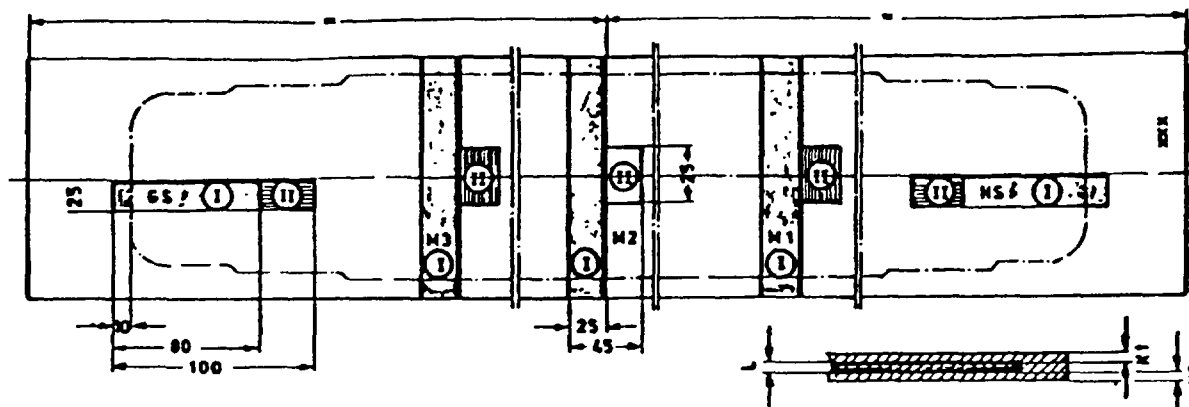
Dim.	Nominal, mm	Testing Equipment/ Test Specification	Testing Process	Test Sample Size, %	Tested By	
					QC*	P*
A	727 ± 0.2	measuring device DOC. YYY	dimensional inspection of outer geometry	RSP	x	
P	69.4 ± 0.1					
M	1.52 ± 0.05					
K	min. 0.25	microscope	Examine cladding and meat thickness by means of sections.			
L	ref. 0.76		Together with the sec- tions, samples shall be obtained for the photo- micrographs (see Inspec- tion Certificate Form B).			
			Testing scope: during qualification, 1 plate per lot; then	1	x	
	no bond defects	clamping device DOC. YYY	bend test at plate sections	RSP	x	
	<u>plate bent:</u>					
	<5 µg U-235 per 929 cm ²	counting apparatus	contamination inspection One fuel plate per batch (100%, if 5 µm is exceeded).			x
	allowable damage Zone 2 <0.08 other <0.13 mm deep	visual light section microscope DOC. YYY	Surface inspection If necessary, measure surface defects.	100	x	

*Tested by QC (QC), Production (P)

INSPECTION CERTIFICATE FORM B, FUEL PLATES

Drawing No: XXX6 (Outer) Rev.
XXX7 (Inner)

Sampling:



Inspection:

1. The plate is to be x-rayed before sampling.
2. The cladding thickness is to be examined along 5 sections (I).
Minimum cladding thickness is 0.25 mm.
Inspection is made by means of microscope.

For NS and GS, a length of at least 19 mm from the edge of the meat is to be examined. In the middle section (M), the total plate width is to be examined.
3. The photomicrographs (200x) of the samples marked II will show the structure of the meat. A general photomicrograph (30x) of cladding and meat thickness shall be made of the same sections.

Results:

(四)

Pos.	Plate No.						
NS	K1						
	K2	min. 0.25					
	L	ref. 0.76					
M1	K1						
	K2	min. 0.25					
	L	ref. 0.76					
M2	K1						
	K2	min. 0.25					
	L	ref. 0.76					
M3	K1						
	K2	min. 0.25					
	L	ref. 0.76					
GS	K1						
	K2	min. 0.25					
	L	ref. 0.76					

INSPECTION CERTIFICATE FORM C, CONTAMINATION TEST

Order No: Key Word: % U-235

Specification: Requirement:

Large surface counter: 810 cm². Calibration plate 7.2 µg U-235 working voltage ... kV

Zero pulses/min Calibration count pulses/min

Type *	Plate No. Element No.	Batch	pulses/min	pulses/min	number side pulses/min	reverse side pulses/min	Result	Date
-----------	--------------------------	-------	------------	------------	------------------------------	-------------------------------	--------	------

Inspector:

Date:

.....
Work Inspector

* I = Inner Plate O = Outer Plate FE = Fuel Element CE = Control Fuel Element

RECORD FORM D, FUEL PLATES FOR FUEL ELEMENTS

Order No: Frame: Enrichment of U-235 %
 Key Word: Material No: Surface:
 Drawing No: Coversheet: Inner plate ☐ Outer plate ☐
 Format: Material No: FE ☐ CE ☐

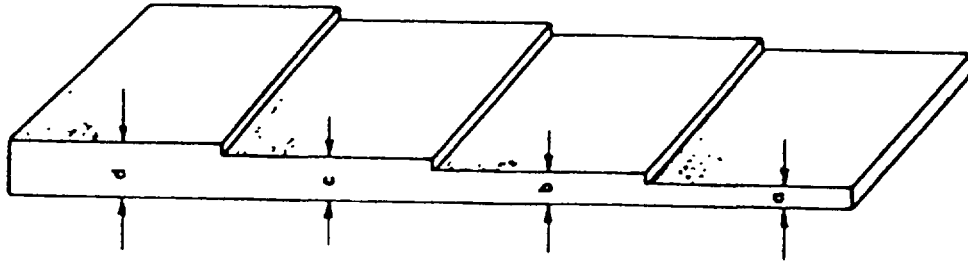
Plate No.	*	Surface defects, µm	Accept	Reject	Plate No.	*	Surface defects, µm	Accept	Reject
_____	—	_____	_____	_____	_____	—	_____	_____	_____

*R = refabricated	from this record, plates	total accepted	total rejected
C = Contamin. tested	accepted: pieces pieces pieces
X = x-rayed	rejected: pieces		
D = dimension			
O = on hand with reservation		
I = inner geometry		Work Inspector	

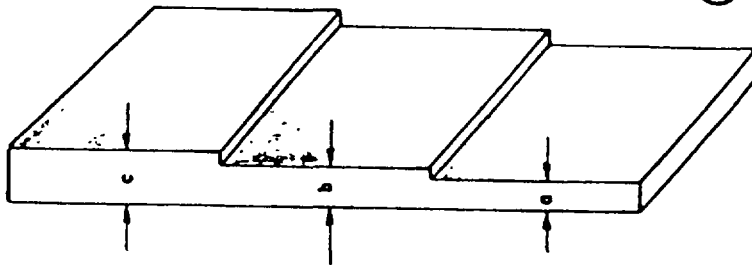
CALIBRATION STEPS (FORM K)

Homogeneity of Fuel Plates

○ four steps

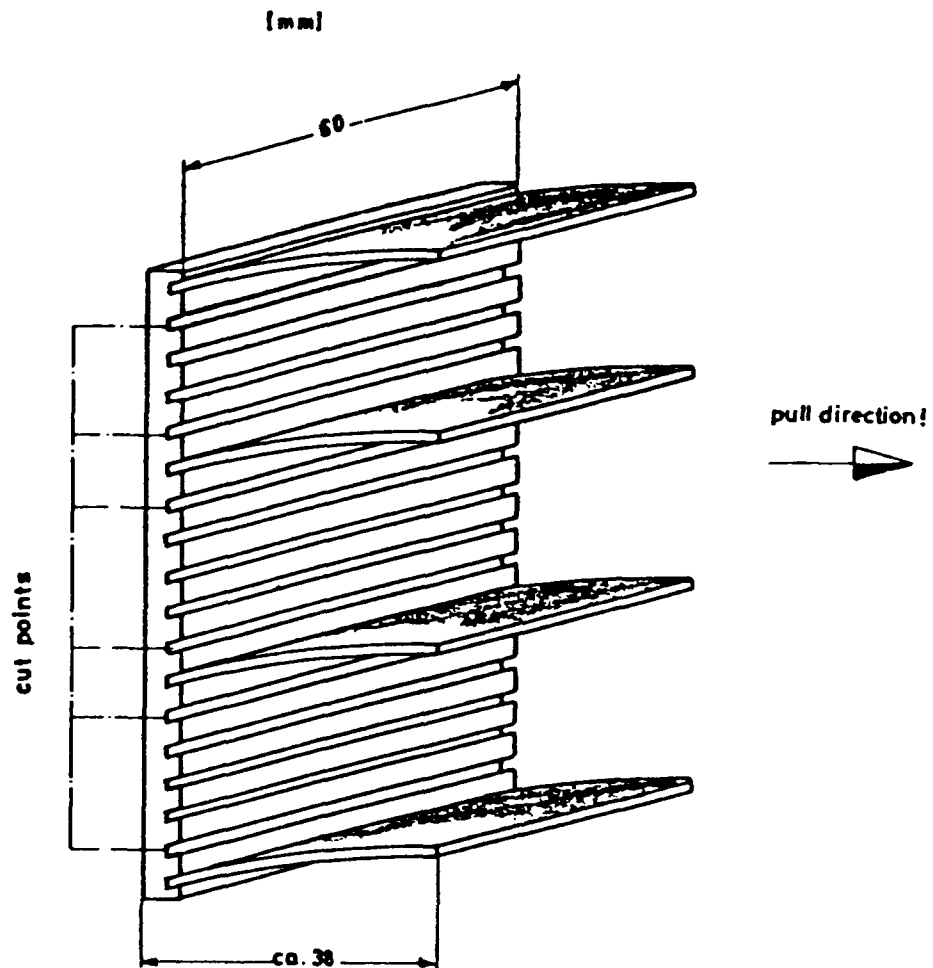


⊗ three steps



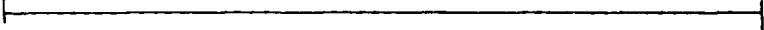
PULL TEST SPECIMEN (FORM E)

Roll Swagging Test on Standard Fuel Elements



INSPECTION CERTIFICATE FORM H, PULL TEST ON ROLL SWAGGING SPECIMEN

6000 Load, N 0



Affix diagram here

Key word/Order No:

Roll swagging specimen No.

.....

Test performed before/
between elements No:

.....

Length of specimen: 60 mm

Load range of test
apparatus: N

Type of apparatus:

.....

Scale of diagram: 1:1

Nominal value: 27 N/mm

Sp. No.	Tear Load, N	Tear Load per mm, N
---------	--------------	---------------------

Inspector:

.....
Work Inspector

INSPECTION CERTIFICATE FORM G, WEIGHTS OF FUEL IN PLATE AND IN ELEMENT

Fuel Element No:

Pos. No.	Plate No.	Core No.	UAl _x Batch No.	U-weight, g	Enrichment, %	U-235 Weight, g
1						
2						
3						
4						
5						
6						
7						
8						
9						
10						
11						
12						
13						
14						
15						
16						
17						
18						
19						
20						
21						
22						
23						

	<u>nominal, g</u>	<u>actual, g</u>	
U-235-weight in fuel-element			fuel element-weight. kg
U-weight in fuel-element	N/A	
average enrichment in fuel-element	N/A		
U-235 weight per plate		N/A	

Date:

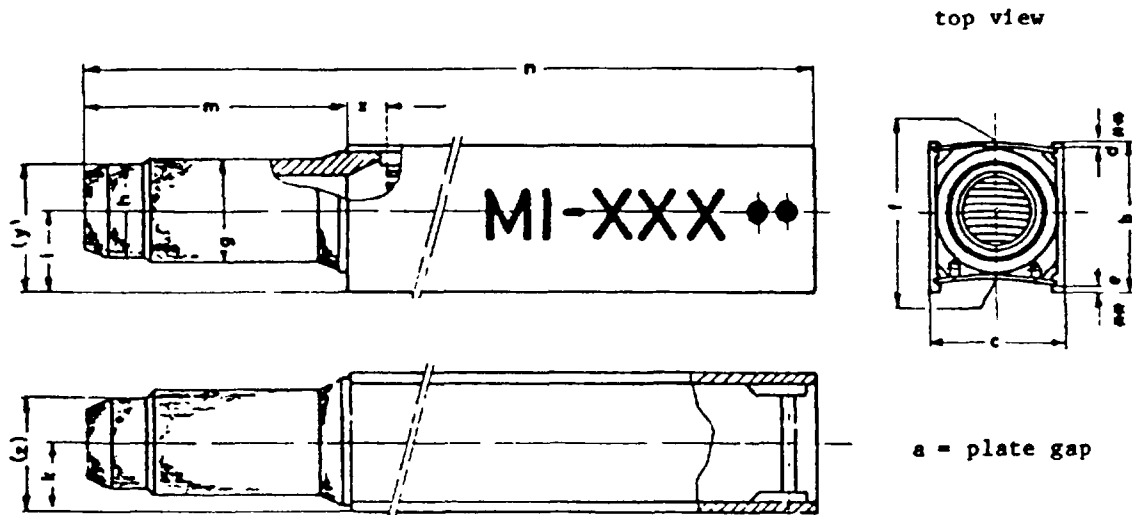
Work Inspector

y

z

INSPECTION CERTIFICATE FORM F, STANDARD FUEL ELEMENT

Ford Fuel Element (18 Plates)



*Measure dimensions "d" and "e" by Dial Gauge on a Measurement Bridge (Form M).

**1. Measure upper flat of element as faces inspector. 2. Turn element 180° and measure again.

Fuel Element No.

Dimension	Nominal, mm	Actual Range, mm	The element is to be free from contamination or damage.
b	79.8 - 80		
c	74.43 - 74.93		
*d	1.16 - 1.36		1
*e	1.37 min.		2
f	76.59 - 77.59		3
g	60.5 - 61.2		4
g	59.75 - 60.25		5
i	43.89 - 44.15		6
**k1	37.22 - 37.47		7
**k2	37.22 - 37.47		8
m	145.5 - 146.5		9
n	872 - 874		10
x	50.65 - 50.95		11
k	Interlocking of end adapter (Form L).		12
			13
			14
	Contamination inspection		15
	of entire surface < 1%		16
			17

Inspector:

Check min. gap with 2.7 mm dia. stainless steel wire before assembling end adapter and handle.

RECORD FORM I, ACCEPTANCE RECORD

Acceptance item: Drawing No: Rev.

Purchaser: pre acceptance ☐ final acceptance ☐

Order No: Specification:

Acceptance inspector:

ACCEPTANCE RESULTS:

On hand: pieces No:

On hand with reservation: pieces No:

Accepted: pieces No:

Accepted with reservation: pieces No:

Rejected: pieces No:

Remarks:

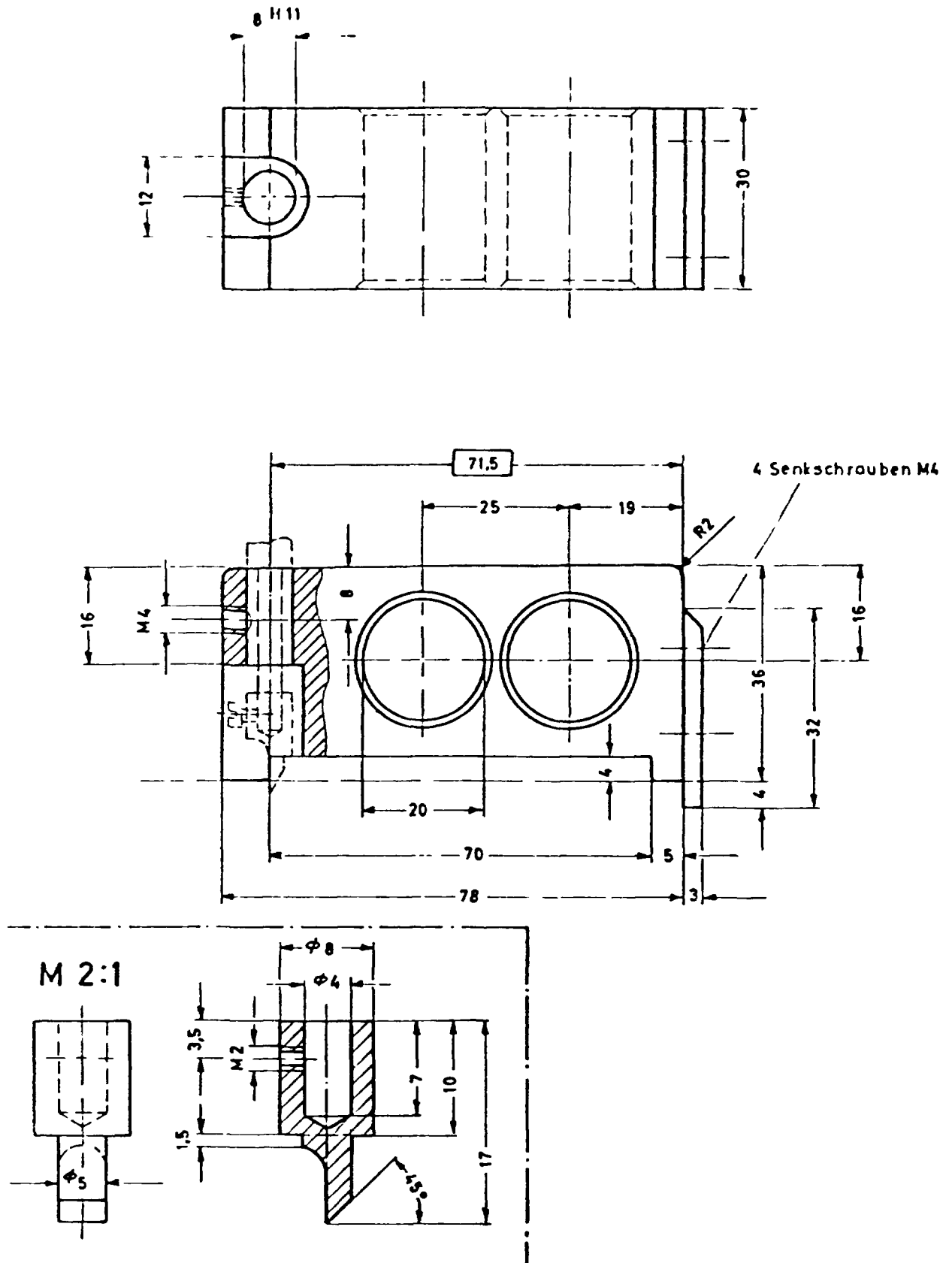
Certificates are to be given to the acceptance inspector.

.....
Acceptance Date

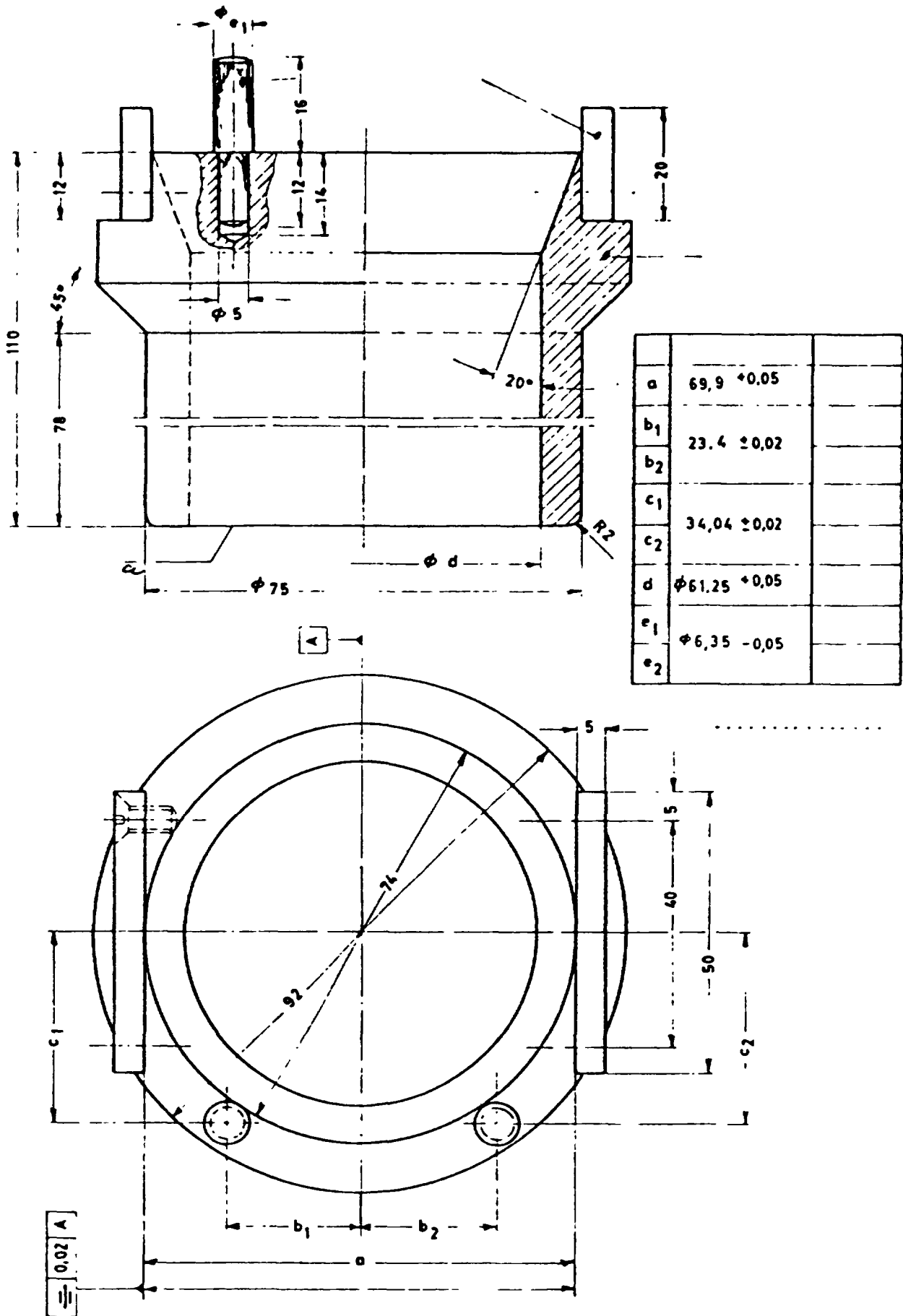
.....
for the Purchaser

.....
Work Inspector

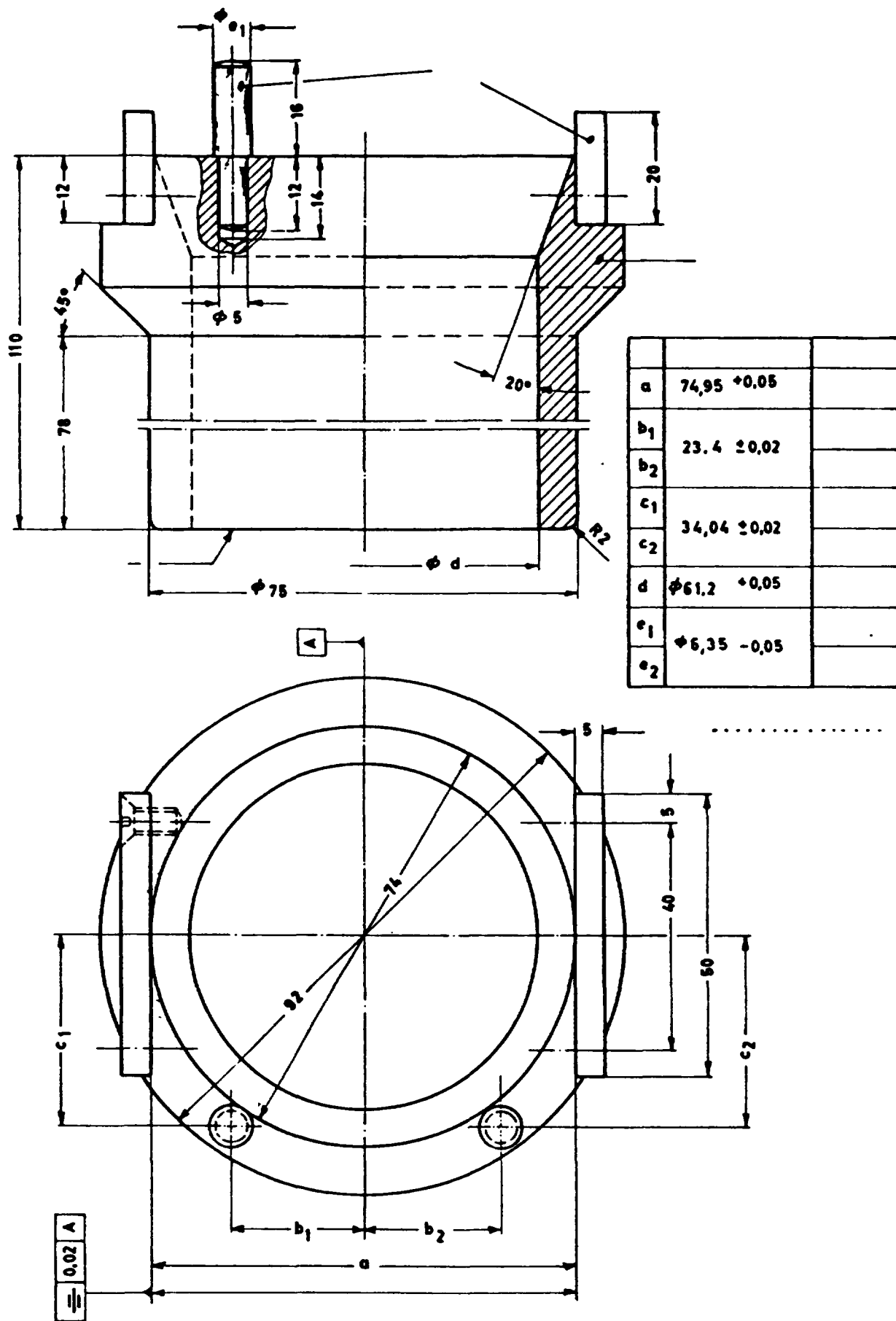
MEASUREMENT BRIDGE (FORM M)



END ADAPTER GAUGE (FORM J)



END ADAPTER GAUGE (FORM L)



LIST OF DOCUMENTS

<u>Contractor No:</u>	<u>Rev.</u>	<u>Document</u>	<u>Purchaser No.</u>	<u>Rev.</u>
Doc. XXX		inspection scheme		
specifications:				
Doc. YYY		specification		
drawings:				
XXX1		standard fuel element		
XXX2		parts list		
XXX3		end adapter		
XXX4		side plate, right		
XXX5		side plate, left		
XXX6		outer fuel plate		
XXX7		inner fuel plate		
XXX8		handle		
XXX9		support plate		
XXX10		roll swagging drawing		

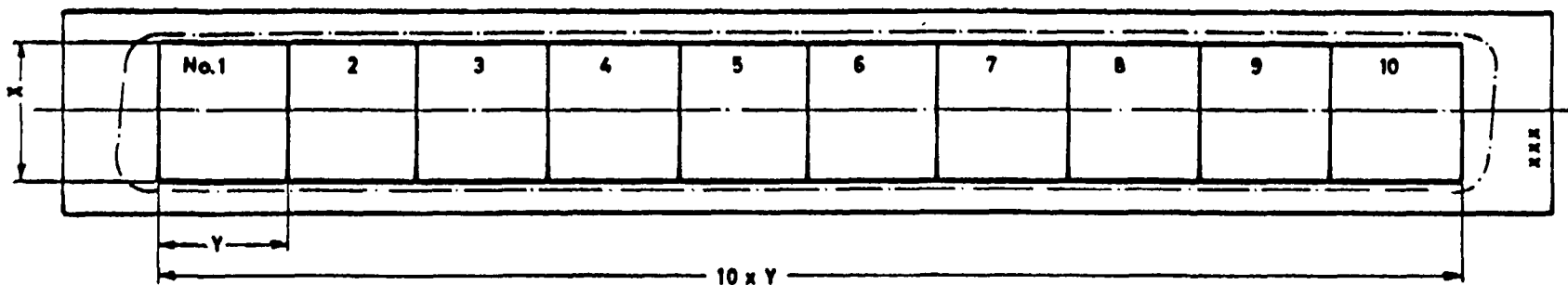
LIST OF REVISIONS

<u>Date</u>	<u>Page</u>	<u>Revision</u>	<u>Approved</u>	<u>Rev.</u>
-------------	-------------	-----------------	-----------------	-------------

Appendix 1

SAMPLING - FORM Q

In the process of qualification, one plate is sectioned and chemically analyzed

[illegible] gU/cm^2 [illegible]

Appendix K-3

FUEL ELEMENTS WITH LEU U_3O_8 -Al FUEL FOR THE DR-3 REACTOR

Appendix K-3.1

SPECIFICATIONS

RISØ NATIONAL LABORATORY
Roskilde, Denmark

Abstract

As part of the Danish RERTR Program, three fuel elements with LEU U_3O_8 -Al fuel and three fuel elements with LEU U_3Si_2 -Al fuel were manufactured by NUKEM for irradiation testing in the DR-3 reactor at the Risoe National Laboratory in Denmark. The specifications for the elements with U_3O_8 -Al fuel are presented here as an illustration only. Specifications for the elements with U_3Si_2 -Al fuel were very similar. In this example, materials, material numbers, documents numbers, and drawing numbers specific to a single fabricator have been deleted.

1.0 GENERAL

1.1 Introduction

This specification describes the production and inspection of the DR-3 fuel element with LEU U_3O_8 -Al fuel.

1.2 Definitions

The fuel element consists of a tubular fuel section, a tubular-unfueled upper section, and an end adapter.

The fuel section consists of four (4) concentrically arranged fuel tubes and an unfueled outer tube. The tubes are fixed at each end with four (4) spacers.

Each fuel tube consists of three (3) fuel plates with aluminum cladding; the plates are connected to each other along longitudinally welded seams.

The upper section of the fuel element contains an emergency cooling spray mechanism and a thermocouple protection tube. A perforated zone (approximately 120 mm in circumference) is located immediately above the fuel section, for the discharge of water.

1.3 Description of the Production Process

1.3.1 Production of the U₃O₈-Al Fuel Core

To guarantee that the U-235 content required for the fuel core is in a homogenous distribution, the U₃O₈ fuel powder and aluminum powder shall be weighed and mixed in portions corresponding to the desired fuel core composition. This composition shall then be cold pressed to form the fuel core.

1.3.2 Production of the Fuel Plates

The fuel plates shall be produced according to the "picture frame technique." In this technique, the fuel core is hermetically enclosed on all sides by the cladding material that is applied by roll bonding. The cladding process is carried out in several steps at temperatures that ensure a perfect metallurgical bond between the fuel and the cladding material. The fuel zone is then calibrated to the required geometry by final cold rolling.

1.3.3 Production of the Fuel Tubes

After bending, three (3) fuel plates of the same width and with the same U content shall be welded together, to form each fuel tube. The fuel tube has uranium-free zones along each of the three longitudinally welded seams.

1.3.4 Production of the Fuel Elements

The individual fuel tubes shall be assembled by mechanical means to form the fuel section. Specifically, the tubes will be pushed into the slots in upper and lower combs, and will be held in these slots by pins or by squeezing the comb material against them. The fuel tube assembly will then be inserted in the unfueled-outer tube and fastened in place by welding the combs to the outer tube. Finally, the upper section and the end adapter are to be welded to the fuel section to complete the fuel element.

2.0 PRODUCT SPECIFICATIONS

2.1 Drawings

The drawings listed in the Appendix are part of this Specification.

2.2 Materials

2.2.1 U₃O₈ Powder

The specifications for the U₃O₈ powder are given in the Appendix.

2.2.2 Al Powder

The specifications for the Al powder are given in the Appendix.

2.2.3 Assembly Parts

The materials for the assembly parts are listed in the Appendix.

2.2.4 Other Materials

Other materials are listed in the Appendix.

2.3 Surface Treatment and Handling

Proper handling and storage shall be ensured through suitable measures. Procedures for surface treatment are listed in the Appendix.

3.0 IDENTIFICATION

3.1 Fuel Core

Each fuel core shall be marked with an identification number.

3.2 Fuel Plate

Each fuel plate shall be marked with an identification number.

3.3 Fuel Tube

After welding, each fuel tube shall be numbered.

3.4 Fuel Element

The fuel element number shall be engraved into the fuel element. Details are given by the corresponding element designation. The numbering shall be provided by the Purchaser.

4.0 QUALITY INSPECTIONS

All quality inspections shall be carried out according to the Inspection Scheme, which is part of this Specification.

4.1 Fuel Core

4.1.1 Analysis of Starting Material

- U_3O_8 powder
- Aluminum powder

4.1.2 Determining U-235 Content

4.1.3 Check of Dimensions

4.1.4 X-Ray Inspection

4.2 Fuel Plate

See Appendix for schematic drawing.

4.2.1 Homogeneity of Uranium Distribution in Fuel Plates

4.2.2 Bond Between Fuel and Cladding Material

All plates with bonding defects shall be rejected.

4.2.3 Internal and External Geometry Dimensions

4.2.4 Contamination of the Fuel Plate Surface

The surfaces of the plates shall be free of foreign materials such as dirt, grease, or slag.

4.2.5 Surface Defects

Levels for permissible surface defects are listed in the Appendix.

4.3 Fuel Tube

4.3.1 Dimensions

The dimensions shall be inspected according to the Inspection Scheme.

4.3.2 Welded Seams

Visual inspections shall be made on the quality of the welded seams. Random-sampled X-ray photographs of individual welded seams are to be made to inspect the position of the core with respect to the welded seams, as well as the quality of the seams.

4.3.3 Visual Inspection of Surface for Damage

(See Section 4.2.5 of this Specification for permissible depth of defects.)

4.4 Outer Tube

4.4.1 Dimensions

The inspection shall be carried out according to the Inspection Scheme.

4.4.2 Welded Seams

Inspections shall be carried out following the procedures described in Section 4.3.2 of this Specification.

4.4.3 Visual Inspection of Surface for Damage

(See Section 4.2.5 of this Specification for permissible depth of defects.)

4.5 Fuel Section

4.5.1 Dimensions

The inspection of the dimensions, especially those of the cooling gaps, shall be carried out according to the Inspection Scheme.

4.6 Fuel Element

4.6.1 Geometry

Each fuel element shall be inspected according to the Inspection Scheme for conformity with the required geometry.

4.6.2 Surface

Each fuel element shall be subjected to a visual check.

5.0 ACCEPTANCE INSPECTION

5.1 Acceptance Inspections by the Producer

The acceptance inspection of the fuel plates, the fuel tubes, the fuel sections, as well as of the fuel element, shall be carried out by the Producer's production-independent Quality Control Office. Bases for the production and inspection are these Specifications and the Inspection Scheme.

The results of the inspections shall be compiled in acceptance records, which are given to the Purchaser.

The acceptance records are part of the Inspection Scheme that is prepared by the Producer and submitted in triplicate to the Purchaser for approval. The Purchaser shall return one copy of the Inspection Scheme, marked with any changes to be made, to the Producer a suitable length of time before start of production.

The purchaser is authorized to appoint representatives who can enter the inspection rooms operated by the Producer's Quality Control Office, and who can observe the inspections or carry out the inspections themselves. These representatives shall follow all instructions relating to technical safety, while on the Producer's property or within areas under the control of the Producer.

The Producer retains the right to refuse entry to any appointed person(s) for valid reasons. The Purchaser or its representatives have the right to take samples from on going production.

5.2 Acceptance Inspections by the Purchaser

When, in accordance with the Delivery Contract, acceptance inspections are to be carried out by the Purchaser or by its representatives, these inspections shall be recorded in the Inspection Plan. A report will be prepared on every acceptance inspection and will be signed by the Purchaser or its representative and by the Producer.

6.0 ACCEPTANCE RECORDS

In conjunction with the intermediate and final acceptances and in accordance with DIN 50049, the following acceptance Inspection Certificates and records will be given to the Purchaser or its representatives in duplicate:

- Certification of the production and inspection of the fuel elements according to this Specification.

- Dimension check of the fuel elements.
- Certification of the U and U-235 contents as well as the degrees of enrichment in the fuel plate and center section, the ratio of total U to Al, and the total weight of the fuel tubes.
- Results of U contamination inspection of fuel plates.
- X-ray films of fuel plates and fuel tubes (1 copy).
- Inspection of the cladding thickness of fuel plates.
- Diagrams from the homogeneity check (1 copy) of the fuel plates.
- Plant certification of the surface treatment of the fuel plates.
- Inspection of the Al powder used for the U_3O_8 -Al mixture.
- Inspection of the U_3O_8 powder used for the U_3O_8 -Al mixture.
- Inspection of the semi-finished parts according to the Parts Lists.

7.0 WARRANTY

The warranty is specified in the Delivery Contract.

8.0 PACKING

After the final inspection, fuel elements shall be packed in plastic foil, the foil will be heat sealed, and the fuel elements will be placed in special transportation containers.

9.0 APPENDIX

9.1 Drawings/Inspection Scheme

9.2 U-235 Content, Surface Coverage, and Enrichment Specifications

9.2.1 U-235 Content

	<u>U-235 Content per Fuel Plate, g</u>	<u>U-235 Content per Fuel Element, g</u>
Format 1	11.89 \pm 5%	180 \pm 3
Format 2	13.96 \pm 5%	180 \pm 3
Format 3	16.03 \pm 5%	180 \pm 3
Format 4	18.12 \pm 5%	180 \pm 3

9.2.2 Surface Coverage with U-235

Nominal value of 33.5 mg U-235/cm²

Zone 1* nominal mg U-235 $\pm 12.5\%$

Zone 2* nominal mg U-235 $+ 16.0\%$
 -100.0%

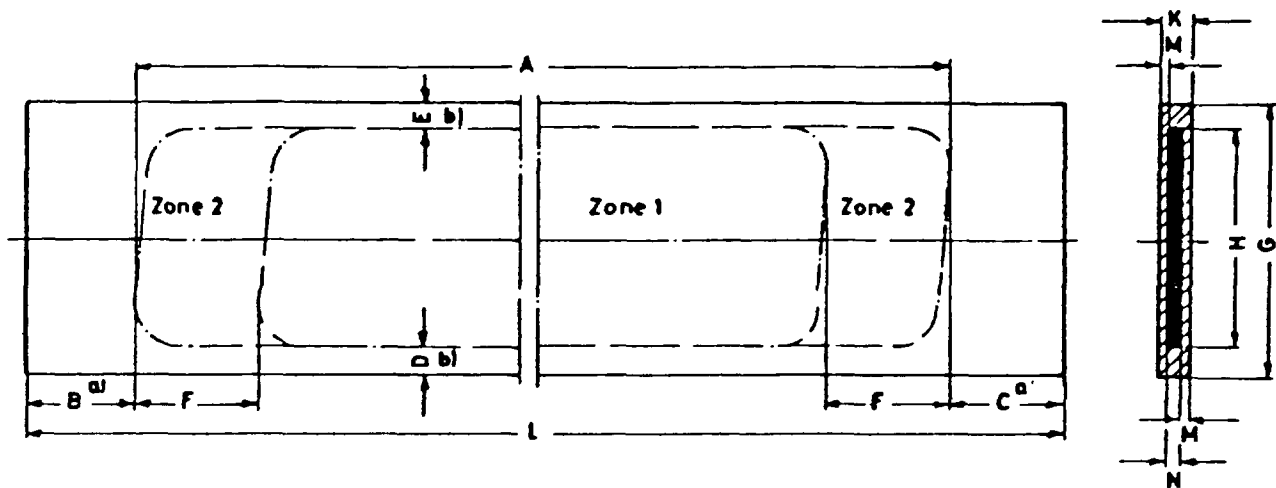
* See Section 9.3, Fuel Plate (schematic drawing)

9.2.3 U-235 Enrichment of 19.75 + 0.2% by Weight - 0.5%

9.2.4 Surface Contamination

The surface contamination must not exceed 10 μ g U-235 per fuel plate.

9.3 Fuel Plate for DR-3 Reactor



Surface defects with a depth of no more than 0.1 mm are acceptable.

$$a_B - C < |3.4|$$

$$b_D - E < |1.6|$$

	<u>Format 1</u>	<u>Format 2</u>	<u>Format 3</u>	<u>Format 4</u>
A	min. 590	min. 590	min. 590	min. 590
B	min. 68	min. 68	min. 68	min. 68
C	min. 68	min. 68	min. 68	min. 68
D	min. 2	min. 2	min. 2	min. 2
E	min. 2	min. 2	min. 2	min. 2
F	max. 30	max. 30	max. 30	max. 30
G	65.3 ± 0.05	75.6 ± 0.05	85.8 ± 0.05	96.1 ± 0.05
H	min. 57.3	min. 67.6	min. 77.8	min. 88.1
K	1.50 ± 0.05	1.50 ± 0.05	1.50 ± 0.05	1.50 ± 0.05
L	746 ± 0.2	746 ± 0.2	746 ± 0.2	746 ± 0.2
M	Zone 1 min. \bar{x} 0.35 ^c Zone 2 min. 0.25			
N	Zone 1 \bar{x} 0.65 ± 0.1 Zone 2 max. 1.05 ^d			

^cIn Zone 1, individual grains may penetrate into the cladding layer of 0.25 or 0.30 mm, provided that the min. average of 0.35 mm is guaranteed.

^dThe max. of 1.05 mm for N in Zone 2 is provided that the min. of 0.25 mm for M in Zone 2 is guaranteed.

9.4 U₃O₈ Powder and Al Powder Specifications

Element	<u>Maximum Impurities in ppm</u>		Element	<u>Maximum Impurities in ppm</u>	
	<u>U₃O₈ Powder</u>	<u>Al Powder</u>		<u>U₃O₈ Powder</u>	<u>Al Powder</u>
Al	100	-	Ti	-	200
B	2	10	V	2	-
Ba	10	-	F	20	-
Be	0.2	-	Zn	-	300
Ca	50	-	Cr-Ni Fe		
Cd	0.5	10	total	150	-
Co	3	30	Individual	-	300
Cu	20	80	Total	-	5000
Fe	-	4000			
K	20	-	Grain	<90 μ m	<150 μ m
Li	5	80	size	(max. 25% by wt. < 40 μ m)	(min. 80% by wt. < 40 μ m)
Mg	50	150			
Mn	5	-			
Na	20	-			
P	100	-			
Si	50	3000			

Density (toluene density) > 8.0 g/cm³

9.5 Materials List

9.6 Surface Treatment

9.6.1 Level Fuel Plates

- Degrease in perchloroethylene vapor
- Mechanical cleaning

9.6.2 Fuel Tubes, Unfueled-Outer Tube, and Combs

- Degrease in perchloroethylene vapor
- Pickle in NaOH (6-10% by wt.) for 1 min. at 60 °C
- Rinse in running water for 1 min.
- Neutralize in HNO₃ (30-50% by wt., density 1.2-1.3 g/cm³) for 1 min.
- Rinse in running water for 5 min.
- Rinse in running, desalted water for 5 min.
- Boil in desalted water for 30 min.
- Dry in air

9.6.3 Upper Section and End Adapter

- Degrease in perchloroethylene vapor
- Pickle in HF/HNO₃ mixture (20 cm³ of HF, 40%, per 1000 cm³ of HNO₃, 20%) for about 10 min. at 20-25 °C
- Rinse in running water for 1 min.
- Pickle in 25% HNO₃ for 2 hours at 20-25 °C
- Rinse in desalted water for 30 min.
- Rinse in running, desalted water for 5 min.
- Brief immersion in hot, desalted water
- Dry in air

9.6.4 Final Cleaning

Before the final visual inspection, every fuel element is rinsed in alcohol.

10.0 LIST OF REVISIONS

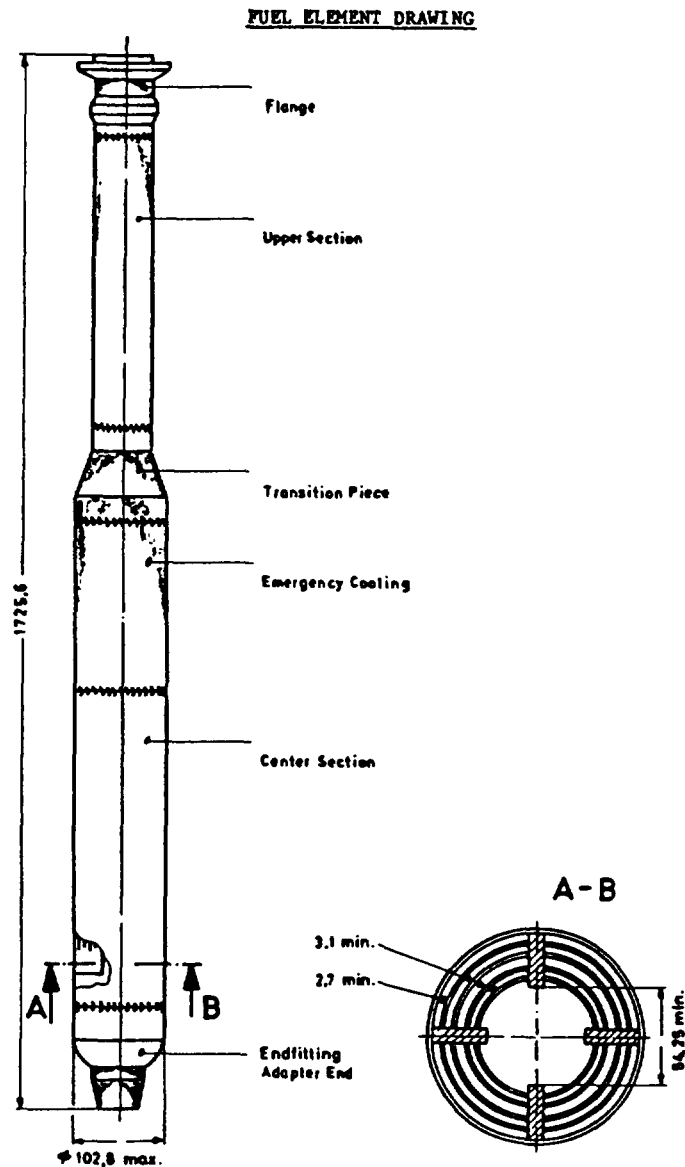
Appendix K-3.2

INSPECTION SCHEME

RISØ NATIONAL LABORATORY
Roskilde, Denmark

Abstract

As part of the Danish RERTR Program, three fuel elements with LEU U_3O_8 -Al fuel and three fuel elements with LEU U_3Si_2 -Al fuel were manufactured by NUKEM for irradiation testing in the DR-3 reactor at the Risoe National Laboratory in Denmark. The inspection scheme for the elements with U_3O_8 -Al fuel is presented here as an illustration only. The inspection scheme for the elements with U_3Si_2 -Al fuel was very similar. In this example, all document numbers, drawing numbers, and form numbers have been deleted or replaced with a generic identification.



INSPECTION SCHEME - OUTLINE

Specification	XXX
Drawings	XXX1 Fuel Element XXX2 Parts List XXX3 Upper Section XXX4 Parts List XXX5 Emergency Cooling XXX6 Flange XXX7 Transition Piece XXX8 Tube XXX9 Emergency-Cooling Tube XXX10 Center Section XXX11 Parts List XXX12 Fuel-Element Tube XXX13 Fuel Plate XXX14 Outer Tube XXX15 Outer-Tube Plate XXX16 Lower Comb XXX17 Upper Comb XXX18 End Adapter XXX19 Core for Fuel Plates

Note: The working documents listed here do not contain information about revision status. This can be taken from the "List of Documents."

U-235 enrichment	$19.75 \begin{smallmatrix} + 0.2 \\ - 0.5 \end{smallmatrix} \text{ wt.}\%$
U-235 content per element	$180 \pm 3 \text{ g}$
U-235 content per fuel plate	Format 1 = $11.89 \text{ g} \pm 5\%$ 2 = $13.96 \text{ g} \pm 5\%$ 3 = $16.03 \text{ g} \pm 5\%$ 4 = $18.12 \text{ g} \pm 5\%$
Surface density of U-235	Nominal value of $33.5 \text{ mg U-235/cm}^2$ Tolerance: Zone 1 nominal $\pm 12.5\%$ Zone 2 nominal $\begin{smallmatrix} + 16.0\% \\ - 100.0\% \end{smallmatrix}$
Number of fuel element tubes and fuel plates in fuel element	4 tubes with 3 plates each for a total of 12 plates

- Tests:
1. End Adapter to Test Sheet No. 1
 2. Comb to Test Sheet No. 2
 3. Upper section to Test Sheet No. 3
 - 3.1 Record Form A, Upper Section
 4. Core to Test Sheet No. 4
 - 4.1. Record Form B, Core for Fuel Plates
 - 4.2 Inspection Certificate Form C, U_3O_8 powder
 - 4.3 Inspection Certificate Form D, Al powder
 5. Fuel Plate to Test Sheet No. 5
 - 5.1 Inspection Certificate Form E, Cladding Thickness
 - 5.2 Calibration Steps
 - 5.3 Inspection Certificate Form F, U Contamination
 - 5.4 Record Form G, Chord Length
 6. Fuel-Element Tube to Test Sheet No. 6
 - 6.1 Inspection Certificate Form H, Fuel-Element Tube
 7. Outer-Tube Plate to Test Sheet No. 7
 8. Outer Tube to Test Sheet No. 8
 - 8.1 Inspection Certificate Form I, Outer Tube
 - 8.2 Inspection Certificate Form J, Weld Seams
 9. Center Section to Inspection Certificate Form K
 - 9.1 Inspection Certificate Form L, Fuel in the Fuel Element
 10. Fuel Element to Inspection Certificate Form M
 11. Balance of Acceptance to Record Form N

Acceptance records and Inspection Certificates according to DIN 50049 (2 each) for:

- Certification of the manufacture and examination of the fuel elements in accordance with the specification.
- Inspection of the dimensions of the Center Section (Form K).
- The Enrichment and the U and U-235 contents of Fuel Plates and Fuel Elements (Form L).
- Inspection of the dimensions of the Fuel Element (Form M).
- X-ray films of Fuel-Element Tubes (1 copy).
- Inspection of the Weld Seams (Form J).
- Testing of the Fuel-Element Tube (Form H).
- Testing of the Outer Tube (Form I).
- Testing of the Fuel Plates for contamination with Uranium (Form F).

- Verification of the cladding thickness of the Fuel Plates (Form E).
- X-ray films of Fuel Plates (1 copy).
- Diagrams from the homogeneity tests (1 copy).
- Surface treatment of the Fuel Plates.
- Al powder used for the U_3O_8 -Al mixture (Form D).
- U_3O_8 powder (Form C).
- Semi-finished products according to the Parts List.
- Record Form N, Acceptance Record.

Test Equipment:

- 1) Reference Gauge (Form X)
- 2) Template (Form P)
- 3) Ring Gauge (Form Q)
- 4) Holding Device (Form R)
- 5) Ring Gauge (Form S)
- 6) Testing Probe (Form T)
- 7) Eccentricity Testing Device (Form U)
- 8) Calibration Gauge (Form V)
- 9) Testing Probe (Form W)

IDENTIFICATION FORM

Order No:

Contractor Order No:

Description:

.....

.....

The elements to be manufactured according to the
description above shall be identified as follows:

Element type:

Numbered from to

Element type:

Numbered from to

Element type:

Numbered from to

RANDOM SAMPLE PROCEDURE (RSP)

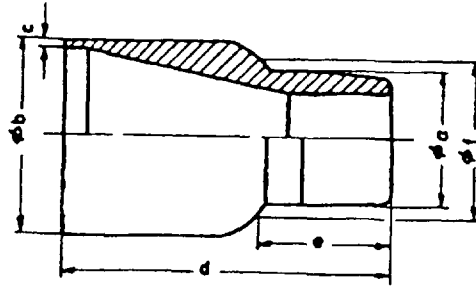
<u>N</u>	<u>n</u>	<u>a</u>	<u>r</u>
0 - 30	3	0	1
31 - 60	6	0	1
61 - 90	9	0	1
91 - 120	12	0	1

If the number of defective items found in a random sample of n items equals a , the related lot of N items shall be considered as good and shall be accepted. If the number of defective items found is equal to or greater than r , the entire lot of N items shall be examined.

N: lot size
n: random sample size
a: acceptance number
r: rejection number

TEST SHEET NO. 1, END ADAPTER

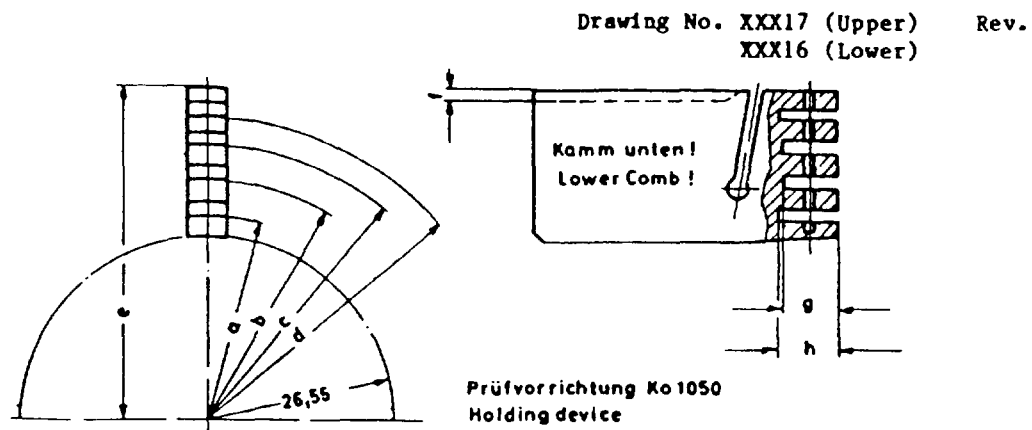
Drawing No. XXX18 Rev.



Dim.	Nominal, mm	Testing Equipment/ Test Specification	Testing Process	Test Sample Size, %	Tested By	
					QC*	P*
			Check all dimensions according to drawing	RSP	x	
a	73 ± 0.1	micrometer	Measure diameter "a"	100	x	
b	$102.4 - 0.3$	micrometer	Measure diameter "b"	100	x	
c	1.5 ± 0.1	micrometer	Measure dimension "c"	RSP	x	
d	137.6 ± 0.2	slide gauge	Measure dimension "d"	100	x	
e	47.6 ± 0.1	Ring Gauge (Form S)	Measure dimension "e"	100	x	
		visual	Check the surface for design according to drawing	100	x	

*Tested by QC (QC), Production (P)

TEST SHEET NO. 2, UPPER COMB/LOWER COMB



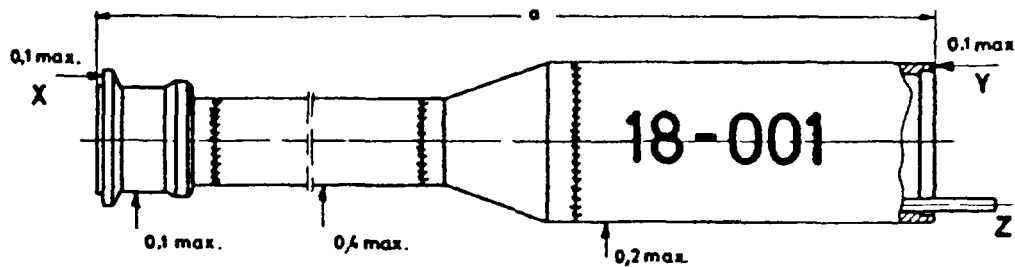
Dim.	Nominal, mm	Testing Equipment/ Test Specification	Testing Process	Test Sample Size, %	Tested By	
					QC*	P*
			Check all dimensions according to the drawing	RSP	x	
a	30.35 ± 0.025	holding device	measure dimensions "a"-"e"	RSP	x	
b	35.275 ± 0.025	(Form R)				
c	40.2 ± 0.025					
d	45.1 ± 0.025					
e	49.6 ± 0.025 (Upper Comb)					
e	49.65 ± 0.025 (Lower Comb)					
f	1.5 ± 0.1	slide gauge	measure dimensions "f"-"h"	RSP	x	
g	9 ± 0.05					
h	10 ± 0.05					

*Tested by QC (QC), Production (P)

TEST SHEET NO. 3, UPPER SECTION

Drawing No. XXX3

Rev.



Dim.	Nominal, mm	Testing Equipment/ Test Specification	Testing Process	Test Sample Size, Z	Tested By QC* P*
			Check all dimensions according to the drawing	RSP	x
		Reference Gauge (Form X) Template (Form P)	Performance test on flange (pegs out of 3 holes)	RSP	x
		Ring Gauge (Form Q)	Inspection of the weld seam diameter	RSP	x
		PVC-Probe	Inspection of the passage (inside diameter) at the Thermocouple guide tube on "Z"	100	x
Lifting the Upper Section with the Calibration Gauge (Form Y), inspect horizontal distances between turning centers.					
	0.1/0.4/0.2	Dial Indicator	Check for eccentricity	100	x
	0.1 max.	?	Check the run-out toler- ances for the "X" and "Y" faces.	100	x
		PVC-Probe 3 mm diameter	Upper surface of the tube insert shall be 3 mm under the upper surface of the top drill holes.	100	x
		PVC-Probe 3 mm diameter	Inspection of the passage (inside diameter) at the emergency cooling tube	100	x
a	792.3 ± 0.6	Slide Gauge	Measure length	100	x
		Visual	Inspection of the weld seams	100	x

*Tested by QC (QC), Production (P)

RECORD FORM A, UPPER SECTION

Part No.	Flange/ Template (Forms X & P)	Weld Seam Diameter Ring Gauge (Form Q)	3 mm Dia. PVC- Probe	Eccentricity** max. 0.1/0.2/0.4	Weld Seam Surface Visual	Front max. 0.1**	Length 792.3±0.5	Upper Section Wire Screen	Emergency Cooling Visual	Weld Seam Visual*	Remarks

*Three wings of inner rings inspected for complete bonding.

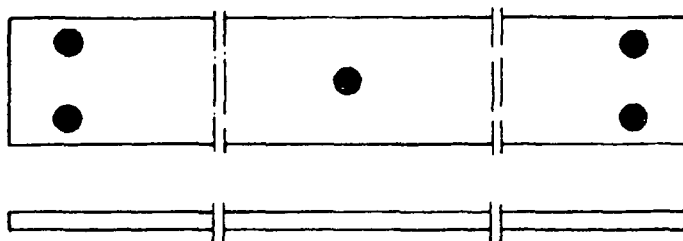
**Examination by Calibration Gauge (Form Y) between points.

Inspector/Date:

TEST SHEET NO. 4. CORE FOR FUEL PLATES

Drawing No. XXX13

Rev.



Dim.	Nominal, mm	Testing Equipment/ Test Specification	Testing Process	Test Sample Size, %	Tested By	
					QC*	P*
		Balance Analysis DOC. YYY	The U-235 content is determined by weighing each fuel core and multiplying this value by the analyzed value of the U and U-235 content.	100	x	
		<u>Alternative:</u> Double Counting- Apparatus DOC. YYY	Determination of the U-235 content by measuring the 185-keV characteristic radiation.	100	x	
		Micrometer	Measure thickness at 5 points (see sketch) and record mean value.	20	x	
		X-ray Film	Check for homogeneity and possible inclusions.	100	x	
			Record fuel core No., fuel core weight, U content, and U-235 content (Form B)	100	x	

*Tested by QC (QC), Production (P)

RECORD FORM B. CORE FOR FUEL PLATES

Key word: Order No: Enrichment of U-235%

batch No: UAl_x -Cermet ☐ U_3O_8 -Cermet ☐

No.	Core No.	Weight, g	U, g	U-235, g	Thickness*, mm	Plate No.	Element No.	Remarks
1								
2								
3								
4								
5								
6								
7								
8								
9								
10								
11								
12								
13								
14								
15								
16								
17								
18								
19								
20								
21								
22								
23								
24								
25								
26								
27								
28								
29								
30								

Corrections: Distribution:

Inspector:

Date:

.....

*Median of 5 tests

INSPECTION CERTIFICATE FORM C, U₃O₈ POWDER

Charge No:

Specification:

U Content wt%

**Analysis Certificate No:

Impurities	Elements	max., ppm	Actual, ppm
	Al	100	
	B	2	
	Ba	10	
	Be	0.2	
	Ca	59	
	Cd	0.5	
	Co	3	
	Cr*	-	
	Cu	20	
	Fe*	-	
	K	20	
	Li	5	
	Mg	50	
	Mn	5	
	Na	20	
	Ni*	-	
	P	100	
	Si	50	
	V	2	
	F	20	
	Σ*	150	

Sieve analysis	Particle size	Actual, %
	< 90 μm	
	< 40 μm ≤ 25%	

Isotope analysis**	U-234, %	U-235, %	U-236, %	U-238, %
--------------------	----------	----------	----------	----------

nom.

act.

The absolute uncertainty of the U-235 weight concentration is

Density nominal: $\geq 8.0 \text{ g/cm}^3$ actual: g/cm^3

Inspector

.....
Work Inspector

INSPECTION CERTIFICATE FORM D, Al POWDER

Purchaser	Charge No.
Purchase Order No.	Date:
Contractor Order No.	Analysis No:
	Specification

Chemical Impurities	<u>Elements</u>	<u>Limit, ppm</u>	<u>Results, ppm</u>
---------------------	-----------------	-------------------	---------------------

B	10
Cd	10
Co	30
Cu	80
Fe	4000
K	80
Li	5
Mg	150
Si	3000
Ti	200
Zn	300

Others	
Individual	300
Total	5000

Particle Size	Grain Size	$\leq 125 \mu\text{m}$
	80%	$\leq 40 \mu\text{m}$

*Determined by inspection sieving with mesh width 125/40 μm .

Manufacturer:

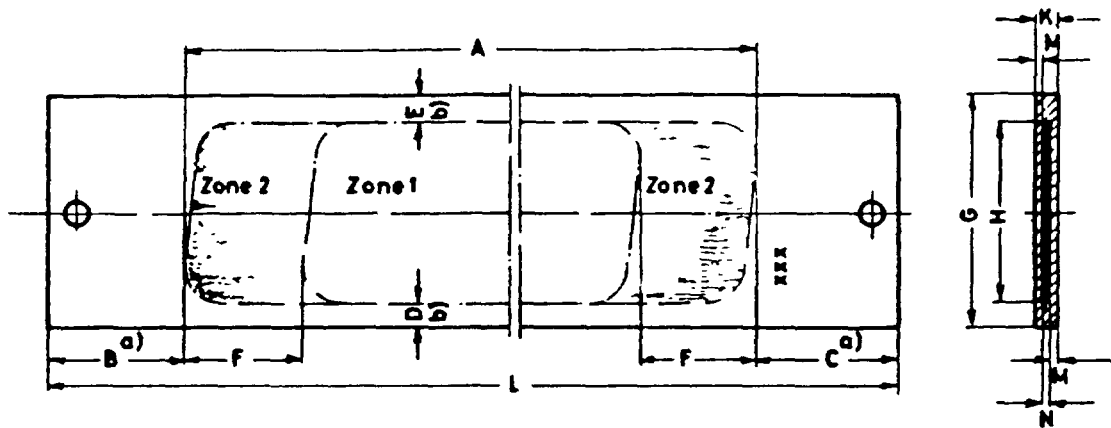
Date

.....
Work Inspector

TEST SHEET NO. 5, FUEL PLATE

Drawing No. XXX13

Rev.



	<u>Format 1</u>	<u>Format 2</u>	<u>Format 3</u>	<u>Format 4</u>
A	min. 590	min. 590	min. 590	min. 590
B	min. 68	min. 68	min. 68	min. 68
C	min. 68	min. 68	min. 68	min. 68
D	min. 2	min. 2	min. 2	min. 2
E	min. 2	min. 2	min. 2	min. 2
F	max. 30	max. 30	max. 30	max. 30
G	65.3 ± 0.05	75.6 ± 0.05	85.8 ± 0.05	96.1 ± 0.05
H	min. 57.3	min. 67.6	min. 77.8	min. 88.1
K	1.50 ± 0.05	1.50 ± 0.05	1.50 ± 0.05	1.50 ± 0.05
L	746 ± 0.2	746 ± 0.2	746 ± 0.2	746 ± 0.2
M	Zone 1 min. \bar{x} 0.35 ^c Zone 2 min. 0.25			
N	Zone 1 \bar{x} 0.65 ± 0.1 Zone 2 max. 1.05 ^d			

^aB - C \leq |3,4|

^bD - E \leq |1,6|

^cIn Zone 1, individual grains may penetrate into the cladding layer of 0.25 or 0.30 mm, provided that the min. average of 0.35 mm is guaranteed.

^dThe max. of 1.05 mm for N in Zone 2 is provided that the min. of 0.25 mm for M in Zone 2 is guaranteed.

Surface defects with a depth of at most 0.1 mm are acceptable.

TEST SHEET NO. 5, FUEL PLATE (CONT.)

Drawing No. XXX13

Rev.

Dim.	Nominal, mm	Testing Equipment/ Test Specification	Testing Process	Test Sample Size, %	Tested By QC* P*
<u>Fuel plate not bent</u>					
	No blisters	Heating 1 h at 425 °C DOC. YYY	Visual evaluation for bond defects (metallur- gical bond) after the heating.	100	x
		X-ray system and template DOC. YYY	X-ray and center	100	x
	Nominal: 33.5 mg U-235/cm ²	X-ray system calibration-steps DOC. YYY	Inspection of the U distribution by means of X-ray absorption. (One line longitudinally per plate.)	RSP	x
	Tolerance: Zone 1 nominal ±12.5% Zone 2 nominal +16% -100%				
D/E	min. 2 D - E ≤ 1.6	X-ray film and template	Inspection of the internal geometry	RSP	x
A	min. 590				
B/C	min. 68 B - C ≤ 3.4				
H	see Table				
K	1.51 ± 0.05	Measuring device DOC. YYY	Inspection of the outer geometry	RSP	x
G	see Table				
L	746 ± 0.2				
M	min. 0.35 (Zone 1) min. 0.25 (Zone 2)	Microscope DOC. YYY	Examine cladding thickness by means of sections (Inspection Certificate Form E).	1	x
<u>Fuel plate bent</u>					
	≤ 10 µg U-235/per plate	Counting Apparatus DOC. YYY	Inspection Certificate (Form F).	1	x
	Plate No. on convex side	Slide Gauge	Measure length (Form G). Check for plate No. position.	100	x
	≤ 0.1 mm deep	Visual light- section microscope DOC. YYY	Surface inspection and, if necessary, measuring of surface defects	100	x

*Tested by QC (QC), Production (P)

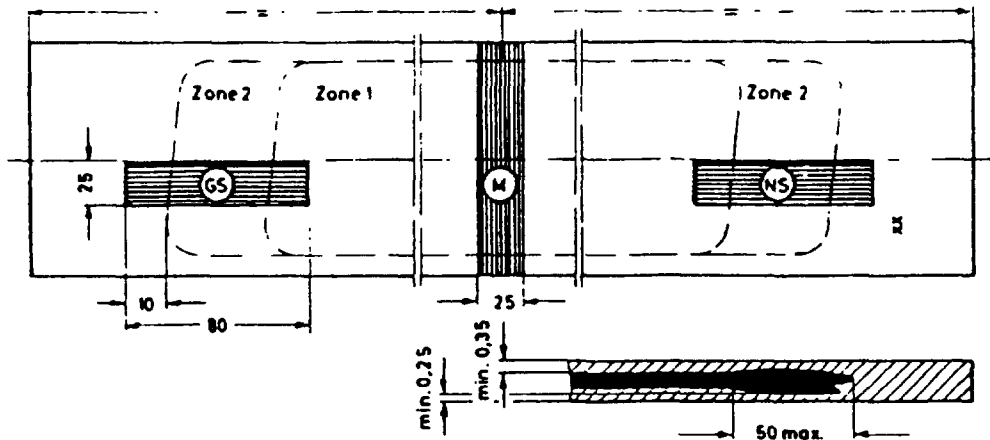
INSPECTION CERTIFICATE FORM E, CLADDING THICKNESS

Order No.

Identification Word:

Sampling

Drawing No. XXX13



In Zone 1, individual grains may penetrate into the cladding layer of 0.25 or 0.35 mm, provided that the min. average of 0.35 mm is guaranteed.

Cladding thickness (nominal), mm

GS		M		NS	
Zone 2	Zone 1	min. average 0.35	Zone 1	Zone 2	
min. 0.25				min. 0.25	

Cladding thickness (actual), mm

Plate No.	Zone 2	Zone 1	Zone 1	Zone 1	Zone 2
	min.	min.	min.	min.	min.

Date:

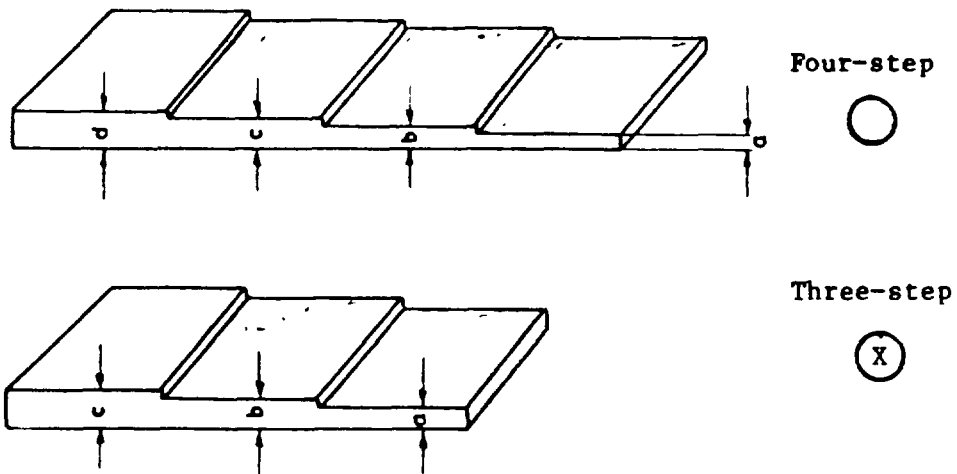
Inspector:

.....

Work Inspector

CALIBRATION STEPS

Homogeneity of Fuel Plates



The thickness dimensions (a, b, c, d) are determined at the beginning of plate production and are included in the appendix to Inspection procedure DOC. YYY.

INSPECTION CERTIFICATE FORM: F, U CONTAMINATION

Plates ☐ Tubes ☐ Fuel Elements ☐

Order No. Identification WordZ U-235

Specification No. Requirement

Inspection system: large-area counter 810 cm² Calibration plate 7.2 µg U-235 Working voltagekV

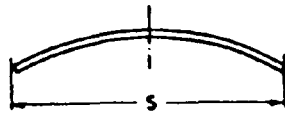
Type**	Plate No. <input type="radio"/>	Tube No. <input type="radio"/>	UA1 _x /U ₃ O ₈ - U _x Si _y Charge No.	Zero rate, pulses/min.	Calibration plate Count rate pulses/min.	Number side pulses/min.	Reverse side pulses/min.	Result: ≤ µg U-235	Date
_____	_____	_____	_____	_____	_____	_____	_____	_____	_____

Inspector

.....
Work Inspector

*I = Inner Plate, O = Outer Plate

RECORD FORM G, CHORD LENGTH

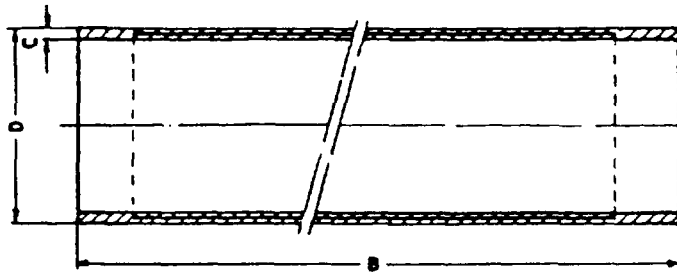


part 1 = 55.0 - 55.5 mm
 2 = 63.5 - 64.0 mm
 3 = 72.0 - 72.5 mm
 4 = 80.5 - 81.0 mm
 Outer tube = 88.3 - 88.7 mm

Part	Plate No.	Numberside, mm	End, mm		Part	Plate No.	Numberside, mm	End, mm
_____	_____	_____	_____		_____	_____	_____	_____

Date/Inspector

TEST SHEET NO. 6, FUEL-ELEMENT TUBE



Drawing No. XXX12 Rev.

part	Diameter (D)
4	92.9-93.5
3	83.1-83.7
2	73.3-73.9
1	63.5-64.1

**Inspection Certificate Form H

Dim.	Nominal, mm	Testing Equipment/ Test Specification	Testing Process	Test Sample Size, %	Tested By QC* P*
B	666.0 \pm 0.1 - 0.4	Slide Gauge	Measure Length**	100	x
C	1.5 \pm 0.04	Wall thickness Micrometer	Measure wall thickness** (3 x top, 3 x bottom)	100	x
D	93.2 \pm 0.3 83.4 \pm 0.3 73.6 \pm 0.3 63.8 \pm 0.3	Slide Gauge	Measure diameter "D" (4 x)**	100	x
	max. 0.3	Measuring Plate Sensor Gauge	Determine max. on edge**	100	x
		Visual	Inspection of the weld seam	100	x
	Defects \leq 0.1 mm deep	Visual, light- section Microscope	Surface inspection for defects and tube identification	100	x
		X-ray film	Inspection of the weld seam quality and dimensions. Meat/weld seam	min. 5	x
		Balance	Determine the tube weight (Form H)	100	x

*Tested by QC (QC), Production (P)

...

Part

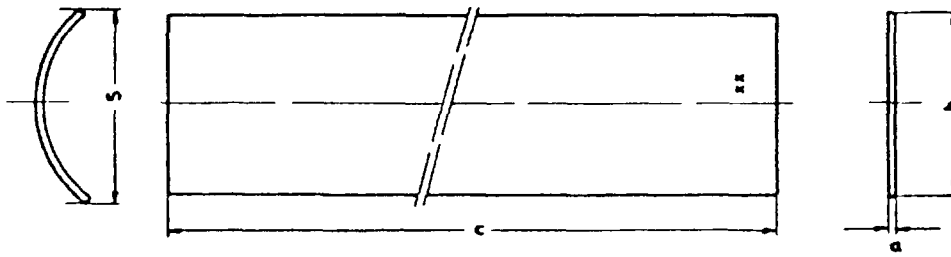
[illegible]

Remarks

..... Inspector Work Inspector

TEST SHEET NO. 7, OUTER-TUBE PLATE

Drawing No. XXX15 Rev.

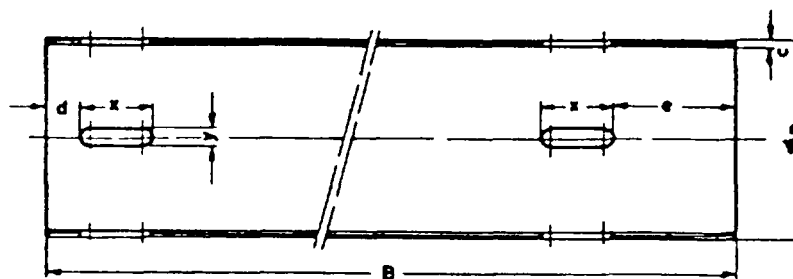


Dim.	Nominal, mm	Testing Equipment/ Test Specification	Testing Process	Test Sample Size, %	Tested By	
					QC*	P*
<u>Plate not bent</u>						
a	1.51 ± 0.03	Micrometer	Measure thickness	RSP	x	
b	105.9 ± 0.1	Slide Gauge	Measure width	RSP	x	
c	860 ± 0.5	Slide Gauge	Measure length	RSP	x	
<u>Plate bent</u>						
	convex slide	Visual	Check for plate No. position	100	x	
S	88.3 - 88.7	Slide Gauge	Measure dimension "S" and record results (Record Form G)	100	x	

*Tested by QC (QC), Production (P)

TEST SHEET NO. 8, OUTER TUBE

Drawing No. XXX14 Rev.



**Inspection Certificate Form H

Dim.	Nominal, mm	Testing Equipment/ Test Specification	Testing Process	Test Sample Size, %	Tested By	
					QC*	P*
			Check all dimensions according to the drawing	RSP	x	
c	1.5 ± 0.04	Wall thickness- Micrometer	Measure wall thickness** (3 x top, 3 x bottom)	100	x	
D	102.6 ± 0.2	Slide Gauge	Measure diameter "D" (4 x) **	100	x	
	max. 0.3	Measuring Plate Sensor Gauge	Determine max. on edge**	100	x	
B	799.3 ± 0.15	Slide Gauge	Measure length	RSP	x	
e	56.9 ± 0.3	Slide Gauge	Measure dimensions "e" and "d"	RSP	x	
d	18 ± 0.1					
x	24 ± 0.2	Reference Gauge (Form Z)	Inspection of the dimensions "x" and "y"	RSP	x	
y	3 ± 0.1					
		Visual	Inspection of the weld seam Inspection of the tube No.	100	x	

*Tested by QC (QC), Production (P)

INSPECTION CERTIFICATE FORM I, OUTER TUBE

No.	Tube No.	Outer Tube			Length, mm 660-660.3	Wall Thickness, mm 1.46 - 1.54	Outer Diameter Nominal	bow, mm max. 0.3	Surface Weld Seam
		No.	No.	No.					

Remarks

.....
Inspector

.....
Work Inspector

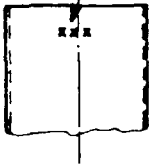
INSPECTION CERTIFICATE FORM J, WELD SEAMS

☐ Fuel Element Tube

Part ☐

Outer Tube ☐

Plate No.



Tube
No.

Weld
Seam

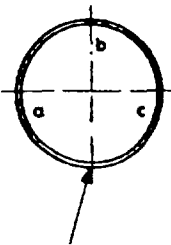
Plate
No.

X-ray
film
desig-
nation

Result

Acceptance

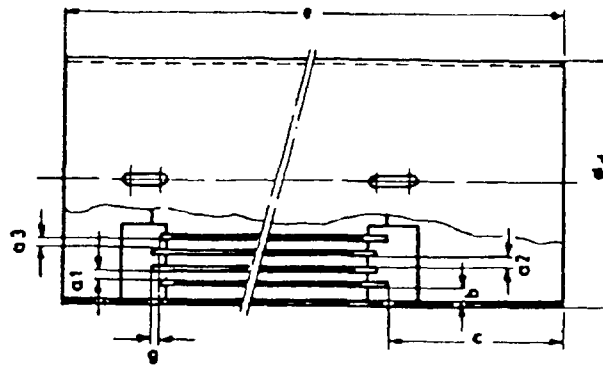
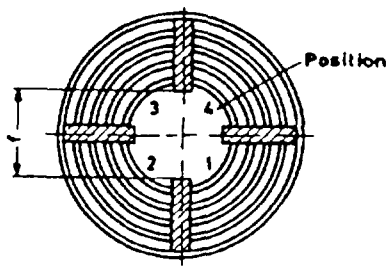
approved rejected



.....
Inspector

.....
Work Inspector

INSPECTION CERTIFICATE FORM K, CENTER SECTION



Center Section No.

.....

Fuel Element Tube Section No. 1

Fuel Element Tube Section No. 2

Fuel Element Tube Section No. 3

Fuel Element Tube Section No. 4

Outer Tube No.

No Impurities

Dimension	nominal, mm	actual, mm
c	87.1 - 87.7	
d	102.8 max.	
e	796.7 - 797.9	
f	54.25 min.	Form V
g	0.9 - 1.1	
bow	≤ 0.7	
Weld Seams	103.4 max.	Form Q
9 mm diameter holes up to start of fuel tube	Testing Probe (Form T) Positions 1 and 2	
Visual inspection	Plate Tube No. location	
Surfaces parallel to within 0.1 mm		
The weld seams are staggered		

Inspector:

.....
Inspector

.....
Work Inspector

INSPECTION CERTIFICATE FORM L, FUEL IN FUEL ELEMENT

Nominal U-235 Content/Center Section:g

Center Section No.

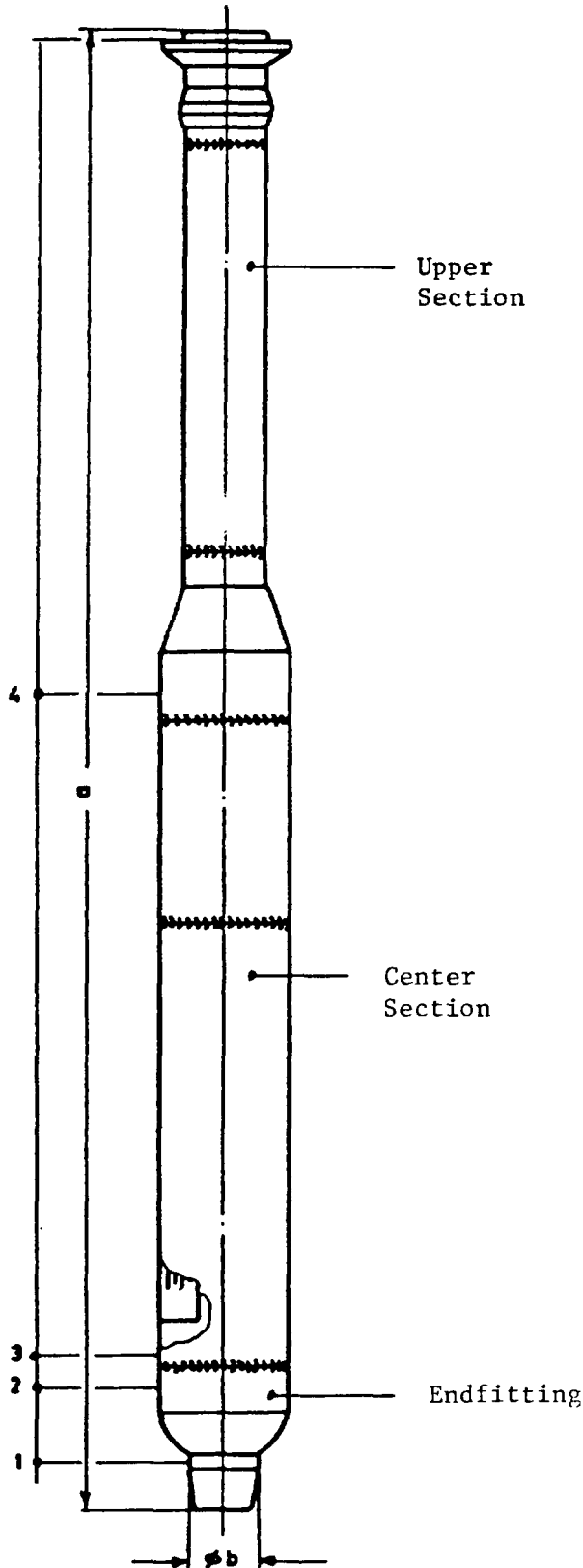
Nominal U-235 Content/Plate:g

Pos.	Plate No.	Core No.	U ₃ O ₈ Charge	U Content	Enrichm., %	U-235 Content, g	U Total to Al, %	Tube Weight, g
Tube Part No. 1								
a	_____	_____	_____	_____	_____	_____	_____	_____
b	_____	_____	_____	_____	_____	_____	_____	_____
c	_____	_____	_____	_____	_____	_____	_____	_____
			Total	_____		_____	_____	_____
Tube Part No. 2								
a	_____	_____	_____	_____	_____	_____	_____	_____
b	_____	_____	_____	_____	_____	_____	_____	_____
c	_____	_____	_____	_____	_____	_____	_____	_____
			Total	_____		_____	_____	_____
Tube Part No. 3								
a	_____	_____	_____	_____	_____	_____	_____	_____
b	_____	_____	_____	_____	_____	_____	_____	_____
c	_____	_____	_____	_____	_____	_____	_____	_____
			Total	_____		_____	_____	_____
Tube Part No. 4								
a	_____	_____	_____	_____	_____	_____	_____	_____
b	_____	_____	_____	_____	_____	_____	_____	_____
c	_____	_____	_____	_____	_____	_____	_____	_____
			Total	_____		_____	_____	_____
Average Enrichment					_____			
Total content in the Center Section						_____	_____	_____

.....
Inspector

.....
Work Inspector

INSPECTION CERTIFICATE FORM M, FUEL ELEMENT



Fuel Element No.

.....

Upper Section No.

End Adapter No.

.....

.....

Inspection of the weld
seam diameter with Ring
Gauge (Form Q)

Inspection of the surface
and the weld seam

Inspection of the 54.3 mm
diameter with testing
probe (Form W)

Inspection of the emergency
cooling tube with 3-mm dia.
PVC testing probe

Inspection of the thermo-
couple guide tube with 3-mm
dia. PVC testing probe

Dim.	nominal, mm	results, mm
a	1724 - 1727.2	
b	72.9 - 73.1	

Check the eccentricity with test
device (Form U)

Measure Pos.	nominal, mm	results, mm
1	max. 1	
2	max. 1	
3	max. 1	
4	max. 1.5	

.....
Work Inspector

RECORD FORM N, ACCEPTANCE RECORD

Acceptance item:

Drawing No:

Rev.

Purchaser: pre acceptance ☐ final acceptance ☐

Order No: Specification:

Acceptance inspector:

ACCEPTANCE RESULTS:

On hand: pieces No:

On hand with reservation: pieces No:

Accepted: pieces No:

Accepted with reservation: pieces No:

Rejected: pieces No:

ACCEPTANCE RECORD:

Type/Format/Part No.

Previously accepted

Accepted above

Accumulated acceptance

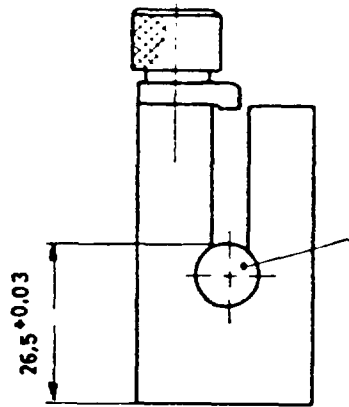
Remarks:

Certificates are to be given to the acceptance inspector.

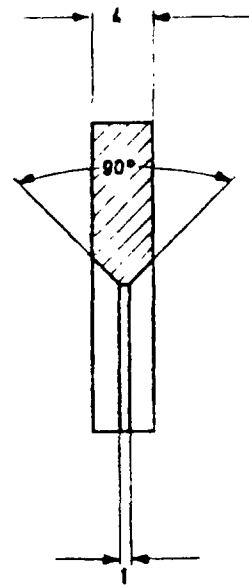
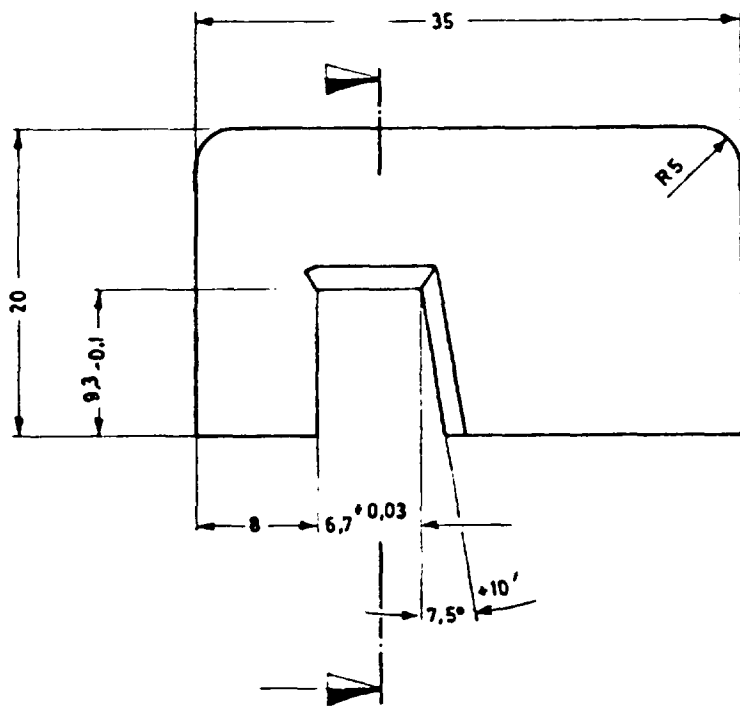
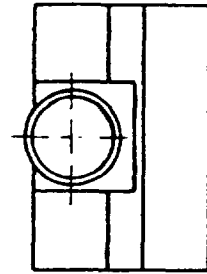
.....
Acceptance Date

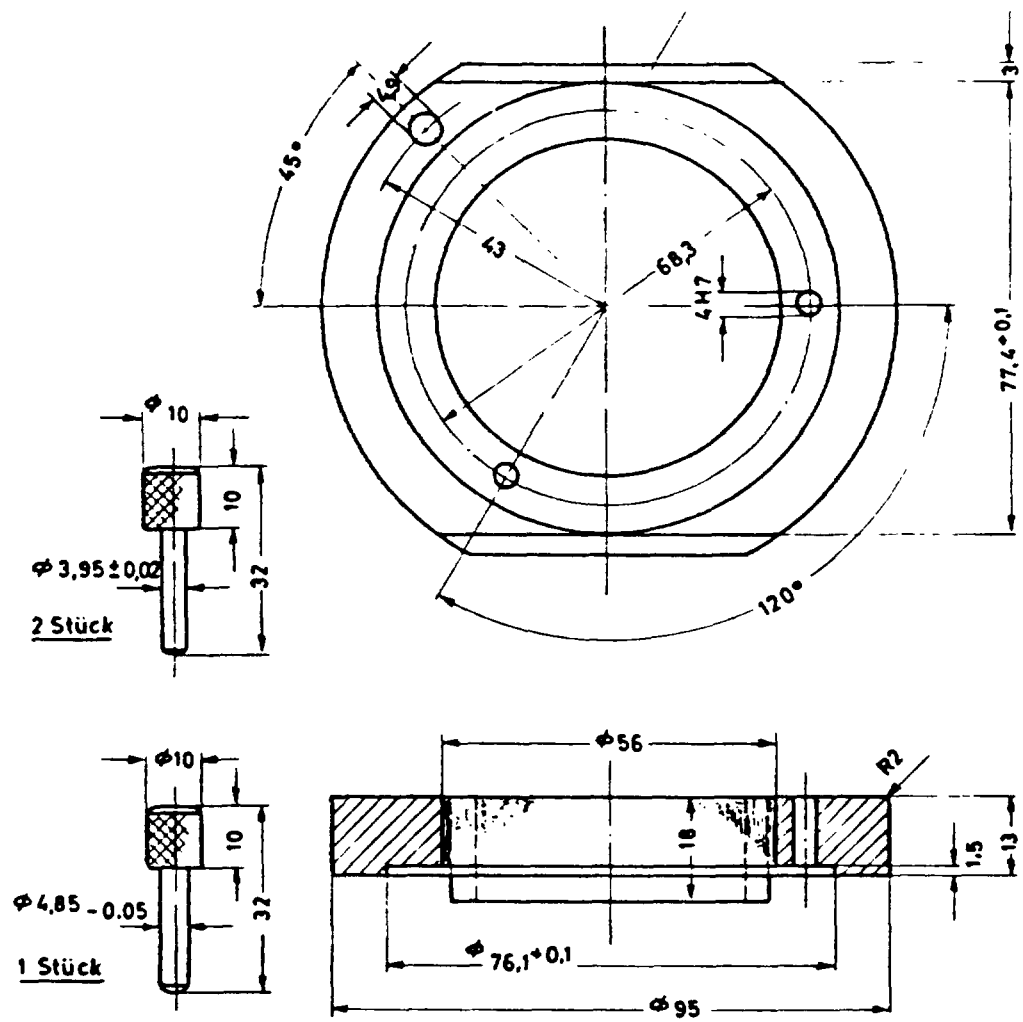
.....
for the Purchaser

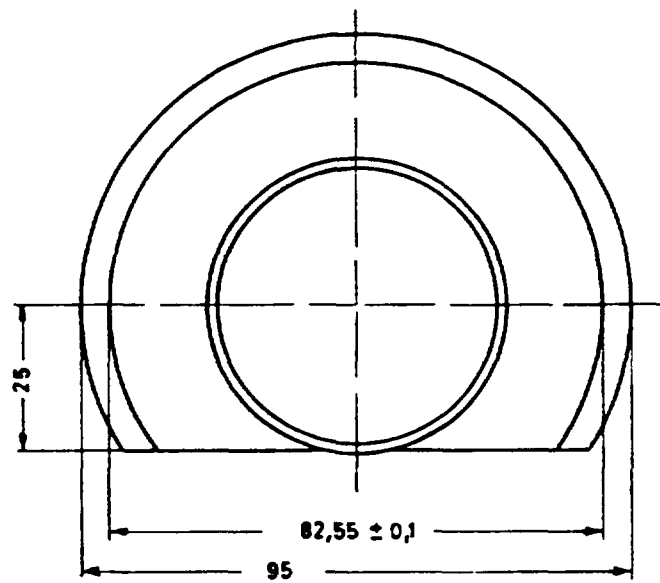
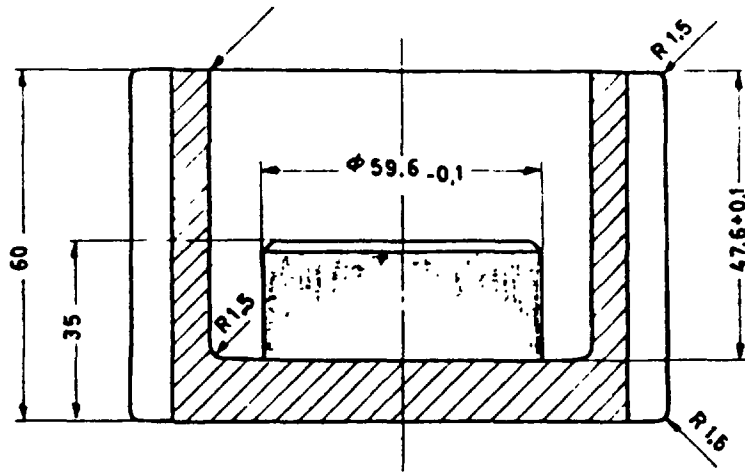
.....
Work Inspector

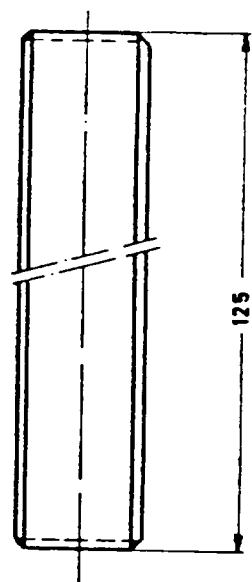
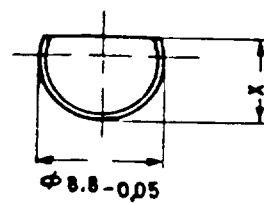
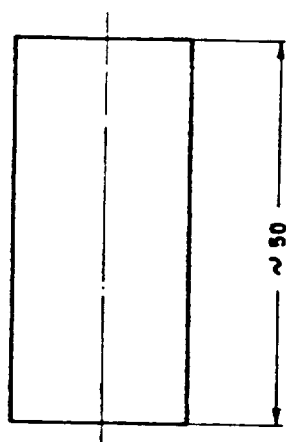
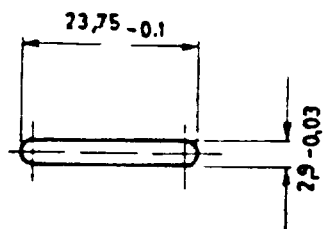
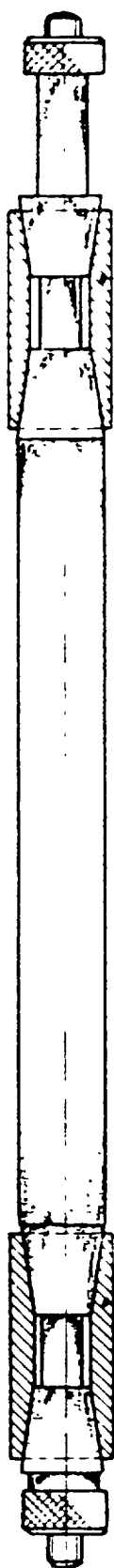


10 ϕ

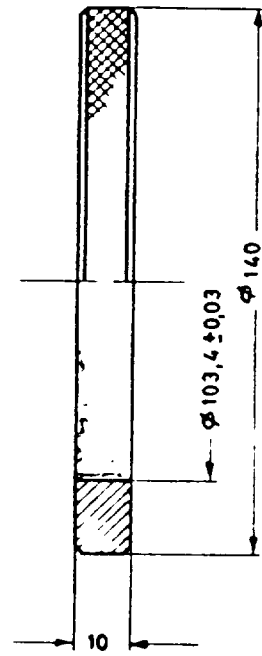
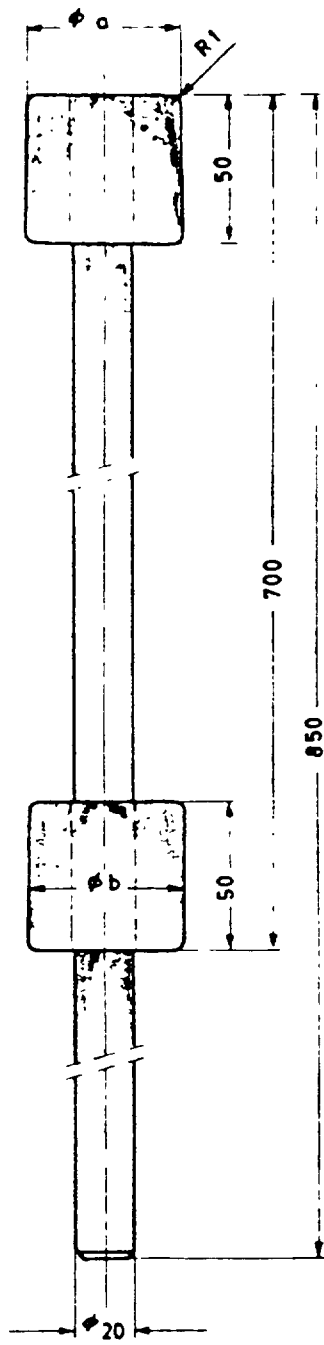


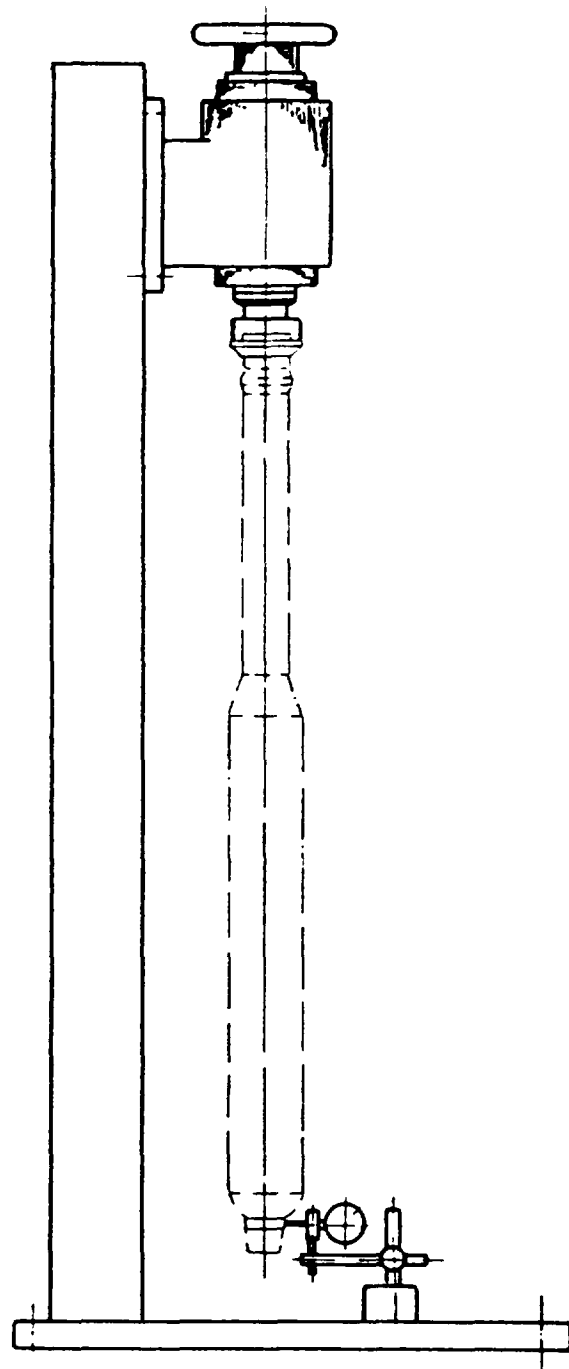
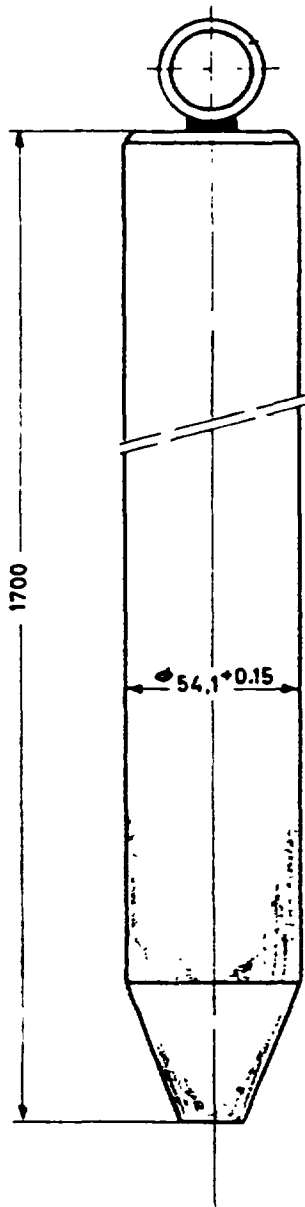






Pos.	X
1	6,2
2	6,8





LIST OF DOCUMENTS

<u>Drawing No.</u>	<u>Document</u>	<u>Rev.</u>	<u>Inspector</u>
Doc. XXX	Inspection Scheme		
Specifications:			
Doc. YYY	Specification		
Drawings:			
XXX1	Fuel Element		
XXX2	Parts List		
XXX3	Upper Section		
XXX4	Parts List		
XXX5	Emergency Cooling		
XXX6	Flange		
XXX7	Transition Piece		
XXX8	Tube		
XXX9	Emergency-Cooling Tube		
XXX10	Center Section		
XXX11	Parts List		
XXX12	Fuel-Element Tube		
XXX13	Fuel Plate		
XXX14	Outer Tube		
XXX15	Outer-Tube Plate		
XXX16	Lower Comb		
XXX17	Upper Comb		
XXX18	End Adapter		

LIST OF REVISIONS

<u>Date</u>	<u>Page</u>	<u>Revision</u>	<u>Approved</u>	<u>Rev.</u>
-------------	-------------	-----------------	-----------------	-------------

Appendix K-4

SPECIFICATIONS FOR FUEL PLATES WITH LEU U_3Si_2 -Al FUEL FOR THE OAK RIDGE RESEARCH REACTOR

ARGONNE NATIONAL LABORATORY
Argonne, Illinois

OAK RIDGE NATIONAL LABORATORY
Oak Ridge, Tennessee

United States of America

Abstract

As part of the RERTR Program, a whole-core demonstration in the Oak Ridge Research Reactor using LEU U_3Si_2 -Al dispersion fuel began in December 1985 and was completed in March 1987. This specification describes the fabrication, inspection, and quality assurance provisions of the fuel plates for the fuel elements and shim rod fuel sections that were used in the demonstration.

1.0 SCOPE

1.1 This specification covers the fabrication, inspection, and quality assurance provisions of aluminum-clad fuel plates containing low-enriched uranium (LEU) for fuel elements and shim rod fuel sections for the Oak Ridge Research Reactor (ORR), a light-water moderated and cooled, 30-MW(th) nuclear reactor. Each fuel-element grouping of fuel plates will contain 17 short and 2 long plates, and each shim-rod-fuel-section grouping of fuel plates will contain 15 short plates. The fuel plates will contain ^{235}U fuel in the form of an aluminum-clad U_3Si_2 -aluminum dispersion. The cladding shall be metallurgically bonded to the fuel core, and the fuel core shall be hermetically sealed.

2.0 APPLICABLE DOCUMENTS

2.1 Applicable Standards

The following documents form a part of this specification except as modified by this specification. Where there is a conflict between the documents cited and the latest revisions thereof, the Contractor shall notify Argonne National Laboratory (ANL), hereinafter referred to as the Laboratory, of the conflict and use the latest revision unless otherwise directed by the Laboratory. NOTE: Contractors located outside the United States territory may submit standards comparable to the U.S. documents listed below to the Laboratory for approval as alternates.

2.1.1 ORNL Drawings

M-11495-OR-004-E
M-11495-OR-012-E

Fuel Plate Details, ORR Fuel Elements
ORR Shim Rod Fuel Section, Fuel Plate
Details

2.1.2 American Society for Testing and Materials Standards

ASTM-B209-70	Aluminum Alloy Sheet and Plate
ASTM-B214-76	Method of Test for Sieve-Analysis of Granular Metal Powders

2.1.3 American Welding Society Standards

AWS-A5.10-69	Aluminum and Aluminum-Alloy Welding Rods and Bare Electrodes
--------------	---

2.1.4 Argonne National Laboratory Documents

AQR-001	Quality Verification Program Requirements
A0004-1020-SA-00	Specification for Low-Enriched Uranium Metal for Uranium-Aluminide and Uranium-Silicide Reactor Fuel Elements

3.0 TECHNICAL REQUIREMENTS

3.1 Materials

The Contractor shall provide a certified report of the chemical analysis of each material listed showing conformance to its respective requirements. The Contractor shall also provide a certified report of the chemical and isotopic analysis of each lot of U_3Si_2 . In addition to other requirements, all materials specified in Paragraphs 3.1.4 and 3.1.5 shall be certified by the Contractor to contain less than 10 ppm boron, 80 ppm cadmium, and 80 ppm lithium. The quantities of these impurities (boron, cadmium, and lithium) in the finished plate shall not exceed those values.

3.1.1 Uranium Metal

The U.S. Department of Energy shall provide the uranium metal needed for the fabrication. The ^{235}U enrichment of the uranium metal shall be 19.75 ± 0.2 wt%. The uranium metal shall meet the technical requirements of ANL specification A0004-1020-SA-00 except for carbon impurity content, which shall be less than 350 ppm by weight.

3.1.2 Uranium-Silicide Powder

3.1.2.1 Uranium silicide, with U_3Si_2 as the primary constituent, shall be produced by melting together uranium metal and high-purity silicon. The silicon content of the uranium silicide, hereinafter called U_3Si_2 , shall be 7.5 ± 0.4 wt%. It is desirable for the silicon content to be close to 7.5 wt%, but in no case should it be less than 7.4 wt%. Except for impurities, whose limits are specified in Subparagraph 3.1.2.2, the balance of the U_3Si_2 shall be uranium.

3.1.2.2 An analysis shall be required for each lot of U_3Si_2 . The impurities in the U_3Si_2 shall not exceed the limits specified in Table 1.

3.1.2.3 As used in the fuel core, the U_3Si_2 powder shall be -100 + 325 mesh (44 to 149 μm) and shall not contain more than 25% of -325 mesh particles, as determined in a standard screening test (ASTM B214-76).

3.1.2.4 A sample with a minimum weight of 10 g shall be obtained from each lot of U_3Si_2 by the Contractor and held at the Contractor's plant for the Laboratory's use. At the time of final delivery, all samples not called for will be considered part of the Contractor's scrap.

Table 1. Maximum Impurity Levels for U_3Si_2 (ppm)

Al	600	Co	10	Li	10
B	10	Cu	80	N	500
C	1000	Fe+Ni	1000	O	7000
Cd	10	H	200	Zn	1000
Other Elements		Individual	500		
		Total	2500		

3.1.2.5 The Contractor shall obtain an independent isotopic analysis of each lot of U_3Si_2 and shall provide to the Laboratory a copy of the results.

3.1.3 Aluminum Powder

3.1.3.1 All aluminum powder shall be atomized spheroidal particles. One hundred percent of the powder shall pass through a 100 mesh (149 μ m) U.S. Standard screen with 80% passing through a 325 mesh (44 μ m) U.S. Standard screen.

3.1.3.2 The chemical composition of the aluminum powder shall be within the limits listed in Table 2.

Table 2. Composition Limits for Al Powder (wt%)

B	0.001 max	Fe	0.400 max	Ti	0.030 max
Cd	0.001 max	Li	0.001 max	Zn	0.030 max
Co	0.001 max	Mg	0.015 max	Al	99.500 min
Cu	0.008 max	Si	0.300 max		

3.1.4 Aluminum Plate and Sheet

The aluminum for the core frames and cladding shall conform to ASTM specification B209-70, alloy 6061-0. The core frames shall be one piece; frames made of multiple pieces welded together are not acceptable.

3.1.5 Aluminum Welding Rods

Aluminum welding rods shall conform to AWS-A5.10-69, Type ER-4043.

3.2 Mechanical Requirements

3.2.1 Fuel Core Fabrication

The fuel core shall consist of 19.75%-enriched U_3Si_2 powder dispersed in aluminum powder. The fuel core shall be fabricated according to standard powder-metallurgical, roll-bonding techniques, modified if necessary, such that excessive oxidation of the fuel core prior to the first hot rolling pass does not occur. The Contractor shall provide to the Laboratory a written procedure for the initial hot rolling step which describes the method used to prevent excessive oxidation or shall provide written certification that the procedure used is the same as that used previously to produce similar U_3Si_2 -Al test elements for the ORR.

3.2.2 Fuel Core Location

3.2.2.1 As verified by fluoroscopic and/or x-radiographic examination, the location of the fuel core shall satisfy either of the following criteria:

3.2.2.1.1 The location of the fuel core shall comply with the requirements specified on the drawings referenced in Section 2.0.

3.2.2.1.2 The outline of the fuel core shall lie within the maximum fuel core dimensions specified on the drawings referenced in Section 2.0, shall be of an area greater than the area of the minimum fuel core dimensions specified on the drawings referenced in Section 2.0, and shall be centered with respect to the edges of the fuel plate. The responsibility for proving that the fuel core area meets this requirement shall lie with the Contractor.

3.2.2.2 The Contractor shall endeavor, through use of adequate compacting pressure and care in assembling the rolling billet, to minimize the occurrence of fuel flakes outside the maximum fuel core dimensions specified on the drawings referenced in Section 2.0. Fuel particles will be allowed in the nominally fuel-free zone except under the following conditions, however:

3.2.2.2.1 Particles (evidenced as white spots on the position radiograph), of any size, closer than 0.5 mm to the ends or edges of the fuel plate or under the comb or plate-identification-number area.

3.2.2.2.2 Particles (white spots) with largest dimension greater than 0.5 mm which are outside the maximum fuel core dimensions specified on the drawings referenced in Section 2.0. Touching particles (white spots) shall be considered to be a single particle for the purpose of determining the largest dimension.

3.2.3 Cladding and Core Thickness Determination

Prior to full production, at least 24 fuel plates shall be manufactured. Two outer fuel plates and two inner fuel plates shall be randomly selected and sectioned as shown in Fig. 1 to verify that cladding and core thicknesses as specified on the drawings referenced in Section 2.0 are met. Further verification of cladding and core thickness shall be demonstrated by randomly selecting

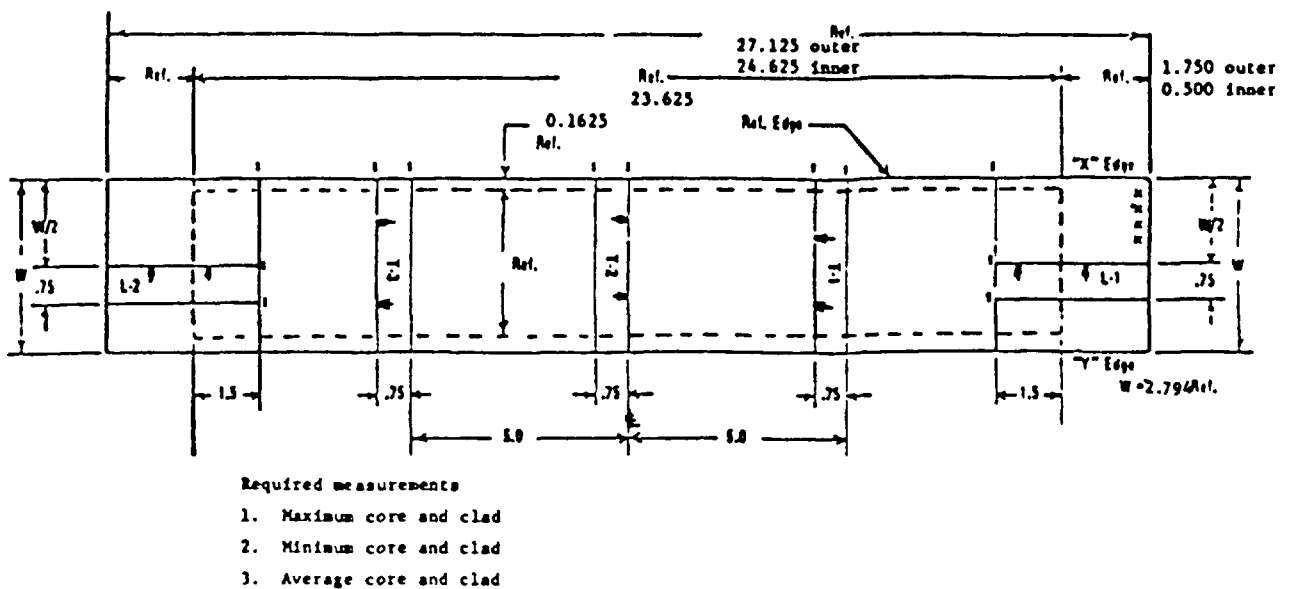


FIG. 1. Typical layout of ORR fuel plates.

one fuel plate from each 100 fuel plates processed. (A plate which has been rejected for reasons not affecting the cladding and core dimensions may be used for this determination.) If production procedures relative to fuel plate fabrication are changed, cladding and core thickness must be requalified.

3.2.4 Cladding Temper

Each fuel plate shall be rolled by a combination of first, hot rolling, and second, cold rolling. The final reduction of the plate thickness shall be accomplished by cold rolling and shall not be less than 4% nor greater than 25% of the final hot-rolled thickness.

3.2.5 Metallurgical Bond

The existence of a metallurgical bond shall be verified by blister test, ultrasonic test, and bending test on a strip sheared from the plate end trimming. The bending test may be replaced by demonstration of at least 40% grain growth across the cladding/frame interface for all plates sectioned to verify fuel core and cladding thickness.

3.3 Physical Properties

3.3.1 Fuel loading

The loading of each fuel plate shall be as specified below. The amount of ^{235}U in the fuel core is to be determined by a uniform, statistically sound sampling procedure, proposed by the Contractor and approved by the Laboratory. The weight of each core shall be measured and recorded to within 0.01 g along with the calculated value of the ^{235}U content. Fuel content may be confirmed by the Laboratory by the use of reactivity measurements.

3.3.1.1 Fuel plates for fuel elements -- Each fuel plate shall contain 17.9 ± 0.35 g of ^{235}U .

3.3.1.2 Fuel plates for shim rod fuel sections -- Each fuel plate shall contain 17.9 ± 0.35 g of ^{235}U unless a smaller loading is specified in the procurement contract.

3.3.2 Homogeneity

The tolerance on the surface density in g/cm^2 of ^{235}U within the maximum fuel core outline shall be $+27 -100\%$ of the nominal value of that spot as measured for any 5/64-inch (2.0-mm) -diam spot. The tolerance on an average ^{235}U surface density within the minimum core outline shall be $\pm 12\%$ of the nominal value. In the area between the maximum and minimum core outlines, the variation of the average shall be within $\pm 12\% -100\%$ of the specified value. These averages shall be measured for a surface area 5/64-inch (2.0-mm) wide and $\sim 1/2$ -inch (12.7-mm) long, or over an equivalent circular surface area of diameter 7/32-inch (5.6 mm). The scans shall be tangent one to the other.

3.4 Dimensional Requirements

3.4.1 Each fuel plate shall be in conformance with the dimensions specified on the drawings referenced in Section 2.0. Preassembly fuel plate width and curvature shall be chosen so that they will be compatible with the value specified for the fuel element or shim rod fuel section in its assembled condition.

3.5 Surface Conditions

3.5.1 Surface Finish

The surface of the finished fuel plates shall be smooth and free of gouges (scratches, pits, or marks) in excess of 0.005 in. (0.127 mm) in depth.

Dents in the fuel plate shall not exceed 0.012 in. (0.3 mm) in depth or 0.25 in. (6.4 mm) in diameter. In the dogboning zone, if there is evidence of dogboning in the plates, surface defects not deeper than 0.003 in. (0.076 mm) are acceptable. No degradation of the fuel plates beyond these limits shall be permitted.

3.5.2 Surface Contamination

The Contractor shall verify that the surface contamination of the fuel plates is less than five micrograms of uranium per square foot (5 μg per 929 cm^2).

3.5.3 General Cleanliness

Precautions must be taken to maintain a high standard of cleanliness during fabrication and assembly to insure that no foreign materials or corrosion products are present in the finished elements. All surfaces must be free from moisture, dirt, oil, organic compounds, scale, graphite, or other foreign matter. Use of graphite for marking purposes is prohibited. The use of abrasives for cleaning the fuel plates or for any other purposes is prohibited, as is any procedure which removes more than 0.0004 in. (0.01 mm) of aluminum from the surface of the finished fuel plates. If any chlorine-bearing material is used for cleaning, it must be completely removed following the cleaning procedure before any elevated temperature treatment or welding. Moreover, the finished element must be free of any chlorine-bearing material.

3.6 Plate Identification

After rolling, a serial number shall be placed on each fuel plate for identification as to U_3Si_2 powder lot number and compact number using procedures approved by the Laboratory. The identification number shall be over the unfueled region of the plate, as shown on the drawings referenced in Section 2.0.

4.0 QUALITY CONTROL AND QUALITY ASSURANCE REQUIREMENTS

4.1 Responsibility

Unless otherwise specified, the Contractor shall be responsible for the performance of all tests and inspections required prior to submission to the Laboratory of any fuel plate for acceptance. However, the performance of such tests and inspections is in addition to, and does not limit, the right of the Laboratory to conduct such other tests and inspections as the Laboratory deems necessary to assure that all fuel plates are in conformance with all requirements of this specification. The Contractor may use either his own or any commercial laboratory acceptable to the Laboratory. Records of all tests and examinations shall be kept by the Contractor, complete and available to the Laboratory as specified in the contract or purchase order.

4.2 Quality Verification Plan

The Contractor shall develop and submit for approval with his bid a quality verification plan fulfilling the requirements of ANL Document AQR-001.

4.3 Prequalification Inspection

Before the contract is awarded, the Laboratory may send a representative to the Bidder's plant to judge the capability of the Bidder to carry out the provisions of the contract and the adequacy of the steps to be taken in executing the quality verification program.

4.4 Manufacturing Procedures

A written general description of the manufacturing procedures, shop drawings, detailed cleaning procedures, and inspection report forms shall be

Table 3. Quality Conformance Inspection

Test	Requirements	Acceptance Criteria	Test Method
Dimension	3.4	4.7.4	4.8.1
Fuel Core Location	3.2.2	4.7.2.1	4.8.2
Cladding and Core Thickness Determination	3.2.3	4.7.2.2	4.8.4
Cladding Temper	3.2.4	4.7.2.3	4.8.5
Metallurgical Bond	3.2.5	4.7.2.4	4.8.6
Surface Finish	3.5.1	4.7.5	4.8.7
Surface Contamination	3.5.2	4.7.5	4.8.8
Cleanliness	3.5.3	4.7.5	4.8.9
Fuel Loading	3.3.1	4.7.3.1	4.8.10
Homogeneity	3.3.2	4.7.3.2	4.8.3

supplied to the Laboratory by the Contractor for approval prior to initiation of any fabrication, and any subsequent changes in the above shall be supplied to the Laboratory for approval prior to their use.

4.5 Quality Conformance Inspections

The tests listed in Table 3 are to be performed by the Contractor and documented in accordance with the requirements of the specification. The Laboratory may observe the performance of these tests and/or audit the documentation of same at any point during the procedure.

4.6 Extent of Inspection

The tests listed in Table 3 are to be performed for each fuel plate except for the following:

Cladding and core thickness determination - At least one randomly-selected plate from each group of 100 plates processed is to be tested.

4.7 Acceptance Criteria

Acceptance and/or rejection criteria for the technical requirements (Section 3.0) are as follows:

4.7.1 Materials

All materials are to be in accordance with the requirements of this specification and the specified standards without exception.

4.7.2 Mechanical

4.7.2.1 Fuel core location -- The fuel core location shall be in accordance with the requirements of Paragraph 3.2.2.

4.7.2.2 Cladding and core thickness determination -- If any plate fails to meet specifications, two more plates randomly selected from the same group of 100 plates are to be sectioned for thickness measurements. If either of the latter two plates fails to meet specifications, all plates manufactured or in the process of manufacture since the last acceptable sectioning shall be rejected.

4.7.2.3 Cladding temper -- Cold reduction shall be in accordance with the requirements of Paragraph 3.2.4.

4.7.2.4 Metallurgical bond -- Plates exhibiting visible raised or blistered areas shall be rejected. Plates exhibiting nonbond indications greater than 2 mm in diameter on the ultrasonic scan record shall

be rejected. Plates showing delamination of the cladding and frame during the bending test shall be rejected.

4.7.3 Physical Properties

4.7.3.1 Fuel loading -- The loading shall, without exception, be within the specified tolerances.

4.7.3.2 Fuel core quality -- Homogeneity and fuel location will be acceptable if they fall within the limits specified in Paragraphs 3.2.2 and 3.3.2.

4.7.4 Dimensional Requirements

All dimensions must be within the tolerances shown on the drawings unless a deviation from these dimensions is granted by the Laboratory.

4.7.5 Surface Conditions

All requirements of the specification are to be met; no non-conformance will be allowed.

4.7.6 Plate Identification

Markings are to be made exactly as approved by the Laboratory.

4.8 Test Methods

All test methods and procedures must be submitted by the Contractor and approved by the Laboratory prior to actual fabrication. Any subsequent changes in the procedures must also be supplied for approval by the Laboratory prior to their use. The granting of any approval or approvals by the Laboratory shall not be construed to relieve the Contractor in any way or to any extent from the full responsibility for delivering fuel plates conforming to all requirements of this specification.

4.8.1 Dimensional

The Contractor shall furnish a written procedure for dimensional examination of the fuel plates. This procedure must be approved by the Laboratory.

4.8.2 Fuel Core Location

The Contractor shall furnish a written procedure for fluoroscopic and/or x-ray examination of the fuel plates. This procedure must be approved by the Laboratory.

4.8.3 Fuel Core Quality

The Contractor shall furnish written procedures for radiography and scanning of the plates. These procedures must be approved by the Laboratory.

4.8.4 Cladding and Core Thickness Determination

Each plate to be examined shall be completely sectioned according to Fig. 1 of this specification.

4.8.5 Cladding Temper

The Contractor shall furnish a written procedure for the Laboratory's approval.

4.8.6 Metallurgical Bond

The Contractor shall furnish a written procedure for the Laboratory's approval.

4.8.7 Surface Finish

The Contractor shall furnish a written procedure for the Laboratory's approval.

4.8.8 Surface Contamination

The Contractor shall furnish a written procedure for the Laboratory's approval.

4.8.9 Cleanliness

The Contractor shall furnish a written procedure for the Laboratory's approval.

4.8.10 Fuel Loading

The Contractor shall furnish a written procedure for the Laboratory's approval.

4.9 Documents

4.9.1 Two certified copies of inspection and test records covering the items listed below shall be supplied the Laboratory. A duplicate copy of the records of each fuel assembly shall be included in the shipping container with the fuel plates.

4.9.1.1 The serial number of each plate within each unit, the calculated fuel loading of uranium and ^{235}U in each fuel plate, and the total calculated loading of U_3Si_2 and ^{235}U . The fuel loadings are to be as specified in Paragraph 3.3.1 of this specification.

4.9.1.2 Data on the examination of the surfaces of the fuel plates as specified in Section 3.5 of this specification.

4.9.1.3 Data regarding the location of fuel cores as prescribed in Paragraph 3.2.2 of this specification.

4.9.1.4 Results of the cladding and core thickness determination as specified in Paragraph 3.2.3 of this specification.

4.9.1.5 Results of the inspection of bonding in each fuel plate examined as specified in Paragraph 3.2.5 of this specification.

4.9.1.6 A certified report of the chemical and isotopic analysis of each U_3Si_2 lot as specified in Paragraph 3.1.2 of this specification.

4.9.1.7 A certified report of the chemical analysis of all other materials used in the fabrication of the fuel plates as specified in Section 3.1 of this specification.

4.9.1.8 A certificate of compliance for each fuel plate unit stating that the element meets all requirements of the contract.

4.9.2 Manufacturing Procedures

The Contractor shall submit to the Laboratory three copies of the manufacturing procedures required by Paragraph 3.2.1 and Section 4.4.

4.9.3 Test Procedures

The Contractor shall submit to the Laboratory three copies of the test procedures required by Section 4.8.

4.9.4 Quality Verification plan

The Contractor shall submit to the Laboratory with the bid three copies of the quality verification plan required by Section 4.2.

Appendix K-5

NOTIONAL SPECIFICATION FOR MTR FUEL PLATES/TUBES AT URANIUM DENSITIES UP TO 1.6 g/cm³

B. HICKEY

Dounreay Nuclear Power Development Establishment,
United Kingdom Atomic Energy Authority,
Thurso, Caithness,
United Kingdom

Abstract

Various representative conditions from the MTR range of specifications are presented. At densities up to 1.2 g U/cc the manufacturing route can be by the traditional casting and rolling process. At densities greater than 1.2 g U/cc the manufacturing route utilises the U₃O₈/Al cermet process.

Included are various representative conditions culled from the MTR range of specifications which might be of interest to a prospective customer.

Note that at densities up to 1.2 g U/cc the manufacturing route can be by the traditional casting and rolling process. At densities greater than 1.2 g U/cc the manufacturing route utilises the U₃O₈/Al cermet process.

- | | | |
|----|-----------------------|---|
| 1. | U235 content | $\pm 2\%$ of nominal value specified. |
| 2. | U Homogeneity | Central region, $\pm 10\%$ (5 mm dia); dogbone, $+ 20\%$ to $- 100\%$ (5 mm dia). |
| 3. | Cladding-material | Can be to 1050 (MTR2) or 6082 (Al 1% Mg). |
| | thickness | The cladding thickness shall be checked by destructive examination to ensure (95% level) that the drawing requirements are satisfied. |
| | bond | The core/clad bond shall be checked by heating each fuel plate/tube to $500^{\circ}\text{C} \pm 10^{\circ}\text{C}$ for 20 minutes. After cooling the plate shall be examined for blisters which, if found, will cause rejection. |
| 4. | Surface contamination | Each finished fuel plate/tube shall be examined for alpha contamination. Any contamination greater than 3.2×10^{-5} grammes/m ² of Uranium (3×10^{-6} g/ft ²) will cause rejection. |
| 5. | Surface finish | Any plate/tube which has a pit, scratch or other blemish greater than 0.076 mm deep over the fuelled area shall be rejected. |

6. Tubes manufactured from fuel plates by welding

The manufacturer shall ensure by sampling (21 samples/tube, 1 tube in 50) that the average weld strength in any fuel tube will be not less than 16.2 kg/cm (350 lbs/in) and that no sample will be less than 27 kg/cm (150 lb/in).
7. Fuel boxes assembled by roll swaging

The manufacturer shall ensure by sampling that the equipment used to swage the joint is normally capable of producing a joint strength of 45 kg/cm (250 lbs/in) and that no joint has a pull out strength of less than 27 kg/cm (150 lbs/in).

Appendix K-6

FABRICATION OF MEDIUM ENRICHED URANIUM FUEL PLATE FOR KUCA CRITICAL EXPERIMENT

Design, fabrication, inspection and transportation

K. KANDA, Y. NAKAGOME, T. SAGANE, T. SHIBATA

Research Reactor Institute,

Kyoto University,

Osaka, Japan

COMPAGNIE POUR L'ETUDE ET LA REALISATION

DE COMBUSTIBLES ATOMIQUES (CERCA)

Créteil, France

Abstract

The design, fabrication, inspection and transportation of fuel elements with MEU UAl_x -Al fuel for the C-core of the KUCA critical facility at the Kyoto University Research Reactor Institute are summarized. The C-core is a mockup of the annular coupled-core design for the 30 MW Kyoto University High Flux Reactor. The fuel elements were fabricated in France by CERCA.

INTRODUCTION

Due to mutual concerns in the USA and Japan about the proliferation potential of highly-enriched uranium (HEU), a joint study program⁽¹⁾ was initiated between Argonne National Laboratory (ANL) and Kyoto University Research Reactor Institute (KURRI) in 1978. In accordance with the reduced enrichment for research and test reactor (RERTR) program, the alternatives were studied for reducing the enrichment of the fuel to be used in the Kyoto University High Flux Reactor (KUHF²).⁽²⁾ The KUHF² has a distinct feature in its core configuration : it is a coupled-core. Each annular shaped core is light-water-moderated and placed within a heavy water reflector with a certain distance between them. The phase A reports of the joint ANL-KURRI program independently prepared by two laboratories in February 1979,^(3,4) concluded that the use of medium-enrichment uranium (MEU, 45%) in the KUHF² is feasible, pending results of the critical experiments in the Kyoto University Critical Assembly (KUCA)⁽⁵⁾ and of the burnup test in the Oak Ridge Research Reactor (ORR).⁽⁶⁾

An application of safety review (Reactor Installation License) for MEU fuel to be used in the KUCA was submitted to the Japanese Government

TABLE 1. SPECIFICATIONS OF MEU FUEL PLATES

plate no.	inner fuel plate					outer fuel plate				
	width of	width of	curvature	Uranium	U-235	width of	width of	curvature	Uranium	U-235
	fuel (mm)	meat (mm)	radius (mm)	(gr)	(gr)	fuel (mm)	meat (mm)	radius (mm)	(gr)	(gr)
1	48.70	39.50	54.4	20.00	8.99	61.16	51.96	133.3	25.96	11.67
2	52.68	43.48	58.2	21.64	9.72	63.15	53.95	137.1	26.94	12.11
3	56.66	47.46	62.0	23.67	10.64	65.14	55.94	140.9	28.51	12.81
4	60.64	51.44	65.8	25.67	11.54	67.13	57.93	144.7	28.99	13.00
5	64.62	55.42	69.6	27.57	12.39	69.12	59.92	148.5	30.12	13.54
6	68.60	59.40	73.4	29.57	13.29	71.11	61.91	152.3	31.04	13.91
7	72.58	63.38	77.2	31.87	14.21	73.10	63.90	156.1	31.92	14.36
8	76.56	67.36	81.0	34.26	15.41	75.09	65.89	159.9	32.85	14.76
9	80.54	71.34	84.8	36.18	16.24	77.08	67.88	163.7	33.89	15.23
10	84.51	75.31	88.6	38.27	17.16	79.07	69.87	167.5	35.55	15.99
11	88.49	79.29	92.4	40.34	18.10	81.06	71.86	171.3	36.49	16.41
12	92.47	83.27	96.2	43.09	19.26	83.05	73.85	175.1	37.10	16.61
13	96.45	87.25	100.0	44.49	19.98	85.04	75.84	178.9	38.25	17.10
14	100.43	91.23	103.8	46.74	20.89	87.03	77.83	182.7	39.68	17.76
15	104.41	95.21	107.6	48.30	21.64	89.02	79.82	186.5	40.69	18.27
16	-	-	-	-	-	91.01	81.81	190.3	41.45	18.63
17	-	-	-	-	-	93.00	83.80	194.1	42.69	19.11

enrichment = 44.87 w%, plate length = 650 mm, meat length = 600 mm

in March 1980, and a license was issued in August 1980. Subsequently, the application for 'Authorization before Construction' was submitted and was authorized in September 1980. Fabrication of MEU fuel elements for the KUCA experiments by CERCA in France was started in September 1980, and was completed in March 1981. The critical experiments in the KUCA with MEU fuel were started on a single-core in May 1981 as a first step. Those on a coupled-core will follow.

The first critical state of the core using MEU fuel was achieved at 3:12 p.m. in May 12, 1981. After that, several experiments were performed as follows : the reactivity effects of the side-plates containing boron burnable-poison, the void reactivities, the temperature coefficients, neutron flux distributions and so on.

FABRICATION OF MEU FUEL ELEMENTS

MEU fuel elements for the KUCA critical experiments were fabricated by Compagnie pour l'Etude et la Réalisation de Combustible Atomiques (CERCA) in France. One fuel element consists of two side-plates and either fifteen or seventeen curved fuel plates. The fuel plate, side-plates, and fuel elements are illustrated in Figs. 2 and 3. The total number of fuel plates fabricated is 294, of 32 different widths. The fuel plates were fabricated by the picture frame technique. The dimension and uranium content of each fuel plate are listed in Table 1.

MEU fuel was supplied from the United States Department of Energy (USDOE) to CERCA for Kyoto University. The nominal enrichment is 45.0 ± 0.4 w/o. The chemical form of the meat (fuel core) is UAl_x -Al dispersion, and the density is about 4.0 g/cm^3 . The Uranium density of the fuel core is 1.69 g/cm^3 and ^{235}U density is 0.7575 g/cm^3 .

The boron loaded side-plates were also fabricated by the picture frame technique. The purity of natural boron contained in the side-plates is more than 98 %.

1. Fabrication Procedures

The fabrication process of the MEU fuel plates is shown in Fig. 1, and the fabrication procedure is as follows ;

- (1) fabrication of U-Al alloy by melting uranium metal and aluminum,
uranium content of UAl_x : 69 ± 3 w/o
- (2) crushing and grinding UAl_x into powder, and sieving,
 UAl_x grain size : $< 40 \text{ } \mu\text{m}$ (40 w/o maximum) and
40 -125 μm (the rest)

Cores

melt and cast UAl_x

crush and grinding into powder

sieving, homogenizing

weighing and blending UAl_x
and Al powders

inspect for U-235 content
and dimensions

Frame

Al sheet cutting into strips

rolling of strip

punch frame

inspect for dimensions

↓
form sandwich (core + frame + cover)

hot rolling

mark identification number

cold rolling

annealing, roller leveling,
dimension checking

cut to size

INSPECTION

- # ultrasonic test
- # radiograph examination
- # fuel homogeneity
- # dimension in flat state
- # surface defects
- # surface contamination
- # cladding thickness (micro-graphs)

↓
curvature of plates

INSPECTION

- # cleanliness
- # surface defects
- # dimension after curving

↓
packaging

shipment

FIG. 1. Fabrication process of MEU fuel plates.

- (3) weighing and blending the UAl_x and aluminum powders for each fuel compact,
- (4) compacting the blended powder,
uranium concentration in the fuel compacts : 42 w/o maximum
- (5) assembling the fuel compact into the aluminum frame and cover plates,
- (6) cladding by hot and cold rolling, and marking,
- (7) annealing at 425 °C for 1 hour to test for blistering,

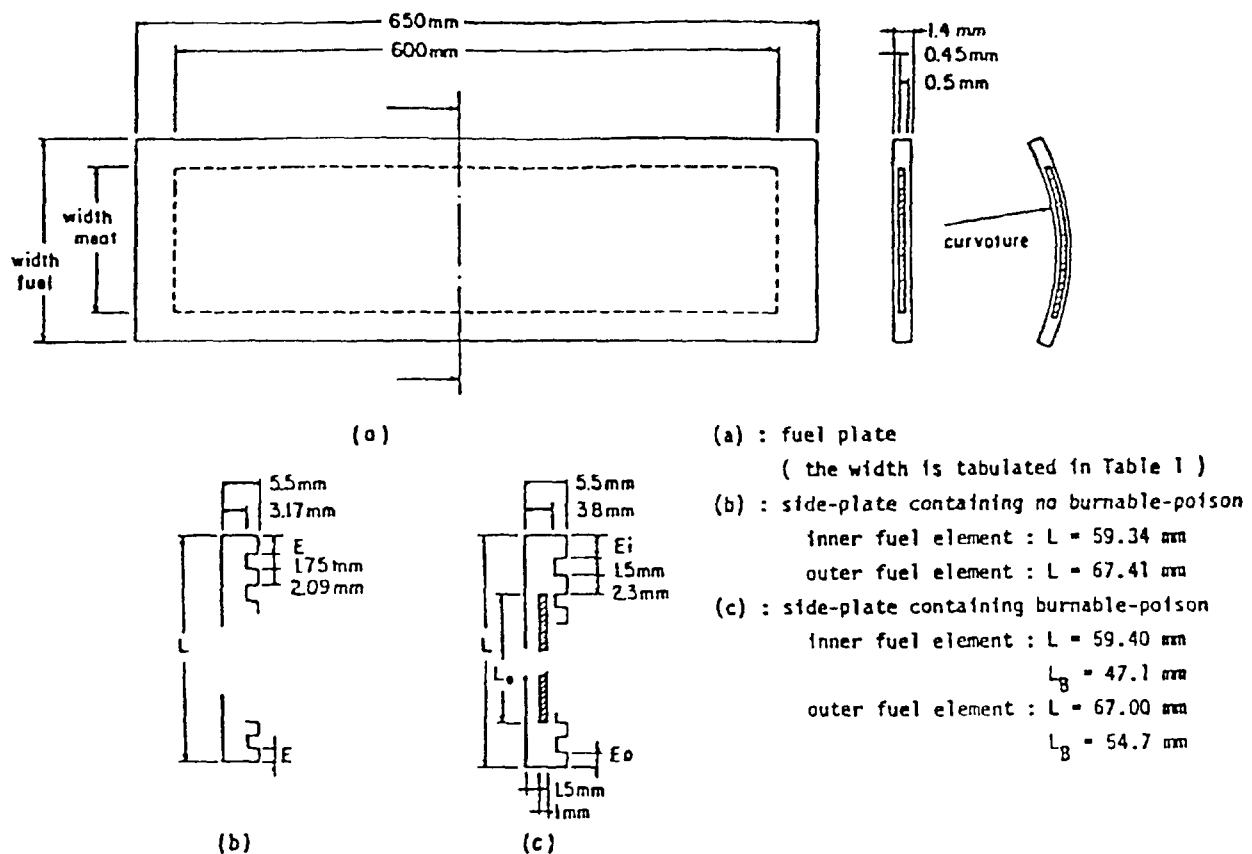


FIG. 2. Illustration of the fuel plates and side-plates.

- (8) cold rolling to specified thickness,
- (9) cutting the plates to specified sizes,
- (10) chemically etching the plate surface,
- (11) curving the plates,
- (12) final cleaning and inspection,
- (13) packaging for shipment.

The fabrication procedure of the boron loaded side-plates is as follows ;

- (1) weighing and blending the natural boron and aluminum powders,
weight of natural boron : $640 \text{ mg} \pm 5 \%$ for outer elements and
 $570 \text{ mg} \pm 5 \%$ for inner elements
boron grain size : $80 \mu\text{m}$ maximum
- (2) assembling the blended powder and silver markers into the aluminum frame and cover plates,
- (3) cladding by rolling,
- (4) annealing at 425°C for 1 hour,
- (5) roller leveling to specified thickness,
- (6) cutting the plates and machining with grooves and engraving to specified sizes,

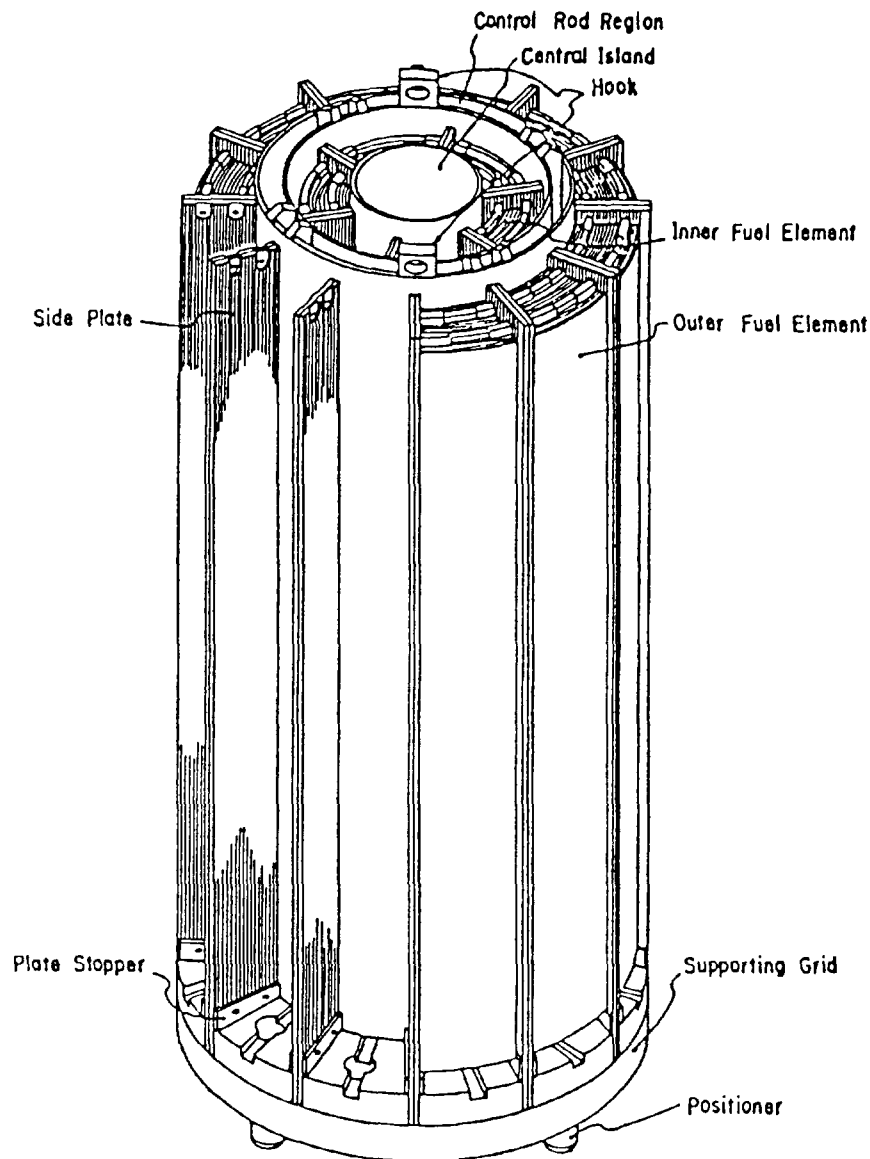


FIG. 3. View of assembled fuel elements.

- (7) chemically etching the plate surface,
- (8) packaging for shipment.

2. Inspection

The actual inspection of the fabrication of MEU fuel elements was performed by Compagnie Générale des Matières Nucléaires (COGEMA) in France, which was chosen by Kyoto University to be the acting inspector. The inspectors of Kyoto University visited CERCA three times - at the beginning of fabrication, mid and final stages -, then Kyoto University authorized the inspection results reported by COGEMA. The Science and Technology Agency of the Japanese Government further inspected the MEU fuel elements in Japan.

The following items were considered in the inspection of the fuel plates ; uranium enrichment from the supplier's report, uranium and aluminum purities by chemical analysis, ^{235}U content in each fuel plate by the gamma-ray counting examination, fuel homogeneity by the X-ray absorption technique, cladding bond integrity by ultrasonic testing, cladding and dog bone thickness by destructive testing, dimension, surface defects, and surface contamination by the alpha counting method.

The inspection items for the side-plates were as follows ; boron and aluminum purities by chemical analysis, boron content in each side-plate by weighing natural boron, boron core location by radiograph examination, cladding bond integrity by ultrasonic testing, cladding and core thickness by destructive testing, dimension, surface condition, and surface contamination by the alpha counting method.

The summary of the inspections for fuel plates and structural parts is shown in Table 2.

The inspection report and records such as X-ray absorption diagrams, radiographs, ultrasonic test diagrams and micro-photographs taken in the destructive testing, were delivered to Kyoto University.

3. Transport of MEU Fuel Elements

MEU fuel elements were transported from CERCA in France to KURRI in Japan as a Type A Fissile Class II Package. Four FS-13 containers were used. These package were certified to satisfy the IAEA requirements of the package design by Ministere des Transports (French Government), Department of Transportation (Government of the United States) and Science and Technology Agency (Japanese Government).

The transport between France and Japan was performed by a cargo plane via Alaska.

TABLE 2. SUMMARY OF THE INSPECTIONS FOR MEU FUEL PLATES AND STRUCTURAL PARTS

(a) MEU fuel plates inspection

Inspection item	Inspection Method	Judgement [*]	Sample Quantity	Report and/or Certificate to be submitted to KU
Material - Uranium Enrichment	Confirmation of USDOE certificate	45.0 ± 0.4 w/o	One per lot	USDOE certificate
Impurities - Aluminum	Confirmation of mill sheet Confirmation of mill sheet	KUCA-spec.-Appendix B KUCA-spec.-Appendices C,E	One per lot One per melting lot	Vendor's mill sheet Vendor's mill sheet
U-235 content in the core	U-235 gamma counting	KUCA-spec.-Appendix D	Each fuel core	U-235 content Core weight Record of the gamma counting
Radiograph examination	Inspection of the fuel core location on the radiograph by matching a gauge Inspection of the existence of foreign substances	Drawing No.1375-001 and KUCA-spec.-Appendix F White spots on the radiographs must be smaller than 0.5 mm dia.	Each fuel core	Record of the fuel core location (Good or No good, or measured values) Record of the white spots radiographs
Cladding bond integrity	Ultrasonic testing	Any defect must be smaller than 1.5 mm dia.	Each fuel plate	Test diagrams
Homogeneity	X-ray absorption	Maximum permissible variation of the uranium concentration in any 10 mm ² surface is +20% (+ 30% on the dog-bone area) relatively to the average loading.	Each fuel plate	Record of X-ray absorption

TABLE 2. (cont.)

(a) MEU fuel plates inspection (cont.)

Inspection item	Inspection Method	Judgement [*]	Sample Quantity	Report and/or Certificate to be submitted to KU
Dimension - Length - Width - Thickness - Curvature	By callipersquare By micrometer (3 points) By micrometer (5 points) By gauge (3 points)	$650 \pm 0.44 \text{ mm}$ Drawing No.1375-001 $1.45 \pm 0.05 \text{ mm}$ Drawing No.1375-002	Each fuel plate	Measured value
Destruction testing	Taking five sections on each fuel plate, which are observed under a light microscope	Local minimum cladding thickness : 0.35 mm Average cladding thickness : $0.45 \pm 0.08 \text{ mm}$	3 fuel plates	Measured value Micro-photographs (magnification : 25)
Appearance - ID No. and U-cut - Surface defects -Surface cleanliness	Visual inspection Visual inspection and light section microscope measurements Visual inspection	ID No. and U-cut must be confirmed. Maximum depth must be 0.12 mm on the core area, and 0.3 mm outside the core limits. Must be clean	Each fuel plate	Results of the inspection Results of the inspection (Good or No good, or measured value) Results of the inspection (Good or No good)
Surface contamination	Alpha counting	Less than $1 \mu\text{gU-235/dm}^2$	10 %	Measured value

* Appendices and drawings are not attached in this document.

TABLE 2. (cont.)

(b) Structural parts inspection

Inspection item	Inspection Method	Judgement [*]	Sample Quantity	Report and/or Certificate to be submitted to KU
Material - Boron purity - Aluminum - Stainless Steel	Confirmation of mill sheet Confirmation of mill sheet Confirmation of mill sheet	More than 98 % KUCA-spec,- Appendix C Z6CN 18-09	One per lot One per melting lot One per lot	Vendor's mill sheet Vendor's mill sheet Vendor's mill sheet
Boron content in the side plate	Weighing	KUCA-spec.- Appendix D	Each side plate	B-10 content Total born content
Radiograph examination	Inspection of the boron core location on the radiograph by matching a gauge	Drawing No.1375-013 and -014	Each side plate	Record of the boron core location (Good or No good, or measured values) Radiographs
Cladding bond integrity (Side plate)	Ultrasonic testing	Maximum area of individual bonding defects : 100 mm ² Maximum length of defect between core and frame : 50 mm total per plate	Each side plate	Ultrasonic test diagrams
Dimension	By callipersquare or micrometer	Drawing No.1375-011,-012 -013,-014,-015,-016 and -017	Each part	Measured value
Destruction testing	Taking three sections on a side plate, which is observed under a light microscope	Cladding thickness and core thickness : Drawing No.1375-013 and -014	One side plate	Measured value Micrographs (Magnification : 12)

TABLE 2. (cont.)

(b) Structural parts inspection (cont.)

Inspection item	Inspection Method	Judgement [*]	Sample Quantity	Report and/or Certificate to be submitted to KU
Surface condition	Visual inspection	ID No. must be confirmed	Each side plate	Results of the inspection
- ID No.				
- Surface defects	Visual inspection and light section microscope measurements	Maximum depth must be 0.25 mm.	Each side plate	Results of the inspection (Good or No good, or measured value)
- Surface cleanliness	Visual inspection	Must be clean	Each part	Results of the inspection (Good or No good)
Surface contamination	Alpha counting	Less than 1 $\mu\text{gU-235}/\text{dm}^2$	10 %	Measured value

* Appendices and drawings are not attached in this document.

REFERENCES

- (1) "Research Reactor Using Medium-Enriched Uranium", (ed. K. Kanda and Y. Nakagome), KURRI-TR-192 (1979).
- (2) SHIBATA, T., "Construction of a High Flux Research Reactor and Conversion of Kyoto University Reactor KUR to a TRIGA Type Pulsed Reactor", Research Reactor Renewal and Upgrading Program, IAEA-214 (1978) 183.
- (3) SHIBATA, T., KANDA, K., "ANL-KURRI Joint Study on the Use of Reduced Enrichment Fuel in KUHFR -- Phase A Report --", (February 15, 1979).
- (4) TRAVELLI, A., STAHL, D., SHIBATA, T., "The U.S. RERTR Program, Its Fuel Development Activities, and Application in the KUHFR", ANS Trans., 36 (1981) 92.
- (5) KANDA, K., KOBAYASHI, K., HAYASHI, M., SHIBATA, T., "Reactor Physics Experiment Using Kyoto University Critical Assembly", J. At. Energy Soc. Japan, 21 (1979) 557, in Japanese.
- (6) SHIBATA, T., TRAVELLI, A., "ANL-KURRI Joint Study on the Use of Reduced Enrichment Fuel in KUHFR -- Status Report on Phase B --", (December 12, 1980).

SPECIFICATIONS FOR FUEL ELEMENTS WITH MEU UAl_x-Al FUEL FOR THE JMTRC REACTOR

R. OYAMADA, Y. YOKEMURA, K. TAKEDA

Oarai Research Establishment,
Japan Atomic Energy Research Institute,
Oarai-machi, Ibaraki-ken,
Japan

Abstract

The JMTRC is a pool-type critical facility operated as a neutronics mockup for the 50 MW JMTR. Prior to conversion of the JMTR to MEU UAl_x-Al fuel, extensive experiments were performed in the JMTRC to validate neutronics codes and obtain nuclear characteristics for the JMTR MEU core.

Specifications for the JMTRC elements with MEU UAl_x-Al fuel are summarized along with the sampling rates for inspection of the materials, parts, and finished elements.

1. Introduction

The JMTRC; a 100 W swimming pool type critical facility, moderated and cooled by light water, and utilizing 90 % enriched uranium-aluminum alloy fuel meat in the ETR-type element, has been operated as a neutronics mock-up for the JMTR (50 MW).

Prior to the JMTR core conversion to the MEU fuel, extensive experiments using the JMTRC are scheduled to validate neutronics calculation code system used for analyzing the JMTR MEU core, and to obtain nuclear characteristics for the JMTR MEU core.

The application of safety review ("Reactor Installation Modification License") for the MEU fuel to be used in the JMTRC was submitted to the Japanese Government in July 1981 and the license was issued in March 1982. Subsequently, the application for "Authorization before Design and Construction Method" was authorized in September 1982.

Fabrication of the MEU fuel elements by NUKEM in the FRG was started in September 1982, and the finished elements are scheduled to be delivered to the JMTRC site in August 1983.

2. Fabrication of MEU Fuel Elements

Fabrication of 31 MEU fuel elements for the JMTRC experiment are in progress in NUKEM.

Content of U-235 per fuel element, uranium density and number of elements to be made are as follows:

Kind of element	^{235}U Content (g/element)	Uranium Density (g/cm^3)	Number
Standard fuel element A	310.0 ± 5.6	1.6	8
Standard fuel element B	280.0 ± 5.0	1.4	10
Standard fuel element C	250.0 ± 4.5	1.3	4
Special fuel element B	280.0 ± 5.0	1.4	2
Special fuel element C	250.0 ± 4.5	1.3	2
Control rod fuel section	205.0 ± 3.7	1.6	5
Total			31

In order to simulate equilibrium core of the JMTR, three kinds of standard fuel elements (A, B, C) and two kind of special fuel elements (B, C) are being fabricated.

Special fuel elements are able to attach and remove the central 5 plates of 19 plates, and they are different from standard fuel element in the structure of the handle at fuel element top.

The standard fuel elements and the control rod fuel sections are illustrated in Figs. 1 and 2, respectively. The structure of the special fuel elements is almost the same as that of the standard fuel elements. The fuel plates were fabricated by the picture frame technique and attached to the side plates by the rollswaging technique.

Summary of the specifications for the JMTRC MEU fuels are as follows;

- ① Uranium Enrichment $45\% \pm 1\text{wt}\%$ with accuracy of $\pm 0.1\%$

② Maximum Impurities (ppm)

UAlx Powder

B = 10	Si = 2000
C = 2000	Zn = 1000
Cd = 10	
Co = 10	Others:
Cu = 80	Individual 500
Fe = 1500	Total 2500
Li = 10	
N = 500	
O = 7000	

Al Powder

B = 10	Ti = 200
Cd = 10	Zn = 300
Co = 10	
Cu = 80	Others:
Fe = 4000	Individual 500
Li = 10	Total 2500
Mg' = 150	
Si = 3000	

③ Grain Size

UAlx Powder

<150 μ m and
up to 50 wt% below 40 μ m

Al Powder

<150 μ m and
up to 80 wt% below 40 μ m

④ Bonding Defect by Ultrasonic Test

<1.0 mm in diameter over
fissile area
<2.5 mm in diameter over
outside fissile area

⑤ Inclusion on Radiograph
(>0.1 mm in diameter)

Inclusions with a diameter
smaller than 0.5 mm are
permissible except:
- 0.4 mm from front of fuel
plate
- 0.4 mm from plate number
- in roll swaged area

For these area, inclusions are
not permissible.

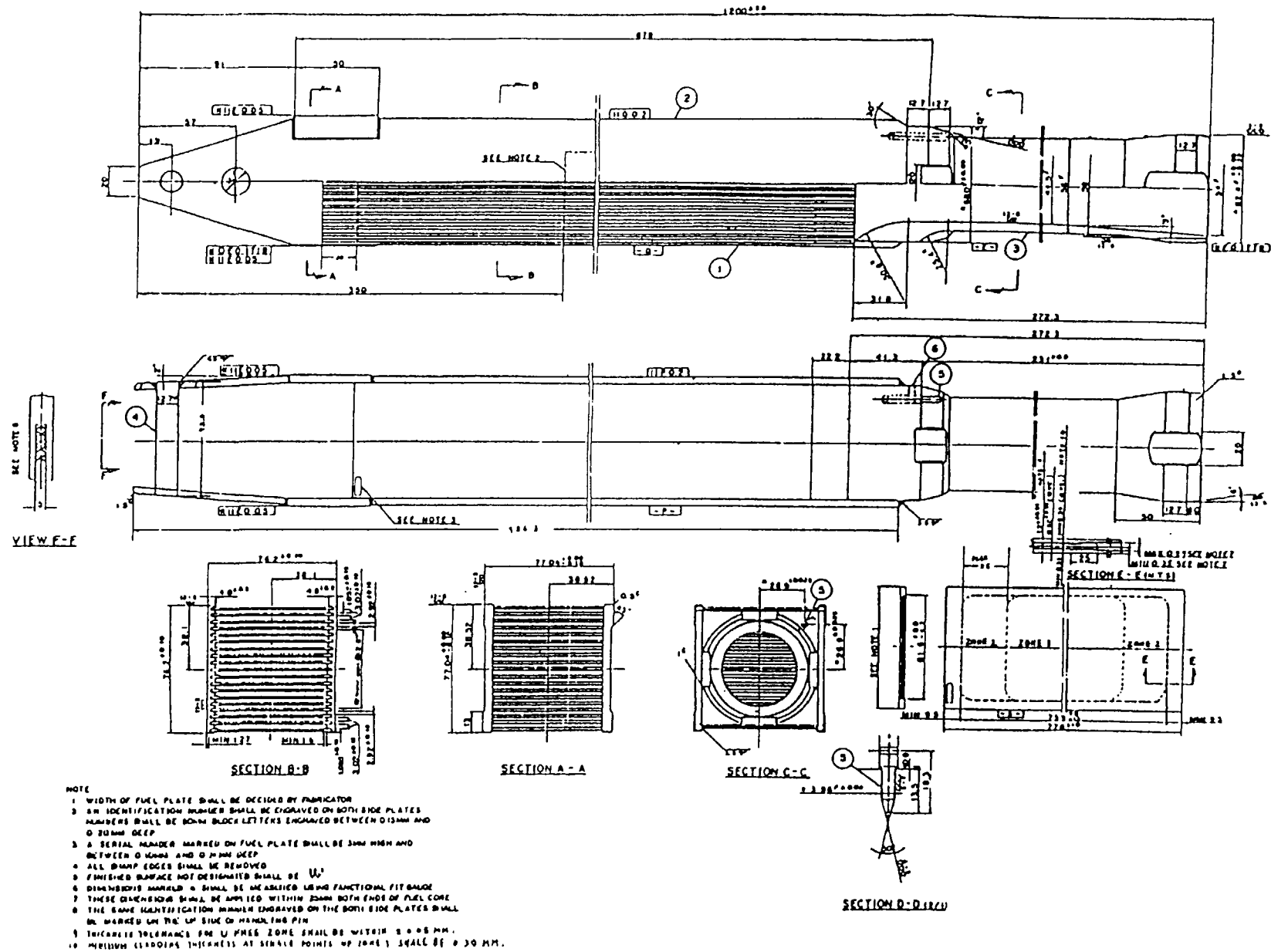
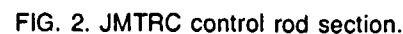


FIG. 1. JMTRC standard fuel element.



- ⑥ Uranium Distribution ± 10 % of average
(+20/-100 % of average for dog bone area)
- ⑦ Surface Contamination ≤ 10 μg of uranium per 900 cm^2
- ⑧ Surface Defect $\leq 80\text{ }\mu\text{m}$ deep over fissile area
 $\leq 200\text{ }\mu\text{m}$ deep over outside fissile area
- ⑨ Void Content in Core 4 to 11 vol. %

3. Inspection

The sampling rates in inspection for the materials, the parts and the finished elements are shown in the following table.

Sampling rate in inspection

	Inspection Item	Fabricator	Inspector		Approval by JAERI*	Remarks
		Sampling Rate	Sampling Rate	Document		
U-metal	Isotopic analysis	1 / batch		○		U-235 enrichment
	Chemical analysis	1 / batch		○		Composition and impurities
UAlx powder	Total U concentration	1 / batch		○		
	Chemical analysis	1 / batch		○		Composition and impurities
	Particle size	1 / batch		○		
Al powder	Chemical analysis	1 / batch		○		Composition and impurities
	Particle size	1 / batch		○		
Structural material	Chemical analysis	each material		○		Composition and boron equivalent
	Mechanical properties	each material		○		
Fuel core	U-235 content	100 %		○	need	
	X-ray diffraction	1 / batch		○		

* For a detailed description of inspection and examination method

Sampling rate in inspection (Continued)

	Inspection Item	Fabricator	Inspector		Approval by JAERI*	Remarks
		Sampling Rate	Sampling Rate	Document		
Fuel plate	Loading of U and U-235			○	need	by document
	Blister test	100%		○		
	Ultrasonic test	100%	10%	○	need	
	Fluoroscopy	100%		○		
	Radiography	100%	10%	○		Film check
	U distribution test	100%	10%	○	need	
	Dimensional inspection	100%	10%	○		100% sampling for removal fuel plates
	Surface contamination	100%	10%	○	need	
	Plate inspection	100%	100%	○	need	Visual inspection
	Cladding and fuel core thickness inspection	**	see 3.3.8	○	need	
	Void content rate	1/batch		○	need	
Fuel element	Dimensional inspection	**	100%	○		
	Water gap measurement	100%	10%	○	need	

* For a detailed description of inspection and examination method.

** According to fabricator's standard.

Sampling rate in inspection (Continued)

	Inspect-on Item	Fabricator	Inspector		Approval by JAERI*	Remarks
		Sampling Rate	Sampling Rate	Document		
	Pull test			○		
	Surface contamination	**	100%	○	need	
	Prepacking inspection	100%	100%	○		Visual inspection
	Loading of U and U-235			○		by document
	Weight of fuel element	100%		○		
	Attaching and removing	100%	100%	○		For special fuel elements
	Inspection of fuel plate					
	Attaching and removing	100%	100%	○		same as above
	Inspection of dummy fuel plates					

* For a detailed description of inspection and examination method.

** According to fabricator's standard.

SUMMARY OF SPECIFICATIONS FOR CANADIAN ENRICHED U-AL PIN-TYPE FUEL

R.D. GRAHAM

Reactor Technology Branch,
Chalk River Nuclear Laboratories,
Atomic Energy of Canada Limited,
Chalk River, Ontario,
Canada

Abstract

A summary is presented of the general specifications which apply to the fabrication of the fuel currently used in the NRX and NRU reactors at the Chalk River Nuclear Laboratories, Canada. The actual specifications would contain much greater detail.

The fuel is a uranium-aluminium alloy pin-type design fabricated by extrusion of the U-Al fuel cores, followed by extrusion cladding with aluminum and weld-sealing the ends of the cladding to aluminum end plugs attached to the fuel cores.

Following is a summary of the general specifications which apply to the fabrication of the fuel currently used in the NRX and NRU reactors at the Chalk River Nuclear Laboratories (CRNL), Canada. The actual specifications would contain much greater detail.

The fuel is a uranium-aluminum alloy pin-type design fabricated by extrusion of the U-Al fuel cores, followed by extrusion cladding with aluminum and weld-sealing the ends of the cladding to aluminum end plugs attached to the fuel cores. Since the uranium concentration and some dimensions vary with different applications of the fuel, these items would be specified in the drawings and purchase orders in each case.

- Aluminum
- for U-Al alloy, fuel cladding, and fuel pin end plugs: a selected form of AA 1050 alloy (minimum 99.5% Al) which specifies maximum permissible percentage of boron, cadmium, copper, and various other elements and both maximum and minimum permissible iron and silicon.
 - a certificate of chemical analysis plus a representative sample (for testing) from each heat, batch, or order to be supplied for approval prior to use.
 - bar or billets to be free of seams, slivers, cracks, grooves, inclusions or other defects which adversely affect subsequent fabrication or irradiation performance.

Uranium	<ul style="list-style-type: none"> - U-235 content: nominal* weight percent $\pm 0.5\%$ in total weight of uranium - certificates of chemical analysis of uranium and of isotopic concentration of U-235 in total uranium to be supplied for approval prior to use.
U-Al Alloy	<ul style="list-style-type: none"> - uranium content in alloy to be nominal* specified weight percent $\pm 1.0\%$ of total alloy weight.
Fuel Core	<ul style="list-style-type: none"> - length: $2743.2 \text{ mm} \pm 1.6 \text{ mm}$ - diameter: nominal* $\pm 0.04 \text{ mm}$ - U-235 to be uniformly distributed along core. <ul style="list-style-type: none"> - uranium concentration at any point to be nominal* weight percent enriched uranium $\pm 1.0\%$ of total alloy weight. - upper limit of U-235 distribution to be confirmed by gamma scanning each core. - the gamma scanning device to be calibrated using a known standard fuel core (provided) with enriched uranium content 1.0% by weight greater than nominal. - cores are to be free of blisters, porosity, inclusions, and surface defects deeper than 0.25 mm. an eddy current device calibrated using a defected standard provided. - fuel cores are to be cleaned and vacuum dried no more than 48 hours prior to extrusion cladding.
Clad Fuel Pins	<ul style="list-style-type: none"> - aluminum billets for cladding are to be cleaned, chemically conditioned (NaOH, then HNO_3) rinsed and vacuum dried no more than 12 hours prior to extrusion. - clad thickness: $0.76 \text{ mm} \pm 10\%$. cladding is to be free of laps, seams, cracks, blisters, inclusions, and any surface defect deeper than 0.10 mm. <ul style="list-style-type: none"> - each clad fuel pin to be inspected visually and using an eddy current device calibrated using a defected standard provided. - finished fuel pins are to be free of sharp bends, and bowing not to exceed 13 mm over length.
Flow Tubes	<ul style="list-style-type: none"> - material either AA 1050 aluminum (minimum 99.5%), or a selected 3.5% magnesium aluminum alloy (with specified maximum impurity levels) depending on application. <ul style="list-style-type: none"> - certificate of chemical analysis plus a representative sample (for testing) from each heat, batch or order to be supplied for approval prior to use. - dimensions as specified (vary with different applications) - inner and outer surfaces to be clean, smooth, and free from seams, slivers, laminations, grooves, cracks

*Nominal values of U-235 content, U content of alloy, and fuel diameter may differ for NRX and NRU, and for different applications within each reactor.

transverse welds, inclusions and other defects deeper than 0.13 mm.

- all tubes to be inspected using an eddy current device calibrated using a defected standard provided.

Handling, Storage, and Shipping - to comply with all applicable government and regulatory agency requirements concerning criticality, health hazards, security, and accountability.

**DETERMINATION OF CLADDING THICKNESS
IN FUEL PLATES FOR MATERIAL TEST
AND RESEARCH REACTORS (MTR)**

T. GÖRGENYI, U. HUTH
NUKEM GmbH,
Hanau, Federal Republic of Germany

Abstract

Methodology for determination of cladding thickness is described. One method involves selective measurements along a sample picking out only locations of minimum cladding thickness. In the statistical method, cladding thickness measurements are carried out in exactly 1 mm intervals on both sides of the 60 mm sample length and the results are plotted on a "probability net." Investigations have shown that the results from the statistical method confirm those of the first method.

1. Introduction

The fissile material in MTR-reactors is 20-93 % enriched uranium in the dispersed form of (UAl_x) , U_3O_8 or U_3Si_2 in aluminium.

These metal-ceramic cores of rectangular shape are sandwiched between aluminium cladding and rolled out by the so called picture frame technique to the thin (approx. 1,3 mm) fuel plates and are finally assembled to the fuel element /1/.

A simplified flow sheet for the production of MTR fuel element, (UAl_x/Al) -type) is shown in Fig. 1, and the cross-section of one fuel plate is illustrated in Fig. 2.

2. Determination of the "Cladding Thickness"

The cladding thickness of the fuel plate is of great importance for the function of the fuel plate in the fuel element, therefore, it is strictly specified. A fuel plate for this specification test is selected

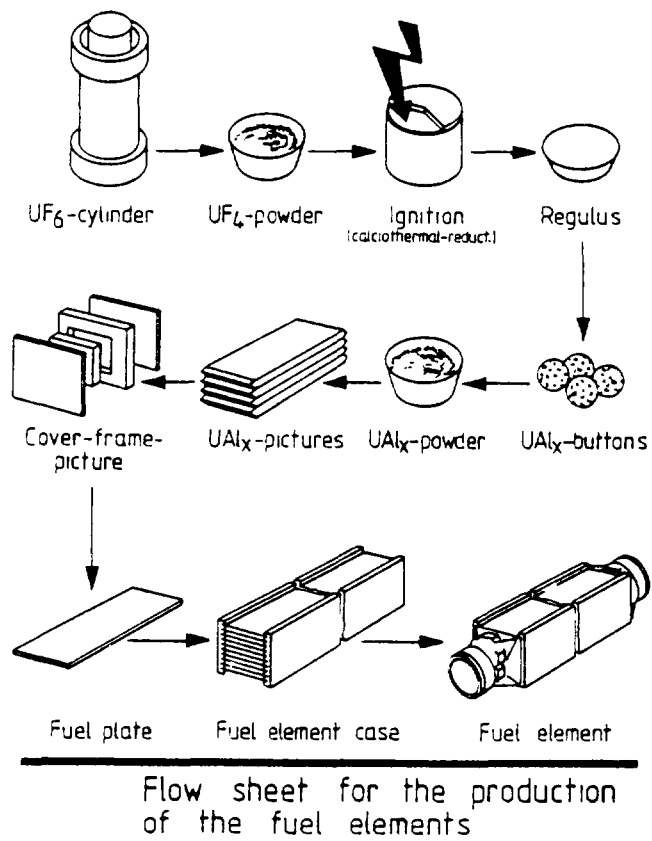


Fig. 1

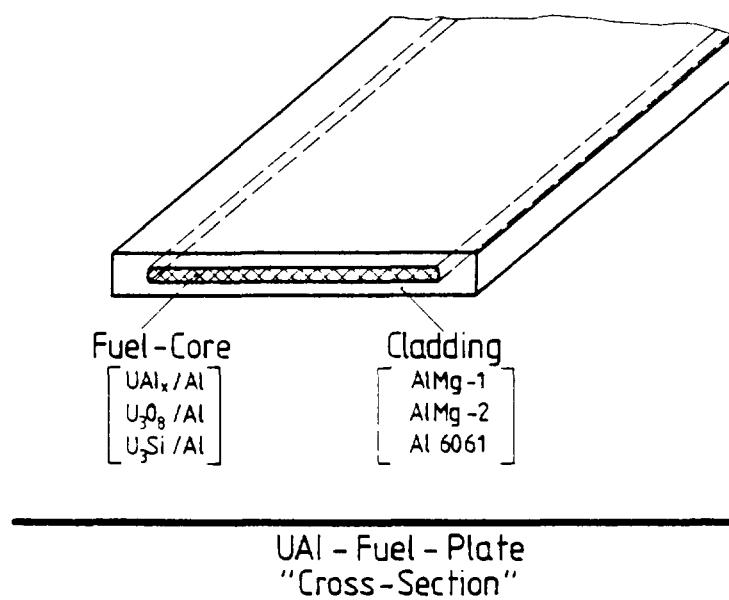


Fig. 2

according to an inspection scheme and three to five specimens are cut out from the plate for the metallographic examinations. Figure 3 demonstrates such a sampling scheme.

The sections to be inspected are first embedded, ground, polished and finally slightly etched. Using a microscope (100 x magnification), the thickness of the cladding can be measured.

There are two ways to carry out the measurement. In the first way a certain number of selective measurements along the slice are carried out picking only locations of minimum cladding thickness. Figure 4 demonstrates such a measurement.

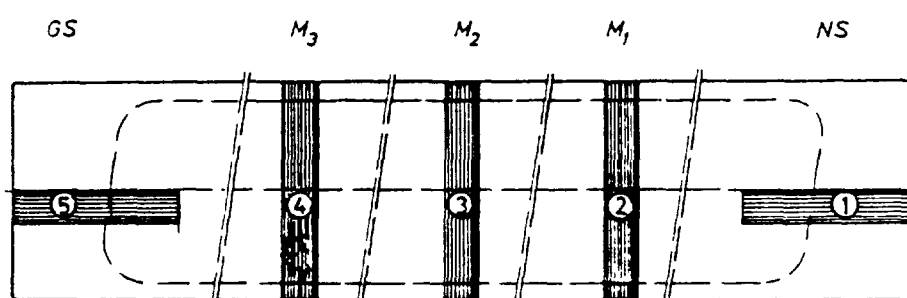


Fig. 3 Sampling scheme for metallographic examination.

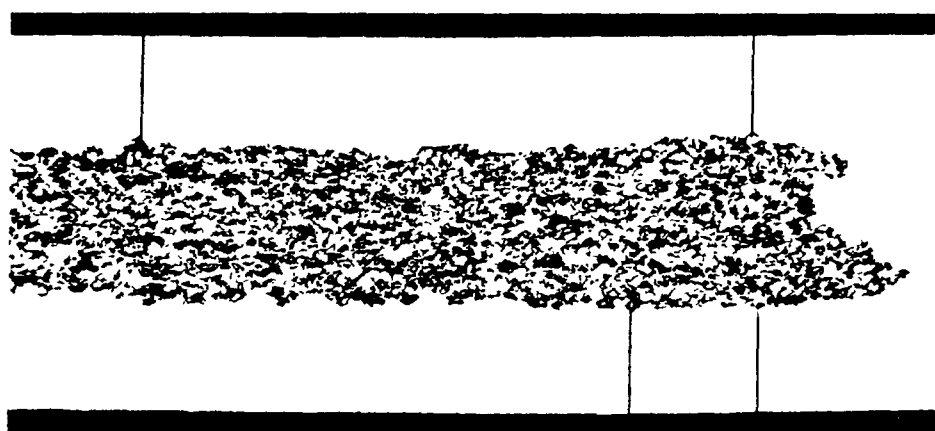


Fig. 4 Selectively measured minimum cladding thickness

The second method was worked out on the statistical basis [2]. In this case the cladding thickness measurements are carried out in exactly 1 mm step intervals on both sides. The slice has the length of approximately 60 mm yielding 60 measuring points ($n = 60$) for each side. Figure 5 illustrates such a measuring scheme.

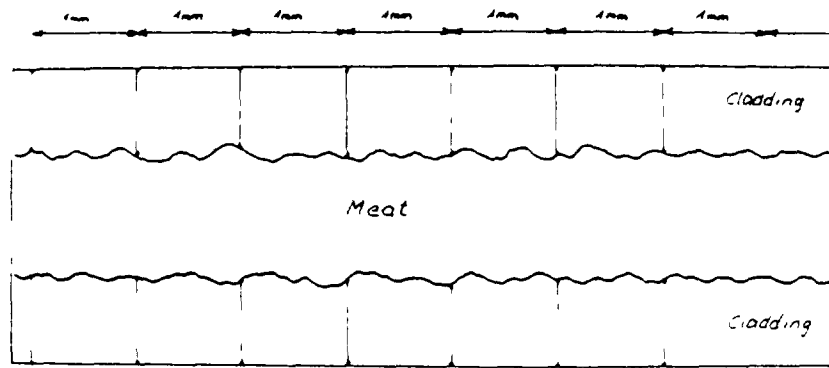


Fig. 5 Cladding thickness measurement on statistical basis.

In order to define some criteria, first of all the type of the distribution function must be known. For this purpose initial measurements of cladding thicknesses (1 mm basis) were carried out. By means of plotting the results on a "probability net" we received the following informations:

- A normal distribution can be assumed (the curve is almost linear). For characterization, therefore, the characteristic parameters of normal distribution, mean value (\bar{x}) and standard deviation (s), can be used.
- Measurements on both sides give a relatively good agreement.

Figure 6 demonstrates the results:

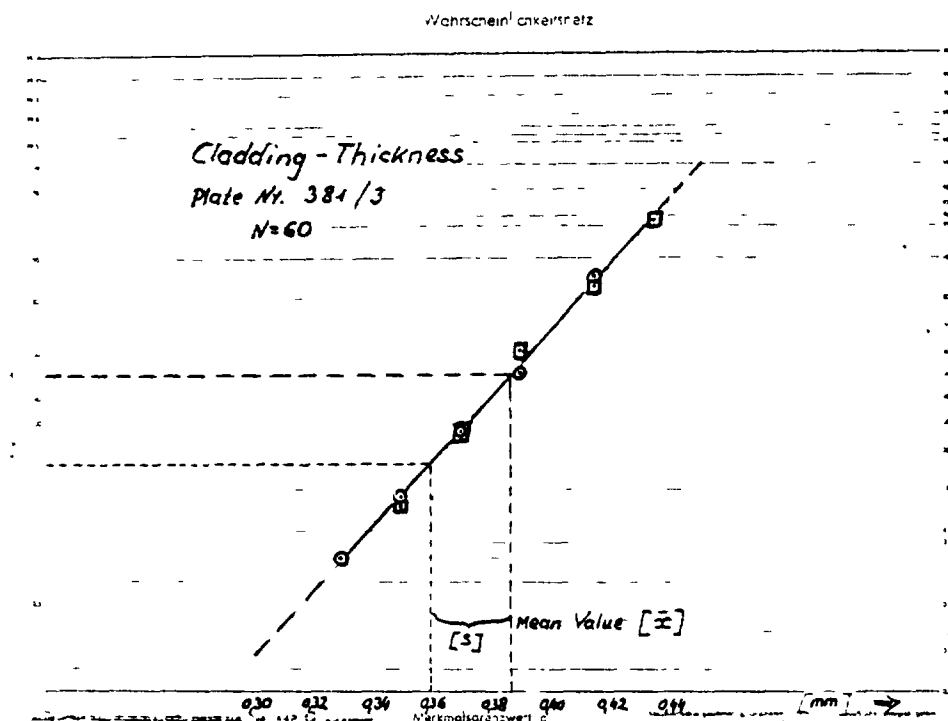


Fig. 6 Plotting the results on a "probability net"

Further investigations have shown, that the results gained from further 60-60 measurements confirm those of the first measurement. The evaluation of such measurements, carried out on one fuel plate with five specimens, is illustrated in Fig. 7

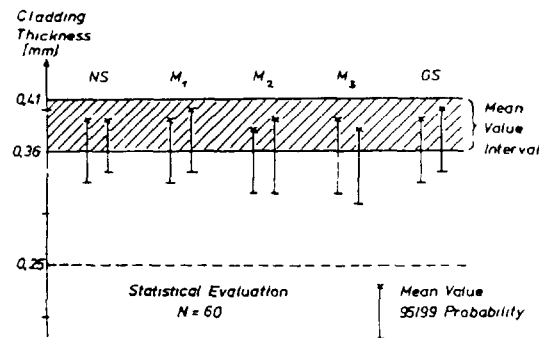


Fig. 7 Statistical evaluation of the results for one fuel plate

The results demonstrate the following:

- The mean cladding thickness values vary between 0,38 and 0,40 mm.
- The lower tolerance limits for a confidence level of 95 % and a portion of 99 % are between 0,31 and 0,34 mm (calculated from fig. 8).
- There is neither a significant difference between NS/GS and M 1-M 3 positions, nor between the upper and lower cladding.

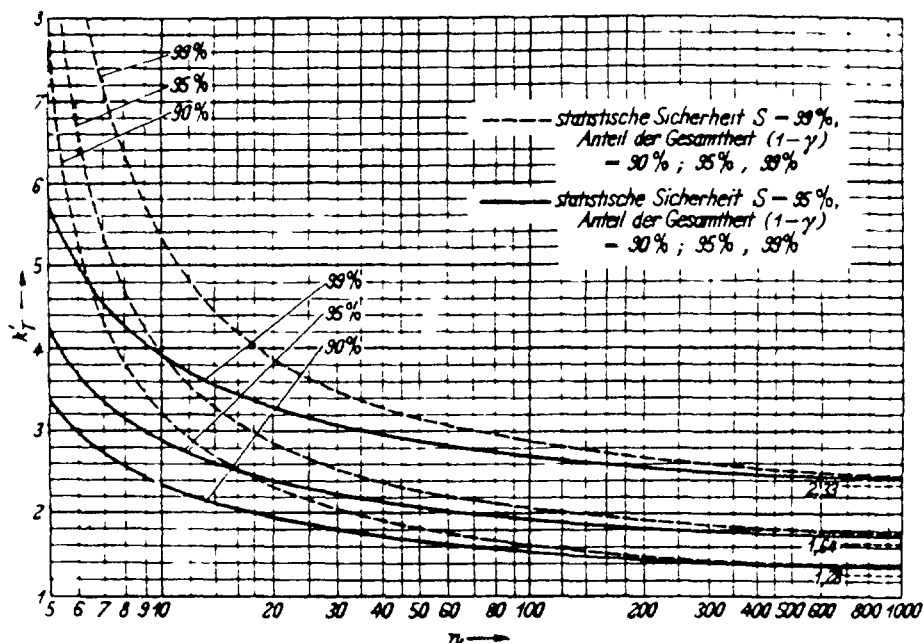


Fig. 8 One side tolerance limits (K_T -Faktors) for the confidence level of 95 % and 99 % and the portions 90 %, 95 % and 99 %.

3. Final Remarks


It is the essential result of these investigations that even with a limited number of measurements a representative statement on the cladding thickness of a fuel plate is possible.

REFERENCES


- /1/ **M. Hrovath** "Report on the status of the German Fuel and Fuel-Element Development Programm";
IAEA-Seminar in Jülich from 14.-18. September 1981;
IAEA-SR-77.
- /2/ **T. Görgenyi and W. Theymann**

"Statistical evaluation of coating thickness measurements"; Paper presented at the Informal Meeting on Quality Control of HTR-Fuels at the Atomic Energy Establishment Winfrith, Dorchester, Dorset, 29 and 30 September, 1970.

HOW TO ORDER IAEA PUBLICATIONS

 An exclusive sales agent for IAEA publications, to whom all orders and inquiries should be addressed, has been appointed for the following countries:

CANADA
UNITED STATES OF AMERICA UNIPUB, 4611-F Assembly Drive, Lanham, MD 20706-4391, USA

 In the following countries IAEA publications may be purchased from the sales agents or booksellers listed or through major local booksellers. Payment can be made in local currency or with UNESCO coupons.

ARGENTINA	Comisión Nacional de Energía Atómica, Avenida del Libertador 8250, RA-1429 Buenos Aires
AUSTRALIA	Hunter Publications, 58 A Gipps Street, Collingwood, Victoria 3066
BELGIUM	Service Courrier UNESCO, 202, Avenue du Roi, B-1060 Brussels
CHILE	Comisión Chilena de Energía Nuclear, Venta de Publicaciones, Amunátegui 95, Casilla 188-D, Santiago
CHINA	IAEA Publications in Chinese China Nuclear Energy Industry Corporation, Translation Section, P O Box 2103, Beijing IAEA Publications other than in Chinese China National Publications Import & Export Corporation, Deutsche Abteilung, P O Box 88, Beijing
CZECHOSLOVAKIA	S N T L, Mikulandska 4, CS-116 86 Prague 1 Alfa, Publishers, Hurbanovo námestie 3, CS-815 89 Bratislava
FRANCE	Office International de Documentation et Librairie, 48, rue Gay-Lussac, F-75240 Paris Cedex 05
HUNGARY	Kultura, Hungarian Foreign Trading Company, P O Box 149, H-1389 Budapest 62
INDIA	Oxford Book and Stationery Co, 17, Park Street, Calcutta-700 016 Oxford Book and Stationery Co, Scindia House, New Delhi-110 001
ISRAEL	YOZMOT (1989) Ltd, P O Box 56055, Tel Aviv 61560
ITALY	Libreria Scientifica, Dott. Lucio de Biasio "aeiou", Via Meravigli 16, I-20123 Milan
JAPAN	Maruzen Company, Ltd, P O Box 5050, 100-31 Tokyo International
PAKISTAN	Mirza Book Agency, 65, Shahrah Quaid-e-Azam, P O Box 729, Lahore 3
POLAND	Ars Polona-Ruch, Centrala Handlu Zagranicznego, Krakowskie Przedmiescie 7, PL-00-068 Warsaw
ROMANIA	Ilexim, P O Box 136-137, Bucharest
RUSSIAN FEDERATION	Mezhdunarodnaya Kniga, Smolenskaya-Sennaya 32-34, Moscow G-200
SOUTH AFRICA	Van Schaik Bookstore (Pty) Ltd, P O Box 724, Pretoria 0001
SPAIN	Díaz de Santos, Lagasca 95, E-28006 Madrid Díaz de Santos, Balmes 417, E-08022 Barcelona
SWEDEN	AB Fritzes Kungl. Hovbokhandel, Fredsgatan 2, P O Box 16356, S-103 27 Stockholm
UNITED KINGDOM	HMSO, Publications Centre, Agency Section, 51 Nine Elms Lane, London SW8 5DR
YUGOSLAVIA	Jugoslavenska Knjiga, Terazije 27, P O Box 36, YU-11001 Belgrade

 Orders from countries where sales agents have not yet been appointed and requests for information should be addressed directly to:



Division of Publications
International Atomic Energy Agency
Wagramerstrasse 5, P.O. Box 100, A-1400 Vienna, Austria